JOURNAL OF FORENSIC SCIENCES

J Forensic Sci, November 2010, Vol. 55, No. 6
doi: 10.1111/j.1556-4029.2010.01493.x
Available online at: onlinelibrary.wiley.com

PAPER

PHYSICAL ANTHROPOLOGY

Victoria A. Smith,[1] *M.N.S.; Angi M. Christensen,*[2] *Ph.D.; and Sarah W. Myers,*[3] *B.S.*

The Reliability of Visually Comparing Small Frontal Sinuses*

ABSTRACT: Several studies have investigated frontal sinus comparison for personal identification. One study addressed the statistical reliability of correct identification using automated digital methods and resulted in a 96% accuracy rate. Missed matches with the digital methods generally involved small, less featured sinuses. This study investigates the hypothesis that human examiners may be able to more accurately identify correct matches than digital methods, even when the comparisons involve small frontal sinuses. Participants were provided two sets of 28 radiographs and were instructed to identify matching radiographs and list the radiographs that did not have a corresponding match. Overall, error rates were low, with correct associations identified at a rate of 0.983. No incorrect associations (''false positives'') were made. Correct association rates were highest among participants ''experienced'' examining radiographs. Results support previous assertions that frontal sinus radiographs are a reliable means of personal identification even when the frontal sinuses are small.

KEYWORDS: forensic science, forensic anthropology, frontal sinus, personal identification

Numerous studies, dating back to the early 1900s, have investigated frontal sinus uniqueness and the use of radiographic comparison for personal identification (1–35). Many of these studies, however, involved small sample sizes in terms of both the number of radiographs examined and the number of participants involved. One study investigated the statistical reliability of correct identification using Elliptic Fourier Analysis and Euclidean distance models on digitized images which resulted in a 96% accuracy rate (8). The remaining 4% largely represented the inability of the computerized models to correctly match small, less featured frontal sinuses. This study investigates the hypothesis that human examiners are able to identify correct matches more accurately than digital methods, even when the frontal sinuses being compared are small or less featured. This, we believe, is both because of the fact that human examiners are more discriminating than digital methods and because humans are able to take into consideration other features present on the radiograph images. Also of interest is the effect, if any, of examiners' experience level on the ability to identify matches.

Materials and Methods

Radiographs were obtained from the University of Tennessee and are images of specimens from the William M. Bass Donated Skeletal Collection taken as part of a previous study (see (8)) in the following manner:

Radiographs were taken of crania with present, complete, and undamaged frontal regions. They were performed at the University of Tennessee Student Health Center using a HoLogic HFQ Series 100 kHz High Frequency machine at the following settings:

KVP (peak kilovoltage): 58–50 kV_{peak}
CM (distance from tube to film): 40 cm
MA (current in the X-ray tube): 75 mA
SEC (exposure time): 65 msec.

Crania were oriented so that the X-ray beam traversed the crania posterior to anterior, with the frontal bone nearest the film to allow minimal distortion and maximum clarity of the frontal sinus. The crania were placed on a foam/cloth ring with the midsagittal plane perpendicular to the X-ray film using the median palatine suture as a guide. When the cranium was viewed from the side, a line perpendicular to the film was in the same vertical plane as nasion and the superior border of the external auditory meatus. Replicate radiographs were taken of each cranium using the same methodology but at a different time so that replicates would not be exact copies and therefore simulated ''antemortem'' and ''postmortem'' images.

For this study, a random sample of 60 pairs of these previously taken radiographs was selected from the collection. From these 60 pairs, the radiographs with the smallest frontal sinuses and lacking visible dental restorations were used to make the matching process as challenging as possible.

Participants of varying backgrounds and levels of experience were solicited to participate in the study including Federal Bureau of Investigation scientists and attendees of the 2008 annual meeting of the American Academy of Forensic Sciences in Washington, D.C. Participants were provided two sets of 28 radiographs labeled A through BB and 1 through 28, an answer sheet/questionnaire, and a light box. They were advised that a ''match'' consisted of one letter or letter combination plus one number and that not all radiographs necessarily had a corresponding match present (there were actually 26 correctly matching pairs and 4 radiographs with

[1]Oak Ridge Associated Universities, 724 S. Saint Asaph Street, B-312, Alexandria, VA 22314.
[2]Federal Bureau of Investigation, Laboratory Division, 2501 Investigation Pkwy, Wuantico, VA 22135.
[3]Emory University, 201 Dowman Drive, Atlanta, GA 30322.
*Presented at the 61st Annual Meeting of the American Academy of Forensic Sciences, February 16-21, 2009, in Denver, CO.

Received 1 July 2009; and in revised form 3 Sept. 2009; accepted 3 Oct. 2009.

no match present). Although the frontal sinuses were presumably the main feature compared, participants were also asked to list any characteristics besides the frontal sinuses that they used to determine matches.

Participants were also asked to provide information regarding their education and background, and to rate their level of experience in both examining radiographs and performing anthropological or skeletal examinations. Experience ratings were defined as "No experience," "Some experience" (I have done this before, but not extensively or routinely), or "Experienced" (I do this as part of my work or have conducted research in this area).

Results

Sixty-five individuals participated in the study. Backgrounds included anthropology, biology, radiology, document examination, geology, photography, chemistry, and odontology and ranged from students to highly experienced professionals. The majority of participants had little or no experience in examining either radiographs or anthropological specimens. Specifically, for examining radiographs, 40 participants reported having "No experience", 17 reported "Some experience", and eight reported being "Experienced". For anthropology/osteology, 33 participants reported having "No experience", 14 reported "Some experience", and 18 reported being "Experienced" (Fig. 1).

Overall, error rates were very low. The correct association rate among all participants was 0.983, with 43 of the 65 participants (66%) correctly identifying all matches. No incorrect associations (i.e., pairing radiographs from different people, or "false positives") were made.

A total of 27 nonassociations (i.e., failure to identify a correct match, or "false negatives") occurred among all participants. Correct association rates were generally higher among those with more experience (Fig. 2) and were highest for those reporting being "experienced" examining radiographs. Participants were given an experience score of 0 (no experience), 1 (some experience), or 2 (experienced) for both their anthropology and radiograph experience as well as for combined experience (up to a score of 4 if the participant reported being an expert in both categories). Correlations were calculated between the type of reported experience and the correct association rate. The correlations were calculated for each type of experience individually as well as combined experience. Only the correlation between radiograph experience and correct associations was significant:

Anthropology experience: $r = 0.0817$, $p = 0.5176$
Radiograph experience: $r = 0.28076$, $p = 0.0224$
Combined experience: $r = 0.17928$, $p = 0.153$

One particular frontal sinus pair was frequently not associated, accounting for 18 of the 27 total nonassociations (Fig. 3). Reasons for this may include the limited number of features of the frontal sinus, differences in cranium position, or radiograph quality.

Other common features participants reported using in the matching process included the following: overall skull shape, bony crests/landmarks/processes, nose shape, orbit shape, venous markings, other paranasal sinuses, trabecular patterns, teeth, and cranial sutures.

Conclusions

Results support previous assertions that frontal sinus radiographs are a reliable means of personal identification. No incorrect associations ("false positives") were made by participants in this study.

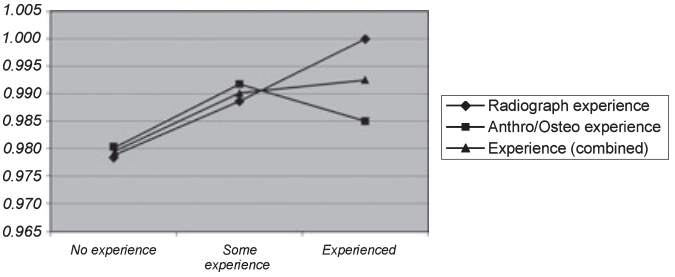

FIG. 1—*Experience levels of participants.*

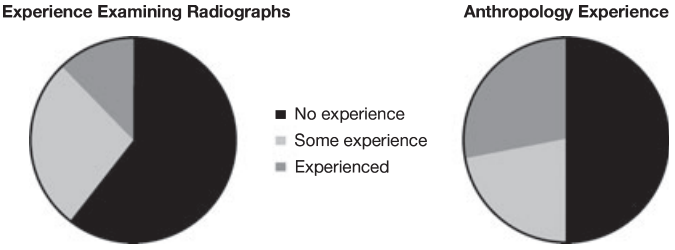

FIG. 2—*Correct association rates by experience level.*

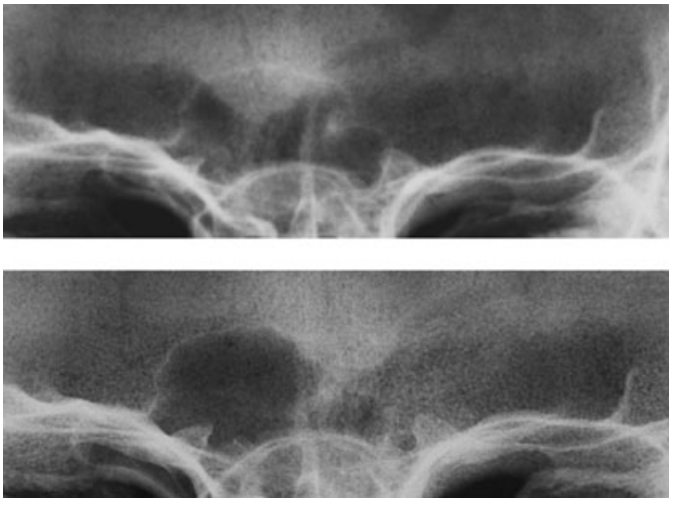

FIG. 3—*Most frequently missed frontal sinus match.*

Correct associations were identified at a rate of 0.983, and this rate was somewhat higher among those with more experience, especially if that experience included radiographic examinations. Moreover, while previous studies have evaluated the technique's reliability using computerized models, our results indicate that traditional visual comparison is highly accurate, even when frontal sinuses are small.

Acknowledgments

We thank Lee Jantz and the University of Tennessee Department of Anthropology for access to the radiographs. We also thank the volunteers who participated in the study, as well as Richard Thomas and Brian Carroll of the FBI Laboratory for reviewing earlier drafts of this manuscript. Kc Wendler and Joshua Friedman assisted with data collection.

References

1. Angual M, Derczy K. Personal identification on the basis of antemortem and postmortem radiographs. J Forensic Sci 1998;43:1089–93.
2. Asherson N. Identification by frontal sinus prints: a forensic medical pilot survey. London, UK: H.K. Lewis & Co. Ltd, 1965.
3. Atkins L, Potsaid MS. Roentgenographic identification of human remains. JAMA 1978;240:2307–8.
4. Brothwell DR, Molleson T, Metreweli C. Radiological aspects of normal variation in earlier skeletons: an exploratory study. In: Brothwell DR, editor. The skeletal biology of earlier human populations. New York, NY: Pergamon Press, 1968;149–72.
5. Buckland-Wright JC. A radiological examination of frontal sinuses in early British populations. Man 1970;5:512–7.
6. Camps FE. Radiology and its forensic application. In: Camps FE, editor. Recent advances in forensic pathology. London, UK: J. & A. Churchill, 1969;149–60.
7. Cheevers LS, Ascencio R. Identification by skull superimposition. Int J Forensic Dent 1977;13:14–6.
8. Christensen AM. Testing the reliability of frontal sinus outlines in personal identification. J Forensic Sci 2005;50(1):18–22.
9. Cryer MH. Some variations in the frontal sinuses. JAMA 1907;48:284–98.
10. Culbert WL, Law FL. Identification by comparison of roentgenograms of nasal accessory sinuses and mastoid processes. JAMA 1927; 88:1634–6.
11. Fischman SL. The use of medical and dental radiographs in identification. Int Dent J 1985;35:301–6.
12. Gulisano M, Pacini P, Orlandini GF, Colosi G. Anatomico-radiological findings on the frontal sinus: statistical study of 520 human cases. Arch Ital Anat Embriol 1987;83(9):9–32.
13. Haglund WD, Fligner CL. Confirmation of human identification using computerized tomography (CT). J Forensic Sci 1993;38:708–12.
14. Hanson CL, Owsley DW. Frontal sinus size in Eskimo populations. Am J Phys Anthropol 1980;53:251–5.
15. Harris AMP, Wood RE, Nortje CJ, Thomas CJ. The frontal sinus: a forensic fingerprint? – A pilot study. J Forensic Odonto-stomatol 1987; 5:9–15.
16. Joblanski NG, Shum BS. Identification of unknown human remains by comparison of antemortem and postmortem radiographs. Forensic Sci Int 1989;42:221–30.
17. Kerley ER, Snow CC. Authentification of John F. Kennedy autopsy radiographs and photographs. Final report to the Select Committee of Assassinations. Washington, DC: U.S. House of Representatives, March 9, 1979.
18. Kirk NJ, Wood RE, Goldstein M. Skeletal identification using the frontal sinus region: a retrospective study of 39 cases. J Forensic Sci 2002;47(2):318–23.
19. Koertvelyessy T. Relationships between the frontal;sinus and climactic conditions: a skeletal approach to cold adaptation. Am J Phys Anthropol 1972;37:161–72.
20. Kullman L, Eklund B, Grudin R. The value of the frontal sinus in identification of unknown persons. J Forensic Odonto-stomatol 1990;8:3–10.
21. Marek Z, Kusmiderski J, Lisowski Z. Radiograms of the paranasal sinuses as a principle of identifying catastrophe victims and unknown skeletons. Arch Kriminol 1983;2:1–6.
22. Marlin DC, Clark MA, Standish SM. Identification of human remains by comparison of frontal sinus radiographs: a series of four cases. J Forensic Sci 1991;36:1765–72.
23. Messmer JM. Radiographic identification. In: Fierro MF, editor. CAP handbook for postmortem examination of unidentified remains. Skokie, IL: College of American Pathologists, 1986;68–75.
24. Murphy WA, Gantner GE. Radiologic examination of anatomic parts and skeletonized remains. J Forensic Sci 1982;27:9–18.
25. Phrabhakaran N, Naidu MDK, Subramaniam K. Anatomical variability of the frontal sinuses and their application in forensic identification. Clin Anat 1999;12:16–9.
26. Quatrehomme G, Fronty P, Sapanet M, Grevin G, Bailet P. Identification by frontal sinus pattern in forensic anthropology. Forensic Sci Int 1996;83(2):147–53.
27. Quatrehomme G, Sapanet M, Bailet P, Grevin G, Boublenza A, Ollier A. Identification by frontal sinus: performance and difficulties. Proceedings of the 6th Annual Meeting of the International Association for Craniofacial Identification; 1995 Nov 8–11; Boca Raton, FL: International Association for Craniofacial Identification, 1995.
28. Reichs KJ. Quantified comparison of frontal sinus patterns by means of computed tomography. Forensic Sci Int 1993;61:141–68.
29. Reichs KJ, Dorion RBJ. The use of computerized axil tomography (CAT) scans in the comparisons of frontal sinus configurations. Canadian Soc Forensic Sci J 1992;25:1–16.
30. Ribeiro FA. Standardized measurements of radiographic films of the frontal sinuses: an aid to identifying unknown persons. Ear Nose Throat J 2000;79:26–33.
31. Schuller A. Das Rontgenogram der Stirnhohle: ein Hilfsmittel fur die Identitatsbestimmung von Schadeln. Monatsschr Ohrenheilkd Laryngorhinol 1921;5:1617–20.
32. Schuller A. A note of the identification of skulls by X-ray pictures of the frontal sinuses. Med J Aust 1943;1:554–7.
33. Strek P, Kaczanowski K, Skawina A, Pitynski K, Kitlinski Z, Mrowka D, et al. The morphological evaluation of frontal sinuses in Human Skulls. Floia Morphol (Warsz.) 1992;51:319–28.
34. Ubelaker DH. Positive identification from the radiographic comparison of frontal sinus patterns. In: Rathbun TA, Buikstra J, editors. Human identification: case studies in forensic anthropology. Springfield, IL: Charles C. Thomas, 1984;399–411.
35. Yoshino M, Miyasaka S, Sato H, Seta S. Classification system of frontal sinus patterns by radiography: its application to identification of unknown skeletal remains. Forensic Sci Int 1987;34:289–99.

Additional information–reprints not available from author:
Victoria A. Smith, M.N.S.
Oak Ridge Associated Universities
724 S. Saint Asaph Street, B-312
Alexandria, VA 22314
E-mail: victoria.smith@orise.orau.gov

JOURNAL OF FORENSIC SCIENCES

J Forensic Sci, November 2010, Vol. 55, No. 6
doi: 10.1111/j.1556-4029.2010.01475.x
Available online at: onlinelibrary.wiley.com

PAPER

PHYSICAL ANTHROPOLOGY; ENGINEERING SCIENCES AND PATHOLOGY/BIOLOGY

Timothy G. Baumer,[1] *M.S.; Marcus Nashelsky,*[2] *M.D.; Carolyn V. Hurst,*[3] *B.A.; Nicholas V. Passalacqua,*[3] *M.S.; Todd W. Fenton,*[3] *Ph.D.; and Roger C. Haut,*[1] *Ph.D.*

Characteristics and Prediction of Cranial Crush Injuries in Children*†

ABSTRACT: This study documents four clinical cases of fatal crush injuries to children between 1.5 and 6 years of age with correlations between modeled stress and clinically observed fracture patterns. The clinical case fractures were concentrated in the basicranium, bridged the impact sites, and traversed the middle cranial fossa in the area of the spheno-occipital synchondrosis. The crushing forces from these cases were recreated on a simplified finite element model of a cranium by applying bilateral pressures to corresponding regions. Numerous trials were run to develop a representative pattern of principal stress directions. In all cases, the highest tensile stresses were located on the basicranium and corresponded to the observed fracture path(s). These results suggest that prefailure stress field diagrams may predict fracture propagation paths, although these will not be exact. Also, these analyses indicate that quasi-static bilateral loading of the cranium may lead to predictable fracture of the basicranium.

KEYWORDS: forensic science, pediatric skull, crushing, quasi-static load, basilar fracture, FE modeling

Fracture interpretation is a necessary component of forensic analysis and contributes to the determination of the cause and manner of death. Skeletonized remains, in particular, lack skin and scalp abnormalities that enhance the complete description of a head injury or injuries. Thus, a clear understanding of fracture propagation becomes vital to the forensic professional. Head injuries are often the result of dynamic forces in which a moving object strikes the cranium at a considerable speed or the cranium makes contact with a static object that causes it to rapidly decelerate (1). In cases of crushing injuries, however, a static load is applied relatively slowly to the cranium, initially causing deformation with eventual fracture if pressure continues or increases. In experimental tests on the effects of bilateral crushing forces on cadaver skulls, Russell and Schiller (2) report that avulsion of the petrous portion, fracture through the dorsum sellae, and principal fracture lines running in the direction of the compressive forces were commonly observed features.

There are several case reports of basilar skull damage in the literature involving both crushing and impulse-based loading scenarios, mainly focusing on adult crania. A study of 15 cases of crushing injuries to adult skulls aged 14–63 and experimentally induced crushing fractures on 11 cadaver crania revealed similarities in basilar fracture patterns (2). However, a study by Harvey and Jones (3) claimed that fractures through both petrous bones were not an indicator of impact site. Another study by Yasue (4) then suggested that the overall path of fracture through the basicranium could, in fact, be related to the region of the skull impacted. More recently, a study by Kroman (5) attempted to produce cranial base (hinge) fractures in two unembalmed cadaver adult human crania specimens using a drop tower. High-speed video demonstrated that fractures initiated at the site of impact and propagated through the middle cranial fossa, with some additional minor fractures surrounding the foramen magnum. In this study, the vaults had been removed so it is unclear if the fractures would have terminated at the points of applied forces (fixture and impactor). Kroman further notes a very wide separation of the failing bones during impact, which no doubt would cause very severe soft-tissue damage in the cranial base. This correlates to the high amount of energy and lethality involved in these scenarios.

It is assumed that fractures will generally follow the path of least resistance, but this path may be different between the child and adult cranium. While all of the aforementioned studies focused on adult crania, some recent case reports on quasi-static loading to the crania of children have also presented observations of basilar fractures (1,6). The trend of quasi-static loading producing basilar fractures in both adults and children may suggest that prediction of these fractures is possible.

The finite element (FE) method is a powerful analytical modeling tool that can be used to determine internal stresses and strains within a complex solid. Several studies have shown that maximum principal stress (or strain) directions from a modeled structure correlate well with areas of experimentally or clinically observed bone fractures (7–9). While modeling of fracture propagation generally

[1]Orthopaedic Biomechanics Laboratories, College of Osteopathic Medicine, Michigan State University, East Lansing, MI 48824.
[2]Department of Pathology, University of Iowa Hospitals & Clinics, University of Iowa, Iowa City, IA 52242.
[3]Department of Anthropology, College of Social Sciences, Michigan State University, East Lansing, MI 48824.

*Funded in part by the National Institute of Justice, Office of Justice Programs, United States Department of Justice (2007-DN-BX-K196).
†Presented in part at the 61st Annual Scientific Meeting of the American Academy of Forensic Sciences, February 16-21, 2009, in Denver, CO.

Received 29 May 2009; and in revised form 12 Aug. 2009; accepted 5 Sept. 2009.

involves high computational costs, one theory suggests that there is a close, although not exact, relationship between prefailure stress trajectories and the ultimate path of propagation. In brief, Frank and Lawn (10) proposed that crack growth occurs in such a way as to maximize the energy dissipation per unit length of growth and that the greatest amount of dissipation occurs when the crack plane is perpendicular to the direction of greatest principal tensile stress. In other words, the directions of principal tensile stress developed on a solid may be a reasonable predictor of propagation direction.

In this study, four cases of childhood fatalities from crushing head injuries inflicted by vehicle tires exhibited similar fracture patterns despite differences in age and magnitude of force. This raised the question as to whether certain fracture patterns are indicative of bilateral crushing injuries and if these could be predicted based on the type of loading and the biomechanical properties of the skull.

Materials and Methods

Four cases of fatal crushing head injuries to young children between 1.5 and 6 years of age under known conditions were used as a baseline for applied forces and resulting fracture patterns. In all cases, the head/skull was run over by a vehicle tire, compressing the head/skull between the vehicle tire and the ground. The contact sites and skull fractures were identified and diagramed during autopsy by the investigating forensic pathologist (M.N.). Biomechanical modeling was then conducted in an attempt to recreate and explain the similarities exhibited in the fracture patterns of these cases.

A simplified model of a skull was created in a FE package (Abaqus v.6.3; Hibbitt, Karlsson & Sorensen, Inc., Pawtucket, RI) (Fig. 1). This model consisted of symmetry about the sagittal plane, but not about the coronal or transverse planes. Each major bone of the vault was modeled separately, assumed to have a uniform thickness, and constrained at the suture joints to form the full cranial model. The base of the cranium was modeled as a flat surface with the same thickness as the vault. The primary landmarks in the basal region were modeled: a hole was added to simulate the foramen magnum, dense oblong extrusions lateral to the foramen magnum were generated to represent the petrous portions, and anterior to the foramen magnum the thickness was reduced to represent the region of the spheno-occipital synchondrosis. This model did not utilize specific, age-dependent material properties for the crania and consisted of simplified, although generally accurate, geometry.

The model was subjected to quasi-static pressures corresponding to the specific exterior injury locations for each case. The magnitude of the pressure applied to the cranial model was the same in each case and was scaled down such that the generated stresses would not cause material failure. By restricting the analyses to the elastic region, the exact material properties were not required for this simple analysis. FE analysis was utilized in an effort to reproduce and examine possible relationships between the theoretical prefailure stresses developed on the modeled crania and the fracture patterns observed clinically. Using some basic stress transformation principles at many predefined locations on the skull (FE), the direction and magnitude of tensile and compressive stresses at each location were determined. The full-field map was then filtered to remove all regions of low stress. Areas of tensile (principal) stress were assumed to be the most likely location(s) of potential fracture, and the general trends produced by the model were examined in comparison with the clinical cases. Numerous trials were run within the elastic (nonfailure) range of bone to develop a representative and clearly characterized pattern of principal stress and strain directions.

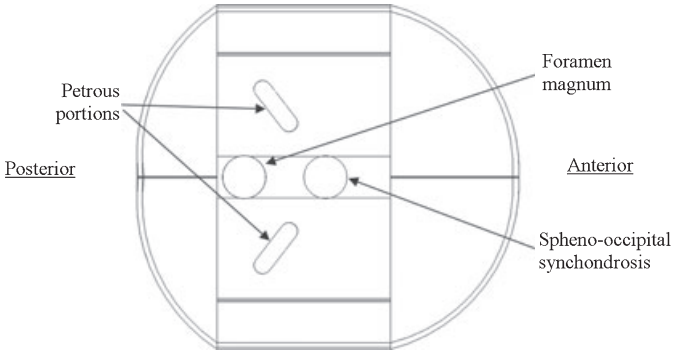

FIG. 1—*Simplified cranial model showing modeled landmarks of the basicranium. View of endocranial surface with vault removed.*

Results

Case 1

A 5-year-old female child was struck by her family's sedan when she fell in an attempt to stop the vehicle after her brother accidentally engaged the transmission. Her head was run over by the right front tire of the car. The autopsy revealed an intact cranial vault with a cranial base fracture that traversed the lateral right anterior cranial fossa, the midline of the middle cranial fossa, and the left lateral aspect of the posterior cranial fossa. This fracture bridged the blunt impact sites on the right anterior and left posterior aspects of the head (Fig. 2).

Case 2

An unhelmeted 6-year-old male was struck by a car while riding his bike. His head was run over by the vehicle's left rear tire.

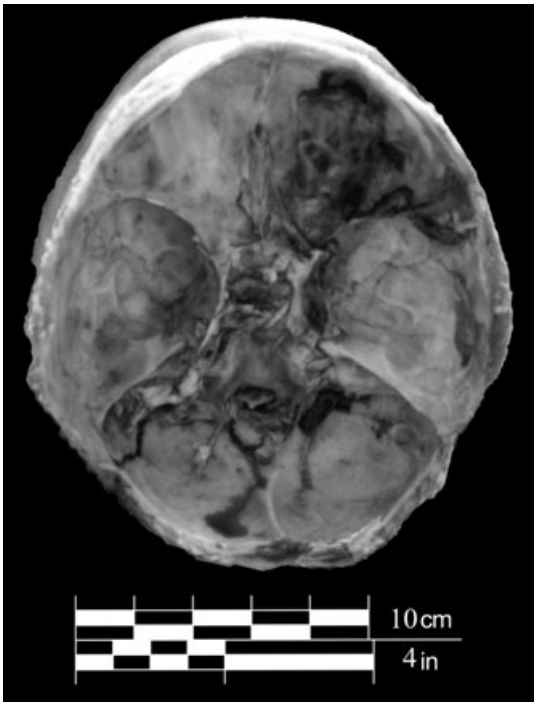

FIG. 2—*Photo taken at autopsy of endocranial base fractures of 5-year-old child from Case 1.*

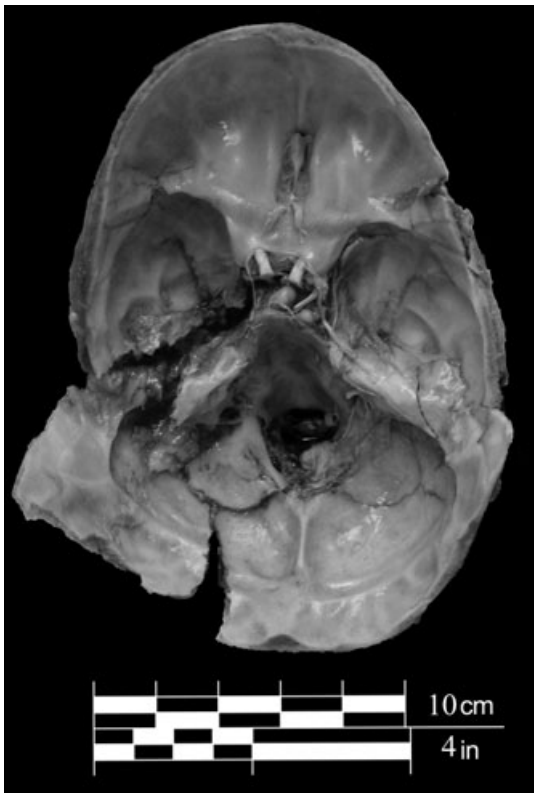

FIG. 3—*Photo taken at autopsy of endocranial base fractures of 6-year-old child from Case 2.*

FIG. 4—*Photo taken at autopsy of endocranial base fractures of 3-year-old child from Case 3.*

Autopsy revealed an intact cranial vault. The cranial base was bisected by a gaping X-shaped fracture centered in the midline of the middle cranial fossa. There were two adjacent arms of the fracture in the right middle cranial fossa. The other two adjacent arms were in the posterior aspect of the left middle cranial fossa and the anterior aspect of the left posterior cranial fossa. This fracture bridged the blunt impact sites on the right anterior and lateral aspects of the head and the left lateral and posterolateral aspects of the head (Fig. 3).

Case 3

A 3-year-old male was run over attempting to run away from a farm grain wagon that had begun to roll. His head was run over by one of the wheels of the wagon. Autopsy revealed gaping linear fractures that traversed the parietal bones and the right and left sides of the frontal bone. One end of each fracture intersected the widely gaping right side of the coronal suture; other ends were continuous with fractures of the cranial base. A dominant cranial base fracture traversed the left petrous bone, the midline of the middle cranial fossa, the anterior aspect of the right middle cranial fossa, and the posterolateral aspect of the right anterior cranial fossa. Additional intersecting fractures were centered in the left middle and posterior cranial fossae (Fig. 4).

Case 4

A 1.5-year-old female was entrapped under a small moving van and her head was run over by the right rear wheel. Autopsy revealed an intact cranial vault but extensive intersecting fractures of the cranial base that predominately traversed the middle and posterior cranial fossae from side to side. A large fracture also bisected the anterior cranial fossae (Fig. 5).

Fracture Pattern Similarities

Each of the cases presented fracture patterns that bridge the impact sites and traversed the middle cranial fossa in the area of the spheno-occipital synchondrosis. Additionally, the damage was concentrated in the basicranium leaving the cranial vault intact in all cases except the 3-year-old boy impacted by the farm grain wagon. Furthermore, general amounts of fracture increased with inferred increase in magnitude of applied force (grain wagon vs. car) or decrease in age.

The four cases presented three contact scenarios with four different fracture configurations, each having commonalities to a single pattern of fracture (described earlier). Specifically, the contact forces in Case 1 were applied primarily to the frontal and occipital bones in a direction between anterior-posterior and lateral (Fig. 6*a*), the contact forces in Cases 2 and 3 were also applied to the frontal and occipital bones but had an additional lateral component (Figs. 7*a* and 8*a*), and the contact forces in Case 4 were applied to the lateral surfaces of the cranial model (Fig. 9*a*).

Modeling of all four cases revealed that the locations of high tensile stress and high tensile strain were the same, and these regions were located on the basicranium. There were some areas of lower tensile stress at the sites of the applied load and in a few areas on the cranial vault, but because of the assumption that failure would occur at locations of high stress, these areas were ignored in this presentation. The maximum tensile stress for all models was similar (standard deviation of ±5%). The tensile

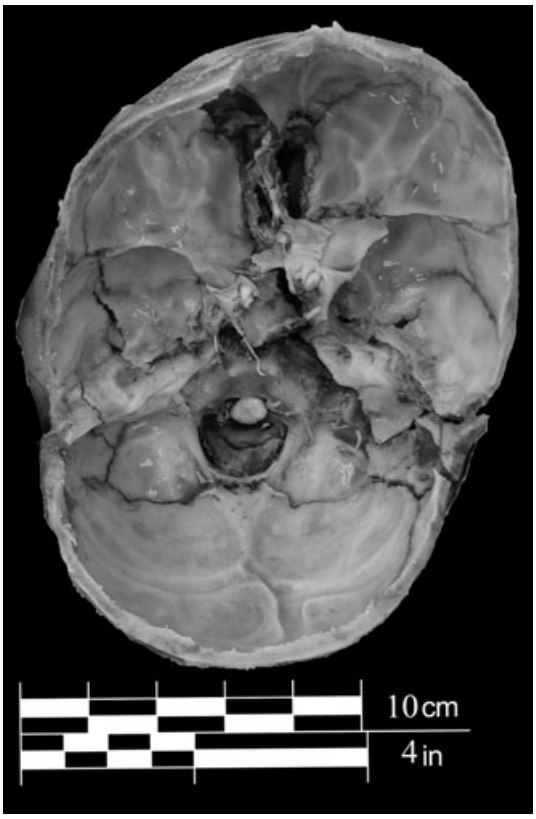

FIG. 5—*Photo taken at autopsy of endocranial base fractures of 1.5-year-old child from Case 4.*

stresses developed on the skull were filtered to display only the highest 20% for correlation to fracture patterns.

Case 1 presented the simplest fracture pattern as a single linear fracture traversing the basicranium from the right greater wing of the sphenoid across the spheno-occipital synchondrosis to the left lateral portion of the occipital, connecting the loading sites (Fig. 6*a*). An overlay of the directions of maximum principal tensile stresses revealed a linear concentration on the right side of the sphenoid and in the area of the spheno-occipital synchondrosis, which correlated well with sections of the observed fracture (Fig. 6*b*).

Cases 2 and 3 presented slightly more complex fracture patterns. In part, the complexity was increased because of the similarities in loading but dissimilarities in fracture (Figs. 7*a* and 8*a*, respectively). A similar fracture in both cases stretched from the right aspect of the sphenoid through the sella turcica and along the superior aspect of the petrous portion of the temporal. The overlay of the directions of maximum principal tensile stresses was identical in both cases because of the similarity of loading patterns. There was correlation between the stress and the fracture for both cases, especially along the line of similar fracture, although each had areas of high stress where fracture did not occur (Figs. 7*b* and 8*b*). Case 4 presented the most complex fracture pattern extending both longitudinally and transversely through the basicranium (Fig. 9*a*). Fractures ran longitudinally across the midline of the anterior cranial fossa and horizontally through the middle and posterior cranial fossa with various areas of comminution. The overlay of the directions of maximum principal tensile stresses revealed an area of complex stress in the same area as the highly comminuted fracture of the right side of the cranial base. Additionally, a more linear pattern of stresses occurred near the fractures on the left side of the skull (Fig. 9*b*).

Discussion

The analyses performed in this study represent a quantitative, theoretical attempt to correlate stress and strain intensities and principal directions to fracture patterns on the skull caused by quasi-static bilateral pressures. A linear, small strain, isotropic, uniform thickness model of a human calvarium was constructed in this study. Analyses of the modeled stresses and the clinically observed fractures suggested that quasi-static bilateral loading of the cranium leads to predictable fracture of the basicranium, although the predictions were not exact. The promising nature of these results suggests that it may be useful to develop a more complex model for a more accurate prediction of fractures on a case-by-case basis.

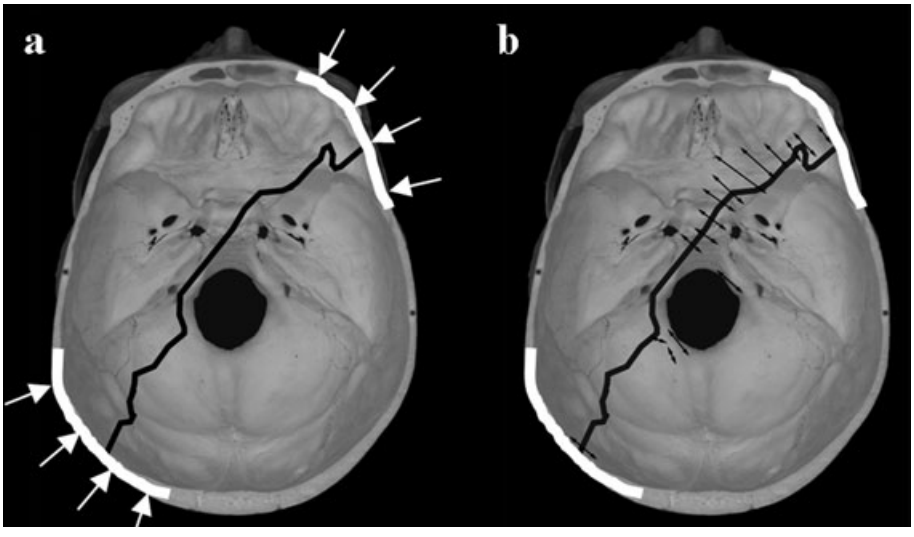

FIG. 6—*(Case 1) Crushing injury to the skull of a 5-year-old. Diagrams of (a) clinically observed fractures and (b) an overlay of the highest 20% of principal tensile stresses produced from a FE model. White cranial margins represent contact of applied forces (ground and tire). The arrows in (b) indicate the directions of tension on the cranium.*

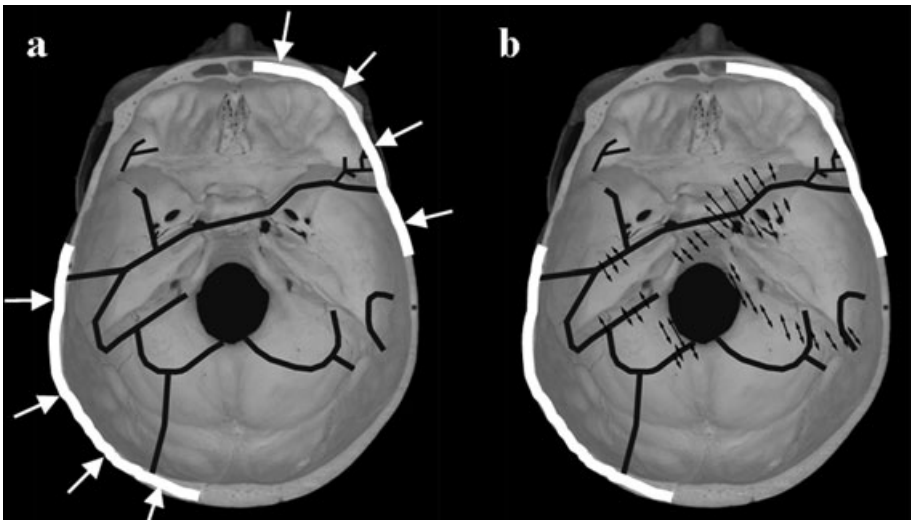

FIG. 7—*(Case 2) Crushing injury to the skull of a 6-year-old. Diagrams of (a) clinically observed fractures and (b) an overlay of the highest 20% of principal tensile stresses produced from a FE model. White cranial margins represent contact of applied forces (ground and tire). The arrows in (b) indicate the directions of tension on the cranium.*

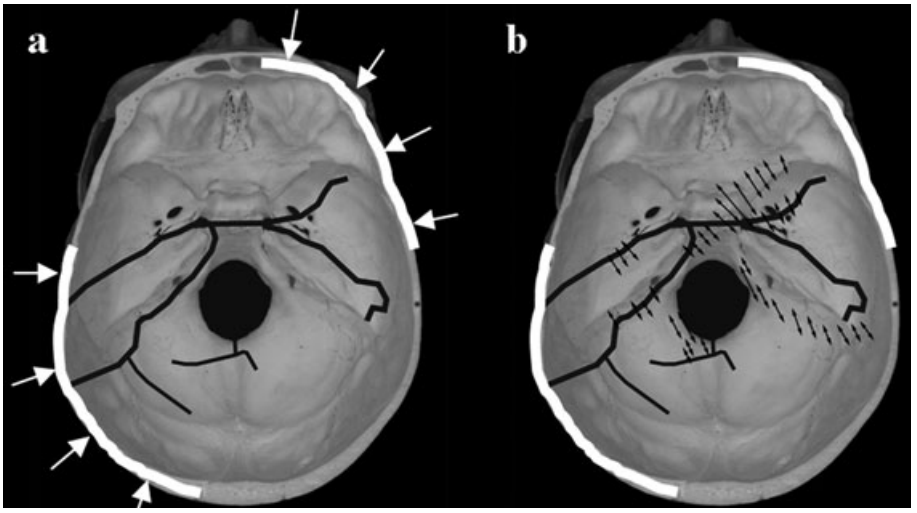

FIG. 8—*(Case 3) Crushing injury to the skull of a 3-year-old. Diagrams of (a) clinically observed fractures and (b) an overlay of the highest 20% of principal tensile stresses produced from a FE model. White cranial margins represent contact of applied forces (ground and tire). The arrows in (b) indicate the directions of tension on the cranium.*

The location of maximum tensile stress would be expected to be the site of fracture initiation, and the location of maximum stress in each of the four models correlated well with the area(s) of fracture in each of the clinical cases. However, Frank and Lawn (10) also suggest that paths of high tensile stress may approximate the path of fracture propagation. In the four cases presented in this study, regions of high tensile stress appeared to follow the path of the fracture extending from the location of maximum stress. Fracture propagation, however, requires increasing levels of stress to overcome the dissipation of energy that occurs with the previous fracturing. These increasing levels of stress may ultimately result in additional fracture sites on the material surface (11). Two or more isolated regions of the skull developed high tensile stresses in Cases 2–4, which may have resulted in multiple sites of fracture initiation with propagation extending from each site. Multiple initiation sites with subsequent propagation joining the sites could explain the complexity of the fractures seen in Cases 2–4, as opposed to the singular region of fracture and stress intensity developed in Case 1. The four cases presented in this study suggest that prefailure stress field diagrams may, in fact, give some insight into the projected fracture propagation paths and, ultimately, fracture patterns developed during quasi-static bilateral loading of the cranium.

The cases and analyses presented in this study supported some general trends for quasi-static bilateral loading scenarios. Autopsy revealed fractures through the middle cranial fossa in the region of the spheno-occipital synchondrosis in all cases. Modeling displayed high tensile stresses through this region in Cases 1–3, with Cases 2 and 3 developing maximum levels of stress at this landmark. However, modeling of Case 4 showed no region of high tensile stress passing through the spheno-occipital synchondrosis. Interestingly, Case 4 involved the youngest child and one of the most massive vehicles (moving van). This result may suggest that the material model should be altered as a function of age, especially for the very young pediatric patient. Autopsies also revealed fractures connecting the loading sites through the basicranium in all four cases. The models showed regions of high tensile stress in this region for

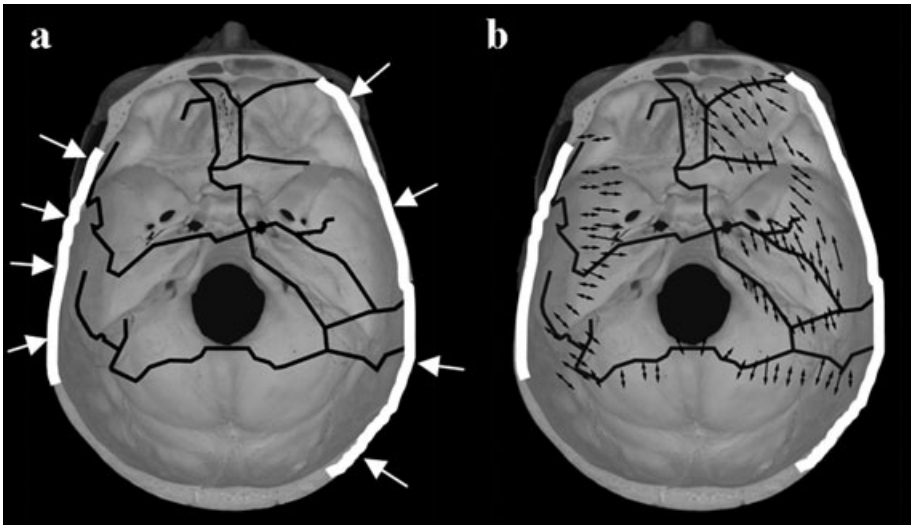

FIG. 9—*(Case 4) Crushing injury to the skull of a 1.5-year-old. Diagrams of (a) clinically observed fractures and (b) an overlay of the highest 20% of principal tensile stresses produced from a FE model. White cranial margins represent contact of applied forces (ground and tire). The arrows in (b) indicate the directions of tension on the cranium.*

Cases 1–3, although the tensile stresses in Case 4 did not seem to follow the same pattern. Intact cranial vaults were also present in three of four cases. The models displayed no significant levels of stress on the vault that would be expected to cause fracture. It is possible that the mass of the vehicle (grain wagon) caused excessive fracture propagation that was not able to be modeled in Case 3. All of the fracture-related observations seen in the current study showed similarities to experimentally developed fractures on adult cadaver skulls (2) suggesting that these patterns of quasi-static loading of the cranium may be somewhat age independent, except for the very young patient, likely as a function of cranial geometry, which would remain essentially the same throughout life.

In summary, a simple model of a cranium subjected to clinically observed bilateral crushing forces was largely able to predict the characteristics of the developed fracture patterns. The results of this study were not meant to propose that the theoretical stresses developed on this simplified cranial model actually predict an arbitrary fracture pattern developed clinically. These results do show that a simplified analysis of tensile stresses developed from some basic information on boundary loads and locations on the cranium could generate patterns of high tensile stress that are consistent with clinical fractures. The four cases, in conjunction with the FE model, suggest that crania subjected to bilateral crushing forces tend to fracture in predictable ways. Further, the regions of high tensile stress that develop between the locations of loading on the pediatric cranium coincide with the locations of tensile fracture.

The predictability of this pediatric cranial fracture pattern has practical application. Medical examiner and coroner death investigations attempt to establish circumstances of injury. In cases of unknown or questionable circumstances, this fracture pattern would suggest a particular mechanism of injury consistent with a heavy wheeled vehicle. The described fracture pattern would be less consistent with other, more common injuries such as those sustained in motor vehicle collisions (ejection or internal tumbling) and in the setting of inflicted blunt trauma. This information may prove relevant in clarifying unexplained perimortem events in cases of crushing injuries to the pediatric cranium, particularly if information from examination of skin and scalp is not possible because of skeletonization.

Acknowledgment

The opinions, findings, and conclusions expressed in this publication are those of the authors and do not necessarily reflect the views of the Department of Justice.

References

1. Duhaime A-C, Eppley M, Margulies S, Heher KL, Bartlett SP. Crush injuries to the head in children. Neurosurgery 1995;37(3):401–7.
2. Russell WR, Schiller F. Crushing injuries to the skull: clinical and experimental observations. J Neurol Neurosurg Psychiatry 1949;12:52–60.
3. Harvey F, Jones A. "Typical" basal skull fracture of both petrous bones: an unreliable indicator of head impact site. J Forensic Sci 1980;25(2):280–6.
4. Yasue M. Clinical and experimental investigation of mediobasal skull fracture. Neurol Med Chir (Tokyo) 1981;21:1041–9.
5. Kroman AM. Fracture biomechanics of the human skeleton [Ph.D. dissertation]. Knoxville (TN): University of Tennessee, 2007.
6. Takeshi M, Okuchi K, Nishiguchi T, Seki T, Watanahe T, Ito S, et al. Clinical analysis of seven patients of crushing head injury. J Trauma 2006;60(6):1245–9.
7. Graham R, Oberlander E, Stewart J, Griffiths D. Validation and use of a finite element model of C-2 for determination of stress and fracture patterns of anterior odontoid loads. J Neurosurg (Spine 1) 2000;93:117–25.
8. Silva M, Keaveny T, Hayes W. Computed tomography-based finite element analysis predicts failure loads and fracture patterns for vertebral sections. J Orthop Res 1998;16:300–8.
9. Doorly M, Gilchrist M. The use of accident reconstruction for the analysis of traumatic brain injury due to head impacts arising from falls. Comput Methods Biomech 2006;9(6):371–7.
10. Frank F, Lawn B. On the theory of Hertzian fracture. Proc R Soc Lond 1967;299(1458):291–306.
11. Paterson M, Wong T. Griffith theory of brittle failure. In: Paterson MS, Wong T-f, editors. Experimental rock deformation—the brittle field. Berlin, Germany: Springer, 2005;45–57.

Additional information and reprint requests:
Roger C. Haut, Ph.D.
Orthopaedic Biomechanics Laboratories
A-407 East Fee Hall
Michigan State University
East Lansing, MI 48824
E-mail: haut@msu.edu

JOURNAL OF FORENSIC SCIENCES

J Forensic Sci, November 2010, Vol. 55, No. 6
doi: 10.1111/j.1556-4029.2010.01411.x
Available online at: onlinelibrary.wiley.com

PAPER

CRIMINALISTICS; PHYSICAL ANTHROPOLOGY

Hwan Young Lee,[1,2] *Ph.D.; Na Young Kim,*[1] *M.S.; Myung Jin Park,*[1] *M.S.; Jeong Eun Sim,*[1] *B.S.; Woo Ick Yang,*[1] *Ph.D.; and Kyoung-Jin Shin,*[1,2] *Ph.D.*

DNA Typing for the Identification of Old Skeletal Remains from Korean War Victims*

ABSTRACT: The identification of missing casualties of the Korean War (1950–1953) has been performed using mitochondrial DNA (mtDNA) profiles, but recent advances in DNA extraction techniques and approaches using smaller amplicons have significantly increased the possibility of obtaining DNA profiles from highly degraded skeletal remains. Therefore, 21 skeletal remains of Korean War victims and 24 samples from biological relatives of the supposed victims were selected based on circumstantial evidence and/or mtDNA-matching results and were analyzed to confirm the alleged relationship. Cumulative likelihood ratios were obtained from autosomal short tandem repeat, Y-chromosomal STR, and mtDNA-genotyping results, and mainly confirmed the alleged relationship with values over 10^5. The present analysis emphasizes the value of mini- and Y-STR systems as well as an efficient DNA extraction method in DNA testing for the identification of old skeletal remains.

KEYWORDS: forensic science, DNA typing, skeletal remains, DNA extraction, mitochondrial DNA, autosomal short tandem repeat, Y-chromosomal short tandem repeat, mini-STR

To identify the remains of service members missing in the Korean War (1950–1953), a population-based, DNA-focused identification system has been implemented since 2000 by the Ministry of National Defense Agency for Killed in Action Recovery and Identification (MAKRI, http://www.withcountry.mil.kr) in Korea. The remains of several missing casualties have been identified and returned to their families on the basis of circumstantial evidence and matching results of mitochondrial DNA (mtDNA) profiles. To match genotyping results, mtDNA profiles from the skeletal remains of missing casualties were compared on a regional scale in a batch mode to the mtDNA profiles obtained from reference samples of biological relatives of supposed victims based on circumstantial evidence and reliable testimonies of surviving witnesses. However, mtDNA testing alone is not sufficiently informative to provide positive identification, and usable references are limited to maternal relatives. Accordingly, analysis of additional genetic markers is required to confirm the alleged relationship between missing casualties and their relatives.

In general, the acquisition of genotyping results for multiple DNA markers from old skeletal remains is assumed to be difficult because of the age and condition of the remains. However, recent advances in DNA extraction techniques and approaches using smaller amplicons have significantly increased the possibility of obtaining DNA profiles from highly degraded skeletal remains (1–13). To facilitate the collection of DNA profiles from the skeletal remains of war victims, a simple and effective DNA extraction method has been developed in Korea, and modified primer sets for analysis of the mtDNA hypervariable (HV) sequence and several mini-short tandem repeat (mini-STR) systems for autosomal STR and Y-chromosomal STR (Y-STR) analysis have been designed (8,12).

Skeletal remains of 21 Korean War victims and 24 samples from biological relatives of the supposed victims were selected and analyzed by employing a recently developed method for efficient DNA extraction and generating autosomal STR and Y-STR results using three commercial STR systems (AmpFlSTR® Identifiler®, AmpFlSTR® MiniFiler™, and AmpFlSTR® Yfiler™; Applied Biosystems, Foster City, CA) and two in-house mini-STR systems (the miniplex NC01 plus and Y-miniplex plus systems) to confirm alleged relationships.

Materials and Methods

Sample Preparation and Pulverization of Skeletal Remains

Long bones were used for the genetic identification of skeletal remains of 21 Korean War victims. To remove potential contamination, the outer surface of bone samples was sanded using a motor drill with a dental bur. Each sample was cut into small pieces using a dental diamond disk and irradiated with ultraviolet (UV)-light at 254 nm and 120,000 μjoules/cm^2 for 2 × 15 min with the bone rotated 180° between each exposure. Three to five pieces of each bone sample were pulverized by cryogenic grinding using liquid nitrogen and a SPEX 6750 Freezer/Mill (SPEX CertiPrep, Metuchen, NJ). The bone powder was transferred to a 15-mL tube and stored at −20°C until DNA extraction.

DNA Extraction from Skeletal Remains

For complete physical dissolution of bone samples, 0.5 g of bone powder was incubated in 15 mL of extraction buffer (0.5 M

[1]Department of Forensic Medicine and Brain Korea 21 Project for Medical Science, Yonsei University College of Medicine, 250 Seongsanno, Seodaemun-Gu, Seoul 120-752, Korea
[2]Human Identification Research Center, Yonsei University, 250 Seongsanno, Seodaemun-Gu, Seoul 120-752, Korea
*Supported by a grant from the Ministry of National Defense Agency for Killed In Action Recovery and Identification (MAKRI) of Korea.

Received 1 April 2009; and in revised form 6 July 2009; accepted 12 July 2009.

EDTA, 0.5% SDS) with 3 mg of proteinase K at 56°C for 48 h. Before recovering DNA from the solution, the sample was further treated with an additional 3 mg of proteinase K at 56°C for 1 h. DNA recovery and purification was performed using a QIAamp® Blood Maxi column (Qiagen, Hilden, Germany) and buffers from the QIAquick® PCR purification kit (Qiagen). Five volumes of buffer PB from the QIAquick® PCR purification kit were added to the solution, and the mixture was passed through a QIAamp® Blood Maxi column. The column was washed with 15 mL of buffer PE from the QIAquick® PCR purification kit, and DNA was eluted using 2 mL of double-distilled (dd) H_2O. The eluted DNA was then concentrated using a QIAamp® Mini spin column (Qiagen) and buffers from the QIAquick® PCR purification kit. Five volumes of buffer PB were added to the 2 mL sample, and the mixture was applied to the QIAamp® Mini spin column. After washing with 750 μL of buffer PE, the final extract was obtained by elution with 50 μL of ddH_2O. The DNA extraction procedure was performed independently at least twice for each sample (see details at http://forensic.yonsei.ac.kr/protocols).

DNA Quantification Using Quantitative Real-Time PCR

Human genomic DNA content was determined using the Quantifiler™ Human DNA Quantification Kit (Applied Biosystems), and 7500 Real-Time PCR System (Applied Biosystems) with modified reduced-scale reactions (14) consisting of 5 μL of primer mix, 6 μL of PCR reaction mix, and 1 μL of DNA extract in a final reaction volume of 12 μL. The set of eight dilutions of standard DNA were used as the DNA quantification standard, and the thermal amplification protocol was performed following the manufacturer's recommendations. All samples were assayed in duplicate, and data collection was conducted at a threshold of 0.2 and a baseline of 3–15. The results for the internal PCR control (IPC) from each assay were monitored to evaluate the presence of PCR inhibitors.

PCR Amplification and Sequencing of mtDNA Hypervariable Regions in Skeletal Remains

To amplify mtDNA HV regions, HV1 (nucleotide position [n.p.] 16024–16365), HV2 (n.p. 73–340), and HV3 (n.p. 438–574) primer pairs were chosen depending on the level of sample degradation and the desired amplicon (Fig. 1). This modified set of primers allowed efficient amplification of mtDNA, with reduced effects of HV1 length heteroplasmy, nucleotide variability, and PCR amplification conditions (Table 1). Among the primers of the Armed Forces DNA Identification Laboratory (AFDIL) (6,7), primers whose efficiencies were influenced by frequent mutations or by PCR conditions were preferentially redesigned. In particular, primers were designed so that the first to third nucleotides from the 3′ end of each redesigned primer were located at nucleotide positions with a low mutation frequency (1.0% or less) in the three major world population groups (European, Asian, and African). In addition, primers that produced amplicons having too much or too little overlap with adjacent PCR products to do direct sequencing of amplicons were also redesigned.

PCR was performed in a reaction mixture of 25 μL total volume containing 2 μL of template DNA, 2.5 U of AmpliTaq Gold® DNA Polymerase (Applied Biosystems), 2.5 μL of Gold ST*R 10× Buffer (Promega, Madison, WI), and 0.6 μM each primer. Thermal cycling was conducted on a PTC-200 DNA engine (MJ Research, Waltham, MA) using the following conditions: 95°C for 11 min; 42 cycles of 95°C for 20 sec, 50°C for 20 sec, and 72°C for 30 sec; and a final extension at 72°C for 7 min. PCR products were purified with the QIAquick® PCR purification kit.

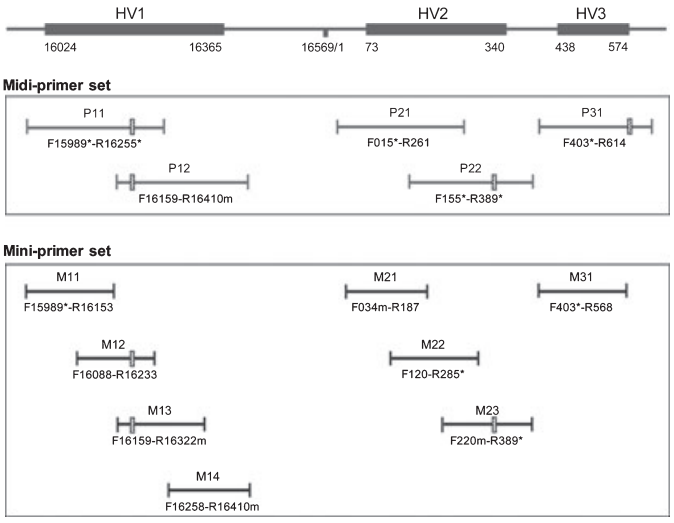

FIG. 1—*Primer schemes for the amplification of mtDNA hypervariable regions from highly degraded specimens. Primer nomenclature designates the 5′ end nucleotide position within the rCRS (26). Primers identical to those of the Armed Forces DNA Identification Laboratory (AFDIL) are indicated with an asterisk (*) and poly C-stretches are indicated by a box.*

TABLE 1—*Primer sequences for amplification and sequencing of the mtDNA control region.*

Primer	Sequence (5′ to 3′)
F15975	CTC CAC CAT TAG CAC CCA AA
F15989*	CCC AAA GCT AAG ATT CTA AT
F16088	TGT ATT TCG TAC ATT ACT GC
F16159	CAT AAA AAC CCA ATC CAC AT
F16258	ACC CCT CAC CCA CTA GGA TA
F16327	CCG TAC ATA GCA CAT TAC AGT C
R16153	CAG GTG GTC AAG TAT TTA TGG
R16233†	TGA TAG TTG AAG GTT GAT TGC TGT
R16255*	CTT TGG AGT TGC AGT TGA TG
R16322m	TGG CTT TAT GTA CTA TGT ACT G
R16410m	GAG GAT GGT GGT CAA GGG A
F015*	CAC CCT ATT AAC CAC TCA CG
F034m	GGG AGC TCT CCA TGC ATT T
F120	CGC AGT ATC TGT CTT TGA TTC C
F155*	TAT TTA TCG CAC CTA CGT TC
F220m	TGC TTG TAG GAC ATA ATA ATA ACA
F314	CCG CTT CTG GCC ACA GCA CT
F403*	TCT TTT GGC GGT ATG CAC TTT
R187	CGC CTG TAA TAT TGA ACG TA
R240*	TAT TAT TAT GTC CTA CAA GCA
R261	GCT GTG CAG ACA TTC AAT TGT T
R285*	GTT ATG ATG TCT GTG TGG AA
R389*	CTG GTT AGG CTG GTG TTA GG
R568	GTG TCT TTG GGG TTT GGT TG
R614	TTT CAG TGT ATT GCT TTG AGG A
R635	GAT GTG AGC CCG TCT AAA CA

*Primers identical to those of the Armed Forces DNA Identification Laboratory (AFDIL) (6,7).

†A mismatched nucleotide of R16233 relative to the rCRS (26) is underlined.

Sequence analysis was performed with the BigDye® Terminator v3.1 Cycle Sequencing Kit (Applied Biosystems) on an ABI 3730 DNA Analyzer (Applied Biosystems). Primers used for sequencing analysis were the same as the primers used in PCR amplification. The sequencing results for mtDNA HV1, HV2, and HV3 were

analyzed using SEQUENCING ANALYSIS Software Version 3.4 (Applied Biosystems) and Sequence Navigator 1.0.1 (Applied Biosystems).

Quality Analysis of mtDNA Sequence Data

To ensure sequencing data quality, duplicate amplifications were sequenced in double strand (e.g., both the forward and reverse directions), and the resultant consensus sequences were used for further analysis. However, separate analysis of the HV segments of mtDNA risks producing artificial recombination (15), and phylogenetic investigations and database screening are known to facilitate the detection of possible errors in a dataset.

Therefore, to confirm the absence of artificial recombination or other errors, the most probable mtDNA haplogroups were estimated using the mtDNAmanager program (http://mtmanager.yonsei.ac.kr) (16). If a certain mtDNA sequence was annotated with the same expected and estimated haplogroups, the sequence was considered to possess the complete mutation motif for the corresponding haplogroup with little possibility of artificial recombination. For data without both of the haplogroup affiliations or that showed discordance between expected and estimated haplogroups, the primary sequence was rechecked for possible errors because of contamination or sample mix-up.

PCR Amplification of Autosomal STRs in Skeletal Remains with a Commonly Used STR Kit

Amplification was performed using the AmpFlSTR® Identifiler® PCR Amplification Kit (Applied Biosystems) with reduced-scale reaction mixtures consisting of 3.8 μL of PCR mix, 2.0 μL of primer mix, 2.5 U of AmpliTaq Gold® DNA Polymerase, and 2.0 μL of template DNA in a final reaction volume of 10 μL. Thermal cycling was conducted on a GeneAmp PCR system 9600 (Applied Biosystems) under the following conditions: 95°C for 11 min, 96°C for 1 min; 10 cycles of 94°C for 30 sec (then ramp 68 sec to 59°C), 59°C for 30 sec (then ramp 50 sec to 70°C), 70°C for 45 sec; 23 cycles of 90°C for 30 sec (then ramp 60 sec to 59°C), 59°C for 30 sec (then ramp 50 sec to 70°C), 70°C for 45 sec, and a final extension at 60°C for 45 min.

PCR Amplification of Autosomal STRs in Skeletal Remains Using Size-Reduced Amplicons

Amplification was performed using AmpFlSTR® MiniFiler™ PCR Amplification Kit (Applied Biosystems) and the in-house miniplex system NC01 plus. To complement the amplification with the commonly used autosomal STR kit, amplification using the AmpFlSTR® MiniFiler™ PCR Amplification Kit was performed with reduced-scale reaction mixtures consisting of 4.0 μL of PCR mix, 2.0 μL of primer mix, 1.5 U of AmpliTaq Gold® DNA Polymerase, and 2.0 μL of template DNA in a final reaction volume of 10 μL. Thermal cycling was conducted on a PTC-200 DNA engine under the following conditions: 95°C for 11 min; 32 cycles of 94°C for 20 sec, 59°C for 120 sec, 72°C for 60 sec; and a final extension at 60°C for 45 min.

To obtain more genetic data from degraded samples using small-size amplicons, amplification using in-house miniplex NC01 plus was performed with reaction mixtures consisting of 2.0 μL of template DNA, 1.5 U of AmpliTaq Gold® DNA Polymerase, 1.0 μL of Gold ST*R 10× Buffer, and an appropriate concentration of each primer in a total volume of 10 μL (Table 2). Thermal cycling was conducted on a PTC-200 DNA engine under the same conditions used for the AmpFlSTR® MiniFiler™ PCR Amplification Kit.

PCR Amplification of Y-STRs in Skeletal Remains with a Commonly Used Y-STR Kit

Amplification was performed using the AmpFlSTR® Yfiler™ PCR Amplification Kit (Applied Biosystems) with reduced-scale reaction mixtures consisting of 3.7 μL of PCR mix, 2.0 μL of primer mix, 4.0 U of AmpliTaq Gold® DNA Polymerase, and 2.0 μL of template DNA in a final reaction volume of 10 μL. Thermal cycling was conducted on a GeneAmp PCR system 9600 under the same conditions used with the AmpFlSTR® Identifiler® PCR Amplification Kit, except that an additional amplification cycle was used (24 instead of 23 cycles of 90°C for 30 sec [then ramp 60 sec to 59°C], 59°C for 30 sec [then ramp 50 sec to 70°C], 70°C for 45 sec).

PCR Amplification of Y-STRs in Skeletal Remains Using Size-Reduced Amplicons

To complement the amplification with the commonly used Y-STR kit, an in-house Y-miniplex plus system was developed, which is capable of amplifying eight Y-STR loci (DYS385, DYS390, DYS391, DYS392, DYS438, DYS439, and DYS635) with reduced PCR product sizes relative to currently used commercial kits (Fig. 2). The amplification was performed with reaction mixtures consisting of 2.0 μL of template DNA, 2.5 U of AmpliTaq Gold® DNA Polymerase, 1.0 μL of Gold ST*R 10× Buffer, and the appropriate concentration of each primer in a total volume of 10 μL (Table 3). Thermal cycling was conducted on a PTC-200 DNA engine under the same conditions as the AmpFlSTR® MiniFiler™ PCR Amplification Kit, except that 33 instead of 32 amplification cycles were used.

Generation and Interpretation of STR Genotype Data in Skeletal Remains

Two separate PCR amplifications were performed for duplicate DNA extracts (1st and 2nd DNA extracts) of each sample of

TABLE 2—*Primer sequences and concentrations of the optimized miniplex NC01 plus system.*

Locus	Dye	Sequence (5′ to 3′)	Final Concentration (μM)
D10S1248	6-FAM	TTA ATG AAT TGA ACA AAT GAG TGA G	1.30
		GCA ACT CTG GTT GTA TTG TCT TCA T*	1.30
D14S1434	VIC	TGT AAT AAC TCT ACG ACT GTC TGT CTG	0.20
		GAA TAG GAG GTG GAT GGA TGG*	0.20
D22S1045	NED	ATT TTC CCC GAT GAT AGT AGT CT	0.13
		GCG AAT GTA TGA TTG GCA ATA TTT TT*	0.13
TPOX	PET	CTT AGG GAA CCC TCA CTG AAT G	0.55
		GTC CTT GTC AGC GTT TAT TTG C	0.55

*The 5′ guanine residue promoting adenylation at the 3′ end of the opposite strand is underlined.

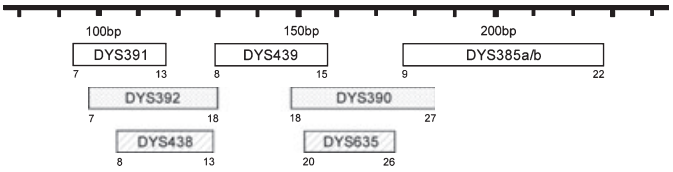

FIG. 2—*Schematic of the Y-miniplex plus system illustrating fluorescent dye labels and relative PCR product size ranges. The upper lane indicates 6-FAM-labeled loci, the middle lane indicates VIC-labeled loci, and the bottom lane indicates NED-labeled loci. PCR product size ranges correspond to the allelic ladder size ranges for the eight loci in the Y-miniplex plus system, but the mobility of DYS439 was modified by adding six hexaethylene oxide (HEO) units to the fluorescence-labeled DYS439 primer.*

skeletal remains. The products of multiplex PCR were analyzed by capillary electrophoresis using the ABI PRISM® 310 Genetic Analyzer (Applied Biosystems). The fragment sizes were determined using GENESCAN® 3.7 software (Applied Biosystems), and the allele designations were made using GENOTYPER® 3.7 software (Applied Biosystems). To confirm data quality, an allele was scored when its peak height was above the interpretational threshold of 75 RFU (i.e., three times the standard deviation of the noise), and alleles with a peak height of ≤15% of the highest allele in each locus were not scored. Then, according to the low copy number DNA interpretation rule (i.e., replicate analyses were performed, with duplicate results obtained prior to reporting alleles) (17), a consensus profile was generated only when an allele was present at least three times in four replicate PCRs.

DNA Typing of the Relatives of the Supposed Victims

On the basis of circumstantial evidence and matching results of mtDNA profiles, 24 biological relatives of the supposed victims were selected for comparative DNA typing with the remains. Blood or buccal swab samples were obtained, and genomic DNA was extracted using a QIAamp® DNA Mini Kit. PCR amplification of the mtDNA was performed using 1–2 ng of template DNA and F15975 and R635 as primers. Primers used for sequencing were F15975, F16327, F155, F314, R16410m, R240, R568, and R635, and detailed protocols for PCR and sequencing of the mtDNA control region are available at http://forensic.yonsei.ac.kr/protocols. STR analyses using AmpFlSTR® Identifiler® and AmpFlSTR® Yfiler™ PCR Amplification Kits were performed with reduced-scale reactions following the manufacturer's recommended thermal amplification protocol. In addition, the analysis using the miniplex NC01 plus system was performed as for skeletal remains, except that 27 cycles of amplification were used during thermal cycling.

Calculation of Likelihood Ratios

To confirm the alleged relationship, the likelihood ratios (LRs) for the proposition that the individuals have the stated relationship versus the proposition that they are unrelated were obtained by multiplying LRs based on autosomal STR, Y-STR, and mtDNA analysis results. LRs based on autosomal STR results were calculated using the AS-STRmanager program (Shin, Korea, unpublished data) and a database of 679 unrelated Koreans according to the method of Buckleton and Triggs (18–20). When calculating the cumulative LRs for autosomal STR using multiple PCR amplification systems, the frequency of the shared loci was considered only once. LRs based on Y-STR and mtDNA results were obtained using the inverse of the frequency of Y-STR and mtDNA haplotypes observed from databases of 708 unrelated Korean males and 593 unrelated Koreans, respectively (21,22), and were estimated by accounting for the uncertainty because of sampling errors (23). To calculate the cumulative LRs including Y-STR data, the Y-STR haplotype was considered only once (24). Accordingly, when using results from both the AmpFlSTR® Yfiler™ and the Y-miniplex plus, a haplotype was obtained from all conclusive loci of the AmpFlSTR® Yfiler™ and the Y-miniplex plus system for each individual sample. In consideration of allelic drop-out, a partial match was allowed for the calculation of Y-STR haplotype frequencies.

Results and Discussion

DNA Extraction and Quantification

To maximize DNA yield, a large-scale silica-based extraction method combined with complete demineralization was employed. Real-time PCR quantification showed that the majority of the tested samples produced 5 ng or more DNA (>100 pg/μl) from 0.5 g of bone powder (Table 4). DNA yields varied slightly between the first and the second extractions, but a consistently high DNA yield was observed in almost all samples except for SR0014 and SR0135 (<30 pg/μL). The IPC assay included in the Quantifiler™ Human DNA Quantification Kit confirmed that PCR inhibitors

TABLE 3—*Primer sequences and concentrations of the optimized Y-miniplex plus system.*

Locus	Dye	Sequence (5′ to 3′)	Final Concentration (μM)
DYS385	6-FAM	GAA GGA AGG AAG GAA GGG AAA*	0.30
		TAA GGG CTG CTG ACC AGA TT	0.30
DYS390	VIC	CTG CAT TTT GGT ACC CCA TA	0.11
		GCA ATG TGT ATA CTC AGA AAC AAG G	0.11
DYS391	6-FAM	TTC AAT CAT ACA CCC ATA TCT GTC	0.36
		GAT AGA GGG ATA GGT AGG CAG GC*	0.36
DYS392	VIC	AAA AGC CAA GAA GGA AAA CAA A	0.12
		GAA ACC TAC CAA TCC CAT TCC TT*	0.12
DYS438	NED	TGG GGA ATA GTT GAA CGG TAA	0.28
		GCT GGG CAA CAA GAG TGA AAC T*†	0.28
DYS439	6-FAM	$(HEO)_6$-ACA TAG GTG GAG ACA GAT AGA TGA T‡	0.12
		GTG GCT TGG AAT TCT TTT ACC C*	0.12
DYS635	NED	GGC TTC TCA CTT TGC ATA GAA TC	0.26
		ACC AGC CCA AAT ATC CAT CA	0.26

*The 5′ guanine residue promoting adenylation at the 3′ end of the opposite strand is underlined.
†Newly designed primer used in the present study.
‡HEO, hexaethylene oxide.

TABLE 4—*DNA concentrations and C_T values for the IPC determined using the Quantifiler™ Human DNA Quantification Kit from 55-year-old skeletal remains (n = 21).*

		First DNA Extraction (50 μL)		Second DNA Extraction (50 μL)	
Number	Skeletal Sample	Concentration (pg/μL)	IPC* (C_T†)	Concentration (pg/μL)	IPC* (C_T†)
1	SR0001	339.5 ± 09.02	27.8 ± 0.00	160.6 ± 24.26	28.1 ± 0.10
2	SR0002	213.5 ± 15.83	27.7 ± 0.01	319.7 ± 53.33	28.1 ± 0.02
3	SR0004	783.6 ± 20.51	27.9 ± 0.16	361.4 ± 09.90	28.1 ± 0.07
4	SR0008	613.6 ± 04.53	28.9 ± 0.01	318.0 ± 14.76	28.1 ± 0.10
5	SR0011	106.1 ± 05.49	28.5 ± 0.03	82.3 ± 20.83	28.2 ± 0.05
6	SR0012	84.3 ± 05.70	27.9 ± 0.06	29.6 ± 03.11	28.0 ± 0.17
7	SR0014	28.7 ± 20.69	28.0 ± 0.03	27.2 ± 16.81	29.5 ± 0.13
8	SR0015	119.0 ± 04.15	28.2 ± 0.06	211.7 ± 11.20	27.7 ± 0.02
9	SR0016	81.5 ± 10.46	28.1 ± 0.08	60.2 ± 06.30	27.4 ± 0.13
10	SR0017	70.6 ± 11.54	27.2 ± 0.08	91.3 ± 30.38	28.6 ± 0.07
11	SR0018	176.2 ± 06.73	28.1 ± 0.06	266.6 ± 01.42	27.7 ± 0.06
12	SR0078	161.8 ± 14.49	28.2 ± 0.08	295.4 ± 14.60	28.2 ± 0.01
13	SR0079	190.7 ± 31.71	28.5 ± 0.20	224.5 ± 03.38	31.3 ± 0.24
14	SR0080	169.2 ± 47.35	28.1 ± 0.10	146.4 ± 04.40	28.4 ± 0.28
15	SR0081	274.4 ± 38.36	28.3 ± 0.03	305.1 ± 59.13	29.0 ± 0.23
16	SR0083	51.2 ± 10.75	27.6 ± 0.15	68.7 ± 18.25	28.4 ± 0.13
17	SR0135	23.5 ± 05.20	27.7 ± 0.01	73.4 ± 17.11	27.6 ± 0.02
18	SR0221	303.1 ± 44.53	27.2 ± 0.01	416.2 ± 48.97	27.5 ± 0.23
19	SR0315	232.9 ± 01.28	28.0 ± 0.10	129.7 ± 15.03	28.0 ± 0.12
20	SR4003	57.3 ± 08.88	30.2 ± 0.09	74.1 ± 05.64	29.2 ± 0.32
21	SR7001	486.8 ± 03.15	27.8 ± 0.14	518.5 ± 82.13	28.2 ± 0.08

*Internal PCR control.
†Threshold cycle for log phase amplification of IPC.

were successfully removed from all of the extracted DNAs, with a majority showing C_T values of <29.

mtDNA Analysis from Skeletal Remains

The mtDNA HV region sequences were successfully determined in all of the 21 skeletal remains using midi- and/or mini-primers. In addition to producing small PCR amplicons, the primers were designed to minimize the effects of nucleotide variability and PCR amplification conditions, and accordingly, the mtDNA sequences of 55-year-old skeletal remains were amplified with ease and high efficiency. Estimation of the most probable mtDNA haplogroups was also successfully performed in all samples, thereby confirming the absence of artificial recombination.

Autosomal STR Genotyping from Skeletal Remains

The success rate of autosomal STR genotype determination was calculated for 21 skeletal remains amplified using two commercial PCR systems (AmpFlSTR® Identifiler® and AmpFlSTR® MiniFiler™) and an in-house PCR system (miniplex NC01 plus) (Tables 5 and 6). Of 15 autosomal STR loci included in the AmpFlSTR® Identifiler® Kit, nine STRs could be re-genotyped using reduced-size amplicons with AmpFlSTR® MiniFiler™ and the miniplex NC01 plus system, which considerably increased the success rate at these loci; all eight AmpFlSTR® MiniFiler™ loci and TPOX in the miniplex NC01 plus system had a success rate of 85% or higher (Table 6). Specifically, the smaller the amplicon size, the higher the success rate increased (57.1% increase for CSF1PO vs. 9.5% increase for D21S11). Moreover, four loci in the miniplex NC01 plus system (including TPOX) showed a 100% success rate in genotyping because of their very small amplicon size. Using the reduced-size amplicons of AmpFlSTR® MiniFiler™ and the in-house miniplex NC01 plus system as a complement to AmpFlSTR® Identifiler®, samples from all 21 skeletal remains produced successful STR typing results (the mean number of successfully genotyped loci was 17.2 out of 18 loci) (Table 5). Significant improvement in the mean number of successfully genotyped loci was observed in samples of lower quality, which demonstrated the usefulness of the mini-STRs in the genotyping of highly degraded

TABLE 5—*Mean number of loci successfully genotyped with the AmpFℓSTR® Identifiler® Kit, AmpFℓSTR® MiniFiler™ Kit, NC01 plus system, AmpFℓSTR® Yfiler™ Kit, and Y-miniplex plus system from 55-year-old skeletal remains.*

		Autosomal STR Loci†			Y-STR Loci‡	
Sample Quality*	No. of Samples	AmpFℓSTR® Identifiler®	AmpFℓSTR® MiniFiler™	NC01 Plus	AmpFℓSTR® Yfiler™	Y-miniplex Plus
Low	7	6.7	12.1	15.7	8.7	11.6
Medium	8	12.0	14.6	18.0	12.4	14.8
High	6	14.8	15.0	18.0	16.5	17.0
Total	21	11.0	13.9	17.2	12.3	14.3

*Sample qualities were classified into three groups according to the number of successfully genotyped loci using the AmpFℓSTR® Identifiler® Kit; low (0–10 loci), medium (11–13 loci), and high (14–15 loci).
†Mean number of autosomal STR loci successfully genotyped using the AmpFℓSTR® Identifiler® Kit and by serially adding the AmpFℓSTR® MiniFiler™ Kit, and the NC01 plus system.
‡Mean number of Y-STR loci successfully genotyped using the AmpFℓSTR® Yfiler™ Kit with or without the Y-miniplex plus system.

TABLE 6—*Success rate of autosomal STR genotype determination using the AmpFℓSTR® Identifiler® Kit, AmpFℓSTR® MiniFiler™ Kit, and NC01 plus system from 55-year-old skeletal remains (*n = *21).*

Locus	Amplicon Size Reduction (bp)	AmpFℓSTR® Identifiler® (%)	AmpFℓSTR® MiniFiler™ (%)	NC01 plus (%)
D3S1358	–	21 (100.0)	–	–
D5S818	–	19 (90.5)	–	–
D8S1179	–	21 (100.0)	–	–
TH01	–	19 (90. 5)	–	–
VWA	–	16 (76.2)	–	–
D19S433	–	20 (95.2)	–	–
D2S1338	183	9 (42.9)	20 (95.2)	–
FGA	87	12 (57.1)	18 (85.7)	–
CSF1PO	201	9 (42.9)	21 (100.0)	–
D7S820	129	13 (61.9)	20 (95.2)	–
D13S317	99	18 (85.7)	20 (95.2)	–
D16S539	157	13 (61.9)	21 (100.0)	–
D18S51	168	10 (47.6)	21 (100.0)	–
D21S11	33	18 (85.7)	20 (95.2)	–
TPOX	148	14 (66.7)	–	21 (100.0)
D10S1248	–	–	–	21 (100.0)
D14S1434	–	–	–	21 (100.0)
D22S1045	–	–	–	21 (100.0)

DNA. Except for SR0014, which had a very low DNA yield, all samples were successfully genotyped at 11 or more loci using AmpFlSTR® Identifiler® and AmpFlSTR® MiniFiler™, and 15 or more loci by adding the miniplex NC01 plus system (the mean number of successfully genotyped loci was 17.6).

Y-STR Genotyping from Skeletal Remains

Although paternal male relatives were reported in only 18 supposed victims, all 21 skeletal remains were genotyped using AmpFlSTR® Yfiler™ and the in-house Y-miniplex plus system. The success rate of Y-STR genotype determination at each locus and the mean number of successfully genotyped loci for each sample were calculated (Tables 5 and 7). On the same principle as for autosomal STR genotyping in skeletal remains, the in-house Y-miniplex plus system considerably increased the success rate at the eight size-reduced loci (e.g., 52.3% increase for DYS392 and 33.4% increase for DYS635), thereby producing an overall success rate of over 70% except for DYS19, DYS448, and DYS389II (Table 7). The mean number of successfully genotyped loci per sample also demonstrated that the use of the in-house Y-miniplex plus system as a complement to AmpFlSTR® Yfiler™ improved the Y-STR genotyping efficiency (14.3 of 17 loci), and this effect was more evident in samples of low quality (Table 5).

TABLE 7—*Success rate of Y-STR genotype determination using the AmpFℓSTR® Yfiler™ Kit and the Y-miniplex plus system from 55-year-old skeletal remains (*n = *21).*

Locus	Amplicon Size Reduction (bp)	AmpFℓSTR® Yfiler™ (%)	Y-miniplex plus (%)
DYS19	–	13 (61.9)	–
DYS389I	–	19 (90.5)	–
DYS389II	–	9 (42.9)	–
DYS393	–	21 (100.0)	–
DYS437	–	16 (76.2)	–
DYS448	–	12 (57.1)	–
DYS456	–	21 (100.0)	–
DYS458	–	21 (100.0)	–
GATA H4.1	–	19 (90.5)	–
DYS385	75	14 (66.7)	15 (71.4)
DYS390	49	16 (76.2)	18 (85.7)
DYS391	59	19 (90.5)	21 (100.0)
DYS392	197	9 (42.9)	20 (95.2)
DYS438	119	15 (71.4)	20 (95.2)
DYS439	89	16 (76.2)	21 (100.0)
DYS635	95	12 (57.1)	19 (90.5)

In comparison with a previous report by the authors using reduced-size amplicons for Y-STR genotyping of skeletal remains (12), the results from the present study confirm the importance of an efficient DNA extraction method in the DNA testing of old skeletal remains, because four of 18 samples in the present study (SR0004, SR0014, SR0015, and SR4003) were from the same batch of bone powder used in the previous study; the numbers of successfully genotyped loci in the four samples were 11, 0, 2, and 13 in the previous report and 12, 5, 11, and 16 in the present study (data not shown).

Assessment of the Alleged Relationship

Based on circumstantial evidence and/or matching results of mtDNA profiles, 21 skeletal remains were matched with 24 corresponding alleged blood relatives. Among the 21 skeletal remains, two (SR0004 and SR0011) were supposedly male siblings and allegedly had a sister in common. Therefore, LRs were obtained for 26 pairs of a victim and a relative, and the resulting values confirmed the alleged relationships for all 25 pairs except for that including SR0014 (Table 8). Poor DNA profiles were obtained from SR0014 because of its extremely low DNA content; SR0014 produced genotype results at 11 autosomal STR loci, but among these, nine were homozygotic, which could be the result of allelic drop-out.

Except for the case of SR0014, all of the remaining 20 skeletal remains and their 23 corresponding relatives shared a common allele at 11 or more autosomal STR loci (16 loci on average), and the LRs for the autosomal STR results were mostly over 250. The use of the reduced-size amplicons of AmpFlSTR® MiniFiler™ as a complement to AmpFlSTR® Identifiler® in the genotyping of skeletal remains increased the cumulative LRs in 20 cases, and the additional use of the in-house miniplex NC01 system significantly increased the cumulative LRs in 18 cases. These results demonstrate the value of mini-STR systems in forensic DNA testing for the analysis of skeletal remains.

In addition, 18 skeletal remains were further compared with their corresponding paternal male relatives using Y-STR genotyping results. Because two skeletal remains were male siblings, 17 pairs of victims and supposed relatives were compared and all except for two (SR0008 and SR0014) showed a match at successfully genotyped loci. Because SR0008 and SR0014 had a one-repeat mismatch at one or two loci (mismatches at DYS389I and DYS448 for SR0008, and a mismatch at GATA H4.1 for SR0014), their LRs were calculated to include the mutation frequencies at each corresponding locus (25). By using AmpFlSTR® Yfiler™ as a complement to the autosomal STR genotyping of skeletal remains, the cumulative LRs were increased in 15 of 17 cases (88.2%), and using the in-house Y-miniplex plus system in addition, 5 of 15 cases showed a further increase in the cumulative LRs (33.3%). On average, LRs were increased 230-fold by adding Y-STR genotype results.

In addition, because 21 skeletal remains were initially coupled with 19 corresponding alleged relatives based on mtDNA-matching results, their mtDNA genotyping results were integrated into the cumulative LRs. On average, LRs were increased 192-fold by adding the mtDNA genotype results. The cumulative LRs confirmed the alleged relationship with final values over 10^5 in all cases

TABLE 8—*Cumulative log likelihood ratios calculated from serially added autosomal STR, Y-STR, and mtDNA analysis results.*

No.	Skeletal Sample	Family Sample	Alleged Family Relationship	Cumulative Log Likelihood Ratio* AmpFℓSTR® Identifiler®	AmpFℓSTR® MiniFiler™	NC01 plus	AmpFℓSTR® Yfiler™	Y-miniplex plus	mtDNA
1	SR0001	FS0011	Brother	−1.6	1.5	0.4	1.8	2.8	5.1
2	SR0002	FS0001	Brother	3.0	3.2	2.4	4.9	4.9	6.9
		FS0001-1	Sister	6.0	6.9	6.5	–	–	8.4
3	SR0004†	FS0016	Sister	1.3	4.0	5.7	–	–	7.7
4	SR0008	FS0009	Brother	7.7	7.7	7.0	5.8	5.8	8.1
5	SR0011†	FS0016	Sister	2.6	4.4	5.6	–	–	7.6
6	SR0012	FS0006	Brother	1.4	1.2	2.7	4.7	5.0	7.3
7	SR0014	FS0015	Brother	−2.4	−2.3	−3.6	−4.5	−4.3	−2.0
8	SR0015	FS0012	Brother	2.5	5.5	6.4	8.1	8.2	10.5
9	SR0016	FS0007	Brother	0.4	4.3	6.1	8.5	8.5	10.8
10	SR0017	FS0003	Brother	2.0	3.9	4.5	6.9	6.9	9.1
11	SR0018	FS0013	Sister	3.6	3.9	4.4	–	–	6.7
12	SR0078	FS7221	Brother	1.8	3.5	4.9	6.8	7.0	9.0
13	SR0079	FS7216	Sister	3.3	5.0	6.5	–	–	8.7
		FS7217	Nephew	2.7	3.0	2.8	5.4	5.4	–
14	SR0080	FS7222	Brother	0.6	5.9	6.4	9.0	9.0	11.4
15	SR0081	FS7218	Brother	1.9	4.6	5.0	7.6	7.6	10.1
16	SR0083	FS7219	Son	2.7	3.1	3.7	5.6	6.2	–
		FS7220	Daughter	2.4	4.0	5.0	–	–	–
17	SR0135	FS7205	Brother	1.0	4.4	4.4	7.0	7.0	9.1
		FS7206	Sister	1.2	3.1	3.5	–	–	5.7
18	SR0221	FS7227	Brother	3.5	5.6	6.0	8.2	8.2	10.5
19	SR0315	FS0019	Sister	1.3	1.3	3.1	–	–	5.4
20	SR4003	FS0020-1	Son	3.3	3.3	3.8	6.3	6.3	–
21	SR7001	FS7001	Sister	0.6	0.6	0.2	–	–	2.6
22	SR0004†	SR0011†	Brother	2.9	5.1	6.1	8.6	8.6	10.6

*The log likelihood ratio in the AmpFℓSTR® Identifiler® column provides the value for AmpFℓSTR® Identifiler® loci alone; values in the AmpFℓSTR® MiniFiler™ column were calculated using the loci from AmpFℓSTR® Identifiler® along with those of AmpFℓSTR® MiniFiler™, etc.

†Skeletal remains of two brothers.

except for SR0014 and SR7001. However, personal effects were found around the remains of SR7001, and the alleged relative and the victim shared a very rare mtDNA haplotype, which confirmed their relationship and ultimately enabled the identification of the remains.

Conclusion

Using a highly effective DNA extraction method and size-reduced PCR fragments along with the application of the low copy number DNA interpretation rule, DNA genotyping can be successfully performed for old skeletal remains. Cumulative LRs obtained from autosomal STR, Y-STR, and mtDNA results confirmed the alleged relationship between missing persons and their relatives with great probabilities. The present analysis emphasizes the value of mini- and Y-STR systems as well as an efficient DNA extraction method in the success and efficiency of forensic DNA testing for the identification of old skeletal remains.

Acknowledgments

The authors thank Seung Hyun Yoon, Young Sub Byun, and Ju Hyun Park (Department of Oral Medicine, Yonsei University College of Dentistry, Seoul, Korea) for the preparation of samples from skeletal remains.

References

1. Höss M, Pääbo S. DNA extraction from Pleistocene bones by a silica-based purification method. Nucleic Acids Res 1993;21:3913–4.
2. Yang DY, Eng B, Waye JS, Dudar JC, Saunders SR. Technical note: improved DNA extraction from ancient bones using silica-based spin columns. Am J Phys Anthropol 1998;105:539–43.
3. Loreille OM, Diegoli TM, Irwin JA, Coble MD, Parsons TJ. High efficiency DNA extraction from bone by total demineralization. Forensic Sci Int Genet 2007;1:191–5.
4. Davoren J, Vanek D, Konjhodzić R, Crews J, Huffine E, Parsons TJ. Highly effective DNA extraction method for nuclear short tandem repeat testing of skeletal remains from mass graves. Croat Med J 2007;48:478–85.
5. Rohland N, Hofreiter M. Comparison and optimization of ancient DNA extraction. BioTechniques 2007;42:343–52.
6. Gabriel MN, Huffine EF, Ryan JH, Holland MM, Parsons T. Improved MtDNA sequence analysis of forensic remains using a ''mini-primer set'' amplification strategy. J Forensic Sci 2001;46:247–53.
7. Edson SM, Ross JP, Coble MD, Parsons TJ, Barritt SM. Naming the dead—confronting the realities of rapid identification of degraded skeletal remains. Forensic Sci Rev 2004;16:64–90.
8. Lee HY, Kim NY, Park MJ, Yang WI, Shin KJ. A modified mini-primer set for analyzing mitochondrial DNA control region sequences from highly degraded forensic samples. BioTechniques 2008;44:555–8.
9. Butler JM, Shen Y, McCord BR. The development of reduced size STR amplicons as tools for analysis of degraded DNA. J Forensic Sci 2003;48:1054–64.
10. Coble MD, Butler JM. Characterization of new miniSTR loci to aid analysis of degraded DNA. J Forensic Sci 2005;50:43–53.
11. Wiegand P, Klein R, Braunschweiger G, Hohoff C, Brinkmann B. Short amplicon STR multiplex for stain typing. Int J Legal Med 2006;120:160–4.
12. Park MJ, Lee HY, Chung U, Kang SC, Shin KJ. Y-STR analysis of degraded DNA using reduced-size amplicons. Int J Legal Med 2007;121:152–7.
13. Mulero JJ, Chang CW, Lagacé RE, Wang DY, Bas JL, McMahon TP, et al. Development and validation of the AmpFlSTR MiniFiler PCR Amplification Kit: a MiniSTR multiplex for the analysis of degraded and/or PCR inhibited DNA. J Forensic Sci 2008;53:838–52.
14. Westring CG, Kristinsson R, Gilbert DM, Danielson PB. Validation of reduced-scale reactions for the Quantifiler Human DNA kit. J Forensic Sci 2007;52:1035–43.
15. Parson W, Bandelt HJ. Extended guidelines for mtDNA typing of population data in forensic science. Forensic Sci Int Genet 2007;1:13–9.

16. Lee HY, Song I, Ha E, Cho SB, Yang WI, Shin KJ. mtDNAmanager: a Web-based tool for the management and quality analysis of mitochondrial DNA control region sequences. BMC Bioinformatics 2008;9:483.
17. Gill P, Whitaker J, Flaxman C, Brown N, Buckleton J. An investigation of the rigor of interpretation rules for STRs derived from less than 100 pg of DNA. Forensic Sci Int 2000;112:17–40.
18. Buckleton J, Clayton T, Triggs CM. Relatedness. In: Buckleton J, Triggs CM, Walsh SJ, editors. Forensic DNA evidence interpretation. Boca Raton, FL: CRC Press, 2005;125–9.
19. Han GR, Lee YW, Lee HL, Kim SM, Ku TW, Kang IH, et al. A Korean population study of the nine STR loci FGA, VWA, D3S1358, D18S51, D21S11, D8S1179, D7S820, D13S317 and D5S818. Int J Legal Med 2000;114:41–4.
20. Han GR, Kwon JS, Yang YS, Choi JH, Kim CY, Shin KJ. Population data of the COfiler STR loci in Koreans. J Forensic Sci 2004;49:176–7.
21. Park MJ, Lee HY, Kim NY, Sim JE, Yang WI, Cho SH, et al. Genetic characteristics of 22 Y-STR loci in Koreans. Korean J Leg Med 2007;31:162–70.
22. Lee HY, Yoo JE, Park MJ, Chung U, Shin KJ. Mitochondrial DNA control region sequences in Koreans: identification of useful variable sites and phylogenetic analysis for mtDNA data quality control. Int J Legal Med 2006;120:5–14.
23. Balding DJ, Nichols RA. DNA profile match probability calculation: how to allow for population stratification, relatedness, database selection and single bands. Forensic Sci Int 1994;64:125–40.
24. Sinha SK, Budowle B, Chakraborty R, Paunovic A, Guidry RD, Larsen C, et al. Utility of the Y-STR typing systems Y-PLEX 6 and Y-PLEX 5 in forensic casework and 11 Y-STR haplotype database for three major population groups in the United States. J Forensic Sci 2004;49:691–700.
25. Sánchez-Diz P, Alves C, Carvalho E, Carvalho M, Espinheira R, García O, et al. Population and segregation data on 17 Y-STRs: results of a GEP-ISFG collaborative study. Int J Legal Med 2008;122:529–33.
26. Andrews RM, Kubacka I, Chinnery PF, Lightowlers RN, Turnbull DM, Howell N. Reanalysis and revision of the Cambridge reference sequence for human mitochondrial DNA. Nat Genet 1999;23:147.

Additional information and reprint requests:
Kyoung-Jin Shin, Ph.D.
Department of Forensic Medicine
Yonsei University College of Medicine
250 Seongsanno, Seodaemun-Gu
Seoul 120-752
Korea
E-mail: kjshin@yuhs.ac

JOURNAL OF FORENSIC SCIENCES

J Forensic Sci, November 2010, Vol. 55, No. 6
doi: 10.1111/j.1556-4029.2010.01433.x
Available online at: onlinelibrary.wiley.com

PAPER

CRIMINALISTICS; PATHOLOGY AND BIOLOGY

Donald J. Johnson,[1,2] *M.S.; Learden K. Matthies,*[3] *M.S.; Katherine A. Roberts,*[1,2] *Ph.D.; and Beatrice Crofts Yorker,*[2] *J.D., R.N., M.S., F.A.A.N.*

Isolation and Individualization of Conceptus and Maternal Tissues from Abortions and Placentas for Parentage Testing in Cases of Rape and Abandoned Newborns*

ABSTRACT: Abortion specimens are often submitted to forensic laboratories as the only piece of physical evidence in rape and incest cases. The recovery of conceptus tissues from this evidence permits the use of paternity testing to evaluate suspects. In cases of abandoned newborns, the recovery of maternal tissue from the placenta allows for the direct comparison of genetic profiles between the suspected mother and the biological mother. We report on the identification and isolation of conceptus tissues from embryonic- and fetal-period abortions, and maternal tissues from delivered placentas, by gross and low-magnification examination with manual dissection. Hundreds of single-source samples have been successfully recovered by this method and short tandem repeat typed using standard forensic procedures. We additionally describe extraembryonic tissues that can be recovered and typed in the absence of the embryo proper. We conclude that an expertise and protocols can be developed by forensic laboratories for the routine analysis of this evidence.

KEYWORDS: forensic science, criminalistics, forensic biology, abortion, embryo, fetus, placenta, short tandem repeat typing, parentage testing

Polymerase chain reaction (PCR)-based, DNA typing methods have greatly expanded the investigative capabilities of forensic laboratories by providing a means to analyze limited samples with discriminating results. These advances have led to the development of standard operating procedures for the analysis of a wide variety of biological samples. However, many forensic laboratories view abortion products and placentas from secundinae as types of evidence beyond their analytical approach. This can be attributed to, in part, the anatomical expertise needed to identify and isolate embryonic, fetal, and maternal structures, in preparation for standard typing procedures. However, through study and practice, an expertise can be developed and the analysis of this evidence can become routine.

The authors have collectively examined several hundred abortion specimens over a 15-year period. Most of the casework has involved the rape of an adult woman, but cases of incest and statutory rape have also been seen. The authors have investigated only one known case of criminal abortion, which involved the investigation of an illegally operated abortion clinic. In our experience, the abortus is usually submitted as the only piece of physical evidence recovered in an investigation. Reportedly, many of the victims in our casework do not initially report the crime because they fear retaliation by the rapist. However, when the victims learn they are pregnant, they then decide to notify the police and have a legal abortion. The authors have also encountered cases where the rape victim had a spontaneous abortion after which she notified the police. The delay of weeks in reporting the crime results in the loss of the other types of sexual assault evidence, thus leaving the abortus as the single piece of physical evidence.

An abortion is the premature stoppage of development and elimination of the products of conception from the uterus (1). An abortion may be spontaneous (occurs by natural causes) or induced (occurs by human intervention). Induced abortions are performed in the United States for medical and elective reasons. Induced abortions are legal in the first trimester (13 weeks), after which the legality varies by state (2). Common methods of inducing abortion are as follows: (i) instrumental evacuation (suction curettage, dilation and curettage [D & C], and dilation and evacuation [D & E], (ii) medical induction by stimulation of uterine contractions and (iii) uterine surgery (hysterotomy and hysterectomy). The abortion method used is primarily based on the gestational age of the conceptus. Instrumental evacuation is used in 97% of abortions and in virtually all pregnancies of less than 12 gestational weeks (2). Instrumental evacuation was the sole method used in the casework of the authors, and most of the abortuses were less than 12 weeks gestation. The majority of submissions in recent years have been embryonic-period (≤56 days) abortions. In these cases, the abortion

[1]School of Criminal Justice and Criminalistics, California State University at Los Angeles, Los Angeles, CA 90032-8163.
[2]College of Health and Human Services, California State University at Los Angeles, Los Angeles, CA.
[3]Los Angeles County Sheriff's Department, Scientific Services Bureau, Los Angeles, CA.

*Part of this research was presented orally at the California Association of Criminalists 106th Semi-Annual Seminar, October 12, 2005, in Los Angeles, CA.

Received 21 Oct. 2008; and in revised form 2 June 2009; accepted 31 July 2009.

procedure typically obliterates the embryo proper. However, extraembryonic tissues can be recovered from these submissions and typed in lieu of the embryo itself. Extraembryonic structures are derived from the fertilized ovum, but not incorporated into the embryo. Extraembryonic structures are referred to as extrafetal structures during the fetal period of development. Extraembryonic/extrafetal structures are genetically identical to the embryo/fetus and include the amnion (synonymous with the amniotic membrane or sac), the chorion (synonymous with the chorionic membrane or sac), the chorionic plate (the part of the chorion related to the placenta), the chorionic villi, and the umbilical cord.

The authors have additionally examined numerous secundinae from cases of abandoned newborns, where the identification of the biological mother is central to the investigation. The secundina constitutes the structures expelled from the uterus after childbirth: the placenta, the fetal membranes (amniotic and chorionic sacs), the umbilical cord, and associated maternal tissue. The placenta in abandoned newborn cases can be a key piece of evidence as it is a source of maternal DNA. The placenta has a fetal component, which consists of the chorionic plate and associated villi, and a maternal component formed by the decidual layer of uterine endometrium that underlies the conceptus. The recovery of maternal tissue from the placenta allows for the direct, one-to-one comparison of the biological mother's DNA profile with that of the putative mother (suspect).

Once the basic patterns of human development are understood, the identification and isolation of tissues are relatively straightforward regardless of the gestational age and developmental state of the conceptus, and the different fragmentation results of the abortion procedures. Given the variation seen in casework, we will describe our basic analytical approach and our findings in general so as to provide the reader with a foundation from which to approach casework.

Materials and Methods

When we began the examination of abortuses in casework, our practice was to identify and separate all maternal, embryo/fetus proper, and extraembryonic/extrafetal tissues present in the specimen. This approach was taken to gain an appreciation of the types and amounts of recoverable tissues. The process is laborious, but is recommended for the trainee. With experience, however, our approach has been simplified. The present practice is to screen the specimen for suitable samples and unusual findings, such as the presence of twins. Once the samples have been chosen and collected, the remainder of the specimen is not further manipulated or examined. This approach is efficient and effective and reduces the risk of contamination.

The authors have found in the analysis of abortuses and secundinae that the structural integrity of the tissues, and the quantity and quality of nuclear DNA, can diminish when the specimens have been refrigerated for more than 1 week or frozen and thawed. The adverse effects of freezing and thawing have been observed after a single cycle. Consequently, the authors instruct investigators to submit the specimens expeditiously in a chilled (on ice), but unfrozen condition. Additionally, the specimens should not be treated with formalin and other fixatives. The analysis of the specimens typically begins on the day of receipt, but if this is impracticable, the specimen is refrigerated at 4°C and examined on the following day.

The initial documentation of the specimens proceeds as with other types of physical evidence. A workstation is prepared, and personal protective equipment is used, appropriate for the handling of potentially infectious materials, particularly volumes of liquid blood. Given the different amounts of tissues submitted, the authors use various types and sizes of sterile disposable containers for the transfer, examination, and sampling of the tissue (e.g., Petri dishes, specimen containers, centrifuge tubes, and microcentrifuge tubes). Additionally, the authors prefer the use of sterile, single-use, disposable instruments (scalpels, forceps, scissors, and probes) to simplify decontamination.

The abortuses are typically enclosed in general use, medical specimen containers of various sizes. The tissues are typically unfixed and within liquid maternal blood. The examination of the unfixed specimens generally begins with decanting the liquid blood into a separate graduated container. The tissue mass is transferred to a tared Petri dish, weighed on a top loading balance, and photographed. The tissue is then examined with a stereomicroscope (EZ4; Leica Microsystems Inc., Bannockburn, IL) using incident and transmitted light, at magnifications up to 50×. Sterile physiological saline (Sigma-Aldrich, St. Louis, MO) is added as needed to the tissue mass to facilitate the examination. The specimen is examined for fragments of the embryo/fetus proper and extraembryonic/extrafetal structures. It is also evaluated for the possibility of twins by evidence of duplicated structures. The tissue fragments are separated with forceps and probe and individually examined. Further dissection is typically unnecessary to obtain a piece of embryonic or fetal tissue. Maternal tissue is also collected should donorship become an issue. The tissue collected for DNA analysis is rinsed with physiological saline, until the discharge is clear, to remove the free blood. The tissue sample is then placed in a tared Petri dish, weighed, and photographed. A piece of the sample is subsequently excised for DNA extraction. The subsample is placed in a tared microcentrifuge tube and weighed on an analytical balance (Discovery series, Ohaus Corporation, Pine Brook, NJ). The tissue sample for DNA analysis can be temporally stored at 4°C for several days or frozen at −20°C until extraction. The remainder of the sample is placed in a separate container and stored frozen. The remainder of the abortion products are returned to the original container and stored frozen. The decanted blood is retained and stored frozen in its container.

The authors have analyzed over 10 fixed specimens, which were reportedly treated with 10% neutral-buffered formalin. The analysis of these specimens begins with decanting the formalin. The tissues are then removed from the container and placed in the center of a square piece of sterile cotton gauze. The corners of the gauze are then brought together and tied to form a sack. The sack is then placed in a wash solution of sterile water or physiological saline, which is repeatedly changed until the discharge is clear and the odor of formaldehyde is faint or unperceivable. The discharge can be brownish in color for several washes because of the elution of fixed blood cells. High-volume washes, relative to the volume of the tissue, are used to increase effectiveness. The use of the cotton gauze sack reduces labor and prevents the loss of tissues through the successive washes. After the abortion products are cleared of formalin, the analysis basically proceeds as with fresh tissue.

The workstation and personal protective equipment used for the examination of secundinae is basically the same as that used for the abortuses. However, the relatively large size of the intact placenta with the fetal membranes often requires the use of a stereomicroscope mounted on a swingarm stand. The analysis of unfixed placentas generally begins with collecting and measuring the liquid blood in the container. The placenta is then transferred to a tared container and weighed on a top loading balance. The specimen is removed from the container and placed on the polyethylene side of a clean sheet of Benchkote (Whatman, Florham Park, NJ) for

photography and examination. The objective of the examination is to identify and sample maternal tissues associated with the placenta, which include the decidua and maternal blood clots. The maternal tissues can generally be separated from the placenta by blunt dissection with forceps and probe; however, fine dissection with a scalpel may sometimes be necessary. Fetal tissue samples are also collected (usually excised pieces of the fetal membranes or umbilical cord), which can serve as references if needed. The authors have examined only one formalin-fixed placenta, which was previously cut into longitudinal sections. The sections were washed of formalin by the method described for the formalin-fixed abortion products.

Once the conceptus and maternal tissues are isolated from the abortus or placenta, the samples can be processed by the same DNA procedures used for other biological samples. We have used an organic procedure to extract most of the tissue samples. The organic procedure includes the following steps: (i) a cell lysis step (incubation of sample in 400 μL of pH 8.0 extraction buffer [10 mM Tris, 10 mM EDTA, 100 mM NaCl, 39 mM dithiothreitol, 2% SDS, 20 μL of 10 mg/mL Proteinase K; all Sigma-Aldrich, St. Louis, MO] for a minimum of 2 h at 56°C), (ii) a phenol/chloroform/isoamyl alcohol (Invitrogen, Carlsbad, CA) extraction step, and (iii) a Centricon® YM-100 (Millipore Corp., Billerica, MA) wash, concentration, and recovery step. A notable difference in the extraction of tissue samples versus physiological stains is the greater resistance of tissue samples to chemical digestion. The authors follow a general-purpose extraction procedure where samples are incubated in the lysis buffer for a minimum of 2 h at 56°C. A 2-h incubation period is generally sufficient to extract most physiological stains; however, the digestion of the tissue samples is typically incomplete at 2 h. To ensure complete lysis, the authors add to the tissue samples another 20-μL aliquot of 10 mg/mL Proteinase K at the end of the 2-h incubation period. The samples are then incubated at 56°C for a total of about 12 h. This modification results in the complete digestion of the tissue samples. Digestion can also be facilitated by cutting the sample into smaller pieces to increase surface area. In addition to the organic procedure, we have recently extracted embryonic/fetal tissue samples with the QIAGEN EZ1 DNA Tissue kit (QIAGEN Inc., Valencia, CA) on the QIAGEN BioRobot EZ1 Workstation (QIAGEN Inc.); and with the DNA IQ™ System (Promega Corp., Madison, WI) on the Biomek 2000 Laboratory Automation Workstation (Beckman Coulter Inc., Fullerton, CA).

The quantification, amplification, and typing of the DNA samples from conceptus and maternal tissues proceeds as with most other DNA samples. Our experience in the analysis of these tissues includes the following: slot blot and real-time PCR DNA quantification methods, and RFLP, AmpliType® PolyMarker+DQA1 (Perkin Elmer, Foster City, CA), and short tandem repeat (STR) typing systems (AmpFISTR® Profiler Plus™, COfiler™, and Identifiler® kits; Applied Biosystems, Foster City, CA). We have not encountered any downstream difficulties with these samples which would require deviation from manufacturer's recommendations and standard forensic procedures.

Results

Our results will be presented in two parts. First, we will describe the basic anatomical findings of the gross and low-magnification examination of abortion products and placentas, which represents a compilation of our casework experience. Second, we will provide qualitative and quantitative data on the STR analysis of abortuses, which includes the DNA yields of 12 recent cases.

Abortuses

The types and amounts of recoverable tissues and organs vary with the developmental state of the conceptus and the abortion procedure. Additionally, the composition of the abortion products can differ between cases of the same developmental state and abortion method, presumably because of variation in the execution of the procedure. Variation is also observed in the composition of abortion products between embryos or fetuses of the same gestational age. This may be attributed to differences in individual developmental rates, but the accuracy of the age estimate must also be considered.

Embryonic Structures

Abortions performed during the embryonic period produce specimens of fine to course pieces of maternal and extraembryonic tissue. Early embryos are typically obliterated by the abortion procedure, because of their small size and delicate structure. For example, human embryos are between 2 and 3.5 mm in greatest length at the beginning of the 4th week, and between 11 and 14 mm in greatest length at the end of the 6th week (3). Moreover, the limb bones of embryos are initially composed of soft tissue, i.e., mesenchyme and cartilage. Contrastingly, late embryos are larger in size and stronger in structure, which has allowed for the recovery of embryonic tissue proper in some cases. At the end of the embryonic period, human embryos are between 27 and 31 mm in greatest length (3), and all major structures are present in their rudimentary form (1). Additionally, the limb bones are beginning to ossify at the end of the embryonic period (1). The authors have recovered upper and lower limbs from abortions reportedly performed at the end of the 8th week. In these cases, individual digits were discernable on the hands and feet under low-power stereomicroscopy.

The recovery of tissues from the embryo proper is, however, the exception with embryonic-period abortions. Typically, only fragments of the amniotic membrane, chorionic membrane, and chorionic villi are found, as to embryonic tissues, in these submissions (see Fig. 1). Occasionally, the yellowish yolk sac is found intact, which can measure about 5 mm in diameter (see Fig. 1). The amniotic membrane may be found in pieces or as a ruptured sac attached at one end to a fragment of the chorion. The amnion at this stage of development is a thin (<1 mm), delicate, transparent membrane, which is basically homogeneous in gross appearance.

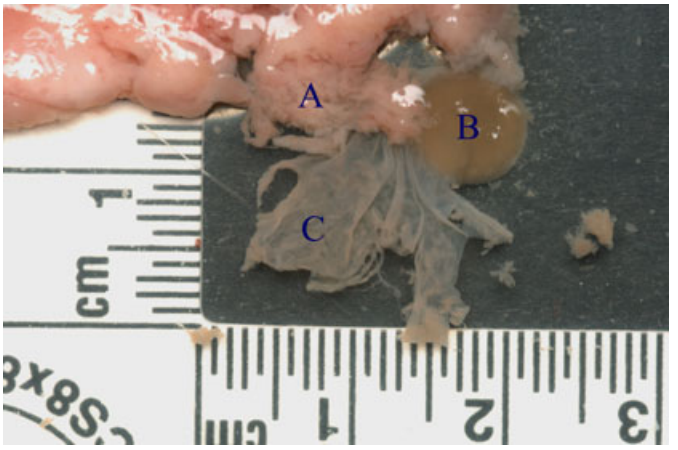

FIG. 1—*Tissue fragments from a late embryonic-period abortion. (A) Villous chorion. (B) Yolk sac. (C) Amnion.*

The membrane has a wispy appearance when floating in solution. Fragments of the embryonic amnion can be greater than 1 cm in length. By comparison, the embryonic chorion is thicker (>1 mm), stronger, and opaque (see Fig. 2). The chorion can appear off-white to pink in color, and occasionally reddish blood vessels can be seen traversing the membrane. The chorion is substantially greater in mass than the embryo and the amnion and shows a greater resistance to tearing. Dissolution of the embryonic chorion by suction curettage produces fine to coarse fragments, with some pieces measuring centimeters in greatest dimension. Pieces of the chorion have been identified in all embryonic-period abortions examined by the authors. The authors have recovered pieces of the chorion from a 4–5-week pregnancy, which was discovered on autopsy of a murdered woman. The fragments of the embryonic chorion are typically covered on one surface with chorionic villi. Chorionic villi cover the entire chorionic sac until the beginning of the 8th week, at which time the villi associated with the decidua capsularis begin to degenerate to form the smooth chorion (1).

Chorion villi are outgrowths of the outer surface of the chorionic membrane (see Fig. 2). Chorionic villi have the same coloration as the chorion and are highly branched structures (see Fig. 3). The "trunk" of the villous "tree" is the main stem villus, which gives rise to numerous branch villi. The branch villi often appear as stout structures with round or blunt ends. Also, branch villi are fairly uniform in width from base to end. Embryonic main stem villi can exceed 5 mm in length. The branch villi are typically shorter than the main stem villus.

Fetal Structures

Fetal-period abortions generally pose few analytical problems. The increased growth and development of the fetus and extrafetal structures facilitates the identification and recovery of the tissue samples. The authors have recovered tissue from the fetus itself in all fetal-period abortions. Fetal-period abortions typically result in the gross fragmentation of the conceptus. The fragments are often large enough to be identified with the unaided eye. Many structures have discernable human features. The cranial, thoracic, abdominal, and pelvic regions are often found as individual pieces. The viscera are typically detached from the body. The brain and other nervous system tissues are occasionally recovered, but rarely intact because of their delicate structure. However, fragments of the head often

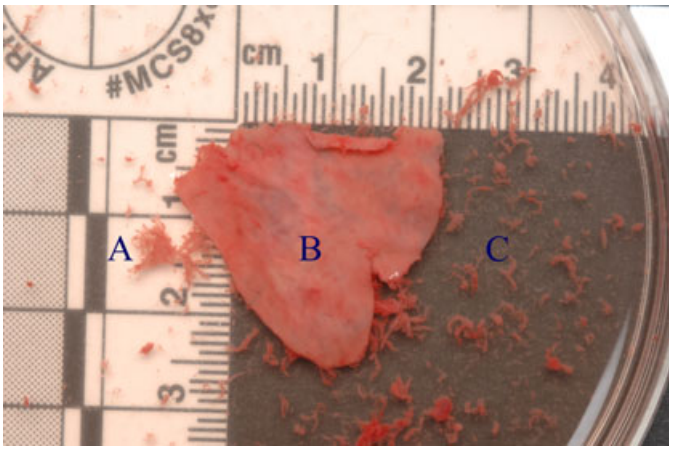

FIG. 2— *Tissue fragments from an early fetal-period abortion. (A) Chorionic villi attached to chorion. (B) Fetus-side of chorionic membrane. (C) Detached chorionic villi floating in saline solution.*

FIG. 3—*Chorionic villi from an early fetal-period abortion.*

contain the bulbous oculi, which appear dark gray to black in color. The limbs are well developed at this period and may be found disarticulated or articulated with the pectoral and pelvic girdles. Intact or fragmented limbs have been found in all fetal-period abortions. The vertebral column is another structure consistently found in fetal-period abortions. The vertebral column is typically fragmented by the abortion procedure, and some fragments may still be attached to cranial, thoracic, and pelvic skeletal structures. The vertebral column can be recognized by the alternating light and dark bands of the vertebral bodies and intervertebral disks.

Remnants of the placenta and fetal membranes can be found in abundance in fetal-period abortion specimens. The fetal placenta is structurally more complex than the embryonic placenta. This difference is apparent even at the gross level. Fragments of the fetal placenta, when viewed under low-power magnification, show densely packed chorionic villi with intricate arborizations. Additionally, the anatomical relationship between the villous chorion and the uterine endometrium shows a greater degree of organization in the fetal placenta, which may present difficulties in separating the fetal and maternal tissues on dissection.

Before the end of the embryonic period, the inner ammonic sac fuses with the chorionic sac to form the single amniochorionic membrane (1). Fragments of the amniochorionic sac can measure centimeters in greatest dimension. However, the enlargement of the sac with the growth of the fetus results in a thinning of the membrane. Pieces of the membrane have been found measuring 1-mm thick. However, despite its thinness, the membrane is relatively strong and resistant to tearing. The membrane in gross appearance is a translucent sheet of tissue, off-white to red in color, and basically homogeneous in structure.

The umbilical cord is another extrafetal structure that can usually be recovered from fetal-period abortion products, and sometimes with embryonic-period abortions. The umbilical cord undergoes development and growth with the embryo/fetus, and as a consequence, its gross appearance will differ with age. The extent of fragmentation of the cord by the abortion procedure will vary between procedures and with the gestational age of the abortus. Segments of the umbilical cord have been recovered from 9- to 12-week abortuses that measure centimeters in length and >5 mm in diameter. The diameter of the cord can exceed 1 cm in later abortions. The normal twisting and bending of the cord can be seen with some fragments. The surface of the cord is covered with an epithelium that imparts a shine. The umbilical cord typically has a mottled appearance: reddish-colored patches against a whitish

background. Fetal blood vessels can sometimes be seen macroscopically within pieces of the cord, which aids in its identification. These blood vessels course parallel to the long axis of the cord.

Decidual Layer of the Uterine Endometrium

Fine to course pieces of the decidual layer of uterine endometrium are routinely found in abortion products (see Fig. 4). Fragments of the decidua can usually be recognized by the folded mucosa, which gives the luminal surface (surface that faces the uterine cavity) a wrinkled appearance at low magnification. Additionally, the luminal surface is marked by numerous holes, which are the openings of the uterine glands. Fragments of the decidua typically have a rough undersurface, often corrugated in appearance, from the mechanical disruption of the fibrous connective tissue layer by the abortion procedure. Decidual tissue is generally darker in color than embryonic tissue. Abortion procedures often fragment the decidua to produce sheets of tissue, which may be confused with pieces of the chorionic membrane to the untrained eye.

The Placenta in Secundinae

The placenta is commonly disk-shaped, 15–20 cm in diameter and 2- to 3-cm thick, with a weight of 500–600 gm (1). In some of our cases of abandoned newborns, the placenta was found attached to the neonate by the umbilical cord. In other cases, the umbilical cord had been severed and the placenta was found separate near the neonate or at a distant location.

With secundinae, the umbilical cord and the ruptured amniochorionic membrane are attached to the fetal surface of the placenta. The amniochorionic membrane extends from the lateral margins of the fetal surface of the placenta. The opposite side (underside) of the placenta is the maternal surface, which has a cobblestone appearance. The "cobblestones" are termed *cotyledons*, and each cotyledon consists of a number of main stem villi with their many branch villi (1). The villi are of fetal origin; however, the surface of the cotyledons is covered by thin grayish shreds of decidua basalis (maternal tissue) that separated from the uterine wall when the placenta was extruded (1). Most of the decidua is temporarily retained in the uterus and is shed with subsequent uterine bleeding (1). We have recovered remnants of the decidua basalis from the cotyledonal surface of fresh placentas in casework, but the dissection was difficult and many of the samples included fetal tissue which resulted in maternal–fetal DNA mixtures. With the majority of submissions, however, large blood clots were found adhering to the maternal surface of the placenta which were easily collected and determined to be of maternal origin.

FIG. 4—*Luminal surface of uterine endometrium.*

Conceptus Tissue and DNA Yields

Late embryonic and early fetal-period abortion specimens typically have a wet weight (not including the decanted blood) of over 100 g. Of the minority of cases where we collected all identifiable pieces of the embryo or fetus, the collective wet weight of the pieces was 1.3–9.4% of the total wet weight of the specimen (minus the decanted blood). However, these specimens included tens of grams of extraembryonic or extrafetal structures. In contrast, maternal tissue can comprise the bulk of early embryonic-period specimens.

Nuclear DNA yields from 12 recent abortion cases are presented in Table 1. Each sample represents a different case. Five unfixed chorionic membrane/villi samples, which ranged in wet starting weight from 0.03 to 0.20 g, were extracted with an organic procedure and gave a range of total DNA yields from 5.2 to 44.0 μg. Three unfixed embryonic/fetal tissue proper samples, which ranged in wet starting weight from 0.02 to 0.23 g, were extracted with an organic procedure and gave a range of total DNA yields from 32.5 to 194.9 μg. Samples from four cases were extracted on a robotic platform. Three formalin-fixed samples were extracted with DNA IQ™ System on the Biomek 2000 Laboratory Automation Workstation. The wet starting weight of these samples ranged from 0.04 to 0.15 g, and the range of total DNA yields was 0.6–1.6 μg. One unfixed chorionic villi sample was extracted with the QIAGEN EZ1 DNA Tissue kit (QIAGEN Inc.) on the QIAGEN BioRobot EZ1 Workstation. The sample had a wet weight of 0.05 g and a total DNA yield of 20.9 μg.

The DNA yields given in Table 1 are typical for unfixed chorion/chorionic villi samples and unfixed embryo/fetus samples—starting with tenths or hundredths of grams of tissue, the DNA yields tend to be in great excess of analytical requirements. The extraction of too much tissue, in fact, can complicate downstream procedures such as DNA ultrafiltration and quantification. In contrast to unfixed samples, the recovery of nuclear DNA from formalin-treated tissues can be problematic. However, micrograms of DNA were obtained from the three formalin-fixed samples given in Table 1, but in amounts less than the unfixed tissue samples (per gram starting weight). In our experience, the ability to obtain nuclear DNA from formalin-fixed tissue appears to be related, at least in part, to the length of time the tissue is exposed to formalin:

TABLE 1—*Nuclear DNA yields in micrograms obtained from unfixed and formalin-fixed prenatal tissues.*

Sample Type	Sample Wet Weight (g)	Total DNA Yield (μg)	Extraction Method
Chorionic villi	0.12	11.0	Organic
Chorionic villi	0.12	5.2	Organic
Rib	0.15	74.0	Organic
Chorionic membrane	0.03	44.0	Organic
Lung	0.02	32.5	Organic
Hand	0.23	194.9	Organic
Chorionic villi	0.20	16.8	Organic
Chorionic membrane	0.20	23.9	Organic
Fixed umbilical cord	0.07	1.2	DNA IQ™ system
Fixed foot bone	0.04	1.6	DNA IQ™ system
Fixed arm muscle	0.15	0.6	DNA IQ™ system
Chorionic villi	0.05	20.9	EZ1 DNA tissue kit

the longer the exposure, the more problematic the analysis by standard forensic methods.

STR Profiles

In the majority of cases, full (13 CODIS STR loci) single-source profiles have been obtained from conceptus and maternal tissue samples that were identified and isolated by the procedures previously described in this article. Tissue samples from some cases, however, have produced partial (< 13) STR profiles as a result of decomposition and formalin-fixation, or have produced mixed STR profiles as a result of incomplete separation of conceptus and maternal tissues. With most mixture cases, however, the separation procedure did enhance the component of interest to produce a DNA mixture profile with a clear major contributor and minor contributor. In many instances, we have been able to recover and type samples from the fetus proper and samples from the extrafetal structures derived from the same pregnancy. In all cases, the STR profile of the fetus was identical to that of the extrafetal tissue. We have not seen evidence of genetic discordance between the tissue types.

The paternity testing of abortuses proceeds as with other cases of disputed fatherhood, but in cases of rape-induced pregnancies, the identification is that of the biological father and the alleged rapist. We routinely use the 13 CODIS STR loci and the CODIS software to calculate the combined paternity index which we report in casework. The comparison of STR profiles for paternity testing on abortion cases has generally been straightforward. In many cases, the obligate paternal allele could be determined for each locus of the abortus profile. In some cases, however, the analysis was complicated by the sharing of alleles by the mother and father at one or more loci. In the analysis of parentage trios, the profile of the alleged father has either been in complete concordance with the genetic profile of the biological father or has differed across many loci. We have not encountered cases where the genotypes of the alleged father and the conceptus mismatch at only one or two loci.

Discussion

An estimated 5% of rapes among women of reproductive age result in pregnancy, and more than 32,000 pregnancies result from rape each year among adult women in the United States (4). The significant occurrence of rape-related pregnancies is reflected in our casework. Over the past decades, crime laboratories in Los Angeles County have received hundreds of abortion specimens from rape and incest cases. Nationally in 1998, 105 newborns (33 deceased and 72 alive) were found abandoned in public places (5). In Los Angeles County, we have assisted with police investigations on illegally abandoned newborns, and in our experience, it is oftentimes difficult to establish maternity by standard STR analysis when limited to reference samples from the newborn and the putative mother. Mitochondrial DNA (mtDNA) analysis can establish a relationship between the suspected mother and infant, but the random match frequency estimates of mtDNA haplotypes do not approach that of STR profiles (6). The placenta is a source of maternal tissue, which can be STR typed and compared directly to the STR profile of the putative mother. This approach circumvents parentage calculations that are often complicated in these cases by the absence of the putative father's profile and the occurrence of common alleles in the profiles of the newborn and suspected mother. The one-to-one comparison of profiles levies the full discrimination power of STR analysis.

Our practice is to sample directly from the embryo or fetus when possible, and the selection of the sample depends on the structures that persist. Given equal amounts, we have found no analytical advantage in choosing one tissue or organ over another. However, an advantage is seen in our approach to recover and type extraembryonic/extrafetal structures in lieu of the absent embryo/fetus, because it has significantly increased the number of cases capable of analysis. The various extraembryonic/extrafetal structures previously described are equally suitable for DNA analysis, providing that any associated maternal tissue has been removed. Additionally, we have not seen evidence of genetic discordance between extraembryonic/extrafetal tissues and the embryo/fetus. However, Reshef et al. (7) describe a condition termed *confined placental mosaicism* (CPM), where the karyotype of the fetus is different from that of the extrafetal tissue. CPM results from a postzygotic, mitotic event that is represented by a trisomic duplication of a paternal or maternal allele. Importantly, Reshef et al. (7) state that STR analysis of postzygote CPM will result in correct allele identification, but with an increase in the intensity of the duplicated allele. Additionally, we have encountered dizygotic twins in casework, and their presence must be considered in the gross examination and STR analysis of abortion products. Ginsberg et al. (8) reported a case of a dizygotic pregnancy within a monochorionic placenta and propose the fusion of early blastomeres as the cause of the chimerism. Ambach et al. (9) reported a case of dizygotic twins fathered by two different men and predict a future increase in such cases.

We cannot overemphasize the importance of educating police departments, coroner's offices, medical facilities, etc. on the evidentiary value of abortuses and secundinae. In our experience over the many years, the value of this evidence is sometimes realized only after it is compromised. Most of our abortus and secundinae caseworks (from local and regional agencies) do not fall within the jurisdiction of a medical examiner or coroner, and for various reasons, which include quality assurance, we have found it prudent to have the expertise in-house. We recommend that the specimens be submitted in their entirety, unless they can be properly documented and sampled by qualified personnel outside of the crime laboratory. Through consultation, study, and practice, an expertise can be developed in the analysis of abortuses and secundinae, which can lead to the successful resolution of many serious criminal offenses.

Acknowledgments

The authors thank Dr. Joseph Peterson for his mentorship and assistance in the preparation of this manuscript. The authors acknowledge the Los Angeles County Sheriff's Department Scientific Services Bureau for its commitment to the advancement of forensic science.

References

1. Moore KL, Persaud TVN. The developing human: clinically oriented embryology. Philadelphia, PA: Saunders, 2003.
2. Beers MH, editor-in-chief. The Merck manual of diagnosis and therapy. Rathway, NJ: Merck Research Laboratories, 1999.
3. Larsen WJ. Human embryology. Philadelphia, PA: Churchill Livingstone, 2001.
4. Holmes MM, Resnick HS, Kilpatrick DG, Best CL. Rape-related pregnancy: estimates and descriptive characteristics from a national sample of women. Am J Obstet Gynecol 1996;175(2):320–5.
5. http://www.babysafe.ca.gov/res/pdf/SSBLaw_Report.pdf (accessed on February 4, 2009).
6. Butler JM. Forensic DNA typing: biology, technology, and genetics of STR markers. Burlington, VT: Elsevier, 2005.

7. Reshef A, Brauner P, Shpitzen M, Gallili N, Marbach A, Motro U, et al. Chorionic villus sampling prior to pregnancy termination, a tool for forensic paternity testing. J Forensic Sci 1999;44(5):1065–8.
8. Ginsberg NA, Ginsberg S, Rechitsky S, Verlinsky Y. Fusion as the etiology of chimerism in monochorionic dizygotic twins. Fetal Diagn Ther 2005;20:20–2.
9. Ambach E, Parson W, Brezinka C. Superfecundation and dual paternity in a twin pregnancy ending with placental abruption. J Forensic Sci 2000;45(1):181–3.

Additional information and reprint requests:
Donald J. Johnson, M.S.
School of Criminal Justice and Criminalistics
Hertzberg-Davis Forensic Science Center
California State University at Los Angeles
1800 Rancho Paseo Castilla
Los Angeles, CA 90032-8163
E-mail: djohnso5@exchange.calstatela.edu

JOURNAL OF FORENSIC SCIENCES

J Forensic Sci, November 2010, Vol. 55, No. 6
doi: 10.1111/j.1556-4029.2010.01464.x
Available online at: onlinelibrary.wiley.com

PAPER

CRIMINALISTICS

Erin J. Lenz,[1,†] *M.S. and David R. Foran,*[2] *Ph.D.*

Bacterial Profiling of Soil Using Genus-Specific Markers and Multidimensional Scaling*

ABSTRACT: Forensic identification of soil based on microbial DNA fingerprinting has met with mixed success, with research efforts rarely considering temporal variability or local heterogeneity in soil's microbial makeup. In the research presented, the nitrogen fixing bacteria rhizobia were specifically examined. Soils were collected monthly from five habitats for 1 year, and quarterly in each cardinal direction from the main collection site. When all habitats were compared simultaneously using Terminal Restriction Fragment Length Polymorphism analysis of the rhizobial *recA* gene and multidimensional scaling, only two were differentiated over a year's time, however pairwise comparisons allowed four of five soils to be effectively differentiated. Adding in 10-foot distant soils as "questioned" samples correctly grouped them in 40–70% of cases, depending on restriction enzyme used. The results indicate that the technique has potential for forensic soil identification, although extensive anthropogenic manipulation of a soil makes such identification much more tentative.

KEYWORDS: forensic science, terminal restriction fragment length polymorphism, rhizobia, bacterial DNA fingerprint, soil microbiology, recombination protein A

Soil has long been considered to be of broad evidentiary value, potentially linking a victim or suspect to a crime scene (1,2). Traditional forensic soil analysis includes observation of color and particle size, assaying chemical features such as pH and organic content, and evaluation of extraneous materials (2). Biological techniques have also been used in an attempt to "fingerprint" soil samples, including surveying pollen (3) or plant wax (4). More recently, the highly variable microbial makeup of soil has been targeted as a tool for its fingerprinting, potentially leading to the identification of a soil's origin (5–11).

Terminal restriction fragment length polymorphism (T-RFLP) analysis has become one of the primary molecular techniques for identifying and differentiating the bacterial content of biological or physical specimens (5,12–15). In this method, a specific segment of DNA is amplified based on conserved primer binding sites for the polymerase chain reaction (PCR), which allows all bacterial strains or species of interest to be scrutinized. One primer carries a 5′ fluorescent tag for subsequent detection (13,14). The amplicons are digested with a restriction enzyme that, based upon sequence variability between the primer sites, produces different-sized products. Digested amplicons are separated and detected via capillary electrophoresis, resulting in a bacterial profile. Specific bacterial strains or species may be identified, or more general overall comparisons between or among samples can be made.

Applying bacterial T-RFLP analysis to soil in a forensic context has met with some, although limited, success. Different soils do generate diverse T-RFLP profiles (11,13,16) and as a rule soil profiles collected within a given site are more similar than are profiles between sites (5,11,15). However, for this technique to be useful forensically, the bacterial content of soil must be relatively homogeneous both spatially and temporally. For instance, it is unlikely that a known soil sample will be collected from the exact same location from which evidentiary material originated. Therefore, if microbial content is heterogeneous over small distances, a DNA profile could erroneously exclude soil from the questioned site. Likewise, known soil samples will rarely be collected immediately after a crime occurs; if the bacterial makeup of soil changes substantially over time, once again the origin of evidentiary soil may be excluded in error.

In an effort to address all of these factors, we recently undertook a spatial and temporal study of soils collected from five different habitats in central Michigan (woodlot, yard, marsh, agricultural field, and a sandy woodlot *c.* 100 miles distant) (11). Soil samples were collected from the same location monthly for 1 year, as well as 10 feet in the cardinal directions every 3 months. The widely utilized 16S ribosomal RNA (rRNA) gene, present in all bacteria, was assayed, and T-RFLP profiles were compared pairwise, based on the similarity of peaks produced.

The results showed that bacterial profiles within a habitat were on average more similar than among habitats. However, there were large levels of variability within habitats both spatially and temporally. Indeed, it was not unusual to find month-to-month similarity values that were lower within a habitat than between habitats, suggesting that the forensic utility of the methodology was limited at best, and might even be misleading. Specific reasons for this are unclear and likely were affected by a variety of factors. Two of the habitats, the yard and agricultural field, were heavily manipulated

[1]Forensic Science Program, School of Criminal Justice, 560 Baker Hall, Michigan State University, East Lansing, MI 48824.
[2]Forensic Science Program, School of Criminal Justice and Department of Zoology, 560 Baker Hall, Michigan State University, East Lansing, MI 48824.

*A portion of this work was presented at the 60th Annual Meeting of the American Academy of Forensic Sciences, February 20, 2008, in Washington, DC.

†Present address: Indiana State Police Laboratory, 550 West 16th Street, Suite C, Indianapolis, IN 46202.

Received 28 May 2009; and in revised form 6 Aug. 2009; accepted 15 Aug. 2009.

anthropogenically (including plantings and/or fertilization), which could easily influence microbial content. The distant sandy woodlot was least similar to the other habitats, which may have resulted directly from remoteness, but could also have been a consequence of geological or meteorological variables. Most importantly, the T-RFLP profiles were extremely "complex," resulting from the very large number of species assayed. The high level of variability within and among habitats indicated that assaying all bacteria present in soil would likely not prove to be a useful tactic for forensic soil comparisons.

Given this, a new strategy for soil bacteria profiling was investigated, in which far fewer species were considered. In this research, the recombination protein A (*recA*) gene specific to the nitrogen-fixing bacteria (rhizobia) was assayed in an attempt to simplify T-RFLP profiles. Rhizobia form root nodules in leguminous plants and vary by habitat and plants species present (17–19). Approximately 75 rhizobial species have been described (20), a subset of which would be expected in any one habitat. The same soil DNAs used in (11) were assayed, again examining bacterial profiles within and among habitats, both spatially and temporally. Profiles were analyzed using multidimensional scaling, which allowed more data from each habitat to be included than did pairwise similarity indices.

Materials and Methods

Soil DNA Isolation and Amplification

Soils were collected from the above-mentioned habitats from September 2004 to August 2005, with DNA extracted thereafter, as detailed in (11). The rhizobial *recA* gene was amplified using forward primer 5′-CATGCRCTGGATCCGGTCTATGC-3′ and reverse labeled primer 5′-[6FAM]CTTGTTCTTGTCGACCTTGACGCG-3′) (18). Twenty microliter amplification reactions included 1 unit of AmpliTaq Gold® DNA Polymerase (Applied Biosystems, Foster City, CA), 1× of the included buffer, 2.5 mM $MgCl_2$, 2 μL of 1 μg/μL bovine serum albumin, 0.2 mM of each dNTP (Promega, Madison, WI), and 2 μM of each primer. Cycling parameters were an enzyme activation step of 10 min at 94°C, followed by 32 cycles of 30 sec denaturation at 94°C, primer annealing at 55°C for 30 sec, and a 45 sec extension at 72°C, with a final extension of 5 min at 72°C. Amplicons were visualized by separating 2 μL of the PCR product on a 2% agarose gel along with a 100 base pair (bp) DNA ladder (New England Biolabs, Beverly, MA). The gel was stained with ethidium bromide, and DNA yields were estimated by comparing the amplicon to the 400-bp size marker that contained *c*. 38 ng of DNA.

T-RFLP Profiling

The remaining PCR product was purified as described in (11). Amplified products were digested with *RsaI*, *MspI*, or *DpnII* (New England Biolabs), using 1 unit enzyme, 1× supplied buffer, 150 ng of PCR product as estimated by gel electrophoresis, and water to 10 μL. Digests were incubated at 37°C overnight, terminated by heating at 75°C for 20 min, purified, and electrophoresed as in (11), with a 10 sec injection time and 35 min separation time.

Analysis of T-RFLP Profiles

T-RFLP profiles were generated with ABI GeneMapper® ID, version 3.1 software (Applied Biosystems, Foster City, CA). Terminal restriction fragments from 40–450 bases with a peak height of at least 50 relative fluorescent units were included. Profiles were aligned and a matrix produced using T-Align (21), based on the presence/absence of shared peaks, with a confidence interval of 0.5 bases. The matrix was exported to Excel (Microsoft, Redmond, WA) as a binary file. Nonmetric multidimensional scaling (MDS) was performed in SPSS® version 15.0 (SPSS Inc., Chicago, IL), examining site heterogeneity, the effect of time, and the ability to differentiate among habitats. MDS is used to create a spatial representation of the data being compared. The program interprets the matrix data based on weighted Euclidean measurements, comparing how similar the samples are, with those having a large number of shared peaks being more similar. A spatial configuration of the samples in two-dimensional space (in this case) is then created. The dimensions have no specific value but simply plot similarities of the samples. This allows complex data sets to be easily visualized, with more similar samples grouping together to form clusters, and dissimilar samples being located further away in the two-dimensional plot.

The 12 monthly main collection sites of all five habitats were first analyzed using MDS as a group, to determine the extent to which the habitats could be differentiated in general. The same data were then analyzed as habitat pairs, generating 30 random comparisons for each of the three restriction enzymes. Next, one of the cardinal direction soils, 10 feet distant from the main collection site, was added into pairwise habitat analyses, acting as a "questioned" sample that should group with the known soils from a habitat if the technique is successful. A questioned soil was rated as grouping correctly if it plotted within 0.5 units of soils from the same habitat, incorrectly if plotted within 0.5 units of soils from a different habitat, and inconclusive if located approximately equidistant between the two.

Results

Amplification of the RecA Gene and T-RFLP Results

RecA was successfully amplified from all but one DNA sample, producing 135 T-RFLP profiles (exemplified in Fig. 1). Comparison of the 12 monthly collected soil DNAs from all habitats produced some generalizable results, in that the sandy woodlot and woodlot tended to plot separately, while the remaining three habitats (agricultural field, marsh, and yard) were not well differentiated (Fig. 2). The restriction enzyme used did not impact the discrimination of habitats. The *DpnII* digested DNAs (Fig. 2*a*) from the

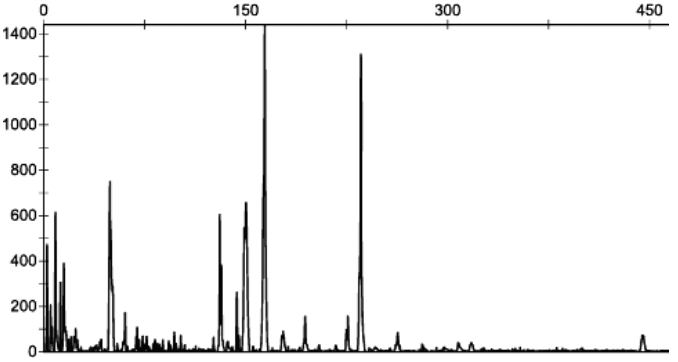

FIG. 1—*An exemplary terminal restriction fragment length polymorphism profile. Fragment size in number of bases is on the* x *axis and relative fluorescence units are on the* y *axis. Fragments between 40 and 450 bases with peaks heights 50 relative fluorescent units and greater were included in the analysis.*

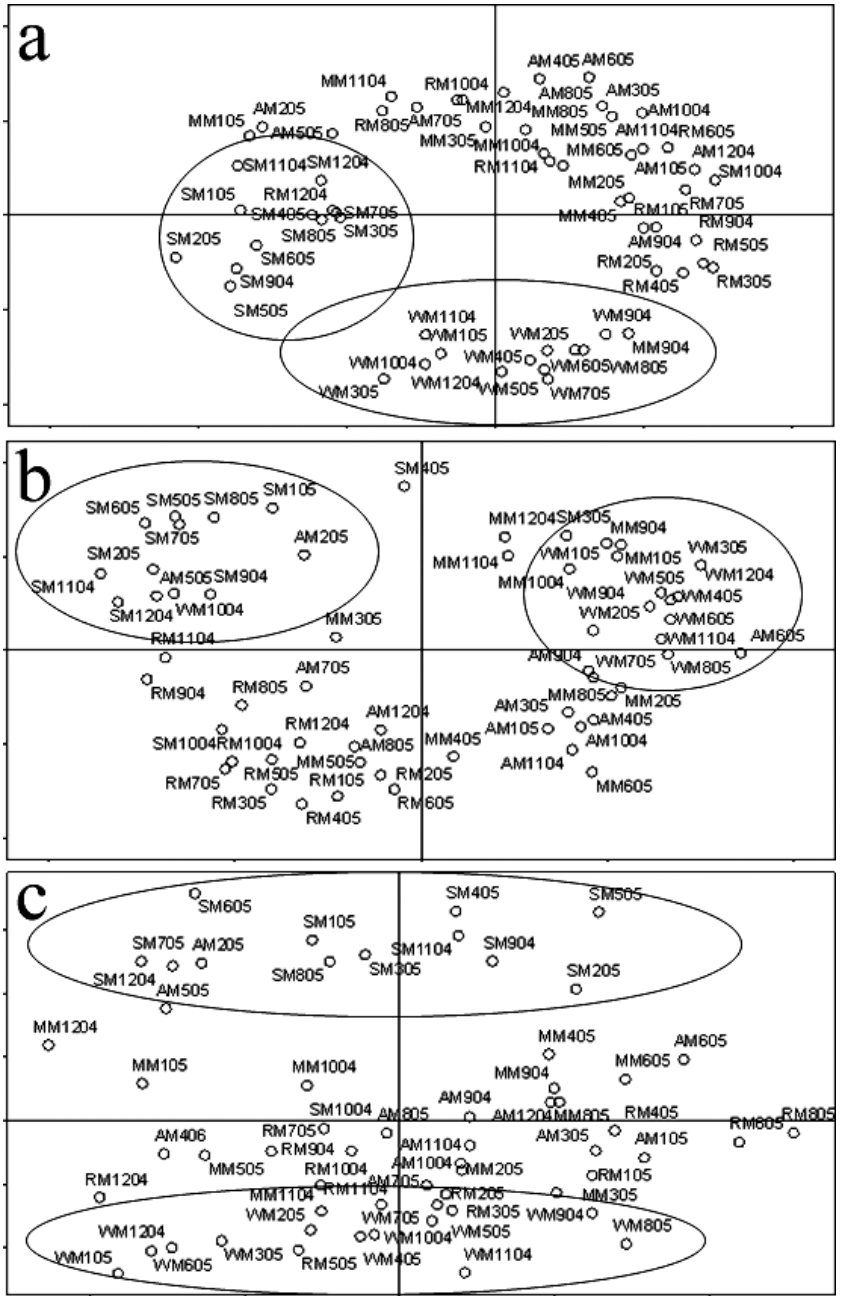

FIG. 2—*Multidimensional scaling plots produced when comparing the main sampling sites on a monthly basis from all habitats. Soils from the two woodlots (S; sandy woodlot, W; woodlot) frequently plotted separately and are circled, while the other habitats (A; agricultural field, M; marsh, R; yard) did not. (a) depicts a DpnII digestion, (b) an RsaI digestion, and (c) an MspI digestion. Month and year of collection are indicated with each plotted point.*

sandy woodlot and woodlot were distinguishable with little overlap from other habitats (the exceptions being soil collected from the marsh in September plotting similarly to woodlot samples, and soil from the yard in December plotting with the sandy woodlot). In contrast, the three other habitats were indistinguishable from each other. DNAs from the sandy woodlot and woodlot digested with *RsaI* (Fig. 2*b*) were also differentiated, with only February and May agricultural field samples and the October woodlot sample grouping with the sandy woodlot, while January, September, and October marsh soils and the June agricultural field sample plotted with the woodlot. Yard soils tended to plot in the lower left quadrant, with the marsh and agricultural field not being differentiated. Plots produced from *MspI* digestions (Fig. 2*c*) generated similar results, again generally differentiating the two woodlots, although agricultural field soils from February and May plotted with the sandy woodlot and woodlot, respectively. However, only one dimension distinguished the habitats, resulting in a wide distribution of plotted points for each habitat along the *x* axis.

Habitats were correctly differentiated for all enzymes when pairwise comparisons were conducted (e.g., Fig. 3*a–c*). The sole exception was the agricultural field, which was indistinguishable from the habitat to which it was compared in ten of twelve plots (e.g., Fig. 3*d*), the exceptions being comparisons with *DpnII* and *RsaI*-digested woodlot soils. Owing to this, the agricultural field was excluded from subsequent pairwise analyses detailed below.

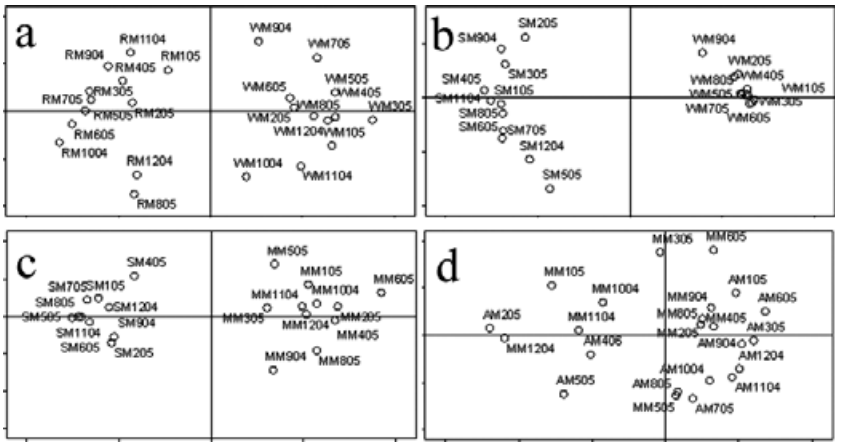

FIG. 3—*Multidimensional scaling plots produced when performing pairwise comparisons of the main sampling sites. (a) shows a DpnII digestion of yard (R) and woodlot (W) soils, (b) an MspI digestion of sandy woodlot (S) and woodlot (W) soils, (c) an RsaI digestion of sandy woodlot (S) and marsh (M) soils, and (d) soils collected from the agricultural field (A) and marsh (M) digested with MspI. Due to the inability to differentiate between habitats, the agricultural field was excluded from further pairwise comparison analysis.*

Inclusion of a Questioned Soil in Pairwise Habitat Comparisons

When 10-foot distant soils were added to the pairwise habitat comparisons described directly above, they grouped with soils originating from the same habitat 40% to 70% of the time depending on the enzyme used (e.g., Fig. 4*a*,*b*). Inconclusive samples (those plotting approximately equidistant between the two habitats) varied from 17% to 47% (Fig. 4*c*), and incorrect grouping ranged from 13% to 23% (Fig. 4*d*). Specifically, the "questioned" soil clustered with the same habitat 70% of the time using *DpnII*, while 17% grouped incorrectly and 13% were inconclusive. *MspI* "questioned" digestions plotted correctly 50% and incorrectly 23% of the time, with the remaining 27% inconclusive. Finally, plots from *RsaI* digestions grouped the "questioned" soil with soils from the same habitat with 40% accuracy, while 13% grouped incorrectly and 47% were inconclusive.

Discussion

Previous research examining the feasibility of using T-RFLP or similar molecular techniques to produce microbial fingerprints of soils has met with, at best, mixed success. Given the very large number of bacterial species/strains that exist in any given soil sample, this may stem, at least in part, from the generation of an exceedingly complicated picture of a soil's bacterial makeup. We thus decided to focus on a more limited bacterial community, with the goal of simplifying and clarifying soil bacterial fingerprints. In addition, multidimensional scaling analysis allowed for a deeper inclusion of available data than did similarity indices, the latter of which only examine profile pairs, multiplying shared peaks by two and dividing by the total number of peaks present in both (22). This may be a major drawback in a forensic context, when the precise origin of a soil sample is unknown. In contrast, MDS can be used to generate a matrix of similarities that are then weighted, with peaks found in multiple habitats accentuated and background "noise" eliminated. The projected similarities are plotted in two-dimensional space, resulting in easy to interpret profiles depicting which soils group similarly.

T-RFLP profiles produced using the rhizobium-specific *recA* gene were less complex than those produced via the bacterial 16S rRNA gene (11), while still generating an adequate number of peaks for comparison. Examining all five habitats at once generally

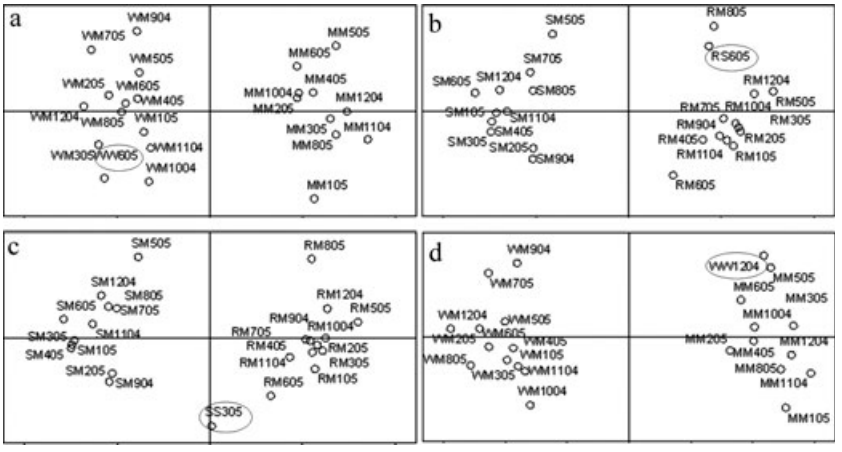

FIG. 4—*Multidimensional scaling plots produced when adding "questioned" soils (circled) collected from the four cardinal directions to pairwise comparisons of the main sampling sites. (a) shows a DpnII digestion of marsh (M) and woodlot (W) soils, (b) an MspI digestion of sandy woodlot (S) and yard (R) soils, (c) an MspI digestion of sandy woodlot (S) and yard (R) soils, and (d) soils collected from the woodlot (W) and marsh (M) digested with DpnII. (a) and (b) represent correct groupings of the questioned soil, (c) portrays an inconclusive result, and (d) an incorrect grouping of the questioned soil with the contrasting habitat.*

produced ambiguous (overlapping) results, although this is perhaps not surprising given a two-dimensional scale with so many habitats and data points. Interestingly, the woodlot and sandy woodlot were effectively differentiated even in the five-way plots, utilizing any of the three restriction enzymes. Only the yard was likewise differentiated, in one instance (*RsaI* digests); the remaining habitats producing broad, overlapping groupings. The specific reason(s) for the differentiation of only the woodlots is unknown, although it is notable that the sandy woodlot was also the most unique habitat based on bacterial 16S rRNA T-RFLP analysis (11). The fact that the sandy woodlot was 100 miles distant from the other habitats indicates that distance might play a large role in bacterial diversity. This has clear forensic implications, wherein large differences in bacterial makeup between questioned and known soil samples may indicate not just habitat variability, but spatial divergence as well. The woodlots were also the least disturbed of the habitats, with the agricultural field being highly manipulated (detailed below), the yard generally being a monoculture that was mowed regularly during the growing season, and the marsh, although much less perturbed, being adjacent to several dwellings.

Overall, it appears that comparing five habitats at a time, each with a dozen soil collection time points, overwhelms the ability to differentiate them in unison. Given this, pairwise habitat analyses were performed, which represent a more realistic forensic scenario as well—where the prosecution claims soil originated from one source while the defense identifies a contrasting location. Pairwise comparison proved much more successful in differentiating soils, again distinguishing both woodlots, but also separating the marsh and yard as well, for all restriction enzymes tested. A major implication of these findings is that known soil samples can potentially be collected well after a crime occurred without detrimental outcomes, given that time/season did not have a substantial negative influence on the ability to group soils from a habitat, even though samples were collected throughout a 1 year period.

In contrast to these four habitats however, the agricultural field was not distinguishable from other habitats in 10 of 12 pairwise comparisons, nor did its soil samples group among themselves. The likely reason for this anomaly is the extreme amount of human manipulation the field experienced, having undergone rounds of tilling, plantings, and fertilization. Soybean (a legume that relies on rhizobia) was sown during the first summer, which was replaced by corn the second summer. The latter crop requires extensive nitrogen fertilization, which took place in the spring prior to its planting. Clearly, all of these could drastically influence the bacterial makeup of the soil. Tilling would also act to mix and homogenize the soil, further altering its bacterial content near the surface where soil collection took place. Such anthropogenic manipulation may explain not only the failure of agricultural field data points to cluster in pairwise comparisons, but also the lack of data clustering in rhizobial profiles seen when all five habitats were compared simultaneously.

The ultimate test of a technique designed for soil identification is determining whether a questioned soil sample correctly groups with known soil from a site, versus soil from an incorrect site. For this, we utilized a subset of the soils obtained 10 feet distant from the main soil collection location and applied them back into 90 pairwise habitat comparisons of main collection sites. These distant soils (acting as the "questioned" samples) were employed as it is possible that known samples will not be collected from the exact spot where a questioned soil originated. It should be noted that the nature of MDS is that all data are utilized, thus these tests did not simply compare the distant soil to the others, but instead reanalyzed the data with the unknown soil's profile incorporated as part of the overall pairwise comparison.

The 10-foot distant questioned soils grouped back with the correct habitat soils 40–70% of the time (dependant on restriction enzyme); however they also grouped with the incorrect soil 13–23% of the time. Inconclusive results (i.e., the questioned sample grouped with neither known soil) were observed 13–47% of the time. There was no clear pattern as to which questioned soil grouped with its respective habitat, and only the marsh samples never incorrectly clustered with the compared habitat. This was surprising given how well four of the habitats were clearly differentiated in pairwise comparisons, or even in five-way comparisons when considering the woodlots. The fact that the marsh did not produce any erroneous results indicates it was more spatially homogeneous than were the other habitats, while still containing enough unique strains of rhizobia to differentiate it. Most importantly, the results clearly indicate that spatial heterogeneity is an extremely important factor in microbial DNA profiling and relatively small distances between soil sampling can have a critical influence on such assays. In contrast, if a questioned soil originated from the same location as the knowns, it seems likely to group with them, even if they were collected at a different time.

Local heterogeneity could stem from a wide range of environmental factors, such as unique plant species, the amount of sunlight reaching the soil, and differing moisture levels. Mummey and Stahl (23) obtained samples from two different types of grasslands in Wyoming and found that similarities within a grassland decreased rapidly at distances >3.6 m. The authors proposed that differences in plant distribution, rooting patterns, or soil organic content could induce different species of bacteria to flourish across such a small area. The results presented here are consistent with this, and local heterogeneity may end up playing a large role in the utility of microbial fingerprinting of soils.

Conclusions

T-RFLP analysis has become a valuable technique in microbial ecology and can be performed quickly and easily with a resolution that allows even related strains of bacteria to be differentiated. Likewise, soils show the potential to be successfully differentiated via T-RFLP, given the right circumstances. The markers utilized (in the current research, rhizobia-specific) must be considered, and the soil cannot have been heavily modified and manipulated between the time when a questioned soil originates and known samples are obtained. If these variables are controlled for, T-RFLP examination appears to have forensic potential. This is not to say, however, that bacterial T-RFLP analysis is ready to be implemented in a forensic setting. Before this can happen, spatial heterogeneity of soil bacteria will need to be better understood, so that known samples, most likely collected some distance from a soil of questioned origin, reliably group together. Further, while the T-RFLP technique is well documented in the peer-reviewed literature, other tenants of Daubert, particularly error rates, will need to be addressed. As bacterial profiling of soil matures in general, genetic identification of soils seems plausible and may offer an objective and reliable method of forensic soil analysis.

Acknowledgments

This study represents the thesis research of E. Lenz in obtaining her Masters degree from Michigan State University. Specials thanks go to Melissa Meyers for her substantial input

into this study. The assistance of Dr. Terry Marsh of MSU for statistical analyses was also greatly appreciated.

References

1. Hopkins DW, Wiltshire PEJ, Turner BD. Microbial characteristics of soils from graves: an investigation at the interface of soil microbiology and forensic science. Appl Soil Ecol 2000;14(3):283–8.
2. Pye K, Blott SJ, Croft DJ, Witton SJ. Discrimination between sediment and soil samples for forensic purposes using elemental data: an investigation of particle size effects. Forensic Sci Int 2007;167(1):30–42.
3. Horrocks M. Subsampling and preparing forensic samples for pollen analysis. J Forensic Sci 2004;49:1024–7.
4. Dawson LA, Towers W, Mayes RW, Hillier S, Fraser A, Craig J, et al. Use of plant wax signatures in understanding soils. Proceedings of the Clay Minerals Group of the Mineralogical Society and the Forensic Science Society—Trace Metals, Isotopes, and Minerals in Forensic Science; 2003 Oct 30; London. London, UK: Mineralogical Society, 2003.
5. Heath LE, Saunders VA. Assessing the potential of bacterial DNA profiling for forensic soil comparisons. J Forensic Sci 2006;51(5):1062–8.
6. DeBruijn FJ. Use of repetitive (repetitive extragenic palindromic and enterobacterial repetitive intergenic consensus) sequences and the polymerase chain reaction to fingerprint the genomes of rhizobium meliloti isolates and other soil bacteria. Appl Environ Microbiol 1992;58: 2180–7.
7. Schwieger F, Tebbe CC. A new approach to utilize PCR single-strand-conformation polymorphism for 16S rRNA gene-based microbial community analysis. Appl Environ Microbiol 1998;64:4870–6.
8. Widmer F, Fließbach A, Laczkó E, Schulze-Aurich J, Zeyer J. Assessing soil biological characteristics: a comparison of bulk soil community DNA-, PLFA-, and Biolog™-analyses. Soil Biol Biochem 2001;33:1029–36.
9. Muyzer G, Smalla K. Application of denaturing gradient gel electrophoresis (DGGE) and temperature gradient gel electrophoresis (TGGE) in microbial ecology. Antonie Van Leeuwenhoek 1998;73:127–41.
10. Casamayor EO, Massana R, Benlloch S, Ovreas L, Diez B, Goddard VJ, et al. Changes in archaeal, bacterial and eukaryal assemblages along a salinity gradient by comparison of genetic fingerprinting methods in a multipond solar saltern. Environ Microbiol 2002;4:338–48.
11. Meyers MS, Foran DR. Spatial and temporal influences on bacterial profiling of forensic soil samples. J Forensic Sci 2008;53(3):652–60.
12. Pesaro M, Nicollie G, Zeyer J, Widmer F. Impact of soil drying–rewetting stress on microbial communities and activities and on degradation of two crop protection products. Appl Environ Microbiol 2004;70:2577–87.
13. Marsh TL. Culture-independent microbial community analysis with terminal restriction fragment length polymorphism. Methods Enzymol 2005;397:308–29.
14. Liu WT, Marsh TL, Cheng H, Forney LJ. Characterization of microbial diversity by determining terminal restriction fragment length polymorphisms of genes encoding 16S rRNA. Appl Environ Microbiol 1997;63(11):4516–22.
15. Blackwood CB, Marsh TL, Sang-Hoon K, Paul EA. Terminal restriction fragment length polymorphism data analysis for quantitative comparison of microbial communities. Appl Environ Microbiol 2003;69(2):926–32.
16. Marsh TL. Terminal restriction fragment length polymorphism (T-RFLP): an emerging method for characterizing diversity among homologous populations of amplification products. Curr Opin Microbiol 1999;2:323–7.
17. http://edis.ifas.ufl.edu/AG152 (accessed April 24, 2010).
18. Perret X, Broughton WJ. Rapid identification of rhizobium strains by targeted PCR fingerprinting. Plant Soil 1998;204:21–34.
19. Spaink HP, Okker RJH, Wijffelman CA, Pees E, Lugtenberg BJJ. Promoters in the nodulation region of Rhizobium leguminosarum. Sym plasmid pRL1JI. Plant Mol Biol 1987;9(1):27–39.
20. http://www.rhizobia.co.nz/taxonomy/rhizobia.html (accessed April 24, 2010).
21. http://inismor.ucd.ie/~talign/index.html (accessed April 24, 2010).
22. Cole JR, Chai B, Marsh TL, Farris RJ, Wang Q, Kulam SA, et al. The Ribosomal Database Project (RDP-II): previewing a new autoaligner that allows regular updates and the new prokaryotic taxonomy. Nucleic Acids Res 2003;31(1):442–3.
23. Mummey DL, Stahl PD. Spatial and temporal variability of bacterial 16S rDNA-based T-RFLP patterns derived from soil of two Wyoming grassland ecosystems. FEMS Microbiol Ecol 2003;46(1):113–20.

Additional information and reprint requests:
David R. Foran, Ph.D.
School of Criminal Justice and Department of Zoology
560 Baker Hall
Michigan State University
East Lansing, MI 48824
E-mail: foran@msu.edu

JOURNAL OF FORENSIC SCIENCES

J Forensic Sci, November 2010, Vol. 55, No. 6
doi: 10.1111/j.1556-4029.2010.01509.x
Available online at: onlinelibrary.wiley.com

PAPER

CRIMINALISTICS

Claude Dalpé,[1] *Ph.D.; Pierre Hudon,*[1,2] *Ph.D.; David J. Ballantyne*[1]*; Darrell Williams,*[3] *Ph.D.; and Denis Marcotte,*[4] *Ph.D.*

Trace Element Analysis of Rough Diamond by LA-ICP-MS: A Case of Source Discrimination?*,†

ABSTRACT: Current profiling of rough diamond source is performed using different physical and/or morphological techniques that require strong knowledge and experience in the field. More recently, chemical impurities have been used to discriminate diamond source and with the advance of laser ablation–inductively coupled plasma–mass spectrometry (LA-ICP-MS) empirical profiling of rough diamonds is possible to some extent. In this study, we present a LA-ICP-MS methodology that we developed for analyzing ultra-trace element impurities in rough diamond for origin determination (“profiling”). Diamonds from two sources were analyzed by LA-ICP-MS and were statistically classified by accepted methods. For the two diamond populations analyzed in this study, binomial logistic regression produced a better overall correct classification than linear discriminant analysis. The results suggest that an anticipated matrix match reference material would improve the robustness of our methodology for forensic applications.

KEYWORDS: forensic science, diamond, laser ablation–inductively coupled plasma–mass spectrometry, profiling, fingerprinting, trace elements

Gem-quality rough diamonds equate to small, highly concentrated forms of wealth that are easily concealed and valued in U.S. dollars for trade around the globe. Their intrinsic beauty as a rare gem has made them highly desired and valued for centuries. These same attributes have also made them highly desirable for theft, for illicit trade and for storage or transfer of wealth (Regrettably the shining light of diamonds has a darker side of theft and other crime. This has been an unfortunate feature of the diamond industry since earliest times; 2001, Sir Alan Grose, personnel communication, Head of Security, De Beers Group, Africa). To combat these problems, the Royal Canadian Mounted Police (RCMP) undertook scientific research into diamond profiling and origin determination to support investigations pertaining to rough diamonds.

The largest consumer markets for diamonds have traditionally been in countries with little or no production, whereas most cutting and polishing occurs in yet other countries where there are skilled workers and/or cheap labor. These two factors necessitate numerous and seemingly convoluted shipments of diamonds as they move quickly through the supply pipeline from mine to market, adding vulnerabilities for loss, theft, or illicit trade. Canada’s diamond industry has grown rapidly. Since the first mine opened in 1998, it has grown to become the fourth largest world producer by value based on 2007 statistics (1). It was during the early years of development when the RCMP first saw the need to develop new tools to safeguard this industry, learning from other countries that had decades of experience.

Physical and optical characteristics, such as morphology, geometric defects, absorption/color, luminescence, etc., have been used to describe diamond populations from different sources for the past century (2). These nonquantitative subjective assessments rely on years of personal experience and study of diamonds from many sources. They require an expertise and knowledge base that is difficult to transfer, is difficult to validate by other experts, and is difficult to assess in a court of law. Objective, quantitative measurements that permit statistical assessment and development of large databases of stones are more easily shared and validated.

As early as the 1940s, Chesley (3) used a semi-quantitative analytical technique called “grating spectrograph” to evaluate the association between the impurities present in rough diamonds and their geographic location. He observed similarities in the presence of some trace elements for diamonds that originated from the same geographic locality. Raal (4) used a “quantitative” spectroscopic technique to assess trace element impurities in rough diamonds and reported the presence of Si, Mg, Al, Ca, Fe, and Cu with the two last elements being linked to the color of some diamonds. A few decades later, a series of studies investigated trace element impurities in rough diamonds for source discrimination using instrumental

[1]Royal Canadian Mounted Police, National Police Services, Forensic Science and Identification Services, Materials Profiling, 1200 Vanier Parkway, Ottawa, Ontario K1A 0R2, Canada.
[2]Department of Mining and Materials Engineering, McGill University, M.H. Wong Building, 3610 rue Université, Montréal, Québec H3A 2B2, Canada.
[3]Royal Canadian Mounted Police, National Police Services, Forensic Science and Identification Services, Integrated Support Services, 1200 Vanier Parkway, Ottawa, Ontario K1A 0R2, Canada.
[4]École Polytechnique, Département des génies civil, géologique et des mines, C.P. 6079, succ. Centre-Ville, Montréal, Québec, Canada.
*Supported in full by the Forensic Science and Identification Services (FS&IS) of the Royal Canadian Mounted Police (Ottawa, Canada).
†Presented in part at the 2008 Winter Conference on Plasma Spectrochemistry, January 6–12, 2008, in Temecula, CA.
Received 9 June 2009; and in revised form 9 Sept. 2009; accepted 13 Sept. 2009.
[Correction added after online publication 30 July 2010: Author affiliation corrected for Pierre Hudon.]

neutron activation analysis (INAA; [5–11]). Sellschop (12, table 4.1) presented a good overall summary of the different trace elements detected in rough diamonds with their range of concentrations mainly defined by those earliest INAA studies noted earlier. However, the minimum detection limit of INAA combined with the low level of impurities in most gem diamonds required studies be based on "bulk" analysis of approximately 1 g of samples sometimes consisting of between 8 and 25 stones analyzed together. Furthermore, INAA can render samples unfit for subsequent analysis because of long-lived isotopes emitting gamma radiation after irradiation and other effects, such as darkening or breakage (6).

As suggested earlier, application constraints must be an integral part of evaluating new forensic methodology. For instance, nondestructive technologies would facilitate access to populations of high value, gem-quality diamonds for study and development of large databases. The vast majority of gem diamonds are void of any sizable inclusions near the surface. Therefore, methods based on analysis of inclusions alone would require destruction of most stones and would not be suitable. The extremely low concentrations of impurities found in gem diamonds require the most sensitive instrumentation with detection limits requiring only the smallest possible samples. Robust analytical methodology, which can be reproduced and validated by others, is most desirable supported by a valid statistical methodology and data analysis to interpret and present the results.

Although trace element analysis is well suited for this application, several other supporting technologies can provide valuable information for source characterization (13). In such context, other chemical characteristics studied include nitrogen content (e.g., nitrogen atomic % [14]); types of mineral inclusions (e.g., eclogitic/peridotitic ratios [15]); chemical/isotope composition of the inclusion [16,17]); and stable isotopic signature of the diamond matrix (e.g., $\delta^{13}C$ and $\delta^{15}N$ [18,19]).

The trace element impurities in natural diamond occur as either inclusions (in the form of crystal/liquid and/or quenched melt) or as foreign atoms substituted into the crystal lattice (e.g., [9,20–22]). Watling et al. (23) were among the first to report the use laser ablation–inductively coupled plasma–mass spectrometry (LA-ICP-MS) to discriminate rough diamond sources based on trace element impurities. They demonstrated significant element ratio differences in Cu, Zn, Y, Zr, W, Pb, and Th for diamond pools originating from Australia, South Africa, China, Zaire, and Russia deposits. Since then, LA-ICP-MS has been used by different academic groups as either "qualitative" (23–25) analysis (i.e., "isotopic ratios of the blank corrected count rates") or "quantitative" (26–29) analysis (i.e., "absolute concentration obtained by external reference calibration procedure") to fingerprint diamond source based on their trace element impurities. These source discrimination studies mentioned earlier were applied to various ore deposits (i.e., kimberlite sources) around the globe but none of them specifically tried to profile alluvial diamonds because it is difficult to verify how many source(s) they can be associated with. It is based on these preliminary studies that the Forensic Science and Identification Services at the RCMP decided in 2003 to evaluate the discrimination power of LA-ICP-MS data for profiling diamond as a forensic tool between well-known kimberlite sources. To facilitate this, trace element concentrations in rough diamonds were measured quantitatively using a commercially available certified reference material (CRM).

In this study, we evaluate how robust the LA-ICP-MS data can be used to discriminate "or profile" rough diamonds from their source of origin. Although other populations have been analyzed, we have chosen to use two diamond populations (ore deposits) and experimental database to test the analytical method. For this study, a total of 140 gem stones originating from two geographic areas have been utilized. One source is from the Canadian Slave Archean craton (approximately 55-Ma-old deposit) and the second one is from the Archean Limpopo Mobile Belt located in South Africa (approximately 500-Ma-old deposit [30]). Two different statistical methodologies were applied to the LA-ICP-MS data to evaluate the potential to discriminate between both diamond populations. A small pool of 10 diamonds was chosen arbitrarily from one population and re-analyzed by LA-ICP-MS to evaluate their probability of belonging to each population and to determine whether subsequent analysis could be correctly matched with original source. A conclusive remark is given regarding future research and development requirements to improve the methodology and discriminating power of LA-ICP-MS data on diamonds.

Analytical Techniques

Analysis of trace elements in diamonds was performed with a 193-nm excimer LA system attached to a double-focusing ICP-MS. The laser consists of a Compex 110 ArF laser mounted to a GeoLas™ 200M Special beam delivery system (Coherent–Lambda Physik–Microlas, Göttingen, Germany). The geometry and optical beam path of the GeoLas™ have been described previously in detail elsewhere (31). The only difference between that described by Günther et al. (31) and the system used in this study is that a 15× reflecting objective was used instead of the original 25× objective to increase the maximum ablation spot from 240 to 400 μm (Ealing Catalog Inc., Rocklin, CA; referred to Schwarzschild objective in Günther et al. [31]). The desired outcome, with this modification being a shallower pit with a larger surface area, minimized penetration depth of the laser beam on the rough diamond surface and minimized fractionation effect (32). An improved 193-nm full reflector aluminum (193-FR/AL) metal dielectric coating was applied on the primary mirror of the 15× reflecting objective to improve the energy density threshold encountered with such a beam delivery system (Princeton Instruments/Acton Optics & Coatings, Acton, MA).

The ICP-MS consists of an Element 2 (Thermo Electron Corporation, Bremen, Germany [33]). The original detection system on the ICP-MS was modified to receive a new state-of-the-art simultaneous electron multiplier and Faraday cup axial detection system (i.e., equivalent to an Element 2 XR instrument). This modification allows the ICP-MS to be operated in a triple detection mode without compromising sensitivity and time acquisition at low resolution (i.e., ions detected per ablation hole and time used for a full mass scan, respectively). Furthermore, the triple detection mode has a linear dynamic range from 0.2 to 10^{+12} counts per second, which is useful for unexpected high signal intensities and protection from detector oversaturation when occasional natural "inclusions" are ablated during the process (e.g., silicate/sulfide inclusions in diamond). Table 1 shows the parameters used for the LA-ICP-MS in this study with some detailed explanations below.

The samples are ablated with the laser in a sample cell using ultra-high purity helium flowing at 0.7 L/min (He grade 5.0). The combination of helium and particles generated by the ablation process was then further mixed outside the sample cell (i.e., 10 cm downstream) to ultra-high purity grade argon gas flowing at 1.035 L/min (Ar grade 5.0) using a "Y" polypropylene connector (Part #53415K143; McMaster-Carr, Aurora, OH). The suspended gas particles from the sample cell were transported to the "Y' and then to the ICP-MS torch inside a 2.8-mm inside/4.0-mm outside diameter clear Teflon-perfluoroalkoxy tubing (Element Scientific

TABLE 1— *Instruments and analytical parameters.*

	Value	Unit
Laser		
Wavelength	193	nm
Pulse frequency	10, 6, 10	Hz*
Voltage on thyratron	24	kV
Spot diameter	17, 250, 333	μm*
Fluence	<1, 5, 6	J/cm^2*
Homogenizer arrays	2 (9 x 9 elements)	Suprasil glass
Reflecting lens (objective)	15x†	
Sample cell volume	22.2	cm^3‡
ICP-MS		
Sample cell gas (He)	0.700	L/min
Mixing gas (Ar)	1.035	L/min
Cool gas	16.0	L/min
Aux gas	0.70	L/min
Plasma RF power	950–1200	watt
Guard electrode	OFF	
Cones	T1001-Ni & T1002A-Ni	Spectron™
Detectors	Type II SEM with Faraday cup	Triple mode§
Dead time	15	ns
Resolution	300	low
Analytical parameters		
Internal calibrating mass	^{13}C,^{51}V	amu¶
Lock mass	^{13}C	amu**
Selected isotopes for analysis	^{7}Li, ^{9}Be, ^{11}B, ^{13}C, ^{23}Na, ^{27}Al, ^{29}Si, ^{31}P, ^{39}K, ^{45}Sc, ^{47}Ti, ^{51}V, ^{55}Mn, ^{59}Co, ^{60}Ni, ^{63}Cu, ^{66}Zn, ^{69}Ga, ^{85}Rb, ^{88}Sr, ^{89}Y, ^{90}Zr, ^{93}Nb, ^{95}Mo, ^{107}Ag, ^{111}Cd, ^{115}In, ^{118}Sn, ^{121}Sb, ^{133}Cs, ^{137}Ba, ^{139}La, ^{140}Ce, ^{141}Pr, ^{146}Nd, ^{147}Sm, ^{153}Eu, ^{157}Gd, ^{163}Dy, ^{165}Ho, ^{166}Er, ^{172}Yb, ^{175}Lu, ^{178}Hf, ^{181}Ta, ^{182}W, ^{208}Pb, ^{209}Bi, ^{232}Th, ^{238}U	amu
Sample/peak	1	
Segment duration	3	msec
Settling time	≤ 50, 20, 1	msec††
Scan type	*ES*can	
Integration type	Peak top	
Total acquisition time	74	s
Number of passes by the mass spectrometer	150	runs

*Parameter used for CRM-S2150 oil, NIST SRM-615 glass, and diamond, respectively (see text for details).
†Reflecting lens with 0.28 numerical aperture, focal length 13.35 mm, and a working distance of 24.5 mm.
‡Cylindrical shape (56 mm ∅).
§Counting, Analog and Faraday cup mode.
¶See text for details.
**Parameters used for "mass locked" with a mass window of 125%, 30 samples/peak, sample time of 3 msec, and an integration type set to "integral."
††Minimum time used for magnet "Fly Back" (from 240 to 7 amu), minimum magnet jump (*B*-jump), and electronic jump (*E*-jump), respectively.

Inc., Omaha, NE). The total flow of the sample gas, or carrying gas, at the ICP-MS torch was 1.735 L/min. The optimized gas flow mixture was obtained by maximizing the peak to background ratio of mass $^{13}C^+$ by ablating a high-purity synthetic chemical vapor deposition diamond (polycrystalline optical grade Diafilm OP; Element Six, New York, NY). Day-to-day tuning procedure on the ICP-MS consisted of maximizing the signal intensity of carbon isotope ($^{13}C^+$) by moving the torch position along the *x*- and *y*-axis once the gas mixture made of Ar and He were stabilized at their setting flow rates (i.e., after approximately 20 min).

Samples, Standards and Quality Control

Two diamond populations originating from two distinct sources were utilized for this study as mentioned earlier (i.e., one from Canada and one from South Africa). These two populations are labeled as KS-1 and KS-2, which refers to kimberlititic source #1 and #2, respectively. KS-1 consisted of 100 rough diamonds and KS-2 consisted of 40 rough diamonds. Rough stones were selected from run of mine productions. With limited knowledge regarding the relationships between trace element profiles versus size or color, all stones chosen where gem quality and in size and color ranges commonly encountered in the illicit trade. Both groups contained stones of different gem quality, size, and shapes. The presence of visible cracks or inclusions could be avoided and would not influence the analysis or data. Categorically, the majority of diamonds are described as good quality and clear of visible inclusions. Figure 1 shows the weight distribution of each diamond population where KS-1 spans a wider range with three separated sub-populations. In this population, 45 stones are ≤0.125 carat, 50 stones are within the range of 0.665–1.167 carat, and five stones are ≥3.995 carat. The KS-2 diamond population has a size range of 0.681–1.205 carat (see insert diagram in Fig. 1). Each diamond was individually washed for 15 min in an ultrasonic bath in *Aqua Regia*, a 3:1 mixture of pure hydrochloric acid (HCl) and nitric acid (HNO_3), respectively (HCl OmniTrace® grade and HNO_3 OmniTrace Ultra™ grade; EM Chemicals Inc., Darmstadt, Germany). The stones were then rinsed in ultra-pure water (Milli-Q™ Academic A10, 18 MΩ cm; Millipore Co., Billerica, MA) and dried for 1 h to overnight using an isotherm forced-air laboratory oven at 70°C in separate 10-mL open beakers.

For quantitative analysis, a CRM oil was used as the main external calibration material (CRM-S21; Conostan® Oil-Analysis

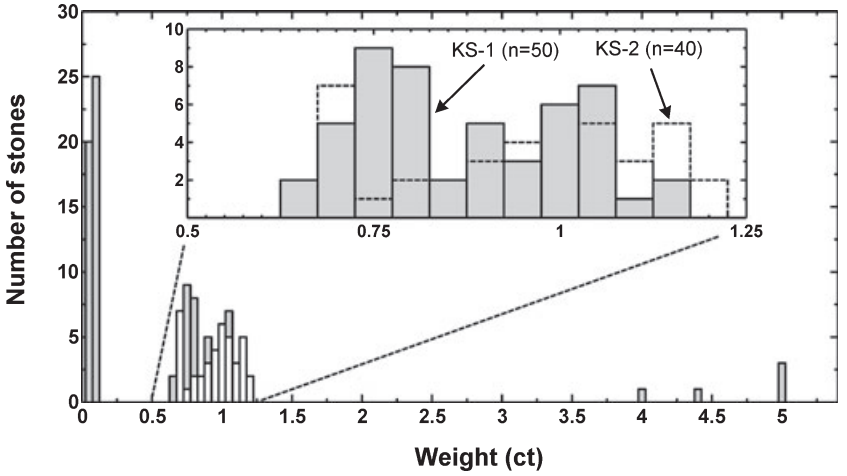

FIG. 1—*Weight distribution of the two diamond populations used in this study (1 carat or ct = 200 mg). In this figure, KS-1 diamonds are represented by gray boxes whereas KS-2 diamonds are represented by white boxes (n = 100 and 40, respectively). The inserted diagram shows a detail weight distribution of the stones within the range of 0.6–1.2 ct for KS-1 (n = 50) and KS-2 (n = 40). Note: For the insert diagram. KS-2 is represented by transparent boxes.*

Standard; SCP Science, Baie-d'Urfé, QC, Canada). This CRM-S21 custom blended oil was doped at 50 μg/g for the following 33 elements: Li, Be, B, Na, Mg, Al, Si, P, K, Ca, Sc, Ti, V, Cr, Mn, Fe, Co, Ni, Cu, Zn, Sr, Y, Mo, Ag, Cd, In, Sn, Sb, Ba, La, W, Pb, and Bi; labeled thereafter as CRM-S2150. For quality assurance, an aliquot of CRM-S2150 oil was analyzed by INAA at École Polytechnique of Montréal (QC, Canada; Table 2). The total carbon concentration was measured by elemental analyzer on two different aliquots in two different laboratories.

To ablate the oil with the excimer laser beam, a special oil-bath reservoir was made for this application. A new oil bath was placed inside the sample cell daily and located as close as possible to the exit port with other samples to be analyzed before starting the ICP-MS instrument (i.e., including the diamond and silicon carbide control samples as described below). Figure 2 shows the different parts required to make the oil-bath reservoir compatible for a stable ablating process under the laser beam. This oil-based calibration technique has been used previously for quantifying trace element concentrations measured by LA-ICP-MS in diamonds (26,27). Furthermore, other applications using liquid calibration for LA-ICP-MS analysis of solid materials were proposed as a useful calibration techniques when no matrix match standards were available (34,35). The oil-bath reservoir was cleaned with ethanol and refilled every day with fresh oil from the original CRM-S2150 bottle. Because a limited number of certified elements are available in the CRM-S2150 oil, a second standard reference material (SRM) made of glass was used in parallel to the oil (i.e., National Institute of Standard and Technology [NIST] SRM-615 glass; Baltimore, MD). The working concentration values were taken from Gao et al. (36). This glass standard allows the calculation of other elements not available from the oil calibration process (i.e., Rb, Zr, Nb, Cs, Ce, Pr, Nd, Sm, Eu, Gd, Dy, Ho, Er, Yb, Lu, Hf, Ta, Th, and U). Furthermore, a synthetic silicon carbide plate grown by chemical vapor deposition was used as quality control (QC; dimensions of the SiC plate: 5 × 5 × 1 mm, labeled thereafter as SiC3; donated by Dr. Thomas Anthony from the Diamond and Ceramic Laboratory, General Electric Global Research, Niskayuna, NY). This SiC3 has been analyzed by INAA with only three elements being detected above the minimum detection limit (i.e., V = 0.23 ± 0.01 μg/g, Mo = 0.25 ± 0.01 μg/g, and W = 0.45 ± 0.02 μg/g; INAA data from École Polytechnique, Montreal, QC, Canada). The two major elements in this glassy material are calculated to be silicon (70.07 wt.%) and carbon (29.93 wt.%) by assuming stoichiometric proportion.

Analytical Procedure

Quality Control

A QC sequence was run twice at the beginning of each day to establish the proper power applied by the radiofrequency (RF) generator to the ICP (so-called "RF forward power"). This was necessary because a linear relationship was found between the measured concentrations of V, Mo, and W in SiC3 and the applied RF power when CRM-S2150 oil was used as the external reference material with carbon as the internal calibrating mass. The two QC sequences are both identical with the exception of the applied RF power (i.e., 1150 and 1000 watts; Table 3). The sequence was first started at 1150 watts by acquiring two CRM-S2150, two SiC3, and then two CRM-S2150 (i.e., QC sequence A). The CRM-S2150 oil reference material was ablated with a fixed 17-μm laser beam diameter positioned in the middle of the 400-μm diameter hole filled with oil. Different pause times were required after ablating samples to re-establish the background level intensities generated by the gas mixture (Table 3). After completing the sequence, the RF power on the ICP-MS was gradually decreased to 1000 watts by 25-watt steps every second. The ICP-MS was kept running at this new condition for 10 min before starting the next sequence to stabilize the gas blank signal intensities. After 10 min, the acquisition of the QC sequence B followed the same sample order as in the previous one (Table 3). Raw data acquired from each sequence were processed separately with carbon (^{13}C) as the internal calibrating mass between CRM-S2150 (external standard) and SiC3 (unknown) using GLITTER™ v. 4.4 (Macquarie University, North Ryde, NSW, Australia; [37]). The calculated data obtained for V and Mo from each QC sequence were plotted against the RF powers as shown in Fig. 3. The optimum $RF_{working}$ value was calculated as the mean value between the RF_{MIN} and RF_{MAX} as shown in Fig. 3 (e.g., $RF_{working}$ = 1081 watts in this case). The QC was considered acceptable when the concentration of vanadium calculated at the $RF_{working}$ value was within approximately 20% of the value obtained by INAA (i.e., $V_{LA\text{-}ICP\text{-}MS}$ between 0.27 and 0.19 ppm). The RF power on the ICP was re-adjusted and kept fixed to the new working value for the rest of the analytical session

TABLE 2—*Major and trace element concentrations of CRM-S2150 oil.*

Element	INAA* (μg/g)	Precision (μg/g)	Certified (μg/g)	Precision † (μg/g)	Used‡ (μg/g)
Ag	51.1	2.6	50	0.15	50.6
Al	50.1	2.5	50	0.15	50.1
B	n.d.		50	0.15	50.0
Ba	32	8	50	0.15	41.0
Be	n.d.		50	0.15	50.0
Bi	n.d.		50	0.15	50.0
Ca	<50		50	0.15	50.0
Cd	49.9	2.5	50	0.15	50.0
Co	47.9	2.4	50	0.15	49.0
Cr	49.1	2.5	50	0.15	49.6
Cu	47	7	50	0.15	48.5
Fe	60	20	50	0.15	55.0
In	50.3	2.5	50	0.15	50.15
K	49	2.5	50	0.15	49.5
La	46.7	2.3	50	0.15	48.4
Li	n.d.		50	0.15	50.0
Mg	<120		50	0.15	50.0
Mn	51.5	2.6	50	0.15	50.8
Mo	49.7	2.5	50	0.15	49.9
Na	50	2.5	50	0.15	50.0
Ni	41	7	50	0.15	45.5
P	n.d.		50	0.15	50.0
Pb	n.d.		50	0.15	50.0
Sb	49.3	2.5	50	0.15	49.7
Sc	51.2	2.6	50	0.15	50.6
Si	n.d.		50	0.15	50.0
Sn	45	12	50	0.15	47.5
Sr	64	15	50	0.15	57.0
Ti	<50		50	0.15	50.0
V	51.1	2.6	50	0.15	50.6
W	49.4	2.5	50	0.15	49.7
Y	n.d.		50	0.15	50.0
Zn	51	2.0	50	0.15	50.5
C_{Total} (μg/g)	EA 849,500§		EA 846,600¶		848,050**

*INAA results from École Polytechnique de Montréal (QC, Canada) with a reported precision of ± 5% on the analysis (n = 1).

†With a reported typical precision of ± 0.3% on certificate of analysis (lot# 050818-3; Conostan® Oil-Analysis Standard; SCP Science, Baie-d'Urfé, QC, Canada).

‡Average values used in this study based on instrumental neutron activation analysis (INAA) results and reported concentrations from certificate of analysis.

§Norwest Labs (Edmonton, AB, Canada).

¶Canadian Microanalytical Service Ltd (Delta, BC, Canada).

**Average carbon concentration value based on external laboratory results.

μg/g, concentration equivalent to part per million (or ppm); INAA, instrumental neutron activation analysis; n.d., not determined; EA, elemental analyzer instrument.

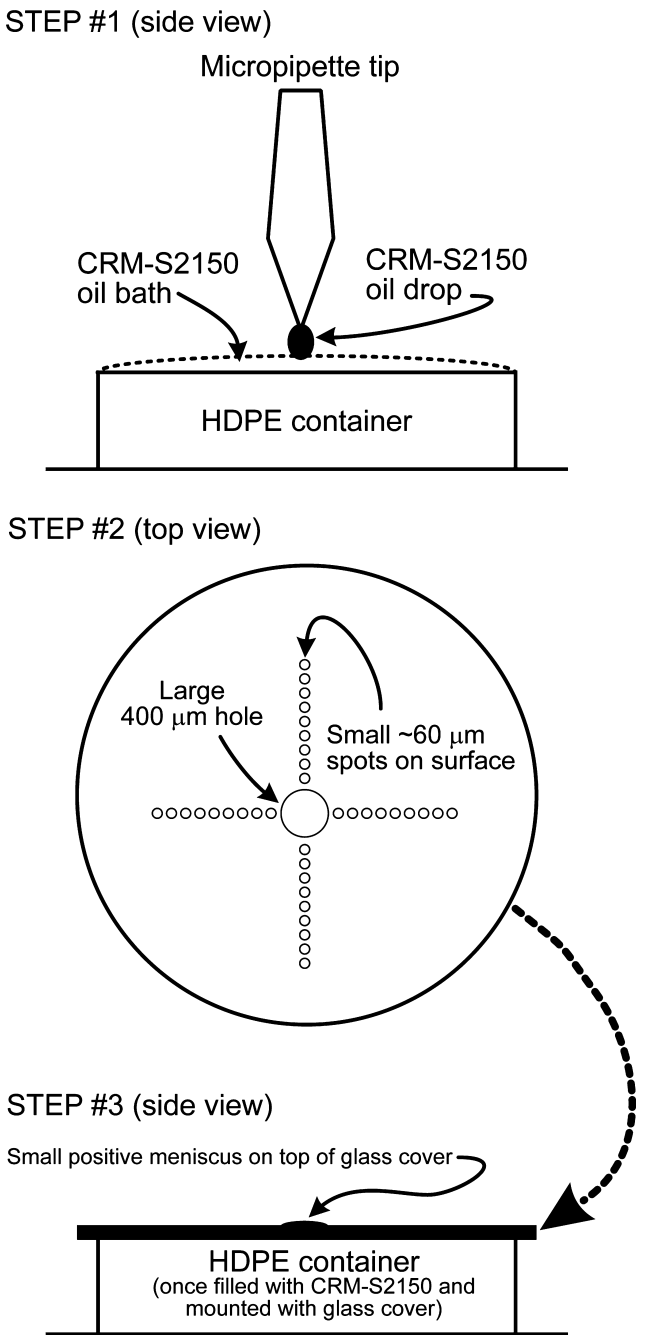

FIG. 2—*Special oil reservoir assembly for LA-ICP-MS analysis. The container is made of high-density polyethylene (HDPE) cap with a volume capacity of approximately 125 μL. In Step #1, the CRM-S2150 oil is poured into the container using a precise micropipette to avoid air bubbles formation. In Step #2, the predrilled glass cover is gently deposit on top of the oil bath with microtweezers (12 mm diameter by approximately 150-μm-thick borosilicate disk with a larger 400-μm diameter predrilled laser hole; cat. no. 12-545-80 [Fisher Scientific, Ottawa, Canada]). In Step #3, no air bubbles should be visible once the predrilled glass cover is sitting on top of the oil bath because air bubbles will create unstable signal during the ablation process. Notes: The approximately 60-μm spots on glass cover forming a cross around the center-hole are used as quick location guides when viewed under the 15× reflecting objective (approximately 20 μm depth). Only the center hole has been ablated through the entire glass cover thickness. All parts were precleaned in* Aqua Regia *before the first use with oil (ultrapure HCl:HNO$_3$ in the ratio of 3:1). Day-to-day cleaning consists of using anhydrous ethyl alcohol before refilling with new oil (see text). Figure not at scale.*

(normally fixed to one day). If the $V_{LA\text{-}ICP\text{-}MS}$ concentration obtained at the $RF_{working}$ was found to be outside the established limits, a new oil batch aliquot was put inside the high-density polyethylene oil container with a new set of sampler and skimmer cones prior to restarting the ICP-MS. After QC acceptance, diamond analyses were completed using the sequence block as described below.

Diamond Analysis

At the beginning of each analytical session, a group of 5–10 cleaned stones were mounted on the bottom of the laser sample cell using reusable adhesive "Bostik™ Blu-Tack" putty, generally with the flattest surfaces facing upward. As mentioned earlier, the

TABLE 3—*Daily QC sequence for diamond analysis by LA-ICP-MS.*

QC Sequence	RF Power (Watt)	Sample Identification	Concentration of Internal Calibrating Mass (μg/g)*	Pause Between Ablating Sample (s)†
A	1150	CRM-S2150-1	848,050	
		CRM-S2150-2	848,050	60
		SiC3-1	299,300	90
		SiC3-2	299,300	60
		CRM-S2150-3	848,050	90
		CRM-S2150-4	848,050	60
B	1000	CRM-S2150-5	848,050	
		CRM-S2150-6	848,050	60
		SiC3-3	299,300	90
		SiC3-4	299,300	60
		CRM-S2150-7	848,050	90
		CRM-S2150-8	848,050	60

*Concentrations used for carbon during the data processing (i.e., applied to ^{13}C as the internal calibrating mass).

†This corresponds to the time period required between the current sample and the previous one to re-establish the background intensities of the different masses analyzed by the ICP-MS.

μg/g, concentration equivalent to part per million (or ppm).

position of the oil-bath reservoir was located near the exit port of the sample cell to minimize potential contamination between samples (i.e., diamond stones and SiC3 were positioned upstream of the helium gas flow inside the sample cell). Table 4 shows a typical analytical sequence used for the diamond analysis (two diamonds in this example here). Typically, each stone was analyzed five times using the parameters described in Table 1. This number of replicates was necessary to attain a representative chemical signature of each sample knowing that some chemical heterogeneity has been observed in some stones during the analytical development of this project as well as by other LA-ICP-MS studies (25,28). That said, it should be noted that all five analyses are treated separately and not averaged (as explained below) and thus treated as independent measurements within that pool of stones.

It is important to note that ablating diamond within an inert gas environment will typically produce a significant carbon deposition around the laser pit. To facilitate focusing and to preclean the sample surface for the next analysis, a preablation procedure of 5–10 pulses was performed. Each analysis location is typically spaced approximately 150 μm from the previous ablation hole. The counting pause delay for the next acquisition begins after this preablation step. Table 4 shows the different pauses used to re-establish the "background" intensities between the different sample types. A longer pause was necessary between the two glassy materials because of the relatively high concentration of trace elements in NIST SRM-615 glass compared to SiC3. We analyzed both NIST SRM-615 and SiC3 glasses to monitor the LA-ICP-MS stability and performance conditions through every analytical session. For each analysis, data for 50 isotopes were acquired by the ICP-MS with a possibility of quantifying 28 of the 33 certified elements directly from the CRM-S2150 oil external standard. It was observed that for some elements, the concentration level was difficult to quantify because of high polyatomic interference levels generated by ablating carbon-rich matrices (e.g., $^{14}N^{15}N$ and $^{13}C^{16}O$ molecule interferences on mass ^{29}Si as well as $^{12}C^{12}C$ on mass ^{24}Mg, $^{12}C^{40}Ar$ on ^{52}Cr, and $^{16}O^{40}Ar$ on ^{56}Fe). The calcium isotope ^{42}Ca was also affected by possible polyatomic interferences (e.g., $^{1}H^{1}H^{40}Ar$, $^{12}C^{14}N^{16}O$ molecules [27]). The internal calibrating mass ^{13}C was selected for the oil and diamonds using the values reported in Table 4. The data reduction and calculation was completed using GLITTER™ software.

As for the other extra isotopes that were not available from the CRM-S2150 oil as mentioned earlier, they were acquired to quantify them when desired, using a two-step calibration procedure where NIST SRM-615 glass was the second SRM with one analyte (isotope) previously determined from the CRM-S2150 oil calibration technique as mentioned earlier (e.g., V or Ba in diamond). However, the results of this two-step calibration procedure are not presented in this discussion. Another calibration procedure that we did consider in this study consists of quantifying all the 49 isotopes in one-step using NIST SRM-615 glass as the main reference

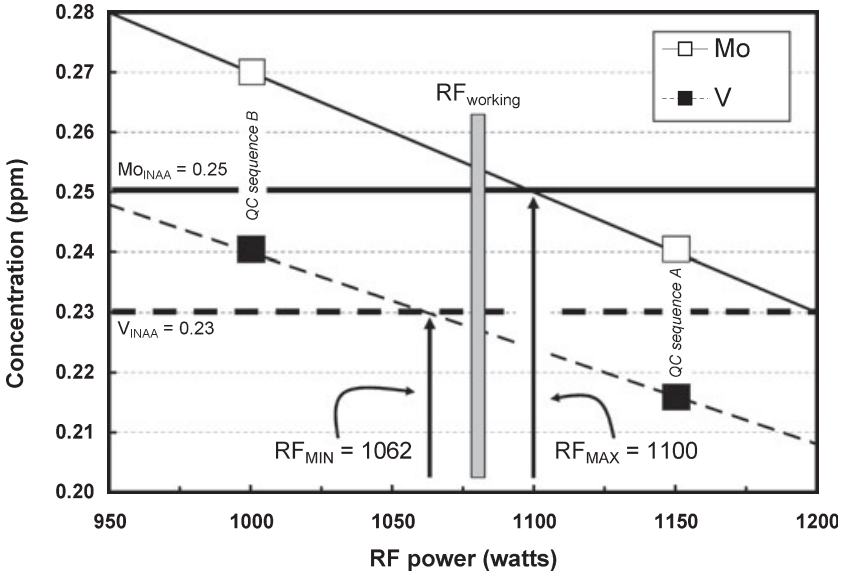

FIG. 3—*Variation of vanadium (V) and molybdenum (Mo) concentrations measured in SiC3 as function of the RF power applied to the ICP. The matching RF power corresponding to where the straight lines from the LA-ICP-MS data intercepts the INAA target concentrations (i.e., 0.23 ± 0.01 μg/g for V and 0.25 ± 0.01 μg/g for Mo). In this example, the RF_{MIN} corresponds to 1062 watts (based on the straight line connecting two concentration values calculated for V) and the RF_{MAX} corresponds to 1100 watts (based on the straight line connecting two concentration values calculated for Mo). A working RF value is then calculated based on those two new RF values (in this case: $RF_{WORKING} = [RF_{MAX\ at\ 1100W\ for\ Mo} + RF_{MIN\ at\ 1062W\ for\ V}] \div 2 = 1081$ watts).*

material for which an apparent carbon concentration was estimated from the CRM-S2150 oil. Figure 4 demonstrates the parameters required to estimate the carbon concentration in NIST SRM-615 glass with vanadium (^{51}V) as the internal calibrating mass between the glass and the CRM-S2150 oil. Based on this relationship, an apparent carbon concentration was estimated to be approximately 30,655 μg/g (i.e., C_{TOTAL} = 30,655 μg/g; see Table 4). We use the term apparent here because we found a value very different than the one reported by Jochum et al. (38) using a secondary ionization mass spectrometer in a similar glass aliquot (results obtained in NIST SRM-614 glass which is equivalent to the NIST SRM-615 sample but with a different wafer thickness [39]). They reported a value of 4.0 μg/g in the molecular form of carbon dioxide (CO_2) which is equivalent to 1.09 μg/g of total carbon (i.e., C_{Total}). Furthermore, the C_{Total} concentration measured in five NIST SRM-614 glass aliquots by elemental analyzer gave 60 ± 5 μg/g (n = 5; using a LECO™ CS-444; CANMET Materials Technology Laboratory, Ottawa, Canada). Based on the different analytical results, it is difficult to determine at this point which carbon value is the most accurate/appropriate one for NIST SRM-614 and/or NIST SRM-615 glasses. However, the intention of using an apparent concentration of 30,655 μg/g in this exercise has no direct implication regarding the conclusion that will be drawn from this study, as will be discussed below. The purpose in this case of using an apparent carbon concentration for NIST SRM-615 glass is not to obtain accurate concentrations (known mass bias) but rather to study consistency of the analytical technique in this research. The mass bias occurs between NIST SRM-615 and CRM-S2150 (i.e., overestimating carbon concentration in NIST SRM-615 using CRM-S2150 in such a case).

Quality and Evaluation Test

Once all the diamonds were analyzed, a "Quality and Evaluation Test (Q&ET)" was performed with a blind test by re-analyzing a small pool of 10 diamonds chosen arbitrarily within the weight range of 0.6–1.2 carat from one of the diamond populations and following the same analytical procedure as described earlier with five replicate analyses per stone (i.e., 50 analyses in total). This test was performed even though we knew the limitations of our current methodology with the external calibration (e.g., possible matrix effects and the absence of some desired elements in the certified oil). We will discuss our results below.

Results and Discussions

A total of 775 analyses were acquired in separate analytical sessions over a period of 9 months to process the two diamond populations (i.e., 535 and 240 analyses from KS-1 and KS-2, respectively). First, we will present the LA-ICP-MS results based on the oil calibration procedure with two statistical methodologies applied to the data to evaluate how distinct they are from each other in terms of chemical fingerprint. The same comparison will be presented for the data obtained from the NIST SRM-615 glass calibration procedure as an exploratory support based on the assumption that we mentioned previously. Discussion of the blind test Q&ET, later in the paper, will compare the probability of this test sample belonging to population KS-1 or KS-2 applying the statistical models developed from either CRM-S2150 or NIST SRM-615 calibration techniques.

Oil Calibration

Table 5 shows the overall results obtained by LA-ICP-MS for each diamond population. The average minimum detection limit was calculated from GLITTER™ based on a formula described by Longerich et al. (40). The difference in average minimum detection limit (MDL_{avg}) between the two diamond populations can be explained by day-to-day instrument conditions (laser and the ICP-MS), total intensity from the ablation process, and the level of gas

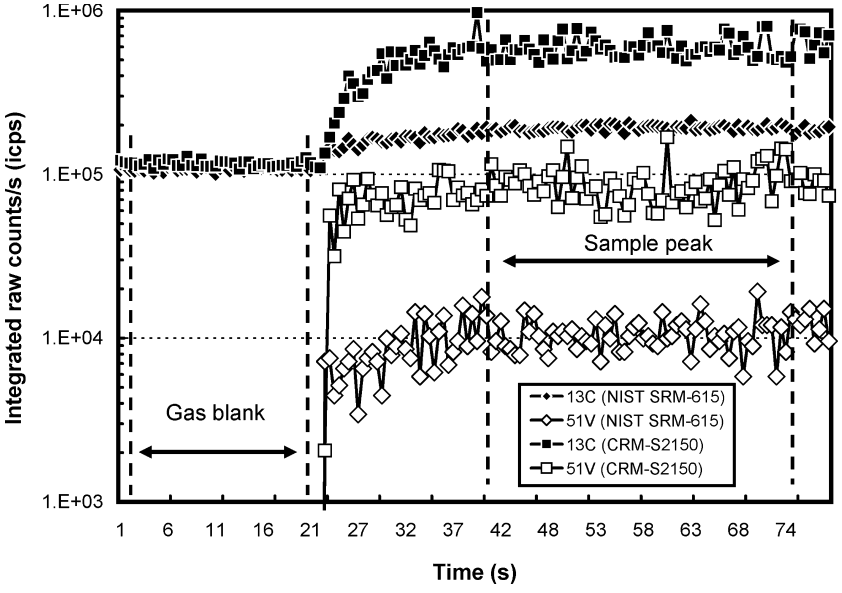

FIG. 4—*Combined time resolved analysis profiles of carbon and vanadium measured in NIST SRM-615 glass and CRM-S2150 oil by LA-ICP-MS. Diamond and square symbols referred to NIST SRM-615 glass and CRM-S2150 oil, respectively. Note the presence of a stable carbon signal on mass $^{13}C^+$ when we started ablating NIST SRM-615 glass with a 250-μm-diameter laser spot. The procedure used to calculate the carbon concentration in the glass ($C_{conc\ in\ NIST\ SRM\text{-}615}$) with the oil was to take the average sample peak intensities of each respective mass to which we subtracted its average gas blank intensities following the relationship: $C_{conc\ in\ NIST\ SRM\text{-}615} = \{[(^{13}C_{icps\ peak} - {}^{13}C_{icps\ blank}) \div (^{51}V_{icps\ peak} - {}^{51}V_{icps\ blank})]_{NIST\ SRM\text{-}615} \div [(^{13}C_{icps\ peak} - {}^{13}C_{icps\ blank}) \div (^{51}V_{icps\ peak} - {}^{51}V_{icps\ blank})]_{CRM\text{-}S2150}\} \times (V_{conc\ in\ NIST\ SRM\text{-}615} \div V_{conc\ in\ CRM\text{-}S2150}) \times C_{conc\ in\ CRM\text{-}S2150}$ (unit in μg/g); where conc stands for concentration (in μg/g), icps represents integrated counts per second.*

TABLE 4—*LA-ICP-MS sequence and calibration steps for diamond analysis.*

Sample Identification	Concentration of Internal calibrating Mass (μg/g)*	Pause Between Ablating Sample (s)†
CRM-S2150-9	848,050	
CRM-S2150-10	848,050	60
CRM-S2150-11	848,050	60
NIST SRM-615-1	*30,655*‡	90
NIST SRM-615-2	*30,655*	60
NIST SRM-615-3	*30,655*	60
SiC3-5	299,300	240
SiC3-6	299,300	60
SiC3-7	299,300	60
DIA-1-1	999,999.9§	90
DIA-1-2	999,999.9	60
DIA-1-3	999,999.9	60
DIA-1-4	999,999.9	60
DIA-1-5	999,999.9	60
CRM-S2150-12	848,050	90
CRM-S2150-13	848,050	60
CRM-S2150-14	848,050	60
NIST SRM-615-4	*30,655*	90
NIST SRM-615-5	*30,655*	60
NIST SRM-615-6	*30,655*	60
SiC3-8	299,300	240
SiC3-9	299,300	60
SiC3-10	299,300	60
DIA-2-1	999,999.9	90
DIA-2-2	999,999.9	60
DIA-2-3	999,999.9	60
DIA-2-4	999,999.9	60
DIA-2-5	999,999.9	60
NIST SRM-615-7	*30,655*	90
NIST SRM-615-8	*30,655*	60
NIST SRM-615-9	*30,655*	60
CRM-S2150-15	848,050	240
CRM-S2150-16	848,050	60
CRM-S2150-17	848,050	60

*Concentrations used for carbon during the data processing (i.e., applied to ^{13}C as the internal calibrating mass).

†This corresponds to the time period required between the current sample and the previous one to re-establish the background intensities of the different masses analyzed by the ICP-MS.

‡Estimated concentration based on CRM-S2150 (using V as internal calibrating mass; see text for more details).

§Concentration obtained by stoichiometric assumption (99.9% pure carbon for gem-quality diamond).

CRM, certified reference material; NIST SRM-615, National Institute of Standard and Technology—Standard Reference Material 615 glass; SiC3, silicon carbide; DIA, diamond.

blank measured by the ICP-MS on each isotope, which affect the MDL. The relative standard deviation in % (RSD%) values observed for KS-1 population are larger in general compared to KS-2 with the exception of a few elements (i.e., Be, Na, V, Mn, Cu, Zn, Cd, Sb, and Bi; Table 5). It is difficult to define the real significance of this difference but it could be the result of a larger diamond population (e.g., 100 stones vs. 40), a larger size distribution (Fig. 1), or it could suggest a wider chemical variation of micro-inclusion compositions in KS-1 diamonds sampled by the LA-ICP-MS, etc. All of these possibilities could affect the overall chemical signature of a population, in such a case the RSD%.

However, by considering only KS-1 diamonds that have similar weight to those in KS-2 (i.e., 50 selected stones from KS-1 population in the range of 0.50–1.25 carat; see inserted diagram in Fig. 1), the RSD% values resulting from this KS-1 subgroup are still predominantly higher to most elements compared to the entire KS-2 diamond population (not shown here). This difference suggests that the chemical signature between those two populations is not a significant function of their dimension (i.e., weight).

The median values of each element are shown in Fig. 5 with other descriptive parameters (box plot diagram). The medians of groups KS-1 and KS-2 for elements B, Na, Al, P, K, Sc, Ti, V, Mn, Co, Cu, Zn, Sr, Sb, Ba, La, and Bi were identified as being statistically significantly different at the 5% level by the Wilcoxon rank-sum test (42); not displayed in Fig. 5). By considering the outliers we can, however, observe an important overlap between the two populations.

Statistical Models

All data were evaluated statistically without using any presumptive filtering, data elimination, or sample averaging from each population (i.e., the "outliers" were not rejected). The statistical methodologies were used (i) to determine the most important discriminating elements of the 775 analyses to remove the collinearity between them (i.e., elements are correlated with one another which do not improve the model); (ii) to determine the chemical signature of each group; and finally (iii) to determine the probability of each Q&ET sample membership based on their chemical signatures. Based on those criteria a "Binomial Logistic Regression (BLR)" and a "Linear Discriminant Analysis (LDA)" methods were applied to the data to answer those questions.

Binomial Logistic Regression

This method is used to analyze the data and to determine the probability of group membership based on the chemical signature of the elements. In logistic regression, the relationship is explained by the following linear equation:

$$Y = b_0 + b_1X_1 + b_2X_2 + \ldots b_nX_n + \epsilon$$

where Y = log(p/(1-p)) is the log odds ratio (or logit) and "p" is the probability of having a "successful" outcome based on the values of the independent variables (i.e., X which is related to the elements [43]). It is used when the dependent variable is binary or represents discrete categorical values that cannot be directly represented by a linear relationship. Choosing KS-1 as the "successful" outcome, positive and negative values of Y indicate observations having a greater probability of belonging to KS-1 or KS-2, respectively.

Scaling

Preliminary analyses indicated that leaving the data "unscaled" resulted in extremely large and unrealistic odds ratios because of concentration range difference (i.e., from approximately 10^{+2}s to $<10^{-3}$ μg/g; as displayed in Fig. 5). Multiplying all the data by 100 prior to the statistical analysis provided a more appropriate scale for the log odds ratio (i.e., logit). With the exception of this step, all BLR analyses were performed using SPSS® Regression Models software using the regression command (version 12; SPSS® Inc., Chicago, IL).

Collinearity

Data were screened for collinearity prior to the statistical analysis as mentioned earlier. Collinearity occurs when an independent variable is correlated with one or more variables (e.g., Al and Mn collinearity observed in different diamond types [11, fig. 1]). The presence of collinearity can lead to larger confidence intervals on

TABLE 5—*Characteristics of element concentration measured in two diamond populations by LA-ICP-MS using the oil calibration procedure (values in μg/g).*

	KS-1 (n = 535)					KS-2 (n = 240)				
	MDL_{avg}	Avg*	Std	RSD%	Med	MDL_{avg}	Avg*	Std	RSD%	Med
Li	0.040	0.159	0.334	210	0.044	0.055	0.070	0.082	118	0.034
Be	4.4E-03	0.011	0.021	191	0.006	5.4E-03	0.027	0.052	194	0.012
B	.011	3.97	4.05	102	2.77	3.4E-03	5.17	3.99	77	4.17
Na	0.0865	38.6	92.0	238	7.95	2.084	29.5	124	420	3.74
Al	0.017	2.64	4.19	158	1.97	0.024	1.92	1.73	91	1.52
P	0.018	7.02	10.9	156	5.51	n.a.	5.36	2.51	47	4.97
K	0.516	64.1	116	181	11.2	1.229	2.19	2.61	119	0.920
Sc	7.7E-03	0.261	0.199	76	0.200	0.024	0.157	0.087	55	0.133
Ti	0.376	1.85	2.52	136	1.09	0.814	3.38	3.27	97	1.92
V	1.0E-03	0.117	0.085	72	0.102	9.4E-03	0.065	0.054	83	0.054
Mn	0.082	0.832	1.15	138	0.320	0.167	4.72	18.8	398	0.475
Co	0.017	0.097	0.276	284	0.033	0.037	0.132	0.283	215	0.057
Ni	0.099	5.33	37.2	699	0.710	0.143	3.19	15.5	487	0.850
Cu	0.013	0.471	1.31	278	0.063	0.023	0.301	1.04	346	0.074
Zn	n.a.	1.24	0.672	54	1.12	3.0E-03	1.06	1.01	96	0.950
Sr	2.3E-03	2.74	23.7	863	0.016	8.0E-03	0.035	0.044	126	0.016
Y	6.5E-04	0.032	0.284	898	0.002	7.3E-04	0.009	0.029	310	0.004
Mo	0.012	0.667	4.35	652	0.022	0.023	0.629	4.01	638	0.057
Ag	0.011	0.015	0.020	127	0.008	0.010	0.015	0.012	79	0.011
Cd	7.5E-03	0.144	0.098	68	0.122	0.012	0.198	0.350	177	0.120
In	5.5E-04	0.006	0.045	711	0.001	1.1E-03	0.013	0.043	329	0.002
Sn	1.8E-03	0.175	1.12	639	0.042	2.7E-03	0.063	0.064	101	0.047
Sb	8.0E-04	0.024	0.023	96	0.018	2.2E-03	0.053	0.063	118	0.039
Ba	3.2E-03	12.6	34.2	272	0.110	3.5E-03	0.074	0.147	199	0.029
La	2.4E-04	0.615	4.58	744	0.006	3.9E-03	0.013	0.032	242	0.005
W	5.3E-03	0.056	0.094	167	0.016	6.4E-03	0.030	0.046	153	0.016
Pb	n.a.	0.128	0.243	190	0.055	n.a.	0.077	0.110	143	0.055
Bi	2.8E-05	0.021	0.019	88	0.017	9.0E-05	0.045	0.057	127	0.031

*Statistic parameters based on the entire population.

MDL_{avg}, average minimum detection limit; Avg, average; Std, standard deviation; RSD%, relative standard deviation in %; med, median value of the entire population; n.a., not available.

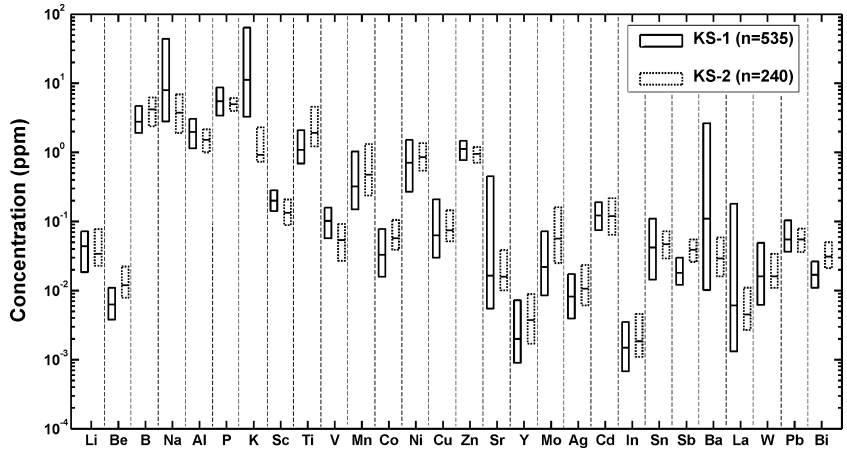

FIG. 5—*Box plot diagram showing the dispersion of trace element concentrations measured in KS-1 and KS-2 diamond populations. The size of the box reported for each element corresponds to the central 50% of the entire population with its lower-end representing the lower quartile (i.e., 25th percentile), the inside line represents the sample median (value that divides in two equal parts the entire data population; 50% above and 50% below) and the top-end representing the upper quartile (i.e., 75th percentile). Note: The extra information available for type of plot, such as the variability of the median between samples for box-to-box comparison (i.e., notches [41]), minimum/maximum values as well as the outliers data are not plotted here for better clarity (generated by Statistic Toolbox™ v5.3 from MATLAB® v7.3.0.267 R2006b; The MathWorks™ Inc., Natick, MA).*

the estimated log odds ratio and individual regression coefficients. Multicollinearity can be detected using "Variance Inflation Factors (VIF)" for each variable (44). The VIF are defined as $1/(1–Rj^2)$ where Rj^2 is the coefficient of determination obtained when regressing linearly variable Xj on all other variables. Multicollinearity is suspected for VIF > 10. The consequences of high multicollinearity are unreliable estimated coefficients, which may lead to incorrect interpretation of a variable's significance. In this procedure, we selected all variables that have a VIF coefficient less than 10. From this step Y, Sr, and Ba were rejected prior to conducting BLR analysis on the data calibrated using the oil. The data were first analyzed using a forward stepwise logistic regression

analysis in which no variables were selected (ref. to a null model). At each stage, the Rao's efficient score statistic is calculated for each individual remaining variable (i.e., 25 remaining elements, such as Li, Be, B, Na, Al, P, K, Sc, Ti, V, Mn, Co, Ni, Cu, Zn, Mo, Ag, Cd, In, Sn, Sb, La, W, Pb, and Bi [45]). The variable with the highest score is added to the model and a new Rao's efficient score is recalculated for the remaining variables. However, after each addition the model is tested for possible variable removal. This process used the significance of the conditional statistic based on the log likelihood ratio (i.e., a close parallel to the R^2 in linear regression model [42]). This process continues until further additions to the model do not provide further benefit to the log likelihood-ratio criteria (i.e., probability of significance should be >90%). The model was evaluated using both the Hosmer & Lemeshow's test and the Nagelkerke's R-square which are an approximation of the variance explained by the model (46,47). From this preliminary analysis, 15 variables demonstrate a significant contribution to the model (i.e., B, Al, P, Sc, Ti, V, Mo, Ag, Cd, In, Sn, Sb, La, W, Bi, and a constant). Once this preliminary process is performed, the residuals were examined to identify which data points presented a poor fit for the model. For example, cases with atypically large residual values were examined carefully as they might be associated with ''outliers'' in the data. After review, all the data were kept for the model, including the ''outliers,'' because there was no significant improvement in the overall final classification results.

Following the forward entry technique, a different operating subcommand was selected under the BLR command to provide a ''backward stepwise entry condition.'' This is the preferred method as it may uncover relationship missed by the forward stepwise inclusion (42). For this condition, the 25 variables were entered into the model together, which is then tested. In this case, the variable with the lowest Rao's score is removed first and then new Rao's scores are recalculated for all the remaining ones. Again, the same process of removing and entering data into the model is tested based on the significance of the conditional statistic (i.e., log likelihood ratio). The process stops after further changes to the model are not likely to benefit the Rao's scores. With this operation, only 14 variables were selected as being significant for the model with the same percentage of correct classification as those obtained under the forward stepwise entry. This latter model was retained and included the following selected variables: B, Al, P, Sc, Ti, V, Mn, Cd, In, Sn, Sb, La, W, Bi, and a constant. As observed here, no collinearity was detected between Al and Mn in those diamonds compared to those referred by Bibby et al. (11). The classification results of KS-1 and KS-2 using the CRM-S2150 oil calibration data are presented under Part A of Table 6. As shown here, a better overall classification for KS-1 diamond analyses (96.1%) was obtained with respect to those of KS-2 (85.8%). The overall correct classification of each individual analysis obtained by BLR is 92.9%, which is a reasonably high rate of classification. Although it is important that the model correctly classify cases, it is equally desirable that designation to a population is based on high probabilities. Figure 6*a* shows the overall predicted probability of each individual analysis. For this type of plot, a data point with a probability greater than the threshold value of 0.5 ($p > 0.5$) has a higher probability to be classified to the right group whereas those equal or less than 0.5 are having a greater probability to be classified to the wrong group based on the statistical model used.

Linear Discriminant Analysis

Discriminant analysis has been widely used for geological and forensic investigations involving either element or isotopic analyses (e.g., [48–53]). The method consists of finding a discriminant function, also called a classification function, based on the variables (i.e., elements) that best describe the difference between a set of population. This is achieved by maximizing the ratio of the ''between-group dispersions'' to the ''within-group dispersions'' of the two populations. Under the assumption of multi-Gaussian distribution with the same within-group dispersion matrix, the discriminant function is linear; otherwise, it is a nonlinear function (54). Linear discriminant function is usually preferred over nonlinear because a smaller number of parameters are required and therefore the analysis is more robust. However, we observed a non normal distribution for some elements (e.g., Ba in KS-1; not shown here); and to reduce departure from the multi-Gaussian distribution criteria, we decided to apply a single power transformation to the original data based on the percentage of well-classified samples. In such a case, we found that elevating all the data to the power of 0.3 was

TABLE 6—*Statistical classification obtained for each individual analysis measured in KS-1 and KS-2 diamonds.*

		KS-1 $_{\text{Predicted}}$	KS-2 $_{\text{Predicted}}$	Correct classification (%)
Part A Based on CRM-S2150 calibration data				
BLR model*	KS-1 $_{\text{Observed}}$	514	21	96.1
	KS-2 $_{\text{Observed}}$	34	206	85.8
		Overall BLR classification		92.9
LDA model†	KS-1 $_{\text{Observed}}$	499	36	93.3
	KS-2 $_{\text{Observed}}$	57	183	76.3
		Overall LDA classification		88.0
Part B Based on NIST SRM-615 calibration data				
BLR model‡	KS-1 $_{\text{Observed}}$	511	24	95.5
	KS-2 $_{\text{Observed}}$	46	194	80.8
		Overall BLR classification		91.0
LDA model§	KS-1 $_{\text{Observed}}$	481	54	89.9
	KS-2 $_{\text{Observed}}$	49	191	79.6
		Overall LDA classification		86.7

*Predicted classification obtained by binomial logistic regression based on 14 elements (B, Al, P, Sc, Ti, V, Mn, Cd, In, Sn, Sb, La, W, Bi, and a constant). Criteria used for model: PIN = 0.05 (probability of score statistic for variable entry), POUT = 0.10 (probability of conditional, Wald), Iterate = 20 (max. set value of iterations), and CUT = 0.5 (cutoff value for classification) under SPSS® regression command.

†Predicted classification obtained by linear discriminant analysis based on 16 elements (V, Sc, P, Sb, Sn, Ba, Mo, B, Ag, W, Ni, Ti, Bi, Cd, Al, and Na).

‡Based on 17 elements (Ag, Al, B, Bi, K, Li, Mn, Na, Pb, Sb, Sc, Si, Sn, Ti, V, W, Y, and a constant).

§Based on 16 elements (V, B, Si, Ba, Mo, Sb, Sn, Sc, Ag, La, W, Cd, Pb, Zn, Ti, Ni).

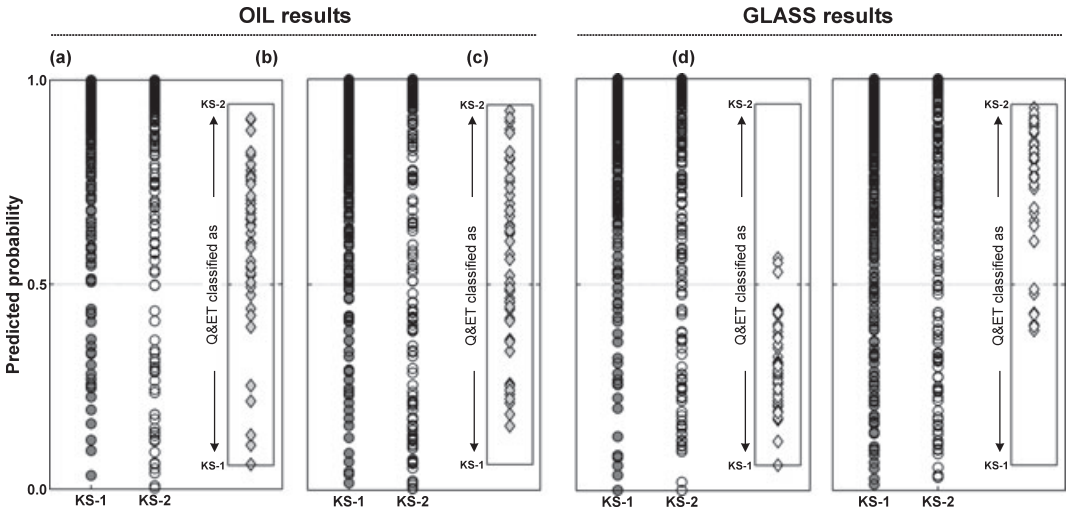

FIG. 6—*Predicted probability and classification results obtained for each individual analysis based on the oil calibration (a,b) and glass calibration (c,d) techniques (n = 535 and 240 for KS-1 and KS-2 populations, respectively). (a) and (c) are showing the results obtained with the BLR models whereas (b) and (d) are the results obtained with the LDA models. The insert diagrams are showing the classification results obtained for each Q&ET analysis based on the BLR and LDA models under different calibration procedures (n = 50). Note: For the insert diagrams, all data points below the 0.5 value classify into the right group (i.e., KS-1) whereas those above 0.5 classify into the wrong group (i.e., KS-2; as indicated by the labels on each end).*

the best compromise (i.e., $element_{concentration}^{0.3}$). This transformation brought the distribution of most elements closer to a "normal distribution" with a better symmetrical shape. Again, we removed Si as mentioned previously because of suspicious polyatomic interference for the CRM-S2150 oil calibration data. To avoid over "parameterization", we selected the most significant variables using a "stepwise" procedure based on the Rao's V criteria (54). From this procedure, the model selected 16 variables that are listed in Table 6. Once the resulted discriminant function was determined, we applied the model to the data to explain and predict the association of a single analysis to one of the two diamond populations based on measured trace element concentrations (i.e., classification analysis). The performance of the LDA was evaluated using a cross-validation procedure (leave-one out) to obtain an unbiased estimate of the LDA percentage of well-classified cases (55).

The final classification results obtained by LDA applied to KS-1 and KS-2 analyses are presented under Part A in Table 6. The LDA shows a better classification results for KS-1 diamonds (93.3%) compared to KS-2 diamonds (76.3%), similar to those results mentioned before with the BLR model. The overall correct classification result of each individual analysis obtained by LDA is 88.0%, which, again, is a reasonably high rate of classification. The dispersion of predicted probabilities obtained for all analyses based on the model is shown in Fig. 6*b*.

For the oil calibration, we observed in each population a greater dispersion of the predicted data in general with the LDA model compared to the BLR (Fig. 7*a*). This indicates that with these data the LDA model is less efficient than the BLR model in recognizing stable characteristics in the training groups used during modeling KS-1 and KS-2.

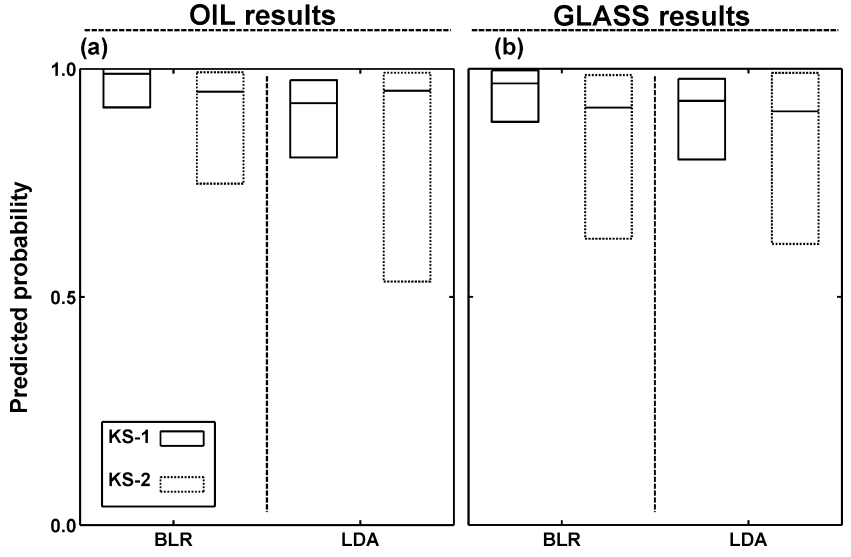

FIG. 7—*Box plot diagrams showing the dispersion of the predicted probabilities for each model based on Fig. 6 data. Note: The same order was kept as in Fig. 6. The size of the box, the sample median, the 25th percentile, and the 75th percentile are described in Fig. 5.*

Glass Calibration

From this procedure, we had the possibility of measuring all isotopes in one step as listed in Table 1 (i.e., 49 isotopes). Unfortunately, most of the "additional" elements that could not be quantified with the oil were found to have their concentration level near or below the minimum detection limit of the instrument (e.g., Ce, Pr, Nd, Sm, Eu, Gd, Dy, Ho, Er, Yb, Lu, Hf, Ta, U, Th). Because of this situation, their contribution was insignificant and, as a result, we removed them from the data prior to statistical analysis. We used, then, the same element list as described in the previous section and checked whether it improved the overall result (i.e., 29 elements including Si for this exercise knowing the potential molecular interferences). Both BLR and LDA were applied to the new data following the same procedure as described previously. The final predicted probabilities obtained for KS-1 and KS-2 diamond populations are depicted in Table 6 (Part B) and Fig. 6*c,d*. The overall classification rates obtained from the quantified with the glass are very similar to those obtained from the oil (i.e., $92.9\%_{\text{CRM-S2150}}$ vs. $91.0\%_{\text{NIST SRM-615}}$ by BLR and $88.0\%_{\text{CRM-S2150}}$ vs. $86.7\%_{\text{NIST SRM-615}}$ by LDA; Table 6). Here then, the glass calibration did not really improve the final overall classification. Furthermore, the BLR model was observed to be not as reliable as the model BLR obtained on the oil calibration data following the Hosmer & Lemeshow's test and the Nagelkerke's *R*-square values. The dispersion of predicted probabilities between KS-1 and KS-2 (Fig. 6*c,d*) is more or less the same to the one obtained by the oil calibration (Fig. 6*a,b*). A similar dispersion of the predicted probability data is observed with the glass calibration compared to the oil ones (Fig. 7*b*). However, the glass calibration did yield some benefits with respect to long-term stability of the data as we will explain below in the Q&ET samples section.

For all the models tested in this study, we observed that B, Sc, Ti, V, Sn, and Sb are among the "common discriminatory elements," which help to differentiate the two diamond populations. This list of elements could be very different if we were to compare two other sources or between one of the key source here and a third one (e.g., [23]).

Q&ET Samples

The 10 "Q&ET" stones all originated from KS-1 population. This information was not divulged to the analyst prior to the test. They were selected and were all of top clarity within the same size range as the KS-2 diamond population (i.e., 0.6–1.2 carat). Table 7 shows the classification results based on each individual analysis or based on stone membership following arbitrary criteria as described in the footnotes. As shown here, the results obtained using BLR were better for the data obtained from the glass calibration procedure than for those obtained from the oil calibration procedure. These results are reported in the insert diagram of Fig. 6*c* where most data are distributed closer to the KS-1 population with only three analyses being classified as KS-2 source. However, it is important to remember that BLR was not very robust for these data as we mentioned previously. The data obtained from the glass-based procedure show that the final results improved for the BLR model (Fig. 6*a* vs. *c*) but not for the LDA model (Fig. 6*b* vs. *d*). In fact, for LDA analysis, it led to incorrect classification for most stones (Fig. 6*d*). These results stress the difficulty to classify correctly the diamonds by their sole chemical characteristics. On the one hand, we observe high Q&ET misclassification rates for LDA with both oil and glass calibrations. On the other hand, BLR classifies well only with the glass calibration. This suggests glass calibration and BLR statistical analysis are preferable to oil calibration and statistical analysis by LDA. However, these results must be considered preliminary given the small representative sample and need to be confirmed by further statistical analysis.

TABLE 7—*Classification results obtained for the Q&ET samples.*

		KS-1 $_{\text{Predicted}}$	KS-2 $_{\text{Predicted}}$	Correct Classification (%)
Part A Based on CRM-S2150 calibration data				
BLR	Q&ET $_{\text{analyses}}$ ‡	10	40	20
model*	Q&ET $_{\text{diamonds}}$ §	2	8	20
LDA	Q&ET $_{\text{analyses}}$ ‡	21	29	42
model†	Q&ET $_{\text{diamonds}}$ §	4	6	40
Part B Based on NIST SRM-615 calibration data				
BLR	Q&ET $_{\text{analyses}}$	47	3	94
model¶	Q&ET $_{\text{diamonds}}$	9	1	90
LDA	Q&ET $_{\text{analyses}}$	7	43	14
model**	Q&ET $_{\text{diamonds}}$	0	10	0

*Results obtained with the BLR model (14 variables; see text for details).

†Results obtained with the LDA model (16 variables; see text for details).

‡Q&ET results based on each individual analysis ($n_{\text{total}} = 50$).

§Q&ET results based on individual stone following the arbitrary criteria of 3⁄5 analyses belong to the correct population ($n_{\text{total}} = 10$; see text for details).

¶Based on 17 variables (see text for details).

**Based on 16 variables (see text for details).

Over the 9-month period, we observed a better stability for V and Mo in SiC3 when NIST SRM-615 was used as the external reference material compared to the CRM-S2150. These observations, however, are not directly translated to the final statistical prediction as shown in Fig. 7*a,b* (i.e., larger data dispersion for the diamond analysis with the glass in general). A better signal stability is good as long as we have a good matrix match, something we did not have at the time of this study but have been developing.

Conclusions

The results obtained in this preliminary study demonstrate the possibility of using chemical impurities as measured by LA-ICP-MS to determine the provenance of a diamond but it requires additional testing from other diamond sources for further validation. The use of two statistical methods confirmed our concerns related to using an oil reference material as opposed to a solid material (e.g., NIST glass). Both statistical methods, BLR and LDA, selected models with a large number of variables (14–17) to achieve a good classification on the training set. A model with a large number of variables often lacks robustness for application to new data. This seems to be the case with the Q&ET as good classification rates were substantially lower for LDA with both calibration and for the BLR with the oil calibration.

There are several reasons why BLR is preferred for this application compared to LDA statistical models. The LDA assumes that the independent variables are normally distributed, have a linear relationship, and have equal within-group variances. The BLR does not have these assumptions as it transforms variables into logits and it can, therefore, accommodate both categorical and continuous independent variables. The BLR assumes, on the other hand, that there is no collinearity between variables (or elements), such as Al-Mn observed in some diamonds (11). However, collinearity is screened prior to the statistical analysis and the "coupled" element being removed to generate the final model.

As well, our results indicate the requirement for a better "reference" material to compare diamond pools analyzed on an extended time period (years) and to facilitate the comparison of results between laboratories. The purpose of this reference material is to generate a better signal stability during the LA-ICP-MS analysis, to have a better control on the matrix effects, and to compare and share some of our LA-ICP-MS results with other laboratories. With this perspective, the RCMP have developing diamond-based standards that would satisfy all these requirements.

Acknowledgments

We specially thank the following people for their support and helpful comments throughout this study: Dr. Jeff Harris from University of Glasgow, Department of Geographical and Earth Sciences (Glasgow, UK) and Drs. John Takos and Esmé Ryan both from Rio Tinto Technical Services (Melbourne, AUS). We particularly thank the following companies for facilitating sample loans and shipment logistics: Rio Tinto (Melbourne, AUS), De Beers–DTC Research Centre (Maidenhead, UK), and BHP Billiton Diamonds Inc. (Yellowknife, Canada). Mrs. Véronique Bouzaglou from École Polytechnique (Montréal, Canada) is thanked for her help in performing linear discriminant analysis on the preliminary LA-ICP-MS data. Two anonymous reviewers are thanked for constructive comments that improved the manuscript.

References

1. http://www.diamondwww.com/presentations/. (accessed July 15, 2010).
2. Wilks E, Wilks J. Properties and applications of diamond. Paperback edn. Oxford: Butterworth-Heinemann Ltd, 1994.
3. Chesley FG. Investigation of the minor elements in diamond. Am Mineral 1942;27:20–36.
4. Raal FA. A spectrographic study of the minor element content of diamond. Am Mineral 1957;42:354–61.
5. Fesq HW, Bibby DM, Sellschop JPF, Watterson JIW. The determination of trace-element impurities in natural diamonds by instrumental neutron activation analysis. J Radioanal Chem 1973;17:195–216.
6. Bibby DM, Erasmus CS, Kable EJD. The determination of trace elements in natural diamonds by instrumental neutron-activation analysis. Randburg, S Africa: National Institute for Metallurgy, Activation Analysis Research Group, University of the Witwatersrand; 1975 May Report No.: 1638.
7. Erasmus CS, Hawkins DM, Kable EJD, Fesq HW, Bibby DM. The identification of diamonds from Premier, Finsch, and Jagersfontein mines by statistical analysis of data obtained from instrumental neutron-activation analysis. Johannesburg, S Africa: National Institute for Metallurgy, Activation Analysis Research Group, University of the Witwatersrand; 1975 Nov. Report No.: 1652.
8. Fesq HW, Bibby DM, Erasmus CS, Kable EJD. Trace elements in diamonds from the Premier, Finsch, and Jagersfontein mines, and their petrogenetic significance. Johannesburg, S Africa: National Institute for Metallurgy, Activation Analysis Research Group, University of the Witwatersrand; 1975 Oct. Report No.: 1636.
9. Fesq HW, Bibby DM, Erasmus CS, Kable EJD, Sellschop JPF. A comparative trace element study of diamonds from Premier, Finsch and Jagersfontein mines, South Africa. Phys Chem Earth 1975;9:817–36.
10. Erasmus CS, Sellschop JPF, Bibby DM, Fesq HW, Kable EJD, Keddy RJ, et al. Natural diamonds–major, minor and trace impurities in relation to source and physical properties. J Radioanal Chem 1977;38:133–46.
11. Bibby DM, Fesq HW, Sellschop JPF. Trace elements in diamonds of different types. Nature 1978;276:379–81.
12. Sellschop JPF. Nuclear probes in physical and geochemical studies of natural diamonds. In: Field JE, editor. The properties of diamond. London: Academic Press Ltd, 1979;107–63.
13. Navon O. Diamond formation in the Earth's mantle. In: Gurney JJ, Gurney JL, Pascoe MD, Richardson SH, editors. The P.H. Nixon volume, Proceedings of the VIIth International Kimberlite Conference; 1998 Apr 11-17; Cape Town, S Africa. Cape Town, S Africa: Red Roof Design cc, 1999;584–604.
14. Kaminsky FV, Khachatryan GK. Characteristics of nitrogen and other impurities in diamond, as revealed by infrared absorption data. Can Mineral 2001;39:1733–45.
15. Taylor LA, Anand M, Promprated P, Floss C, Sobolev NV. The significance of mineral inclusions in large diamonds from Yakutia, Russia. Am Mineral 2003;88:912–20.
16. Cartigny P. Stable isotopes and the origin of diamond. Elements 2005;1:79–84.
17. Stachel T, Aulbach S, Brey GP, Harris JW, Leost I, Tappert R, et al. The trace element composition of silicate inclusions in diamonds: a review. Lithos 2004;77:1–19.
18. Cartigny P, Harris JW, Taylor A, Davies R, Javoy M. On the possibilities of a kinetic fractionation of nitrogen stable isotopes during natural diamond growth. Geochim Cosmochim Acta 2003;67:1571–6.
19. Bulanova GP, Pearson DG, Hauri EH, Griffin BJ. Carbon and nitrogen isotope systematics within a sector-growth diamond from the Mir kimberlite, Yakutia. Chem Geol 2002;188:105–23.
20. Sellschop JPF. Nuclear probes in physical and geochemical studies of natural diamonds. In: Field JE, editor. The properties of diamond. London: Academic Press Ltd, 1990;107–63.
21. Navon O, Hutcheon ID, Rossman GR, Wasserburg GJ. Mantle-derived fluids in diamond micro-inclusions. Nature 1988;335:784–9.
22. Klein-Ben David O, Izraeli ES, Hauri E, Navon O. Fluid inclusions in diamonds from Diavik mine, Canada and the evolution of diamond-forming fluids. Geochim Cosmochim Acta 2007;71:723–44.
23. Watling RJ, Herbert HK, Barrow IS, Thomas AG. Analysis of diamonds and indicator minerals for diamond exploration by laser ablation–inductively coupled plasma mass spectrometry. Analyst 1995;120: 1357–64.
24. Watling RJ. Novel applications of laser ablation–inductively coupled plasma mass spectrometry in inorganic analytical chemistry. Rapid Commun Mass Spectrom 1996;10:130–7.
25. Resano M, Vanhaecke F, Hutsebaut D, De Corte K, Moens L. Possibility of laser ablation-inductively coupled plasma-mass spectrometry for diamond fingerprinting. J Anal At Spectrom 2003;18:1238–42.
26. Jackson SE, Davies RM, Griffin WL, O'Reilly SY, Doyle B [abstract]. Quantitative LAM-ICPMS analysis of trace elements in diamonds. In: Ninth Annual VM Goldschmidt Conference, Abstract #7361; 1999 Aug 22-27; Cambridge, MA. Houston, TX: LPI Contribution No. 971, Lunar and Planetary Institute, 1999 (CD-ROM).
27. Rege S, Jackson S, Griffin WL, Davies RM, Pearson NJ, O'Reilly SY. Quantitative trace-element analysis of diamond by laser ablation inductively coupled plasma mass spectrometry. J Anal At Spectrom 2005;20:601–11.
28. Weiss Y, Griffin WL, Elhlou S, Navon O. Comparison between LA-ICP-MS and EPMA analysis of trace elements in diamonds. Chem Geol 2008;252:158–68.
29. McNeill J, Pearson DG, Klein-BenDavid O, Nowell GM, Ottley CJ, Chinn I. Quantitative analysis of trace element concentrations in some gem-quality diamonds. J Phys Condens Matter 2009;21(36), doi:10.1088/0953-8984/21/36/364207.
30. Field M, Scott Smith BH. Contrasting geology and near-surface emplacement of kimberlite pipes in Southern Africa and Canada. In: Gurney JJ, Gurney JL, Pascoe MD, Richardson SH, editors. The J.B. Dawson. Vol. 1. Proceeding of the VIIth International Kimberlite Conference; 1998 Apr 11-17; Cape Town, S Africa. Cape Town, S Africa: Red Roof Design cc, 1999;214–37.
31. Günther D, Frischknecht R, Heinrich CA, Kahlert H-J. Capabilities of an argon fluoride 193 nm excimer laser for laser ablation inductively coupled plasma mass spectrometry microanalysis of geological materials. J Anal At Spectrom 1997;12:939–44.
32. Mank AJG, Mason PRD. A critical assessment of laser ablation ICP-MS as an analytical tool for depth analysis in silica-based glass samples. J Anal At Spectrom 1999;14:1143–53.
33. Feldmann I, Tittes W, Jakubowski N, Stuewer D, Giessmann U. Performance characteristics of inductively coupled plasma mass spectrometry with high mass resolution. J Anal At Spectrom 1994;9:1007–14.
34. Günther D, Frischknecht R, Müschenborn H-J, Heinrich CA. Direct liquid ablation: a new calibration strategy for laser ablation-ICP-MS microanalysis of solids and liquids. Fresenius J Anal Chem 1997;359:390–3.
35. Boué-Bigne F, Masters BJ, Crighton JS, Sharp BL. A calibration strategy for LA-ICP-MS analysis employing aqueous standards having modified absorption coefficients. J Anal At Spectrom 1999;14:1665–72.
36. Gao S, Liu X, Yuan H, Hattendorf B, Günther D, Chen L, et al. Determination of forty-two major and trace elements in USGS and NIST

SRM glasses by laser ablation-inductively coupled plasma-mass spectrometry. Geostand Geoanal Res 2002;26:181–96.
37. Achterbergh E, Ryan CG, Jackson SE, Griffin WL. Appendix III. Data reduction software for LA-ICP-MS. In: Sylvester P, editor. Laser-ablation-ICPMS in the Earth Sciences. Ottawa, Canada: Mineralogical Association of Canada, Short Course Series, 2001;29.
38. Jochum KP, Stoll B, Herwig K, Willbold M, Hofmann AW, Amini M, et al. MPI-DING reference glasses for *in situ* microanalysis: new reference values for element concentrations and isotope ratios. Geochem Geophys Geosyst 2006;7(2):Q02008, doi:10.1029/2005GC001060.
39. Kane JS. A history of the development and certification of NIST glass SRMs 610-617. Geostand Geoanal Res 1998;22:7–13.
40. Longerich HP, Jackson SE, Günther D. Laser ablation inductively coupled plasma mass spectrometric transient signal data acquisition and analyte concentration calculation. J Anal At Spectrom 1996;11:899–904.
41. McGill R, Tukey JW, Larsen WA. Variations of boxplots. Am Stat 1978;32:12–6.
42. Wilcoxon F. Individual comparisons by ranking methods. Biomet Bull 1945;1:80–3.
43. Menard SW. Applied logistic regression analysis. 2nd ed Series: Quantitative applications in the social sciences. Vol. 106. Thousand Oaks, CA: Sage Publications Inc., 2002.
44. Neter J, Wasserman W, Kutner MH. Applied linear statistical models: regression, analysis of variance, and experimental designs, 3rd edn. Homewood, IL: Irwin, 1990.
45. Rao CR. Advanced statistical methods in biometric research. New York, NY: J. Wiley, 1952.
46. Hosmer DW, Lemeshow S. Applied logistic regression, 2nd edn. New York, NY: Wiley, 2000.
47. Nagelkerke NJD. A note on a general definition of the coefficient of determination. Biometrika 1991;78:691–2.
48. Herz N. Dean NE. Stable isotopes and archeological geology: the Carrara marble, northern Italy. Appl Geochem 1986;1:139–51.
49. Marshall BT, Herman JS. Trace element distribution in the soils above deeply weathered pegmatites, Virginia, USA: implications for exploration. Appl Geochem 1986;1:681–90.
50. Sandercock PML, Du Pasquier E. Chemical fingerprinting of unevaporated automotive gasoline samples. Forensic Sci Int 2003;134:1–10.
51. Lambrakis N, Antonakos A, Panagopoulos G. The use of multicomponent statistical analysis in hydrogeological environment research. Water Res 2004;38:1862–72.
52. Goodpaster JV, Sturdevant AB, Andrews KL, Brun-Conti L. Identification and comparison of electrical tapes using instrumental and statistical techniques: I. Microscopic surface texture and elemental composition. J Forensic Sci 2007;52:610–29.
53. Aziz N, Greenwood PF, Grice K, Watling RJ, van Bronswijk W. Chemical fingerprinting of adhesive tapes by GCMS detection of petroleum hydrocarbon products. J Forensic Sci 2008;53:1130–7.
54. Cooley WW, Lohnes PR. Multivariate data analysis. New York, NY: Wiley, 1971.
55. Piraux F, Palm R. Étude empirique des estimateurs des taux d'erreur en analyse discriminante. Rev Statist Appl 2001;49:71–85.

Additional information and reprint requests:
Claude Dalpé, Ph.D.
Research Scientist
Royal Canadian Mounted Police—National Police Services
Forensic Science and Identification Services
Materials Profiling
1200 Vanier Parkway
Ottawa, Ontario K1A 0R2
Canada
Email: claude.dalpe@rcmp-grc.gc.ca

JOURNAL OF FORENSIC SCIENCES

J Forensic Sci, November 2010, Vol. 55, No. 6
doi: 10.1111/j.1556-4029.2010.01476.x
Available online at: onlinelibrary.wiley.com

PAPER

CRIMINALISTICS

Doris Färber[1]*; Andrea Seul*[1]*; Hans-Joachim Weisser,*[2] *Ph.D.; and Michael Bohnert,*[2] *M.D.*

Recovery of Latent Fingerprints and DNA on Human Skin*

ABSTRACT: The project "Latent Fingerprints and DNA on Human Skin" was the first systematic research in Europe dealing with detection of fingerprints and DNA left by offenders on the skin of corpses. One thousand samples gave results that allow general statements on the materials and methods used. The tests were carried out according to a uniform trial structure. Fingerprints were deposited by natural donors on corpses. The latent fingerprints were treated with magnetic powder or black fingerprint powder. Afterward, they were lifted with silicone casting material (Isomark®) or gelatine foil. All lifts were swabbed to recover DNA. It was possible to visualize comparable and identifiable fingerprints on the skin of corpses (16%). In the same categories, magnetic powder (18.4%) yielded better results than black fingerprint powder (13.6%). The number of comparable and identifiable fingerprints decreased on the lifts (12.7%). Isomark® (14.9%) was the better lifting material in comparison with gelatine foil (10.1%). In one-third of the samples, DNA could be extracted from the powdered and lifted latents. Black fingerprint powder delivered the better result with a rate of 2.2% for full DNA profiles and profiles useful for exclusion in comparison with 1.8% for the magnetic powder traces. Isomark® (3.1%) yielded better results than gelatine foil (0.6%).

KEYWORDS: forensic science, fingerprints, DNA, human skin, adhesive powder, silicon, gelatine foil

In postmortem casework, evidence of offender contact on the skin surface of the homicide victim has to date in Europe been regarded as almost impossible to detect, as indeed has forensic analysis of such evidence. The search for fingerprints left by the offender on the skin of the victim has repeatedly been discussed in relevant publications (1–17).

In 2000, the Crime Scene Unit at the German Federal Criminal Police (Bundeskriminalamt) began a series of trials supported by various federal police offices and institutes of forensic medicine aimed at detecting and recovering latent fingerprints on the skin of corpses by using adhesive powders (18). During the course of the trials, the question arose as to whether an offender's DNA could be recovered and typed from the lift of a fingerprint on the victim's skin. This was possible during some pretests that were conducted under laboratory conditions (19).

The initial successes at a national level for the recovery of fingerprints and for the typing of DNA on human skin were the bases of a project funded by the AGIS program of the European Union (EU). The project objectives were verification of the results of the German test series to visualize latent fingerprints on human skin with common adhesive agents, determination of suitable and easy to use instruments, proof of the possibility of recovering "offender's" DNA from fingerprints placed on skin, exploration of best extraction method for DNA typing with regard to inhibition problems caused by the adhesive powders, and development of a standardized method/recommendation.

[1]German Federal Criminal Police, Wiesbaden, Germany.
[2]University Hospital Freiburg—Institute of Forensic Medicine, Albertstr. 9, Freiburg 79104, Germany.
*Financial support from the AGIS programme, European Commission—Directorate-General Justice, Freedom and Security.

Received 23 April 2009; and in revised form 22 July 2009; accepted 5 Sept. 2009.

It was the first systematic research carried out in Europe dealing with this topic and the first study involving four countries (Austria, Denmark, Germany [project management], and the United Kingdom) and a project time of 2 years. The large number of samples (1000) gave results that allow general statements on the materials and methods used.

Materials and Methods

The trials were carried out in the respective local morgues of the project partners (Germany: Institute of Forensic Medicine at the University Hospital of Freiburg; Austria: Department for Forensic Medicine at the Medical University of Vienna and the Pathology Department at the State Clinic in St. Pölten; the United Kingdom: University of Oxford School of Anatomy, Physiology & Genetics, Medical Sciences Teaching Centre; Denmark: Faculty of Health Sciences, Department of Forensic Medicine) in accordance with the ethical standards on human experimentation (Declaration of Helsinki 1983).

In each of the participating countries, 250 fingerprints were placed on and recovered from 10 corpses, so that a total of 1000 fingerprints and lifts were analyzed. In the project, 18 male and 22 female corpses were processed. The age of the deceased ranged from 15 to 98 years. The deceased were not obvious victims of crime.

When the project began, a uniform trial structure was established, to which all participants were to adhere.

Preparation

The partners were issued with a "starter kit" containing all materials needed along with equipment to avoid contamination and to create equal conditions for the fingerprint and DNA recovery.

Besides, a full protective clothing set (suit, gloves, face mask, shoe protection) each team received:

- Magnetic powder and magna brush (Hans Stöckle GmbH, München, Germany),
- Black fingerprint powder and disposable fiberglass brushes (Armor Holdings Forensics, Jacksonville, FL),
- Isomark® pistol, cartridge, nozzles (Isomark Ltd, Nuneaton, U.K.),
- Gelatine foil (Teiva s.r.o. GmbH, Prague, Czech Republic),
- Air-permeable containers for storing lifts.

If the corpse had already been refrigerated, it was left in a warmer environment for at least 4 h to allow moisture to dissipate. The skin had to be dry when placing the fingerprints. The skin temperature of the corpses ranged from 15 to 25°C. The ambient temperature ranged from 17 to 25°C.

DNA samples were taken from each depositor and each corpse by taking oral mucous samples.

Fingerprint Placement

With regard to the whole project, 26 different natural depositors were involved. The donors had not been picked out for special selection criteria, but by their affiliation to the partners'' institutions. If possible, the fingerprints were placed on smooth and undamaged parts of the skin on the limbs (forearm, lower leg, and foot) of the corpses. The areas of deposition were marked, and every print was given an individual number. The fingerprints were placed groomed, using a body's own perspiration and sebum adhesions. For this purpose, the fingerprint depositor wiped his or her fingers across his forehead and neck. When placing the fingerprints, the pressure was subjectively firm and exerted for several seconds.

Fingerprint Detection

Between 30 and 60 min passed before the search and recovery of latents started. Protective clothing was worn by the participants at all stages in the fingerprint recovery process to prevent contamination with foreign DNA.

Previously unused powder was applied to all fingerprints. Five hundred and five fingerprints were treated with magnetic powder using a magnetic plunger (''magna brush''). The magnetic plunger was cleaned before treating a new fingerprint area. Analogous to this, 495 fingerprints were treated with black fingerprint powder using disposable fiberglass brushes. Both powders were carefully applied with gentle strokes to avoid over-powdering. Excessive black fingerprint powder was wiped off the fiberglass brush before powdering to distribute the powder evenly and to minimize background staining. It was kept in mind that too many strokes could brush away cells from the fingerprints, which could have meant a loss of DNA.

Preserving Latents

First of all, all areas where fingerprints were deposited were photographed with a digital SLR camera with a macro lens. Photographs were taken as follows:

- Photograph of complete body,
- Close-up shot of the areas marked,
- Each recovered fingerprint, even those which were not suitable for analysis, was photographed twice with a measuring scale 1:1 (first on the skin, second on the lift).

Image processing (enhancement of fingerprints) followed the various project partners'' standard operating procedures.

Fingerprint and DNA Recovery

Five hundred and thirty-eight fingerprints were lifted with white Isomark®, a silicone-based two-component casting material, 462 with gelatine foil. The lifts were packed in air-permeable containers and forwarded to the Institute of Forensic Medicine, University Hospital of Freiburg for DNA analysis.

DNA Typing

To carry out DNA typing cellular material attached to the gelatine foils and Isomark® casts was transferred to sterile cotton buds moistened with high performance liquid chromatography (HPLC) water by wiping over the fingerprint area.

To limit the loss of DNA during processing, organic extraction with subsequent ethanol precipitation was initially chosen. While those samples treated with black fingerprint powder provided interpretable, amplified DNA results, in those samples treated with magnetic powder, inhibition of the PCR was observed. Even when cleaned with column chromatography (Chromaspin 100), the inhibitor could not completely be removed. Cleaning also resulted in a considerable loss of DNA, which had a negative effect on the DNA profiling. As a consequence, an extraction method had to be found, which would remove the inhibitor without the loss of a significant amount of DNA. Following various trials, NucleoSpin® Tissue XS kits (Macherey-Nagel, Düren, Germany) were chosen. With this method, following cell lysis, the DNA is attached to a silica membrane, washed, and released using an elution buffer. The advantage of this process over the majority of other extraction kits is the very small elution volume of 10–30 μL, a consequence of binding the DNA to a membrane, which is only a few mm^2, and also the elimination of inhibitors, which was confirmed by real-time PCR.

It was then possible to reduce the number of samples that produced no results. An increase in samples giving the corpse's profile compared to organic extraction was also a result of improved extraction.

Organic Extraction Method

An organic extraction process was used on the first 193 samples to release DNA from each of the samples. This was carried out by placing the samples in 500 μL of stain extraction buffer and adding 10 μL of proteinase K (20 mg/mL). The samples were then incubated in a shake incubator overnight at 56°C. This was followed by a phenol/chloroform/isoamyl alcohol extraction and then a chloroform/isoamyl alcohol extraction and finally an ethanol precipitation to which 10 μg tRNA was added as a carrier. After washing with 70% ethanol and drying the DNA, the DNA was re-suspended in HPLC water.

Extraction with NucleoSpin® Tissue XS kit

The remaining 807 samples were processed using the NucleoSpin® Tissue XS kit. Samples were incubated overnight at 56°C with 160 μL of the lysis buffer, to which 8 μL proteinase K (20 mg/mL) was added. The extraction protocol provided by the manufacturer was slightly modified because of the small amount of DNA expected. First, a more rigorous extraction buffer CF from Macherey-Nagel GmbH & Company was used for cell lysis. Second, the wash buffer B5 was split. The first washing was carried out with a final ethanol concentration of 80% (B5.1), the second washing with 60% ethanol (B5.2) to enhance DNA elution with buffer BE. Third, for a complete removal of residual ethanol, DNA solution was incubated at 75°C for 8 min with open lid in a shaking incubator.

Evaluation and Statistical Methods

The analyses of the recovered fingerprints were carried out by the project partners" fingerprint experts in accordance with their respective regulations. Each print was classified twice, once on skin and once on the lift. To keep the results consistent, the following scoring system was used:

- Identification
- Elimination
- Indication of touch
- No trace

The DNA traces were analyzed according to the following categories:

- No result (A)
- Complete DNA profile of the corpse (B)
- Partially interpretable mixed trace (C)
- Completely interpretable mixed trace (D)
- Complete donor DNA profile (E)

To assign traces to these categories, eight genetic marker systems were used (Amelogenin, TH01, VWA, FGA, D3S1358, D8S1179, D21S11, and SE33).

Statistical data preparation was carried out by using SPSS software (Statistical Package for Social Scientists, Version 14, SPSS Inc., Chicago, IL). The results are provided here with descriptive statistics. The results were also statistically checked with regard to their dependency on each other and to their significance. However, the tests predominantly confirmed the results of the relative frequencies. Therefore, this article will do without a full description of the statistical analyses performed and will only point out selected methods when appropriate.

Results

The individually numbered traces were listed in an "Evidence Record" with their locations on the corpses and the recovery materials used. On a second form, information regarding the deceased persons and the condition in the mortuaries was recorded. For evaluation purposes, the information was managed by using a MS Access database.

Preliminary Remark

Neither gender nor age of the deceased had a significant impact on the fingerprint and DNA results. Evaluation of the results showed no significant influence exerted by either the ambient temperature or the temperature of the donors" fingers within the temperature ranges encountered.

Dactyloscopic Analyses

On examination of corpses" skin, 16% of the fingerprints deposited would have been suitable for elimination or identification (Figs. 1 and 2). The results are given in Table 1. Comparison of the latent results "skin" and "lift" showed that no latent with "no result on skin" was improved to a usable dactyloscopic result by lifting (either "elimination" or "identification"). Only one latent was improved from "elimination" on skin to "identification" on the lift. Merely, three latents (of 1000), which were assessed as "indication of touch" on the skin, were put in the category "elimination" on the lift, i.e., these latents improved from an unusable to a usable dactyloscopic result.

FIG. 1—*Fingerprint on human skin, made visible with magnetic powder.*

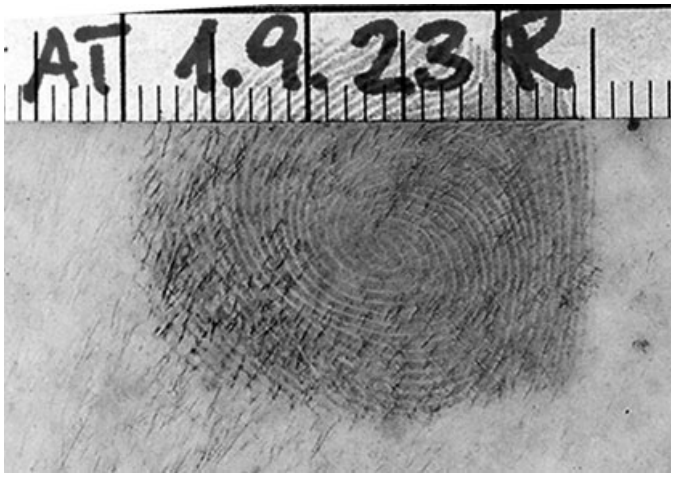

FIG. 2—*Fingerprint on human skin, made visible with black powder.*

TABLE 1—*Fingerprint results on skin.*

	Frequency	Percent
No result	502	50.2
Indication of touch	338	33.8
Elimination	69	6.9
Identification	91	9.1

The results of fingerprint evaluation (on the skin) with regard to different adhesion agents are given in the cross-tabulation (Table 2). In our trials, magnetic powder turned out to be the better adhesion agent. Then, 18.4% of the latents treated with magnetic powder were categorized as "elimination" or "identification" compared to 13.6% of the black fingerprint powder dusted traces. Regarding the lifting materials tested, better results for fingerprints were obtained with Isomark® casting material. Seventy-seven (14.9%) of the Isomark® castings were suitable for "elimination" or "identification," whereas only 44 (10.1%) of the gelatine lifts were. In terms of dactyloscopic analysis, the combination "magnetic powder & Isomark®" yielded the best results ("elimination" + "identification" = 17%). The least promising combination is that involving black fingerprint powder and gelatine foil ("elimination" + "identification" = 8%).

Identifiable prints could be visualized on all body areas tested. It was noted that "bony" areas such as feet, shanks, and forearms yielded better results than more "fleshy" areas such as thighs and upper arms (i.e., foot = 26.9% "elimination" + "identification";

TABLE 2—*Fingerprint results on skin regarding adhesion agents.*

Fingerprint Results on Skin		Adhesion Agents: Black Fingerprint Powder	Adhesion Agents: Magnetic Powder	Total
No result	Number	257	245	502
	% Results on skin	51.2	48.8	100.0
	% Adhesion agent	51.9	48.5	50.2
	% Total number	25.7	24.5	50.2
Indication of touch	Number	171	167	338
	% Results on skin	50.6	49.4	100.0
	% Adhesion agent	34.5	33.1	33.8
	% Total number	17.1	16.7	33.8
Elimination	Number	36	33	69
	% Results on skin	52.2	47.8	100.0
	% Adhesion agent	7.3	6.5	6.9
	% Total number	3.6	3.3	6.9
Identification	Number	31	60	91
	% Results on skin	34.1	65.9	100.0
	% Adhesion agent	6.3	11.9	9.1
	% Total number	3.1	6.0	9.1

TABLE 3—*Overall DNA results.*

	Frequency	Percent
No results (A)	645	64.5
Profile victim (B)	269	26.9
Incomplete mixed trace (C)	66	6.6
Completely interpretable mixed trace (D)	7	0.7
Donor's DNA (E)	13	1.3

upper arm = 4% "elimination" + "identification"). The location had no impact on the DNA results.

DNA-Typing

Considering the DNA results, overall it was possible to extract DNA from one-third of the samples. Twenty samples (2%) were suitable for eliminating or identifying a perpetrator (Table 3).

Regarding the DNA typing, both statistical tests and mean value comparison confirm the findings concerning the relative frequencies in as much as DNA analysis of traces treated with black fingerprint powder (2.2%) yielded better results with both extraction methods than magnetic powder (1.8%). However, the results of magnetic powder and black fingerprint powder converge in the *T*-Test with the extraction method using the NucleoSpin® kit (organic method: mean value black powder 1.63, mean value magnetic powder 1.29; NucleoSpin®: mean value black powder 1.58, mean value magnetic powder 1.38). The DNA typing was successful with 17 of the Isomark® castings in the categories "completely interpretable mixed trace" and "donor's DNA", when compared to three of the gelatine foil traces (Table 4).

To evaluate the results for DNA regarding the combination of the adhesive powder used with the lifting agents, mean value comparison was carried out. It was found that all combinations differed significantly from each other. Here, the best results were obtained by the "black fingerprint powder–Isomark®," combination (4.2%). The "magnetic powder–Isomark®," combination, which ranked best with regard to latent print analysis, was statistically the second best combination in terms of DNA analysis (2.2%).

DNA Results in Relation to Visual Aspects of the Latents

The question was whether or not DNA results depend on the quality of dactyloscopic results. To clarify this, two groups were formed during the statistical evaluation: "latent print not visualized" (category "no result") and "latent visualized" (categories "indication of touch" + "elimination" + "identification").

TABLE 4—*DNA results regarding lifting material.*

DNA Results		Lifting Agent: Isomark®	Lifting Agent: Gelatine Foil	Total
No results	Number	258	387	645
	% Results DNA	40.0	60.0	100.0
	% Lifting agent	48.0	83.8	64.5
	% Total number	25.8	38.7	64.5
Profile victim	Number	221	48	269
	% Results DNA	82.2	17.8	100.0
	% Lifting agent	41.1	10.4	26.9
	% Total number	22.1	4.8	26.9
Incomplete mixed trace	Number	42	24	66
	% Results DNA	63.6	36.4	100.0
	% Lifting agent	7.8	5.2	6.6
	% Total number	4.2	2.4	6.6
Complete interpretable mixed traces	Number	5	2	7
	% Results DNA	71.4	28.6	100.0
	% Lifting agent	0.9	0.4	0.7
	% Total number	0.5	0.2	0.7
Donor's DNA	Number	12	1	13
	% Results DNA	92.3	7.7	100.0
	% Lifting agent	2.2	0.2	1.3
	% Total number	1.2	0.1	1.3

To measure the dependency of the groups in relation to DNA results, Pearson's correlation coefficient was applied. According to this, the hypothesis that a visible fingerprint generates better DNA results can be ruled out. In this project, statistics showed that dactyloscopic (i.e., visual) results were completely independent of DNA results and are therefore irrelevant as indicators. Whether or not the fingerprint/contact can be visualized or not is completely irrelevant for the results of a DNA analysis.

Discussion

Our study was the first empirical research concerning the detection of fingerprints on human skin with common and well-known crime scene examination equipment in Europe. Moreover, this is the first study that evaluated the sequence of fingerprint and DNA recovery on the skin of corpses. The EU-AGIS project has shown that it is possible to visualize a considerable number of latent fingerprints on the skin of corpses, which are potentially useful in eliminating or identifying a possible offender. The project was also successful in demonstrating that it is possible to recover "offender's" DNA from fingerprints placed on the skin of corpses, to remove this from latent lifting agents, and to extract it independently of the adhesion agent used. It is hoped that the results of this project will encourage the use of this procedure in postmortem casework.

The relatively small number of interpretable DNA profiles (2%), which would have identified/eliminated the donor (categories D and E samples), might be a result of a loss of DNA for the following reasons:

- The transfer of cells from the fingertips to the skin of the corpse is dependent on the intensity of the contact process (pressure, period of time) and the individual differences in the skin.
- The donor cells placed on the skin of the corpse were then transferred to gelatine foil or Isomark® casts.
- Cells were transferred yet again to swabs for DNA extraction.
- As described earlier, the DNA extraction method strongly influenced the quality and quantity of isolated DNA and its ability to be typed.

All the earlier points cause a loss of cells or DNA, which can mean that a sample may no longer contain enough DNA for analysis. Hence, further research will be necessary to enhance the DNA results. Particularly, the recovery of the "offender's" cells (directly) from the skin of the victim and the subsequent DNA extraction has to be improved.

It is recommended to use the combination of "magnetic powder–Isomark®." This combination delivered the best fingerprint results and was statistically the second best variation for the DNA analysis. The application of magnetic powder is preferred by the project partners who found the handling more practicable because of less abrasion and less over-powdering. As a rule, during postmortem casework, the complete corpse is tape lifted. Based on the results of the EU-AGIS project and depending on the status of investigations, for example, if there are indications that the body was transported, one should refrain from taping such areas of the body and prioritize the search for fingerprints and/or offender's DNA in these areas. Additionally, it is worth noting that whether the fingerprint/indication of touch can be visualized or not has no bearing whatsoever on the DNA analysis results. For this reason, the powdered areas with no fingerprint result should be treated with DNA recovery methods for later analysis.

Because of the success of the project and the remaining questions raised during the course of the trials, we have applied for EU funding for a follow-up project.

Acknowledgments

We thank our project partners Wolfgang Ostermann, Johann Kaufmann (both Federal Police of Lower Austria, Crime Scene Unit); Rikke Fink, Flemming Rahbek-Fabricius (both Danish National Police, Fingerprint Unit); Jane Stevenson, David Mallett (both LGC Forensics); and John Smith (formerly of LGC Forensics, now University of Westminster). We thank the institutes where the trials have been carried out for their kind co-operation.

References

1. Shin DH, Argue DG. Identification of fingerprints left on human skin. Can Soc Forensic Sci 1976;9:81–4.
2. Agdal N. Fingerprints on a dead body: a new approach. Forensic Sci 1977;9(2):105–7.
3. Dalrymple BE, Duff JM, Menzel ER. Inherent fingerprint luminescence—detection by laser. J Forensic Sci 1977;22:106–15.
4. Mooney DJ. Fingerprints on human skin. Identification News 1977;59:5–8.
5. Adcock JM. The development of latent fingerprints on human skin. J Forensic Sci 1978;22:599–605.
6. Hammer H-J, Linder R. The demonstration of fingerprints on human skin. Forensic Sci Int 1980;16:35–41.
7. Menzel ER. Laser detection of latent fingerprints on skin. J Forensic Sci 1982;27(4):918–22.
8. Haslett M. Fingerprints from skin using Magna Brush technique. Ident News 1986;34(2):7–8.
9. Delmas BJ. Postmortem latent print recovery from skin surfaces. J Forensic Ident 1988;38(2):49–56.
10. Allman DS, Pounds CA. Detection of fingerprints on skin. Forensic Sci Rev 1991;3(2):83–9.
11. Bettencourt DSA. Compilation of techniques for processing deceased human skin for latent prints. J Forensic Ident 1991;41(2):111.
12. Donche A, Hebrard J. Fingerprint detection methods on skin: experimental study on 16 live subjects and 23 cadavers. J Forensic Ident 1994;44 (6):623–7.
13. Sampson WC. Latent fingerprint evidence on human skin, Part 1. J Forensic Ident 1996;46(2):96–100.
14. Wilkinson DA, Watkin JE, Misner AH. A comparison of techniques for the visualization of fingerprints on human skin including the application of iodine and a-naphthoflavone. J Forensic Ident 1996;46(4): 432–47.
15. Wilgus G. Latent print recovery from human skin. J Forensic Ident 2002;52(2):133–5.
16. Sampson WC, Sampson KL. Recovery of latent prints from human skin. J Forensic Ident 2005;55(3):362–85.
17. Trapecar M, Balazic J. Fingerprint recovery from human skin surfaces. Sci Justice 2007;47(3):136–40.
18. Lenertz O, Schönborn S, Bohnert M. Daktyloskopische Spuren auf menschlicher Haut—Ergebnisse einer praxisorientierten Versuchsreihe. Arch Kriminol 2002;210:129–36.
19. Färber D, Schönborn S. Sichtbarmachung daktyloskopischer und DNA-Spuren auf menschlicher Haut. Polizei Heute 2004;2:42–3.

Additional information and reprint requests:
Michael Bohnert, M.D.
University Hospital Freiburg
Institute of Forensic Medicine
Albertstr. 9
Freiburg 79104
Germany
E-mail: michaelbohnert@mac.com

JOURNAL OF FORENSIC SCIENCES

J Forensic Sci, November 2010, Vol. 55, No. 6
doi: 10.1111/j.1556-4029.2010.01484.x
Available online at: onlinelibrary.wiley.com

PAPER

CRIMINALISTICS

R. Maggie Connatser,[1] Ph.D.; Sharka M. Prokes,[2] Ph.D.; Orest J. Glembocki,[3] Ph.D.; Rebecca L. Schuler,[3] B.S.; Charles W. Gardner,[3] Ph.D.; Samuel A. Lewis, Sr.,[1] M.S.; and Linda A. Lewis,[1] Ph.D.

Toward Surface-Enhanced Raman Imaging of Latent Fingerprints*

ABSTRACT: Exposure to light or heat, or simply a dearth of fingerprint material, renders some latent fingerprints undetectable using conventional methods. We begin to address such elusive fingerprints using detection targeting photo- and thermally stable fingerprint constituents: surface-enhanced Raman spectroscopy (SERS). SERS can give descriptive vibrational spectra of amino acids, among other robust fingerprint constituents, and good sensitivity can be attained by improving metal-dielectric nanoparticle substrates. With SERS chemical imaging, vibrational bands' intensities recreate a visual of fingerprint topography. The impact of nanoparticle synthesis route, dispersal methodology–deposition solvent, and laser wavelength are discussed, as are data from enhanced vibrational spectra of fingerprint components. SERS and Raman chemical images of fingerprints and realistic contaminants are shown. To our knowledge, this represents the first SERS imaging of fingerprints. In conclusion, this work progresses toward the ultimate goal of vibrationally detecting latent prints that would otherwise remain undetected using traditional development methods.

KEYWORDS: forensic science, latent fingerprints, fingerprint degradation, surface enhanced Raman spectroscopy, enhancement factor, dispersible Raman substrates, dielectric core–metal shell nanowires, macro-Raman chemical imaging

Latent eccrine fingerprints deposited on many surfaces may sometimes go undetected once prints age over a few hours, especially when exposed to sunlight. The ability to develop latent fingerprints is often influenced by many factors including print-type (clean/eccrine through oily/sebaceous), humidity, light, surface matrix, etc. (1). Recent findings on the fundamental chemistry of superglue fuming, a prominent method for developing prints on nonporous surfaces, revealed methods capable of enhancing the ability to develop latent fingerprints that would otherwise go undetected (2). This enhancement, which involves fuming with acetic acid vapors prior to superglue fuming, was not highly effective on fingerprints exposed to high energy (UV/blue light) radiation from sun or fluorescent lighting, especially on surfaces containing iron (III) because of the catalyzed photodegradation of a lactate anion, which is the major cyanoacrylate polymerization initiator (3). In addition, the enhancement method is not easily amenable to field applications. Thus, a real need exists to detect latent fingerprints on all surfaces regardless of the print type or environmental exposure factors. This work on latent print detection will lead to a better understanding of fingerprint degradation chemistry. It will also facilitate a new, complementary method for Raman-based latent print visualization by utilizing the surface enhancement phenomenon to achieve sensitive chemical imaging-based latent print detection for field applications. To accomplish this goal, the project was divided into two phases. The objective of the first part, described herein, was to study the fingerprint chemistry and decomposition with respect to Raman detection and enhancement methods with an aim to eventually validate the concept of a transportable macro-Raman system. The second part, fully fieldable imaging of prints, relies on the development of a dispersible surface-enhanced Raman spectroscopy (SERS) reagent system of intense inherent sensitivity currently being researched in our laboratories. The current time to image a single print is 30 sec based on the narrow vibrational band at 1129 cm^{-1} and 10–30 min to create a full spectral profile of the print. In our SERS substrate development, this procedure is common practice to fully characterize the substrate's performance and look for any potential contaminants. In the field/forensic laboratory setting, this long acquisition time would only be done if unknowns were suspected and the practitioner desired vibrational information to use in an attempt to identify non-fingerprint materials.

Raman spectroscopy is executed when the inelastically scattered photons from a molecule are collected and their energy differences translated into a wavenumber spectrum indicative of the vibrating bonds within the molecule (4). Surface enhancement results when an analyte molecule's proximity with a metal surface allows the amplification of two electromagnetic fields: the one impinging on the molecule and the one scattered by the molecule (5). Additionally chemical enhancement may be achieved between analyte and metal through the quenching of fluorescence, a significant source of nondescript background in Raman (6). However, chemical interactions are also detrimental in some cases because of the repulsion between molecule and metal surface and steric obstruction of the metal surface by nonanalyte ambient molecules.

[1]Oak Ridge National Laboratory, 1 Bethel Valley Road, Bldg. 4500N, Room F56, MS 6120, Oak Ridge, TN 37831.
[2]Naval Research Laboratory, 4555 Overlook Avenue SW, Bldg. 208, Code 6876, Washington, DC 20375-0001.
[3]ChemImage Corporation, 7301 Penn Avenue, Pittsburgh, PA 15208.
*Presented in part at the International Association for Identification Annual Conference, August 17–22, 2008, in Louisville, KY.

Received 25 May 2009; and in revised form 10 Aug. 2009; accepted 11 Sep. 2009.

The role of Raman spectroscopy as a forensic tool has already been well established in terms of drug identification, document and currency verification, and, most prominently, art and archeology verification and dating (7–11). SERS of amino acids has found broad application in the study of protein folding investigations and simply in detecting certain proteins in an aqueous environment (12). Urea and lactic acid separately have also been evaluated using Raman as specific markers of physiologic imbalance in diabetes and muscle conditions, respectively (13,14). Raman detection was even pioneered in fingerprint and contaminant detection on a spot detection basis in 2004 (15). Despite these prior uses of Raman spectroscopy for nonimaging fingerprint forensics and the Raman detection of prominent components of eccrine prints in biomedicine, no confluence of these streams of research has yet occurred to produce Raman chemical imaging detection of latent fingerprints. In the research described herein, preliminary groundwork toward developing a technique aimed at using surface-enhanced Raman imaging of latent fingerprints is presented.

The science of retrieving latent fingerprints or their images has been well established and continues to improve as new technologies arise in the fundamental fields of science, such as physics, chemistry, and biology. The last two decades have seen the forensic field begin to reap more direct and immediate benefits from advances in fundamental biochemical and analytical chemical research. A few examples of these new technologies include advanced fluorescent tagging, DNA mapping and matching, and the use of data mining techniques in combination with extensive fingerprint databases to electronically catalog latent prints and comparatively identify them (16–18). Vibrational spectroscopic analysis of fingerprints can benefit the forensic community by offering a means of identification and isolation of a latent print from its background that does not rely solely on physical means of development (i.e., one lacking descriptive chemical information). The narrow vibrational bandwidths of analyte molecules allows discernment of, for instance, a vibrational band of urea from a closely related vibrational band of the amide bonds in the wooden surface on which the print is deposited. Using chemical signatures to discern on-ridge from off-ridge would allow imaging of prints irrespective of chemical pretreatment with fuming or dyes. Using the weak but perceptible Raman signature of amino acids and urea would ameliorate the need for oils within the print to preserve moisture and protect the lactate ion, a component proven in our earlier work to act as the main initiator in the polymerization of cyanoacrylate vapors (2,3). Optical vibrational spectroscopic has previously been reported utilizing Fourier transform infrared (FTIR) spectroscopy to image latent prints on highly reflective surfaces and on tapes/gels using an attenuated total reflectance cell (19). Reconstructed images comprise an intensity map of one or more regions of vibrational spectrum indicative of a fingerprint. However, the FTIR-based spectral interrogation described does not utilize portable instrumentation, and IR in general suffers from water signal background to a greater extent than Raman. The work presented also conveys results on the technological background of SERS chemical imaging. SERS is evaluated for creating a chemical image of latent prints by following a characteristic spectral signal from print components. Raman imaging data, illustrating the ability to co-identify contaminants within a print, i.e., drugs of abuse or explosive residue, is also presented.

Materials and Methods

Artificial Fingerprint Solution

In order to perform multiple sequential analyses on eccrine fingerprint material with the possibility of increasing concentrations of the components, an artificial fingerprint solution was identified and is discussed at length elsewhere (20). Briefly, the process included a compilation and evaluation of literature recipes to yield an optimized single complete surrogate eccrine recipe. A reference was found that identified and quantified (in μmoles/print) the individual amino acids and urea found in a thumbprint deposited on a glass surface (21). The Geigy Scientific Tables were consulted for the nonamino acid composition of eccrine secretions, reported in mg/L (22). Calculations were performed to correlate the amount of urea and total amount of all amino acids found in one print, as reported by Hamilton, with the overall concentrations of those substances found in eccrine sweat, as reported in the Geigy Scientific (21,22). According to the urea data, one print consisted of 23.92 μL of sweat; based on the amino acid data, one print contained 31.89 μL of sweat. The average of these values, 27.91 μL of sweat per print, was employed for all conversion calculations used to create a "recipe" for an artificial eccrine-fingerprint solution currently in press in a forthcoming Journal of Forensic Sciences article detailing fingerprint component degradation studies (20).

Instrumentation and Chemicals

Several Raman instruments were used during the course of this developmental work. For initial surveys of SERS activity of individual fingerprint components with silver and gold nanocomposite substrates, a JYHoriba LabRam was used with a thermoelectrically cooled CCD detector, notch filter for rejection of Rayleigh scatter and laser line, and a 632.8-nm helium–neon laser. Laser power at sample is 8.9 mW, and sample acquisitions were all set to 1 sec, unless otherwise noted. For experiments with gold nanocomposite substrates, a Dilor Raman spectrometer was used that employed a triple monochromator wavelength selection with laser line rejection and a liquid nitrogen cooled CCD camera. Both of these instruments use versions of LabSpec software (JYHoriba, Inc., Edison, NJ). Raman images were collected by co-authors R. Schuler and C. Gardner at ChemImage Corporation's Pittsburgh, PA, location on a FALCON® Microscope Raman and Fluorescence Imaging System while an ORNL prototype imager was being constructed. The FALCON® system utilizes a liquid crystal tunable filter (LCTF) for collected scattered wavelength selection. These systems also have a thermoelectrically cooled CCD. Raman chemical images are created by such a system as follows: the impinging laser light is expanded to 20 mm diameter, light is collected over a narrow wavelength range defined by the LCTF, and an image at essentially a single wavelength of Raman scattered light is created and stored. The LCTF then tunes to another wavelength and the process is repeated, stacking "single" Raman wavenumber images on top of each other until a hyperspectral cube is created. In this cube, the *X* and *Y* axes define an intensity map of the sample's Raman scatter signal at a particular wavenumber electromagnetic region. The *Z* direction illustrates the Raman spectrum from single spots once the cube is constructed via LCTF tuning across whatever wavenumber regions are defined by experimental parameters. The difference in this type of imaging as contrasted with conventional Raman rastering or mapping is the speed with which the image can be collected in a situation where the target analyte is known, and therefore a predetermined spectral region can be targeted by the LCTF. Conventional rastering or mapping creates a Raman image by collecting an entire Raman spectrum at each of many spots across the sample, after which the intensity map is reconstructed by following defined wavenumber regions from within the *X–Y* grid of whole spectra. This approach is more suitable for gaining descriptive information from maps of unknown

substances as it is more time consuming than large field of view imaging using known wavenumber regions of interest for analytes, in our case fingerprint materials. For SERS response screening, 1 mM solutions of the fingerprint components were prepared individually in 18 MΩ deionized water from a Millipore Elix® system (Millipore, Inc., Billerica, MA). All chemicals were procured from Sigma–Aldrich (St. Louis, MO) and used as received.

SERS Reagents and Nanoparticle Dispersal

Several incarnations of surface-enhanced Raman substrates were employed, falling into three categories. (i) Advanced, nondispersible substrates were used for proof-of-principle demonstrates supporting SERS chemical imaging of fingerprint material deposited directly onto the substrate. (ii) Conventionally prepared silver colloidal solutions were utilized for solution screening of eccrine fingerprint component chemicals at concentrations of 10^{-3} M and diluted to 10^{-4} M when combined with colloid. Conventional colloids were also heavily used in early dispersal studies and solvent exchange tests. (iii) Finally, four types of advanced solution-based substrates were tested, of which only silver-coated gallium oxide nanowires yielded as sensitive or more sensitive SERS responses when compared with conventional colloid. Nanocomposites of silver metal vapor deposited onto the elastomer polydimethylsiloxane used in the initial proof of concept experiments were previously characterized by Sepaniak et al. (23–26). The bulk Sylgard polymer was mixed in a 10:1 ratio with curing agent, degassed under vacuum, poured onto a $1'' \times 3''$ microscope slide, and cured at 70°C for 1 h. The slide was then inverted in a physical vapor deposition unit, and silver metal was deposited in a sublimed plume from a resistively heated tungsten boat at a pressure of 2×10^{-6} Torr. This substrate, although beneficial in its solid phase extraction and slow silver oxidation characteristics, is nondispersible and therefore not amenable to field use. Conventional silver colloidal solutions were used for screening the individual components of eccrine prints. These spherical particles were reduced with trisodium citrate or with sodium borohydride using silver nitrate as a feedstock with stirring at temperatures of 90°C and in an ice bath, respectively. Further details of these preparations have been exhausted in the literature (27–29). Preparation of geometrically shaped silver nanoparticles for SERS enhancement included rods, cubes, triangular nanoprisms, and silver-coated dielectric core nanowires may also be found in the literature (30–33). Only the nanowires possessing a dielectric core produced results equal or superior to the conventional colloid; thus, the material preparation is included herein. Dielectric core–metal shell nanowires were prepared at the Naval Research Laboratory via thermal vapor liquid solid deposition of Ga_2O_3 onto gold catalyst spots in a tube furnace (33). Silver was vacuum sputtered onto the nanowires at a nominal thickness of 6 nm. A full description and analysis of the nanowires' preparation and fundamental properties is available in Reference (33). Scanning electron micrographs of the triangular nanoprisms demonstrating their prohibitively dilute solutions were collected at the ORNL High Temperature Materials Laboratory on a HF3300 TEM/STEM operated at 300 kV. The SEM of dielectric core–metal shell nanowires was collected by Sharka Prokes at the Naval Research Laboratory.

Dispersal solvent and method were important parameters to SERS reagent development. Two factors govern solvent selection: volatility and interaction with the metal nanoparticles. All solvents were HPLC grade and used as is from the manufacturer, Fisher Scientific. Dispersal of nanoparticle solutions must be a nearly dry spray from an instrument that is field portable. The dispersed nanoparticle solvent must meet two requirements: (i) high volatility to mitigate pooling which can compromise SERS enhancement due to the overaggregation of metal nanoparticles. If extensive enough, pooling can also lead to wash-off or blurring of the latent print ridges; and (ii) low Raman activity to promote negligible spectral background. As for the dispersal instruments, the earliest trials utilized citrate or borohydride reduced conventional colloid, nanocubes, and triangular nanoprisms in aqueous matrices dispersed through a CETAC® high-performance nebulizer (CETAC Technologies, Inc., Omaha, NE). Next, a commercial grade airbrush by Pasqual® (Paasche, Inc., Chicago, IL) was employed. Finally, a commercially available aerosol propellant (Preval®, CA Acquisition, LLC, Coal City, IL) which can be made to interface with a refillable glass reagent bottle was utilized with nonaqueous dispersal solvents to form the current iteration of a field-ready implement for deploying SERS enhancing reagent onto surfaces containing latent fingerprint material. Representations of the three dispersal instruments are shown in Fig. 1. The high performance, expensive, and time-intensive CETAC® nebulizer required compressed gas as a propellant. This system can disperse a wide range of solvents, with a water load up to 100%. The higher throughput airbrush required DC power, but did not require feed gas. This system can disperse SERS substrate solutions containing up to a 40% water load without over-wetting the target. The cheapest delivery system required the most volatile dispersal solvents for SERS dispersal, such as ethyl acetate, with low concentrations of acetone or ethanol and only traces of water to prevent over-wetting.

Results and Discussion

Surface-enhanced Raman shows promise for chemical imaging of latent prints (either eccrine or sebaceous in nature), as well as print contaminants. The data represented in Figs. 2 and 3 illustrate how Raman chemical imaging, using the hydrocarbon band from skin oils at 2900 cm^{-1}, can be used to create a detailed picture of a fingerprint and possible contaminants therein. Although the SERS chemical image collected in Fig. 2 was of a fingerprint placed onto an elastomer-metal nanocomposite SERS substrate, a print

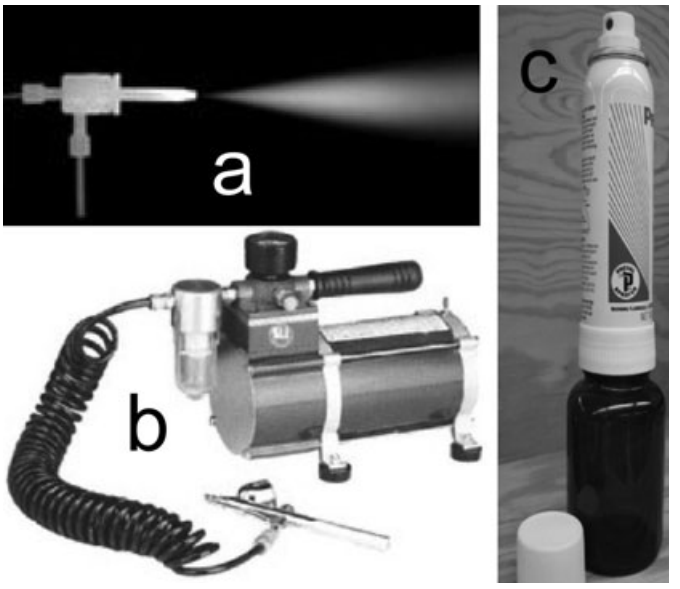

FIG. 1—*SERS substrate dispersal tools. (a) CETAC high performance nebulizer is expensive, time intensive, requires compressed gases. (b) Increased throughput airbrush requires DC power but no feed gas. (c) Cheapest, most portable sprayer system requires use of most volatile dispersal solvents.*

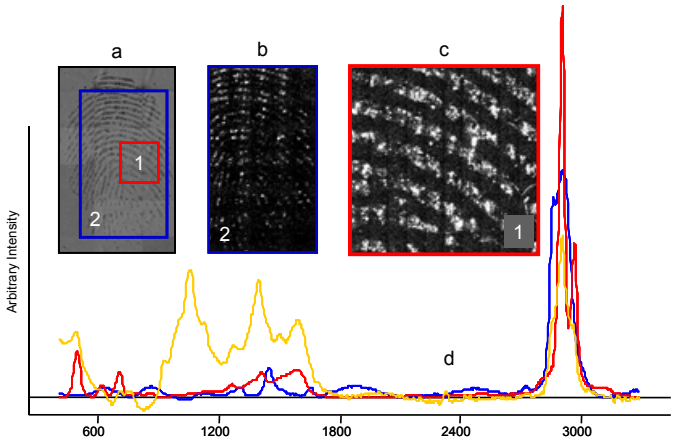

FIG. 2—*SERS chemical images of a sebaceous print deposited onto silver-elastomer substrate. (a) 1.25× magnified brightfield camera image of the fingerprint, showing regions 1 and 2 from which other panels were extracted spectrally based on vibrational band at 2900 cm^{-1}. (b) 5× magnified Raman chemical image of area shown in rectangle 2 of panel (a). (c) 20× magnified SERS chemical image of regions 1 shown in panel (b). (d) shows Raman signals from fingerprint oil (gray trace), SERS substrate background (middle trace, broad hump centered at 1600 cm^{-1}), and the difference between the two (lowest trace, sharp band at 1600 cm^{-1}).*

collection geometry unusable for latent prints, the chemical image created serves as a formidable proof that sufficiently sensitive dispersible SERS substrates could facilitate print imaging on remote evidentiary surfaces. Figure 3 is a conventional Raman image of fingerprint oils and added pharmaceutical dust (acetaminophen) deposited directly onto a completely clean, highly reflective surface to demonstrate the capability of vibrational spectroscopy for discerning latent prints from informative contaminant spectra. The phenomenon of surface-enhancing Raman scatter is necessary to increase the scattering efficiency of fingerprint components to the point that scatter can be detected from light or partial prints, heat or photodegraded prints, as well as from nonideal remote surfaces or dielectric environments. Enhancement is achieved by introducing analyte into close proximity with a roughened metal surface or clusters of noble metal nanoparticles. Interaction with impinging laser light initiates a coherent oscillation parallel to the surface in the valence electrons of the metal. These plasmon bands enhance both the electromagnetic fields impinging on and scattered by the analyte molecules (34). Chemical effects, such as electrostatic, steric, or even covalent bonding can alternately improve the enhancement via charge transfer fluorescence quenching. By the same token, the enhancement factor can be compromised by the chemical effect when analyte molecules are effectively excluded from electromagnetically favorable loci among the nanoparticles or nano-roughness of a metal surface. This chemical inhibition of SERS enhancement makes selection of a dispersal solvent critical. It was found that a regime to remove SERS active nanoparticles from their native aqueous solution and into a more volatile solvent via incremental increases in solvent polarity alleviated spectral background because of residual reductant and facilitated better dispersal characteristics. Solvent exchange steps included centrifugation to gravitationally concentrate the particles into a small volume of their original water-based synthesis solution. This step was followed by sonication to achieve mixing into clean, deionized water free of reductant residuals. This water rinse was repeated, and after removing the second rinse, ethanol was introduced as the sonication solvent. The particles were then centrifuged for removal from the ethanol and introduced into ethyl acetate, which served as the final dispersal solvent. The resulting solution was approximately 25% ethanol and 75% ethyl acetate with traces of water. This solution dissipated the nanoparticles onto test surfaces without pooling while maintaining ample wetness to prevent the dangers of aerosolized metal nanoparticles.

SERS uses a myriad of different metal-dielectric combination substrates, including nanocomposites of polymer and metal, solution-prepared metal colloids of varied geometries, and sol–gel materials in fluid clusters or adsorbed on flat surfaces. Figure 4 illustrates several points relevant to discussion. First, the magnitude of conventional Raman signal for neat fingerprint components is easily matched by using surface-enhanced Raman for solutions of components orders of magnitude lower in concentration (10^{-5} M with silver-elastomer nanocomposite and 10^{-4} M with colloid). The highlighted vibrational regions indicate how, despite different vibrational broadening effects because of substrate adsorption and analyte molecule orientation, common vibrational signatures can be followed from Raman to different surface enhancing substrates. For the practical purpose of imaging latent fingerprints, the employment of dispersible Raman enhancing metal nanoparticle systems is required.

Micrographs of the dispersible SERS substrates studied for latent print analysis are shown in Fig. 5 and were collected with scanning or tunneling electron microscopes. Microscopy has the great benefit of revealing morphology of SERS substrates after they have been dispersed, crucial information to a technique that relies on particle spacing for efficacy. Even a cursory evaluation of the contrast between Fig. 5*b* with Fig. 5*a* and the inset SEM in Fig. 5*c* reveals one cause for lack of sensitivity of the dispersed advanced materials: spacing. Even long periods of dispersal (30 min to cover a square inch) of triangular nanoprisms do not yield the dense cross-covered nanoparticle layer necessary to yield sensitive, uniform image-creating enhancements. The advantages in increased Raman enhancement purported for the geometrical nanoparticles in their respective synthetic reports relative to the conventional spherical colloid were not realized in our studies. The nanowires did, however, demonstrate a potentially higher response factor despite being too diffuse to facilitate collection of a complete fingerprint image. We speculate that the loss of Raman signal enhancement factor relative to original investigators' reports of sensitivity is because of the process of dispersal itself. For SERS reagents usually tested in solution or tethered to a surface in a self-assembled monolayer, the process of dispersal would render individual nanoparticles too far from each other for enhancement or in an unfavorable dielectric environment such as a solvent cage. This comparison of dispersible SERS substrates shows conventional silver colloid deposited onto glass using a droplet nebulizer, Fig. 5*a*, and gallium oxide nanowires coated with silver and dropped onto a surface, Fig. 5*c*, as giving greater coverage than the advanced substrate in Fig. 5*b*, solution-prepared nanotriangular prisms, also dried from a droplet. The inset shows coverage within aggregates on the nanoscale superior to Fig. 5*b* and equal to Fig. 5*a*, but micro- and milliscale coverage is still insufficient for imaging complete or even partial latent prints. Figure 6*a* shows the single spectrum for eccrine print material at real concentrations deposited on smooth glass with conventional spherical colloid as the SERS reagent. The majority of the bands present are because of the ubiquitous Raman background from the citrate reduction of the colloid. Also shown in Fig. 6*a* is the result that, despite being unable to image, we have achieved the collection of a SERS spectrum from an aggregate of nanowires on a porous galvanized metal pipe that was previously coated with 5× concentrated eccrine fingerprint solution. Such an aggregate is shown in the 80× magnified microscope picture in Fig. 5*c*, along with an SEM of an aggregate of nanowires and a

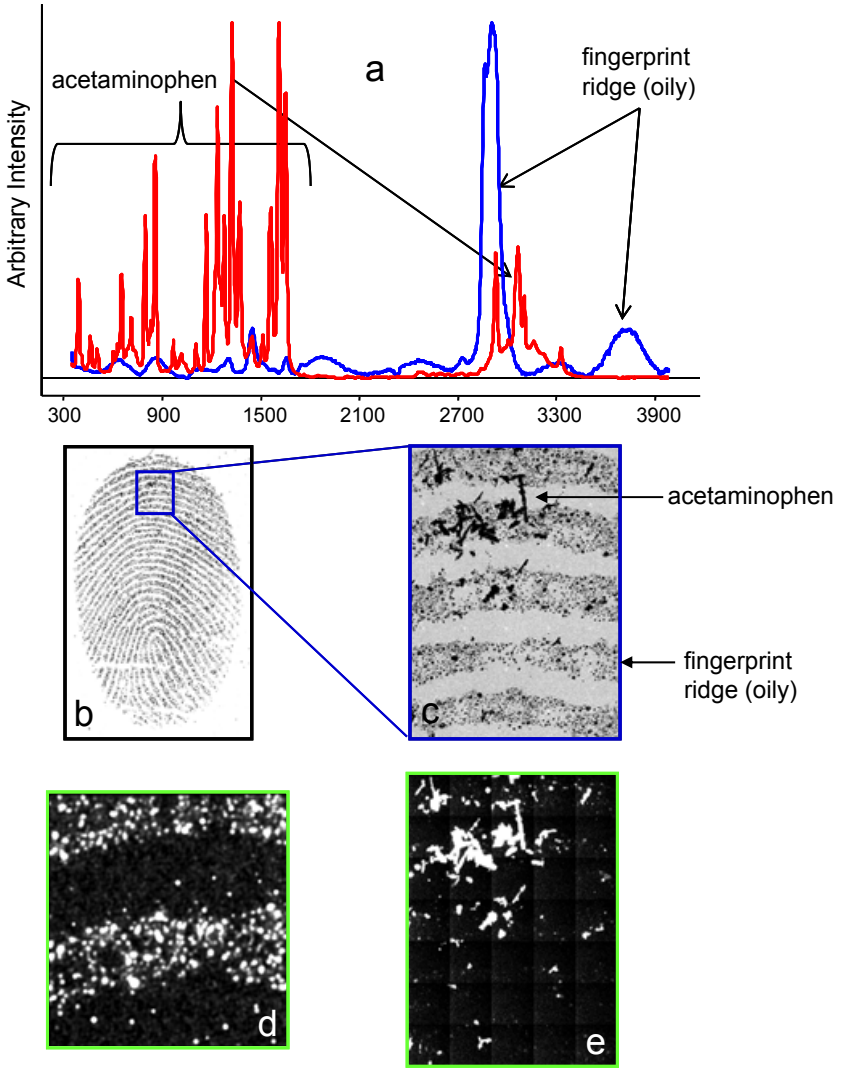

FIG. 3—*Raman chemical imaging of a sebaceous fingerprint doped with acetaminophen and placed on a clean, highly reflective slide. (a) Overlaid Raman spectra of fingerprint oil and acetaminophen to represent potential drug-related latent print contaminants. (b) 1.25× magnification of brightfield image of print/drug. (c) 5× magnification of zoom camera brightfield image of region of print/drug. (d) 20× magnification Raman chemical image montage of fingerprint ridges, 2900 cm^{-1} image extract. (e) 5× magnification of Raman chemical image of acetaminophen on fingerprint, 2940 cm^{-1} image extract.*

schematic depicting nanowire make-up. The absolute magnitudes of signal intensity cannot be compared between the spectra from conventional colloid (Fig. 6*a*) and a nanowire aggregate (Fig. 6*b*), because of the collection at different impinging wavelengths (633 nm for Fig. 6*a*, 532 nm for Fig. 6*b*) on different instruments. Nonetheless, the response from the artificial solutions indicates promise in the optimization of the nanowires for higher surface coverage and extension of the nanowires' improved signal to noise in the detection of real prints. Currently, however, the conventional spherical colloid works best for our purposes because it can be prepared and sprayed in much higher particle densities for better surface coverage with similar enhancements.

SERS screening was conducted on eccrine fingerprint components in an effort to assess these individual compounds for their contribution to the total vibrational scatter signals from the prints. Two separate facts led to this choice of eccrine screening. First, the absence of oils to retain moisture and slow photodegradation of the lactate anion results in eccrine prints being the most difficult to retrieve. Second, because SERS is used in protein analysis to detect amino acids, we hypothesized that this technique could also be used to detect amino acids and other eccrine print components. This focus on clean (i.e., not oily), pure eccrine prints is not so much a requirement of this niche technique, it is a demonstration that during development researchers are targeting the more difficult of the two types of prints for detection. In fact, some of the most common contaminants (blood, drugs, and explosives) are actually easier to detect than the eccrine fingerprint constituents themselves. Several of the initial test solutions, all at 1×10^{-4} M concentration in deionized water, yielded some vibrational bands when assayed on silver as well as gold nanocomposite. Table 1 enumerates all the vibrational bands and likely structural assignments detected for individual components of fingerprints in water (35). Bands in italics were detectable above the level of noise only with silver substrates, even when the wavelength of the Raman initiating laser was chosen to better align with gold substrates at 785 nm. However, none of the print components yielded spectra from gold substrates that even approached the response of the components on silver. Although using the SERS signature of aggregate surface amino acid moieties is well established in the literature for discerning protein conformational changes, amino acids tend to give weak to modest SERS response when deposited onto a surface in high micromolar

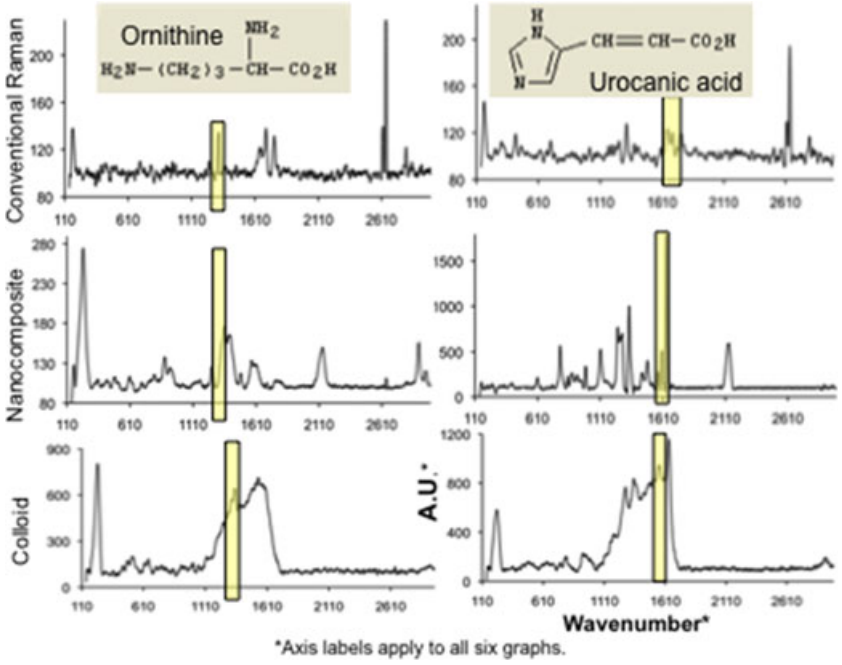

FIG. 4—*Activity for fingerprint components using conventional Raman, silver-elastomer nanocomposite and silver colloid substrates. Sample concentrations were neat, 1×10^{-5}M, and 1×10^{-4}M, respectively. Vibrational bands highlighted by box are distinctive to each analyte across substrate types.*

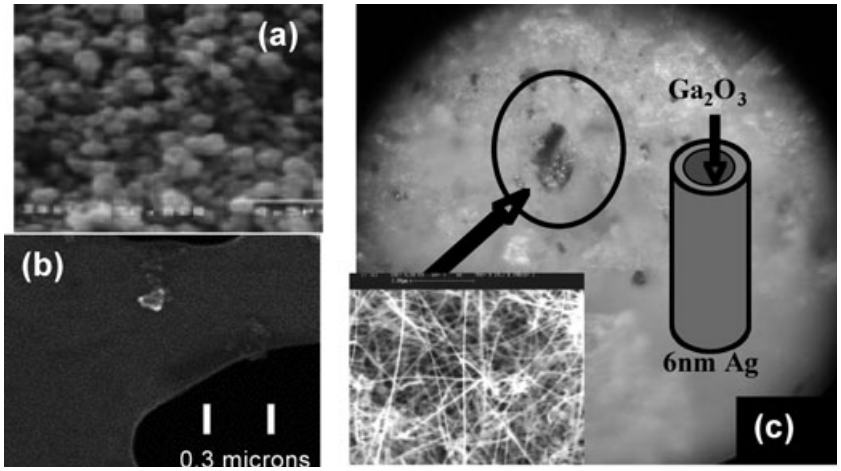

FIG. 5—*Comparison of dispersible SERS substrates. (a) Conventional silver colloid deposited onto glass using a droplet nebulizer. (b) Advanced substrate, solution-prepared nanotriangular prisms, dried from a droplet onto SEM mesh. (c) Gallium oxide nanowires coated with silver and dropped onto PVC that was previously coated with 5× concentrated eccrine fingerprint solution. Inset shows coverage within aggregates on the nanoscale superior to (b) and equal to (a), but micro- and milliscale coverage is still insufficient for imaging latent prints.*

total amino acid concentrations as in latent fingerprints. None of the print components yielded spectra from gold substrates, at either wavelength, that approached the response obtained when employing silver. These results indicate that, with sufficient coverage by high Raman enhancement factor nanoparticles dispersed without chemical inhibition onto surfaces with latent prints, SERS chemical imaging should be possible.

The relatively nontoxic nature of metal colloids in their SERS format and the portability of Raman spectrometers and imaging units all point toward high feasibility of a fully fieldable method. Hence, an investigation was initiated into the application of SERS imaging to detecting difficult prints, even on porous surfaces because of the depth of focus and other physical microproperties including wettability, hydrophobicity, and curvature. The experiments in this paper proved the concept of SERS fingerprint imaging (Figs. 2 and 3) and laid the groundwork (Figs. 4, 5, 6; Table 1) for an emerging technology with the *potential* capacity to discern otherwise irretrievable prints and many classes of information-rich print contaminants, such as drugs or explosives, all based on their inherent chemical vibrational signal and the intense possibility of enhanced Raman scatter (1×10^7 increases in Raman signals for surface enhancement have been shown by multiple groups) (6). This potential must be tested against traditional methods as improved SERS substrates are developed. On the heat and light exposed, porous, and overall low total material content prints we have been targeting, we do not observe the darkened print image optically resulting from Physical Developer solutions from the fingerprint treated with SERS enhancement reagent, even when

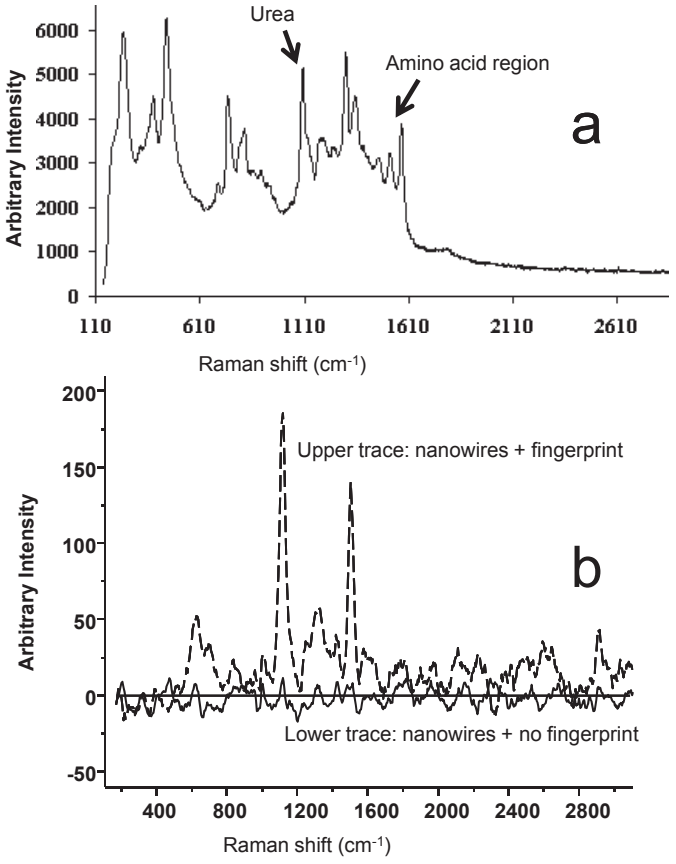

FIG. 6—*Comparison of simple colloid and advanced SERS nanoparticles. (a) Spectrum from eccrine print material detected at realistic concentration with conventional silver colloid.*
**Note that a significant background is present from the silver reducing citrate solution. (b) Spectrum of 5× concentrated eccrine material on porous steel with nanowires from NRL.*
**Note much lower background and less overall signal.*

examined under a reflected ultraviolet imaging system. The applicability of SERS imaging for widespread fingerprint detection relies on dispersed SERS reagents offering 1×10^7 scatter signals quoted in the academic SERS literature for nondispersed reagents. Finally, Fig. 6 also helps illustrate the feasibility of this technique, as it shows a surface-enhanced Raman response of 5× concentrated eccrine fingerprint material that has been deposited on polyvinyl chloride tubing filled with a low explosive and subsequently ignited. The fingerprint solution and SERS reagent nanowires were deposited, dried, and the scattering measured after the model miniature ignition event. The response shown demonstrates that bands representative of such relevant background interferents as explosives are discernible from fingerprint spectral responses. Evidentiary information beyond collection of the latent fingerprint image could be gleaned from the careful characterization of these interferent spectra, as well as spectra from other potential fingerprint contaminants such as drugs of abuse, bioterror agents or residues, or high explosives. The practicality and reliability of a dual-duty application of SERS imaging for fingerprints and their contaminants is being explored further as our group continues to develop the SERS macro-Raman imaging technique. The success of SERS chemical imaging of latent fingerprints relies heavily upon the creation of a high enhancement factor SERS metal nanoparticle substrate that retains its field-amplifying characteristics upon dispersal. The synthesis and testing of just such an improved SERS reagent will be founded upon the preliminary studies related here, and this is the current occupation of our research efforts. Once more adequate SERS reagent sensitivity is achieved, comparison studies to gauge this new niche technique's overall utility versus established methods will be executed and reported.

Conclusion

This work fills an important niche for chemically imaging clean, aged or new, latent fingerprints, especially on difficult surfaces or exposed to conditions that would render a latent print undetectable

TABLE 1—*Results of surface-enhanced Raman spectroscopy (SERS) screening of individual fingerprint components at 0.1 mM in water using silver and gold nanocomposite substrates and 633 nm or 785 nm wavelength illumination lasers, respectively. Results in italics were only attainable using silver with a 633-nm laser.*

Fingerprint Component	SERS Vibrational Bands (cm^{-1})	Likely Structural Assignment
Leucine	451–678, *~1450*	Amine
Glucose	1223–1416, 1472–1667, 2078–2142	Carbonyl
Glutamic acid	1577–1612	Carboxylic acid, amine
Histidine	550, 1481–1542, 1577–1612	Amine, amide, carboxylic acid
Threonine	450–720	Amine
Ornithine	1407–1469, 1504–1551	Carbonyl
Urocanic acid	~1250, 1308–1374, 1608–1673	Carboxylic acid, amine, vinyl
Creatinine	550, 1229–1632	Amine
Tyrosine	*875,* 1445–1598	*Benzene ring stretching,* Amine
Uric acid	1427–1664	Carboxylic acid, amine
Urea	451–769, 1100	Carboxylic acid, amine (double)
Propionic acid	800, 2275	Hydrocarbon, carboxylic acid
Isovaleric acid	1100	Hydrocarbon, carboxylic acid
n-Hexanoic acid	800, 900, 1200, 1375, 1625	Hydrocarbon, carboxylic acid
Isobutyric acid	800, *1100*	Hydrocarbon, carboxylic acid
Acetic acid	800, *1100*	Hydrocarbon, carboxylic acid
n-Butyric acid	800, *1100*	Hydrocarbon, carboxylic acid
Aspartic acid	*~1475–1580*	*Carboxylic acid*
Serine	*550*	*Amine*
Pyruvic acid	*~1475–1580*	*Carboxylic acid*
Lactic acid	*~1475–1580*	*Carboxylic acid*
Isoleucine	*451–575, 1450*	*Amine*
Glycine	*1670*	*Amide*

using traditional print development techniques. In order to continue progress on this effort beyond the proof-of-concept and process development steps reported herein, our on-going work targets the macro-Raman instrument design, testing, and especially further SERS reagent optimization for latent-print detection applications. A distinction of surface-enhanced Raman imaging relative to FTIR imaging reports and other, more conventional methods of print visualization is that the amino acids in eccrine fingerprints can be targeted, instead of relying on the response or reactivity of oils' common hydrocarbon signal being used to create the image. The differences between FTIR and SERS imaging emerge in an examination of the background and reflectivity requirements of infrared imaging. Although the Fourier transform math can alleviate much of the background created by moisture in the vibrational absorbance spectrum, some sensitivity is lost in the averaging. What's more, the most compelling fingerprint images have been collected from highly reflective surfaces such as aluminum cans and surfaces that do not create a broad IR background including some polymers. Our technique seeks to address porous or granular surfaces, especially those marred during thermal events. The narrow Raman bands allow slightly more straightforward spectral identification and subtraction of polymer background bands without loss of analyte information. Finally, the surface enhancement phenomenon does not benefit IR absorption, so the only mechanism of increasing optical signal collected is longer image acquisition times, more powerful lamps, or IR tagging of fingerprint constituents. Future work will specifically improve the degree of Raman enhancement for urea and amino acids. Thereby, the ridge/furrow contrast, fingerprint chemical content, and ridge detail may be improved for an increase in sensitivity of the SERS chemical imaging technique.

Acknowledgments

We gratefully acknowledge microscopy support by Jane Y. Howe at the High Temperature Materials Laboratory at Oak Ridge National Lab.

Supported by grants from the National Institute of Justice, the Office of Naval Research, and the Technical Support Working Group.

References

1. Lee HC, Gaensslen RE. Methods of latent fingerprint development. In: Lee HC, Gaensslen RE, editors. Advances in fingerprint technology, 2nd edn. Boca Raton, FL: CRC Press, 2001;105–75.
2. Lewis LA, Smithwick RW, DeVault GL, Bolinger B, Lewis SA. Processes involved in the development of latent fingerprints using the cyanoacrylate fuming method. J Forensic Sci 2001;46(2):241–6.
3. Wargacki SP, Lewis LA, Dadmun MD. Understanding the chemistry of the development of latent fingerprints by superglue fuming. J Forensic Sci 2007;52(5):1057–62.
4. Colthup NB, Daly LH, Wiberly SE. Introduction to infrared and Raman spectroscopy. New York, NY: Academic Press, 1975.
5. Andersen PC, Rowlen KL. Brilliant optical properties of nanometric noble metal spheres, rods, and aperture arrays. Appl Spectrosc 2002;56(5): 124A–35A.
6. Kneipp J, Kneipp H, Kneipp K. SERS—a single-molecule and nanoscale tool for bioanalytics. Chem Soc Rev 2008;37(5):1052–60.
7. Bell SEJ, Fido LA, Sirimuthu NMS, Speers SJ, Peters KL, Cosbey SH. Screening tablets for DOB using surface-enhanced Raman spectroscopy. J Forensic Sci 2007;52(5):1063–67.
8. White PC. *In situ* Surface Enhanced Resonance Raman Scattering (SERRS) spectroscopy of biro inks—long term stability of colloid treated samples. Sci Justice 2003;43(3):149–52.
9. Noonan KY, Beshire M, Darnell J, Frederick KA. Qualitative and quantitative analysis of illicit drug mixtures on paper currency using Raman microspectroscopy. Appl Spectrosc 2005;59(12):1493–97.
10. Edwards HGM, Domenech-Carbo MT, Hargreaves MD, Domenech-Carbo A. A Raman spectroscopic and combined analytical approach to the restoration of severely damaged frescoes: the Palomino project. J Raman Spectrosc 2008;39(4):444–52.
11. Shi J, Li T, Feng M, Mao Z, Wang C. Study of the corrosion from the printing plates of "Guan Zi" by Raman spectroscopy. J Raman Spectrosc 2006;37(8):836–40.
12. Grosserueschkamp M, Friedrich MG, Plum M, Knoll W, Naumann RL. Electron transfer kinetics of Cytochrome c probed by time-resolved surface-enhanced resonance Raman spectroscopy. J Phys Chem B 2009; 113(8):2492–97.
13. Han HWA, Yan XL, Dong RX, Song W, Yang M. Analysis of serum from type II diabetes mellitus and diabetic complication using surface-enhanced Raman spectra (SERS). Appl Phys B 2009;94(4):667–72.
14. Chowdhury MH, Gant VA, Trache A, Baldwin A, Meininger GA, Coté GL. Use of surface-enhanced Raman spectroscopy for the detection of human integrins. J Biomed Opt 2006;11(2):024004.
15. Day JS, Edwards HGM, Dobrowski SA, Voice AM. The detection of drugs of abuse in fingerprints using Raman spectroscopy I: latent fingerprints. Spectrochim Acta A 2004;60(3):563–8.
16. Sapse D, Petraco NDK. A step on the path in the discovery of new latent fingerprint development reagents: substituted Ruhemann's purples and implications for the law. J Mol Model 2007;13(8):943–8.
17. Legendre M, Pochet N, Pak T, Verstrepen KJ. Sequence-based estimation of minisatellite and microsatellite repeat variability. Genome Res 2007;17(12):1787–96.
18. Iqbal F, Hadjidj R, Fung BCM, Debbabi M. A novel approach of mining write-prints for authorship attribution in e-mail forensics. Digit Invest 2008;5(Suppl.1):S42–S51.
19. Grant A, Wilkinson TJ, Holman DR, Martin MC. Identification of recently handled materials by analysis of latent human fingerprints using infrared spectromicroscopy. Appl Spectrosc 2005;59(9): 1182–87.
20. DePaoli G, Lewis SA, Schuette EL, Lewis LA, Connatser RM, Farkas T. Photo- and thermal degradation studies of select eccrine fingerprint constituents. J Forensic Sci 2010 May 4. [Epub ahead of print]
21. Hamilton PB. Amino-acids on hands. Nature 1965;205(4968):284–5.
22. Lentner C, editor. Sweat. Geigy Scientific Tables Volume I, 8th edn. West Caldwell, NJ: Ciba-Geigy Limited, 1981.
23. Connatser RM, Riddle LA, Sepaniak MJ. Metal-polymer nanocomposites for integrated microfluidic separations and surface enhanced Raman spectroscopic detection. J Sep Sci 2004;18:1545–50.
24. Connatser RM, Cochran M, Harrison RJ, Sepaniak MJ. Analytical optimization of nanocomposite surface-enhanced Raman spectroscopy/scattering detection in microfluidic separation devices. Electrophoresis 2008;29(7): 1441–50.
25. Giesfeldt KS, Connatser RM, De Jesus MA, Lavrik NV, Dutta P, Sepaniak MJ. Studies of the optical properties of metal-pliable polymer composite materials. Appl Spectrosc 2003;57(11):1346–52.
26. Giesfeldt K, Connatser RM, De Jesus MA, Dutta P, Sepaniak MJ. Gold-polymer nanocomposites: studies of their optical properties and their potential as SERS substrates. J Raman Spectrosc 2005;36(12): 1134–42.
27. Munro CH, Smith WE, Garner M, Clarkson J, White PC. Characterization of the surface of a citrate-reduced colloid optimized for use as a substrate for surface-enhanced resonance Raman-scattering. Langmuir 1995;11(10):3712–20.
28. Keir R, Sadler D, Smith WE. Preparation of stable, reproducible silver colloids for use as surface-enhanced resonance Raman scattering substrates. Appl Spectrosc 2002;56(5):551–9.
29. Hayat MA, editor. Colloidal gold: principles, methods, and applications, Volume 1. San Diego, CA: Academic Press, Inc., 1989.
30. Ibrahim A, Oldham PB, Stokes DL, Vo-Dinh T, Loo BH. A comparison of enhancement factors for surface-enhanced Raman scattering using visible and near-infrared excitations. J Mol Struct 2005;735:69–73.
31. Sherry LJ, Chang S, Schatz GC, Van Duyne RP, Wiley BJ, Xia Y. Localized surface plasmon resonance spectroscopy of single silver nanocubes. Nano Lett 2005;5(10):2034–38.
32. Metraux GS, Mirkin CA. Rapid thermal synthesis of silver nanoprisms with chemically tailorable thickness. Adv Mater 2005;17(4):412–5.
33. Prokes SM, Glembocki OJ, Rendell RW, Ancona MG. Enhanced plasmon coupling in crossed dielectric/metal nanowire composite geometries and applications to surface-enhanced Raman spectroscopy. Appl Phys Lett 2007;90(9):093105.

34. Moskovits M, Suh J. Surface-enhanced Raman spectroscopy of amino-acids and nucleotide bases adsorbed on silver. J Amer Chem Soc 1985; 107(34):6826–29.
35. Socrates G. Infrared and Raman characteristic group frequencies, 3rd edn. Chichester, UK: John Wiley & Sons, Ltd., 2001; 51,53,107–9,125,129,132,143–4,151–2,157–61.

Additional information and reprint requests:
R. Maggie Connatser, Ph.D.
Oak Ridge National Laboratory
NTRC Bldg., 2360 Cherahala Blvd.
Knoxville, TN 37932
E-mail: connatserrm@ornl.gov

JOURNAL OF FORENSIC SCIENCES

J Forensic Sci, November 2010, Vol. 55, No. 6
doi: 10.1111/j.1556-4029.2010.01528.x
Available online at: onlinelibrary.wiley.com

PAPER

DIGITAL & MULTIMEDIA SCIENCES

Denis Trček,[1,2] *Ph.D.; Habtamu Abie,*[3] *Ph.D.; Åsmund Skomedal,*[3] *Ph.D.; and Iztok Starc,*[1,2] *B.Sc.*

Advanced Framework for Digital Forensic Technologies and Procedures*

ABSTRACT: Recent trends in global networks are leading toward service-oriented architectures and sensor networks. On one hand of the spectrum, this means deployment of services from numerous providers to form new service composites, and on the other hand this means emergence of Internet of things. Both these kinds belong to a plethora of realms and can be deployed in many ways, which will pose serious problems in cases of abuse. Consequently, both trends increase the need for new approaches to digital forensics that would furnish admissible evidence for litigation. Because technology alone is clearly not sufficient, it has to be adequately supported by appropriate investigative procedures, which have yet become a subject of an international consensus. This paper therefore provides appropriate a holistic framework to foster an internationally agreed upon approach in digital forensics along with necessary improvements. It is based on a top-down approach, starting with legal, continuing with organizational, and ending with technical issues. More precisely, the paper presents a new architectural technological solution that addresses the core forensic principles at its roots. It deploys so-called leveled message authentication codes and digital signatures to provide data integrity in a way that significantly eases forensic investigations into attacked systems in their operational state. Further, using a top-down approach a conceptual framework for forensics readiness is given, which provides levels of abstraction and procedural guides embellished with a process model that allow investigators perform routine investigations, without becoming overwhelmed by low-level details. As low-level details should not be left out, the framework is further evaluated to include these details to allow organizations to configure their systems for proactive collection and preservation of potential digital evidence in a structured manner. The main reason behind this approach is to stimulate efforts on an internationally agreed "template legislation," similarly to model law in the area of electronic commerce, which would enable harmonized national implementations in the area of digital forensics.

KEYWORDS: forensic science, digital forensics, service-oriented architectures, sensor networks, forensic procedures, admissible evidence

Modern communication technology has caused significant societal and cultural changes. Our personal and professional lives depend on various communication networks and services, and even the most vital infrastructures are no exception. One of the most important challenges, present and future, is therefore that of developing methods and measures to deal with threats, ranging from terrorism, organized crime, and natural disasters to electronic intrusions (1).

Just as a large part of our lives takes place in cyberspace, so do more and more criminal activities. Criminal investigations and law enforcement have to deal with these radical changes, which is not an easy task. In the past, criminal investigations relied on physical evidence, eyewitnesses, and confessions (2). But the first important element, physical evidence, is nonexisting in cyberspace. What remains is only information in binary form, stored on media that range from semi-conductors to magnetic and optical media.

Therefore, the critical element in criminal investigations and law enforcement, physical evidence, is being replaced by information in digital form, digital evidence. This digital evidence is mainly in the form of (or kept primarily in) various log files. But things are becoming harder because of the emergence of ubiquitous computing where a significant number of computing devices will not possess such capabilities—a typical example is sensor networks. On top of this, a few years ago collection of digital evidence was possible by seizing the suspected computing devices. Today, the evidence has to be collected in environments that have to remain operational during investigation (e.g., in an air-traffic control system).

This new situation requires appropriate changes in dealing with evidence that is the task of digital forensics, which is still in its infancy (2,3). Developing this field of science further requires strict adherence to the main goal of forensic investigation, which is the identification of the responsible party (or parties) through a trail of admissible evidence (2).

This paper presents a novel approach to technological and procedural elements, both of which are needed in these new circumstances. In section two, the field of digital forensics is presented to provide the common basis for new solutions in the subsequent sections. Section three presents the new approaches to procedural and technological solutions. Through a top-down approach, it first gives a conceptual framework for forensic readiness procedures, which addresses both organizations and their systems' ability to collect proactively, and preserve potential digital evidence in a structured way for possible later use. Next, it describes a refinement of a structured conceptual framework through inclusion of security services and mechanisms. This is followed by a new technological solution that is intended for deployment in operating pervasive computing environments. Finally, there is a discussion in the fourth section that is followed by conclusions in the fifth section.

[1]Faculty of Computer and Information Science, University of Ljubljana, Tržaška c. 25, 1000 Ljubljana, Slovenia.
[2]FAMNIT, University of Primorska, Glagoljaška 9, 6000 Koper, Slovenia.
[3]Norwegian Computing Center, P.O. Box 114, Blindern, NO-0314 Oslo, Norway.

*Supported by grant BI-NO/07-09-003, research program funding P2-0359, and by DESDIFOR project.

Received 24 Feb. 2009; and in revised form 26 Aug. 2009; accepted 6 Sept. 2009.

Fundamentals of Digital Forensics and Forensics Readiness

Digital forensics consists of two basic elements: the technology that enables it and procedural steps that have to be followed if the whole investigative process is to result in evidence that will be admissible in court. With these, an attack is analyzed and therefore a structure of a typical attack should be presented first.

An Outline of a Typical Attack

According to Stephenson (4), an attack consists of the following typical steps:

- Reconnaissance—In this step, an attacker selects a victim and collects as much data about it as possible with emphasis on weaknesses. Typical tools used in this step are nslookup/dig, whois, ping, traceroute, and information provided on web pages. Already for this step, the investigator starts to identify possible objectives of an attack, but usually this step provides little evidence, because the collection of most of the evidence of this step would require access to the attacker's computer.
- Footprinting and enumeration—After identifying the target, the attacker starts getting details of the victim's system: the network structure (architecture), operating systems, available services (applications), deployed firewalls, and intrusion detection systems (IDS). Typical tools used in this phase include traceroute and nmap. In this step, the attacker is often starting to deploy intermediate hosts and attacking the victim from those hosts. Evidence of this step is usually also limited, because many of the tools used in this phase can be used in a stealth mode.
- Probing for weaknesses—In this step, the attacker is likely to leave traces on remote machines. Some most frequently performed attacks (buffer overflows, denial of service, and exploitation of weak passwords) require port scanning, and collecting details of operating systems and applications (brand and version, revision, configuration). These events will leave traces in logs and other places.
- Penetration—Here, the attacker realizes her/his objective and can often leave evidence. Traces are now generated in system logs, firewall logs, IDS logs, and elsewhere.
- Gaining the objective—In this step, the final objective is achieved which ranges from completely evident, intentionally nonstealth activity (e.g., web page defacement and computer interoperability) to intentionally stealth activities (unauthorized access to data, e.g., phishing and credit cards number stealing).
- Cleanup—A skilled attacker will do as much as possible to erase the evidence, but eliminating evidence totally is often impossible. Even in a case of stealth operation (when stealing, e.g., credit card numbers), traces will exist in the attacker's computer and any involved intermediate hosts. Last but not least, the golden rule of forensics is Locard's exchange principle, which states that it is impossible for a criminal to act, especially considering the intensity of a crime, without leaving traces of presence (5).

Digital Forensics Principles and Existing Methodologies

To achieve investigative objectives, the forensic procedure follows the following steps: preservation of evidence, examination of the evidence, extraction of relevant data, analysis of extracted data, and production of properly documented interpretation (6). These steps are quite aligned with one of the first procedural frameworks, established in 2001 by the Digital Forensics Research Workshop (DFRWS [7]). DFRWS developed one of the first models for digital investigative process, which included the following steps (2,7): identification, preservation, collection, examination, analysis, presentation, and decision. But in general, computer forensics has as yet no established firm standards that are comparable to those developed through decades in other areas that rest on physical evidence like blood- or DNA-based forensics (8). So the standards of digital forensic procedures are still evolving, and some improvements can be found in the literature (1,9–19).

With each investigative process, after the misuse has been detected, preservation of data must take place first. Therefore, the original data have to be copied, and the investigation has to be performed on the copies. Further, original data (i.e., their integrity) have to be preserved in a safe place according to defined procedures, which typically include sealing of the original medium, performing procedures with the participation of at least two investigators, and producing and signing a document about the original data archiving procedure. As a proof of integrity, strong one-way hash functions are used to obtain fingerprints of files, directories, partitions, or whole media (these fingerprints of originals are then compared with produced duplicates). After preservation is performed, analysis takes place. During the analysis, which goes backward from the victim to an attacker and which often requires additional extraction of data from intermediate devices, the two kinds of information threads (scenarios) emerge (4). The first one (primary evidence) is a potential explanation of what has happened. The second one (supporting evidence) is potential verification of the first. In an ideal case, the complete chain of evidence is obtained. However, in the majority of cases gaps will exist. This chain and the collected evidence will have to be supplemented by additional corroboration steps to prove the identity and the action of the suspects. Only after these steps, the complete chain can be effectively presented in court.

Summing up, each investigative step has to follow these investigative objectives (9):

- Development of evidence that links the attacker to the victim.
- Development of evidence for every step in the attack chain that corroborates other steps.
- Development of evidence leads to support traditional investigative techniques.
- Development of evidence that corroborates traditionally developed evidence.

The whole investigative process should provide sufficient ground for an investigator to clearly justify, and confirm by experimental demonstrations, the theory of what has happened and that other alternative theories presented by opponents can be refuted (20). This sounds familiar to the scientific community, and indeed, the forensic principles are the same—theories have to be proved by experiments and if refuted, a new theory has to be used; so forensics is using scientific methodologies to support criminal investigations. When two theories are available about a given case and neither can be determined to be better, or more plausible, the Occam's Razor principle is applied. This means that the simpler theory is chosen (20).

Although the field of digital forensics is rapidly evolving, the development of such theories with a variety of practical techniques and tools to support correctness of investigative findings is still seen as an important research problem. There exists a body of literature describing different areas and aspects of digital forensics, including time stamping evidence correlation (21–23), improving the efficiency and accuracy of a stego (forensic) web search engine

(24), efficient technique for enhancing forensic capabilities of Ext2 file system (25), IP tracebacking (26–28), reconstructing system state for forensic analysis (19), packet tagging for evidence source verification (29), cognitive-mapping based investigation into digital security incidents (18), and conducting forensic investigations into cyber attacks on automobile in-vehicle networks (30).

Digital forensic readiness (DFR) is one of the few proposed frameworks discussed in the forensics literature. It was proposed by Tan (31) to meet two objectives for systems used in digital investigations: (i) costs should be minimized for incident responses and (ii) an environment's ability to collect digital evidence should be maximized. He described many specific techniques for achieving DFR including logging techniques, IDS' data usage, forensic acquisition, and evidence handling. DFR relates to another field within digital forensics, postmortem analysis, by increasing the availability and quality of the raw traces that are needed for investigating an incident postmortem.

Rowlingson (32) described how DFR can be built into an enterprise's forensics program and outlines 10 steps to achieve forensic readiness. He suggested that enterprises should be actively collecting potential evidence, such as log files, network traffic records, e-mail, and telephone records, prior to involvement in an investigation. Further, there exists a body of literature describing different aspects of DFR, including policies for enhancing DFR (33), incorporating forensic readiness into existing response plans (34,35), making sure forensic readiness leads to sound investigation (36), ensuring that hardware devices used to capture forensic evidence are reliable enough to enforce forensic readiness (13), specifying digital forensics policy approach (14), proposing a network forensic readiness as a solution to digital forensic investigations that have become too resource intensive to encourage broad application to the growing numbers of computer crimes (13), and making DFR as a component of information security (15).

As illustrated previously by the wide variety of studies, there is no agreed upon methodology or approach to enable DFR within organizations. Because of this, there is a need for a structured approach that consists of procedures and methods for analyzing the potential evidence need of organizations, collecting proactively and preserving potential digital evidence, and ensuring that actions are targeted toward the most critical disputes and crimes. As a result, we were motivated to investigate and develop a structured approach to DFR with a general aim to develop forensic readiness methodology as a contribution to the advancement of the field.

Improved Approaches to Digital Forensics

In the previous section, we have described the current state in the field. Now to properly base future research and trends in digital forensics (to predict it), the following trends that can already be identified have to be taken into account:

1. First, the development of information communication technology goes into services-oriented architectures (SOAs). This means chaining of services from various security realms, where an attack can be, in the worst case, automatically chained (as opposed to current situation, where each host has to be actively included in the attack by an attacker).
2. Second, networked information systems are being extended with sensor networks that lack computational resources (processing power, memory resources, and communication capabilities). However, these devices are expected to outgrow soon all other kinds of devices in global networks.
3. Third, a large part of systems in current networks cannot be simply turned off or seized for investigations but has to remain operational (e.g., power grids controlling networks). Thus, this has to be taken into account from a technological, as well as a procedural, point of view.
4. And finally, what is probably most surprising is the fact that the primary function of the majority of logging mechanisms in computer systems was not designed with the intention of supporting forensic investigations, but basically system administration (kernel and system logs) and ease of use (history data, meta-data).

Procedural Part

DFR involves adapting organizations by configuring their systems to the proactive collection and preservation of potential digital evidence in a structured manner (the business requirement to collect and use digital evidence has been recognized in, e.g., [37]). To meet such business requirements, to leverage DFR procedures and best practices in the contemporary environments, and to limit the cost of implementing DFR, it is important that these organizations make investments and that they acquire readiness incrementally. This in turn requires a structured DFR procedural approach that builds on relevant standards and best practices and that maximizes the capability and efficiency of service providing organizations for proactively collecting and preserving digital evidence (17).

Implementation of a universal DFR in different organizations should be guided on an international (e.g., by the minimal set of requirements on privacy), national, or macro level by legislation and culture (e.g., by concrete legislation on privacy issues), and on a micro level by the nature of each organization (e.g., by concrete procedural coverage of privacy issues between employer and employees). So the forensic community should define and acknowledge such universal standards if effective methods that enable admissible proofs are to be implemented (14).

Figure 1 depicts the proposed conceptual framework for DFR procedures, while each level is more precisely described in the following text:

- Universal or international-level requirements: This level is about analysis of the problem domain at the highest, general level on how to extract, analyze, and preserve all forms of digital evidence proactively. In spite of variations in local situations, a number of aspects of DFR are universal. The general requirements for this abstraction level include the following:
  - Guidelines for preserving digital evidence, including processes, procedures, and suggestions as to how technology solutions can be used.
  - The provision of digital evidence without violating (or even being perceived to violate) privacy concerns (social acceptability).
  - An identification and classification of potential digital evidence sources, and enumeration of technologies and processes for utilizing these sources.
  - Guidance on when and how to report incidents to law enforcement agencies, including contents and formats of reports, criteria for reporting, and standardization of the interaction between affected parties and law enforcement agencies.

There are additional requirements to the ones listed earlier such as preparing for incident response, criteria for escalation, awareness building, etc. (see [31,32]).

- National-level requirements: An analysis of legal requirements and constraints on the collection and preservation of potential

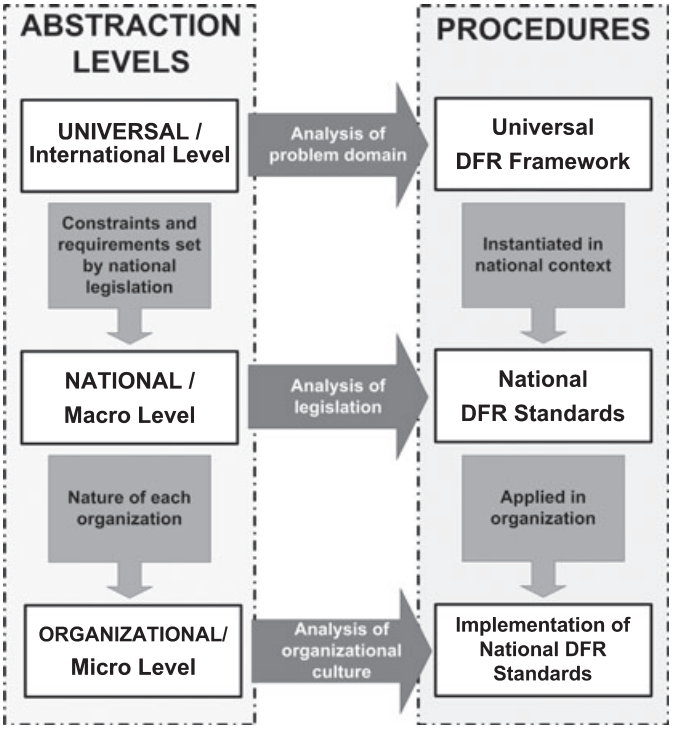

FIG. 1—*A framework for forensics readiness procedures.*

digital evidence in the applicable legal context is the task of this level. National legislation sets requirements (e.g., concerning integrity protection of evidence) and constraints (i.e., what can be collected lawfully) on DFR procedures and practices are considered here. Different jurisdictions set different requirements on how digital evidence should be collected and preserved. Any viable structured approach to DFR must therefore take the applicable legislation into account when shaping the needed policies.

- Organizational-level context: This level deals with methods for analyzing the organizations' need for digital evidence (e.g., the dialogue between employers and employees, and views on privacy, various in different cultures). Organizations have different needs for digital evidence and have different capabilities for collecting and preserving specific evidence. Further, organizations are exposed to different types of crimes or to the same type with different risk factors and have therefore different needs for digital evidence. Moreover, they have different capabilities when it comes to collecting and preserving specific evidence.

The proposed framework (see Fig. 2) addresses all this by providing procedural steps that can be adjusted to different legal contexts and customized to each organization's needs and requirements. It provides structural approaches for DFR for different legal contexts and cultures, and its instantiation provides guidelines to organizations on how to implement a proactive DFR. The universal DFR framework provides a common base that is universal and a method for forming this base, crafting a national guideline for DFR, through analysis of relevant legislations. Because the nature of crimes and disputes is in a constant state of flux, this common base is extendable to support the addition of new types of crime and dispute.

For organizations implementing forensic readiness, this framework provides the DFR process model with associated procedural guideline documentation. Figure 3 depicts this process model with

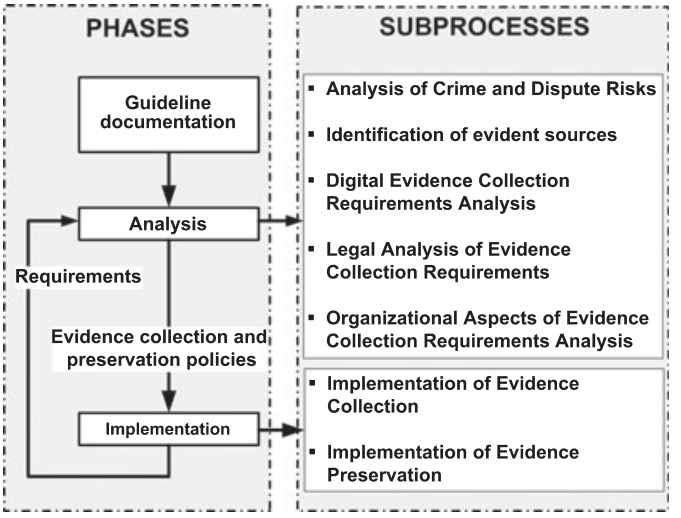

FIG. 2—*An overview of the components of process model.*

its phases and subprocesses. The process guides organizations through the steps required to implement DFR, and the guideline documentation provides guidance in the steps of the process. This answers the questions what to do and how to do it. That is, the framework provides both requirements and guidance. Additionally, as the framework was to be applied to a national context, as a proof of concept it has identified constraints and requirements for proactive digital evidence collection set by Norwegian legislation (the detailed description and theoretical foundation of the process model have yet to be addressed).

From DFR to Forensic Services and Mechanisms

To further refine the requirements from the DFR framework, we propose that this refinement is carried out on two further levels: security services and security mechanisms. There are several approaches possible, e.g., "security functions," at one or more levels of abstraction. We have chosen the security services structure initially proposed by Muftic et al. (38) for open distributed systems and combined it with the relevant components of an overall system. For security mechanisms, a structure similar to that defined in Muftic et al. (38) is used as this has an appropriate level of abstraction without defining a particular set of mechanisms at this stage.

For now, we assume that for each service, there will exist at least one mechanism that (i) can be applied to implement the service, and (ii) the strength of mechanism (SoM) function can be derived that maps a mechanism according to evaluation criteria to a scale of "strength." This function works as an abstraction to formulate dependencies between the services and mechanisms. To summarize, the output from the framework shall be taken as input to select security services which again is refined by making a selection of the appropriate security mechanisms within the implemented system. The overall process is presented in Fig. 3.

Some generic requirements for the selection of services for each component should be available to ensure a level of consistency appropriate for DFR implementations. Bearing in mind the dependencies between security services from the lattice structure defined in Muftic et al. (38), we propose a general structure for the selection of security services and minimum SoM values (per service and component) as shown in Table 1.

The underlying principle here is that the forensics component is the most sensitive part of the system. This is the part that has

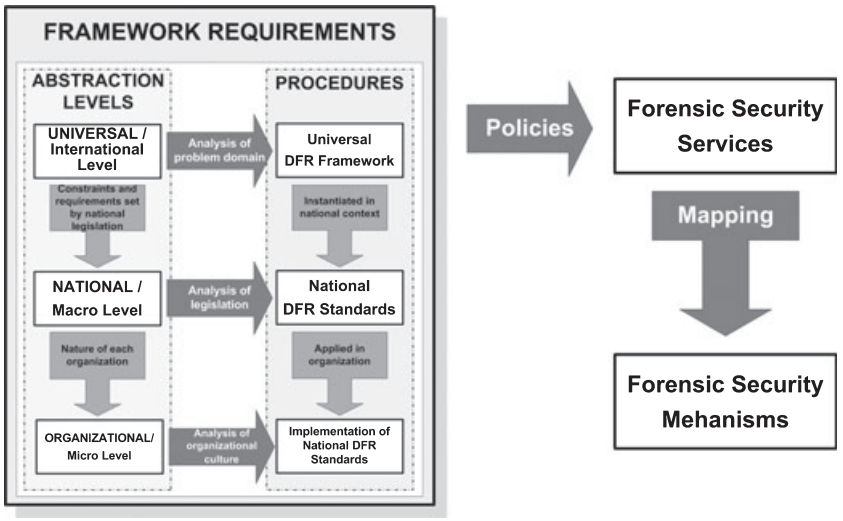

FIG. 3—*From conceptual to operational level.*

TABLE 1—*The strength of mechanism at level* n *for component* c; *SoM (*n, c*) = {l, m, h}, (low, medium, high), requirements can be mandatory (M), recommended (R) or optional (O).*

	Service Level							
	1	2	3.1	3.2	4	Supportive		
System Component	Authentication	Access Control	Integrity	Confidentiality	Nonrepudiation	Accountability	Audit	Spec
Application	l – (R)	l – (R)	l – (R)	l – (O)	l – (O)	l – (O)	l – (O)	m – (O)
System	m – (M)	m – (M)	m – (M)	m – (O)	m – (O)	m – (R)	m – (O)	m – (O)
Sec Mgmt	h – (M)	h – (M)	h – (M)	m – (R)	m – (O)	m – M)	m – (M)	m – (O)
Forensics	h – (M)	h – (M)	h – (M)	m – (R)	h – (R)	h – (M)	h – (M)	m – (O)

direct legal implications for all users (39). This is always the case, and it is independent of direct, or indirect legal, or contractual consequences of how applications are used. Hence, the forensics component also needs the strongest protection. For this component, we propose to have all mechanisms with a high strength except for the confidentiality service. This may be relaxed as it is much more important to know who accessed forensics data and that they are not manipulated. It is also important to have a strong accountability service for the forensics component as this will provide data of who investigated what data and when. Hence, this collected data (internal audit and accountability) needs to be combined with a (strong) nonrepudiatory service. The motivation for this would be to have in place several structured technical measures that prevent false evidence being presented in court. Application requirements are much more specific and influenced by business needs. The consequence is that this component has less mandatory requirements and normally no general requirement for medium- or high-level mechanisms. The end system and security management component have increasing needs for strong mechanisms; internally the services are structured accordingly so that the "base services" are stronger than the higher-level services. Based on these observations, we are able to formulate some structural relationships between the SoM of the security services applied in an overall system.

Security services depend on each other: a security service at service level n will depend on services at the lower level $n-1$, $n-2$, etc. In the original work by Muftic et al. (38), this was formulated as the "lattice structure of security services." The structure was augmented with a method to evaluate the strength and effectiveness of a mechanism. Here, the refinement is different as we introduce a function that simply evaluates the SoM for a mechanism that implements a service for a component.

Definition 1. For a security service at service level n within the component c, $\mathrm{SoM}(n, c) = S$, where $S = \{s_1, s_2, \ldots, s_3\}$ is the set of possible strengths.

Based on this, we can formulate a principle of consistency. This principle means that one should base strong walls on strong foundations, and there is little point in a strong roof on weak walls.

Definition 2. A component c is consistent if there exists an SoM for all n such that $\mathrm{SoM}(n-1, c) \geq \mathrm{SoM}(n, c)$.

Still there is a need to make the components of the system as independent of each other as possible. A component at a "lower" architectural level should only not need to have stronger mechanisms that the "higher" components.

Definition 3. Component independence means that a service at level n for a component at level c does not require $\mathrm{SoM}(n, c) \geq \mathrm{SoM}(n, c+1)$.

In addition, we define the following structural properties of a system:

Definition 4. The overall system is sound if there exists an SoM for all n and all c such that all components are consistent, and $\mathrm{SoM}(n, c) \leq \mathrm{SoM}(n, c+1)$.

Definition 5. The overall components' strength is the lowest SoM found in the chain from security services level $l = 1$ to service $l = 4$ for a given component. That is, the overall components' strength is given by

$$\mathrm{Strength}_c = \min(\mathrm{SoM}(l, c)) \text{ for } l = 1,\ldots, 4 \text{ and a given component } c$$

Hence, even if different components of the system can be viewed quite independently of each other, by combining the concepts of consistency with strength of a component we can conclude that an SoM value of s_i is needed throughout all four security service levels to achieve a forensics component with strength of s_i. That is:

In a consistent system with a security forensics component $\mathrm{strength}_4 = s_i$, all security services need to be implemented with $\mathrm{SoM}(n, 4) = s_i$ in the forensics component.

An interpretation of this is that the SoM of the nonrepudiatory service in the forensics component becomes the best practice marker for the overall system. If we, for the sake of argument, assume that the SoM value of the nonrepudiatory service is a very sensitive parameter in a system, then it should be set to s_i = high. If this system in addition is sound, the consequence is that it becomes necessary to implement all services within the forensics component with $\mathrm{SoM}(n, 4)$ = high, even if other components may have lower SoM values for nonrepudiation.

This may appear somewhat unpleasant for developers and system owners, but it is important to consider the relationships between the services and their role within the overall system. As an example, assume the mapping SoM: {l, m, h}. For a sound system with forensics component $\mathrm{strength}_4 = m$, the table of SoM values can be selected as shown in Table 2.

As the SoM values fall off when the service level increases, this system is sound, but it is another discussion whether this is a type of system that is normally implemented. An example of a system that is not sound is shown in Table 3.

Here, the system is not consistent or sound for several reasons: The authentication mechanism for security management is weaker than both the access control service and system component authentication. The access control mechanism for forensics is weaker than the integrity mechanism, and the access control is stronger for security management than for forensics.

For further mapping from services to mechanisms, we provide an outline of a structure in Table 4.

For practical use of these structural relationships, taxonomy of strengths, mechanism, and their evaluation criteria are needed. This area is for further study, but a good starting point for such evaluations can be found in similar taxonomies (40) for dynamic properties of distributed security services.

In the following, we provide a detailed account for how new integrity services can be made highly secure and scalable for SOA environments.

Technological Part

Digital forensic investigations start with preservation of data in a controlled environment with authorized users after an incident has happened. Strong one-way hash functions are routinely deployed in this step to assure integrity of the original data and its copies. Integrity of data with possible investigation in mind should be addressed when the computing system is deployed for the first time. However, if the solution is to be accepted in reality, it has to be applicable without significant overhead in terms of required software upgrades and required system resources.

For this purpose, multilevel keyed message authentication codes (MACs) are proposed. Immediately after data have been generated, their integrity has to be preserved. The best mechanism for this purpose would be, from the cryptographic strength point of view, digital signatures. However, they would require excessive resources if, basically, each data stream and file in a system should be processed periodically this way. Taking into account that keyed strong one-way hash functions like MD5 are routinely deployed for MACs in real-time exchange of packets in networks, they are acceptable also for the purpose of digital forensics. But the final goal remains digitally signed data. To counter digital signatures'

TABLE 2—*Example of a sound system.*

	Service level				
	1	2	3.1	3.2	4
System component	Authentication	Access Control	Integrity	Confidentiality	Nonrepudiation
Application	m	m	l	–	–
System	m	m	l	l	–
Sec Mgmt	h	h	m	m	l
Forensics	h	h	h	h	m

TABLE 3—*Example of an inconsistent system.*

	Service Level				
	1	2	3.1	3.2	4
System Component	Authentication	Access Control	Integrity	Confidentiality	Nonrepudiation
Application	m	l	–	–	–
System	h	m	–	–	–
Sec Mgmt	m	h	m	–	–
Forensics	m	m	h	–	–

TABLE 4—*Example mechanisms with S_i = high.*

Security Service Level	Mechanism, SoM(*n, c*) = h	Security Assurance Level
1. Authentication	One-time password (Lamport's scheme with SHA-256)	Qualified certificates
2. Access Control	ACL or RBAC	EAL 3+
3. 1 Integrity	ICV with SHA-256	Qualified certificates
3. 2 Confidentiality	AES-256	Qualified certificates
4. Nonrepudiation	e-signature (2K RSA, SHA-256)	EAL 4

disadvantage, they are applied only at the second level (or at the third level) on the MAC that is derived from the MACs generated at a lower level (see Fig. 4).

Further, contemporary computing systems are mainly endangered remotely, over the network. This means that attacks are "injected" through their TCP/IP stacks, which is the main concern of SOAs. To counter this situation, network data streams have to be captured before they enter (and after they leave) the system. In Linux, for example, this means capturing data at the IP level in the kernel space where the network module is implemented. Many technical solutions already exist for this purpose, or minimal modifications to Linux kernel are required (41). Similar solutions can be implemented in Windows environments by deploying DLLs and registry start-up entries.

Now to complete the whole technological solution, a forensic daemon (in UNIX system parlance) is needed. This daemon has the following functions:

- First, at system boot time the daemon is started (before networking is enabled) where the forensics system administrator has to be authenticated and authorized before typing in the integrity key that is used for keyed MACs. Further, the administrator types in the locations where keyed MACs will be stored and where the second-level keyed MACs will be produced and signed. It is also wise if the private key that is used for signing is not available in any (encrypted) file on the system. This key should be invoked from a smart card and available in plaintext only during the signing in the RAM of the system, where the daemon is running. The even better approach is to perform signing on the smart card, so the private key never leaves the tamper resistant area.
- The daemon starts keyed hashing of the network related data stream, and all selected files (directories) on the system. After a predefined amount of time (first-level MACing interval and second-level MACing with signing interval), the generated hashes are hashed again, and the result is digitally signed.
- First-level and second-level MACs together with the second-level signatures are duplicated at a safe (remote) place, preferably on inerasable media like recordable CDs or DVDs.

This leveled MAC approach can be also deployed in IDS, of which one example is SNORT (42). These systems capture every packet that traverses the network at the link layer. However, deployment of IDS needs significant expertise, and they are therefore used in larger networks, while smaller organizations rarely deploy them. Further, such systems are almost never deployed in home networks or for individual networking with, for example palmtops. There are also legal obstacles to wider deployment of IDS. Because they disclose the complete content of communication, sensitive personal data may be disclosed, which is a serious legal issue (43). And "lack of due care and attention to the legal rules surrounding the collection and uses of digital evidence can not only make the evidence worthless, it can leave investigators vulnerable to liability in countersuits" (16).

Therefore, our preference for forensics integrity is the deployment of leveled MACs with a specialized system daemon (service). This daemon can be easily realized, especially if it does not have to do anything with the content of communication. More precisely, the daemon leaves the contents of files intact and just produces admissible traces of their integrity. So when a warrant for an investigation is obtained, the content of recent and archived files can be disclosed, while their changes and modifications can be effectively traced and proved. In addition, the deployed daemon supports investigations in real-time and reduces the need for seizure, or turning off, of the attacked system. Further, as digital evidence is very

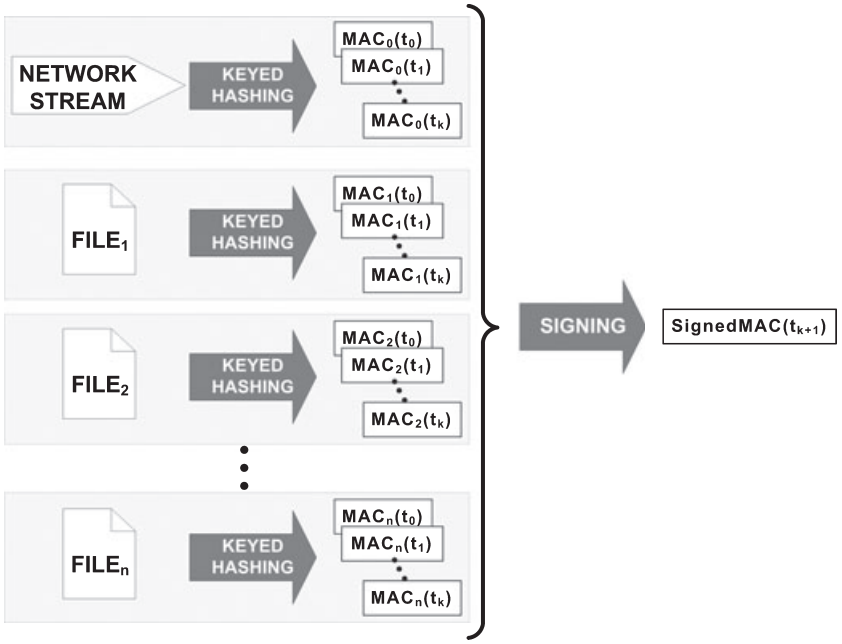

FIG. 4—*Leveled MACs—the first k time intervals keyed MACs are produced, which are afterward digitally signed every (k+1)th interval.*

volatile, the previous solution significantly reduces its volatility. This approach also addresses sensor networks—when deployed as SOAs, sensors will be accessible through so-called wrapped architectures (44). These architectures will enable communications with the specialized daemon. But even if only sensors as such are used, the last hop can be controlled by the proposed daemon.

It should be added that the concept of using keyed MACs for system files integrity is not new—it has been applied more than a decade ago in Tripwire (41). However, Tripwire was intended to support administrators to discover possible breaches and did not focus on steps that are needed for forensic investigations (leveled MACs that are digitally signed, support for inclusion of not only files, but also network streams, and daemon application for ease of deployment in a wide variety of environments, including personal networks and weak devices like palmtops). And finally, in the extreme cases, where it is necessary to preserve each and every packet at Gb speeds, specialized solutions have been developed and can be applied (45).

Discussion

On one hand, SOAs provide customized services to boost personal and business productivity, but they have raised significant concerns regarding forensics investigations for a service. The concern is exacerbated further with the advent of more complex services that involve multiple service providers, as it raises the potential of personal information being shared across these providers in ways that were not intended by the owner of the information. The SOA system architecture also creates risk—one prominent area of risk being the difficulty of understanding and addressing internal and external threats to confidential, personal, or proprietary data, the compromising of which could cause significant harm to individuals or to the organization.

Hence, increasing awareness and understanding of DFR in the SOA environment are essential, not to mention "Internet of things." We therefore need a structure for overall understanding of DFR procedures to support forensics implementation issues in "next-generation forensics aware SOA and Internet of things" (appropriate abstraction serves this purpose [11,17,45]). Our conceptual framework for forensics readiness procedures therefore provides levels of abstraction that allow investigators to perform routine investigations, without becoming overwhelmed by low-level details.

On the other hand, the architecture and bits on SOA are particularly revealing and add more grist to the mill of evidence building around the compelling economics that bind together open source products and SOA activities. Our methodological approach in digital forensics strikes the balance between these two.

Now focusing on the existing forensic technology and products, the following representatives have to be mentioned:

- Media Exploitation Kit, such as Bootable CD (and external USB/Firewire Drive), automatically copies contents of hard disk to external drive and requires little training.
- Advanced Forensic Format, which is an open and extensible disk image storage format.
- Open Digital Forensic Framework (ODFF), which is open plug-in framework for analysis techniques.
- Automated Data Reduction System that identifies unknown files and clusters them.
- Multiple-drive Analysis System, which allows for interactive analysis and collaboration and can correlate computers together.

Carrier states that few published comparisons of open source and commercial forensic software exist (he maintains a Web site of open source forensic tools organized into Windows-based and Unix-based tools [46]). Manson et al. (47) compare an open source tool to two commercial tools, and the advantages and disadvantages of all three tools, and they agree with Carrier's (48) conclusion that confidence in forensic tools will increase through publication, review, and formal testing. It is also stated that open source software continues to be one of the most widely used tools in computer forensics (49,50). Manson et al. (47) point out the importance of both open and proprietary programs working together to validate each other's results so that justice can be done to those who deserve it. However, for this to happen, the authors argue that proprietary software users must have an open mind and must try other tools, preferably open source tools, to validate their results. Geiger and Cranor in their evaluation of six counter-forensic privacy tools (51), highlight significant shortfalls in the methods and implementations of the tools. In Geiger and Cranor (51), a crime scene acquisition of an open source tool to perform a smart-phone internal memory acquisition has been described as beneficial. If an open source tool creates the same evidence as a proprietary tool, the open source tool's code can be analyzed and proved to be working correctly. Therefore, the proprietary tool's code can be assumed to also work correctly without inspection because of the identical outcome (52). Finally, an extensive overview of the next generation tools can be found in Richard and Roussev (53).

Notwithstanding all this, there is still a need for a structured approach, which will provide guidance on how organizations can configure their systems and adapt their organizations proactively to collect and preserve potential evidence according to applicable international and national legislation. Furthermore, such structured approach provides clarification of requirements and constraints set by the applicable legislation on proactive collection and preservation of potential digital evidence that is missing in these tools.

Last but not least, it is worth to compare this framework to established best practices guides (e.g., [54,55]), which heavily rely on existing standards (56). These guides are important documents; however, our proposed framework presents complementary improvements to both of them. First, it emphasizes the importance of defining an internationally agreed upon template that would enable harmonized national and organizational derivatives for treatment of digital forensics. Second, the proposed framework builds on a proactive approach. In the both previously mentioned documents, postfestum activities are considered—these are activities that start with seizing of the evidence. Such focus on seizure of digital evidence is often impossible in emerging environments, because services have to remain operational (examples include air-traffic control systems, power grids, SCADA systems, etc.). Therefore, and third, our framework presents a leveled MAC architectural approach that is suitable for a wide range of digital devices and which means one important low-level step in proactive collection of admissible evidence.

Conclusions

This paper presents current methodological and procedural approaches in digital forensics. Based on them, and taking into account current trends and requirements, such as SOAs, sensor networks, and 24/7 interoperability requirements, a new architectural technological solution is presented that addresses the core forensic principles at its roots. It deploys leveled MACs and digital signatures to provide more reliable data (data integrity) and to significantly ease forensic investigations into the attacked system under

operating conditions. In addition, using a top-down approach, this paper also gives a conceptual framework for forensics readiness procedures that provides levels of abstraction and procedural guides embellished with a process model that allow investigators perform routine investigations, without becoming overwhelmed by low-level details. The framework allows adapting service organizations to configure their systems for proactive collection and preservation of potential digital evidence in a structured manner. Finally, this paper describes how this structured approach is further refined to include security services and mechanisms.

Last but not least, one important intention behind the proposed approach is to initiate work on an internationally agreed "template" in the area of digital forensics, similarly to UNCITRAL model law on electronic commerce (57). This model law is an internationally agreed basis for derivation of national legislations in the area of e-commerce, which has significantly eased and supported promotion of commerce in cyberspace. As our intention is to foster and orchestrate forensics activities in cyberspace, it is reasonable to expect that a similar framework in the area of digital forensics would be another successful story, which certainly holds true for UNCITRAL model law on e-commerce.

References

1. Abie H, Skomedal A. A conceptual formal framework for developing and maintaining security-critical systems. International Journal of Computer Science and Network Security 2005;5(12):89–98.
2. Rogers M. The role of criminal profiling in the computer forensics process. Comput Secur 2003;22(4):292–8.
3. Kruse WJ, Heiser JG. Computer forensics: incident response essentials. New York, NY: Addison-Wesley Professional, 2002.
4. Stephenson P. End-to-end digital forensics. Computer Fraud and Security 2002;2002(9):17–9.
5. Trček D. Managing information systems security and privacy. Heidelberg/New York: Springer, 2006.
6. Wang SJ. Measures of retaining digital evidence to prosecute computer-based cyber-crimes. Computer Standards & Interfaces 2007;29(2):216–23.
7. Palmer G, editor. A road map for digital forensic research (Report From the First Digital Forensic Research Workshop (DFRWS)). Utica, NY: AFRL/IFGB; 2001 Nov. Report No.: DTR-T001-01 FINAL.
8. Hunter W. Forensics: The science of crime-solving series. Philadelphia, PA: Ser. Mason Crest Publishers, 2005.
9. Stephenson P. Analysis and correlation. Computer Fraud and Security 2002;2002(12):16–8.
10. Stephenson P. A formal model for information risk analysis using colored petri nets. In: Jensen K, editor. Proceedings of the Fifth Workshop and Tutorial on Practical Use of Coloured Petri Nets and the CPN Tools (CPN '04); 2004 Oct 8–11; Aarhus, Denmark. Aarhus, Denmark: CPN Group-Department of Computer Science/University of Aarhus, 2004;167–84.
11. Brinson A, Robinson A, Rogers M. A cyber forensics ontology: creating a new approach to studying cyber forensics. Digit Invest 2006;3(Suppl. 1):37–43.
12. Ieong RSC. FORZA—Digital forensics investigation framework that incorporate legal issues. Digit Invest 2006;3(Suppl. 1):29–36.
13. Endicott-Popovsky B, Frincke DA, Taylor CA. A theoretical framework for organizational network forensic readiness. J Comput 2007;2(3):1–11.
14. Taylor C, Endicott-Popovsky B, Frincke DA. Specifying digital forensics: a forensics policy approach. Digital Investigation 2007;4(Suppl. 1):101–4.
15. Grobler T, Louwrens B. Digital forensic readiness as a component of information security: best practice. In: Venter H, Eloff M, Labuschagne L, Eloff VSR, editors. New approaches for security, privacy and trust in complex environments (IFIP International Federation for Information Processing). Boston, MA: Springer, 2007;13–24.
16. Ryan DJ, Shpantzer G. Legal aspects of digital forensics. Washington, DC: The George Washington University, 2002.
17. Pollitt MM. An ad hoc review of digital forensic models. Proceedings of the Second International Workshop on Systematic Approaches to Digital Forensic Engineering (SADFE 2007); 2007 Apr 10–12; Seattle, WA. Washington, DC: IEEE Computer Society, 2007;10–2.
18. Rekhis S, Krichene J, Boudriga N. Cognitive-maps based investigation of digital security incidents. In: Rekhis S, Krichene J, Boudriga N, editors. SADFE 2008. Proceedings of the 2008 Third International Workshop on Systematic Approaches to Digital Forensic Engineering; 2008 May; Oakland, CA. Washington, DC: IEEE Computer Society, 2008;25–40.
19. Goel A, Farhadi K, Po K, Feng W. Reconstructing system state for intrusion analysis. ACM SIGOPS Operating Systems Review 2008;42(3):21–8.
20. Cohen F. Digital forensics. Network Sec 2000;2000(1):18–20.
21. Schatz B, Mohay G, Clark A. A correlation method for establishing provenance of timestamps in digital evidence. Digit Invest 2006;3(Suppl. 1):98–107.
22. Willassen SY. Timestamp evidence correlation by model based clock hypothesis testing. Proceedings of the 1st International Conference on Forensic Applications and Techniques in Telecommunications, Information, and Multimedia and Workshop; 2008 Jan 21–23; Adelaide, Australia. Brussels, Belgium: ICST, 2008;Article No 15.
23. Case A, Cristina A, Marziale L, Richard GG, Roussev V. FACE: Automated digital evidence discovery and correlation. Digit Invest 2008;5(Suppl. 1):S65–75.
24. Patel A, Shah M, Chandramouli R, Subbalakshmi KP. Covert channel forensics on the internet: issues, approaches, and experiences. International Journal of Network Security 2007;5(1):41–50.
25. Barik MS, Gupta G, Sinha S, Mishra A, Mazumdar C. An efficient technique for enhancing forensic capabilities of Ext2 file system. Digit Invest 2007;4(Suppl. 1):55–61.
26. Goodrich MT. Probabilistic packet marking for large-scale IP traceback. IEEE/ACM Transactions on Networking (TON) 2008;16(1):15–24.
27. Sung M, Xu J, Li J, Li L. Large-scale IP traceback in high-speed internet: practical techniques and information-theoretic foundation. IEEE/ACM Transactions on Networking (TON) 2008;16(6):1253–66.
28. Lu L, Chan MC, Chang EC. A general model of probabilistic packet marking for IP traceback. Proceedings of the 2008 of the ASIAN ACM Symposium on Information, Computer and Communications Security; 2008 Mar 18–20; Tokyo, Japan. New York, NY: ACM;179–88.
29. Shue CA, Gupta M, Davy MP. Packet forwarding with source verification. Computer Networks 2008;52(8):1567–82.
30. Nilsson DK, Larson UE. Conducting forensic investigations of cyber attacks on automobile in-vehicle networks. Proceedings of the 1st International Conference on Forensic Applications and Techniques in Telecommunications, Information, and Multimedia and Workshop; 2008 Jan 21-23; Adelaide, Australia. Brussels, Belgium: ICST 2008;Article No 8.
31. Tan J. Forensic readiness. Cambridge, MA: @stake Inc., 2001, http://www.arcert.gov.ar/webs/textos/forensic_readiness.pdf (accessed August 13, 2009).
32. Rowlingson R. A ten step process for forensic readiness. Int J Digit Evid 2004;2(3):1–28.
33. Yasinsac A, Manzano Y. Policies to enhance computer and network forensics. Proceedings of the 2001 IEEE Workshop on Information Assurance and Security; 2001 June 5–6; West Point, NY. IEEE, 2001.
34. Wolfe-Wilson J, Wolfe HB. Management strategies for implementing forensic security measure. Info Tech Sec Report 2003;8(2):55–64.
35. Rogers MK, Seigfried K. The future of computer forensics: a needs analysis survey. Comput & Secur 2004;23(1):12–6.
36. Carrier B, Spafford E. Getting physical with the digital investigation process. Int J Digit Evid 2003;2(2):???–???.
37. Yasinsac A, Erbacher RF, Marks DG, Pollitt MM, Sommer PM. Computer forensics education. IEEE Sec & Priv 2003;1(4):15–23.
38. Muftic S, Patel A, Sanders P, Colon R, Heijnsdijk J, Pulkkinen U. Security architecture for open distributed systems (Wiley Series in Communications & Distributed Systems). Chichester, England: John Wiley & Sons, 1993.
39. Garber L. Computer forensics: high-tech law enforcement. IEEE Computer 2001;34(1):22–7.
40. Savola R, Abie H. On-line and off-line security measurement framework for mobile ad hoc networks. Journal of Networks Special Issue on Security of Wireless Communication System 2009;4(7):565–79.
41. Gene HK, Spafford EH. The design and implementation of tripwire: a file system integrity checker. Proceedings of the 2nd ACM Conference on Computer and Communications Security; 1994 Nov 2–4; Fairfax, VA. New York, NY: ACM 1994;18–29.
42. Roesch M. SNORT—Lightweight intrusion detection system for networks. Proceedings of the 13th USENIX Conference on System Administration; 1999 Nov 7–12; Seattle, WA. Berkeley, CA: USENIX Association, 1999;229–38.

43. Data Protection Directive 95/64/EC. Official Journal of the European Communities L281, European Commission. 1995.
44. Trček D. Services deployment methodologies for weak processing devices: an analysis. In: System theory and applications. Proceedings of the 11th WSEAS International Conference on Systems; 2007 Jul 23–25; Agios Nikolaos, Greece. Stevens Point, WI: WSEAS Press 2007;357–60.
45. Morariu C, Stiller B. DiCAP: distributed packet capturing architecture for high-speed network links. 33rd Annual IEEE Conference on Local Computer Networks (LCN); 2008 Oct 14–17; Montreal, Canada. IEEE Computer Society, 2008;168–75.
46. Open Source Forensics: Open Source Tools, http://www.opensourceforensics.org/tools/index.html.
47. Manson D, Carlin A, Ramos S, Gyger A, Kaufman M, Treichelt J. Is the open way a better way? Digital forensics using open source tools. Proceedings of the 40th Hawaii International Conference on System Sciences; 2007 Jan 3–6; Waikola Village, Hawaii. Washington, DC: IEEE Computer Society 2007;266b.
48. Carrier B. Open source digital forensics tools: the legal argument. Cambridge, MA: @stake Inc., 2002.
49. Byfield B. The two-edged sword: Legal computer forensics and open source. News Forge 2005;???:???–???.
50. Gyger A. Sleuthkit/Autopsy: an open source forensic package. February 15, 2006.
51. Geiger M, Cranor LF. Scrubbing stubborn data. IEEE Sec & Priv 2006;4(5):16–25.
52. Distefano A, Me G. An overall assessment of Mobile Internal Acquisition Tool. Digit Invest 2008;5(Suppl. 1):S121–7.
53. Richard GG, Roussev V. Digital forensics tools: the next generation. In: Kanellis P, editor. Digital crime and forensic science in cyberspace (N/A). Hershey, PA: Idea Group Publishing, 2006;76–81.
54. Scientific Working Group on Digital Evidence. Best practices for computer forensics, Version 2.1 (July 2006), http://www.enfsi.eu/get_doc.php?uid=326 (accessed August 13, 2009).
55. ENFSI. Guidelines for best practice in the forensic examination of digital technology, FIT-2005-001, No. 6, http://www.swgde.org/ (accessed August 13, 2009).
56. ISO/IEC. General requirements for the competence of testing and calibration laboratories, ISO/IEC 17025, 2nd edn. Geneva, Switzerland: ISO, 2005.
57. UNCITRAL. Model law on electronic commerce. Vienna, Austria: United Nations Commission on International Trade Law (UNCITRAL), 1996.

Additional information and reprint requests:
Denis Trček, Ph.D.
Faculty of Computer and Information Science
University of Ljubljana
Tržaška c. 25, 1000 Ljubljana
Slovenia/EU
E-mail: denis.trcek@guest.arnes.si

JOURNAL OF FORENSIC SCIENCES

J Forensic Sci, November 2010, Vol. 55, No. 6
doi: 10.1111/j.1556-4029.2010.01467.x
Available online at: onlinelibrary.wiley.com

PAPER

ENGINEERING SCIENCES: PATHOLOGY/BIOLOGY

Jimmy L. Smart,[1] *Ph.D.*

Estimation of Time of Death With a Fourier Series Unsteady-State Heat Transfer Model

ABSTRACT: The purpose of this study was to return to fundamental principles of heat transfer and derive a suitable model to establish a firm basis for constructing a postmortem human cooling curve. A Fourier Series Model was successfully applied to unsteady heat transfer within a wooden cylinder in controlled laboratory conditions. Wood has similar thermal diffusivity properties as human tissue. By manipulation of the model, sensitivity analyses were performed to observe the impact of changes in values of input variables. Variables of initial temperature of the cylinder and ambient surrounding temperature were shown to be very sensitive and have the most impact upon predictive results of the model. The model was also used to demonstrate the existence of an initial temperature plateau, which is often the subject of controversy in estimating time of death. Finally, it was demonstrated how the Fourier Series Model can be applied to estimate time of death for humans.

KEYWORDS: forensic science, forensic pathology, postmortem cooling curve, time of death, unsteady-state heat transfer, Fourier series heat transfer model, temperature plateau, body temperature after death

Historically, estimation of time of death has always been a valuable forensic tool. Can you imagine an early caveman touching his deceased clansman and upon sensing the cold corpse, concluding the man had been dead for some time. In England, 925 AD, St. John of Beverly was appointed "keeper of the pleaser of the crown", later to be shortened to "crowner", then finally to "coroner". Even at that time, only crude "forensic" tools of rigor mortis and corpse warmth were used to gage time of death. It was not until 1600 that the first criminal autopsy was conducted by a French physician, Ambrose Pare (1,2).

By 1811, an English physician named John Davey had formulated his famous law based upon the principle of algor mortis (slow cooling of a warm-blooded corpse). Davey's Law states that 1.5°F is lost per hour as measured in the armpit. Therefore, at least in theory, it should be possible to record the temperature of a corpse, and having knowledge of the heat loss rate curve, be able to estimate time of death. In reality, the heat loss rate curve is not strictly linear and is complicated by many factors.

Over the past 100 years, there have been numerous models proposed to estimate time of death. As Kaliszan et al. (3) points out in a recent review article, no single model or method allows the postmortem interval to be defined with absolute precision. Results of these models can be useful to crime scene investigators but are generally not strictly admissible into courts of law. There is too much error and variability associated with these current models.

Much work has been carried out by various investigators to construct a suitable model for predicting time of death. Though the scope of this article is not aimed at a survey of existing methods, some excellent approaches and summaries are available in references (4–11). In 1948, Sellier (12) made use of an infinite cylinder Fourier series to mathematically explore how variables might affect the rate of a human cooling curve. This current investigation uses a similar Fourier Series Model and expands upon earlier ideas.

One of the few published accounts of time of death estimation, which included actual errors, was conducted by two forensic pathologists upon 100 bodies (13). Based upon a single rectal temperature and judgment of an experienced pathologist, only 11 cases were estimated correctly (<5% error), when compared to the actual known elapsed times. In 35 of the 100 cases, the error was <10%, and in 70 of the 100 cases, the error was <30%.

Approach

Most of the existing time-of-death models are either empirically derived or based upon some simple questionable mathematical formula. The Fourier Series Model used in this investigation is based upon fundamental principles of conductive heat transfer. This approach provides a firm foundation upon which to build an ultimate predictive model for estimating time of death. Starting from the most basic equation of steady-state heat conduction in one dimension, Fourier's rate equation states that the heat flux per unit area normal to the x-direction of heat flow is proportional to the temperature gradient in the x-direction. This statement can be compactly expressed as $\frac{q_x}{A} = -k\,\frac{dT}{dx}$, where q_x is the heat transfer rate in the x-direction, A is the area normal to the direction of heat flow, k is the proportionality constant called the thermal conductivity, and dT/dx is the temperature gradient in the x-direction. Because the human torso can be approximated as a cylinder, it is appropriate to expand the one-dimensional Fourier's rate equation and express it in cylindrical coordinates. The result is shown as

[1]Department of Chemical & Materials Engineering, University of Kentucky, 4810 Alben Barkley Drive, Paducah, KY 42002.

Received 2 July 2009; and in revised form 26 Aug. 2009; accepted 7 Sep. 2009.

Eq. 1, below. Because the loss of temperature from a human body is inherently an unsteady-state process, the term on the RHS of Eq. 1 represents the change of body temperature over time. The subsequent partial differential equation can be solved for heat transfer in the radial direction with use of a Fourier series, shown as Eq. 2. This exact series solution is for an infinitely long cylinder. An infinite cylinder is an idealization that permits the assumption of one-dimensional conduction in the radial direction. Of course, the human torso is not an infinite cylinder, but typical torso ratios of cylinder length/cylinder diameter of 2–3 provide a reasonable estimate of radial heat flow (with subsequent temperature loss) from the postmortem human torso.

Methods

Experimental

A wooden cylinder was constructed to mimic the approximate proportions of a small human torso (0.22 m diameter by 0.44 m length). Some initial testing was performed with raw tree trunks and then with pressure-treated fence posts. In both cases, these specimens contained too much moisture, severely cracked upon heating and were unusable. Next, a wooden cylinder was constructed from kiln-dried lumber, containing an estimated moisture content of 10–15%. Standard $2' \times 10'$ yellow pine planks of lumber were joined and clamped together using a minimal amount of polyurethane construction adhesive. The subsequent integrous block of wood was turned on a lathe to yield the final wooden cylinder for testing. A hole was drilled parallel to the axis of the cylinder from the face of one end of the cylinder, located about 1/3 of the cylinder radius from centerline. The hole was drilled to approximate the depth and location of the anus of a human torso.

The cylinder was placed in an oven thermostatically controlled to a temperature of 37°C. It required about 2 days for the cylinder to attain this final temperature throughout its volume. The cylinder was quickly removed from the oven and a thermocouple wire supported within an insulated fiberglass rod was inserted into the "rectum." About 2–3 min elapsed between time of cylinder removal from the oven and temperature capture of the first data point. This operation was quickly performed in an effort to capture any early temperature plateau effects. Under conditions of free convection, the cylinder was suspended over a laboratory bench, and data capturing software was used to monitor temperature decay each min. Ambient temperature conditions within the laboratory were carefully controlled (near temperatures of 21°C). In other experiments, the wooden cylinder was placed directly on the laboratory bench, covered with a blanket in some cases and subjected to conditions of forced convection with use of a pedestal fan.

Thermal diffusivity of a material is a measure of the rate at which heat is lost from the material to its cooler surroundings; it is the ratio of thermal conductivity to the product of density and heat capacity, or $\alpha = k/(\rho\, C_p)$, where α is the thermal diffusivity with units of m^2/s, k is the thermal conductivity with units of W/(m K), ρ is the density with units of kg/m^3, and C_p is the heat capacity with units of J/(g K). Interestingly enough, it was discovered that the thermal diffusivity of the human body and wood are very similar. Their individual values of thermal conductivity, density, and heat capacity are significantly different, but the ratios of the values combining to form the overall thermal diffusivity are of the same approximate magnitude. For example, typical values for average thermal properties of the lower human torso are $k = 0.40$ W/(m K), $\rho = 880$ kg/m^3, and $C_p = 3.41$ J/(g K); they combine to equal a thermal diffusivity of 0.13×10^{-6} m^2/s (14). A typical value for thermal diffusivity of wood is reported to be 0.16×10^{-6} m^2/s (15). However, there is some variation within specific wood species. For the yellow pine wood of our particular cylinder, $k = 0.12$ W/(m K), $\rho = 661.8$ kg/m^3, and $C_p = 3.00$ J/(g K); they combine to form a thermal diffusivity of 0.06×10^{-6} m^2/s.

Fourier Series Heat Transfer Model

The heat equation for heat conduction analysis in a cylindrical body, written in cylindrical coordinates, is (16):

$$\frac{1}{r}\frac{\partial}{\partial r}\left(k\,r\frac{\partial T}{\partial r}\right) + \frac{1}{r^2}\frac{\partial}{\partial \phi}\left(k\frac{\partial T}{\partial \phi}\right) + \frac{\partial}{\partial z}\left(k\frac{\partial T}{\partial z}\right) + \dot{q} = \rho\, C_p\frac{\partial T}{\partial t} \tag{1}$$

The exact solution for uniform initial temperature and convective boundary conditions can be written as a Fourier series (17):

$$\theta = \sum_{n=1}^{\infty} C_n \exp\left(-\lambda_n^2 \hat{Fo}\right) J_o\left(\lambda_n r^*\right) \tag{2}$$

where, $\boldsymbol{\theta} = (T - T_\infty)/(T_{\text{initial}} - T_\infty)$ or unaccomplished temperature change; T_∞ = ambient temperature; F_o = Fourier number, $\alpha t/(V/A)^2$; α = thermal diffusivity, $k/(\rho C_p)$; r_o = outside cylinder radius; $r^* = r/r_o$.

$$C_n = \frac{2}{\lambda_n}\frac{J_1(\lambda_n)}{J_o^2(\lambda_n) + J_1^2(\lambda_n)}$$

The Biot number, Bi, is calculated as $h(V/A)/k$, where h is the heat transfer coefficient, V is the volume of the solid cylinder, A is the surface area of the cylinder, and k is the thermal conductivity of the cylinder. The eigenvalues, λ_n, are positive roots of the transcendental equation, $\text{Bi} = \lambda_n\, [J_1(\lambda_n)/J_o(\lambda_n)]$. Tabulated values of the first four roots of this equation are listed in Table A-13 of reference (17). These roots can also be determined by using Excel SOLVER to find the eigenvalues as solutions to the equation, $\text{Bi} = \lambda_n\, [J_1(\lambda_n)/J_o(\lambda_n)]$.

The quantities J_1 and J_o are Bessel functions of the first kind. Tabulated values for these functions are listed in Table I of reference (17). These Bessel functions can also be solved directly with the Excel worksheet function, BESSELJ(x,n), where x is the eigenvalue and n is the order.

Several terms within the Fourier series, i.e., the RHS of Eq. 2, are summed to provide a value for the LHS or $\boldsymbol{\theta}$. $\boldsymbol{\theta}$ is called the unaccomplished temperature change. Once $\boldsymbol{\theta}$ is determined, temperature within the cylinder, T, can be found at any time t.

Because the ratio of cylinder length/cylinder diameter is only 2, the wooden cylinder cannot be modeled as an infinite cylinder. Therefore, instead of using the radius r to calculate the Fourier number for the infinite cylinder case, the ratio V/A was substituted (18). Table 1 lists the variable values used in the Fourier Series Model.

Results

Model Application

See Fig. 1 for experimental data collected from the wooden cylinder under conditions of the base case (suspended cylinder), the cylinder resting on a laboratory bench, the cylinder covered with a

TABLE 1—*Variables used in Fourier Series Model.*

	Wood Cylinder	Human Torso (raw model)	Human Torso (adjusted model)
r, radius, m	0.109	0.15	0.20
L, length, m	0.441	0.61	0.61
W, weight, kg	10.85	N/A	N/A
T_i, initial temp, °C	37.0	37.0	37.0
T_∞, ambient temp, °C	21.0	23.9	22.5
r, anus, m	0.042	0.05	0.07
k, W/(m K)	0.120	0.40	0.36
ρ, kg/m^3	661.8	880	890
C_p, J/(kg K)	3000	3400	3530

fleece blanket, and the cylinder subjected to forced convection from use of a pedestal fan. This plot is provided to show the variability in rate of temperature decay from the test cylinder in a variety of "field conditions." The base case provides a basis for our theoretical mathematical model (to follow), the cylinder resting on a bench corresponds to a human body found resting on the ground, the fleece blanket corresponds to a human body found resting on the ground with minimal clothing, and use of the pedestal fan corresponds to a human body found on the ground with a slight breeze blowing across the body.

The Fourier Series Model was fitted to experimental temperature decay data collected from the base case of suspended wooden cylinder under conditions of free convection. A three-term Fourier model was used to judge how each variable affected the fit of the model to the experimental data. The coefficient of determination, R^2, commonly used in statistical analysis, was used to judge how change in a variable influenced the model fit. According to Fig. 2, the model provided a good fit, with an R^2 of 0.990. Note, in the modeling application, no effort was made to model the early stages of temperature decay. This early time period is called the "temperature plateau effect" and will be addressed later. Most investigators ignore this early time period as it is difficult to model and often not known or even especially relevant when establishing a temperature decay curve. See reference (4) for further discussion.

Sensitivity Analysis

There are many variables that affect the shape of the temperature decay curve. Various investigators (4,12,19) have attempted to assess the importance of these variables relative to each other. In an effort to understand the influence of each variable, a sensitivity analysis was performed on the variables associated with the temperature decay of the wooden cylinder. This sensitivity analysis is shown in Fig. 3.

As demonstrated by Al-Alousi (20), where he examined 117 forensic cases, and also by other investigators (4), there is much variability and large standard deviations from temperature averages across various individual postmortem cooling curves. The cooling curve problem is difficult to model. Why so? The use of a Fourier Series Model as applied to controlled laboratory conditions was used in an effort to answer this question. Sensitivity analyses were performed on all major variables associated with the model. Once sensitive variables were identified, a closer look was taken at each

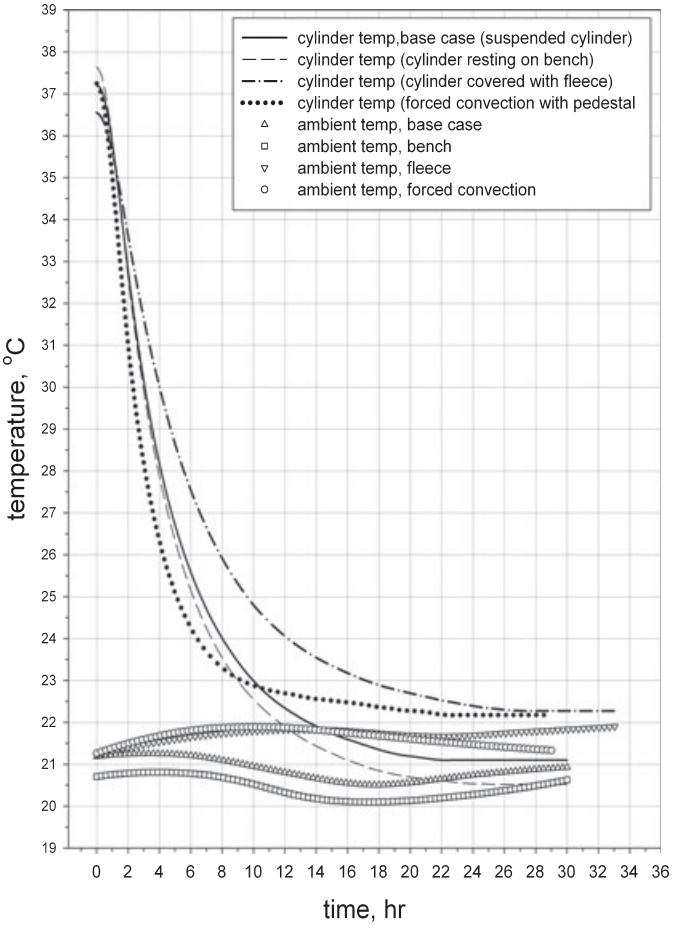

FIG. 1—*Temperature decay of wooden cylinder under various conditions.*

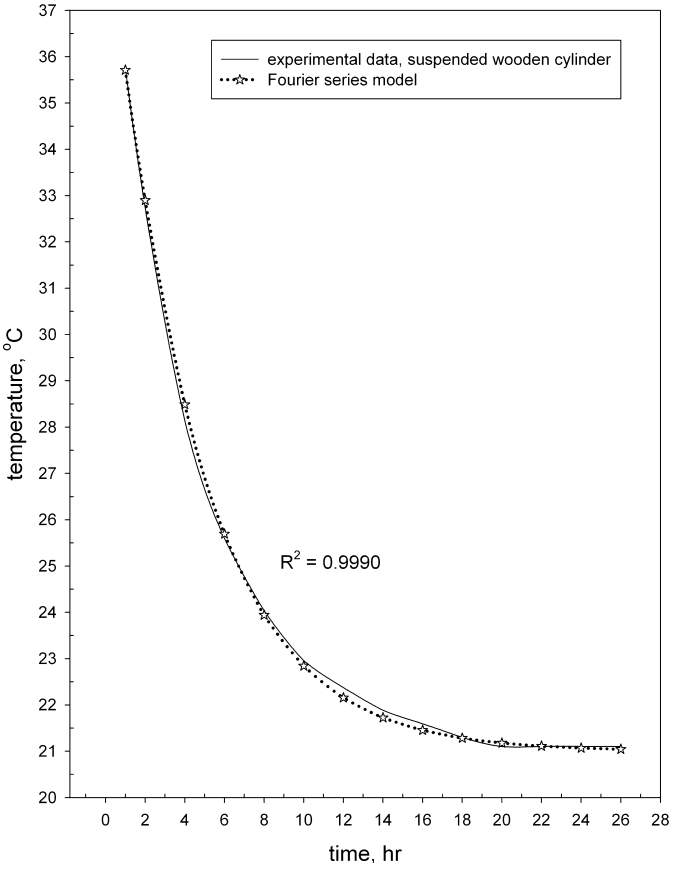

FIG. 2—*Application of the Fourier Series Model to cooling curve of suspended wooden cylinder.*

variable to explain how they might affect the predictive power of the model. Initially, one might think the variable thermal conductivity of body tissue, as reported by several investigators (14,21), might explain the wide variability between individual cooling curves. However, our sensitivity analysis (see Fig. 3) showed that the variables of thermal conductivity, and even specific heat, did not significantly affect the cooling curve.

The primary variables exercising the most influence on the cooling curve are initial body temperature and ambient surrounding temperature conditions. The sensitivity analysis reveals that it is absolutely critical when constructing a predictive model to know these temperature conditions. Note in Fig. 3 that the temperature sensitivity curves are not symmetrical. Because of this nonsymmetry, if errors were to be made when exercising the predictive model, it appears to be somewhat more advantageous to overestimate the initial temperature and underestimate the ambient temperature conditions.

As can be seen in Fig. 1, even in a thermostatically controlled room, there are some small fluctuations in ambient temperature as a result of normal cycling of a heating/cooling unit. In the literature (22), there are solution templates for the Fourier series heat transfer model with conditions of variable ambient temperature. However, in our case where the ambient temperature underwent a slight cycle, it is believed that these solutions add another level of complexity and are unnecessary because of the fact that the effects of the rise and fall of the ambient temperature curve essentially cancel out each other. In other cases, where the temperature is linearly increasing or decreasing, exact solution templates for the Fourier series heat transfer model are also available (22).

Discussion

Temperature Plateau Effect

Examination of the cooling curves of the test cylinder shown in Fig. 1 reveals a slight temperature plateau effect. This plateau effect is because of the fact that initially, there is no temperature change and there is no temperature gradient. This corresponds to the case of a human body, as the temperature does not change immediately upon death; the postmortem temperature decay curve is initially flat or only slightly changing. Shortly after time zero (when a person dies or our cylinder is removed from the oven), it takes a brief period for a temperature gradient to become established. In our model, the plateau effect is dependent primarily upon the cylinder radius and the thermal diffusivity of the cylinder material. This temperature plateau effect has been the subject of much controversy over decades of forensic research associated with estimation of time of death in humans. Some investigators report the effect is just a natural phenomenon associated with heat transfer (as is demonstrated with our wooden cylinder). Other investigators (23–25) insist some heat is produced after somatic death as a result of anaerobic and aerobic metabolic processes. Therefore, it is argued that these processes will significantly distort the temperature plateau effect.

Most models used by previous investigators to estimate time of death ignore the temperature plateau effect. With use of the Fourier Series Model, the temperature plateau effect can be captured. The effect of additional terms in the Fourier series is demonstrated in Fig. 4. With use of spreadsheet software, it is easy and convenient to incorporate additional terms into the Fourier series. With use of a five-term model, a smooth curve is fitted to the temperature

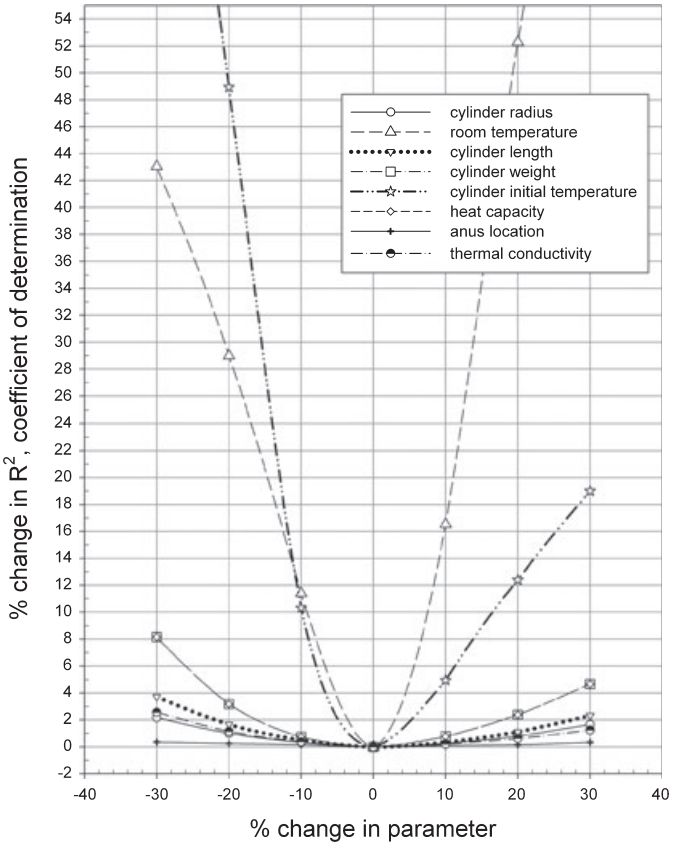

FIG. 3—*Sensitivity analysis.*

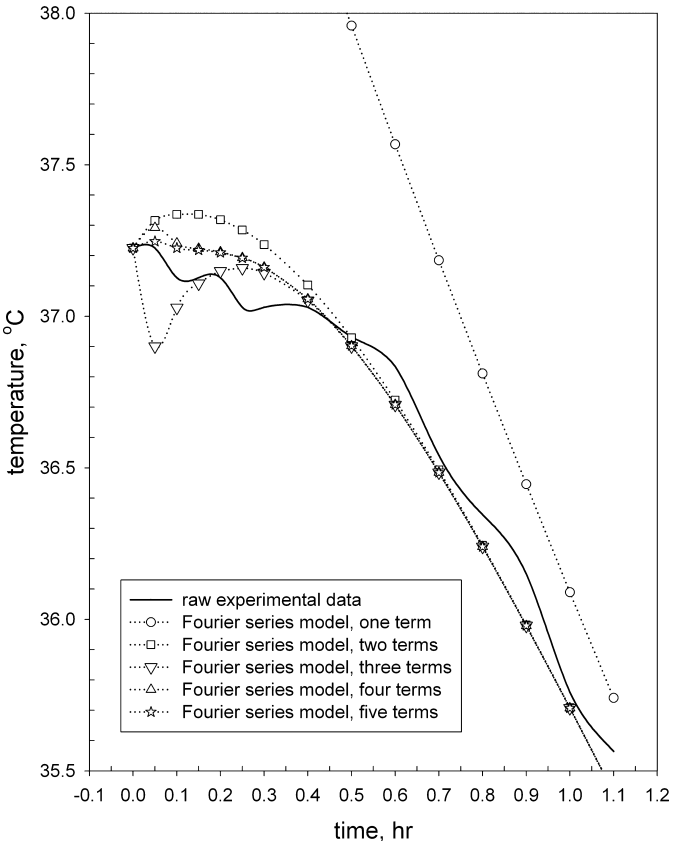

FIG. 4—*Influence of additional terms in the Fourier Series Model.*

plateau. Many investigators are content to offer models equivalent to the sum of the first two or three terms of the Fourier series (4,5,20). Even in this current experimental work with a small diameter wooden cylinder, limiting the description to two terms in the Fourier series gives <0.3°C error in the temperature plateau region.

Modifications of the Fourier Series Model to Accommodate Changes in Surrounding Ambient Conditions

In our carefully controlled experimental conditions, temperature decay within the wooden cylinder was studied while the cylinder was suspended in still air. These conditions define our base case. For forensic studies of corpses, conditions certainly deviate from our base case. The human body is usually found resting on a firm surface, is seldom discovered as a naked body, and some slight conditions of forced convection (wind or air conditioning) may be present.

According to Fig. 1, there are some slight differences between the cooling curves of the base case of our wooden cylinder suspended in air versus the same cylinder resting on a laboratory bench (a thermally indifferent base). By making a slight adjustment of adding 0.8°C to the ambient room temperature conditions, the cylinder bench cooling curve was adjusted up to be essentially congruent to the suspended cylinder curve. This adjustment was incorporated into the Fourier Series Model when applying it to applications for a postmortem human cooling curve, as bodies are usually discovered on a thermally indifferent base.

Correction factors were not attempted to fit the Fourier Series Model to other conditions indicated in Fig. 1. Henssge (4) has performed extensive testing to establish corrective factors for bodies with various layers of clothing, bodies in water, and moving air. These corrective factors are applied to conditions other than his base case: a naked body resting on its back on a thermally indifferent base in a closed room. Henssge`s corrective factors were applied to what he calls the "Newtonian cooling coefficient", which is the slope of the cooling curve. It is not clear whether Henssge's correction factors could be adapted to the Fourier Series Model. Corrective factors for other conditions will be determined in our additional investigations.

Suggested Application of the Fourier Series Model to Describe the Postmortem Human Cooling Curve

Thermal properties of a human torso have been estimated according to body type. Table 2 and Fig. 5 have been constructed from assigning proportions of various types of tissue (lung, pelvic organ, gastrointestinal organs, subcutaneous fat, etc.) that comprise various body types. Individual literature values of thermal conductivity, density, and heat capacity for various tissues are available (14). According to the sensitivity analysis shown in Fig. 3, the Fourier Series Model is not especially sensitive to variation of these properties. Also, it is convenient that the body weight of the torso does not have to be known, because values of density can be estimated from Fig. 5. Body type (lean–normal–obese) can be estimated from physical inspection of the corpse.

TABLE 2—*Thermal properties of materials.*

	Wood (yellow pine)	Human Tissue (lean)	Human Tissue (average)	Human Tissue (obese)	Human Tissue (very obese)
k, W/(m K)	0.120	0.36	0.40	0.36	0.34
ρ, kg/m^3	61.8	891	880	870	873
C_p, J/(kg K)	3000	3519	3414	3252	3083

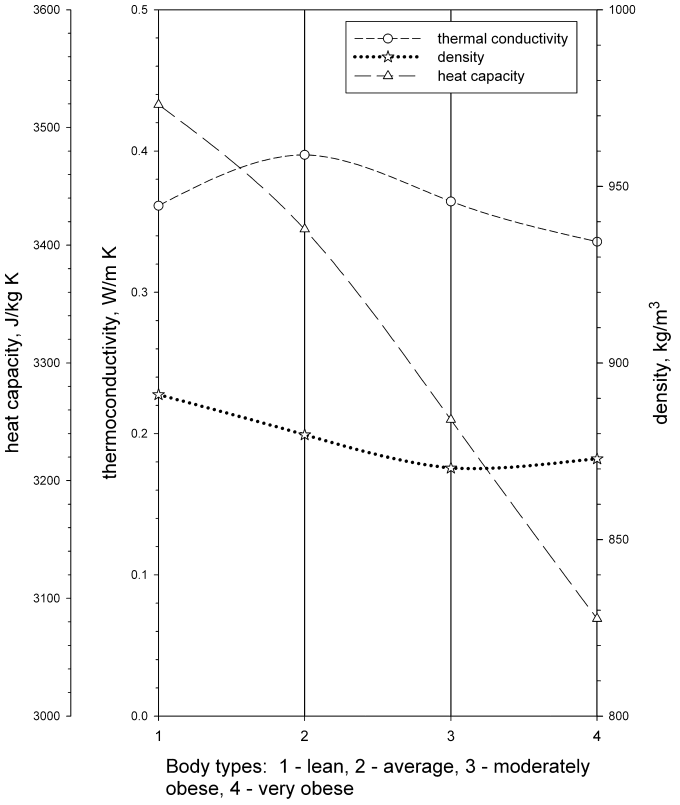

FIG. 5—*Estimated thermal properties of a human torso; based upon actual data from Reference (14).*

As cylinder diameter is an important input variable into the Fourier Series Model, it necessary to determine the diameter of the torso. This can be carried out by measuring the circumference of the torso at an average location and calculating an equivalent diameter. Again, from the sensitivity analysis of Fig. 3, the model is relatively insensitive to errors in torso radius.

Given the sensitivity of the model to changes in temperature, how can we ensure these critical temperature variables are closely tracked? In most cases, the initial body temperature is not known. It can typically vary between reported values of 34.2°C (hypothermia) and 37.7°C, with even excursions up to 104.2°C when drugs, fever, or body trauma are involved (4). Often, unless the body is in a thermostatically controlled room or in a large body of water, some variations in ambient temperature conditions will occur. For forensic modeling, if a normal-size body (normal posture, normal initial body temperature, and minimal clothing) is discovered in an ordinary, small to moderately sized thermostatically controlled room, a predictive model stands a good chance of providing a close estimate as to time of death. If that same body is discovered outside, under conditions of variable weather and wind (forced convection effects), a predictive model may not be so reliable.

The Fourier Series Model cannot be used if significant information about the cooling curve is not known. There must be confidence in the average temperature value of the surroundings (ambient conditions). The following conditions will also render the model unreliable: strong solar radiation, if the condition of the body is unusual or different than normal, if the body is moved from its original location, and if there are strong climatic changes or cooling conditions present.

The following procedure is recommended for application of the Fourier Series Model to the forensic scene of a recently discovered human corpse. Note the environment, including ambient temperature conditions, position and condition of corpse, clothing, and relative torso size (lean, average, medium, moderately obese, and very obese). Take a rectal temperature and note the time. Leave the body as found; do not disturb any existing conditions; discourage any area activity until the investigation is complete. Continue to take a rectal temperature reading every 2 h until the body temperature achieves steady-state conditions. If this is not practical, collect as much of the cooling curve as possible. Plot these temperature points; this is called the field data curve. Measure torso length and determine an equivalent torso diameter. Using an initial body temperature of 37°C and estimated physical properties of torso, set up a five-term Fourier Series Model on a spreadsheet. Adjust the input parameters to the model based upon amount of body clothing, size and condition of the body, and any other mitigating factors. Apply corrective factors to the model to account for any layers of clothing or moving air conditions. Exercise the model to generate a postmortem cooling curve; this is called the model curve. Now, superimpose the model curve upon the actual field data curve to check for fit. Because the model is very sensitive to ambient temperature conditions, adjust this value in the model (typically ± 0–20%) to improve the fit between model and field data curves. For final fit improvement, the initial temperature condition of 37°C might be adjusted a bit (between 36°C and 39°C), because the model is also very sensitive to this variable. The final model curve thus generated represents the postmortem cooling curve and can now be used to estimate exact time of death.

Application of the Fourier Series Model to Literature Values of Postmortem Human Cooling Curve Data

The Fourier Series Model was applied to actual literature data of postmortem human cooling. Lyle's data (26) is commonly used by investigators in modeling the temperature decay curve of postmortem cooling. With Lyle, as with other data sources, the torso diameter is not reported. Unfortunately, this key value will have to be assumed for inclusion into the Fourier Series Model. Also, Lyle does not report body type. An average body type (see Fig. 5 for thermal properties) and a torso diameter of 0.3 m were assumed. Refer to Table 1 for values of other variables assumed in the execution of the raw model. Results of the raw Fourier Series Model are illustrated in Fig. 6. In the absence of vital torso diameter and body type information, the model fit to the literature data is not particularly good. By assuming a larger diameter torso, a decreased value of ambient temperature conditions, and a lean body type, the fit of the adjusted Fourier Series Model to the Lyle data is significantly improved (R^2 = 0.9844).

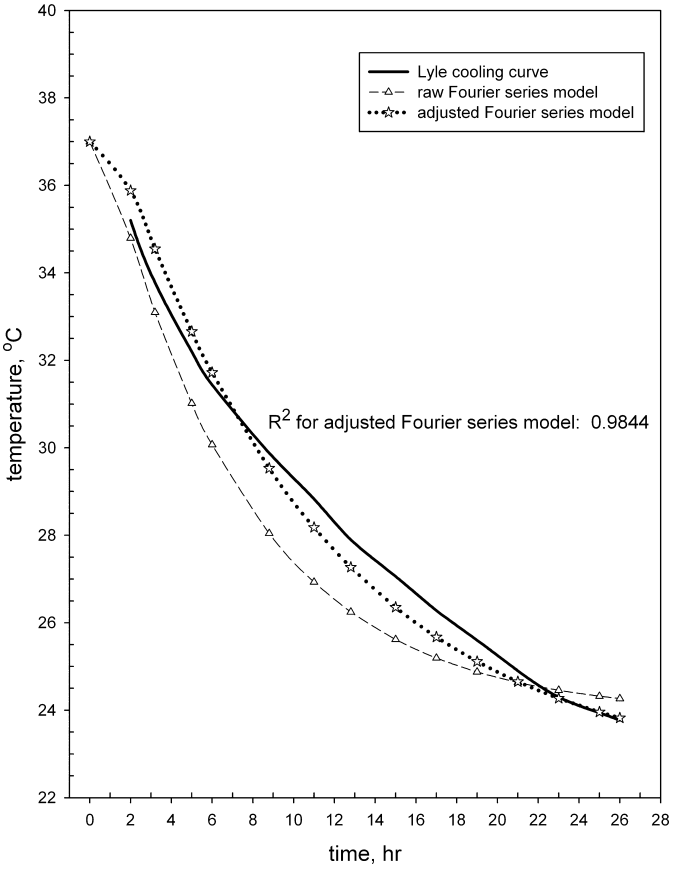

FIG. 6—*Application of Fourier Series Model to postmortem cooling curve (Lyle data).*

Conclusions

The purpose of this investigation was to return to fundamental principles of heat transfer and derive a suitable model to establish a firm basis for constructing a postmortem human cooling curve. A Fourier Series Model was successfully applied to unsteady heat transfer within a wooden cylinder in controlled laboratory conditions. By manipulation of the model, sensitivity analyses were performed to observe the impact of changes in values of input variables. Variables of initial temperature of the cylinder and ambient surrounding temperature were shown to be very sensitive and have the most impact upon predictive results of the model. Finally, it was demonstrated how the Fourier Series Model can be applied to estimate the time of death for humans. The model was applied to a postmortem human cooling curve from existing literature values. Even though the model was tested against one set of field data from literature, much more testing is required to truly validate use of the model under various field conditions. Also, unfortunately, there is no torso diameter data reported in existing field data literature. Other pathologists and crime scene investigators are invited to collect field data—along with torso diameter measurements—to validate the model and improve its predictive powers. The Fourier Series Model, Eq. 2, works well for idealized, controlled laboratory conditions. In the end, for the model to be useful to practitioners, it will necessarily have to be modified and adapted to realistic field conditions. To date, investigation is continuing in our laboratory to further refine the model to predict time of death under other conditions besides natural convection of a naked body resting on a thermally indifferent base. This includes conditions of various levels of clothing and forced convection.

Nomenclature

A surface area, m^2
A thermal diffusivity, $k/\rho C_p$, m^2/s
Bi Biot number, dimensionless
C_p heat capacity, J/(g K)
$\hat{F}o$ fourier number, $\alpha t/r_o^2$, dimensionless
h heat transfer coefficient, W/(m^2 K)
J joule(s)
J_1, J_o bessel functions of the first kind.
k thermal conductivity, W/(m K)

K Kelvin
LHS left hand side
λ_n eigenvalues; positive roots of the transcendental equation, $\mathrm{Bi} = \lambda_n [J_1(\lambda_n)/J_o(\lambda_n)]$
m meter
n order of Bessel function or summation of terms in the Fourier series.
ϕ phi-direction in cylindrical coordinates
q_x heat transfer rate in the x-direction, watts
$\dot{q}$ rate of heat generation, watts
RHS right hand side
r radius, m
ρ density, kg/m^3
T temperature within the cylinder at a position r and at time t, °C
T_{initial} initial uniform temperature of the cylinder, °C
T_∞ ambient temperature conditions surrounding the outside of the cylinder, °C
t time, s
θ unaccomplished temperature change, $(T - T_\infty)/(T_{\text{initial}} - T_\infty)$, dimensionless
V volume, m^3
W watt(s), J/s
x one-dimensional x-direction in Cartesian coordinates
z z-direction in cylindrical coordinates

References

1. Sachs JS. Corpse: nature, forensics, and the struggle to pinpoint time of death. Cambridge, MA: Perseus Books, 2001.
2. Miller H. What the corpse revealed: murder and the science of forensic detection. New York, NY: St Martin's Press, 1999.
3. Kaliszan M, Hauser R, Kernbach-Wighton G. Estimation of the time of death based on the assessment of post mortem processes with emphasis on body cooling. Legal Med 2009;11:111–7.
4. Henssge C. The estimation of the time since death in the early postmortem period, 2nd edn. London: Arnold Publishing, 2002.
5. Marshall TK, Hoare FE. Estimating the time of death: the rectal cooling after death and its mathematical expression. J Forensic Sci 1962;7:56–81.
6. Marshall TK. Estimating the time of death: the use of body temperature in estimating the time of death. J Forensic Sci 1962;7:211–21.
7. Marshall TK. Estimating the time of death: the use of the cooling formula in the study of postmortem body cooling. J Forensic Sci 1962;7:189–210.
8. Marshall TK. Temperature methods of estimating the time of death. Med Sci Law 1965;5(4):224–32.
9. Marshall TK. The use of body temperature in estimating the time of death and its limitations. Med Sci Law 1969;9(3):179–82.
10. Brown A, Marshall TK. Body temperature as a means of estimating the time of death. J Forensic Sci 1974;4:125–33.
11. Mall G, Eisenmenger W. Estimation of time since death by heat flow finite-element model. part I: method, model, calibration, and validation. Leg Med 2005;7:1–14.
12. Sellier K. Determination of the time of death by extrapolation of the temperature decrease curve. Acta Med Leg Soc 1948;2:279–301.
13. James W, Knight B. Errors in estimating time since death. Med Sci Law 1965;5:111–6.
14. Werner J, Buse M. Temperature profiles with respect to inhomogeneity and geometry of the human body. J Appl Physiol 1988;65:1110–8.
15. US Department of Agriculture editor. Physical properties and moisture relations of wood. In: The encyclopedia of wood. New York, NY: Skyhorse Publishing, 2007;17
16. Incropera FP, DeWitt DP. Fundamentals of heat and mass transfer. New York, NY: J Wiley & Sons, 2002.
17. Schneider PJ. Conduction heat transfer. Addison-Wesley: Reading, MA, 1955.
18. Welty JR, Wicks CE, Wilson RE, Rorrer G. Fundamentals of momentum, heat, and mass transfer, 4th edn. New York, NY: John Wiley & Sons, 2001.
19. Kanawaku Y, Kunetake J, Komiya A, Maruyama S, Masato F. Effects of rounding errors on postmortem temperature measurements caused by thermometer resolution. Int J Legal Med 2007;121:267–73.
20. Al-Alousi LM. A study of the shape of the post-mortem cooling curve in 117 forensic cases. Forensic Sci Int 2002;125:237–44.
21. Hatfield HS, Pugh LGC. Thermal conductivity of human fat and muscle. Nature 1951;24:918–9.
22. Carslaw HS, Jaeger JC. Conduction of heat in solids, 2nd edn. Oxford: Clarendon Press, 1959.
23. Nokes LDM, Hicks B, Knight BH. The post mortem temperature plateau—fact or fiction? Med Sci Law 1985;25:263–4.
24. Lundquist F. Physical and chemical methods for the estimation of the time of death. Acta Med Leg Soc 1959;9:205–13.
25. Hutchins GM. Body temperature is elevated in the early postmortem period. Hum Pathol 1985;16(6):560–1.
26. Lyle HP, Cleveland FP. Determination of the time of death by body heat loss. J Forensic Sci 1956;1:11–24.

Additional information and reprint requests:
Jim Smart, Ph.D.
Department of Chemical & Materials Engineering4810 Alben Barkley Drive
University of Kentucky
Paducah, KY 42002
E-mail: jsmart@engr.uky.edu

JOURNAL OF FORENSIC SCIENCES

J Forensic Sci, November 2010, Vol. 55, No. 6
doi: 10.1111/j.1556-4029.2010.01505.x
Available online at: onlinelibrary.wiley.com

PAPER

GENERAL

Kristen L. Tregar,[1,2] *M.S. and Gloria Proni,*[1] *Ph.D.*

A Review of Forensic Science Higher Education Programs in the United States: Bachelor's and Master's Degrees*

ABSTRACT: As the number of forensic science programs offered at higher education institutions rises, and more students express an interest in them, it is important to gain information regarding the offerings in terms of courses, equipment available to students, degree requirements, and other important aspects of the programs. A survey was conducted examining the existing bachelor's and master's forensic science programs in the U.S. Of the responding institutions, relatively few were, at the time of the survey, accredited by the forensic science Education Programs Accreditation Commission (FEPAC). In general, the standards of the responding programs vary considerably primarily in terms of their size and subjects coverage. While it is clear that the standards for the forensic science programs investigated are not homogeneous, the majority of the programs provide a strong science curriculum, faculties with advanced degrees, and interesting forensic-oriented courses.

KEYWORDS: forensic science, education, survey, bachelor's program, master's program

The number of higher education forensic science degree and certificate programs is rapidly expanding. As recently as 1975, there were only 21 colleges or universities offering degrees in forensic science (1). These programs were limited to bachelor's degrees, master's degrees, and several different doctoral degrees. However, as of 2007, there were 120 colleges or universities offering a wide variety of programs, including undergraduate and graduate certificates, associate degrees, bachelor's degrees, master's degrees, and doctoral degrees. There has been speculation that popular television shows, such as *CSI: Crime Scene Investigation*, are partly responsible for the increase in student interest (2). It was reported in *USA Today* that in 2004, forensic science was the most popular undergraduate major for the second year in a row at West Virginia University (2).

A 2002 Technical Working Group for Education and Training in Forensic Sciences (3), promoted by the National Institute of Justice, proposed guidelines for educational forensic science programs that served as a foundation for the Forensic Science Education Programs Accreditation Commission (FEPAC) that accredits colleges and universities, which have forensic science programs available to their students. FEPAC was initially developed as an ad hoc committee of the American Academy of forensic sciences, which then evolved into a standing committee, and, finally, into a commission, composed of five forensic science educators.

At the time of our research, 15 institutions of the 120 offering forensic science programs had received FEPAC accreditation for their programs, although this number has since increased (26 in May 2009). Although FEPAC accreditation is a major step toward creating national standards for forensic science programs, the availability of such accreditation is relatively new. Although the goal of this study is to provide a snapshot of the current data regarding the programs that were surveyed as they stand now, it is noteworthy to mention that the recent report by the National Association of Sciences (4), finding the forensic science system "fragmented," calls for major reforms in the field in general and with forensic science education and training in particular. Clearly, the call is to provide personnel with improved educational and training backgrounds. The report also calls for mandatory certification and accreditation, which it states should be the responsibility of a National Institute of forensic science.

In 1977, Peterson and De Forest (5) surveyed 22 forensic science/criminalistics degrees in the U.S. and provided a snapshot of the condition and needs of forensic science education. At that time, also the quality and standards of the programs were not uniform, and the authors wished for accreditation and improvements in many programs' aspects.

A 1988 study (6) indicated that the preferred educational background for an entry-level forensic scientist was a bachelor's degree with a strong chemistry component followed by a master's degree in forensic science. Siegel also found that bachelor's degrees in forensic science were not preferred because the general feeling was that these degree programs did not provide sufficient "hard science" courses.

Also in 1988, a study (7) was published that attempted to assess whether or not the graduate forensic science programs available at that time were meeting the needs of the community. Again, it was found that a strong chemistry background was preferred so much, so that approximately half of the managers who responded to the survey preferred to hire individuals with a B.S. in chemistry than

[1]John Jay College of Criminal Justice, Science Department, 445 West 59th Street, New York, NY 10017.
[2]Masters School, Science Department, 49 Clinton Avenue, Dobbs Ferry, New York, NY 10522.
*Presented at the 61st Annual Meeting of the American Academy of Forensic Sciences, February 16–21, 2009, in Denver, CO.

Received 16 April 2009; and in revised form 12 Aug. 2009; accepted 15 Aug. 2009.

individuals with an M.S. in forensic science. Additionally, graduate internships were found to be of significant importance to most laboratory supervisors.

These findings were reiterated by Furton et al. (8), who surveyed laboratory directors. In this study, the authors found that 63% of their respondents required B.S. degrees. Once again, a strong preference was observed for "hard science" courses and a B.S. in chemistry, with bachelor's degrees in forensic science not preferred by laboratory directors.

In 2009, Quarino and Brettell (9) provided an assessment of forensic science education, its historical prospective, and the needs for forensic science graduates. Moreover, the manuscript discusses the future of forensic science education stating that the overall quality of the programs has dramatically improved in the last decade or so.

This study was designed primarily to acquire and catalog data regarding the 120 higher education facilities that offer programs in forensic science. These programs range from undergraduate certificates to doctoral degrees but in this manuscript, only data relative to bachelor's and master's programs are presented. The survey sections requested data on curriculum, number of laboratory hours, prerequisites, and FEPAC accreditation status. Questions regarding postgraduate employment tracking were also included in each program section. The study sought to obtain information that could subsequently be used by institutions to maintain and improve the quality of their programs and by students to have a unified idea about the course offerings available in forensic science education.

Methods

The research was performed as an electronic survey designed using a website called SurveyMonkey®(10). To facilitate completion of data analysis, the amount of time for which the survey was open to participants was limited. The survey was first made available to participants in early October 2007 and was subsequently closed to participants in March 2008. The survey questions and format were designed using methods suggested by Posavac and Carey (11).

Contact information of the 120 institutions offering forensic science programs was obtained using the American Academy of Forensic Scientists website and Internet searches, such as Google. This contact information was entered into a spreadsheet to facilitate usage for mailings and participation tracking.

To gain as much information as possible on the programs offered, the scope of the survey was relatively wide. The electronic version of the survey allowed the participant to skip questions, which were not applicable to their program. To encourage electronic participation, solicitations to participate were sent via e-mail. However, if a participant requested a paper copy of the survey, one was mailed to them with a return envelope.

Results

Over the course of 6 months of data collection, 41 responses (34%) to the survey were obtained. Because of the manner in which the survey was designed, it was possible for participants to omit questions that did not apply to their program or to which they did not have a response. As a result, the number of respondents for each section of the survey varies.

Faculty and Facility Information

Of the 120 institutions surveyed, 37 completed the Faculty and Facility Information section (31%). It was observed that the number of faculty in any given forensic science department varied widely, from as few as one faculty member to as many as 40. The majority of departments were comprised of more than 10 faculty members, although departments of 3–5 or 6–10 members were represented by only slightly fewer departments.

The responding departments varied in the number of tenured faculty they employed, from zero tenured faculty to as many as 20 tenured faculty members. Additionally, the number of adjunct faculty members varied widely, ranging from 0 to 25. In the majority of cases, tenured faculty members outnumbered adjunct faculty members, although in 12 cases (33%), the number of adjuncts was higher when compared to the number of tenured faculty. The number of tenured versus adjunct faculty was the same in only one case. The vast majority of institutions reported having only one to two faculty members, if any, with a bachelor's degree as their highest obtained degree. Similarly, most institutions replied that one to two faculty members had master's degrees as their highest obtained degree. Ten institutions (27%) reported having one to two faculty members holding doctoral degrees, while an additional 10 institutions (27%) reported three to five faculty members with doctoral degrees. Nine institutions (24%) reported 5–10 faculty members with doctoral degrees, and five institutions (14%) replied they had more than 10 faculty members with doctoral degrees.

In 24 cases (65%), the doctoral faculty outnumbered the faculty members with master's degrees, while in four cases (11%), the number of faculty with master's degrees outnumbered those with doctoral degrees. In three cases (8%), the number of faculty with doctoral degrees was equal to those with master's degrees.

Eighteen of 37 respondents (49%) noted that 76–100% of their faculty had attended industry conferences in the last 5 years, with the American Academy of forensic sciences Annual Meeting being the most commonly attended by all respondents. Six of 37 respondents (16%) replied that none of their faculty had attended an industry conference in the last 5 years. Additionally, 14 of 37 respondents (38%) noted that 76–100% of their faculty had published in a peer-reviewed journal within the last 5 years. The *Journal of Forensic Sciences* was the most common journal noted. Twelve of 37 respondents (32%) noted that none of their faculty had published in a peer-reviewed journal in the last 5 years.

Twelve institutions (32%) replied that 76–100% of their faculty worked currently, or had previously worked, in a public or private sector laboratory that specialized in the analysis of forensic materials, while six institutions (16%) noted that none of their faculty had this experience. One respondent (3%) replied that it "didn't matter" whether or not faculty members had worked in this type of environment. In contrast, only four institutions (11%) noted that 76–100% of their faculty had worked as independent consultants in the field of forensic science, while 12 institutions (32%) replied that none of their faculty had this experience.

The remaining questions in this section of the survey asked about the facilities available to students. Twelve of the 37 responding institutions (32%) replied that they had no laboratory space dedicated for use by their forensic science students. Sixteen responding institutions (43%) had one to two dedicated laboratories, while four (11%) noted between 3 and 10 dedicated laboratories, as presented in Fig. 1. The colleges and universities that do not have dedicated facilities may or may not share laboratories with other majors.

Almost all responding institutions (30 of 37—81%) have gas chromatography equipment available for use by their students, while 29 (78%) offer mass spectroscopy, 26 (70%) have high-performance liquid chromatography, 25 (68%) offer ultraviolet spectroscopy, 24 (65%) offer infrared spectroscopy, 23 (62%) have

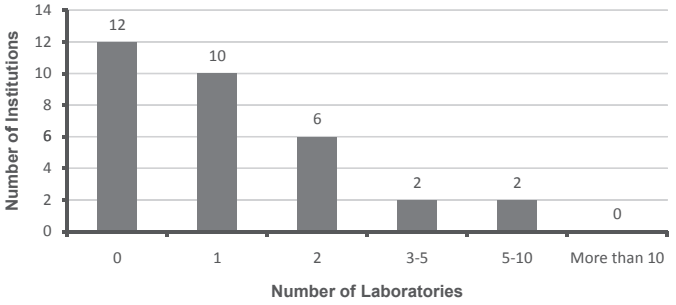

FIG. 1—*Number of laboratories dedicated to forensic science courses.*

polarized light microscopes, and 19 (51%) have nuclear magnetic resonance equipment available. Only 13 institutions (35%) noted that their students had access to a scanning electron microscope (Fig. 2).

Bachelor's Degrees

Twenty-two institutions (54%) replied in the affirmative that they offer bachelor's degrees. Four (18%) of the responding institutions have programs that have been accredited by FEPAC, while the remaining 18 are not accredited. Of those 18 which are not accredited (82%), 12 (67%, or 55% of total sample in this section) stated they were either currently in the process of being accredited, or intended to initiate the process. The remaining six institutions (34%, or 27% of the total sample in this section) do not intend to pursue FEPAC accreditation.

Over the last 5 years, there has been a slight increase in the number of applicants to the responding institutions' programs, although a slight majority of institutions noted a consistent level of more than 50 applicants per year over the last 5 years. Two institutions (9%) noted more than 200 applicants were accepted in each of the last 5 years, while the remaining responding institutions primarily noted levels on the order of 1–20 students per year.

Additionally, it was noted by the respondents that over the last 5 years, the slight majority of the students have been female, with only one institution (5%) noting 60–70% male enrollment in 2007. All other respondents noted less than 60% male enrollment for each year over the last 5 years, with at least two institutions (9%) noting 90–100% female enrollment over the last 5 years.

Despite relatively high enrollment numbers, most responding institutions noted zero to five graduates for each of the last 5 years, with no more than six institutions (27%) noting 5–10 graduates in any given year—this occurred once in 2005. No institution noted more than 30 graduates in any of the last 5 years. Of the institutions surveyed, only seven (32%) responded that they track post-graduate employment. Of those seven, most noted zero to five graduates had gone on to work in the forensic science field. Only one institution (14%) noted that 5–10 of its graduates had gone on to work in the field in 2006 and 2007. No institution noted more than 10 graduates finding employment in the forensic science field.

Ten of 22 responding institutions (46%) noted their program was comprised of 20–30 courses, with the range from as few as six courses to as many as 42. Ten institutions (46%) also noted that 10–15 of the courses they offered were laboratory courses. One institution (5%) did not offer laboratory courses as part of their bachelor's degree. The maximum number of laboratory courses listed was 32. Twelve of 22 respondents (55%) noted their average laboratory class length was 2–3 h.

The majority of institutions (82%) require general biology and general chemistry as part of their standard curriculum. Most schools (64%) also require general physics and organic chemistry. Statistics is required by 55% of responding institutions, while calculus and biochemistry are required by 50%. Physical chemistry is required by 41% of responding institutions. Only one respondent (5%) noted that none of these courses was required by their institution (Fig. 3). One institution (5%) requires bachelor's degree students to write a thesis.

Forensic-oriented subjects available to students in the responding bachelor's degree programs varied widely and are grouped in Fig. 4. Eighty to 90% of responding institutions require courses in

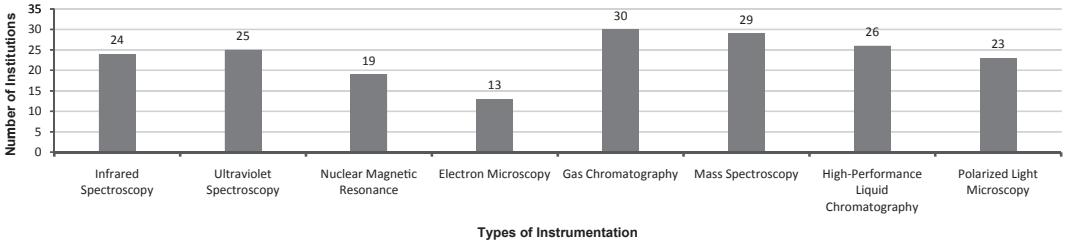

FIG. 2—*Instrumentation available.*

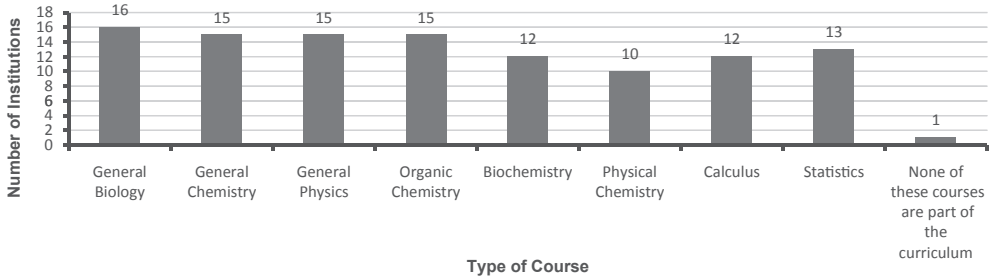

FIG. 3—*Science course required in the forensic science majors investigated.*

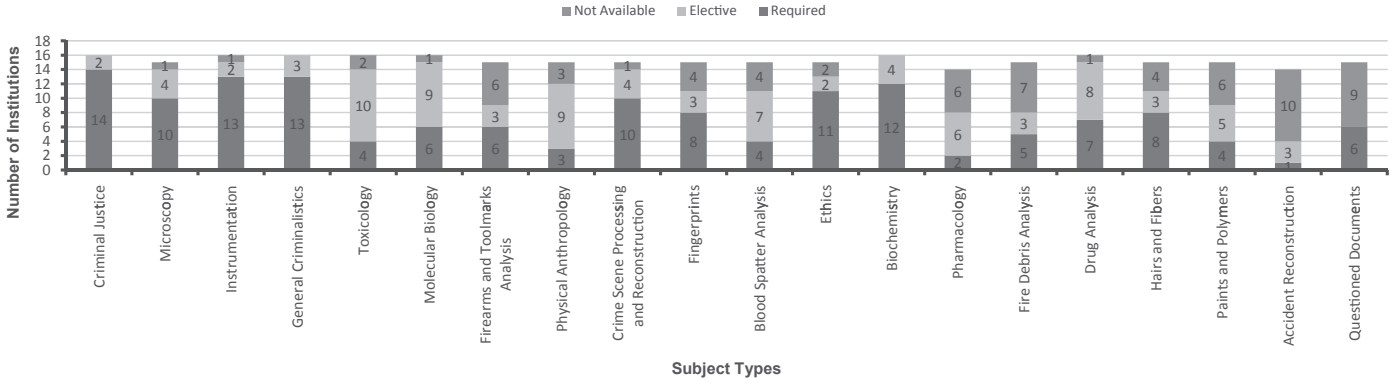

FIG. 4—*Forensic-oriented subjects offered in the forensic science majors investigated.*

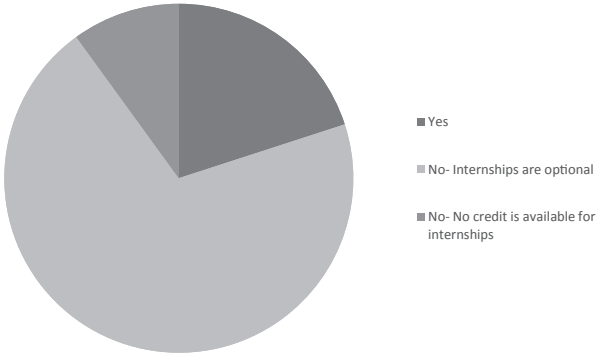

FIG. 5—*Internship requirements.*

criminal justice, instrumentation, and general criminalistics. Seventy to 80% of respondents require microscopy, crime scene processing, ethics, and biochemistry. Only two subjects were available at all the responding institutions: general criminalistics and biochemistry. All other subjects had at least one institution at which they were not available. Toxicology and physical anthropology are offered primarily as elective courses. Pharmacology, accident reconstruction, and questioned documents were among the least available.

All responding institutions give credit for internships, with 11 of 22 (50%) requiring internships for completion of the bachelor's degree (Fig. 5). The required internships varied widely in length from as few as 30 contact hours up to 450 h. Eighteen of 22 responding institutions (82%) noted their programs were designed for individuals seeking entry into the field, while 10 institutions (46%) responded that their program was appropriate for individuals interested in seeking a higher degree. Fifteen of 22 institutions (68%) responded that their bachelor's degree program prepared students for work as a technician, while 14 of 22 (64%) responded that their programs prepared students for low-level analyst positions. Five institutions (23%) felt their program prepared students for mid-level analyst positions, and one respondent (5%) felt their bachelor's degree program prepared their students for supervisory positions.

Master's Degrees

Of 33 anticipated respondents, 12 institutions (36%) replied in the affirmative that their institutions offer master's degrees. Only one responding institution (8%) had acquired FEPAC accreditation, while the remaining 11 (92%) had not. All 11 had either started the application process, or intended to apply for accreditation.

Most institutions noted more than 50 applicants in each of the last 5 years. Of those applicants, fewer than 50 were accepted in any given year, with 7–9 of 10 institutions accepting 30 or fewer applicants per year.

Over the last 5 years, the number of institutions reporting 90–100% of their students were female has increased from one to four. In fact, only one institution (8%) reported a majority of male students at any time over the last 5 years. The remaining institutions all reported at least a 50–50% distribution of male-to-female students.

Beginning in 2003, five institutions (42%) reported zero to five graduates. This trend continued through 2004, with the number of graduates increasing in 2005 to 5–10 graduates. This figure was reported by four institutions (33%) in 2005 and 2007. One institution (8%) reported more than 30 graduates in a given year, 2006. Additionally, in 2005, one institution (8%) noted 20–30 graduates. Of the responding institutions, six (50%) tracked their graduates. Of these, one institution (17%) consistently reported 10–15 of their graduates working in the field each year from 2003 to 2007. The remaining institutions who responded (83%) noted between 0 to 5 or 5 to 10 graduates going on to work in the field in each of the last 5 years.

Six responding institutions (50%) have a thesis option available to their students but do not require one. Four (33%) require a thesis to complete the master's degree. One respondent (8%) has no thesis option.

A significant majority of responding institutions (75%) responded that their master's degree program is comprised of 10–15 courses. Two responding institutions (17%) require only 5–10 courses, and one (8%) requires 20–30 courses to complete the master's degree.

Three institutions (25%) noted that zero to five of the courses included in the master's degree were laboratory courses, while seven (58%) noted their program included 5–10 laboratory courses. No institutions offered more than 10 laboratory courses as part of the master's degree. The lowest number of laboratory courses offered was two, reported by one institution (8%). Laboratory class periods varied in length from 1 to 2 h to more than 5 h, with 2–3 h being the most common. An even distribution was observed across several of the other laboratory lengths. However, two respondents (17%) noted 1–2 h, 3–4 h, and more than 5 h.

The institutions were asked to note which courses were prerequisites for their master's degree program. Only 10 institutions (83%) responded to this question. Of those 10, 100% require general biology, general chemistry, and organic chemistry. Eighty percent require biochemistry and calculus, while 70% require general physics and statistics. Only 40% require physical chemistry, and only

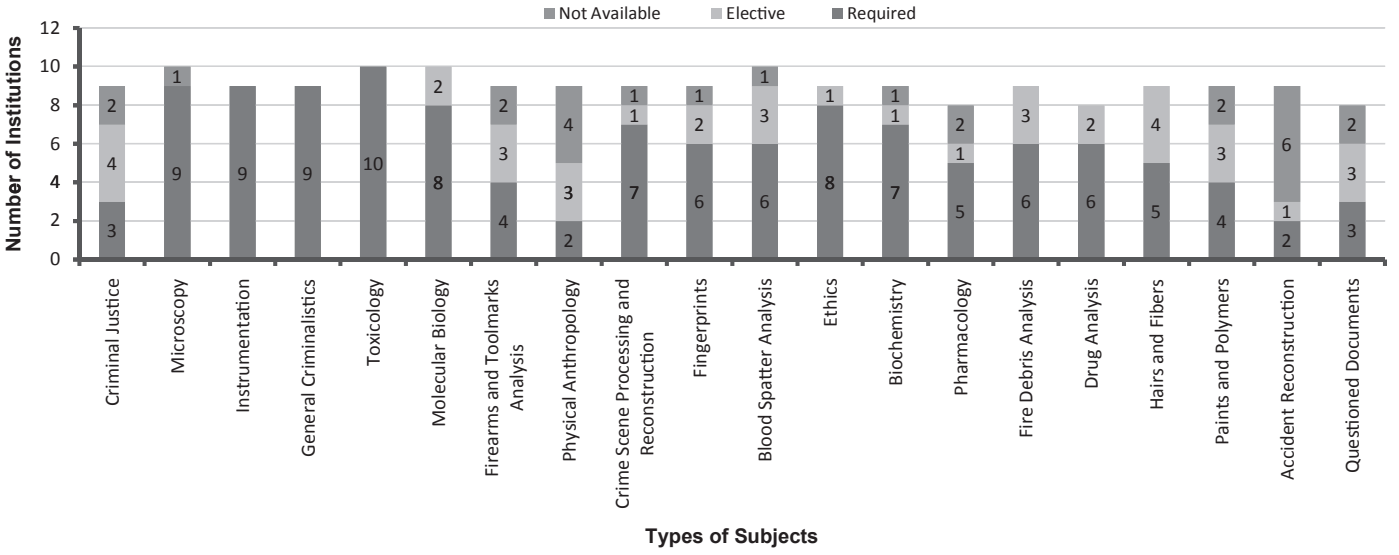

FIG. 6—*Courses offered in the master's programs investigated.*

30% require English. Only one institution (10%) required all courses listed as prerequisites.

Subjects included as part of the master's degree varied, although all questioned subjects were required by at least one institution. Again, only 10 respondents completed this question. Instrumentation, general criminalistics, and toxicology were required by 100% of responding institutions. Microscopy was required by nine institutions (90%) and unavailable at the remaining institution. Ethics was also required by nine institutions (90%), but was offered as an elective by the remaining institution. Physical anthropology and accident reconstruction were the least available, being offered at only five (50%) and three (30%) institutions, respectively. The results are summarized in Fig. 6.

Only two of 10 respondents (20%) noted that their institution required an internship for completion of the master's degree. These internships varied in length from 90 h to 10 weeks. One institution (10%) noted that no credit was available for internships. The remaining seven institutions (70%) offer credit for internships but do not require them.

Ten of 10 responding institutions (100%) noted that their program was intended for individuals seeking entry into the field. Fifty percent of institutions also noted their program was appropriate for individuals already working in the field, or individuals who intended to pursue a higher degree. No respondents believed that their degree was appropriate for an individual who intended to pursue teaching, and only one respondent (10%) believed that their degree was appropriate for individuals interested in management. Seven of 10 respondents (70%) noted they believed their program prepared its students for position as mid-level analysts. Six of 10 (60%) responded that their program prepared students for positions as low-level analysts, while four (40%) stated their program prepared students for positions as technicians. Three of 10 respondents (30%) responded that they believed their program prepared students academic posts or positions as high-level analysts. Only one institution (10%) responded that their program qualified students for supervisory positions.

Discussion and Conclusion

This study received a favorable response rate of 34%, which is considered high for this type of survey analysis. Higgins and Selavka (7) noted a 15% return rate from the surveys used in their study of graduate programs, and Furton et al. (8) noted a similar response rate for their survey of crime laboratory directors. The higher response rate could potentially be attributed to the use of electronic media for the survey as Furton et al. (8) noted that their response rate of 15% was "less than hoped for, but was in keeping with 10–15% return rate typical for mailed surveys."

It is evident from the obtained results that a large variance in non-FEPAC-accredited forensic science higher education programs exists. In the bachelor's degree section of the survey, there was a substantial degree of variation. A majority of 82% were observed only in response to three questions: whether or not the program was accredited (primarily not), what courses were required for this program (general biology and general chemistry), and who the program was intended for (individuals seeking entry into the field). Despite the fact that the only two subjects which all of the programs have in common are biology and chemistry, the programs, requiring several "hard" science courses, provide rigorous scientific coursework to the participants.

It was observed that subjects included in the bachelor's and master's degrees varied considerably in terms of availability and whether or not the subject was required. For the bachelor's degrees, all subjects included in the survey (criminal justice, microscopy, instrumentation, toxicology, molecular biology, crime scene processing, ethics, drug analysis) were required by at least one institution, and yet, almost all the included subjects were listed as unavailable at a minimum of one institution (with the exception of general criminalistics and biochemistry). In the master's degree programs, the same subjects were all again required by at least one institution (instrumentation, criminalistic, toxicology, molecular biology, ethics, fire debris analysis, drug analysis, hairs and fibers, microscopy and crime scene processing, fingerprints, blood spatter analysis, biochemistry) and were more widely available than in the bachelor's degree programs. However, once again, more than half the subjects were unavailable at one institution or more.

The size and scope of the various programs also seemed to vary greatly. The number of accepted students varied considerably, with as few as 0–10 to more than 200 in any given year. The majority of the faculty members at the surveyed institutions hold a doctoral degree and are in tenured or tenure-track positions. The level of

participation to conferences and publication of the faculties at these institutions is quite high. In addition, the majority of the forensic programs have dedicated facilities and instrumentation available. Internships are generally required by the majority of the bachelor's programs in order to graduate.

The most continuity observed between programs was in their student demographics. It was also noticed that over the last 5 years, the majority of students entering forensic science programs were female.

The data collected and examined regarding B.S. and M.S. programs in forensic science tend to show a great variance in programs in all areas from laboratory facilities, number of faculty, educational level of faculty members, and instrumentation available. The mandatory accreditation recommended by the National Association of Scientists necessarily would have the effect of creating more standardized program offerings and would help to ensure the success of the academic mission of producing more well-trained practitioners. However, despite the common perception that forensic science students are not, at the present time, well prepared to serve the needs of that community because of the uneven standards, such perception misses the mark. It is noteworthy to mention that despite the overall variations between the programs, the majority of the institutions investigated provide the scientific coursework deemed necessary by laboratory directors (8), faculties with advanced degrees, and large portions of laboratory hands-on experiences to the participants. Certainly, mandatory accreditation would assist laboratory directors and other forensic personnel in their confidence that graduates of forensic higher education programs have the skills necessary to contribute to the field at large.

Acknowledgments

The authors are grateful to Dr. E. Champeil and S. Sherbell for helpful discussion.

References

1. Kobilinsky L, Sheehan FX. The desirability of a Ph.D. program in forensic science. J Forensic Sci 1984;29(3):706–10.
2. Willing R. 'CSI effect' has juries wanting more evidence. USA Today 2004; Sect. 1A.
3. Technical Working Group for Education, Training in forensic sciences. Education and Training in forensic science: A Guide for forensic science Laboratories, Educational Institutions, and Students. Washington, DC: National Institute of Justice, US Department of Justice Office of Justice Programs DC, 2002.
4. Committee on Identifying the Needs of the Forensic Science Community, Community on Science, Technology, and Law Policy and Global Affairs, Committee on Applied and Theoretical Statistics Division and Engineering and Physical Sciences. Strengthening Forensic Science in the United States: A Path Forward. Washington, DC: National Research Council of the National Academies, National Academies Press, 2009.
5. Peterson JL, De Forest PR. The status of forensic science degree programs in the United States. J Forensic Sci 1977;22(1):18–33.
6. Siegel JA. The appropriate educational background for entry level forensic scientists: a survey of practitioners. J Forensic Sci 1988;33(4):1065–8.
7. Higgins KM, Selavka CM. Do forensic science graduate programs fulfill the needs of the forensic science community? J Forensic Sci 1988;33(4):1015–21.
8. Furton KG, Hsu YL, Cole MD. What educational background do crime laboratory directors require from applicants? J Forensic Sci 1999;44(1): 128–32.
9. Quarino L, Brettell TA. Current issues in forensic science higher education. Anal Bioanal Chem 2009;394(8):1987–93.
10. SurveyMonkey.com LLC, Palo Alto, CA.
11. Posavac EJ, Carey R. Program Evaluations: Methods and case studies. New Jersey: Pearson Prentice Hall, 2006.

Additional information and reprints requests:
Gloria Proni, Ph.D.
Associate Professor
John Jay College of Criminal Justice
Science Department
445 West 59th Street #4405
New York, NY 10019
E-mail: gproni@jjay.cuny.edu

JOURNAL OF FORENSIC SCIENCES

J Forensic Sci, November 2010, Vol. 55, No. 6
doi: 10.1111/j.1556-4029.2010.01504.x
Available online at: onlinelibrary.wiley.com

PAPER

GENERAL

Silvia Tambuscio,[1,2] *M.D.; Elie Boghossian,*[1] *B.Sc.; and Anny Sauvageau,*[1,3] *M.D., M.Sc.*

From Abstract to Publication: The Fate of Research Presented at an Annual Forensic Meeting

ABSTRACT: In forensic sciences, the fate of abstracts presented at international meetings has not yet been assessed. The purpose of this study is to estimate publication ratio and evaluate possible predictors of publication after the 58th edition of the 2006 American Academy of Forensic Sciences annual meeting. Section of the meeting, type of presentation (oral platform or poster), number of authors per abstract and per paper, time span to publication, countries involved, and journal of publication were tabulated. A total of 623 abstracts were presented, from which 102 were subsequently published as a full paper. The overall publication rate was 16.4%, ranging from 3.4% (jurisprudence) to 28.8% (toxicology). The type of presentation (oral platform or poster) did not significantly affect the outcome of the abstract. However, a higher number of authors, foreign authors, and international collaboration were found to be good predictive factors of publication.

KEYWORDS: forensic science, bibliometry, meeting abstracts, publication ratio, international collaboration, peer-review, number of authors

Scientific presentations at professional organization meetings provide a valuable forum for rapid dissemination of latest research and new knowledge to a large and interested audience (1–4). Meetings attendees often assume that information contained in an abstract presentation is of equal value to studies published in peer-reviewed journals (4). However, peer-reviewed publications allow a more rigorous evaluation of the design, methods and conclusions of a paper than abstract acceptance, as conference scientific committees decide on abstract acceptance or refusal based on limited information contained in the abstract itself (1,2,5). Although acceptance of an abstract at the American Academy of Forensic Sciences (AAFS) meeting is prestigious, publication in a peer-reviewed journal remains the ultimate validation of research findings. The usefulness of research reports presented in abstract form at scientific meetings is a concern (3,6).

A possible measurement of quality of abstracts presented in scientific meetings is the abstract to publication ratio, representing the proportion of abstracts published in peer-reviewed journals (5,7). This ratio has been studied for several international meetings, ranging from 8.5% to 78% (2–5,8–20).

In forensic sciences, the fate of abstracts presented at international meetings has not yet been evaluated. The aim of this study is to estimate publication ratio and time span to publication as well as to appraise possible predictors of publication for forensic sciences meetings.

[1]Laboratoire de sciences judiciaires et de médecine légale, Montreal, Canada.
[2]Private consultant in legal medicine for the court of Padua, Italy.
[3]Office of the Chief Medical Examiner, Edmonton, Canada.

Received 21 May 2009; and in revised form 3 Aug. 2009; accepted 15 Aug. 2009.

Materials and Methods

The AAFS meeting was chosen for this study as in our opinion, it represents one of the most important international meetings in forensic sciences. All abstracts of the 58th edition of the 2006 AAFS annual meeting, in Seattle, were searched in the PubMed database of the National Library of Medicine for subsequent corresponding published paper in peer-reviewed journals. The search in PubMed was performed using multiple strategies, beginning with the lead author and then, if necessary, combinations of co-authors, title, and keywords. Papers found on PubMed were closely compared to the proceeding abstracts to confirm correspondence of both. The complete abstract search was done by an undergraduate student. Two forensic experts then double-checked the search, one reviewing 10% of abstracts and the other reviewing all published abstracts and 10% of unpublished ones. For a few problematic abstracts, full-length articles were screened by the three judges and a consensus decision was achieved. Furthermore, abstracts from three sections of the AAFS meeting, namely engineering sciences, jurisprudence, and questioned documents, were also searched through the FORS Forensic Bibliographic Database. Finally, for all published and unpublished abstracts, the following variables were compiled: section of the meeting, type of presentation (oral platform or poster), number of authors per abstract and per paper, time span to publication, countries involved, and journal of publication. The reported data were statistically analyzed using the SPSS Statistics 17.0 software.

Results

For the 58th edition of the 2006 AAFS annual meeting, 623 abstracts were presented at the meeting, from which 102 were subsequently published as a full paper in a peer-reviewed journal.

TABLE 1—*Publication ratio.*

	Meeting Abstracts	Published Abstracts	Publication Ratio (%)
AAFS meeting—all sections	623	102	16.4
Criminalistics	174	38	21.8
Engineering sciences	37	3	8.1
General	54	5	9.3
Jurisprudence	29	1	3.4
Odontology	46	9	19.6
Pathology/biology	107	17	15.9
Physical anthropology	84	11	13.1
Psychiatry & behavioral science	16	1	6.3
Questioned documents	24	2	8.3
Toxicology	52	15	28.8

AAFS, American Academy of Forensic Sciences.

TABLE 2—*Publication ratio in relation to type of presentation.*

	Publication Ratio (%)		
	Oral	Poster	*p*
AAFS meeting—all sections	17.2	14.6	0.4219
Criminalistics	23.6	18.8	0.4512
Engineering sciences	8.3	–	0.7633
General	8.1	11.8	0.6636
Jurisprudence	3.7	–	0.7819
Odontology	19.5	20.0	0.9792
Pathology/biology	21.2	7.3	0.0559
Physical anthropology	18.9	3.2	0.0403
Psychiatry & behavioral science	7.1	–	0.6963
Questioned documents	9.5	–	0.5766
Toxicology	23.1	34.6	0.3585

AAFS, American Academy of Forensic Sciences.

TABLE 3—*Average number of authors.*

	Meeting Abstract	Unpublished Abstract	Published Abstract
AAFS meeting—all sections	2.9	2.7	3.7
Criminalistics	3.4	3.1	3.8
Engineering sciences	2.1	2.0	3.3
General	2.3	2.2	2.8
Jurisprudence	1.8	1.6	6.0
Odontology	2.4	2.1	3.0
Pathology/biology	3.2	3.0	4.2
Physical anthropology	2.5	2.5	2.7
Psychiatry & behavioral science	3.3	3.2	4.0
Questioned documents	2.3	2.4	1.0
Toxicology	3.5	3.4	4.7

AAFS, American Academy of Forensic Sciences.

TABLE 4—*Time span to publication.*

	Number of Months to Publication (average ± standard deviation)
AAFS meeting—all sections	10 ± 9
Criminalistics	8 ± 9
Engineering sciences	8 ± 1
General	16 ± 6
Jurisprudence	11*
Odontology	7 ± 7
Pathology/biology	12 ± 10
Physical anthropology	12 ± 9
Psychiatry & behavioral science	21*
Questioned documents	11 ± 8
Toxicology	13 ± 10

*Only one published paper for this section.
AAFS, American Academy of Forensic Sciences.

The majority of those papers were published in the AAFS's journal, the *Journal of Forensic Sciences* (64.7%).

Publication Ratio

The overall publication rate was 16.4%, ranging from 3.4% (for the Jurisprudence section) to 28.8% (for the Toxicology section). Table 1 illustrates detailed results for each section of the meeting. Although Criminalistics ranged second considering the publication rate (21.8%), in absolute number, it published more papers than all other sections. Of the 38 papers published by the Criminalistics section, about half were directly or indirectly related to DNA or RNA (21 papers), whereas the other half were not (17 papers).

Type of Presentation

In general, oral presentations were more likely to be later published than poster presentations, with respective publication ratios of 17.2% and 14.6% (Table 2). However, this difference was not statistically significant ($p = 0.4219$). The only exception appeared in the Physical Anthropology section, with a statistically significant difference for the publication ratios of oral (18.9%) and poster (3.2%) presentations.

Number of Authors

Overall, the average number of authors per abstract was of 2.9. This number of authors per abstract was higher for published abstracts (3.7) compared to unpublished ones (2.7) (Table 3). This difference was statistically significant ($p = 0.0001$).

Time Span to Publication

The time span to publication averaged 10 ± 9 months (Table 4). Among the published articles, 13% were published before the AAFS conference, 52% were published within a year, and 75% within 1.5 years.

Countries Involved and International Collaboration

As expected, American authors outnumbered foreigners at this American meeting (USA 76%, other countries 20%, and international collaboration 4%). Publication ratio, however, was highest for abstracts written in international collaboration (37%), followed by abstracts from non-USA authors (21%), whereas USA authors presented the lowest publication rate (14%) (Table 5). Statistical analysis revealed a strong association between the geographic source and the publication ratio ($p = 0.0021$; non-USA vs. USA $p = 0.0538$, international collaboration vs. USA $p = 0.0012$). Publication rates for non-USA countries are compared in Table 6.

Discussion

Since the 1950s, scientists have been noticing that not more than half of the papers presented at scientific meetings are ultimately

TABLE 5—*Countries involved and their publication ratio.*

	Meeting Abstract	Unpublished Abstract	Published Abstract
AAFS—all sections			
USA	472	406 (86.0%)	66 (14.0%)
Non-USA	124	98 (79.0%)	26 (21.0%)
International collaboration	27	17 (63.0%)	10 (37.0%)
Criminalistics			
USA	147	118	29
Non-USA	20	16	4
International collaboration	7	2	5
Engineering sciences			
USA	25	24	1
Non-USA	10	8	2
International collaboration	2	2	0
General			
USA	42	40	2
Non-USA	10	8	2
International collaboration	2	1	1
Jurisprudence			
USA	24	24	0
Non-USA	5	4	1
International collaboration	0	0	0
Odontology			
USA	28	26	2
Non-USA	16	10	6
International collaboration	2	1	1
Pathology/biology			
USA	66	57	9
Non-USA	34	27	7
International collaboration	7	6	1
Physical anthropology			
USA	67	60	7
Non-USA	12	9	3
International collaboration	5	4	1
Psychiatry & behavioral science			
USA	13	12	1
Non-USA	2	2	0
International collaboration	1	1	0
Questioned documents			
USA	18	16	2
Non-USA	6	6	0
International collaboration	0	0	0
Toxicology			
USA	42	29	13
Non-USA	9	8	1
International collaboration	1	0	1

AAFS, American Academy of Forensic Sciences.

TABLE 6—*Non-USA countries involved and their publication ratio.*

	Meeting Abstract	Published Abstract	Publication Ratio (%)
Canada	28	3	10.7
Italy	20	2	10.0
China	14	1	7.1
United Kingdom	12	5	41.7
France	8	3	37.5
Netherlands	7	2	28.6
Switzerland	5	4	80.0
Australia	5	2	40.0
Germany	4	1	25.0
Belgium	3	3	100.0
Other Countries	18	0	–
Total	124	26	21.0

being published as full-text articles in peer-reviewed journals (21,22). Hence, quality evaluation and outcome of scientific meetings have become an increasing topic of interest bringing diverse medical specialties to evaluate the fate of their research.

Publication Ratio

The AAFS publication rate was 16%. The majority of published papers appeared in the *Journal of Forensic Sciences*. This comes as no surprise because the policy of AAFS is to request presenters to submit their papers for publication in the *Journal of Forensic Sciences* within 6 months of the meeting.

Publication ratios have been studied for several scientific meetings outside forensics (Table 7). Those ratios are highly variable from one scientific organization to the next, ranging from 8.5% to 78%. Almost all those studies, however, presented a publication ratio of more than 30%. The AAFS publication rate of 16% is therefore much more inferior to what was expected. The reasons underlying the observed lower publication ratio in forensics as compared with the other medical specialties are difficult to explain. A survey sent to the abstracts' authors could have been an interesting approach, revealing specific reasons for the nonpublication as full-paper articles. Nevertheless, it remains a necessity, as a scientific field, to improve this publication ratio. Generally, it has been emitted that the reasons for the nonpublication of abstracts are multifactorial, habitually depending on the author's resources (whether financial, human, etc.) or his behavior (as in studies providing negative or statistically nonsignificant results are less encouraging to publish), the quality of abstracts (some abstracts may not fit higher requirements of the journal reviewers), and mostly lack of time to achieve a full-text article after the meeting (1–4,9).

One factor is probably important in explaining the low publication rate at the AAFS compared to other scientific meetings: the fraction of academic presenters at the AAFS is probably on the low side compared to other meetings compiled in Table 7. Academia provides powerful incentives for peer-reviewed publication, almost to the extent of "publish or perish." Private practice forensic scientists (psychiatrists, questioned document examiners, engineers) and public sector medical examiners and laboratory offer no rewards for publication. In keeping with that, it is interesting to note that in this study, the sections with the highest publication rates are mostly those with higher academically based members.

The lack of incentives for publication may therefore be a major factor in the low publication rates at the AAFS. On the other hand, there are several incentives for presentation. AAFS (and its sections) creates incentives to present at the annual meeting through promotion criteria. Furthermore, some certification bodies (like ABC) award points toward recertification for these presentations. Doctors, dentists, and lawyers can get continuing education credits toward maintenance of certification in the same way. Agencies which pay to send people to meetings also often require that a presentation be given to justify the costs. Unfortunately, these incentives do not carry over to converting the presentations to peer-reviewed publication. To help our field of science to continue to grow and develop, it may be useful that some incentives to publications are put in place.

Type of Presentation

At the AAFS meeting, the type of presentation does not seem to be a predictor of publication. Indeed, there was no statistical difference between the publication ratio of oral (17.2%) and poster (14.6%) presentations. This is in keeping with a previous study, conducted by Ng et al. (2) following an American Urological Association meeting, revealing that podium presentations are not more likely to be published. However, a study by Gilbert and Pitkin (1), after a Society for Maternal-Fetal Medicine meeting, differs from the prior assertion and effectively identifies plenary session

TABLE 7—*Comparative publication ratio of other scientific organizations.*

Reference	Scientific Organization	Year(s)	Publication Ratio (%)
19	Journées Françaises de Radiologie (JFR96)	1996	8.5
18	American Society of Health System Pharmacists (ASHP)	1994	11
17	North American Congress of Clinical Toxicology (NACCT)	2001	24.1
4	Radiological Society of North America (RSNA)	1993	33
9	American Academy of Orthopaedic Surgeons	1996	34.2
5	Royal Australian and New Zealand College of Radiologists (RANZCR)	1996–1999	35
4	American Society of Neuroradiology (ASNR)	1993	37
2	American Urological Association (AUA)	1998–2000	37.8
3	European Congress of Radiology (ECR)	2000	39
15	North American Spine Society (NASS)	1990–1992	40
12	European Society of Anaesthesiologists (ESA)	1995	42.2
8	Society for Academic Emergency Medicine (SAEM)	1991	45
10	Paediatric Orthopaedic Society of North America (POSNA)	1991–1994	45
13	Perinatal Society of Australia and New Zealand (PSANZ)	1997	45
15	International Society for the Study of the Lumbar Spine (ISSLS)	1991–1993	45
15	Scoliosis Research Society (SRS)	1991–1993	47
16	Arthroscopy Association of North America (AANA)	1991–1993	50.9
11	American Pancreatic Association (APA)	1994–1995	54.3
11	European Pancreatic Club (EPC)	1994–1995	59.7
16	American Orthopaedic Society for Sports Medicine (AOSSM)	1990–1993	68.1
14	Otorhinolarygological Research Society (ORS)	1978–1995	69.09
20	American Society of Clinical Oncology (ASCO)	1984	78
	Average publication ratio		41.7

presentations as a predictor of further publication compared to slide or poster presentations with an odds ratio of 2.57. Therefore, it seems that the predictive value of oral versus poster presentation differs depending on the medical specialty and the meeting. Considering the publication ratio as a marker of quality, poster and oral presentations seem to be of similar value at the AAFS meeting.

Number of Authors

In the last 25 years, the average number of authors per article has doubled in North-American forensic science (23). This significant augmentation in the average number of authors per article is not specific to our field. In fact, this seems to be a generalized trend in science, as demonstrated by Shaban (24) in a study of authorship in prestigious journals from 1950 to 2005: the number of authors per article increased over time in a linear fashion while the number of single-author articles decreased. Several authors have discussed the ethical issues related to this situation, with particular attention toward the problem of gift and ghost authorship (23,25–27).

In this study, the average number of authors in published abstracts (3.7) clearly surpassed the one for unpublished abstracts (2.7), suggesting this factor holds a positive effect on publication ratio. Indeed, working in teams may increase the productivity of research, permitting an adequate share-out of the work and a pooling of skills and resources. As far as we know, this study is the first of its type to ever consider the number of authors as a predictor of publication. Although we fully agree that the increase in the number of authors in the recent decades raises several important ethical questions, team work is an important aspect of science that should not be discouraged.

Time Span to Publication

Furthermore, previous authors have noted that the abstracts ultimately published in indexed journals are majorly in print with an average time course of 9.5 months and within 4 years of abstract presentation (20,28–32). Following the AAFS conference, 75% of the abstracts were published in a peer-reviewed journal within 1.5 years, with a mean time lag of 10 months after presentation. This data proves to be concordant with the other medical fields. Nonetheless, the relatively shortness of our follow-up period since the presentation of abstracts at the AAFS meeting in February 2006 may lead to a minor underestimation of the publication ratio. As already mentioned, a further small but significant quota of articles is published 2–4 years after a scientific meeting (1,4).

Countries Involved and International Collaboration

In this study focusing on an American meeting, 75.8% of abstracts were presented by USA authors, with a lower publication ratio for these local authors (14%) compared to foreigners (21%). This tendency for local authors presenting more abstracts yet generating a lower publication ratio was also observed in a previous study by Miguel-Dasit et al. (3) in a European radiologic meeting, Europeans were proportionately more represented among abstract presenters but had a lower publication ratio than American authors.

International collaboration has been proven to be an efficient mean to advance research and to enhance publication capacity (3,23,33). In keeping with the latter, a high rate of subsequent publication for abstracts presented in an international collaboration setting was noticed in this study (37.0% compared to 14% for USA-only authors). Therefore, international collaboration seems an effective predictor of publication outcome.

Study Limitation

This study is the first to study the fate of abstract in forensic sciences. Further studies are needed before a good picture of our science field could be drawn and compared to our scientific fields. This study has some selection bias that also needs consideration. The AAFS was chosen but other forensic meetings should be studies as well. The 2006 meeting may not have been representative of all other AAFS meetings. Furthermore, as the assessment of the publication status was mainly accomplished consulting the PubMed browser, articles published in journals not included in the Medline database were initially ruled as unpublished. For this reason, an improved research strategy was adopted by the authors who

consulted the FORS Forensic Bibliographic Database for three sections of the AAFS meeting, namely engineering sciences, jurisprudence, and questioned documents. An additional published article in engineering sciences was found through this search motor, proving the presence of a minor selection bias.

Conclusion

Forensic scientists are encouraged to publish their findings, as abstracts that fail to attain subsequent publication remain valueless in forensic sciences, their data being hardly accessible and of dubious validity owing to lack of rigorous peer-review. As good predictors of publication are a higher number of authors and international collaboration, authors are incited to work in teams, locally and internationally, to increase the productivity of research. Research teams must be careful, however, to avoid gift authorship.

Acknowledgment

The authors gratefully thank Dr. Marie-Josée Perron, forensic odontologist, for her help in this project.

References

1. Gilbert WM, Pitkin RM. Society for Maternal-Fetal Medicine meeting presentations: what gets published and why? Am J Obstet Gynecol 2004;191(1):32–5.
2. Ng L, Hersey K, Fleshner N. Publication rate of abstracts presented at the annual meeting of the American Urological Association. BJU Int 2004;94(1):79–81.
3. Miguel-Dasit A, Martí-Bonmatí L, Aleixandre R, Sanfeliu P, Bautista D. Publication of material presented at radiologic meetings: authors' country and international collaboration. Radiology 2006;239(2):521–8.
4. Marx WF, Cloft HJ, Do HM, Kallmes DF. The fate of neuroradiologic abstracts presented at national meetings in 1993: rate of subsequent publication in peer-reviewed, indexed journals. Am J Neuroradiol 1999;20(6):1173–7.
5. Bydder SA, Joseph DJ, Spry NA. Publication rates of abstracts presented at annual scientific meetings: how does the Royal Australian and New Zealand College of Radiologists compare? Australas Radiol 2004;48(1):25–8.
6. McCormick MC, Holmes JH. Publication of research presented at the pediatric meetings. Change in selection. Am J Dis Child 1985;139(2): 122–6.
7. Walby A, Kelly AM, Georgakas C. Abstract to publication ratio for papers presented at scientific meetings: how does emergency medicine compare? Emerg Med 2001;13(4):460–4.
8. Weber EJ, Callaham ML, Wears RL, Barton C, Young G. Unpublished research from a medical specialty meeting: why investigators fail to publish. JAMA 1998;280(3):257–9.
9. Sprague S, Bhandari M, Devereaux PJ, Swiontkowski MF, Tornetta P 3rd, Cook DJ, et al. Barriers to full-text publication following presentation of abstracts at annual orthopaedic meetings. J Bone Joint Surg Am 2003;1:158–63.
10. Jackson KR, Daluiski A, Kay RM. Publication of abstracts submitted to the annual meeting of the Pediatric Orthopaedic Society of North America. J Pediatr Orthop 2000;20(1):2–6.
11. Timmer A, Blum T, Lankisch PG. Publication rates following pancreas meetings. Pancreas 2001;23(2):212–5.
12. Castillo J, Garcia-Guasch R, Cifuentes I. Fate of abstracts from the Paris 1995 European Society of Anaesthesiologists meeting. Eur J Anaesthesiol 2002;19(12):888–93.
13. Davies MW, Dunster KR, East CE, Lingwood BE. Fate of abstracts published in the proceedings of the first annual Perinatal Society of Australia and New Zealand Congress in 1997. J Paediatr Child Health 2002;38(5):501–6.
14. Roy D, Sankar V, Hughes JP, Jones A, Fenton JE. Publication rates of scientific papers presented at the Otorhinolarygological Research Society meetings. Clin Otolaryngol Allied Sci 2001;26(3):253–6.
15. Wang JC, Yoo S, Delamarter RB. The publication rates of presentations at major Spine Specialty Society meetings (NASS, SRS, ISSLS). Spine 1999;24(5):425–7.
16. Yoo S, Oh G, Wang JC. Publication rates of presentations made at annual meetings of the American Orthopaedic Society for Sports Medicine and the Arthroscopy Association of North America. Am J Orthop 2002;31(6):367–9.
17. Smollin CG, Nelson LS. Publication of abstracts presented at 2001 NAACT. J Med Toxicol 2006;2(3):97–100.
18. Byerly WG, Rheney CC, Connelly JF, Verzino KC. Publication rates of abstracts from two pharmacy meetings. Ann Pharmacother 2000;34(10):1123–7.
19. Arrivé L, Dono P, Lewin M, Dahan H, Monnier-Cholley L, Tubiana JM. Publication rate of original papers orally presented at the Journées Françaises de Radiologie 1996. J Radiol 2001;1:1719–22.
20. De Bellefeuille C, Morrison CA, Tannock IF. The fate of abstracts submitted to a cancer meeting: factors which influence presentation and subsequent publication. Ann Oncol 1992;3(3):187–91.
21. Liebesny F. Lost information: unpublished conference papers. In: Proceedings of the International Conference on Scientific Information; 1958 Nov 16-21; Washington, DC. Washington, DC: The National Academies Press, 1959;475–9.
22. Oseman RH. Conferences and their literature. London, England: Library Association Publishing, 1989.
23. Sauvageau A, Desnoyers S, Godin A. Mapping the literature in forensic sciences: a bibliometric study of North-American journals from 1980 to 2005. Open Forensic Sci J 2009;2:41–6.
24. Shaban S. Multiple authorship trends in prestigious journals from 1950 to 2005. Saudi Med J 2007;28(6):927–32.
25. Benos DJ, Fabres J, Farmer J, Gutierrez JP, Hennessy K, Kosek D, et al. Ethics and scientific publication. Adv Physiol Educ 2005;29(2):59–74.
26. Jones AW. The distribution of forensic journals, reflections on authorship practices, peer-review and role of the impact factor. Forensic Sci Int 2007;3:115–28.
27. Rennie D, Flanagin A. Authorship! Authorship! Authorship! Guests, ghosts, grafters, and the two-sided coin. JAMA 1994;271:469–71.
28. Scherer RW, Dickersin K, Langenberg P. Full publication of results initially presented in abstracts: a meta-analysis. JAMA 1994;272:158–62.
29. Yentis SM, Campbell FA, Lerman J. Publication of abstracts presented at anaesthesia meetings. Can J Anaesth 1993;40:632–4.
30. Juzych MS, Shin DH, Coffey JB, Parrow KA, Tsai CS, Briggs KS. Pattern of publication of ophthalmic abstracts in peer-reviewed journals. Ophthalmology 1991;98:553–6.
31. Meranze J, Ellison N, Greenhow DE. Publications resulting from anesthesia meeting abstracts. Anesth Analg 1982;61:445–8.
32. Goldman L, Loscalzo A. Fate of cardiology research originally published in abstract form. N Engl J Med 1980;303:255–9.
33. Pao ML. Global and local collaborators: a study of scientific collaboration. Inf Process Manag 1992;28(1):99–109.

Additional information and reprint requests:
Anny Sauvageau, M.D., M.Sc.
Office of the Chief Medical Examiner
7007, 116 Street
Edmonton, Alberta T6H 5R8
Canada
E-mail: anny.sauvageau@gmail.com

JOURNAL OF FORENSIC SCIENCES

J Forensic Sci, November 2010, Vol. 55, No. 6
doi: 10.1111/j.1556-4029.2010.01492.x
Available online at: onlinelibrary.wiley.com

PAPER

ODONTOLOGY

Dirk T. van der Meer,[1] *D.M.D.; Paula C. Brumit,*[1] *D.D.S.; Bruce A. Schrader,*[1] *D.D.S.; Stephen B. Dove,*[2] *D.D.S., M.S.; and David R. Senn,*[1] *D.D.S.*

Root Morphology and Anatomical Patterns in Forensic Dental Identification: A Comparison of Computer-Aided Identification with Traditional Forensic Dental Identification*

ABSTRACT: An online forensic dental identification exercise was conducted involving 24 antemortem–postmortem (AM–PM) dental radiograph pairs from actual forensic identification cases. Images had been digitally cropped to remove coronal tooth structure and dental restorations. Volunteer forensic odontologists were passively recruited to compare the AM–PM dental radiographs online and conclude identification status using the guidelines for identification from the American Board of Forensic Odontology. The mean accuracy rate for identification was 86.0% (standard deviation 9.2%). The same radiograph pairs were compared using a digital imaging software algorithm, which generated a normalized coefficient of similarity for each pair. Twenty of the radiograph pairs generated a mean accuracy of 85.0%. Four of the pairs could not be used to generate a coefficient of similarity. Receiver operator curve and area under the curve statistical analysis confirmed good discrimination abilities of both methods (online exercise = 0.978; UT-ID index = 0.923) and Spearman's rank correlation coefficient analysis (0.683) indicated good correlation between the results of both methods. Computer-aided dental identification allows for an objective comparison of AM–PM radiographs and can be a useful tool to support a forensic dental identification conclusion.

KEYWORDS: forensic science, forensic identification, forensic odontology, dental radiography, ImageTool, UT-ID Index

Forensic dental identification plays an important role in establishing the identity of unknown decedents because of the individuality of dental patterns, the resiliency of dental structures to withstand extreme conditions, and the accessibility of AM dental records (1–4). Dental comparisons are utilized for victim identification following multiple fatality incidents including the September 2001 terror attacks and the 2005 Hurricanes Katrina and Rita. In Thailand, following the 2004 Indian Ocean tsunami, *c.* 80% of the non-Thai victims were identified by dental information (5,6). Forensic dental identification can be an important identification method in smaller-scale cases, which involve single or multiple fatalities including motor vehicle crashes, smaller-scale airplane crashes, structural fires, and whenever decomposed or skeletonized bodies are found (7).

Human identification using forensic odontology is a reliable and efficient method but is contingent on the individual nature of dental and anatomical features compared between antemortem (AM) and postmortem (PM) radiographs. Identification is more challenging in cases in which either no AM dental restorations exist or no PM restorations remain after events resulting in fragmentation or prolonged extreme heat exposure. Root morphology, bone trabecular patterns, sinus morphology or other distinctive radiographic characteristics can be useful anatomical features for comparisons in these cases. There is limited research using identification cases in which either restorations are not present or coronal structures are missing PM and cannot be compared for identification.

Sholl (8) conducted a comparison study using dental radiographs from dried skulls. The success rates for matching the dental radiographs with no dental restorations varied from 63.6% to 100%, and participants believed that root morphology and alignment had been the greatest aid to matching and not crown morphology. A Web-based study that evaluated dental identification error rates when forensic odontologists compared radiographs from actual forensic dental identification cases determined an overall mean accuracy of 85.5%, and researchers concluded that comparing digital radiographs via the internet was a valid, accurate, and reliable method (9).

Digital subtraction radiography involves the superimposition of registered radiographs and pixel by pixel subtraction of gray scale values allowing for quantification of image similarity. Digital subtraction radiography can be effectively used in dentistry to evaluate radiographic changes in periodontal bone height, endodontic lesions, external root resorption, and other radiographically detectable pathologies (10–13). Subtraction radiography can also be used to compare dental films for identification purposes (14,15).

[1]Center for Education and Research in Forensics (C.E.R.F.), University of Texas Health Science Center at San Antonio, 7703 Floyd Curl Drive, San Antonio, TX.

[2]Department of Dental Diagnostic Science, University of Texas Health Science Center at San Antonio, TX.

*Portions of the results were given in oral presentation at the 61st Annual Meeting of the American Academy of Forensic Sciences, February 16–21, 2009, in Denver, CO.

Received 16 July 2009; accepted 3 Oct. 2009.

Lehmann (16) determined that cross covariance coefficient (CCC) was an appropriate statistical tool when used with digital subtraction radiographic comparisons. UTHSCSA ImageTool Version 3.0 (developed at the University of Texas Health Science Center at San Antonio, Texas) is a general purpose digital imaging and analysis software program. ImageTool with UT-ID plugin compares dental radiographs by registering to correct for differences in projection geometry and digitally subtracting the images. UT-ID generates a normalized coefficient of similarity (UT-ID Index), which is based on the CCC. Flint (17) determined that there was a significant difference in UT-ID Index values between images taken at different times from the same individual and those from different individuals, and that the UT-ID Index thresholds for positive identification varied by dental region. Clinical trials using actual forensic cases are needed to investigate both the usefulness of subtraction radiography as well as the error rates for traditional visual identification by forensic odontologists, especially in difficult cases that contain no dental restorations.

Methods

Twenty-four pairs of AM–PM dental periapical radiographs were randomly selected from actual forensic dental identification cases completed at the Bexar County Forensic Sciences Center, San Antonio, Texas between the years 1999 and 2008. These consisted of sixteen positive identification pairs (radiographs originated from the same person) and eight exclusion pairs (radiographs originated from different persons). The original radiographs included a mixture of analog and digital formats, and for those cases that original analog films were still available the films were digitized using an Epson flatbed scanner at a resolution of 300 pixels per inch. Personal information was redacted, radiograph images were assigned a random number and all images were saved in both Joint Photographic Experts Group (JPEG) and Tagged Image File (TIF) digital formats. Using Adobe Photoshop CS3, dental coronal structures and dental restorations were cropped from the radiographs (see Fig. 1). A Web-based forensic dental identification exercise was constructed and hosted by HostedTest™ (http://www.hostedtest.com; Irvine, CA). Anonymous data was collected from the volunteers who participated (see Table 1). Respondents were asked to complete the exercise a second time after a 1 month washout period to test for intra-examiner reliability using a respondent-generated ten character password to match the first and second scores. Each case was represented by one AM and one PM radiograph (see Fig. 2). The 24 AM–PM radiograph pairs were presented in random order for each participant, and the participants were asked to conclude identification status based on the guidelines of the American Board of Forensic Odontology (see Table 2, http://www.abfo.org). For purposes of this study, "Positive" and "Possible" responses were pooled and equally weighted, while "Insufficient Evidence" responses were disregarded. Approximately 750 invitations requesting volunteers to participate in the online exercise were sent by e-mail to members of the American Society of Forensic Odontology, the British Columbia Forensic Odontology Response Team and other professional contacts.

The same images were analyzed using ImageTool Version 3.0 with UT-ID plugin. Analysis of the radiograph pairs was performed on a Toshiba Satellite notebook computer using Windows Vista

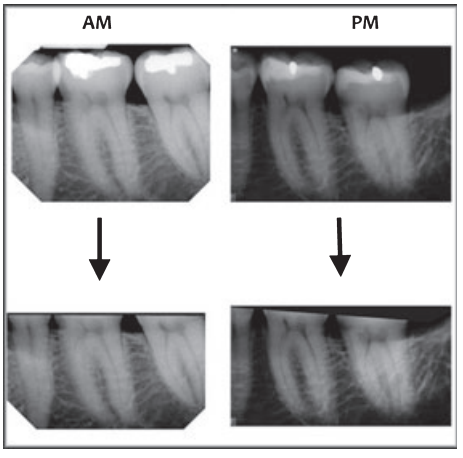

FIG. 1—*Uncropped and cropped antemortem–postmortem radiograph pair.*

TABLE 1—*Respondent data collected for online comparison exercise.*

Category	Options
Profession	Dentist
	Hygienist
	Dental assistant
	Other (specify)
Experience in forensic dental identification	25 or more identifications
	5–24 identifications
	1–4 identifications
	None
Country of residence	(Specify)

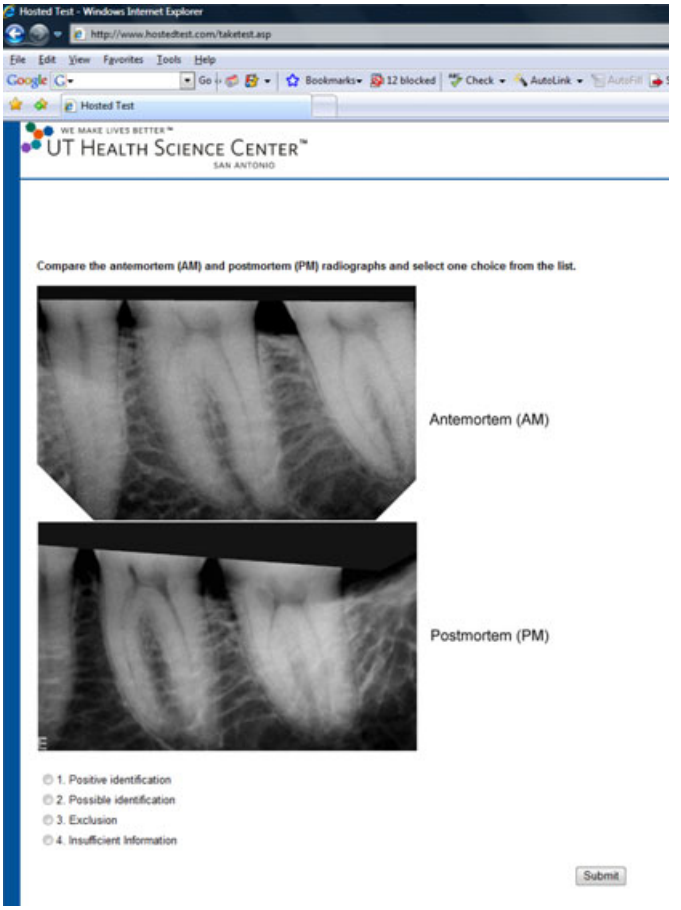

FIG. 2—*Sample screenshot from online comparison exercise.*

TABLE 2—*Conclusion levels available to the participants.*

Level	Description
Positive Identification	Antemortem (AM) and postmortem (PM) evidence are from the same individual
Possible Identification	AM and PM evidence have consistent features, but owing to quality of evidence it is not possible to conclude a positive identification
Exclusion	AM and PM evidences are clearly inconsistent

Ultimate operating system. Each pair of AM–PM radiographs was adjusted for similar resolution and pixel matrix. Using ImageTool UT-ID plugin, the radiographs were then registered to correct for varying projection geometries prior to subtraction radiography and pixel by pixel image comparison techniques to determine the UT-ID index score (see Fig. 3). Ten trials were performed for each radiograph pair to generate a mean UT-ID index score and standard deviation. Each radiograph was also compared against itself for UT-ID Index score.

Results

One hundred and ninety-nine volunteers from eleven different countries responded to the online comparison exercise (see Table 3). One hundred and forty-seven were dentists (73.9%) (see Table 4). A wide range of experience levels was represented ranging from no experience to 25 or more previously completed forensic dental identifications (see Table 5). Seventy of the respondents (35.2%) were dentists, who had completed 25 or more forensic dental identifications. The mean accuracy for all experience levels combined was 86.0% (standard deviation 9.2%) with a sensitivity of 85.9% (SD 14.6%) and a specificity of 86.1% (SD 14.7%) (See Table 6). Kruskal–Wallis analysis of variance (ANOVA) found no statistically significant differences in the mean accuracy scores of the four experience levels. Thirty-nine respondents completed the exercise a second time with a congruence of the first and second answers of 87.4%. Receiver operator curve (ROC) was plotted and the area under the curve (AUC) calculated at 0.978.

UT-ID Index scores were generated for 20 of the 24 radiograph pairs but could not be generated for four of the radiograph pairs because of several factors including poor image quality and widely disparate projection geometries. In total, 13 "True Positive" pairs and 7 "True Exclusion" pairs were used. Mean UT-ID Index scores for the "True Positive" pairs was 0.763 (SD 0.135) and for the "True Exclusion" pairs was 0.427 (SD 0.225). Using the UT-ID Index threshold levels for positive identification as suggested by Flint (17) (see Table 7), sensitivity was 53.8% and specificity was 100%. However, considering the proposed threshold for positive identification for mandibular premolars is 0.650 and that for mandibular molars is 0.800 and given the close anatomical proximity of these regions such that a posterior mandibular periapical radiograph could contain both premolars and molars, when the proposed threshold for both mandibular areas is set at 0.700, sensitivity is 76.9% (three fewer false negatives) while specificity remains unchanged at 100%. This represents a mean accuracy of 85.0%. ROC was plotted and the AUC calculated at 0.923. When each radiograph was compared against itself, UT-ID Index scores of 1.00 were consistently achieved.

Discussion

The mean accuracy of 86.0% (SD 9.2%) for odontologists comparing cropped radiograph pairs online compares well with the previous online identification exercise by Pretty (9) in which respondents compared multiple AM–PM films from each identification case and had a mean accuracy of 85.5%. In this study, no significant difference in the mean accuracy scores was detected between all experience levels indicating dental knowledge was not

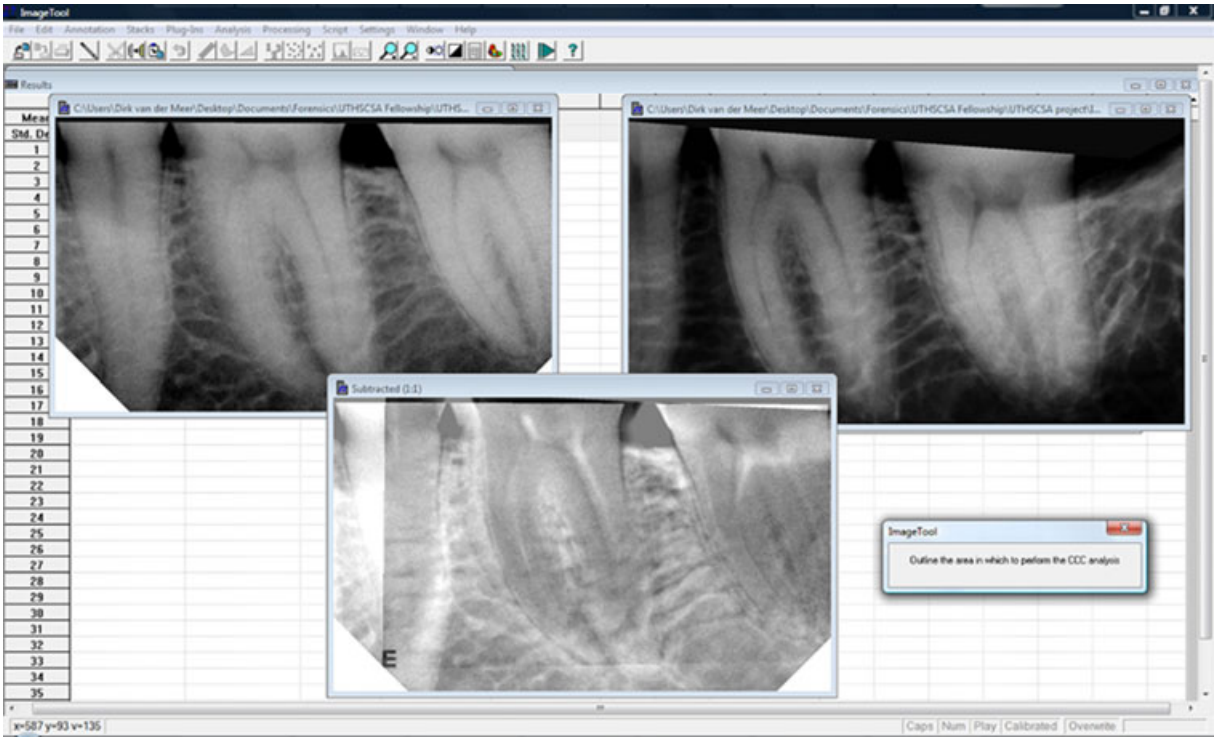

FIG. 3—*Sample screenshot from ImageTool UT-ID. (Left—antemortem; Right—postmortem; Bottom Center—Subtracted image).*

TABLE 3—*Respondents by country.*

Country	Number Respondents	Percent
USA	134	67.3
Canada	50	25.1
New Zealand	4	2.0
Belgium	3	1.5
Switzerland	2	1.0
France	1	0.5
Ireland	1	0.5
England	1	0.5
Taiwan	1	0.5
Japan	1	0.5
Australia	1	0.5

TABLE 4—*Respondents by profession.*

Country	Number Respondents	Percent
Dentist	147	73.9
Hygienist	23	11.6
Dental Assistant	22	11.1
Dental Receptionist	3	1.5
Coroner	1	1.0
Forensic lab Tech	1	0.5
Office Manager	1	0.5
Student Intern	1	0.5

TABLE 5—*Experience level of respondents (number of forensic dental identifications performed).*

Number of Identifications	Number of Respondents	Percent of Total Respondents (%)
25 or more	74	37.2
5–24	40	20.1
1–4	34	17.1
None	51	25.6
Total	199	100

TABLE 6—*Mean accuracy by respondent answer (online exercise).*

Respondent Answer	Mean Accuracy (%)	Standard Deviation (%)
Positive ID	97.3	4.9
Possible ID	89.1	14.0
Exclusion	76.4	15.6
Total mean accuracy	86.0	9.2

TABLE 7—*Proposed UT-ID Index thresholds for positive identification [Flint (17)].*

Oral region	UT-ID Index
Maxillary molar	0.750
Maxillary premolar	0.775
Maxillary anterior	0.700
Mandibular premolar	0.650
Mandibular molar	0.800
Mandibular incisor	0.725

the primary factor in determining an identification conclusion. This can be partly explained by the fact that as all coronal and restorative information was cropped from the AM-PM radiograph pairs, the comparisons were essentially based on pattern recognition and not knowledge of dental restorations. When respondents answered "Positive Identification", the mean accuracy was 97.3% (SD 4.9%), but when respondents answered "Possible Identification," the mean accuracy was 89.1% (SD 14.0%) indicating a positive correlation between conclusion confidence and accuracy (See Table 6). When respondents answered "Exclusion," mean accuracy was 76.4% (SD 15.6%) indicating a higher rate of False Negatives (lower negative predictive value) than False Positives.

TABLE 8—*Comparison online responses and UT-ID Index.*

AM–PM Radiograph Pair	Online Result (% Correct)	UT-ID Index (Std Dev)
1 (Positive)	76.0	0.707 (0.0231)
2 (Positive)	55.8	0.746 (0.0375)
3 (Exclusion)	78.9	0.611 (0.0735)
4 (Exclusion)	57.4	0.167 (0.0661)
5 (Positive)	75.4	
6 (Positive)	95.2	0.527 (0.0408)
7 (Exclusion)	91.6	
8 (Positive)	90.5	
9 (Positive)	53.4	0.838 (0.0476)
10 (Positive)	95.8	0.914 (0.0295)
11 (Positive)	65.4	0.667 (0.0090)
12 (Positive)	86.5	0.813 (0.0461)
13 (Exclusion)	90.6	0.118 (0.0775)
14 (Exclusion)	34.9	0.657 (0.2010)
15 (Exclusion)	81.3	0.502 (0.0988)
16 (Positive)	73.3	
17 (Positive)	81.2	0.832 (0.0230)
18 (Exclusion)	94.7	0.317 (0.0651)
19 (Positive)	78.0	0.786 (0.0294)
20 (Positive)	73.4	0.910 (0.0411)
21 (Positive)	90.2	0.802 (0.0569)
22 (Positive)	15.7	0.486 (0.0315)
23 (Exclusion)	96.3	0.619 (0.1170)
24 (Positive)	68.8	0.886 (0.0156)

AM–PM, antemortem–postmortem.

The online exercise generated a response rate of *c.* 27% indicating that e-mail invitation and anonymous online participation is an effective method to recruit participants. A limitation of this Web-based comparison study is that as respondents used their own personal computers, screen size and quality would have varied between participants and may have affected response results. In addition, the images posted for comparison were static and the respondents could not magnify, brighten or otherwise digitally assist the radiograph image quality to improve the comparison. This differs from an actual dental identification in which the forensic odontologist has access to digital imaging software to select image contrast, brightness, and magnification to enhance comparison. Further studies are needed using standardized digital media for all participants.

Results from 20 of the 24 AM–PM radiograph pairs were used to compare the online exercise responses with ImageTool UT-ID Index scores (see Tables 8 and 9, Fig. 4). Mean accuracy scores were similar between both methods, but ImageTool UT-ID had greater specificity and poorer sensitivity than odontologists comparing the same pairs online. ROC AUC results indicate good discrimination ability of both the online respondents and ImageTool with UT-ID plugin. Spearman's rank correlation coefficient (0.683) indicates good correlation between the results of both methods.

Four of the radiograph pairs could not be used for comparison revealing the limitations of the ImageTool UT-ID algorithm. Several strict parameters are required prior to image comparison in order for ImageTool to generate a UT-ID Index score. Images must be of similar pixel array (most images were cropped to about 600×400 pixels at 300 ppi) with similar diagnostic quality contrast. Projection geometries must be within an acceptable range as widely disparate projection geometries between the AM and PM images introduces greater error to the UT-ID Index calculation.

TABLE 9—*Comparison online responses and UT-ID Index. (results from 20 AM–PM radiograph pairs)*

	Online (Std Dev)	UT-ID Index
Mean accuracy	84.8% (9.7%)	85.0%
Sensitivity	85.1% (15.0%)	76.9%
Specificity	84.4% (16.4%)	100.0%
ROC AUC	0.978	0.923
Spearman's Rank CC (ρ)	0.683	

AM–PM, antemortem–postmortem; ROC, receiver operator curve; AUC, area under the curve.

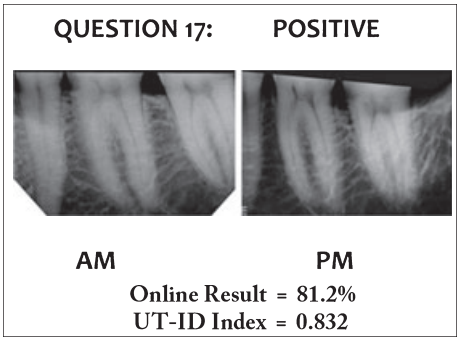

FIG. 4—*Results comparison for antemortem–postmortem radiograph pair #17.*

The same four nonvariant, coplanar points must be clearly identifiable on both AM and PM images. Common features used include root tip apices and interproximal cemento-enamel junctions. These points are used to register the images to correct for slight differences in projection geometry. Inability to clearly identify all four points in both films (because of poor image quality or overlapping anatomical structures) introduces error into UT-ID calculation. Other factors that appeared to hinder UT-ID Index calculation included excessive image compression (as when a lossy format file such as JPEG is repeatedly opened and saved) and digitization of an analog radiograph by means of unscaled digital photography or scanning with uncalibrated equipment with resultant loss of scale.

In consideration of both Daubert standards and recent recommendations from the National Academy of Sciences (NAS) (18), the criteria on which forensic conclusions are based should include objective measurements with established error rates. ImageTool with UT-ID plugin can quantify image similarity between AM and PM dental radiographs from actual forensic cases supporting the identification conclusion of a forensic odontologist comparing the same radiograph pairs by traditional visual means. This fulfills some of the Daubert and NAS standards. Owing to factors that impede the calculation of a UT-ID Index score (such as excessive image compression, widely disparate projection geometries and lack of common, nonvariant anatomical structures), traditional visual identification is more reliable on a wider range of AM–PM image pairs than comparison with ImageTool UT-ID.

Ethics

This study was determined exempt by the Institutional Review Board, University of Texas Health Science Center, San Antonio (Protocol number HSC20080538E).

Acknowledgments

Project funded by a research grant from the American Society of Forensic Odontology.

References

1. Pretty IA, Sweet D. A look at forensic dentistry—part 1: the role of teeth in the determination of human identity. Br Dent J 2001;190(7): 359–66.
2. Avon SL. Forensic odontology: the roles and responsibility of the dentist. J Can Dent Assoc 2004;70(7):453–8.
3. Nuzzolese E, Di Vella G. Future project concerning mass disaster management: a forensic odontology prospectus. Int Dent J 2007;57:261–6.
4. Rothwell BR. Principles of dental identification. Dent Clin North Am 2001;45(2):253–70.
5. Petju M, Suteerayongprasert A, Thongpud R, Hassiri K. Importance of dental records for victim identification following the Indian Ocean tsunami. Public Health 2007;121:251–7.
6. Schuller-Gotzburg P, Suchanek J. Forensic odontologists successfully identify tsunami victims in Phuket, Thailand. Forensic Sci Int 2007; 171(2–3):204–7.
7. Pinchi V, Zei G. Two positive identifications assessed with occasional dental findings on non-dental x-rays. J Forensic Odontostomatol 2008; 27(2):34–8.
8. Sholl SA, Moody GH. Evaluation of dental radiographic identification: an experimental study. Forensic Sci Int 2001;115:165–9.
9. Pretty IA, Pretty RJ, Rothwell BR, Sweet D. The reliability of digitized radiographs for dental identification: a Web-based study. J Forensic Sci 2003;48(6):1325–30.
10. Hekmatian E, Sharif S, Khodaian N. Literature review digital subtraction radiography in dentistry. Dent Res J 2005;2(2):1–9.
11. Mikrogeorgis G, Lyroudia K, Molyvdas I, Nikolaidas N, Pitas I. Digital radiographic registration and subtraction: a useful tool for the evaluation of the progress of chronic apical periodontitis. J Endod 2004;30(7):513–7.
12. Zamani NA, Hekmatian E, Sadraie V. Comparative study of accuracy of digital radiography and digital subtraction radiography in detection of simulated lesions on alveolar crest of dried human mandible. Res J Biol Sci 2008;3(8):953–6.
13. Gegler A, Mahl CEW, Fontanella V. Reproducibility of and file format effect on digital subtraction radiography of simulated external root resorptions. Dentomaxillofac Radiol 2006;35:10–3.
14. Anderson L, Wenzel A. Individual identification by means of conventional bitewing film and subtraction radiography. Forensic Sci Int 1995;72:55–64.
15. Dove B, McDavid WD, Hamilton KE. Analysis of sensitivity and specificity of a new digital subtraction system. Oral Surg Oral Med Oral Pathol Oral Radiol Endod 2000;89:771–6.
16. Lehmann T, Sovakar A, Schmitt W, Repges R. A comparison of similarity measures for digital subtraction radiography. Comp Biol Med 1997;27(2):151–67.
17. Flint DJ, Dove BS, Brumit PC, White M, Senn DR. Computer-aided dental identification: an objective method for assessment of radiographic image similarity. J Forensic Sci 2009;54(1):177–84.
18. Strengthening forensic science in the United States: a path forward. Washington, DC: National Research Council of the National Academies, 2009.

Additional information and reprint requests:
Dirk van der Meer, D.M.D
Box 208
Armstrong, BC V0E 1B0
Canada
E-mail: dirk@sunwave.net

JOURNAL OF FORENSIC SCIENCES

J Forensic Sci, November 2010, Vol. 55, No. 6
doi: 10.1111/j.1556-4029.2010.01491.x
Available online at: onlinelibrary.wiley.com

PAPER

ODONTOLOGY

Matthew R. B. Blenkin,[1] *M.Sc. and Wendell Evans,*[2] *D.D.Sc.*

Age Estimation from the Teeth Using a Modified Demirjian System*

ABSTRACT: The estimation of age at time of death is often an important step in the identification of human remains. The purpose of this study was to test the applicability of the Demirjian system on a sample of the Sydney child population and to develop and test age-prediction models using a large sample of Sydney children (1624 girls, 1637 boys). The use of the Demirjian standards resulted in consistent overestimates of chronological age in children under the age of 14 by as much as a mean of 0.99 years. Of the alternative predictive models derived from the Sydney sample, those that provided the most accurate age estimates are applicable for the age ranges 2–14 years, with *R*-square = 0.94 and a 95% confidence interval of ±1.8 years. The Sydney-based standards provided significantly different and more accurate estimates of age for that sample when compared to the published standards of Demirjian.

KEYWORDS: forensic science, age estimation, dental development, Demirjian, forensic odontology, scoring system

The estimation of age at time of death is an important step in the identification of human remains. If age at time of death can be estimated accurately, it will significantly narrow the field of possible identities that may have to be compared to the remains to establish a positive identification.

Over the years, many authors have realized the utility of systems of age estimation based upon the actual development of the teeth. As early as 1935, Schour and Hoffman (1) found that the pattern of calcification of the dentition under normal conditions acts as a reliable indicator of the pattern of growth, shortly after which the pattern of dental development was used to estimate age (2).

It was the relative consistency of the pattern of tooth development that contributed to the widespread use of dental development-based age-estimation systems (3–5). It is well established that the progressive cusp-to-apex calcification pattern of teeth surpasses all other anthropological and forensic methods of estimating chronological age in children under the age of 14 (6). Demirjian had theorized that while the pattern of development remains reasonably consistent between populations, the rate of development varies somewhat from region to region (7,8).

While most researchers have sought to develop age-estimation systems based on dental development (2,7,9–15), others have simply sought techniques to predict a level of maturity of an individual relative to an average (or expected) level of development for a given age (16–19). While it was the intent of this latter group of authors to provide norms for the ages of attainment of specific stages of tooth development and root resorption, their results have been widely used in reverse to estimate chronological age from a given stage of dental development.

Demirjian et al. (7) sought to develop a method of estimating dental maturity based upon consideration of stage of development in each tooth present in the jaws of selected subjects. Their intent was to develop charts that would allow for the conversion of dental maturity scores to estimates of subject age and that these estimates could be used in clinical and forensic settings to determine chronological age. Their method, which refers to eight tooth

TABLE 1—*Age distribution of cases in the Sydney sample.*

	Female	Male	Total
Years	*n* (%)	*n* (%)	*n* (%)
0–2.4	37 (1.1)	62 (1.9)	99 (3.0)
2.5–3.4	90 (2.8)	114 (3.5)	204 (6.3)
3.5–4.4	107 (3.3)	106 (3.3)	213 (6.5)
4.5–5.4	109 (3.3)	123 (3.8)	232 (7.1)
5.5–6.4	86 (2.6)	80 (2.5)	166 (5.1)
6.5–7.4	103 (3.2)	118 (3.6)	221 (6.8)
7.5–8.4	101 (3.1)	117 (3.6)	218 (6.7)
8.5–9.4	103 (3.2)	150 (4.6)	253 (7.8)
9.5–10.4	114 (3.5)	140 (4.3)	254 (7.8)
10.5–11.4	92 (2.8)	110 (3.4)	202 (6.2)
11.5–12.4	102 (3.1)	83 (2.5)	185 (5.7)
12.5–13.4	86 (2.6)	66 (2.0)	152 (4.7)
13.5–14.4	85 (2.6)	76 (2.3)	161 (4.9)
14.5–15.4	81 (2.5)	65 (2.0)	146 (4.5)
15.5–16.4	89 (2.7)	62 (1.9)	151 (4.6)
16.5–17.4	74 (2.3)	42 (1.3)	116 (3.6)
17.5–18.4	54 (1.7)	50 (1.5)	104 (3.2)
18.5–19.4	57 (1.7)	34 (1.0)	91 (2.8)
19.5–20.4	36 (1.1)	27 (0.8)	63 (1.9)
20.5–21.4	13 (0.4)	12 (0.4)	25 (0.8)
21.5–22.4	3 (0.1)	0 (0.0)	3 (0.1)
22.5–23.4	1 (0.0)	1 (0.0)	2 (0.1)
Total	1623 (49.8)	1638 (50.2)	3261 (100)

[1]Royal Australian Navy, Health Centre Cerberus, HMAS Cerberus, Vic. 3920, Australia.
[2]University of Sydney, Building C24A, 1 Mons Road, Westmead, NSW 2145, Australia.
*Presented at the Australian and New Zealand Forensic Science Society Biannual Conference, April 1–9, 2006, in Fremantle, Western Australia.

Received 26 July 2009; and in revised form 7 Sept. 2009; accepted 27 Sept. 2009.

developmental stages, was more simplified than the approach previously published by Moorrees et al. (13), which was based on 14 stages.

The written descriptions of the eight stages were modified in a later paper by Demirjian to provide further clarification of their defining features (20).

It has been widely reported that this method gave a valid estimate of chronological age only when applied to French-Canadian children, being the population on which the system is based. However, results from studies on population samples of different genetic heritage show that this method did not accurately predict chronological age (12,21–36).

The purpose of this study was (1) to test the applicability of the Demirjian system in Australia on a Sydney-based sample and (2) to develop and test a new age-prediction model on material from this sample.

Materials and Methods

The material for this study, orthopantomographs (OPGs), was obtained from records of patients who had attended public dental clinics in the Sydney region, NSW. A convenience sample of 3261 cases were selected relating to 1623 females and 1638 males, of unknown racial background, aged between 1 and 23 (Table 1).

The tooth images in the lower right quadrant of each OPG were each assessed and rated according to the Demirjian system (Fig. 1) by two examiners (MB and NA) who were blinded to the age of the subjects. The examiners had previously become calibrated in the application of the Demirjian system through duplicate scorings of 200 OPGs. Intra- and inter-observer agreement was assessed through the kappa statistic.

The alphanumeric ratings were later converted to numerical scores (see Table 2 for conversion scheme).

For each case, the sum of the set of scores is termed the Simple Maturity Score (SMS); the maximum score per case is 56 and is attained when all teeth (excluding third molars) are assessed as fully developed.

Development of the Analysis

The cases were sorted by gender and one-third each of the male and female cases were selected (the development sample), and

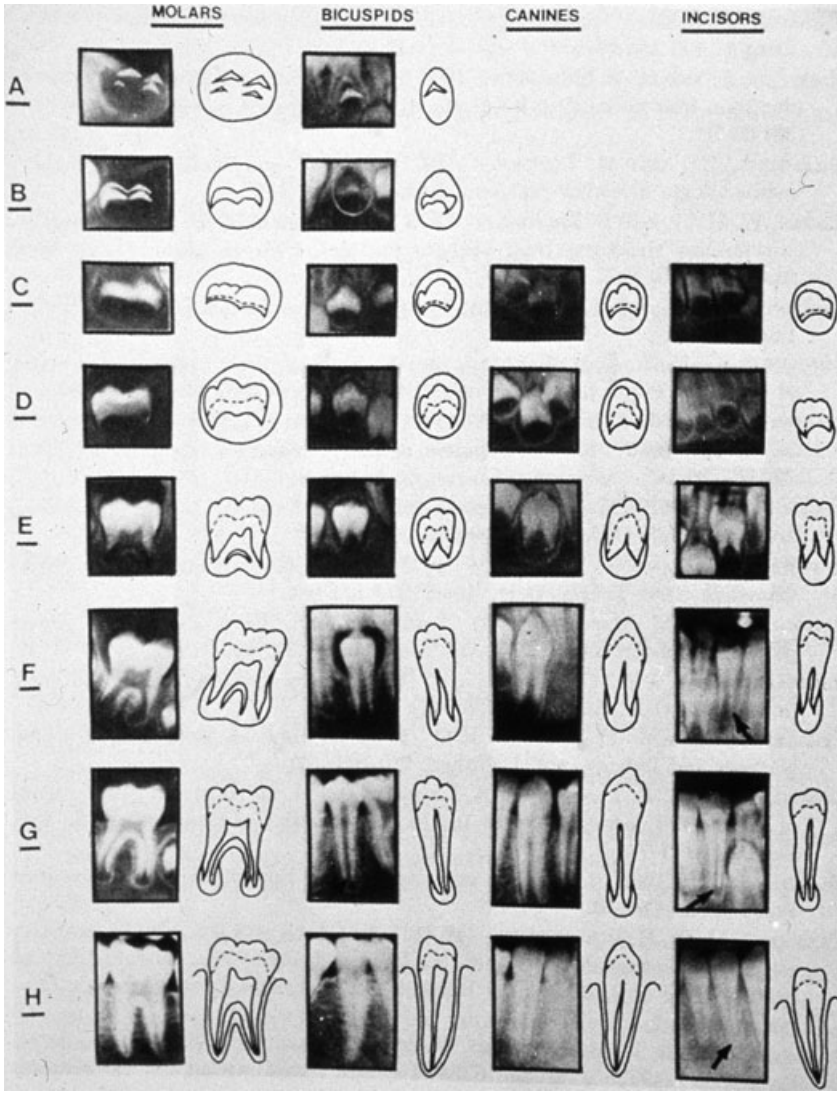

FIG. 1—*The Demirjian system for rating eight developmental stages for permanent molars and premolars, and six stages for canines, and incisors (from Demirjian '76). Reprinted from Figure 1 from Demirjian, A., Goldstein, H., and Tanner, JM. "A New System of Dental Age Assessment." Human Biology, Vol. 45. Copyright © Wayne State University Press, with the permission of Wayne State University Press.*

TABLE 2—*Conversion table—from Demirjian rating to Maturity Score (After Demirjian 1976).*

Demirjian Rating	Maturity Score
0	0
A	1
B	2
C	3
D	4
E	5
F	6
G	7
H	8

SMS was regressed against case age using the least squares method to derive gender-specific age-predictive models. The additional variables, in this study SMS multiplied by themselves to varying powers, were introduced into the regression model one at a time to find the model that best described the relationship between predicted age and SMS. The number of powered predictors did not exceed 5 (i.e., SMS^5). The model selected as best fit was that in which the terms, entered in order of their increasing power, continued to contribute significantly to the explanation of the variance. These equations were then used to predict the ages of the remaining two-thirds of cases (the validation sample).

Next, predicted age was compared with actual age, and mean differences were calculated for each gender-specific age group. The differences were evaluated by means of the *t*-test.

In addition, the predicted ages for the cases were derived separately using (a) the Schour and Massler (b) method and the Demirjian Canadian population-based predictive tables. Respective mean differences from actual age were also calculated.

Final age-prediction curves for both genders were constructed using SMS derived from the entire sample. However, as SMSs of 56 relate to fully developed dentitions and cannot be used to discriminate between ages younger than age 15 and are of no use above this age, the dataset was truncated to include only those cases that had a total SMS of 55 or less. Hence, the total number of cases was reduced to 2587 (1363 male and 1224 female).

Gender-specific 95% confidence intervals were derived using the square root of the residual error from the ANOVA outputs of the regression calculations (12).

Clearance to conduct this study was obtained from the Westmead Scientific Advisory Committee.

Results

The kappa statistic values for intra- and inter-observer agreement were 0.80 and 0.65, respectively, and said to indicate substantial reliability beyond chance.

Table 3 shows that age prediction of cases in the validation sample derived from the use of the Demirjian conversion tables, compared with predictions based on SMS, was more accurate for children aged 13 and 14 only, but not for the younger children. Across all ages and both genders, the Demirjian age predictions underestimated the true age by nearly 0.6 years. Discrepancies between actual age and that predicted according to Schour and Massler for 1-year-olds and children aged 3–5 were less than those predicted from SMSs. However, across all ages, it is seen that the mean discrepancies between actual and predicted age were substantially less overall when those predictions were derived from SMS rather than from either of the other two systems ($p < 0.000$) (Table 4).

TABLE 3—*Age- and gender-specific mean differences between actual age and predicted age according to SMS, the method of Schour and Massler, and the Demirjian conversion tables.*

Mean Overestimate of Predicted Age by Model (Years)						
	SMS		Schour & Massler		Demirjian	
True Age (Years)	Female	Male	Female	Male	Female	Male
1	−1.52	−0.72	0.00	0.25	−2.10	−1.35
2	−0.32	−0.10	0.02	0.11	−0.52	−0.56
3	−0.03	0.00	0.15	0.13	0.01	−0.17
4	−0.07	−0.15	0.19	0.22	−0.16	−0.44
5	−0.23	−0.24	0.12	0.22	−0.72	−0.88
6	−0.27	−0.22	−0.14	0.00	−0.87	−1.01
7	−0.06	−0.33	0.02	0.08	−0.58	−1.03
8	0.06	0.16	0.20	0.33	−0.41	−0.45
9	−0.23	−0.15	0.15	0.33	−0.68	−0.77
10	−0.08	0.01	0.44	0.78	−0.53	−0.70
11	−0.45	0.24	0.37	1.16	−0.94	−0.48
12	−0.48	0.07	0.57	0.98	−0.99	−0.66
13	−0.05	0.58	1.32	1.34	−0.66	−0.16
14	0.37	0.55	−0.80	0.89	−0.28	−0.17
15			0.53	1.52	0.52	0.65
16			−0.13			
17						
Overall	−0.08	0.06	0.25	0.43	−0.57	−0.59
t statistic for comparison with SMS			7.85*	13.00*	46.68*	67.21*

SMS, Simple Maturity Score.
*$p < 0.000$.

The regression equations, based on the entire dataset, developed to describe the relationship between chronological age and SMS age follow:

Male,

$$y = -2.042579201 + 0.416441557x - 0.009307122x^2 + 0.000128194x^3$$

Female,

$$y = -1.914675804 + 0.421823224x - 0.010273636x^2 + 0.000141442x^3$$

TABLE 4—t-*Test statistics in relation to overall mean prediction errors for given models.*

t-Test Statistics* for Comparison Between Models				
Method Used	Demirjian—Male (M CPA)	Demirjian—Female (F CPA)	Schour & Massler—Male (M S&M)	Schour & Massler—Female (F S&M)
Present study—male (M SMS)	67.21	–	13.00	–
Present study—female (F SMS)	–	46.68	–	7.85

CPA, Canadian Predicted Age; SMS, Simple Maturity Score.
*All significant, $p < 0.000$.

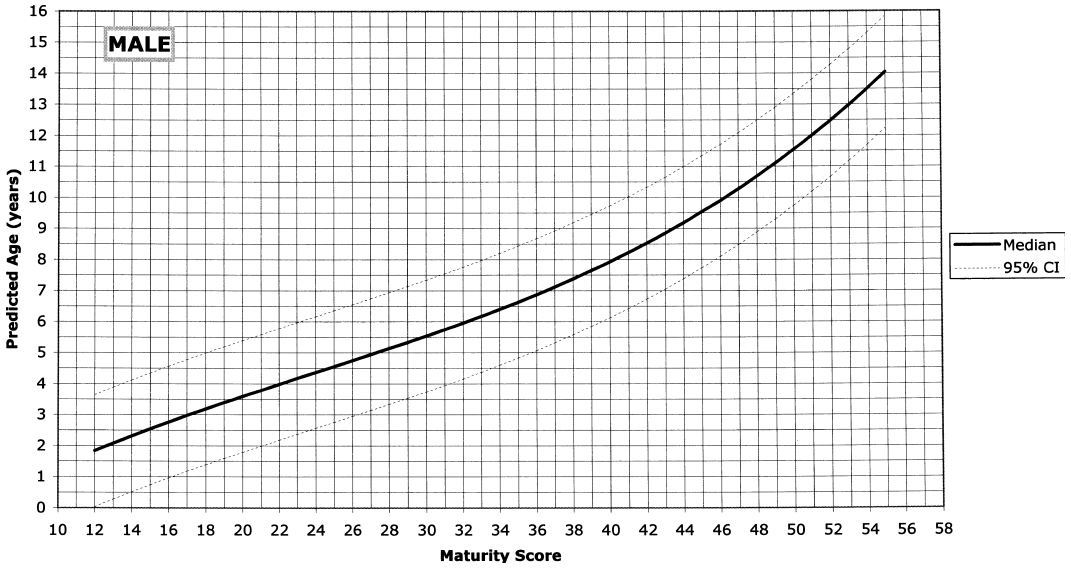

FIG. 2—*Regression curve for age in years against Simple Maturity Score (SMS) for males.*

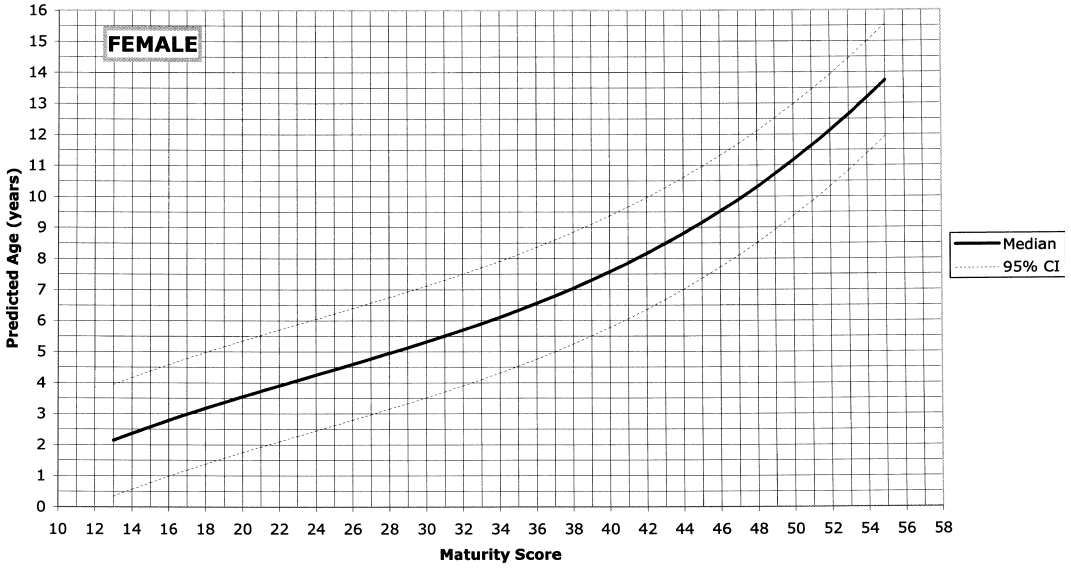

FIG. 3—*Regression curve for age in years against Simple Maturity Score (SMS) for females.*

where y is age in years and x is the SMS. The R-square value for both equations is $R = 0.94$.

The respective regression lines and the 95% confidence limits are shown in Figs. 2 and 3. Each regression line describes a very gentle s-shaped curve. The 95% confidence interval, uniform over the entire range of ages, and based on the residual error from the ANOVA output, is the predicted age ±1.8 years for both genders.

Discussion

These results demonstrate that the Demirjian standards are not applicable to an Australian sample of unknown racial composition because, on average, they underestimate chronological age by 0.6. The findings are consistent with those of McKenna et al. (25), who applied the Demirjian system to a sample of South Australian children.

Demirjian had theorized that while the pattern of development remains reasonably consistent between populations, the rate of development varies somewhat from region to region (7,8).

The *t*-test results confirmed a significant sex dimorphism as reported by others (13,17,37–40). This finding was the driver for the separate male and female regression models developed and published here.

While the reported 95% confidence intervals of age estimates associated with some methods of age-estimation range from ±1 to ±20 years, those based upon dentition development average about ±2 years (14). The results of the present study are consistent with these latter findings.

Increasing global mobility has led to the intermixing of gene pools resulting in less distinct racial traits. Most studies involving methods that focus on dental development have aimed to select racially homogeneous samples in the hope of limiting the

variability associated with rate of dental maturation. This approach may not be reasonable, however, given that one such study revealed that significant variation can even exist within what was thought to be a ''fairly homogeneous'' population (41). Therefore, if significant variations in the rate of dental development occur between (and within) different populations, and as a significant proportion of the Australian population is comprised of subgroups born in many other countries, the variation found within an Australian sample may well be much larger than the variation reported in countries with less genetically mixed populations. Moreover, the greater the variation, the wider the confidence intervals associated with predictive models.

This multicultural nature of Australian society means that unless the genetic or racial origin of the victim is known or suspected, and that appropriate conversion tables for that specific group can be used, reliance will have to be placed on standards that, as discussed earlier, are probably associated with broader error margins around any given age estimate.

Acknowledgments

The authors acknowledge the assistance of Dr. Nec Andrews (NA) and Dr. Dave Grayson in the conduct of this research project.

References

1. Schour I, Hoffman JM. Demonstration of 16-micra rhythm in normal stratification of enamel and dentin in man and other mammals. In: Proceedings of the Thirteenth General Meeting - International Association for Dental Research; 1935 March 16–17. J Dent Res 1935;15(3):161.
2. Schour I, Massler M. The development of the human dentition. J Am Dent Assoc 1941;28:1153–60.
3. Garn SM, Lewis AB, Polacheck DL. Variability of tooth formation. J Dent Res 1959;38:135–48.
4. Liliequist B, Lundberg M. Skeletal and tooth development, a methodologic investigation. Acta Radiol 1971;11:97–112.
5. Stewart TD. New developments in evaluating evidence from the skeleton. J Dent Res 1963;42:264–73.
6. Sopher IM. Forensic dentistry. Springfield, IL: Charles C. Thomas, 1976.
7. Demirjian A, Goldstein H, Tanner JM. A new system of dental age assessment. Hum Biol 1973;45:211–27.
8. Demirjian A. Dentition. In: Falkner F, Tanner JM, editors. Human growth, vol 2. New York, NY: Plenum Publishing, 1986;269–300.
9. Calonius PE, Lunin M, Stout F. Histologic criteria for age estimation of the developing human dentition. Oral Surg Oral Med Oral Pathol Oral Radiol Endod 1970;29:869–76.
10. Gleiser I, Hunt E. The permanent first molar: its calcification, eruption and decay. Am J Phys Anthropol 1955;13:253–81.
11. Gustafson G, Koch G. Age estimation up to 16 years-of-age based on dental development. Odont Revy 1974;25:297–306.
12. Liversidge HM, Molleson TI. Developing permanent tooth length as an estimate of age. J Forensic Sci 1999;44:917–20.
13. Moorrees CF, Fanning E, Hunt E. Age formation stages for ten permanent teeth. J Dent Res 1963;42:1490–502.
14. Mörnstad H, Staaf V, Welander U. Age estimation with the aid of tooth development: a new method based on objective measurements. Scand J Dent Res 1994;102:137–43.
15. Wolanski N. A new method for the evaluation of tooth formation. Acta Genet Stat Med 1966;16:186–97.
16. Anderson DL, Thompson GW, Popovich F. Age of attainment of mineralization stages of the permanent dentition. J Forensic Sci 1976;21:191–200.
17. Fanning E. A longitudinal study of tooth formation and root resorbtion. N Z Dent J 1961;57:202–17.
18. Logan WHG, Kronfeld R. Development of the human jaws and surrounding structures from birth to the age of fifteen years. J Am Dent Assoc 1933;20:379–427.
19. Nolla CM. The development of the permanent teeth. ADC ASDC J Dent Child 1960;27:254–66.
20. Demirjian A. New systems for dental maturity based on seven and four teeth. Ann Hum Biol 1976;3:411–21.
21. Davidson LE, Rodd HD. Interrelationship between dental age and chronological age in Somali children. Community Dent Health 2001;18:27–30.
22. Davis PJ, Häag U. The accuracy and precision of the Demirjian system when used for age determination in Chinese children. Swed Dent J 1994;18:113–6.
23. Eid RMR, Simi R, Friggi MNP, Fisberg M. Assessment of dental maturity in Brazilian children aged 6 to 14 years using Demirjian's method. Int J Paediatr Dent 2002;12:423–8.
24. Loevy H. Maturation of the permanent teeth in black and Latino children. Acta Odontol Scand 1983;4:732–9.
25. McKenna CJ, James H, Taylor JA, Townsend GC. Tooth development standards for South Australia. Aust Dent J 2002;47:223–7.
26. Mörnstad H. The validity of four methods for age determination by teeth in Swedish children: a multicentre study. Swed Dent J 1995;19:121–30.
27. Nyström M. Dental maturity in Finnish children, estimated from the development of seven permanent mandibular teeth. Acta Odontol Scand 1986;44:193–8.
28. Staaf V, Mörnstad H, Welander U. Age estimation based on tooth development: a test of reliability and validity. Scand J Dent Res 1991;99: 281–6.
29. Tompkins RL. Human population variability in relative dental development. Am J Phys Anthropol 1996;99:79–102.
30. Willems G, Van Olmen A, Spiessens B, Carels C. Dental age estimation in Belgian children: Demirjian's technique revisited. J Forensic Sci 2001;46: 893–5.
31. Maber M, Liversidge HM, Hector MP. Accuracy of age estimation of radiographic methods using developing teeth. Forensic Sci Int 2006;159 (Suppl 1):S68–73.
32. Tunc ES, Koyuturk AE. Dental age assessment using Demirjian's method on northern Turkish children. Forensic Sci Int 2008;174(1):23–6.
33. Mani SA, Naing L, John J, Samsudin AR. Comparison of two methods of dental age estimation in 7-15-year old Malays. Int J Paediatr Dent 2008;18(5):380–8.
34. TeMoananui R, Kieser J, Herbison GP, Liversidge HM. Estimating age in Maori, Pacific Island and European children from New Zealand. J Forensic Sci 2008;53(2):401–4.
35. Cameriere R, Ferrante L, Liversidge HM, Prieto JL, Brkic H. Accuracy of age estimation in children using radiograph of developing teeth. Forensic Sci Int 2008;176(2–3):173–7.
36. Lee SE, Lee SH, Lee JY, Park HK, Kim YK. Age estimation of Korean children based on dental maturity. Forensic Sci Int 2008;178(2–3):125–31.
37. Garn S, Lewis A, Koski P, Polacheck D. The sex difference in tooth calcification. J Dent Res 1958;37:561–7.
38. Rosen AA. Chronological development of the dentition of medically indigent children: a new perspective. ASDC J Dent Child 1981;48:437–42.
39. Sapoka AA, Demirjian A. Dental development of the French Canadian child. J Can Dent Assoc 1971;7:100–4.
40. Thompson GW, Anderson DL, Popovich F. Sexual dimorphism in dentition mineralization. Growth 1975;39:289–301.
41. Nyström M. Comparisons of dental maturity between the rural community of Kuhmo in northeastern Finland and the city of Helsinki. Community Dent Oral Epidemiol 1988;16:215–7.

Additional information and reprint requests:
Matthew R. B. Blenkin, M.Sc. (Dent)
c/- Dental Department
HMAS Stirling
Garden Island, WA 6958
Australia
E-mail: matt.blenkin@bigpond.com

JOURNAL OF FORENSIC SCIENCES

J Forensic Sci, November 2010, Vol. 55, No. 6
doi: 10.1111/j.1556-4029.2010.01465.x
Available online at: onlinelibrary.wiley.com

PAPER

PATHOLOGY/BIOLOGY

Hirotaro Iwase,[1] *M.D., Ph.D.; Daisuke Yajima,*[1] *M.D., Ph.D.; Mutsumi Hayakawa,*[1] *M.D., Ph.D.; Seiji Yamamoto,*[2] *M.D., Ph.D.; Hisako Motani,*[1] *D.D.S., Ph.D.; Ayaka Sakuma,*[1] *D.D.S.; Shiori Kasahara,*[1] *B.S.; and Hisao Ito,*[2] *M.D., Ph.D.*

Evaluation of Computed Tomography as a Screening Test for Death Inquest

ABSTRACT: The Japanese method of inquest, which depends mostly on external examinations, may misdiagnose a considerable number of accidental deaths and suicides as death by disease. We conducted computed tomography (CT) scans of 80 cases for which police concluded death by disease or natural causes based on police investigations into the circumstances and results from external examinations. The cause of death was clearly determined by CT scan in 17 of 80 cases. Ten cases underwent autopsy after the police suspected criminality based on results of the CT examinations. The results suggest CT scan may be a tool for preventing a number of overlooked crimes and accidents in Japan. However, it cannot be a perfect tool for discerning between death by disease and other causes of death without cooperation from the investigative agencies and subsequent forensic examinations such as autopsy and toxicological tests.

KEYWORDS: forensic science, computed tomography, inquest, medicolegal autopsy, forensic radiology

Diagnostic imaging techniques, including computed tomography (CT), magnetic resonance imaging (MRI), and echography (ultrasonic imaging), are being introduced to the field of forensic medicine throughout the world (1–3). The primary objective of postmortem imaging diagnoses is to supplement information from autopsy, centeses, and other forensic examinations to establish causes of death more properly (4–8), improve the precision of individual identification (9–13), and identify victims following catastrophic disasters (14,15).

One of the advantages of CT lies in its ability to easily detect foreign objects in the body, overt fractures, and bleeding within the skull (4). However, even the most sophisticated multidetector row CT has difficulty diagnosing myocardial infarctions, stasis, or anemia or distinguishing between pneumonia and pulmonary edema (4). Regarding traumatic injury, CT can sometimes miss such cases as rib fractures (5), cervical spine injury (16–18), cardiac rupture (16,19), hollow viscus injury (16,20), diaphragmatic injury (16,19), and hemomediastinum (19). CT may indeed be helpful for emergency physicians, but for forensic medicine its reliability is sometimes doubtful when used as evidence in courtroom testimony (16,21). The recent trend, therefore, is to determine the cause of death with a combination of CT and other forensic examinations instead of CT alone (5).

In Japan, diagnostic imaging techniques were gradually introduced to the field of forensic medicine in the latter half of the 20th century (3,18,20,22,23). However, forensic autopsies are conducted at an extremely low rate in Japan, and diagnostic imaging techniques are expected to be employed from a different perspective than in other countries. Some purport that CT should be used as a screening test prior to autopsy to discern between death by disease (i.e., natural death) and other causes of death, with the goal of preventing overlooked crimes and accidents, even in the limited number of autopsies that are conducted. Diagnostic imaging introduced in postmortem inspections may be more useful than the current method to improve the accuracy of death inquests.

Japanese methods of death inquests are unique, still in the developmental stages, and therefore not very systematic. Japan introduced a Chinese inquest system in the 18th century. This classical method of inquest did not adopt autopsy to determine cause of death, instead judging criminality and subsequent penalties based solely on external examinations. In the second half of the 19th century, the Japanese government attempted to introduce a medicolegal autopsy system adopted from European countries, in which the cause of death is determined by forensic autopsy. However, such a system was not actually adopted in Japan because of the shortfall of human resources and the uncomfortable feelings related to autopsy among the common people. After World War II, the General Headquarters of the Supreme Commander of Allied Powers (GHQ) found flaws in the Japanese death inquest system and ordered the Japanese government to introduce a medical examiner/coroner system identical to that in the United States. In the initial plan, an authorized medical examiner was tasked with conducting autopsies for unknown causes of death regardless of criminality. Together with the investigative information obtained from police, the medical examiner would then ascertain the likely cause of death to be used for subsequent judgments in criminality and general precautions for public health.

The Japanese government, however, did not modify their system as instructed by the GHQ. They instead decided to conduct conventional forensic autopsies in cases that the police had judged to be

[1]Department of Legal Medicine, Graduate School of Medicine, Chiba University, Chiba, Japan.
[2]Department of Radiology, Chiba University Hospital, 1-8-1 Inohana, Chuo-ku, Chiba, Japan.

Received 17 June 2009; and in revised form 31 July 2009; accepted 15 Aug. 2009.

criminal based on their brief initial investigation (i.e., external examination of the body and situational investigations). For cases that the police had judged to be noncriminal, an authorized medical examiner was permitted to conduct an administrative autopsy at his or her discretion and from the public health perspective. An arbitrary, double-standard forensic autopsy system was therefore created in Japan that was separated into two autopsy systems: forensic and administrative. A systemic change in the ways in which autopsies were conducted was never fully realized. Additionally, the administrative autopsy system was implemented only in large cities, such as Tokyo, Osaka, Kobe, and Yokohama, and not allocated to most of the cities where 80% of the people in Japan reside, including Chiba Prefecture, where our department is located. Consequently, the autopsy rate of unnatural death cases reported to police is 20–30% in the designated areas where the administrative autopsy system is applied, whereas the autopsy rate of unnatural death cases reported to police in the remaining areas is on the order of 4%. In Chiba, with a population of 6 million, about 7000 unknown causes of death are reported to the police each year, of which only about 200 cases suspected as criminal by police are scheduled for medicolegal autopsy.

Chiba Prefecture has only one university with forensic courses. Additionally, the department has only one table for autopsy. For this reason, autopsies are very often limited to cases that are highly suspected of criminality in the inquest. In areas such as Chiba where no administrative autopsy system has been adopted, the police determine the criminality of a case prior to autopsy to reveal the cause of death. Their determination is usually based only on the results of external examinations by a nonforensic physician and on their own investigations into the circumstances (Fig. 1). This is one of the traits that maintain the classical style of Chinese inquest introduced to Japan in the 18th century. An autopsy is conducted if the case is suspected to be criminal in the inquest; if not, most cases are treated as death by disease without being autopsied. This is a scientifically groundless approach. External examinations can reportedly detect only 8.4% of the causes of death, and the results from the circumstances can reveal 65.3% of them (24). However, there is some concern that those cases judged as death by disease without being verified by forensics actually include criminal and accidental deaths, thereby overlooking many cases suspected of criminality or accidents. These flaws in the Japanese inquest system have recently been reported and debated in the National Diet (Japan's bicameral legislature).

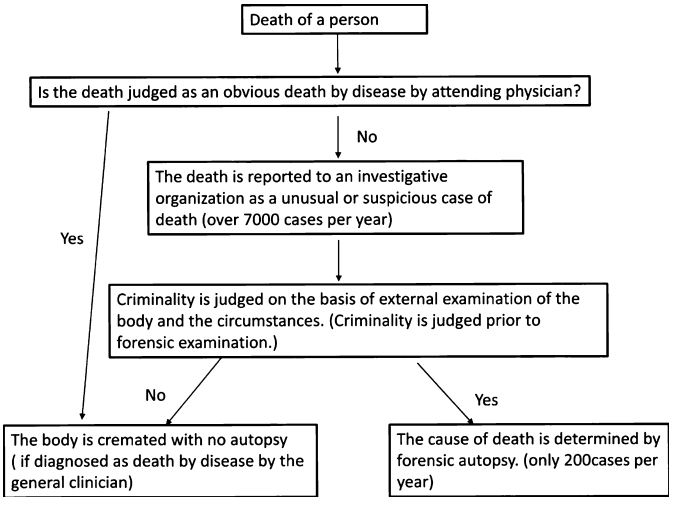

FIG. 1—*Death inquests in Chiba Prefecture. In the regions that do not adopt the medical examiner system, the cases with unknown causes of death reported to the police are judged on whether they are criminal based on the results of external examinations of the body and the circumstances. If the case is suspected of involving a crime, a forensic autopsy will then be conducted. In other cases, including suicide or accidental death, the body will be cremated without forensic examination.*

To look at the issues in the Japanese death inquest system from the scientific perspective, our department conducted 20 postmortem examinations using a rental mobile CT system in 2003. We found that CT scan is effective for accurately diagnosing causes of death compared with a conventional approach solely dependent on external examination (23). We also installed a pre-owned CT adjoining our autopsy room in January 2005. Since that time, until April 2009, we conducted a comparative study between all autopsy reports and CT images obtained from over 600 forensic autopsy cases (18). Meanwhile, we conducted CT scans in collaboration with the police for cases that were previously not scheduled for autopsy because the police suspected no foul play.

In this study, we sought to determine whether CT is appropriate as a screening test to discern between death by disease (i.e., natural death) and other causes of death in the cases for which the police initially determined that no forensic autopsy was necessary because of their noncriminality. We also attempted to determine what factors are important in using CT scans for screening.

Methods

Since August 2006, the Department of Legal Medicine of the Graduate School of Medicine, Chiba University, has posted on our Website (http://www.m.chiba-u.ac.jp/class/houi/CT/index.html) that we will perform free postmortem CT scans of bodies that do not qualify for forensic autopsies, upon request of the bereaved families or the police.

The CT scanner used in this study was a CT-W950SR (Hitachi Medico Co., Ltd., Tokyo, Japan, 1990). The head, neck, chest, and abdomen were scanned at 1-cm intervals with a simple bedside protocol (head and neck: 170 mA, 120 kV, 4.0 sec; chest: 110 mA, 120 kV, 2.0 sec; and abdomen: 140 mA, 120 kV, 2.0 sec). Interpretation of postmortem scans requires skills in image analysis different from those required for antemortem interpretation (2). Skilled techniques were necessary to compare anatomical consequences with diagnostic imaging when interpreting the postmortem CT images. Therefore, we assigned our experienced forensic pathologists to interpreting both the autopsy information and images from an identical case. When we encountered a difficult case, we asked our radiologists for advice and cooperated with them for judgment. We received 84 requests between August 2006 and March 2009. Ages ranged from 2 months to 90 years (average, 55.7 years), with 69 men and 15 women. Five cases were highly decomposed after a span of more than 4 days since death. The remaining cases were estimated to be within 3 days after death. Seventy-three cases were found lifeless indoors, three of which were found in the bathtub, and 11 were found outdoors, three of which were found in a ditch or on the beach.

Three cases were scanned based on requests made by the bereaved families through the police. The remaining cases were direct requests from the police. The police requested that we perform our examinations mainly because they thought that unconfirmed causes of death would be an obstacle when explaining the deaths to the bereaved, or because they were unsure of a causal relationship between the cause of death and reported external causes, in which the deceased had fallen down or received minor injuries a few days before death but with no major injuries

observed externally. The above 84 cases included four that were initially considered death by unforeseen accident (two cases were crushing deaths, one was death after being hit by a train, and one was death by falling). The police suspected no foul play based on the circumstances. Therefore, a forensic autopsy could not be conventionally ordered. We excluded these four cases from this study because we believed that they were not suitable for determining the efficacy of CT scanning when discerning between death by disease and other causes of death. Of these 80 cases, external examinations revealed that no overt injuries were responsible for the death. The physicians, including clinicians who were nonexperts in forensics, conducted these inquests and estimated all of the cases to be death by disease or natural death, and no autopsies were ordered.

The study protocol was approved by the Ethical Review Board of the Graduate School of Medicine, Chiba University.

Results

The cause of death was definitively determined with CT scan in 18 of the 80 cases. The breakdown of the 18 cases was the following: brain hemorrhage (four cases), subdural hematoma (three cases), cardiac tamponade caused by cardiac rupture or by ascending aortic rupture (three cases), subdural hematoma combined with a ruptured aneurysm of the thoracic aorta (one case), a needle-shaped object reaching the heart (one case) (Fig. 2), and tension pneumothorax (one case) (Fig. 3). None of these 18 cases was badly decomposed. One case of suspected brain hemorrhage and one case of suspected hemorrhagic infarction were observed in the five cases that were examined 4 days or longer after death, but neither of these two causes of death could be determined definitively because of the faint images attributed to decomposition. Calcified coronary arteries were observed in 22 cases, but these alone were not sufficient for us to identify the cause of death as ischemic cardiac disease because the degree of luminal obstruction and cardiac muscle fibrosis could not be assessed. Trapped fluids were observed on one side of the chest cavity in one case, but the nature of the fluids could not be accessed by CT alone. We therefore performed thoracentesis to confirm purulent fluids. The cause of death proved to be empyema.

In drowning cases, a ground-glass appearance can be observed in the lungs independent of gravitational forces, and fluids are sometimes trapped in the paranasal sinuses (25). Similar findings were obtained in the cases where the body was discovered in a bathtub, in a ditch, and on the beach (Fig. 4). However, these findings did not help to conclude that the cause of death was drowning. An autopsy should be performed in such cases to determine the presence of plankton in the organs. In ten cases, an autopsy was ordered after the police suspected criminality from the results of our CT examinations. In eight of these cases, our CT examinations revealed that some sort of external cause was likely to be responsible for the death. The breakdown of these cases was the following:

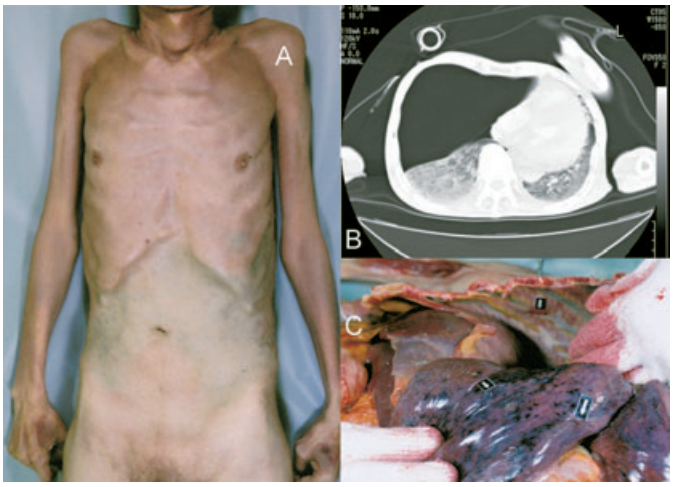

FIG. 3—*A case of traumatic tension pneumothorax. An 88-year-old man was found lifeless at home by his family. He was recently predisposed to easily falling down. Inquest showed no overt damage on the external surface. Police suspected no foul play, and the doctor who witnessed the inquest also determined that the patient likely died from disease. A computed tomography scan in our department showed a tension pneumothorax in the chest (B) and rib fractures. The subsequent autopsy found the rib fractures and the associated pulmonary contusion (C) despite no apparent damage on the surface (A).*

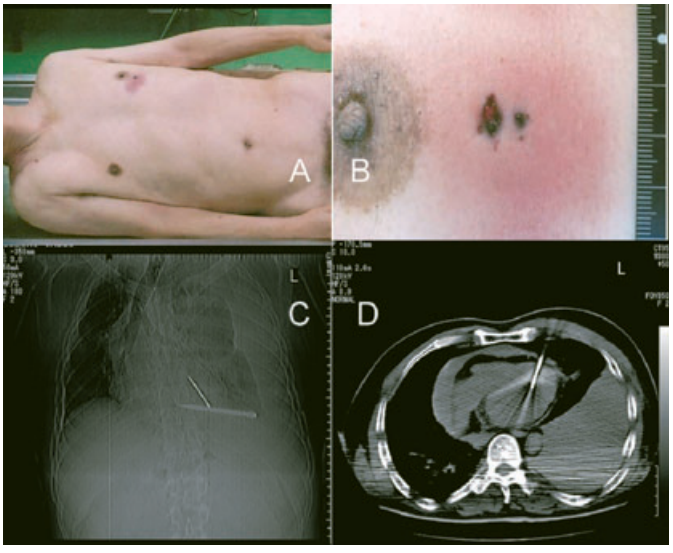

FIG. 2—*A case of a stab wound to the heart. A 60-year-old man was found lifeless at home by his wife. External examination showed only minor lesions similar to excoriation on the left anterior chest skin (A,B), which were considered likely to be a chest bruise caused by a fall when he died suddenly from heart disease. A computed tomography scan in our department found the apical part of an awl reaching the heart (C,D), which led to an autopsy. Later, the cause of death was judged as suicide when a note implying suicide was found.*

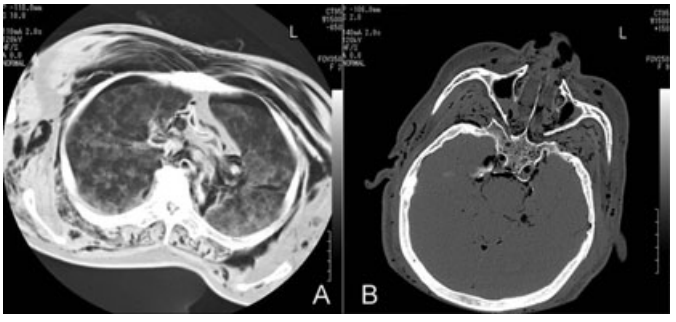

FIG. 4—*A case of suspected drowning. A 72-year-old man with a history of cervical spine surgery was found lifeless in an irrigation ditch. Based on the circumstances, the police suspected no foul play. A forensic autopsy could not be legally ordered. Our computed tomography scan showed a ground-glass appearance in the lungs that was independent of gravitational forces (A), and a small amount of fluid was trapped in the paranasal sinuses (B). The summer season hastened decomposition of the body, and putrefactive gas was observed subcutaneously just 1 day after death.*

FIG. 5—*A case of foreign bodies in the pharynx and larynx. A 74-year-old man was found at home about 5 days after death. No foul play was suspected, so police at first determined that a forensic autopsy was not necessary. However, our computed tomography scan showed a coin-like shadowing in the pharynx. A forensic autopsy was then ordered, but the autopsy could not confirm the cause of death.*

subdural hematoma (four cases), a needle-shaped object reaching the heart (one case) (Fig. 2), suspected traumatic tension pneumothorax (one case) (Fig. 3), foreign bodies in the pharynx and larynx (one case) (Fig. 5), and possible injuries to abdominal organs (one case).

Discussion

In this study, we established the cause of death by CT examination alone in 18 (22.5%) of 80 cases. In Denmark, a diagnostic rate regarding the cause of death with CT alone was reported to be 30% in 150 cases examined with both autopsy and CT (26). Similarly, we established the cause of death with CT alone in 28.9% of 342 cases examined with both CT and autopsy. Therefore, the diagnostic rate regarding the cause of death using CT together with external examination was estimated to be 20–30%. CT alone could not identify the cause of death in over 70% of the cases, possibly because the imaging findings were not helpful for definitive diagnoses of ischemic cardiac disease, chemical addiction, metabolic disorders including diabetic coma, and inflammatory entities such as pneumonia and peritonitis. For example, our CT examinations revealed calcified coronary arteries in 22 cases, but these alone were not sufficient to diagnose ischemic cardiac disease because the extent of luminal obstruction and cardiac muscle affected was not assessable. CT is generally excellent at detecting severe traumas (27,28), but it alone is insufficient for accurately diagnosing the cause of death. A survey of the literature indicated that a subarachnoid hemorrhage observed on CT is not necessarily the cause of death (29). Moreover, it is indicated that CT cannot forensically detect other important findings such as minor bleeding and pale organs from exsanguination (21), and CT also may miss cervical spine injuries, cardiac ruptures, injuries to hollow organs (16), diaphragmatic injuries, and hemomediastinum (19).

To achieve a more accurate diagnosis regarding the cause of death without autopsy, additional needle biopsies (7,8) and angiography (6) are recommended. Introducing MRI (30) also appears promising for diagnosing myocardial infarction. In Japan, however, needle biopsies and angiography, as well as forensic autopsy, require court-issued warrants, the attendance of a police official, or the consent of the bereaved family. It should be noted, therefore, that the above two examinations, if conducted without proper authorization, would conflict with the law against destruction of corpses. As for MRI, it is time-consuming and expensive to perform the procedure. In addition, image reading of postmortem MRI requires special skills and experience. Therefore, MRI would be difficult to use regularly for the diagnosis of the cause of death.

Notably, of the 80 cases in this study that police concluded as death by disease with no element of criminality in their initial investigations, eight (10%) were reconsidered for autopsy after the external causes were revealed in our CT examinations. These cases were later judged as death by suicide or accident with no suspected element of criminality. However, the presence of these cases indicates that under the current Japanese death inquest system, a considerable number of accidental or suicidal cases might have been misdiagnosed as death by disease. A death from cardiac disease or subarachnoid hemorrhage is often accompanied by bruises on the head and chest from falling down, and so many of the bodies may have slight abrasions and/or subcutaneous bleeding. Once we become accustomed to these types of injuries at the time of inquest, we are less likely to suspect that minor trauma observed in the external examination can be the cause of death. In cases of subdural hematomas induced by head injuries, abrasions and discolored areas are only slightly observed or sometimes not observed at all (Fig. 6), and most of these cases are likely to be overlooked and diagnosed as death by disease. These results make CT look promising because it could reveal overlooked crimes or accidents.

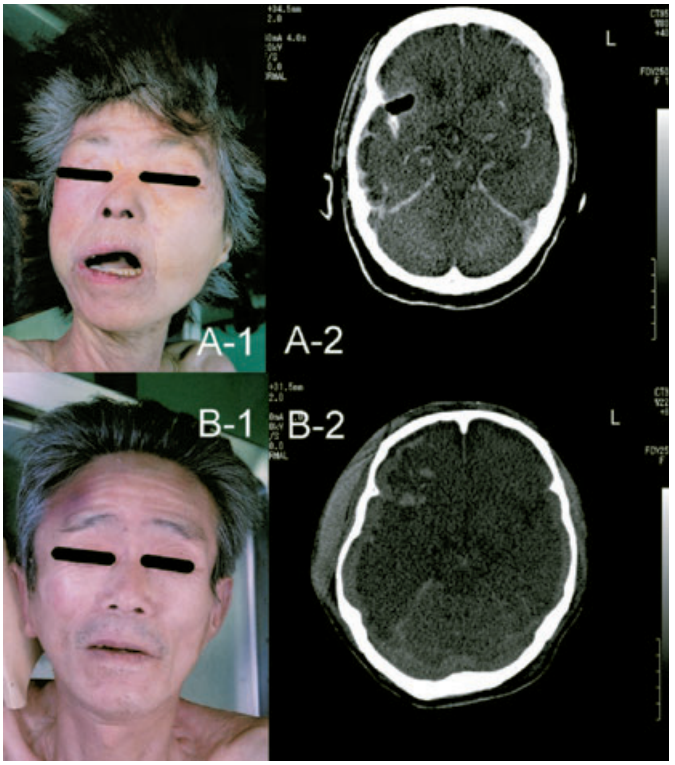

FIG. 6—*The following two cases were at first not judged as criminal by the police based on the circumstances and external examination of the body, so they were assumed to be death by disease. Our computed tomography (CT) scan showed subdural hematomas. It was suspected that death was related to traumatic causes, which led to an autopsy. (A) A 77-year-old woman lived a solitary life and was found lifeless on the bed in her room when her daughter visited her. External examination showed no appreciable damage over the entire body, including face (A-1). Our CT scan showed a subdural hematoma around the left frontal lobe (A-2) and a ruptured aneurysm of the thoracic aorta. (B) A 60-year-old man was found lifeless on the bed in his room. The day before his death, he drank alcohol and another man carried him home. No great craniofacial damage was observed with the exception of a discolored area on the right lateral forehead (B-1). Our CT scan showed a subdural hematoma in the right temple (B-2).*

However, CT also has a few major forensic flaws. Myocardial infarction, intramuscular bleeding caused by cervical compression, and poisoning are difficult to discern by CT. CT also cannot distinguish between pneumonia and pulmonary edema (4), and it may miss cervical cord damage caused by disk rupture (18), cardiac ruptures, injuries to hollow organs (16,20), diaphragmatic injuries, and mediastinal bleeding (19). In fact, we also faced difficulties determining myocardial infarction, chemical addiction, cervical spine injuries, and injuries to hollow organs using CT. Therefore, we cannot exclude the possibility that we may have overlooked poisoning or other criminal activity.

Based on our experience, we discuss below how to perform an ideal screening test with CT and whether systematic CT screening should be conducted before or after notifying the police.

When we are to judge, prior to a notice of unnatural death, whether or not to notify the police based only on the diagnosis of cause of death made by a physician with CT, we will not have to report the case to the police only when more than one healthcare professional follows the patient's disease course until death occurs in the hospital and when death can be objectively confirmed as death by disease or natural causes. If a physician fails to satisfy the above two requirements and attempts to determine the cause of death from CT results as a paid trustee practice without filing a report with the police or obtaining information from investigative agencies, then he will assume considerable risk in exchange for the cost of examining the body. Such a physician is likely to make an erroneous judgment in the cause of death and overlook a crime or accident much more readily than the police who could determine that the death is caused by foul play based on their independent examinations of the external surface of body and circumstances.

We actually experienced some misjudgments and near-miss cases based on diagnostic imaging regarding the forensic autopsy cases we conducted. These included a death from subarachnoid hemorrhage caused by injuries in the vertebral arteries and their branches caused by blows to the face (Fig. 7) and a fatal case of a patient with a history of liver cancer who died from spleen trauma caused by blows to the abdomen (Fig. 8). If we had not shared this information with investigative authorities, the victim may have then been misdiagnosed with death by disease and cremated or buried with no autopsy evidence preserved. Furthermore, poisoning is extremely difficult to diagnose with imaging. Notably, many of the murder-for-insurance cases overlooked in the past were misdiagnosed as death by disease and went unreported to the police, even though the victims were taken to the hospital shortly after death and were examined by a physician.

It is challenging to determine who should interpret postmortem CT images. The radiologists familiar with CT images of living patients would not be able to diagnose the correct cause of death from postmortem CT because of lack of experience. We should expect radiologists or forensic pathologists to be familiar with postmortem CT interpretation through experiences in comparing autopsy and CT findings.

The use of CT screening to diagnose causes of death requires prior notification of the investigative agencies and cooperation between the agencies and physicians, with the exception of cases in which the fatal case involves an in-hospital death which can be obviously concluded as death by disease. On this basis, no autopsy may be needed for some cases (20–30%) that can be definitively confirmed as death by disease. When CT screening results suggest extrinsic factors affecting the cause of death, medicolegal autopsy will almost always be indispensable for preserving evidence for trial (16). When CT scan reveals no findings that can be related to cause of death, forensic examinations, including autopsy and blood and urine tests, will be necessary because of the possibility of poisoning and intervertebral disc injury. Autopsy will be needed to confirm whether external forces pertain to the cause of death even if CT reveals such findings as subarachnoid hemorrhage or ruptured aortic aneurysm suggesting death by disease. CT alone cannot exclude abdominal and head trauma as being involved in the cause of death when the situation prior to death is not clear.

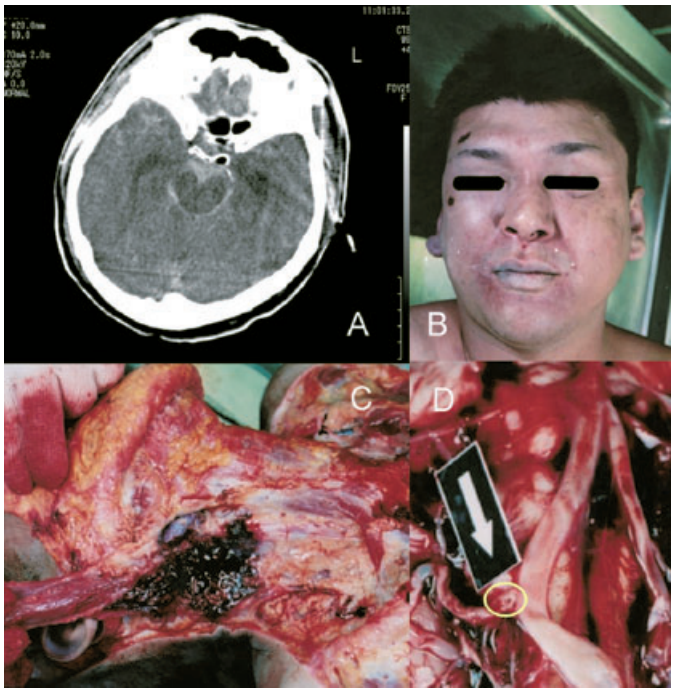

FIG. 7—*A case of traumatic subarachnoid hemorrhage nearly misdiagnosed as death by disease. A 32-year-old man in cardiopulmonary arrest was taken to the hospital by ambulance. Based on the head computed tomography images scanned at the hospital, the doctor diagnosed a subarachnoid hemorrhage caused by ruptured aneurysms at the base of the brain. However, the doctor reported the case to the police because the situation prior to death was unknown. Police investigation revealed that the man suddenly became unconscious after receiving several blows to the face. A forensic autopsy was then ordered. The autopsy showed an abrasion on the face (B), bleeding in the muscles of the right lateral neck region (C), and damage to the right posterior inferior cerebellar artery (arrow D). The cause of death was then determined to be traumatic subarachnoid hemorrhage caused by blows to the head and neck area.*

An interesting question is whether the introduction of CT screening will contribute to a reduction in the number of autopsies performed. Our study suggests the opposite—the number of autopsies may increase; when positive cases suggestive of death caused by external forces are ordered to include an autopsy, the number of autopsies is expected to increase by about 10% of the number reported to police. In cases in which the situation prior to death is unknown, or CT cannot detect the cause of death, and autopsies are to be performed. Thus, 70–80% of those cases reported to police for which the cause of death cannot be obviously considered as death by disease need to have an autopsy. In either event, the total number of autopsies is expected to increase rather than decrease when CT screening is introduced in the Japanese forensic procedure. If physicians and medical examiners employ CT screening without adequate facilities or personnel for autopsies, they will either need to reduce the number of reports to the police or limit the number of autopsies conducted after the report regarding cases in which CT cannot detect the cause of death. In either situation, an accurate diagnosis of the cause of death will not be assured.

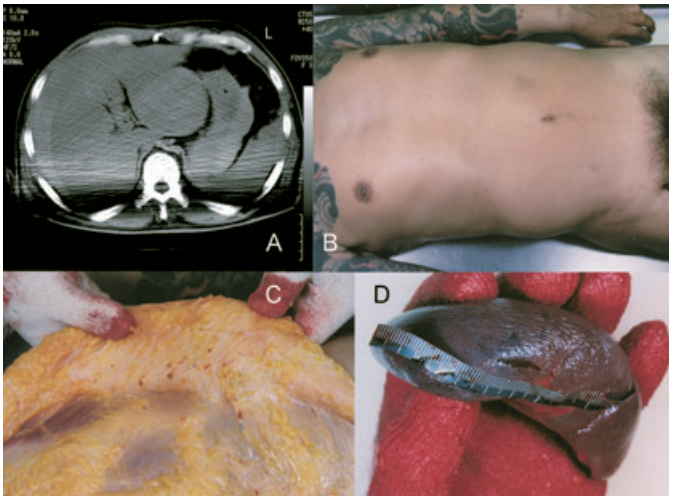

FIG. 8—*A case of misdiagnosed spleen rupture. A 55-year-old man complained of a stomach ache and subsequently suffered cardiopulmonary arrest. He was taken to the hospital by ambulance and later confirmed dead. A computed tomography scan in the hospital showed a large tumor in the liver and bleeding in the abdomen (A). With no external damage observed in the abdominal area (B), the doctor determined that the man died from blood loss caused by a ruptured hepatoma and did not report the case to the police. Immediately before the body was taken to the crematorium, those involved informed the police that the man had been beaten, which led to a forensic autopsy. The autopsy showed a subcutaneous dot hemorrhage, suggesting external forces applied to the abdomen (C), and damage was observed in the spleen (D). These findings indicated that the cause of death was a spleen rupture attributed to blunt force injuries to the abdomen.*

In the former situation, physicians may be asked to assume responsibility for failing to report if they should overlook suspected criminal or accidental cases. Unless an efficient autopsy system is adequately established, the introduction of CT screening would be of minimal value for ensuring safety and protecting the rights of the population.

Diagnostic imaging technologies are being introduced worldwide in the area of forensic medicine. Currently, various approaches are being taken in different countries with respect to applying these technologies. Some countries utilize imaging as a tool for optimizing diagnosis in combination with autopsy and other methods of forensic examination, and some countries use imaging for screening in postmortem inspections. When attempting to use CT as a screening tool for distinguishing between death by disease and other causes of death in Japan, not only its advantages but also its disadvantages and limits must be sufficiently considered. Autopsy, drug testing, and other complementary investigations should also be consolidated to detect elements suggestive of crimes, accidents, and epidemic diseases. These efforts and approaches will be indispensable in creating a social framework that truly contributes to public health.

References

1. Rutty GN, Morgan B, O'Donnell C, Leth PM, Thali M. Forensic institutes across the world place CT or MRI scanners or both into their mortuaries. J Trauma 2008;65:493–4.
2. O'Donnell C, Woodford N. Post-mortem radiology—a new sub-specialty? Clin Radiol 2008;63:1189–94.
3. Uchigasaki S, Oesterhelweg L, Sperhake JP, Püschel K, Oshida S. Application of ultrasonography to postmortem examination. Diagnosis of pericardial tamponade. Forensic Sci Int 2006;162:167–9.
4. Poulsen K, Simonsen J. Computed tomography as routine in connection with medico-legal autopsies. Forensic Sci Int 2007;171:190–7.
5. Cattaneo C, Marinelli E, Di Giancamillo A, Di Giancamillo M, Travetti O, Vigano' L, et al. Sensitivity of autopsy and radiological examination in detecting bone fractures in an animal model: implications for the assessment of fatal child physical abuse. Forensic Sci Int 2006;164:131–7.
6. Grabherr S, Djonov V, Yen K, Thali MJ, Dirnhofer R. Postmortem angiography: review of former and current methods. AJR Am J Roentgenol 2007;188:832–8.
7. Aghayev E, Thali MJ, Sonnenschein M, Jackowski C, Dirnhofer R, Vock P. Post-mortem tissue sampling using computed tomography guidance. Forensic Sci Int 2007;166:199–203.
8. Weustink AC, Hunink MG, van Dijke CF, Renken NS, Krestin GP, Oosterhuis JW. Minimally invasive autopsy: an alternative to conventional autopsy? Radiology 2009;250:897–904.
9. Dedouit F, Telmon N, Costagliola R, Otal P, Florence LL, Joffre F, et al. New identification possibilities with postmortem multislice computed tomography. Int J Legal Med 2007;121:507–10.
10. Kirchhoff S, Fischer F, Lindemaier G, Herzog P, Kirchhoff C, Becker C, et al. Is post-mortem CT of the dentition adequate for correct forensic identification?: comparison of dental computed tomograpy and visual dental record. Int J Legal Med 2008;122:471–9.
11. Ferrant O, Rougé-Maillart C, Guittet L, Papin F, Clin B, Fau G, et al. Age at death estimation of adult males using coxal bone and CT scan: a preliminary study. Forensic Sci Int 2009;186:14–21.
12. Aka PS, Canturk N, Dagalp R, Yagan M. Age determination from central incisors of fetuses and infants. Forensic Sci Int 2009;184:15–20.
13. Rocha Sdos S, Ramos DL, Cavalcanti Mde G. Applicability of 3D-CT facial reconstruction for forensic individual identification. Pesqui Odontol Bras 2003;17:24–8.
14. Blau S, Robertson S, Johnstone M. Disaster victim identification: new applications for postmortem computed tomography. J Forensic Sci 2008;53:956–61.
15. Sidler M, Jackowski C, Dirnhofer R, Vock P, Thali M. Use of multislice computed tomography in disaster victim identification—advantages and limitations. Forensic Sci Int 2007;169:118–28.
16. Molina DK, Nichols JJ, Dimaio VJ. The sensitivity of computed tomography (CT) scans in detecting trauma: are CT scans reliable enough for courtroom testimony? J Trauma 2007;63:625–9.
17. Phal PM, Riccelli LP, Wang P, Nesbit GM, Anderson JC. Fracture detection in the cervical spine with multidetector CT: 1-mm versus 3-mm axial images. AJNR Am J Neuroradiol 2008;29:1446–9.
18. Iwase H, Yamamoto S, Yajima D, Hayakawa M, Kobayashi K, Otsuka K, et al. Can cervical spine injury be correctly diagnosed by postmortem computed tomography? Leg Med (Tokyo) 2009;11:168–74.
19. Aghayev E, Christe A, Sonnenschein M, Yen K, Jackowski C, Thali MJ, et al. Postmortem imaging of blunt chest trauma using CT and MRI: comparison with autopsy. J Thorac Imaging 2008;23:20–7.
20. Yamazaki K, Shiotani S, Ohashi N, Doi M, Kikuchi K, Nagata C, et al. Comparison between computed tomography (CT) and autopsy findings in cases of abdominal injury and disease. Forensic Sci Int 2006;162:163–6.
21. Thomsen AH, Jurik AG, Uhrenholt L, Vesterby A. An alternative approach to Computerized Tomography (CT) in forensic pathology. Forensic Sci Int 2009;183:87–90.
22. Iwase H, Yamada Y, Ootani S, Sasaki Y, Nagao M, Iwadate K, et al. Evidence for an antemortem injury of a burned head dissected from a burned body. Forensic Sci Int 1998;94:9–14.
23. Hayakawa M, Yamamoto S, Motani H, Yajima D, Sato Y, Iwase H. Does imaging technology overcome problems of conventional postmortem examination? A trial of computed tomography imaging for postmortem examination. Int J Legal Med 2006;120:24–6.
24. Biggs MJ, Brown LJ, Rutty GN. Can cause of death be predicted from the pre-necropsy information provided in coroners' cases? J Clin Pathol 2008;61:124–6.
25. Levy AD, Harcke HT, Getz JM, Mallak CT, Caruso JL, Pearse L, et al. Virtual autopsy: two- and three-dimensional multidetector CT findings in drowning with autopsy comparison. Radiology 2007;243:862–8.
26. Leth PM, Christoffersen S. Computerized tomography in forensic autopsies. Ugeskr Laeger 2008;170:444–7.
27. Hoey BA, Cipolla J, Grossman M, McQuay N, Shukla PR, Stawicki SP, et al. Postmortem computed tomography, ''CATopsy'', predicts cause of death in trauma patients. J Trauma 2007;63:979–85.
28. Thali MJ, Yen K, Schweitzer W, Vock P, Boesch C, Ozdoba C, et al. Virtopsy, a new imaging horizon in forensic pathology: virtual autopsy by postmortem multislice computed tomography (MSCT) and magnetic

resonance imaging (MRI)-a feasibility study. J Forensic Sci 2003;48: 386–403.
29. Opeskin K, Silberstein M. False positive diagnosis of subarachnoid haemorrhage on computed tomography scan. J Clin Neurosci 1998;5: 382–6.
30. Jackowski C, Christe A, Sonnenschein M, Aghayev E, Thali MJ. Postmortem unenhanced magnetic resonance imaging of myocardial infarction in correlation to histological infarction age characterization. Eur Heart J 2006;27:2459–67.

Additional information and reprint requests:
Hirotaro Iwase, M.D., Ph.D.
Department of Legal Medicine
Graduate School of Medicine
Chiba University, 1-8-1 Inohana
Chuo-ku, Chiba City
Chiba 260-8670
Japan
E-mail: iwase@faculty.chiba-u.jp

JOURNAL OF FORENSIC SCIENCES

J Forensic Sci, November 2010, Vol. 55, No. 6
doi: 10.1111/j.1556-4029.2010.01511.x
Available online at: onlinelibrary.wiley.com

PAPER

PATHOLOGY/BIOLOGY; ANTHROPOLOGY

Henry P. Schwarcz,[1] *Ph.D.; Kristina Agur,*[1] *B.Sc.; and Lee Meadows Jantz,*[2] *Ph.D.*

A New Method for Determination of Postmortem Interval: Citrate Content of Bone*

ABSTRACT: Few accurate methods exist currently to determine the time since death (postmortem interval, PMI) of skeletonized human remains found at crime scenes. Citrate is present as a constituent of living human and animal cortical bone at very uniform initial concentration (2.0 ± 0.1 wt %). In skeletal remains found in open landscape settings (whether buried or not), the concentration of citrate remains constant for a period of about 4 weeks, after which it decreases linearly as a function of log(time). The upper limit of the dating range is about 100 years. The precision of determination decreases slightly with age. The rate of decrease appears to be independent of temperature or rainfall but drops to zero for storage temperature <0°C.

KEYWORDS: forensic science, time since death, cortical bone, citrate, hydroxyapatite, storage temperature

The determination of the time since death (postmortem interval, PMI) is an important component of the forensic study of human remains and may contribute significantly to the correct attribution of the circumstances of death. Many methods have been developed for the determination of PMI. In general, these can be divided into two classes depending on the stage of decomposition of the cadaver: early period while soft, readily biodegradable tissues are still present and late period when only skeletal remains are present. Swift (1) has summarized both types of methods and notes that "When decomposition has advanced, entering the late PMI and resulting in only skeletal elements, dating of the PMI becomes much more difficult". In the present study, we have developed a method of determining PMI based on the analysis of bone that is specifically applicable to this later period of decomposition.

Various analytical methods have been developed that are applicable to this time interval based on the analysis of bone, including changes in histological appearance (2), measurement of nitrogen or amino acid content (3), or by the reaction of bone tissue with luminal, a fluorescent reagent specific for hemoglobin (4). None of these methods appears to provide the desired level of precision of determination of PMI (a few weeks to months). A somewhat more promising technique is the measurement of the decrease in excess ^{14}C activity present in tissues that was generated by nuclear weapons testing in the 1950s. The excess ^{14}C activity in the atmosphere (and thus in most food and drink) has been decaying with an apparent half-life of about 20 years. However, the rate of turnover of carbon (in collagen) is only between 3% and 5% per year for adults with the result that the average ^{14}C level in modern bone averages over a 5- to 30-year time period (5).

In view of the absence of accurate methods for PMI determination, it would appear important to try to develop a new method for the late postmortem period. Such a method would be widely applicable to distinguish ancient skeletal remains from more recently deceased human material that could have forensic implications. If a new method was sufficiently accurate, it could contribute evidence to the identification of murder victims and their assailants, including constituting evidence admissible in legal proceedings.

A major challenge in developing such a method is that it should be applicable to skeletal material found in settings that vary widely in climate history and physical characteristics (burials, surficial deposits, etc.). In this study, we report a new method that appears to have these characteristics, which is easily applied to even small samples of skeletal material and which provides dates with moderately high accuracy and precision. The method is based on the observation that the citrate molecule, which is present in living bone at a constant, well-defined concentration, disappears from bone postmortem at a well-defined rate that does not appear to depend strongly on the storage environment, within specified limits.

Citrate in Bone

Bone is a composite material consisting of hydroxyapatite (HA) crystals associated with protein, principally collagen in the form of discrete fibrils. Since the 1940s, it has been known that living bone contains between 1.5 and 2.0 wt% of citrate, a tricarboxylic acid that is a key component of the so-called Krebs (or citric acid) cycle, essential to the metabolism of all cells. Approximately 90% of the total body content of citrate is present in bone. This surprisingly high concentration in bone was first observed by Dickens (6)

[1]School of Geography and Earth Sciences, McMaster University, Hamilton, ON, L8S 4K1, Canada.
[2]Coordinator, Forensic Anthropology Center, Department of Anthropology, University of TN, 250 South Stadium Hall, Knoxville, TN 37996-0720.
*Research supported by grants to HPS from the Social Sciences and Humanities Research Council and the Natural Sciences and Engineering Research Councils of Canada.

Received 19 Aug. 2009; and in revised form 28 Sept. 2009; accepted 8 Oct. 2009.

and subsequently studied by many authors shortly after WW II (e.g., 7–9).

The function of citrate in bone was hinted at in studies by Neuman and Neuman (10) who noted that citrate was one of a series of organic molecules that could inhibit the growth of HA crystals from supersaturated solutions, thus preventing excessive growth of the nanometer-sized HA crystals essential to the native fabric of freshly formed bone. Further support for this notion was suggested by Hendricks and Hill (11) who suggested that the surface area of HA crystals in bone was sufficiently large that all the citrate in bone could be accommodated as a monomolecular layer adsorbed on HA crystals. Taylor (9) suggests that citrate adsorbed on HA is an inadvertent consequence of the normal level of citrate in serum.

After about 1975, interest in the role of citrate in bone waned, and many recent texts on bone do not identify citrate as a major constituent although it is much more abundant than some noncollagenous proteins, such as osteopontin that are thought to inhibit the growth of HA (12).

Factors Influencing the Concentration of Citrate in Bone

Earlier studies used somewhat less accurate methods of determining citrate levels than those currently available and appeared to show variable concentrations depending on sex or age. However, more recently, using enzymatic citrate determinations, Knuuttilla et al. (13) showed that variations in citrate content of bone were not age or sex dependent. Gibbs (14) showed that trabecular bone from a large number of recently embalmed individuals contained 1.5 ± 0.1 wt% citrate, while in the present study, we have shown that citrate in cortical bone averages 2.0 ± 0.1 wt% regardless of sex or age. Thus, while there are clear differences in the citrate content of different types of bone (trabecular, cortical), it appears that the concentration of a specific type of bone is quite uniform and does not vary significantly, at least among adults. There is some indication that citrate content is related to the total mineral content of the bone, and therefore, immature, partially mineralized bone might contain less citrate (research in progress). Osteoporotic bone might also have anomalously low concentrations owing to deficiency of HA. Corresponding skeletal components in other vertebrates (e.g., pig, cow) also contain almost identical citrate concentrations, showing that uptake of citrate from blood is a general characteristic of all bone and not restricted to humans. Therefore, it was feasible in this study to use pig bones as a proxy for human material.

Disappearance of Citrate Postmortem

The unpublished study of Gibbs (14) found that the citrate content of human bone buried for >100 year was <1% of the initial content (usually a few parts per million). No other published studies have investigated this obscure point, but it opened up the possibility that if the loss of citrate from bone was gradual, then it could be used as a forensic tool to determine PMI. The study of Gibbs unfortunately did not examine younger burials (a few years or less), so it was not apparent at what point citrate began to be lost.

Goals of this Study

From the previous studies we see that (i) citrate content in specific living bony tissue is uniform regardless of sex and age and (ii) citrate concentration decreases postmortem in buried skeletons. The goal of this study was to test whether we could therefore use the residual content of citrate in a bone sample as an index of the time since death. That is, we would have to develop a relationship of the form

$$C(t)/C_0 = f(t) \quad (1)$$

where C_0 = the initial citrate content, C(t) is the residual citrate content at time = t, that is, the PMI, and f(t) is some function of t to be determined. To establish and validate this method, we must accomplish the following tasks:

- develop a methodology for determining citrate concentrations in bone,
- determine the degree of variation of citrate concentration in living human bone,
- determine the lifetime and decay history of citrate concentration in bone [that is, determine f(t)],
- test the method using forensic or other samples of known PMI,
- identify factors (if any) that could affect f(t).

In order for this method to be effective in a wide range of settings, it will be necessary to establish that f(t) is not strongly dependent on the local climate or storage conditions of the skeleton. If such dependence is observed, it still might be possible to "tune" the method so that it is applicable in a specific region for specific types of occurrences, although this would obviously complicate the application of the method.

Samples Used

All the samples used in this studied are portions of rib bones, either from pigs or from humans. Based on the expected range of concentration in bone, we established that samples of 50 mg of cortical bone would be adequate for the determination of citrate concentration, although larger samples could, in principle, be used for establishing the age of bones near the limit of the method (as citrate approaches zero concentration). Four types of samples were used.

Artificially Prepared Samples of Pig Bones

Whole sections of ribs from a pig purchased at a local grocery store in Knoxville with flesh attached were buried to a depth of approximately 20 cm in a part of the Anthropological Research Facility (ARF) at the University of Tennessee, Knoxville. At this relatively shallow depth, we assume that decomposition occurred in an aerobic environment. A total of six fresh pig rib samples were buried in April 2008. The samples were recovered and frozen (−20°C) at 1-month intervals. One additional sample was frozen at the start of the procedure to be used as a control. The samples were shipped in cooled but not frozen containers by overnight courier to Hamilton and were then immediately frozen pending further analysis.

Human Bones Stored in a Laboratory Setting (HBLS)

To determine the extent to which the storage environment might influence the loss of citrate, we established an experimental storage site in a laboratory, with the assistance of Prof. Anne Agur, Department of Anatomy, University of Toronto. The materials were rib sections removed from recently deceased cadavers. Each rib was defleshed and cut into five 4-cm segments, for a total of 10 rib segments for each subject. One segment was placed in a freezer (−20°C) immediately following excision, and each remaining rib segment was placed in a glass jar in a fume hood kept at room

temperature (23°C) inside a well-ventilated fume hood in the Department of Anatomy. These bone segments were removed and placed in the freezer at 1–4, 6, 8, 10, and 12 weeks postexcision. The procedures for handling and analyzing these samples were approved by the medical ethics committees of both the University of Toronto and McMaster University.

Forensic Bone Samples

Samples of human skeletal material were made available to us by various researchers and police units in the United States and Canada. The list of samples and estimated PMI as provided by the donors is shown in Table 1. Note that these samples came from locations ranging across the North American continent, from California to northwestern Ontario, and therefore encompass a wide range of climatic settings. None of these samples represent burials but were rather found as scatters or well-defined deposits on the ground surface. In some cases, some light covering material (wood, soil, vegetation) overlay the skeletal material.

Cadavers Stored in the Field Under Controlled Conditions

At the ARF, donated cadavers are placed on the ground surface or buried and allowed to decompose for varying lengths of time and then prepared for subsequent forensic study to calibrate forensic analytical methods. We obtained three specimens of rib bone from cadavers that had been processed at ARF, representing postmortem storage intervals up to several years. For these samples, we had complete records of when the samples had been removed from the field and processed; they were subsequently stored in a dried but not frozen condition, prior to the samples being removed for this study.

Analytical Procedures

If necessary, each sample was defleshed, either in the McMaster Stable Isotope Research Laboratory or (for the HBLS series) at the University of Toronto Department of Anatomy. The cleaned bone was defatted by soaking in a 1:1 mixture of chloroform and ethanol for about 1 h. The cleaned, defatted bone samples were then powdered in a liquid nitrogen–cooled grinding device and reduced to particles <10 μm in size. A 50-mg aliquot of the powder was placed in a 50-mL centrifuge tube to which was added 2 mL of 1.0 M HCl, and this was set in a water bath held at 60°C for 1 h; this procedure dissolves the HA component of the bone and liberates citrate into the solution phase. The sample was then brought to pH = 5 by dropwise addition of 0.5 M KOH and spun at 1200 *g* for 5 min, causing the collagen to form a pellet. The clear supernate was decanted into a fresh tube and stored at 4°C until analysis for citrate.

TABLE 1—*Forensic samples studied: T(ave) = average annual temperature at site; T(max) = maximum annual temperature; T < 0 = number of months at site when temperature is <0°C.*

Sample	Location	PMI (y)	Skeletal element	Sex
C-91-129	Santa Barbara, CA	17	Cranium	M
FF	Atascadero, CA	8	rib	M
Jane Doe	Mammoth Lakes, CA	6	femur	F
JD	Lawrence Co., SD	5	femur	M
MM	Thunder Bay, ON	?	rib	M
ARF	Knoxville, TN	see text	rib	M

Citrate was determined using the citrate lyase method described by Moellering and Gruber (15) using analytical kits obtained from Xygen Diagnostics Inc. (Burgessville, ON). The enzyme converts citrate to a mixture of oxaloacetate and pyruvate; these react with NADH. The amount of citrate is monitored by detection of the decrease in UV absorption by NADH at 340 nm using a UV spectrophotometer (Cary 5000 UV-Vis; Varian Inc., Palo Alto, CA). This reaction was calibrated using Na citrate stock solution and yielded a linear response over the range from 0.4 to 0.0001 mg/mL citrate.

Although we did not carry out specific tests of reproducibility of the method, this can be inferred from our analyses of the HBLS series because there was essentially no change in the citrate content of these samples over the duration of the experiment (see below for discussion). Table 2 shows the successive analyses for citrate in these essentially identical aliquots of human rib. The average error for the four data sets is ±0.0031 wt% citrate. This can be taken as the expected error in the analysis of well-conserved samples.

Analytical Results and Discussion

Initial Citrate Concentration of Cortical Bone

In Table 3, we show the range of citrate concentrations observed in all the fresh cortical bone (human and pig) samples that were frozen immediately or very soon after death. In all cases, the concentration is quite uniform, averaging 1.96 ± 0.06 wt%. The human samples are all from mature individuals, and the data do not reflect

TABLE 2—*Samples studied in University of Toronto experiment (HBLS), showing citrate content analyzed for each sample after given intervals. Because these samples showed very little variation with time, they were used to estimate the replication error, as shown.*

Sample	Citrate (wt%)	Time (days)
UofT1-1	1.967	0.01
UofT1-2	1.963	14
UofT1-3	1.963	28
UofT1-4	1.962	42
UofT1-5	1.962	56
UofT1-6	1.959	70
UofT1-7	1.958	84
Average	1.962	
SD	0.003	
UofT2-1	1.986	0.01
UofT2-2	1.985	14
UofT2-3	1.985	28
UofT2-4	1.982	42
UofT2-5	1.981	56
UofT2-6	1.99	70
Average	1.985	
SD	0.003	
UofT3-1	1.854	0.01
UofT3-2	1.854	14
UofT3-3	1.852	28
UofT3-4	1.85	42
UofT3-5	1.852	56
UofT3-6	1.853	70
Average	1.853	
SD	0.002	
UofT4-1	2.011	0.01
UofT4-2	2.013	14
UofT4-3	2.002	28
UofT4-4	2.01	42
Average	2.009	
SD	0.005	
Average SD	0.0031	

TABLE 3—*Initial citrate concentration in bone samples (human and animal). All samples were frozen soon after death.*

Sample	Citrate (wt%)
UofT samples	
1	1.967
2	1.986
3	1.854
4	2.011
ARF pig	1.974
Average	1.958 ± 0.061

possibly lower values in immature humans whose bone is not yet fully mineralized.

Based on this observation, it appears that we can assume a uniform initial citrate concentration C_0 for human cortical bone. This is essential for the application of the proposed method of PMI determination as expressed in Eq. (1).

Experimental Observation of Citrate Loss in Buried Bone

Pig bones with flesh attached were buried at the ARF and recovered at 1-month intervals for 6 months. The analyses of these samples are shown in Table 4. Citrate concentration in these buried bones remained essentially constant for the first month and presumably for a short time thereafter. Subsequently, citrate concentration began to decline significantly and, by the end of experiment (6 months storage time), had dropped to about 50% of its initial value of 2.0 wt%. By excluding the data for the period from 0 to 30 days, we can fit the data with a logarithmic curve

$$C(t) = -0.56 \log t + 20.803 \quad r^2 = 0.919 \qquad (2)$$

where C = citrate in wt% and t = time in days (Fig. 1). Unfortunately, the initial samples are not spaced sufficiently closely to identify the point at which the logarithmic decrease in citrate begins, but back extrapolation of Eq. 1 suggests that citrate concentration begins to drop off starting about 30 days after death.

Eq. 2 does not conform to the model expressed by Eq. 1 because there appears to be an initial period during which essentially no citrate is lost. As we shall see, this appears to be generally valid for all burial or exposed storage settings and must reflect a time needed for activation of the process, which eventually leads to citrate loss.

Extrapolation of Eq. 2 suggests that it should be possible to use citrate measured in bones to determine PMI ≤ 1000 days. Therefore, the citrate determination method does have promise to extend PMI determinations into the hitherto previously inaccessible time range after the loss of soft tissues.

Human Bones Stored in a Laboratory Setting (HBLS)

The data for these experiments are shown in Table 2 and plotted on Fig. 2. To our surprise, we found that when stored in open glass jars for extended periods of time, there was essentially no loss of citrate from human bone. Indeed, as noted earlier, we could use these data to establish the precision of analysis of citrate inasmuch as the loss was undetectable. It is clear from this experiment that something about the nature of the storage environment has a profound effect on the rate of loss of citrate. As we shall see, this fact is equally dramatically shown by forensic samples as well as exposed human cadaver samples from the ARF, all of which underwent significant citrate loss that approximated the trend of Eq. 2.

TABLE 4—*Pig bones buried at ARF: citrate analyses versus time.*

Sample #	Citrate (wt. %)	Time (days)
Tennessee 0	1.974	0.01
Tennessee 1	1.945	30
Tennessee 2	1.821	60
Tennessee 3	1.745	90
Tennessee 4	1.702	120
Tennessee 5	1.590	150
Tennessee 6	1.470	180

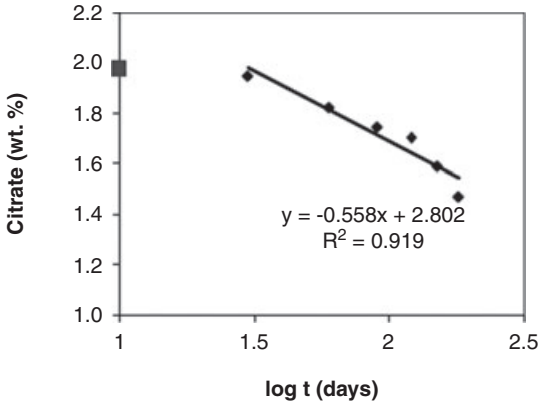

FIG. 1—*Variation in citrate in pig bones plotted versus log t (days). A regression line has been constructed through all but the t = 0 point (shown as square).*

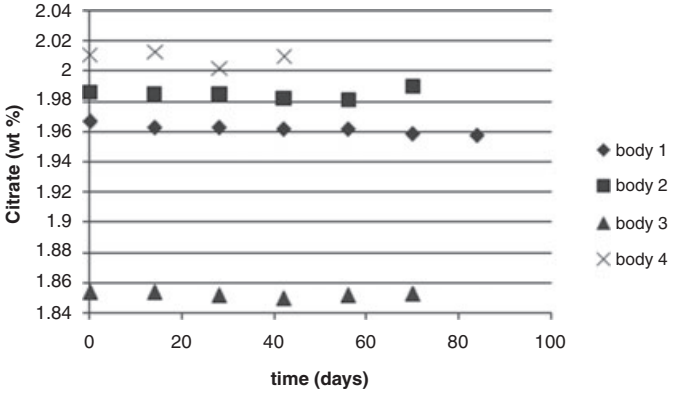

FIG. 2—*Samples stored at University of Toronto (HBLS), showing lack of variation in citrate content with time. Experiment extends well beyond the point (approximately 30 days) at which significant decline is expected based on ARF series.*

In effect, these data are telling us something about the otherwise unidentified mechanism of citrate loss from bone. We can speculate that this involves exposure to soilborne organisms that are able to enter the bone and to consume citrate. In general, studies of soil show that almost all catabolism (oxidation) of organic matter is mediated by microorganisms. Inorganic oxidation by reaction with O_2 in or above the soil is always much slower than heterotrophic activities of bacteria, fungi, etc. Additionally, the samples in the HBLS experiment were kept free of moisture except for what might have been still present in the living bone (because the samples were not dehydrated before storage). Generally, in most "wild" environments (except for arid or frozen settings), liquid water could penetrate the somewhat porous structure of partly decayed bone and stimulate biodegradation of citrate and other molecules.

TABLE 5—*Forensic samples: citrate content and estimated PMI as provided by donors.*

Sample	Citrate (wt%)
C-91-129	0.504
FF	0.677
Jane Doe	0.766
JD	0.762
Femur	0.465
Mandible	0.762
MM	1.52

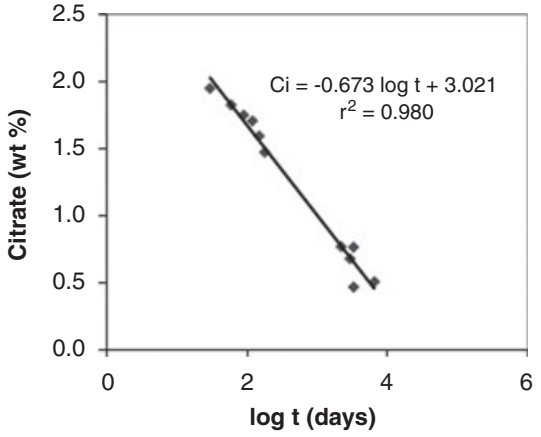

FIG. 3—*Variation in citrate content of forensic samples in addition to ARF buried pig bones. As in Fig 1., regression line excludes t = 0 point.*

Forensic Samples; Temperature Correction

The analytical data for these samples are shown in Table 5. The data are plotted on Fig 3., together with the data from the ARF experiment previously discussed. These additional data extend to much longer times but generally conform to the same trend as defined by the ARF data. We can fit the entire data set to a single relationship:

$$C(t) = -0.647 \log t + 20.971 \; r^2 = 0.991 \qquad (3)$$

There is a considerable scatter of the data points about the line, which may be in part attributable to the variability of the environmental conditions at the site where the samples resided postmortem. In particular, we expect that, whatever the mechanisms are that result in the loss of citrate, these are greatly reduced or completely interrupted when the sample is stored below 0°C and all water in and around the sample is frozen. Therefore, we expect that citrate loss occurs only in the part of the year when T > 0°C.

We can use this fact to modify the expected time-trend of citrate content in bone as follows: Instead of using the total PMI = t as the independent variable, we substitute t*, which is defined as

$$t* = t(1 - [w/12]) \qquad (4)$$

where w = number of months in each year when T < 0°C.

Two of the forensic samples analyzed in this study experienced subzero temperatures for extended periods: Jane Doe from Mammoth Lakes, CA, and JD from Lawrence Co., SD. At both sites, T < 0°C for approximately 4 months of the year; the corrected points are shown on Fig. 4. This slightly alters the correlation between citrate content and time:

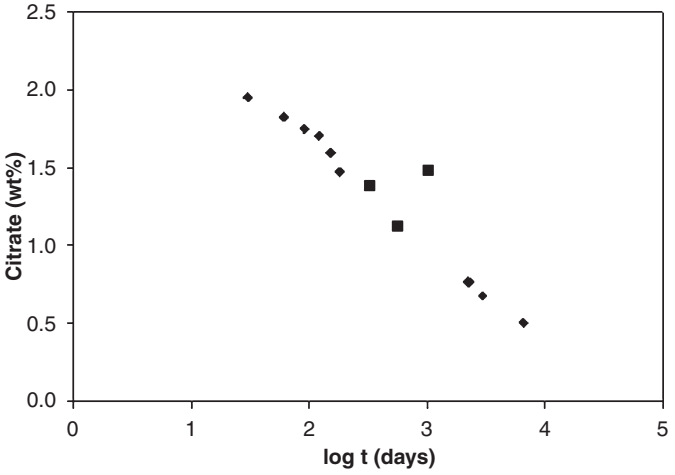

FIG. 4—*Variation in citrate content of forensic samples corrected for time when T < 0°C and including data for ARF pig bones (excluding t = 0). Also shown (squares) are data for exhumed human remains from ARF (Table 6; see text).*

$$C(t) = -0.661 \log t + 20.99 \; r^2 = 0.986 \qquad (5)$$

We suggest that this equation could be used for determining PMI, where subzero temperatures have been encountered at the recovery site.

No estimate of PMI was available for forensic sample MM. The victim was found in the vicinity of Thunder Bay, ON, where the temperature is <0°C for 4.5 months, t* = 0.625 t. The estimated PMI for this individual is therefore 275 days. This result is anomalous because the sample was recovered in June, 2000. The individual had been buried in a pit filled with a white chalky material, which was identified by mass spectrometry to be lime [$Ca(OH)_2$]. Evidently, burial in this material had significantly inhibited the loss of citrate from these bones both during burial and afterward.

Interments at ARF

We also analyzed rib samples from a series of individuals, which had been interred at the ARF at the University of Tennessee at Knoxville. The dates of death of these samples were known accurately, but for some of them, the detailed times when the samples were transferred from the ARF to a processing facility there were not recorded.

However, for three of the samples, we were provided with values for the time elapsed from death until the pickup from the ground surface. After the samples have been exhumed, they are stored, cleaned, and then taken to the collection. This places them in a condition similar to the HBLS samples, which would be expected to slow down the citrate loss rate. Table 6 compares the

TABLE 6—*Exhumed human remains from ARF: citrate analyses for three individuals for whom time of recovery from facility was known. Calculated PMI values are derived from citrate content using Eq. 5.*

	Citrate (wt%)	Known PMI (days)	Calculated
PMI (days)			
52–04	1.12	556	692
57–05	1.48	1010	198
85–06	1.38	324	280

calculated time using Eq. 5 with the known time from death until exhumation. For two of the samples (52–04 and 85–06), there is good agreement between calculated and observed PMI values (within *c.* 10%), whereas one of the samples (57–05) has a much higher citrate content than would be expected for the reported time since recovery. We have no explanation for this discrepancy. These data are shown on Fig. 4.

Conclusions

Effect of Storage Conditions

We have observed that citrate content of bones decreases with remarkable regularity in a series of samples collected from a wide variety of settings. It appears that the storage conditions (temperature, relative humidity, depth of burial, etc.), within broad limits, do not greatly influence the rate of citrate loss. The one exception to this observation has been that there is no loss of citrate at temperatures below 0°C. As well, the forensic sample from Thunder Bay, ON, stored in a pit in contact with large amounts of calcium hydroxide apparently experienced much less loss of citrate, even given the broad limits placed on the true PMI. To better understand the variation in conditions, Table 1 shows the average and estimated maximum summer temperature at each site where a sample (forensic or experimental) was stored. The average temperatures range from 9 to 16°C, but this does not appear to affect the fit of the data to the relationship between time and citrate content. For example samples FF and JD, which differ the most in storage temperature, both lie exactly on the trend line fitted to the total data set.

Limit of the Method

From Eq. 5 and assuming that $t = t^*$, we see that citrate content is expected to approach zero at approximately 95 years. This is the expected lifetime for samples stored at $T > 0$. For sites where $T < 0$ for some part of the year, the potential lifetime is longer. We would assume, however, that samples left resting on the surface for this long would begin to degrade in other ways (see, e.g., Trueman et al. [16]) including extensive recrystallization of HA with consequent release of adsorbed citrate. Therefore, depending on the conditions of storage, it is difficult to predict the very long-term behavior of citrate, although it is reasonable to suppose that the rate of decline might increase somewhat.

Precision of the Method

The high degree of correlation of citrate content with log t suggests that the method would be a quite robust technique for determining PMI in the period beyond the loss of soft tissues. Because the correlation is with log t, the error will increase with age. From Eq. 5, and assuming that the only source of error is the analytical error in citrate (±0.003%), then the error is approximately 1% of the age. Therefore, at an age of 10 years, the expected error in PMI is about 1 month. This is almost certainly an underestimate of the true error, as shown from the scatter of data around the regression line (Fig. 3). A better estimate of the error will emerge as further samples of known PMI are analyzed. The precision of this method cannot be easily compared with bomb-spike radiocarbon dating, the only other method applicable in this time range, because errors in the latter depend critically on the nature of the material dated (e.g., the chronological age of the victim). In general, however, citrate analysis appears to be a more robust method and less subject to untestable assumptions about the sample material.

Further Tests of the Method

We have demonstrated that the citrate content of bone can be used to estimate PMI up to a limit of about 100 years with a minimum estimated error of 1% of the age. Having demonstrated the principle of the method, it will be necessary to test the method against further samples of known PMI and especially samples that have been properly stored subsequent to collection. At present, all the forensic samples used in calibrating the method were stored in a dry but not frozen state in various crime laboratories around the U.S. Likewise, the test samples from the ARF were not frozen subsequent to curation. Even though the HBLS study suggested that no citrate loss occurs when the samples have not been exposed to moist soil at $T > 0$°C, it is not clear that samples that were once in the latter state do not continue to lose citrate during storage even though they have been kept dry and out of contact with soil. Hopefully, through collaboration with legal authorities interested in the potential application of this method, we will be able to obtain further samples that were frozen immediately on collection and kept frozen until shortly before analysis.

Acknowledgments

The authors thank Dr. Anne Agur of the Department of Anatomy, University of Toronto, for her assistance in the preparation and storage of bone samples for this study. The following people kindly donated forensic samples for analysis: the late Prof. Philip Walker, University of California at Santa Barbara; Paulette Peterson, DCI Forensic Laboratory, Pierre SD; Sgt. Paul Dostie, Mammoth Lakes Police Department, Mammoth Lakes, CA; and Prof. Eldon Molto, Department of Anthropology, University of Western Ontario. We thank Martin Knyf for assistance in analysis of the samples for citrate. We acknowledge the assistance of Rebecca Wilson and Sandy Cridlin at the ARF for their assistance. We thank Arpad Vass for constructive suggestions on this study.

References

1. Swift B. The timing of death. In: Rutty G, editor. Essentials of autopsy practice. Berlin: Springer, 2006;189–214.
2. Specht S, Berg W. Untersuchungen zur Bestimmung der Liegezeit von Skeletteilen. Dtsch Z Gerichtl Med 1958;47:209–41.
3. Knight B, Lauder I. Practical methods of dating skeletal remains: a preliminary study. Med Sci Law 1967;7:205–9.
4. Introna F, Di Vella G, Campobasso CP. Determination of postmortem interval from old skeletal remains by image analysis of luminol test results. J Forensic Sci 1999;44:535–8.
5. Hedges REM, Clement JG, Thomas CD, O'Connell TC. Collagen turnover in the adult femoral mid-shaft: modeled from anthropogenic radiocarbon tracer measurements. Am J Phys Anthrop 2007;133: 808–16.
6. Dickens J. The citric acid content of animal tissues with reference to its occurrence in bone and tumor. Biochem J 1941;35:1011–23.
7. Dixon HR, Perkins TF. Citric acid and bone metabolism. Biochem J 1952;52:260–5.
8. Kenny A, Draskóczy P, Goldhaber P. Citric acid production by resorbing bone in tissue culture. Am J Physiol 1959;197:502–4.
9. Taylor TG. The nature of bone citrate. Biochim Biophys Acta 1960;39:148–9.
10. Neuman WF, Neuman MW. The chemical dynamics of bone mineral. Chicago, IL: University of Chicago Press, 1958.
11. Hendricks SB, Hill WL. The nature of bone and phosphate rock. Proc Natl Acad Sci USA 1950;36:731–7.

12. Jahnen-Dechent W. Lot's wife's problem revisited: how we prevent pathological calcification. In: Bauerlein E, editor. Biomineralization progress in biology, molecular biology and application. Weinheim: Wiley-VCH, 2004;245–67.
13. Knuuttilla M, Lappalainen R, Alakuijala P, Lammi S. Statistical evidence for the relation between citrate and carbonate in human cortical bone. Calcif Tiss Int 1985;37:363–6.
14. Gibbs LM. What's sex in the East is not necessarily sex in the West: citrate, sex, and human skeletal remains [dissertation]. Hamilton, ON: McMaster University, 1991.
15. Moellering H, Gruber W. Determination of citrate with citrate lyase. Anal Biochem 1966;17:369–76.
16. Trueman CNG, Behrensmeyer AK, Tuross N, Weiner S. Mineralogical and compositional changes in bones exposed on soilsurfaces in Amboseli National Park, Kenya: diagenetic mechanisms and the role of sediment pore fluids. J Archaeol Sci 2004;31:721–39.

Additional information and reprint requests:
Henry P. Schwarcz, Ph.D.
University Professor Emeritus
School of Geography and Earth Sciences,
McMaster University
Hamilton, ON L8S 4K1
Canada
E-mail: schwarcz@mcmaster.ca

JOURNAL OF FORENSIC SCIENCES

J Forensic Sci, November 2010, Vol. 55, No. 6
doi: 10.1111/j.1556-4029.2010.01501.x
Available online at: onlinelibrary.wiley.com

PAPER

PATHOLOGY/BIOLOGY

Kusum D. Jashnani,[1] *M.B.B.S., M.D.; Smita A. Kale,*[1] *M.B.B.S., M.D.; and Asha B. Rupani,*[1] *M.B.B.S., M.D.*

Vitreous Humor: Biochemical Constituents in Estimation of Postmortem Interval*,†

ABSTRACT: Analysis of biochemical constituents of the vitreous humor can be useful in determining the postmortem interval as there is proportionate postmortem rise of potassium and fall in sodium concentration. We studied 120 autopsy cases to determine the utility of potassium, sodium, calcium, and chloride levels, and sodium/potassium ratio in estimating the postmortem interval. There was a linear relationship between vitreous potassium concentration and postmortem interval, whereas an inverse relationship between vitreous sodium/potassium ratio and postmortem interval was noted. Other factors like age, sex, cause of death, season of death, and refrigeration of sample did not influence the vitreous humor potassium values. Using the statistical tools, a new formula was derived to determine the postmortem interval based on the potassium concentration and a review of previous literature is presented. Hence, the findings of this study supported a central role of vitreous humor biochemistry in many postmortem forensic and pathological evaluations.

KEYWORDS: forensic science, vitreous humor, postmortem interval, potassium levels, sodium/potassium ratio, statistical analysis

Postmortem interval (PMI) is the interval between death and the time of postmortem examination. Determination of PMI is essential in many criminal forensic investigations as well as in certain natural deaths (1,2). In spite of its great importance, determining the accurate time of death is a recurring problem. Over the last few decades, extensive work has been carried out to determine the PMI from various physical changes as well as from the study of changes in biochemical constituents in various body fluids like blood, cerebro-spinal fluid, and vitreous humor (VH) immediately or shortly after the death (1–3). Analysis of chemical changes in the intraocular fluid, after death was introduced by Naumann (4) and has since aroused a great deal of interest (5). In VH, a postmortem rise of potassium and fall in sodium concentration proportional to PMI has been reported (2,6–8). It can also be useful to the pathologists as an important adjunct to confirm an antemortem diagnosis like diabetes or as a potential source of DNA (9,10). We therefore undertook this study to understand the relevance of this correlation between PMI and VH constituents in Indian conditions.

Materials and Methods

The objectives of this study were to determine the utility of biochemical constituents of VH like potassium, sodium, calcium, and chloride in estimating the PMI and to study the relationship between ratio of postmortem vitreous sodium/potassium concentration and PMI. We also wanted to analyze the correlation between VH potassium and other variables like age, gender, cause of death, effects of seasonal variations, and refrigeration of the sample.

The present study was a prospective study in which VH samples were collected from 120 autopsies conducted at our hospital during a period of 15 months, from April 2006 to June 2007. The autopsy subjects were all hospital deaths with known time of death and involved resuscitation attempt. The excluding criteria were pediatric cases and cases for eye donation. Written consent was taken from the relatives. The relevant clinical data were obtained from the medical records at the hospital.

In each case, about 3–4 mL of VH from one eye, either left or right, was aspirated by making a puncture 5–6 mm away from the sclero-corneal junction by using a 10 mL syringe and a 21-gauge needle. Normal saline was replaced in the vitreous body for cosmetic purpose (11). Careful and gentle suction was applied, and residual fluid was left during sampling to avoid detachment and contamination by retinal cells. Cloudy fluid or any fluid containing particulate matter was rejected. The specimen obtained was placed in a clean rubber-stoppered small glass bulb with a proper label. The samples were processed in the biochemistry laboratory within 1 h of collection on working days. On nonworking days and emergency hours, the samples were stored at 4°C and subsequently analyzed. The samples were centrifuged at 2000 rotations per minute for 5 min, and the supernatant was used for the estimation of potassium, sodium, calcium, and chloride ions. Sodium and potassium levels were determined by flame photometry FLM3 (Radiometer, Bronshoj, Denmark), calcium by Olympus AU4OO (Olympus, Nyon, Switzerland), and chloride by Biolyte 2000 (Biocare, Hsinchu, Taiwan). While measuring all the four biochemical constituents, known normal and abnormal quality control samples of

[1]Department of Pathology, Topiwala National Medical College and B Y L Nair Charitable Hospital, Mumbai Central, Maharashtra 400 008, India.

*Funding provided by the Nair Golden Jubilee Research Fund (NGJRF) of Topiwala National Medical College, Mumbai, India.

†Presented at the State Level Conference of Pathology, MAPCON 2007, October 4–7, 2007, in Navi Mumbai, India; and at the Staff Society Meeting of the Topiwala National Medical College, November 2007, in Mumbai, India.

Received 24 May 2009; and in revised form 9 Aug. 2009; accepted 27 Sept. 2009.

TABLE 1—*Table showing vital statistics of the four major electrolytes (1,14).*

Electrolyte	Normal value (mmol/L)	Range (mmol/L)	Mean	SD	*p*-Value
Potassium	5–8	4.80–45.60	11.06	6.36	8.08E–19 (<0.05)
Sodium	118–154	106–165	131.93	12.26	0.093
Calcium	6–8	5.40–10.10	7.20	0.81	0.127
Chloride	114	69–192	95.54	14.35	0.347
Na/K ratio	–	0.17–30	13.90	4.85	5.58E–18 (<0.05)

SD, standard deviation.

Bio-Rad Company (Irvine, CA) were used. The sodium and potassium levels were calculated in all 120 subjects, calcium in 113 subjects, and chloride in 119 subjects. The above investigations could not be performed in all cases because of insufficient quantity of the VH.

Statistical tests used were linear regression correlation analysis and Pearson's correlation tests to establish the correlation between individual vitreous biochemical constituents and the PMI and their significance (12,13). The linear regression formula to estimate the PMI using individual vitreous biochemical constituent was derived.

Results

The results of the biochemical estimation of the four electrolytes in VH are shown in Table 1. In this study, observations were made up to 50 h postmortem. During the studied postmortem period, the vitreous potassium represented a consistently linear rise with increasing PMI (Table 2). The linear rise of vitreous potassium was consistent in the early PMI with the range of scatter increasing in the later postmortem hours especially after 20 h (Fig. 1). The slope of regression line for postmortem vitreous potassium rise with the increasing PMI was 0.929 mmol/L per hour with a 0 h "y" intercept at 2.616 mmol/L. We also found that the measured postmortem VH potassium and estimated potassium values as per time of death showed good correlation (*p*-value of 2.30E-11 [<0.05]).

Measurement of sodium up to 50 h after death showed little change. The linear regression graph between time since death and postmortem VH sodium was horizontal, suggesting no correlation between the two and also not statistically significant with the *p*-value of 0.093 (Fig. 2, Table 1). However, it was observed that the sodium to potassium ratio was indirectly proportional to PMI (Fig. 3). This was also statistically significant with a *p*-value of 5.58E-18 (<0.05). The vitreous calcium and chloride concentration did not change significantly following death according to the PMI and were not statistically significant (Table 1).

In this study, the age of the deceased varied from 15 to 88 years with mean of 51.5 years (SD = 17.65). The linear regression graph between postmortem VH potassium and age of deceased was horizontal, suggesting no correlation between the two (*p*-value of 0.631). Seventy percent were men and 30% were women. No correlation was observed between postmortem VH potassium and sex of deceased (*p*-value of 0.382). The samples were collected throughout the year in all seasons with 55.8% of the samples in monsoon and 30.8% and 13.4% during winter and summer, respectively. The season had no effect on the postmortem VH potassium value (*p*-value of 0.984). Of the samples, 64.2% were refrigerated at 4°C and analyzed subsequently and 35.8% of the samples were analyzed immediately within 1 h of the collection. It was observed that refrigeration of the sample did not affect postmortem VH potassium value (*p*-value of 0.336). The majority of the causes of death were related to infectious diseases (92%), with septicemia and tuberculosis the major causes of death followed by intrapulmonary hemorrhages in acute febrile illness and pneumonia. The cause of death had no effect on postmortem VH potassium value as in each case the *p*-value was more than 0.05. Antemortem blood sodium and potassium values were available in

TABLE 2—*Table showing correlation between time since death and postmortem vitreous humor potassium.*

Variables		Time Since Death	Postmortem K
Time since death	PC	1.000	0.698*
	p-Value		8.08E–19 (<0.05)
Postmortem K	PC	0.698*	1.000
	p-Value	8.08E-19 (<0.05)	

*Correlation is significant at the 0.01 level (2-tailed). PC, Pearson correlation.

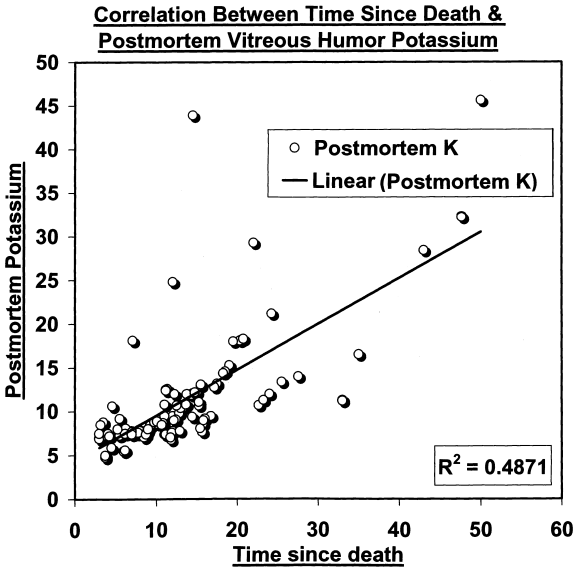

FIG. 1—*Linear regression graph showing correlation between time since death and postmortem vitreous humor potassium.*

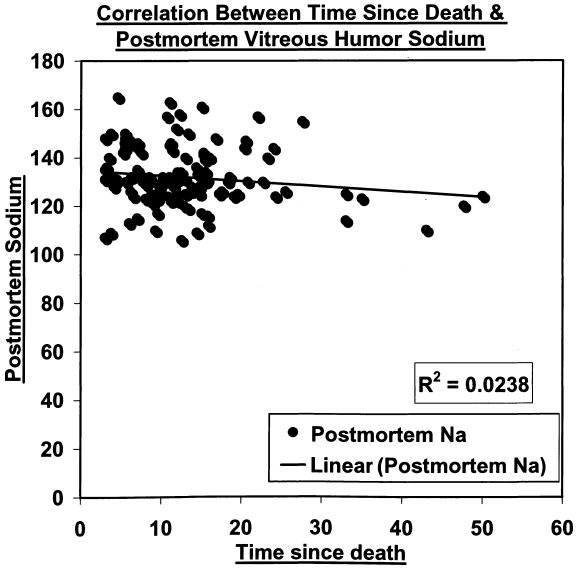

FIG. 2—*Linear regression graph showing correlation between time since death and postmortem vitreous humor sodium.*

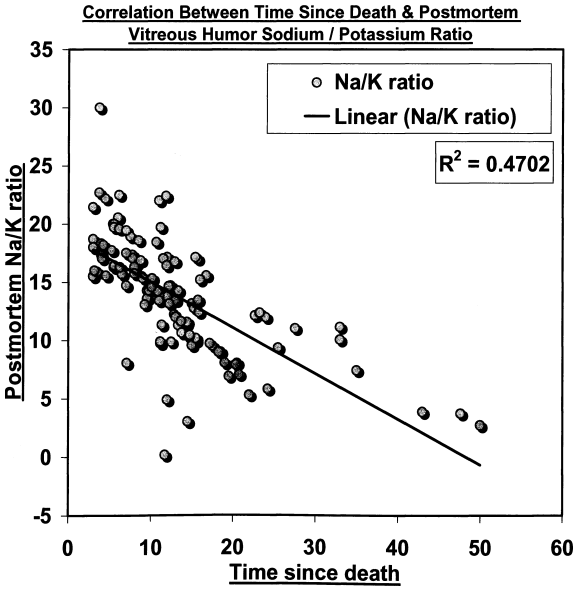

FIG. 3—*Linear regression graph showing correlation between time since death and postmortem vitreous humor sodium/potassium ratio.*

TABLE 3—*Comparison between antemortem blood and postmortem vitreous humor values of various variables.*

	Variables	No.	Mean	SD	*t*-Value	*p*-Value
Comparison between	Antemortem Na	59	133.37	10.45	1.984	0.052
	Postmortem Na	59	129.95	10.33	Difference is not significant	
Comparison between	Antemortem K	59	5.22	5.59	−5.256	2.20E-06 (<0.05)
	Postmortem K	59	11.79	8.00	Difference is significant	

59 cases (50%). Antemortem blood sodium values and postmortem VH sodium values were almost similar (*p*-value of 0.052), but a significant difference was observed between antemortem blood potassium values and postmortem VH potassium values (Table 3). Antemortem calcium and chloride levels were available only in two and one case, respectively, and hence, the correlation studies could not be carried out.

Discussion

VH is a colorless, jelly-like, hydrophilic gel within the vitreous body, around 4–5 mL in quantity (14). It is preferred for postmortem investigations because of its large volume and easy accessibility (2). It contains 99% water and solids in the form of macromolecular and low molecular weight constituents, such as sugars, urea, creatinine, and electrolytes. The various electrolytes that can be measured in VH are sodium, potassium, chloride, calcium, and magnesium (15,16). VH is relatively inert and only slightly influenced by sudden fluctuations in the blood chemistry (2). The concentration of sodium is equal to that of plasma indicating passive diffusion. The potassium concentration of VH is slightly higher than the plasma because of an active transport of potassium across the ciliary body into the posterior chamber and through the anterior capsule of the lens and passive diffusion through the posterior capsule of the lens into the vitreous body (5). After death, there is steady potassium leak through the cell membrane to approach equilibrium with the plasma in the postmortem period, which helps to estimate the PMI. Numerous workers have demonstrated the linear relationship between increase in vitreous potassium concentration and increasing PMI (7).

In this study, the postmortem VH potassium values ranged between 4.80 and 45.60 mmol/L and there was a linear rise of vitreous potassium in the early PMI. These results were similar to the previous reports in literature (2,7). The slope of regression line for postmortem vitreous potassium rise with increasing PMI was 0.929 mmol/L per hour with a 0 h "y" intercept of 2.616 mmol/L (Fig. 1). Similarly, 0 h "y" intercept of 4.2 mmol/L has been reported by James et al. (17) The variation in experimental methods and the sample characteristics may account for the differences noted with the slopes in various studies. It is essential that the slope of regression line be relatively steeper because flatter slopes tend to overestimate the time since death based on the obtained regression line and equation. Many equations and corresponding formulas have been reported in literature to precisely estimate the PMI based on postmortem vitreous potassium concentration. Many of these equations are based on the linear regression model on the assumption that the postmortem increase in the vitreous potassium is proportional with time and changes at a constant rate. The earliest and widely used equation was developed by Sturner and Gantner (5).

$$\text{PMI (hours)} = (7.14 \times \text{K}^+) - 39.1$$

A primary disadvantage of this equation was that a flat slope was reported with this equation and significant difference was observed between actual postmortem potassium and estimated potassium value. Accurate PMI estimation was possible with sudden and traumatic deaths when compared to the hospital deaths where severe antemortem electrolyte imbalance often upset the potassium values considerably (5). Later, Madea et al. (18) devised another equation.

$$\text{PMI (hours)} = (5.26 \times \text{K}^+) - 30.9$$

The linear regression derived by Madea et al. (18) had a steeper slope and they suggested that Sturner's equation systemically overestimated the PMI because of the flat slope, while their equation with a steeper slope had no systematic deviations. They concluded that when using vitreous potassium in estimation of the PMI, equation with a steeper slope should be preferred to avoid any systematic overestimation as a result of flatter slopes. Recently, James et al. (17) also devised an equation for the estimation of PMI based on postmortem potassium concentrations.

$$\text{PMI (hours)} = (4.32 \times \text{K}^+) - 18.35$$

In spite of all conflicting reports in literature regarding the different 95% confidence intervals and the best equation for practical use in PMI estimation, there is wide consensus on the linear increase in postmortem vitreous potassium with increasing PMI (17,18). In this study, antemortem serum potassium, when available, reflected the expected postmortem rise in vitreous values. By using statistical tools, we derived the following formula:

$$\text{K}^+ = 2.616 + 0.929\ (\text{PMI in hours})$$

$$\text{PMI (hours)} = 1.076\,(\text{K}^+) - 2.815$$

Thus, the measurement of VH potassium possesses inherent technical advantages and surmounts exterior influences offering an exciting new tool for future forensic studies. While in investigations the PMI has been used as independent and potassium as dependent variable in the linear regression analysis, the recent use of potassium as independent variable has been useful for more accurate death time estimation as the use of sodium/potassium ratio in our study (8,19). Also as the Figs. 1 and 3 show, the various amount

of scatter indicates that no one test can confidently predict the PMI. James et al. (17) in their study of 100 autopsy cases observed that using both potassium and hypoxanthine measurements to estimate the PMI were associated with increased accuracy in all circumstances.

Vitreous sodium, calcium, and chloride concentration had no role in estimating PMI in this study as also mentioned by other investigators (15). Dufour reported (20) no significant change in postmortem vitreous calcium when compared to antemortem serum calcium.

The postmortem VH sodium to potassium ratio varied from 0.17 to 30.00, with the mean of 13.90 (SD = 4.85) and it was observed that the ratio was indirectly proportional to the PMI. This observation is similar to the one of Singh et al. (21), who found the ratio useful in their 1026 cases where it decreased rapidly from mean value of 24.22 ± 7.59 at PMI of <3 h to mean value of 14.93 ± 4.47 at postmortem interval of 15–18 h and then at a progressively slower rate to mean value of 6.95 ± 1.88 at postmortem interval of 60–66 h. They also observed that the relationship of ratio with environmental temperature, age, gender, and cause of death was highly significant. Postmortem interval could be predicted from vitreous sodium/potassium electrolytes concentration ratio, with standard error of estimate 0.18 h (21). Hence, besides potassium concentration, sodium/potassium ratio can also be utilized as an additional parameter for PMI estimation.

Antemortem blood sodium and potassium values were available in 59 cases (50%). Antemortem blood sodium values and postmortem VH sodium values were almost similar (p-value of 0.052), but significant difference was observed between antemortem blood potassium values and postmortem VH potassium values. From these observations, evaporation can be dismissed as the cause of rise in the vitreous potassium concentration after death as no similar type of change has been demonstrated in the sodium concentration. These findings support the previous observation that sodium has no role in estimating PMI. Jaffe in his study (22) also eliminated evaporation as a cause of postmortem rise of vitreous potassium by demonstrating the stability of sodium and chloride concentrations.

In this study, age of deceased varied from 15 to 88 years with mean of 51.5 (SD = 17.65). The linear regression graph between postmortem VH potassium and age of deceased was horizontal, suggesting no correlation between the two (p-value of 0.631). This result is in accordance with the result of Garg et al. (2) However, a study by Coe suggested that age of the individual may have some effect on the vitreous potassium (23).

No correlation was observed between postmortem VH potassium and sex of deceased (p-value of 0.382), which is in accordance with the result of Garg et al. (2). Singh et al. (21) observed gender variation in sodium/potassium ratio. They proposed that abundant subcutaneous tissue in women retains body heat for longer period, which heightens the process of decomposition, thereby probably enhancing the process of diffusion of electrolytes (21).

During monsoon, 55.8% of the samples were collected and 30.8% and 13.3% were collected during winter and summer, respectively. It was observed that there was no effect of season of death on postmortem VH potassium value (p-value of 0.984). Similar results were obtained by others who commented on the lack of influence of environmental temperature (2), although vitreous potassium concentrations in Bray's study (24) were found to be lower in the cold weather. Komura and Oshiro (25) were among the early investigators to suggest a significant influence of ambient temperature on vitreous potassium concentration. They found that the bodies at warmer temperatures had higher vitreous potassium levels than those present at lower temperature. This study was carried out in Mumbai, a city on the western coast of India, where temperature difference seen between the different seasons is not much. This can explain the lack of influence of environmental temperature on postmortem VH potassium value. In this study, 35.8% of the samples were analyzed immediately within 1 h of collection and 64.2% of the samples were refrigerated at 4°C and analyzed subsequently. It was observed that refrigeration of sample did not affect postmortem VH potassium value (p-value of 0.336). This result is similar to that of Garg et al. (2) However, others have reported that freezing and thawing can cause increase in potassium concentration, other chemical analytes, and osmolality (26,27). The body temperature at the time of death in cases of infectious diseases was not taken into consideration and would require further studies.

Septicemia and tuberculosis were major causes of death among the deceased followed by intrapulmonary hemorrhages in acute febrile illness and pneumonia. It was observed in our study that cause of death has no effect on postmortem vitreous potassium value. Among other studies in the literature, based on cases of sudden deaths after chronic diseases, Madea et al. (18) suggested 95% limits of confidence in the range of ±34 h up to 120 h postmortem. This discrepancy may be a result of antemortem electrolyte imbalances caused by the chronic diseases. Potassium values in burn cases were found to be higher than the nonburn cases by Garg et al. (2).

It is necessary to remove all of the fluid from the eye that can be aspirated because the VH next to retina has a different concentration of solutes than in the central portion of the globe until putrefaction sets in. Therefore, an accurate measure of the vitreous level of a solute requires a total removal of the VH as is possible as also stressed by Lie without forceful aspiration (28). Also the vitreous must be aspirated slowly to avoid tearing loose fragments of tissue. Such tissue fragments grossly distort the electrolytes in the vitreous as it is from such cells that most of the electrolytes are derived. Hence, while aspiration, we left behind a residual VH to avoid contamination.

Studies in the past have demonstrated that the values of potassium manifest in the vitreous will vary with the instrumentation used to measure the concentration (29,30). However, we were unable to explore this aspect in our study. The most important concern in utilizing vitreous biochemistry for crucial forensic pathology determinations arises from the observed between eye differences at identical PMI (13,31). However, we did not measure VH electrolytes in both eyes but aspirated VH from either the left or right eye, which ever was convenient.

To conclude, the results of this study show that VH potassium and sodium/potassium concentration ratio play a significant role in estimating the PMI. The sodium, calcium, and chloride levels have no role in estimating PMI. Other factors like age, sex, cause of death, season of death, and refrigeration of sample does not influence VH potassium values. Once obtained, VH may be refrigerated for lengthy periods without deterioration. Evaporation can be dismissed as the cause of the rise in the VH potassium concentration after death as no similar changes were demonstrated in the sodium concentration. Unique advantages of this method are that it is extremely simple, requiring inexpensive apparatus for the collection of sample and its processing. The findings of this study support a central role of VH biochemistry in many postmortem forensic and pathological evaluations.

References

1. Narayan Reddy KS. The essentials of forensic medicine and toxicology, 24th edn. India: Sugandhadevi K, 2005.

2. Garg V, Oberoi SS, Gorea RK, Kiranjeet K. Changes in the levels of vitreous potassium with increasing time since death. JIAFM 2004;26(4): 136–9.
3. Madea B, Musshoff F. Postmortem biochemistry. Forensic Sci Int 2007;3:165–71.
4. Naumann HN. Postmortem chemistry of the vitreous body in man. Arch Ophthalmol 1959;62:356–63.
5. Sturner WQ, Gantner GE Jr. The postmortem interval. A study of potassium in the vitreous humor. Am J Clin Pathol 1964;42:137–44.
6. Prasad BK, Choudhary A, Sinha JN. A study of correlation between vitreous potassium level and post mortem interval. Kathmandu Univ Med J 2003;1(2):132–4.
7. Lange N, Swearer S, Sturner WQ. Human postmortem interval estimation from vitreous potassium: an analysis of original data from six different studies. Forensic Sci Int 1994;66:159–74.
8. Madea B, Rödig A. Time of death dependent criteria in vitreous humor: accuracy of estimating the time since death. Forensic Sci Int 2006;3:87–92.
9. Péclet C, Picotte P, Jobin F. The use of vitreous humor levels of glucose, lactic acid and blood levels of acetone to establish ante mortem hyperglycemia in diabetics. Forensic Sci Int 1994;65(1):1–6.
10. Stolyszewski I, Niemcunowicz-Janica A, Pepiński W, Spólnicka M, Zbiec R, Janica J. Vitreous humour as a potential DNA source for postmortem human identification. Folia Histochem Cytobiol 2007;45(2): 135–6.
11. Finkbeiner WE, Ursell PC, Davis RL. Autopsy pathology: a manual and atlas, 1st edn. Philadelphia, PA: Churchill Livingstone, 2004.
12. Park K. Park's Textbook of preventive and social medicine, 19th edn. India: Bhanot Publishers, 2007.
13. Singh G. Freely available statistical software on internet. Internt J Med Simul 2009;2:2.
14. Albert DM, Jakobiec FA. Principles and practice of ophthalmology, basic sciences, 2nd edn. Philadelphia, PA: WB Saunders Company, 1994.
15. Farmer JG, Benomran F, Watson AA, Harland WA. Magnesium, potassium, sodium and calcium in postmortem vitreous humor from humans. Forensic Sci Int 1985;27(1):1–13.
16. Pounder DJ, Carson DO, Johnston K, Orihara Y. Electrolyte concentration differences between left and right vitreous humor samples. J Forensic Sci 1998;43(3):604–7.
17. James RA, Hoadley PA, Sampson BG. Determination of postmortem interval by sampling vitreous humor. Am J Forensic Med Pathol 1997; 18(2):158–62.
18. Madea B, Henssge C, Hönig W, Gerbracht A. References for determining the time of death by potassium in vitreous humor. Forensic Sci Int 1989;40(3):231–43.
19. Muñoz JI, Suárez-Peñaranda JM, Otero XL, Rodríguez-Calvo MS, Costas E, Miguéns X, et al. A new perspective in the estimation of postmortem interval (PMI) based on vitreous. J Forensic Sci 2001;46(2):209–14.
20. Dufour DR. Lack of correlation of postmortem vitreous humor calcium concentration with ante mortem serum calcium concentration. J Forensic Sci 1982;27(4):889–93.
21. Singh D, Prashad R, Sharma SK, Pandey AN. Double logarithmic, linear relationship between postmortem vitreous sodium/potassium electrolytes concentration ratio and time since death in subjects of Chandigarh zone of northwest India. JIAFM 2005;27(3):159–65.
22. Jaffe FA. Chemical postmortem changes in the intraocular fluid. J Forensic Sci 1962;7:231–7.
23. Coe JI. Vitreous potassium as a measure of the postmortem interval: an historical review and critical evaluation. Forensic Sci Int 1989;42(3): 201–13.
24. Bray M. The eye as a chemical indicator of environmental temperature at the time of death. J Forensic Sci 1984;29(2):396–403.
25. Komura S, Oshiro S. Potassium levels in the aqueous and the vitreous humor after death. Tohoku J Exp Med 1977;122(1):65–8.
26. Bray M. The effect of chilling, freezing and rewarming on the postmortem chemistry of vitreous humor. J Forensic Sci 1984;29(2):404–11.
27. Gagajewski A, Murakami MM, Kloss J, Edstrom M, Hillyer M, Peterson GF, et al. Measurement of chemical analytes in vitreous humor: stability and precision studies. J Forensic Sci 2004;49(2):371–4.
28. Lie JT. Changes of potassium concentration in the vitreous humor after death. Am J Med Sci 1967;254(2):136–43.
29. McNeil AR, Gardner A, Stables S. Simple method for improving the precision of electrolyte measurements in vitreous humor. Clin Chem 1999;45:135–6.
30. Coe JI, Apple FS. Variations in vitreous humor chemical values as a result of instrumentation. J Forensic Sci 1985;30(3):828–35.
31. Mulla A, Massey KL, Kalra J. Vitreous humor biochemical constituents: evaluation of between-eye differences. Am J Forensic Med Pathol 2005; 26(2):146–9.

Additional information—reprints not available from author:
Kusum D. Jashnani, M.B.B.S., M.D.
8, Ashirwad, 1st Floor
Opposite Kakad Industrial Estate
L. J. Cross Road-3, Mahim
Mumbai 400016
India
E-mail: kusumjash@hotmail.com

JOURNAL OF FORENSIC SCIENCES

J Forensic Sci, November 2010, Vol. 55, No. 6
doi: 10.1111/j.1556-4029.2010.01489.x
Available online at: onlinelibrary.wiley.com

PAPER

PATHOLOGY/BIOLOGY

Jonathon Herbst,[1] *M.D.; Calle Winskog,*[1] *M.D.; and Roger W. Byard,*[1,2] *M.B.B.S., M.D.*

Cardiovascular Conditions and the Evaluation of the Heart in Pregnancy-Associated Autopsies

ABSTRACT: Pregnancy-associated death is defined as the death of a woman from any cause during pregnancy or in the year after delivery. This review concentrates on cardiac conditions that may result in pregnancy-associated death including, but not limited to, acute myocardial infarction, endocarditis, peripartum cardiomyopathy, and prolonged QT syndrome. Lethal vascular conditions may also occur involving arterial dissection and thromboembolism, on occasion exacerbated by hypercoagulability, and altered hormonal and physiologic states. The autopsy evaluation of these patients includes a careful assessment of the medical history particularly for prior pregnancy-related conditions, fetal loss, and episodes of unexplained collapse. A family history of sudden death at an early age may be significant. At autopsy, evaluation for underlying syndromes such as Marfan, or evidence of intravenous narcotism should be undertaken. Autopsy examination involves careful dissection of the heart and vessels with consideration of conduction tract studies and possible genetic evaluation for prolonged QT syndrome.

KEYWORDS: forensic science, forensic pathology, pregnancy, autopsy, cardiac, sudden death, cardiomyopathy, dissection, myocardial infarct, thromboembolism, postpartum

Medical examiners and forensic pathologists must have a clear understanding of lethal cardiac conditions associated with both pregnancy and the postpartum period, as cardiovascular conditions account for a substantial proportion of fatalities in this group of women (1). Carter and Rutty found the most common direct cause of maternal death in the United Kingdom over a 3-year period from 1997 to 1999 to be pulmonary thromboembolism (1). Acute myocardial infarction, endocarditis, valvular heart disease, and arrhythmias are among other conditions that may also cause death (2–5). Whitehead et al. (6) studied pregnancy-related mortality because of cardiomyopathy from 1991 to 1997 and noted that this accounted for 7.7% of deaths, with the percentage of deaths because of cardiomyopathy increasing since the previous decade. Despite this, most reviews have not focussed on cardiovascular conditions.

The evaluation of possible cardiac death associated with pregnancy first requires an understanding of the various terminologies that may be used, such as maternal death, pregnancy-related death, late maternal death, and pregnancy-associated death. Pregnancy-associated death will be the term used in this paper as this covers "the death of a woman, from any cause, while she is pregnant or within 1 year of the termination of pregnancy, regardless of the duration and site of pregnancy" (7). Maternal death is the "death of a woman while pregnant or within 42 days of the termination of pregnancy, irrespective of the duration and the site of the pregnancy, from any cause related to or aggravated by the pregnancy or its management, but not from accidental or incidental causes" (8), and pregnancy-related death refers to the "death of a woman while pregnant or within 42 days of the termination of pregnancy, irrespective of the cause of death" (8). Finally, late maternal death refers to "death of a woman from direct or indirect obstetric causes more than 42 days but <1 year after termination of the pregnancy" (8). Thus, pregnancy-associated death appears to be the most inclusive term. As cardiac deaths may occur well after 42 days, this terminology allows the inclusion of those patients.

It is important to clarify two additional definitions. Direct obstetric deaths are "those resulting from obstetric complications of the pregnant state (pregnancy, labor, and puerperium), from interventions, omissions, incorrect treatment, or from a chain of events resulting from any of the above" (8). Indirect obstetric deaths are "those resulting from previous existing disease or disease that developed during pregnancy and which was not due to direct obstetric causes, but which was aggravated by physiologic effects of pregnancy"(8).

This review will begin with those entities, which would be the most apparent on gross examination such as acute myocardial infarction or coronary artery dissections. As the paper continues, we explore those entities that may not be apparent to the naked eye such as arrhythmogenic disorders, and amniotic and air embolism for which the heart or vessels may appear grossly normal.

Acute Myocardial Infarction—Coronary Artery Pathology

In 1996, Roth and Elkayam reported 123 pregnancies complicated by 125 myocardial infarctions (9). The overall maternal death rate was 21%. Fifty-four percent of all patients had coronary artery evaluation either by angiography or at autopsy. Of those who had anatomic evaluation of the cardiac vessels, 16% were complicated by dissection, most of which occurred in the immediate postpartum

[1]Forensic Science SA, 21 Divett Place, Adelaide, SA, 5000, Australia.
[2]Discipline of Pathology, The University of Adelaide, Frome Rd, Adelaide, SA, 5005, Australia.

Received 29 May 2009; and in revised form 6 Aug. 2009; accepted 26 Sept. 2009.

period. Aneurysms were noted in 4% of the patients and coronary artery spasm in 1%. Interestingly, 29% of the coronary arteries evaluated anatomically were found to be normal. Coronary thrombus without atherosclerotic heart disease was detected in 21% of the patients.

In 2008, Roth and Elkayam published a further review, from 1995 to 2005, in which 96 of 103 (93%) pregnancies complicated by myocardial infarction had received coronary evaluation either by angiography or at autopsy (10). Twenty-eight patients had coronary artery dissection (27%) compared to 16% in the previous study. Thirteen percent of patients in the later study had normal vessels. The mortality rate had decreased to 11% in the 2008 review from 21% in the previous study. The finding of coronary thrombosis without atherosclerotic heart disease occurred in 8% of the patients.

Research into the etiology of dissections suggests that hemodynamic and increased progesterone levels (10) could lead to loss of integrity of the intimal layer of vessels and contribute to such vascular events (11,12). A 1967 study by Menalo-Estrella et al. (13) examined the histology of the aorta in pregnancy and found changes in the elastic and reticular fibers. Such vascular changes, in combination with arterial blood pressure changes, could account for dissections, particularly if these occur in more than one vessel.

The unique stresses and changes in physiology in the pregnant state may also be important factors in the development of acute myocardial infarction because of causes other than dissection. Pregnancy results in increases in blood volume, resting cardiac output, stroke volume, and heart rate (5,14,15). Roth noted that 84% of myocardial infarctions were anterior in location in nonsurvivors of acute myocardial infarction (9). The stage of pregnancy at the time of infarction is also an important factor, with mortality higher during the peripartum period (18%) than in the antepartum (9%) or postpartum periods (9%) (10).

James et al. (2) examined myocardial infarctions in the United States from 2000 to 2002. By reviewing pregnancy-related discharge records, they found 859 patients with acute myocardial infarction, with 44 deaths caused by acute myocardial infarction resulting in a case fatality rate of 5.1% and an overall mortality rate of 0.35 per 100,000 deliveries. They also noted that anterior wall infarction was more common than lateral- or inferior wall infarcts with subendocardial infarction present in 37% of the patients. The authors noted that these data might not include those women who died outside hospital. Risk factors for myocardial infarction included black race, age >35 for any race, hypertension, thrombophilia, diabetes mellitus, smoking, pre-eclampsia, blood transfusion, and postpartum infection (2).

Diagnosis

Before incising the coronary arteries at autopsy, their epicardial courses should be followed to check for any extravasated blood relating to possible dissection. The origin and ostia of the coronary arteries should be examined, and they should then be cross-sectioned at short intervals (1–2 mm) with careful attention being paid to the presence or absence of thrombus. It is important not to be deceived by the normal appearance of the coronary arteries, as an acute thrombus may be present in an apparently normal vessel.

Other arteries are also vulnerable to dissection during pregnancy, presumably from similar mechanisms, and this may involve pulmonary, splenic or other visceral vessels with lethal outcomes. These vessels should also be carefully sectioned at autopsy.

It is important, even in young mothers to examine particularly the anterior aspect of the myocardium and to take additional sections from this area for histology looking for changes of acute and chronic ischemic damage such as contraction band necrosis and fibrosis (15,16). As previously discussed, myocardial infarction can occur with seemingly normal coronary arteries, and so careful inspection of the myocardium is warranted regardless of the coronary artery findings.

Peripartum Cardiomyopathy (PPCM)

PPCM has a reported incidence of 1 in 3000 to 1 in 15,000 pregnancies in the United States (17). This is a unique disease entity that can display features of dilated cardiomyopathy, but is unique in the definitional use of its time at onset, and possible underlying etiologies. However, some authors relate that PPCM and cardiomyopathy that begins earlier in pregnancy may represent a continuum of disease (18). Still, unique definitions for the diagnosis were established at a workshop in 2000 (19). The pathology of PPCM was reported by Gouley et al. (20) in 1937. In this paper, a series of women with cardiomyopathy late in their pregnancies are described; four of the seven patients died and had autopsies. The original descriptions of the autopsies document mural thrombi associated with embolism to various organs and tissues including the brain, lung, and mesentery.

According to a workshop in 2000, the criteria for the diagnosis of PPCM include the development of congestive heart failure secondary to decreased left ventricular systolic function in the last month of pregnancy, or within 5 months of delivery, absence of pre-existing cardiac dysfunction, absence of a determinable cause of cardiomyopathy, and additional echocardiogram findings including depressed shortening fraction or ejection fraction (19).

Proposed mechanisms for PPCM include myocarditis, autoimmunity, apoptosis related, infection, and other etiologies including microchimerism (21). Other possibilities include drug-induced, familial, or nutritional factors (22). Ansari et al. (21) report unique autoantibodies against human cardiac tissue in those with PPCM but not in those with idiopathic dilated cardiomyopathy. Endomyocardial biopsies from 26 patients with PPCM have revealed viral genomes in eight patients (30.7%) that were associated with interstitial inflammation. The viral genomes included parvovirus B19, human herpes virus 6, EBV, and CMV (23). A study by Felker et al. (24) found myocarditis to be present in 62% of the patients based on endomyocardial biopsy.

Several studies have also demonstrated a high incidence of thromboembolism in patients with PPCM. A clinical or pathological suspicion of PPCM should, therefore, lead a pathologist to carefully examine the vasculature including the pulmonary arteries, coronary arteries, and cerebral and limb vessels (14,25–32). Conversely, the finding of pulmonary thromboembolism should raise the possibility of PPCM. In Whitehead et al.'s (6) study among PPCM deaths, eight patients (5%) had pulmonary or cerebrovascular thromboembolism. Ro et al. (22) report that mortality caused by embolic events associated with this condition may be as high as 30%. Thromboemboli may develop because of the hypercoagulable state of pregnancy complicated by static flow through a poorly contracting heart (33). These conditions can lead to intracardiac thrombosis, which can subsequently embolize to peripheral locations in the body (25,26,30).

Cardiomyopathy is one of the few pregnancy-related (sic) deaths that has been increasing in incidence since 1979 (6,34). PPCM was the leading cause of pregnancy-related (sic) death in North Carolina from 1993 to 1997, accounting for 26 deaths (35). Studies have demonstrated a mortality rate ranging from 9% to 56% (18,36).

Diagnosis

In Gouley et al.'s original study, the heart weights at autopsy ranged from 450 to 500 g with histologic evidence of widespread and severe focal inflammatory reactions, often with necrosis followed by fibrosis. Other microscopic findings included focal myocardial degeneration and/or dissolution (20). Myocarditis is one of many postulated causes of PPCM. More recently, O'Connell et al. evaluated 14 patients with PPCM and compared the characteristics to 55 patients with idiopathic dilated cardiomyopathy. They noted that findings such as myocyte hypertrophy, nuclear hyperchromaticity, and interstitial fibrosis were similar, with the exception of myocarditis that was seen in 29% of patients with PPCM, compared to only 9% of those with idiopathic dilated cardiomyopathy (37). Myocarditis was defined as interstitial and perivascular lymphomononuclear infiltration in the presence of myocyte necrosis, with or without fibrosis. Carter and Rutty describe no characteristic features that were absolutely diagnostic of this entity but noted that on endomyocardial biopsy, the findings may include focal fibrosis, variability in myocyte caliber, and scattered chronic inflammatory cells (1).

Valvular Heart Disease and Endocarditis

Deaths in patients with mitral stenosis are rare (38) although a review of cardiovascular surgery over the period 1984 to 1996 reported a mortality rate of 9% during pregnancy. This mortality rate may reflect the fact that these were high-risk patients refractory to conventional therapies. Surgical techniques may also have been refined and improved since the period of study (39). Mitral regurgitation with the associated findings of either rheumatic heart disease or mitral valve prolapse is usually not as problematic as mitral stenosis (4).

Aortic regurgitation without left ventricular dysfunction and pulmonary stenosis are generally well tolerated during pregnancy (4). Other congenital malformations, including those with previous surgical repair, may also be seen, and aortic stenosis may present with varying degrees of severity.

In 1991, Clark stratified mortality risk groups into low, intermediate, and high risk based on particular cardiac conditions (40). High-risk conditions were defined as those with a mortality risk of 25–50% and included conditions with severe outflow obstruction such as severe aortic stenosis and marked pulmonary hypertension. Colman et al. described pulmonary vascular obstructive disease, Marfan syndrome with a dilated aortic root, severe aortic stenosis, and severe systemic ventricular dysfunction, as conditions with high enough risk to warrant avoidance of pregnancy and the consequent high risk of mortality (41).

A review examining bacterial endocarditis in 68 pregnancies calculated a maternal death rate of 22% with an associated fetal mortality rate of 14.7% (42). Valve-specific mortality was highest for aortic valve disease at 42%. The authors also noted that 27% of patients were associated with postpartum endocarditis (42). Montaya et al. (3) reported a case of endocarditis occurring during pregnancy in a woman with a history of intravenous drug use and a bicuspid aortic valve.

Diagnosis

Given the possibility of endocarditis, it is important to examine the valves closely and to particularly assess the anatomy and integrity of the leaflets and cusps. Needle track marks can be looked for in the context of a history of intravenous drug use (42). Additionally, high-risk conditions such as mitral incompetence, aortic stenosis, and Marfan disease should be specifically sought. Valvular heart disease also carries the risk of thromboembolism and stroke, and so vascular evaluation at sites removed from the heart is also required. Additionally, special attention should be placed to the right-sided valves when given a history of IV drug use.

Arrhythmias Including the Long QT Syndrome (LQTS)

Rashba et al. conducted a retrospective analysis during pregnancy of women either with hereditary long QT syndrome or with relatives with this disorder. Three affected first-degree relatives died during the postpartum period of presumed LQTS. Additional events noted in this study included two probands with aborted cardiac arrest before pregnancy, two during pregnancy, and seven in the postpartum period (43).

Seth et al. also examined LQTS in pregnant and nonpregnant women, and their conclusions were that while there is a reduced risk of cardiac events during pregnancy, there is increased risk in the 9-month period postpartum. Specifically they noted a 2.7-fold increased risk of a cardiac event and a 4.1-fold increased risk of a life-threatening cardiac event (defined in their study as aborted cardiac arrest or LQTS-related death), during this time. The risk for cardiac events in the postpartum period was especially evident in those with the LQT2 genotype. Those with LQT1, LQT3 or non-genotyped cases had a lower annual cardiac event rate (5).

The explanation why the postpartum period may be more conducive for a fatal arrhythmogenic event secondary to LQTS involves the heart rate. During pregnancy, there is a baseline increase in heart rate, which brings with it a shortening of the QT interval (i.e., producing a relative protective effect during pregnancy). However, in the postpartum period, as cardiac physiology returns to normal and the heart rate slows back to the baseline, there will be an increase in the QT interval. Several authors hypothesize that a stressful event such as caring for a newborn baby in the postpartum state could provoke a fatal event (5,44). In a study of LQTS by Schwartz et al. (44), 80% of the patients with events that occurred after auditory stimuli had LQT2. Other possible considerations for the increased events in the postpartum period include decreased levels of estrogen (5). Seth et al. (5) further state that decreased estrogen levels seen as during breastfeeding may lead to increased adrenergic activity and lead to increased myocyte excitability. This could lead to increased adverse events in the postpartum period (5).

Other arrhythmias may cause death during pregnancy. Brodsky et al. (45) reviewed ventricular tachycardia and noted two deaths out of 26 reported cases. The two deaths included one described by Rally and Walters (46) of a 19-year-old woman with symptomatic paroxysmal ventricular tachycardia that developed in the sixth month of pregnancy, who died suddenly 3 weeks after therapy. Postmortem examination revealed a structurally normal heart. Another case involved a woman who survived a myocardial infarct with ventricular fibrillation at 6 months gestation only to die 3 months later while still pregnant and in hospital awaiting labor. An autopsy demonstrated thrombotic occlusion of the circumflex artery (47). Arrhythmias may also be seen in conjunction with congenital heart disease. Other conditions that can result in sudden unexpected death are catecholaminergic polymorphic ventricular tachycardia (CPVT), Congenital short QT syndrome, and Brugada syndrome (48,49).

Diagnosis

A history of arrhythmia should be looked for at the time of medical record review. In addition to careful dissection of the heart

TABLE 1—*Time-related vulnerability to certain conditions in pregnancy.**

Early-mid pregnancy
Cardiomyopathies (other than PPCM), clinical congestive heart failure
Acute myocardial infarction
High-risk valvular heart disease
Pulmonary thromboembolism
Endocarditis
Viral myocarditis
Peripartum
Acute myocardial infarction specifically involving coronary dissections
PPCM
Amniotic fluid embolism
Air embolism
Pulmonary thromboembolism
Endocarditis
Viral myocarditis
Postpartum
PPCM
Long QT syndrome
Acute myocardial infarction
Endocarditis
Viral myocarditis

PPCM, peripartum cardiomyopathy.

*Conditions may be listed in more than one category, as death may be because of that condition at various points of time. The table displays those entities that commonly cause death at certain timeframes of the pregnant state. Other entities, not listed need to be considered in the appropriate setting.

with routine histologic sampling, Schandl and Collins (16) recommend evaluation of the conduction system in the maternal autopsy. If a structurally normal heart is found at autopsy, molecular testing for LQTS and other cardiac conditions that can result in sudden death, i.e., CPVT, should be considered. Molecular testing for LQ genotypes may also be of considerable benefit to the family. Testing for LQTS requires DNA, and specimens should be sent to a specialist laboratory. Suitable specimens include whole blood collected in EDTA tubes. Additionally, tissues such as frozen heart, liver, or spleen tissues are also suitable specimens (49). Of these tissues, 5–10 g should be flash-frozen at −80°C (49). Formalin-fixed, paraffin-embedded tissues are suboptimal for postmortem genetic testing (50).

Hypercoagulable States of Pregnancy, Amniotic Fluid, and Air Embolism

In addition to the earlier conditions that may predispose to thromboembolism, hypercoagulability may also occur because of changes in the levels of coagulation factors, as well as to physical effects relating to pregnancy. Alterations may occur in concentrations of von Willebrand factor, Factor VIII, fibrinogen, and other factors. Protein S may decrease in concentration, and there may be increased resistance to protein C (51). Plasminogen activator inhibitors 1 and 2 are increased in concentration (52). On a physical level, the gravid uterus may compress pelvic vessels leading to venous stasis, as may decrease ambulation.

The antiphospholipid syndrome (APS) may also cause a prothrombotic state resulting in recurrent early pregnancy loss of the fetus, with both venous and arterial thrombi (53). Those with known APS can be managed with anticoagulation during future pregnancies; however, in 6% of the patients, APS presents *de novo* during pregnancy or the puerperium (54).

Several recent papers have described the approach to amniotic fluid and air embolism (15,55). The former condition is associated with a high mortality, and clinical findings can include disseminated intravascular coagulation, pulmonary edema, hemorrhage, and signs that should be apparent at autopsy. There may be a clinical record of seizures or respiratory failure; however, the typical history is usually that of sudden cardiovascular collapse. Risk factors are more likely in multiparous patients, with a rapid labor (15). The mechanism required for the development of amniotic fluid embolus is the entry of amniotic fluid directly into the maternal circulation. This usually occurs at the lower uterine segment or endocervix. The taking at autopsy of tissue sections for histologic evaluation of these areas is recommended (15,16,55). Another possible mechanism leading to the catastrophic consequences of amniotic fluid embolus is a maternal anaphylactic reaction to fetal antigens (56). An elevated serum tryptase can, therefore, support the diagnosis of amniotic fluid embolus (55,56).

Air embolism must be another consideration for sudden unexpected death following cardiovascular collapse. The lethal mechanism involves air entering the maternal circulation. Here, the portal of entry may be secondary to placental abruption, or occur during intercourse (15). The result is that air enters the uterine cavity and gains entry to the uterine venous drainage. From there, air proceeds via the usual circulatory pathways to the right side of the heart and ultimately can become lodged in the pulmonary vasculature.

Diagnosis

The investigation into pulmonary thromboembolism requires careful evaluation of the pulmonary arteries in addition to the veins of the legs and pelvis, with multiple tissue specimens for histology. Anatomic conditions such as patent foramen ovale may lead to paradoxical embolism with stroke (52).

For amniotic fluid embolus, multiple lung sections should also be examined. The classical finding is squamous cells in the pulmonary circulation. One must be wary that squamous cells may also be because of contamination. More convincing material is fetal material, debris, mucin or lanugo. Finding a response to this foreign material by leukocytes is still more convincing.

Special stains can be useful in the evaluation of foreign material in the lungs. Stains employed can include alcian blue pH 2.5 for the evaluation of mucin, and low and high molecular weight keratin stains (AE1/AE3) for squamous cells (55). The Attwood stain may prove of additional benefit (15). The characteristics of this stain include staining mucin green, squamous cells red, and fibrin red. Polarization is also a useful technique for the detection of lanugo hairs (15). A recently described immunostain TKH-2 can also be employed and is a sensitive method to detect meconium and amniotic fluid derived mucin (57). A serum tryptase should also be performed and can be supportive of the diagnosis (55,56).

For the diagnosis of air embolism, ancillary techniques grossly include opening the heart initially under water, as any air bubbles would be expected to rise. Additionally, Christiansen and Collins (15) recommend examining the vasculature of the pelvis for air bubbles. Consideration should be given to saving frozen sections of lung tissue. These frozen section slides could then be used to look for air emboli. Air and fat emboli may look the same histologically, so the presence of a negative fat stain would be useful in concluding that air is present. One must be careful not to overinterpret emboli after cardiopulmonary resuscitation with fractures, as fat emboli may be a secondary phenomenon.

Conclusions

Pregnancy is associated with a range of cardiovascular and hematologic conditions that may interact to cause sudden and unexpected death in apparently healthy young women. A methodical

approach to the cardiovascular examination will assist in capturing the major unique disease entities that occur during this period. There is overlap with sudden unexpected death in nonpregnant persons, certainly in regard to the molecular genetic evaluation. Vulnerability to certain conditions varies at different stages of pregnancy Table 1, and the autopsy evaluation requires a stepwise assessment of the heart and vasculature as outlined in Table 2.

TABLE 2—*Guide to cardiac evaluation in the pregnancy-associated autopsy.*

Medical record review
History of congenital heart disease/cardiac surgery
Previous history of arrhythmia, collapse, thrombosis
Previous history of fetal loss/pregnancy-related problems
Family history of sudden death
Previous electrocardiographs
Previous obstetric history including C-section or difficult labor
General examination
Evidence of possible syndromes, e.g., Marfan
Track marks for intravenous drug use
Signs of congestive heart failure
Signs of endocarditis, including infarcts in susceptible organs (i.e., kidneys, spleen, extremities or digits)
Signs of disseminated intravascular coagulation that may be indicative of either Amniotic fluid embolus or sepsis
Heart
Weight
Standard full dissection
Photographic documentation of abnormalities
Valves
Careful examination for stenosis/incompetence
Congenital abnormalities
Vegetations
Coronary arteries
Check for dissection (more than one vessel may be involved)
Section at short intervals (1–2 mm) to evaluate for thrombosis (a thrombus may be present in otherwise normal vessels)
Myocardium
Liberal histologic sampling (particularly the anterior wall) to check for myocardial infarction/ischemia
Histologic evaluation for cardiomyopathies
Routine sampling of right ventricle for evaluation of arrhythmogenic right ventricular dysplasia (ARVD)
Consider histology of the conduction system
Consider viral culture of myocardium if the gross findings are negative
Serum viral cultures
Pulmonary arteries
Thromboemboli
Vessel wall dissection
Pulmonary artery examination for peripheral thromboemboli
Multiple sections for microscopic evidence of thromboemboli
Signs of pulmonary hypertension, including atheroma
Signs of amniotic fluid embolus
Squamous cells in pulmonary vasculature, mucin, lanugo, +/− inflammatory response to aforementioned features
Stains to assist include:
Alcian blue ph 2.5
Keratins (AE1/AE3)
Attwood stain
Immunostain TKH-2
Serum tryptase level
Hemosiderin-laden macrophages in congestive heart failure
Vasculature elsewhere
Vessel wall dissection
Vascular examination for thrombus
Molecular/Genetic
Consider long QT syndrome testing and testing of first-degree relatives
Consider testing for catecholaminergic polymorphic
Ventricular tachycardia (CPVT), short QT syndrome, and Brugada syndrome.

CPVT, catecholaminergic polymorphic ventricular tachycardia.

References

1. Carter N, Rutty GN. The maternal death. In: Ruddy GN, editor. Essentials of autopsy practice: recent advances, topics and developments. London, UK: Springer-Verlag, 2004;73–92.
2. James AH, Jamison MG, Biswas MS, Brancazio LR, Swamy GK, Myers ER. Acute myocardial infarction in pregnancy: a United States population-based study. Circulation 2006;113:1564–71.
3. Montoya ME, Karnath BM, Ahmad M. Endocarditis during pregnancy. South Med J 2003;96:1156–7.
4. Elkayam U, Bitar F. Valvular heart disease and pregnancy Part I: native valves. J Am Coll Cardiol 2005;46:223–30.
5. Seth R, Moss AJ, McNitt S, Zareba W, Andrews ML, Qi M, et al. Long QT syndrome and pregnancy. J Am Coll Cardiol 2007;49:1092–8.
6. Whitehead SJ, Berg CJ, Chang J. Pregnancy-related mortality due to cardiomyopathy: United States, 1991–1997. Obstet Gynecol 2003;102: 1326–31.
7. Atrash HK, Rowley D, Hogue CJ. Maternal and perinatal mortality. Curr Opin Obstet Gynecol 1992;4:61–71.
8. International statistical classification of diseases and related health problems. 10th revision, 2nd edn. Geneva, Switzerland: World Health Organization, 2004.
9. Roth A, Elkayam U. Acute myocardial infarction associated with pregnancy. Ann Intern Med 1996;125:751–62.
10. Roth A, Elkayam U. Acute myocardial infarction associated with pregnancy. J Am Coll Cardiol 2008;52:171–80.
11. Madu EC, Kosinski DJ, Wilson WR, Burket MW, Fraker TD Jr, Ansel GM. Two-vessel coronary artery dissection in the peripartum period. Case report and literature review. Angiology 1994;45:809–16.
12. Klutstein MW, Tzivoni D, Bitran D, Mendzelevski B, Ilan M, Almagor Y. Treatment of spontaneous coronary artery dissection: report of three cases. Cathet Cardiovasc Diagn 1997;40:372–6.
13. Manalo-Estrella P, Barker AE. Histopathologic findings in human aortic media associated with pregnancy. Arch Pathol 1967;83:336–41.
14. Abboud J, Murad Y, Chen-Scarabelli C, Saravolatz L, Scarabelli TM. Peripartum cardiomyopathy: a comprehensive review. Int J Cardiol 2007;118:295–303.
15. Christiansen LR, Collins KA. Pregnancy-associated deaths: a 15 year retrospective study and overall review of maternal pathophysiology. Am J Forensic Med Pathol 2006;27:11–9.
16. Schandl CA, Collins KA. Maternal autopsy. In: Collins KA, Hutchins GM, editors. Autopsy performance and reporting, 2nd edn. Northfield, IL: College of American Pathologists, 2003;135–47.
17. Mehta NJ, Mehta RN, Khan IA. Peripartum cardiomyopathy: clinical and therapeutic aspects. Angiology 2001;52:759–62.
18. Elkayam U, Akhter MW, Singh H, Khan S, Bitar F, Hameed A, et al. Pregnancy-associated cardiomyopathy: clinical characteristics and a comparison between early and late presentation. Circulation 2005;111: 2050–5.
19. Pearson GD, Veille JC, Rahimtolla S, Hsia J, Oakley CM, Hosenpud JD, et al. Peripartum cardiomyopathy. National Heart Lung and Blood Institute and Office of Rare Diseases (National Institutes of Health) workshop recommendations and review. JAMA 2000;283:1183–8.
20. Gouley BA, McMillan TM, Bellet S. Idiopathic myocardial degeneration associated with pregnancy and especially the puerperium. Am J Med Sci 1937;19:185–99.
21. Ansari AA, Fett JD, Carraway RE, Mayne AE, Onlamoon N, Sundstrom JB. Autoimmune mechanisms as the basis for human peripartum cardiomyopathy. Clin Rev Allergy Immunol 2002;23:289–312.
22. Ro A, Frishman WH. Peripartum cardiomyopathy. Cardiol Rev 2006; 14:35–42.
23. Bultmann BD, Klingel K, Nabauer M, Wallwiener D, Kandolf R. High prevalence of viral genomes and inflammation in peripartum cardiomyopathy. Am J Obstet Gynecol 2005;193:363–5.
24. Felker GM, Jaeger CJ, Klodas E, Thiemann DR, Hare JM, Hruban RH, et al. Myocarditis and long-term survival in peripartum cardiomyopathy. Am Heart J 2000;140:785–91.
25. Box LC, Hanak V, Arciniegas JG. Dual coronary emboli in peripartum cardiomyopathy. Tex Heart Inst J 2004;31:442–4.
26. Nishi I, Ishimitsu T, Ishizu T, Ueno Y, Suzuki A, Seo Y, et al. Peripartum cardiomyopathy and biventricular thrombi. Circ J 2002;66:863–5.
27. Sanchez-Rubio Lezcano J, Galache Osuna JG, Marquina Barcos A, Calvo Cebollero I, Diarte de Miguel JA, Placer Peralta LJ. Miocardiopatía periparto con trombosis biventricular. An Med Interna 2004;21:498–500.
28. Quinn B, Doyle B, McInerney J. Postnatal pre-cordial pain. Pulmonary embolism or peripartum cardiomyopathy. Emerg Med J 2004;21:746–7.

29. Kaufman I, Bondy R, Benjamin A. Peripartum cardiomyopathy and thromboembolism; anesthetic management and clinical course of an obese, diabetic patient. Can J Anaesth 2003;50:161–5.
30. Gagne PJ, Newman JB, Muhs BE. Ischemia due to peripartum cardiomyopathy threatening loss of a leg. Cardiol Young 2003;13:209–11.
31. Helms AK, Kittner SJ. Pregnancy and stroke. CNS Spectr 2005;10:580–7.
32. Silwa K, Skudicky D, Bergemann A, Candy G, Puren A, Sareli P. Peripartum cardiomyopathy: analysis of clinical outcome, left ventricular function, plasma levels of cytokines and Fas/Apo-1. J Am Coll Cardiol 2000;35:701–5.
33. Brown CS, Bertolet BD. Peripartum cardiomyopathy: a comprehensive review. Am J Obstet Gynecol 1998;178:409–14.
34. Berg CJ, Atrash HK, Koonin LM, Tucker M. Pregnancy-related mortality in the United States, 1987–1990. Obstet Gynecol 1996;88:161–7.
35. Buescher PA, Harper M, Meyer RE. Enhanced surveillance of maternal mortality in North Carolina. N C Med J 2002;63:76–9.
36. James PR. A review of peripartum cardiomyopathy. Int J Clin Pract 2004;58:363–5.
37. O'Connell JB, Costanzo-Nordin MR, Subramanian R, Robinson JA, Wallis DE, Scanlon PJ, et al. Peripartum cardiomyopathy: clinical, hemodynamic, histologic, and prognostic characteristics. J Am Coll Cardiol 1986;8:52–6.
38. Hameed A, Karaalp IS, Tummala PP, Wani OR, Canetti M, Akhter MW, et al. The effect of valvular heart disease on maternal and fetal outcome of pregnancy. J Am Coll Cardiol 2001;37:893–9.
39. Weiss BM, Von Segesser LK, Alon E, Seifert B, Turina MI. Outcome of cardiovascular surgery and pregnancy: a systematic review of the period 1984-96. Am J Obstet Gynecol 1998;179:1643–53.
40. Clark SL. Cardiac disease in pregnancy. Obstet Gynecol Clin North Am 1991;18:237–56.
41. Colman JM, Sermer M, Seaward PG, Siu SC. Congenital heart disease in pregnancy. Cardiol Rev 2000;8:166–73.
42. Campuzano K, Rogue H, Bolnick A, Leo MV, Campbell WA. Bacterial endocarditis complicating pregnancy: case report and systematic review of the literature. Arch Gynecol Obstet 2003;268:251–5.
43. Rashba EJ, Zareba W, Moss AJ, Hall WJ, Robinson J, Locati EH, et al. Influence of pregnancy on the risk for cardiac events in patients with hereditary long QT syndrome. Circulation 1998;97:451–6.
44. Schwartz PJ, Priori SG, Spazzolini C, Moss AJ, Vincent GM, Napolitano C, et al. Genotype phenotype correlation in the long-QT syndrome: gene-specific triggers for life-threatening arrhythmias. Circulation 2001;103:89–95.
45. Brodsky M, Doria R, Allen B, Sato D, Thomas G, Sada M. New-onset ventricular tachycardia during pregnancy. Am Heart J 1992;123:933–41.
46. Rally CR, Walters MB. Paroxysmal ventricular tachycardia without evident heart disease. Can Med Assoc J 1962;86:268–73.
47. Curry JJ, Quintana FJ. Myocardial infarction with ventricular fibrillation during pregnancy treated by direct current defibrillation with fetal survival. Chest 1970;58:82–4.
48. Chugh SS, Kelly KL, Titus JL. Sudden cardiac death with apparently normal heart. Circulation 2000;102:649–54.
49. Ackerman MJ, Tester DJ, Driscoll DJ. Molecular autopsy of sudden unexplained death in the young. Am J Forensic Med Pathol 2001;22:105–11.
50. Carturan E, Tester DJ, Brost BC, Basso C, Thiene G, Ackerman MJ. Postmortem genetic testing for conventional autopsy-negative sudden unexplained death. Am J Clin Path 2008;129:391–7.
51. Clark P, Brennand J, Conkie JA, McCall F, Greer IA, Walker ID. Activated protein C sensitivity, protein C, protein S and coagulation in normal pregnancy. Thromb Haemost 1998;79:1166–70.
52. Treadwell SD, Thanvi B, Robinson TG. Stroke in pregnancy and the puerperium. Postgrad Med J 2008;84:238–45.
53. Wilson WA, Gharavi AE, Koike T, Lockshin MD, Branch DW, Piette J-C, et al. International consensus statement on preliminary classification criteria for definite antiphospholipid syndrome. Arthritis Rheum 1999;47:1309–11.
54. Gomez-Puerta JA, Cervera R, Espinosa G, Bucciarelli S, Font J. Pregnancy and puerperium are high susceptibility periods for the development of catastrophic antiphospholipid syndrome. Autoimmun Rev 2006;6:85–8.
55. Marcus BJ, Collins KA, Harley RA. Ancillary studies in Amniotic fluid embolus: a case study and review of the literature. Am J Forensic Med Pathol 2005;26:92–5.
56. Benson MD, Lindberg RE. Amniotic fluid embolism, anaphylaxis, and tryptase. Am J Obstet Gynecol 1996;175:737.
57. Kobayashi H, Ooi H, Hayakawa H, Arai T, Matsuda Y, Gotoh K, et al. Histological diagnosis of amniotic fluid embolism by monoclonal antibody TKH-2 that recognizes NeuAc α 2-6GalNAc epitope. Hum Pathol 1997;28:428–33.

Additional information and reprint requests:
Jonathon Herbst, M.D.
Forensic Science South Australia
21 Divett Place
Adelaide, SA 5000
Australia
E-mail: herbst.jonathon@saugov.sa.gov.au

JOURNAL OF FORENSIC SCIENCES

J Forensic Sci, November 2010, Vol. 55, No. 6
doi: 10.1111/j.1556-4029.2010.01490.x
Available online at: onlinelibrary.wiley.com

PAPER

PATHOLOGY/BIOLOGY

Henry J. Carson,[1] *M.D.*

Patterns of Ecchymoses Caused by Manner of Death and Collateral Injuries Sustained in Bruising Incidents: Decedent Injuries, Profiles, Comparisons, and Clinicopathologic Significance

ABSTRACT: We investigated how ecchymoses could be used to predict other injuries, or help establish the cause of death. Ecchymoses, fractures, lacerations, abrasions, and other data were recorded. Eleven percent of decedents had ecchymoses. Motor vehicle accident by car (MVA-C) was the most common cause of ecchymoses and showed the most collateral injuries. Decedents of natural causes were more likely to have ecchymoses without collateral injuries. There appeared to be two groups of decedents with ecchymoses: one group is younger, comprised of victims of MVA-C and homicides, with more injuries related to ecchymoses than others; another is an older group of victims of other accidents, natural causes, and suicide. There were no indeterminate causes of death among decedents with ecchymoses. Therefore, ecchymoses may be a surrogate marker to direct the pathologist to continue to seek a cause of death should be seen, even if the case, otherwise, appears to be indeterminate.

KEYWORDS: forensic science, accidents, indeterminate, homicide, ecchymosis, natural death

Contusions or ecchymoses are common in clinical medicine. They are often indicators of domestic, sexual, or child abuse (1–3). In the event of fatality, they are no less important in forensic pathology. We investigated situations, where contusions and ecchymoses could be used to predict other injuries, estimate the sequence of injuries, or help establish or corroborate cause and manner of death.

A *contusion* is an extravasation of blood to mechanical trauma. It may occur in skin, solid organs, or viscera. In the skin, the injury is usually discolored blue or purple from blood that has extravasated because of blunt force trauma (4,5). A contusion may be considered an injury by itself and does not involve a secondary component; technically, there should be no breakage of the skin caused by the infliction of a contusion.

An *ecchymosis* refers to any extravasation of blood by any type of injury, including punctures (e.g. phlebotomy) or incisions (e.g. surgery). *Ecchymosis* is, therefore, a more-general term for extravasated blood than is *contusion*, which has a specific mechanism. Some authorities note that an ecchymosis may extend from a contusion when blood spreads under the skin beyond the site of blunt force injury because of gravity and anatomic barriers, causing extravasated blood to migrate from its original site. In the living patient, these injuries are often seen in the lower extremities and ankles (6). Thus, an ecchymosis may create an area of skin discoloration that is larger than the site of blunt force trauma from a contusion and may be remote from the initial injury site. A petechia is a small ecchymosis. Because an ecchymosis does not require mechanical injury to cause it, an ecchymosis can also form spontaneously in a living patient as a result of a medical condition, such as thrombocytopenia or other bleeding diathesis (7) and can be identified on mucous membranes. Contusions would be unlikely to form in mucous membranes, as direct blunt force trauma to an internal mucous membrane site is uncommon. Ecchymoses may also form because of skin fragility and tissue looseness, particularly important in assessing skin discolorations of the elderly.

Contusions and ecchymoses reflect antemortem events, because blood circulation is necessary for them to form. The mechanism of formation of an ecchymosis is the same as a contusion or bruise on the living body, i.e. hemorrhage into soft tissue that sustains blunt force trauma because of injury to the blood vessels. However, a contusion may be deformed in other ways (raised, depressed, spreading, fixed), while an ecchymosis is almost always flat. Contusions (used interchangeably with the term *bruising*) are also used as a clinical term associated with a living patient, who can have resolution of the injury over time by degradation of blood components, healing, and resolution. Postmortem, contusions or ecchymoses are fixed owing to death and lack of mechanisms for healing and resolution.

An exception to the previous terminology is described in the brain, where a cerebral contusion represents a permanent injury that is fixed because of death, and may be related to the cause of death. A contusion of the brain involves visible bleeding on the surface of the brain without damage to the leptomeninges (4,8,9). Thus, in the brain there is an anatomic similarity to a skin/soft tissue contusion, in that bleeding occurs under an anatomic barrier, but differs in that the cerebral contusion is visible and can be fatal when it extends

[1]Linn County Medical Examiners Office, 930 1st Street SW, Cedar Rapids, IA 52404.

Received 27 April 2009; and in revised form 21 July 2009; accepted 26 Sept. 2009.

into the contiguous submembranous parenchyma, the brain. We will be addressing external skin and soft tissue contusions and ecchymoses in this study, although intracranial hemorrhages will be noted as they occur from case to case.

Contusions and ecchymoses can be isolated or part of a pattern of injury, as occurs in domestic abuse, elder abuse, accidents, or even natural disease (e.g. bleeding diatheses, drug reactions, or infectious diseases) (1–3,7,10–14). Contusion and ecchymoses can be because of many etiologies and can be associated with virtually any mechanism of injury or cause of death. While considered an injury by themselves, contusions or ecchymoses can occur in conjunction with other trauma in forensic pathology that causes both rupture of blood vessels and deformation of other anatomy (2,3,9,12). For example, a contusion may be associated with tearing of the skin and may be legally considered a "contused wound" (15).

Contusions and ecchymoses are especially useful in death investigation because they are in plain sight on the external examination of the body and are routinely documented. They may also be associated with injuries or conditions that are not initially obvious. We reviewed autopsy cases to assess what patterns of ecchymoses emerged in various circumstances and to determine if there were consistent patterns of bruising that could be useful to anticipate or seek other injuries, or to deduct hypotheses regarding the sequence of injuries cause or manner of death.

As our cases were all examined postmortem, we used the term *ecchymosis* for our findings, as it can be difficult to determine which contusions were results of direct blunt force trauma versus hemorrhagic spread from any cause. Therefore, the term *ecchymosis* can be more comprehensive. In either situation, however, the presumptive underlying injury was blunt force trauma. The new question we brought to this study was what collateral and/or related injuries could be found with the subcutaneous bleeding and bruising that we examine almost daily in forensic pathology, and what other injuries could we expect or should we seek when faced with ecchymoses that can be readily visible from the external examination?

Methods

Cases from an 11-year period, 1997–2008, were reviewed. Cases were performed by the Linn County Medical Examiner Office, Linn County IA, and for several contiguous counties. All autopsies were performed by the author, facilitating diagnostic consistency. Any case in which ecchymoses were recorded was collected. Data were recorded from the reports, including age, gender, cause and manner of death, circumstances of different types of accidents, ecchymoses and other injuries (details following), and any other clinically or pathologically useful information, such as use of drugs or alcohol, or special circumstance (e.g. passenger in a vehicle rather than driver). Comprehensive toxicological studies were regrettably not routinely performed on all cases, as the ancillary studies to the autopsy were limited at the request of the county medical examiners, many of whom were under financial constraints to preserve limited county resources. The toxicological screens that were performed were full panels of 20 items if performed on blood, or a seven-analyte screen if performed on urine (amphetamine, barbiturate, benzodiazepine, cannabinoids, opiates, tricyclics, and cocaine).

All decedents had ecchymoses to be included in the study. The sites of the lesions were described in the column following the demographic data. The sites of any fractures, lacerations, and abrasions were recorded in subsequent columns. Other data, described earlier, were recorded in the next column, and the cause of death as determined by the autopsy or clinical records were recorded in the last column based on the autopsy findings. Sizes of ecchymoses were not recorded for this study as this assessment would require proportional hazards regression analysis to evaluate and were beyond the scope of our available methodologies.

The decedents were divided by manner of death, and in the case of accidents, subdivided by circumstances of the accidents: motor vehicle accidents in cars (MVA-C), motor vehicle accidents in other vehicles (MVA-O), and other accidents not involving motor vehicles (OA). The other traditional manners of death were recorded. The injuries sustained by each individual were then tracked from the site of ecchymosis across the columns of other injuries to determine if there were corresponding collateral injuries and if they were related to the site of the ecchymosis. If the injuries were internal and could only be discovered by the autopsy, the internal injuries were recorded with the external or palpable injuries, separated by semicolons.

In many cases, although ecchymoses were identified and there were other injuries found, they might not have been related. These data were tabulated in terms of correlation of ecchymoses with other types of injuries and of other injuries without corresponding ecchymoses.

Ethics

Ethical standards were maintained. There was no human or animal experimentation, and no decedent identifiers are present in any of the cases used in the study.

Statistics

Parametric data such as age and numbers of injuries were compared using t-tests. Nonparametric data were compared using two-tailed Fisher's exact test for chi-square 2×2 contingency tables. Differences were considered significant if the probability of random distribution was the traditional value of <5%. When there appeared to be consistent patterns of significance between groups based on a particular quality or measure, these groups were consolidated to make comprehensive comparisons between related groups.

Sequential injuries were estimated when hemorrhages could not be associated with the injury, thus implying that circulation had ceased and the damage was inflicted postmortem, or that one injury was fatal and further bleeding was not possible.

Results

From the 11-year period, 401 autopsies were reviewed. There were 44 cases in which ecchymoses were documented (11%). There were 22 men and 22 women, mean ages 45 and 47, respectively. As described earlier, the manners/circumstances of death divided into six categories: MVA-C, $n = 18$, 10 women and 8 men, mean age 37 (Table 1); MVA-O, $n = 4$, all men, mean age 59 (Table 2); OA, $n = 7$, four women and three men, mean age 52 (Table 3); homicides, $n = 5$, three women and two men, mean age 31 (Table 4); suicides, $n = 3$, all men, mean age 47 (Table 5); and natural deaths, $n = 7$, five women and two men, mean ages 65 (Table 6). Accidents were divided into three categories, MVA-C, MVA-O, and OA, and reported as such because they seemed distinctive in terms of the circumstances involved in the accidents. Statistical analysis demonstrated some differences (following).

There were no cases of indeterminate cause of death.

TABLE 1—*Ecchymoses, motor vehicle accidents, car.*

No.	Age	Sex	Ecchymoses	Fractures	Lacerations	Abrasions	Other	COD
1	80	F	Arm, hip, flank				Cerebral edema, hemorrhage	Closed head trauma (passenger)
2	53	M	Orbits, face	Orbits, skull	Head, face, elbow	Arms, leg	Fatty liver, marijuana, hydrocodone	Multiple injuries
3	48	F	Breast; small intestine	Orbit, skull, leg, ribs	Head, face, flank, legs; spleen, brainstem	Flank, leg		Multiple injuries
4	48	M	Scalp, face	Ribs	Face; lung		Cerebral edema	Closed head trauma
5	44	F	Ankle	Arm, legs, sternum	Face, back, arm, legs; lungs, liver	Face, back	AOD, torn pericardium with displaced heart	Multiple injuries
6	43	F	Orbit, torso, extremities	Arms, legs, ribs, spine	Orbit, head, breasts, legs; liver, spleen	Breasts, chest abdomen, legs	Transected spinal cord, aorta, esophagus	Multiple injuries
7	42	F	Wrist, elbow	Arm	Arm, scalp	Head, neck, arm, scapula, legs	AOD, EtOH 280	Multiple injuries
8	40	F	Head, torso, extremities	Arm, leg, ribs	Head, face, chest, abdomen, arms, legs	Face, chest, abdomen, arms, legs	SAH, splenic rupture	Multiple injuries
9	38	M	Shoulder, chest, arm	Face, skull, arms, leg, ribs	Face, leg, arm; brain, artery, liver, spleen,	Face, chest, shoulder, abdomen, arms, leg	Hemothorax, hemo-pericardium, ASCVD	Multiple injuries
10	34	M	Orbit, face, abdomen		Arm, leg; spleen	Face, chest, abdomen, leg	EtOH 264, AOD, SAH	Multiple injuries
11	32	F	Face	Skull, leg	Face; brainstem, aorta	Face		Multiple injuries
12	30	F	Orbits	Skull		Face		Skull fracture
13	26	M	Orbits, legs	Legs, ribs	Abdomen, legs	Abdomen	EtOH 222	Multiple injuries
14	24	M	Head, chest, abdomen, arms, legs	Skull, arms, legs	Face, neck, chest, abdomen, arms, legs; brain	Chest, abdomen, arms, legs	Open cranium, brain lost, EtOH 240	Multiple injuries
15	23	F	Legs	Skull	Orbit			Skull fracture
16	21	M	Face	Skull		Face, shoulders, arms	AOD, intracranial hemorrhage	Multiple injuries
17	19	F	Orbits, leg	Orbit, leg, skull	Face, leg; brain, liver, spleen	Face, leg	Subdural hemorrhage	Multiple injuries
18	18	M	Orbits	Skull, ribs	Arms; aorta	Face, shoulder, arm, flank, hip	Partial AOD, heart displaced into chest, marijuana	Multiple injuries

Mean age, in years; M, male; F, female; AOD, atlanto-occipital dislocation; SAH, subarachnoid hemorrhage; EtOH, ethanol (in mg/dL); COD, cause of death.

TABLE 2—*Ecchymoses, motor vehicle accidents, motorcycle, and other vehicle.*

No.	Age	Sex	Ecchymoses	Fractures	Lacerations	Abrasions	Other	COD
1	66	M	Shoulders, arm	Skull, shoulders, ribs	Face, neck, shoulder; lung, brain	Orbit, neck, arm, leg	AOD, ASCVD severe, fatty liver, 268 EtOH	Multiple injuries (tractor)
2	61	M	Face	Legs, ribs, sternum	Head, leg	Head, face, chest, arms, flank, leg	Internal chest hemorrhage, fatty liver, 2-artery bypass, SAH	Multiple injuries
3	57	M	Arms	Ribs	Intercostal	Face, leg	SAH, fatty liver	SAH
4	50	M	Face, abdomen, flank, leg	Rib, legs	Leg	Face, abdomen, flank, leg	EtOH 199, AOD, SAH, ASCVD	Multiple injuries

Mean age in years; M, male; F, female; AOD, atlanto-occipital dislocation; ASCVD, arteriosclerotic cardiovascular disease; SAH, subarachnoid hemorrhage; EtOH, ethanol (in mg/dL); COD, cause of death.

TABLE 3—*Ecchymoses, other accidents.*

No.	Age	Sex	Type	Ecchymoses	Fractures	Lacerations	Abrasions	Other	COD
1	74	F	Fall (collapse)	Scalp, axilla, abdomen, flanks, leg (mixed ages)				Epidural hematoma, AOD; citalopram 278 ng/mL (nL < 120 ng/mL)	AOD, epidural hematoma
2	68	F	Fall (stairs)	Chest, flank, arm (mixed ages)	Skull	Head, arm		ASCVD, pneumonia, fatty liver, subdural hematoma	Skull fracture, intracranial hemorrhage
3	66	M	Fall (grain elevator)	Face, head, neck	Ribs		Face	Myeloma, pulmonary edema	Suffocation in grain
4	53	F	Fall (stairs)	Orbits	Skull, ribs	Scalp	Abdomen	Fatty liver, ASCVD, EtOH 188, intracranial hemorrhage	Skull fracture, intracranial hemorrhage
5	41	M	Fall (crane)	Abdomen, leg	Face, arm, legs	Face, neck, knee; liver	Head, neck, arm	AOD, heart into chest, hemothorax	Multiple injuries
6	35	F	Multiple drugs	Arms, leg				Multiple drugs, asthma	Multiple drug intoxication
7	28	M	Multiple drugs	Legs				Multiple drugs	Multiple drug intoxication

Mean age in years; M, male; F, female; nL, normal; AOD, atlanto-occipital dislocation; ASCVD, arteriosclerotic cardiovascular disease; EtOH, ethanol (in mg/dL); COD, cause of death.

TABLE 4—*Ecchymoses, homicides.*

No.	Age	Sex	Ecchymoses	Fractures	Lacerations	Abrasions	Other	COD
1	48	M	Orbits	Teeth	Head, neck	Neck, shoulder	Severed carotid artery	Exsanguination
2	39	M	Orbit	Skull			Intracranial hematoma	Skull fracture, hemorrhage
3	30	F	Orbits	Skull	Face, head	Neck	Subdural hematoma	Skull fracture, hemorrhage
4	18	F	Shoulder, abdomen, legs		Head; liver		Incisions, stabs; heart, lungs	Multiple injuries
5	18	F	Shoulder, arm, legs	Skull	Brain	Neck, legs	Hemorrhage	Multiple injuries

Age in years; M, male; F, female; COD, cause of death.

There was no significant difference between the total number of men or women in the study, the distributions of genders among the manners of death, or between the ages of men or women in any group or taken together.

Among the groups, however, there were differences between the ages of the decedents (Table 7). Decedents of MVA-O, OA, and natural etiologies were older than decedents of MVA-C and homicide at significant levels. There was no significant difference between the ages of decedents of MVA-O, OA, natural, and suicide nor were there differences between the ages of decedents of MVA-C and homicides. Taken together, the mean age of decedents of MVA-O, OA, natural, and suicide etiologies was 58 years and was significantly older than decedents of MVA-C and homicides, 36 years ($p = 0.0001$).

The external anatomic locations of the different injuries are summarized (Table 8). By inspection, we can see that in decedents of MVA-C, facial lacerations, abrasions, and sometimes ecchymoses frequently occurred together; skull fractures were often without related injuries; and extremities virtually all presented with every type of injury, including ecchymosis, fracture, laceration, and abrasion. Among decedents of MVA-O, abrasions were common in most sites and also tended to occur with lacerations and ecchymoses of the extremities. Among decedents of OA, the orbit tended to develop all four types of injuries. Among decedents of homicides,

TABLE 5—*Ecchymoses, suicides.*

No.	Age	Sex	Ecchymoses	Fractures	Lacerations	Abrasions	Other	COD
1	61	M	Orbits	Skull	Head, brain		ASCVD with grafts	Gunshot wound
2	42	M	Chest (shotgun)	Skull	Head, brain		Depression	Gunshot wound
3	38	M	Orbits	Skull	Head, brain		Fatty liver	Gunshot wound

Mean age in years; M, male; ASCVD, arteriosclerotic cardiovascular disease; COD, cause of death.

TABLE 6—*Ecchymoses, natural.*

No.	Age	Sex	Ecchymoses	Fractures	Lacerations	Abrasions	Other	COD
1	86	F	Face		Face		Diabetes	CVA
2	83	F	Arms				Gallbladder carcinoma	CHF
3	74	M	Abdomen, groin, legs				Parkinson's disease	Pneumonia
4	67	F	Breast, abdomen, arms, legs				Emphysema	Pneumonia
5	52	F	Legs (mixed ages)				Seizure disorder	Seizure
6	50	M	Arm, abdomen, flank				ASCVD, esophageal cancer, diabetes	ESLD
7	41	F	Orbits, neck, arm		Nose, lip		EtOH 289, gastritis, varices, fatty liver	GI bleed

Mean age in years; M, male; F, female; ASCVD, arteriosclerotic cardiovascular disease; EtOH, ethanol (in g/dL); COD, cause of death; CVA, cerebrovascular accident; CHF, congestive heart failure; ESLD, end-stage lung disease; GI bleed, gastrointestinal hemorrhage.

TABLE 7—*Decedents by manner of death and mean age.*

Manner, Age	MVA-C, 37	MVA-O, 52	OA, 52	Homicide, 31	Suicide, 47	Natural, 65
MVA-C, 37		0.01	0.04	NS	NS	0.0006
MVA-O, 52	0.01		NS	0.007	NS	NS
OA, 52	0.04	NS		0.04	NS	NS
Homicide, 31	NS	0.007	0.04		NS	0.004
Suicide, 47	NS	NS	NS	NS		NS
Natural, 65	0.0006	NS	NS	0.004	NS	

Manner, manner or circumstances of death; mean age in years; MVA-C, motor vehicle accident, car; MVA-O, motor vehicle accident, other vehicle; OA, other accident; Mean age in upper row reported in years; NS, not significant.

ecchymoses were often distributed in different parts of the body. Among three decedents by suicide, all suffered gunshot wounds to the head, so their injuries of ecchymoses, fractures and lacerations, mostly to the head, were similar. Among decedents of natural deaths, all had ecchymoses only and distributed over many parts of the body, especially the extremities.

All decedents had ecchymoses to be included in the study. Other injuries appeared to depend on the manner or circumstances of death. The confluence of ecchymoses and collateral injuries is summarized (Table 9). MVA-C decedents had the most ecchymoses with collateral injuries, $n = 38$, followed by decedents of MVA-O, $n = 11$; homicides, OA, $n = 7$; $n = 6$; suicides, $n = 3$; natural, $n = 2$. The cases with the most ecchymoses and unrelated or no collateral injuries were decedents of natural disease, $n = 14$; followed by OA, $n = 12$; MVA-C, $n = 7$; homicide $n = 7$; and MVA-O $n = 4$. In short, decedents of MVA-C, OA, and suicides were highly likely to have mixed presentation of ecchymoses and collateral injuries; decedents of natural disease were highly likely to have ecchymoses without collateral injury; and decedents of homicides of MVA-O were about equally likely to have related collateral injury or not.

All individual ecchymoses among the decedents were recorded regarding concurrent presence of ecchymoses with and without collateral injuries among all decedents. An anatomic distribution of these injuries in relation to each other is shown in Figure 1. (The use of the body diagram is by permission of the American Society of Clinical Pathologists.) Major confluence required three or four related injuries; unrelated simply meant any injuries that did not overlap with each other anatomically. Two patterns emerged. The first pattern was the presence of ecchymoses with collateral injuries in the form of abrasions, lacerations, or abrasions that were observed in concert or continuity with the ecchymoses. Because evidence of life was present with these injuries (circulation, bruising, contusions), it is possible to consider these injuries as concurrent with the manner/circumstances of death and possibly contributory. For example, there was a decedent of MVA-C (e.g. Table 1, case 2) with orbital ecchymoses and orbital fractures, or another decedent of MVA-C (Table 1, case 6) with orbital ecchymoses and lacerations would be examples of decedents with ecchymoses and collateral related injury relationships that occurred during life. There is no Table to show these relationships. This absence is because among decedents with ecchymoses and collateral injuries, there were no significant differences between any of the groups based on manner or circumstances of death and the likelihood of ecchymoses coinciding with related injuries. In short, ecchymoses with collateral injuries were as likely in any group based on manner/cause of death and might have been considered contributory to that cause of death.

However, the second type of relationship between ecchymoses and collateral injuries were those in which ecchymoses occurred without related collateral injury. The distributions of these injuries are summarized by manner/circumstances of death (Table 10). Such decedents may have had immediately lethal injuries, and did not survive long enough to have hemorrhage and form ecchymoses at a given injury site, or an injury followed the cessation of vital functions including circulation, preventing hemorrhage at the site

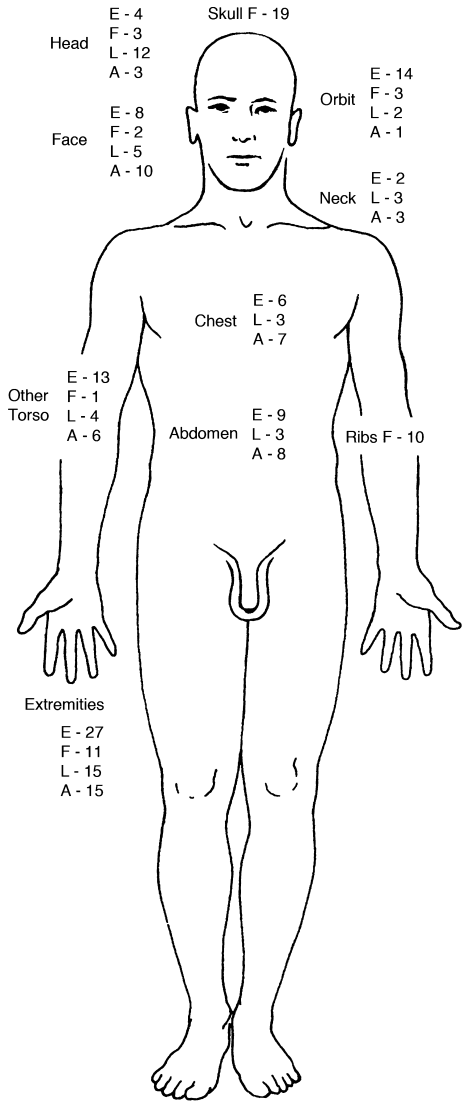

FIG. 1—*Distribution of ecchymoses (E), fractures (F), lacerations (L), and abrasions (A) by anatomic site.*

from marking it. Examples of such decedents are from MVA-C (Table 1, Case 11), where ecchymoses and lacerations occurred on the face (collateral, related injury), but a fracture of the leg was not accompanied by collateral or related injury. One might conclude that the facial injury was first and contributed to death, while the leg fracture was secondary and did not contribute to death.

In this group, there were significant differences between decedents with ecchymoses who lacked collateral related injuries. As noted, the differences between these groups are reported in Table 10. Decedents of OA were more likely to have ecchymoses without collateral, related injuries than decedents of MVA-C and MVA-O. It is also noteworthy that decedents of OA and natural causes tended to have multiple bruises of different ages and stages of resolution, suggestive of repeated injury rather than a single terminal incident. Decedents of natural causes were more likely to have ecchymoses without collateral, related injuries than decedents of MVA-C, MVA-O, homicide, and suicide. Taken together, decedents of MVA-C, MVA-O, homicide, and suicide were more likely to have related, collateral injures than those of OA or natural deaths, implying that the succession of injuries in the previous group were concurrent and contributory to death, while those among OA and natural deaths were subsequent or noncontributory to death.

Other correlations are summarized in Table 11. In general, decedents of natural diseases and OAs had significantly fewer injuries than those with traumatic manners or circumstances of death. There

TABLE 8—*External anatomic distributions of injuries by manner/circumstances of death.*

Site	Ecchymoses	Fractures	Lacerations	Abrasions
Motor vehicle accident—car				
Face	4	1	9	9
Orbit	7	3	2	
Head	2		5	1
Skull		10		
Neck			1	
Chest	3		3	6
Ribs		6		
Spine		1		
Abdomen	2		3	6
Other torso	5		2	5
Extremities	11	10	11	11
Motor vehicle accident—other vehicle				
Face	2		1	3
Orbit				1
Head				1
Skull		1		
Neck				1
Chest				1
Ribs		2		
Abdomen	1			1
Other torso	2	1	2	
Extremities	3		2	3
Other accident				
Face	1	1	1	1
Orbit	1			
Head	2	2	1	1
Skull		2		
Neck	1		1	1
Chest	1			
Ribs		2		
Abdomen	2			1
Other torso	3			
Extremities	5	1	2	
Homicide				
Face			1	
Orbit	3			
Head		1	3	
Skull		3		
Neck			1	1
Abdomen	1			
Other torso	2			1
Extremities	2			1
Suicide				
Face				
Orbit	2			
Head			3	
Skull		3		
Neck				
Chest	1			
Natural				
Face	1		2	
Orbit	1			
Neck	1			
Abdomen	3			
Other torso	1			
Extremities	6			

All decedents had ecchymoses. Not all decedents had ecchymoses at all listed sites in the rows, however. The empty cells in the ecchymoses columns for some manners and circumstances of death are because of this fact.

TABLE 9—*Correlations of ecchymoses and collateral injuries.*

Manner	EFLA	EFL	ELA	EFA	FLA	EA	EL	EF	FA	LA	FL	UR
MVA-C	11	4	3	2	2	1	2	2		6	5	7
MVA-O	2		1	1	2	2			1		2	4
OA					1	1	2	2	1		2	12
Homicide	2					1	1	1			1	7
Suicide		3										
Natural							2					14

Manner, manner or circumstances of death: MVA-C, motor vehicle accident, car; MVA-O, motor vehicle accident, other vehicle; OA, other accident.

Types of injuries and groupings of related injuries in columns: E, ecchymoses; F, fracture; L, laceration; A, abrasion; UR, unrelated, i.e. one injury with no associated collateral injury. Types of injuries connected in terms of relationship between other kinds of injuries.

TABLE 10—*Significance of frequency of ecchymoses without collateral related injuries (suggests death occurred before collateral or related injury could bleed/bruise, or initial injury was lethal by itself).*

Manner	MVA-C	MVA-O	OA	Homicide	Suicide	Natural
MVA-C		NS	0.0001	NS	NS	0.0001
MVA-O	NS		0.0001	NS	NS	0.0114
OA	0.0001	0.0001		NS	NS	NS
Homicide	NS	NS	NS		NS	0.0207
Suicide	NS	NS	NS	NS		0.0103
Natural	0.0001	0.0114	NS	0.0207	0.0103	

Manner, manner or circumstances of death; mean age in years; MVA-C, motor vehicle accident, car; MVA-O, motor vehicle accident, other vehicle; OA, other accident; mean age in upper row reported in years; NS, not significant.

There were no differences between decedents of any group with ecchymoses and related or collateral injuries.

TABLE 11—*Correlations between relative significant prevalence of specific injuries or diseases based on different manners/circumstances of death.*

Finding	More Prevalent	Less Prevalent	*p*-Value
Injury to orbit(s)	NS		
Skull fracture	MVA-C	Natural	0.0202
	Homicide	Natural	0.0455
	Suicide	Natural	0.0083
Brain injury	MVA-C	Natural	0.0267
	Homicide	Natural	0.0455
	Suicide	Natural	0.0083
	Suicide	OA	0.0333
	MVA-O	OA	0.0333
AOD	NS		
Internal lacerations	MVA-C	Natural	0.0202
	Suicide	Natural	0.0083
	Suicide	OA	0.0333
Other disease	Natural	Homicide	0.0013
	Natural	MVA-C	0.0001
	MVA-O	MVA-C	0.0008
	MVA-O	Homicide	0.0079
	Suicide	MVA-C	0.0035
	Suicide	Homicide	0.0179
	OA	MVA-C	0.0145
Multiple injuries	MVA-C	All others	0.0014
Drugs or alcohol	NS		

MVA-C, motor vehicle accident, car; MVA-O, motor vehicle accident, other vehicle; OA, other accident; AOD, atlanto-occipital dislocation.

were no differences of prevalence based on manner or circumstances of death for some recurring injuries or conditions: injuries to the orbit(s), atlanto-occipital dislocation, and presence of drugs or alcohol.

Discussion

The definitions provided in the Introduction have a fascinating history. *Ecchymosis* is a Greek word adapted to English in 1541 (16). *Bruise* comes from an old English term, *brysan*, meaning to crush or bruise, probably merged with a French word *briesier-e*, which means to break or shatter (17). *Contusion* possibly has the most elaborate etymology. Its roots are Latin, *contusionem*, meaning to crush or bruise and passes from Latin through French to our modern English form, *contusion*. Adopted into English, it early graced part 2 of Shakespeare's *Henry VI* in 1593, per character Yorke: "That Winter Lyon, who in rage forgets Aged *contusions*, and all brush of Time; And like a Gallant, in the brow of youth Repaires him with Occasion." (Italics added) (18). *Contusion* is further a term for this injury with legal standing, established in Ansley v. Travelers Ins. Co., 27 Tenn. App. 720, 173 S.W.2d 702,704: "To bruise; to injure or disorganize a part of without breaking the skin" (15).

The preceding data show that these colorful injuries can be correlated with the incidence of injuries and manner or circumstances of death. These findings can be used to assess severity and relative importance of injuries associated with ecchymoses in death, and to guide one as regards what to seek in the presence of ecchymoses.

Surprisingly, as common an injury as an ecchymosis is among the living, they are seen in a relatively small numbers of forensic cases, 11% in our study. The study is limited, however, because minor injuries not obviously related to an incident may have been overlooked and not become part of the autopsy report. Men were as common as women to have ecchymoses, and there was no difference between their ages (45 or 47 years). However, injuries by manners or circumstances of death tended to merge in some characteristics. Considering Table 7, decedents of MVA-O, OA, natural causes, and suicide were of comparable ages, 58 years, and significantly older than victims of MVA-C and homicide, 36 years. This difference could be because of the associations of younger people with violent death (19) compared to an older population that is at risk for death from natural disease. We were interested that our group, MVA-O, tended to be middle- or older-aged men, mean 59 years, rather than the younger population often associated with motorcycle or other non-car vehicular accidents, e.g. recreational vehicles.

As described, decedents of MVA-O were all older middle-aged men, mean 52 years; as suicides were all men, of younger middle age, mean 47 years. We note that there were other MVA-O and suicides in our study group. However, among suicides for example, only these three had ecchymoses and could be included in the study. In one case, the ecchymosis was on the chest and corresponded to the compression and heat of a shotgun; in the others, the ecchymoses were because of placement of a handgun, which allowed bleeding into the subcutaneous tissue.

As Tables 1, 3, 4, and 6 show, all other manners and circumstances of death were divided among men and women, and no preference was shown for one gender or the other.

The anatomic distribution of ecchymoses, referenced in Table 8, shows some recurrent patterns. In MVA-C, one might expect the greatest confluence of multiple injuries, and Table 8 corroborates this expectation. The face and head had many corresponding ecchymoses, fractures, lacerations, and abrasions. The chest, abdomen, and other torso had moderate injuries and corresponding ecchymoses. Ecchymoses to extremities had extensive overlap of all forms of injury. By contrast, victims of MVA-O tended to have overlapping injuries in the torso and extremities only. They were prone to abrasions and lacerations. The last among accidents, those who

suffered OA, had the greatest confluence of injury in the face and head, as well as in the extremities.

The overlap of types of injuries is shown in Table 9 and simplified in Chart 3. Interestingly, ecchymoses without collateral injury were a common finding, although the combined effect of multiple injuries was more common. (This chart also does not include the double-injury overlaps, as an all-inclusive chart would be too crowded and unwieldy.)

In any kind of accident, the extremities were by far the most likely to have collateral injuries associated with ecchymoses, noted elsewhere in the literature regarding the humerus and ankle (20,21). Other correlations depended on the type of accident, detailed earlier.

Other studies have occasionally observed internal contusions, aside from the commonly described cerebral contusions (9,14). We curiously had only one case of visceral contusion (Table 1, patient 3, a 48-year-old woman with an ecchymosis of the small intestine following MVA-C). Other organ damage occurred in many settings, however, but tended to be lacerations from direct trauma or shock waves of injuries. Apparently, isolated internal ecchymoses are a rare finding.

Among victims of homicides and suicides, there was no systematic confluence of collateral injuries. Natural deaths showed almost exclusively external ecchymoses with no collateral injuries, except two cases with facial lacerations.

Table 9 affirms the previous findings but quantifies the overlap of types of injury without referencing their particular anatomic sites. As expected, MVA-C has the greatest number and types of concurrent injuries, and likewise natural disease has the greatest number of unrelated injuries with no corresponding injuries ($n = 14$). The group of decedents from OAs approaches this number of decedents with unrelated injuries and no corresponding injuries ($n = 12$), but a few correlated injures are seen. For MVA-O, homicide, and suicide, there is no particular pattern of correlated ecchymoses and injury types.

As noted in Results, there were no differences between decedents with ecchymoses in continuity with other injury based on injury class. However, as summarized in Table 10, several groups had ecchymoses without collateral injury. The striking finding here was the consistent difference between natural death and every other manner or circumstance of death of OA. These two groups were similar in that collateral injuries did not occur or did not occur in continuity with other injuries, so other injuries possibly did not contribute to death.

The comparison of other clinical data with injuries summarized in Table 11 showed two major patterns. Decedents of natural causes and OAs were far less likely to have skull fractures, brain injuries, or internal lacerations compared to other decedents; and other diseases were significantly more common in decedents of natural disease, MVA-O, and suicide. Interestingly, drugs or alcohol were not significantly more common in any group of decedents compared to any other. Specific findings are described in Table 11.

In summary, ecchymoses and their collateral injuries appeared to distribute into two groups with areas of overlap. The first group was younger, comprised of victims of MVA-C and homicide, who suffered more injuries of all types related to ecchymoses than others. We attribute this finding to the more-severe injuries sustained in these manners and circumstances of death compared to other. There were few differences among these decedents, because many injuries were essentially concurrent and could contribute to death. Victims of all types of accidents had more head and face injuries than others. Ecchymoses with collateral injuries to the extremities were common in all groups.

The second, older group included victims of MVA-O, OA, natural causes, and suicide. Victims of natural deaths understandably had the most ecchymoses that were unrelated to other injuries, and paradoxically, victims of OA also had many ecchymoses unrelated to other injuries. We interpret these findings to suggest that the ecchymoses may have been unrelated to the fatal accident or disease, and this observation may be corroborated by the different ages of ecchymoses encountered in these decedents, a factor not seen in the more-violent deaths of the younger group, where the ecchymoses were generally fresh and related to the fatal injuries. Other disease was predictably more common among decedents of natural death but also of MVA-O and suicide. Use of drugs or alcohol interestingly did not seem to predominate in any group, including any kind of accident, although this observation may be biased by the lower rate of toxicological screening in our cohort.

It is also interesting that there were no indeterminate causes of death among decedents with ecchymoses. In cases where the ecchymoses would be related to the manner of injury and death, it is logical that these cases would not be indeterminate. In other situations, it would seem likely that at least some cases would be indeterminate, but this outcome was not demonstrated in our data. Therefore, ecchymoses may be a useful surrogate marker of the likelihood of being able to determine a cause of death, and to direct the pathologist to continue to seek a cause of death should ecchymoses be seen, even if the case otherwise appears to be indeterminate.

References

1. Jessee SA. Physical manifestations of child abuse to the head, face, and mouth: a hospital survey. ASDC J Dent Child 1995;62:245–9.
2. Hahn YS, Raimondi AJ, McLone DG, Yamonouchi Y. Traumatic mechanisms of head injury in child abuse. Childs Brain 1983;10:229–41.
3. Mancino P, Parlavecchio E, Melluso J, Monti M, Russo P. Introducing colposcopy and vulvovaginoscopy as routine examinations for victims of sexual assault. Clin Exp Obstet Gynecol 2003;30:40–2.
4. Armbrustmacher V, Hirsch CS. Trauma of the nervous system. In: Spitz WU, Spitz DJ, editors. Spitz and Fisher's medicolegal investigation of death, guidelines for the application of pathology to crime investigation, 4th edn. Springfield, IL: Charles C. Thomas Publisher, 2006;994–1077.
5. DiMaio DJ, DiMaio JM. Blunt trauma wounds. In: DiMaio DJ, DiMaio JM, editors. Forensic pathology, 2nd edn. New York, NY: Elsevier Science Publishing Inc, 2001;91–116.
6. Dickey JW Jr. Drifting hematomas. Surg Gynecol Obstet 1979;148:209–12.
7. Hathaway WE. Easy bruising in children. Postgrad Med 1977;61:224–6.
8. Illustrated Stedman's medical dictionary, 26th edn. Baltimore, MD: Williams and Wilkins, 1995;390.
9. Hirsch CS, Kaufman B. Contrecoup skull fractures. J Neurosurg 1975;42:530–4.
10. Roy P, Bonello L, Torguson R, de Labriolle A, Lemesle G, Slottow TL, et al. Impact of ''nuisance'' bleeding on clopidogrel compliance in patients undergoing intracoronary drug-eluting stent implantation. Am J Cardiol 2008;102:1614–7.
11. Seeley BM, Denton AB, Ahn MS, Maas CS. Effect of homeopathic Arnica montana on bruising in face-lifts: results of a randomized, double-blind, placebo-controlled clinical trial. Arch Facial Plast Surg 2006;8:54–9.
12. Antonelli V, Cremonini AM, Capobassi A, Pascarella R, Zofrea G, Servadei F. Traumatic encephalocele related to orbital roof fractures: report of six cases and literature review. Surg Neurol 2002;57:117–25.
13. Harrison-Woolrych M, Hill GR, Clark DW. Bruising associated with sibutramine: results from postmarketing surveillance in New Zealand. Int J Obes (Lond) 2006;30:1315–7.
14. Dodd KT, Mundie TG, Lagutchik MS, Morris JR. Cardiopulmonary effects of high-impulse noise exposure. J Trauma 1997;43:656–66.
15. Black HC, Nolan JR, Nolan-Haley JM, Connolly MJ, Hicks SC, Alibrandi MN. Black's law dictionary, 6th edn. St. Paul, MN: West Publishing Company, 1996;330.

16. Simpson JA, Weiner ESC, editors. The Oxford English dictionary, 2nd edn, Volume V, Dvanda-Follis. Oxford, UK: Clarendon Press, 1989;50.
17. Simpson JA, Weiner ESC, editors. The Oxford English dictionary, 2nd edn, Volume II B.B.C.-Chalypsography. Oxford, UK: Clarendon Press, 1989;596–7.
18. Simpson JA, Weiner ESC, editors. The Oxford English dictionary, 2nd edn, Volume III, Cham-Creeky. Oxford, UK: Clarendon Press, 1989;857.
19. Cothren CC, Moore EE, Hedegaard HB, Meng K. Epidemiology of urban trauma deaths: a comprehensive reassessment 10 years later. World J Surg 2007;31:1507–11.
20. Meyer NJ, Lyon RM. Lateral elbow ecchymosis as a clinical sign of lateral humeral condylar fractures. Am J Orthop 2003;32:260–1.
21. Auletta AG, Conway WF, Hayes CW, Guisto DF, Gervin AS. Indications for radiography in patients with acute ankle injuries: role of the physical examination. AJR Am J Roentgenol 1991;157:789–91.

Additional information—reprints not available from author:
Henry J. Carson, M.D.
Linn County Medical Examiners Office
930 1st Street SW
Cedar Rapids, IA 52404
E-mail: hjcmd@earthlink.net

JOURNAL OF FORENSIC SCIENCES

J Forensic Sci, November 2010, Vol. 55, No. 6
doi: 10.1111/j.1556-4029.2010.01500.x
Available online at: onlinelibrary.wiley.com

PAPER
PATHOLOGY/BIOLOGY

Karen M. Kester,[1] *Ph.D.; Mary H. Toothman,*[1] *M.S.; Bonnie L. Brown,*[1] *Ph.D.; W. Scott Street, IV,*[2] *Ph.D.; and Tracey D. Cruz,*[1,3] *Ph.D.*

Recovery of Environmental Human DNA by Insects*,†

ABSTRACT: We tested the hypotheses that foraging insects can acquire human DNA from the environment and that insect-delivered human DNA is of sufficient quantity and quality to permit standard forensic analyses. Houseflies, German cockroaches, and camel crickets were exposed to dusty surfaces and then assayed for human mitochondrial and nuclear loci by conventional and qPCR, and multiplex STR amplification. Over two experiments, 100% of insect groups and 94% of dust controls tested positive for human DNA. Of 177 individuals, 33–67% tested positive and 13 yielded quantifiable human DNA (mean = 0.022 ± 0.006 ng; mean dust control = 2.448 ± 0.960 ng); four had at least one positive allele call for one or more locus; eight others showed multiple peaks at some loci. Results imply that application to routine forensic casework is limited given current detection methodology yet demonstrate the potential use of insects as environmental samplers for human DNA.

KEYWORDS: forensic science, forensic entomology, human DNA dust, surveillance, environmental sampling, mitochondrial DNA, nuclear DNA, quantitative polymerase chain reaction, short tandem repeats

Insects were first used in modern forensic investigations in the late 19th century and are now used routinely in homicide and other medico-legal investigations (1–3). Most recently, casework and simulated studies based on short tandem repeat (STR) analysis of DNA extracted from the gut contents of larval blow flies have demonstrated that blow flies can provide molecular evidence for the identification of both victims and criminals (4–6). Owing to the advances in molecular genotyping and the application of methods for low copy number DNA forensic analysis, the routine use of insects in casework is likely to expand (7).

The employment of free-roaming arthropods as environmental samplers for the surveillance of biothreats has been the focus of our research for several years. Insects passively acquire or ingest multiple organic and inorganic materials while foraging in the environment, and these materials can be easily harvested for analyses using a variety of detection methodologies (8). In particular, scavenging insect species are adept at locating organic materials and may be useful for collecting environmental samples when stealth is indicated. Further, depending on the material of interest and the detection methodology employed, foraging insects may provide more informative samples than traditional sampling methods. This study investigates the potential use of three common insect species, the common housefly, the German cockroach, and a camel cricket, as collectors of human DNA that may be relevant to the surveillance of humans and human activity in enclosed structures. Two of these species, the housefly and German cockroach, are synanthropic, i.e., highly adapted to living in close association with humans and human dwellings, and are also cosmopolitan, i.e., the same species occurs throughout the world.

Recently, Toothman et al. (9) reported that 97% of 36 environmental swab samples collected from dusty surfaces from multiple locations within a large academic building tested positive for human mitochondrial DNA (mtDNA) or human nuclear DNA. Samples yielded human DNA at levels (0.2–1.1 pg per cm^2) high enough to permit detection using standard forensic techniques, and 61% of samples contained human DNA of adequate quality to permit STR analysis with interpretable results. No obvious trends in human DNA quantity or quality were detected with respect to human traffic level and visual dust levels. Results of this study provide control data for interpreting results of the study reported herein; both studies were conducted concurrently, and samples were taken from the same locations and at the same time.

We hypothesized that insects could acquire human DNA from dust while foraging in an indoor environment and, further, that insect-delivered human DNA would be of sufficient quantity and adequate quality to permit standard forensic analyses. Two manipulative experiments were performed to test the effect of insect species and sampling location on recovery of human DNA from insect foragers. The effects of human traffic level and apparent dust level on recovery of insect-borne human DNA were also examined to determine whether resulting samples could provide information about the relative number of past or present human inhabitants. Human DNA recovered from insects was subjected to qualitative and quantitative analyses using conventional and quantitative polymerase chain reaction (qPCR) methods for nuclear and

[1]Department of Biology, Virginia Commonwealth University, 1000 W. Cary Street, Richmond, VA 23284-2012.
[2]Department of Statistical Sciences and Operations Research, Virginia Commonwealth University, 1015 Floyd Avenue, Richmond, VA 23284-3083.
[3]Department of Forensic Science, Virginia Commonwealth University, 1000 W. Cary Street, Richmond, VA 23284-2012.

*Funded by The Johns Hopkins University Applied Physics Laboratory, Award Number 8821816, to KMK and BLB.
†Presented in part at the Annual Meeting of the Entomological Society of America, November 16–19, 2008, in Reno, NV.

Received 21 Mar. 2009; and in revised form 30 Aug. 2009; accepted 11 Sept. 2009.

mitochondrial loci, and by multiplex STR amplification followed by ultrathin and capillary electrophoresis. As we report here, results support our hypotheses and, in so doing, demonstrate the use of free-roaming insects for the surveillance of humans and human activity in inaccessible locations and collection of molecular evidence in general.

Experimental Insects

The common housefly, *Musca domestica* L. (Diptera: Muscidae), occurs wherever humans and domesticated animals reside and is considered the most widely distributed synanthropic insect species in the world. Eggs are oviposited in decaying organic material on which developing larvae feed until pupation. Adults, which live 2–3 weeks depending on environmental conditions and food supply, are diurnal scavengers with sponging mouthparts and feed on liquids or solids liquefied by saliva or vomitus (10). As demonstrated by the number of human (11,12) and veterinary pathogens (13) that have been recovered or mechanically vectored, the housefly is a superb environmental sampler.

The German cockroach, *Blattella germanica* L. (Blattodea: Blattellidae), is cosmopolitan and synanthropic and often abundant in urban dwellings. Development time from egg to adult is highly dependent on temperature and relative humidity and ranges from 54 to 215 days (14). Both nymphal and adult roaches have chewing mouthparts and are nocturnal scavengers. Similar to the housefly, numerous microorganisms of human or animal importance have been recovered from the German cockroach (15,16).

Camel crickets (= cave crickets), *Ceuthophilus* spp. (Orthoptera: Rhaphidophoridae), inhabit dark, cool, and damp environments including basements, barns, and caves. Omnivorous nymphs and adults have chewing mouthparts and are nocturnal scavengers; cave-dwelling species venture outside of caves to forage for food (17). Although no single *Ceuthophilus* species is reported to be cosmopolitan, members of the same genus typically have similar behaviors and life histories.

Materials and Methods

Insects

Houseflies and cockroaches originated from colonies maintained at North Carolina State University, and camel crickets were first-generation laboratory-reared offspring of locally collected wild parents. Insects were housed and offered appropriate diets and water *ad libitum*. Houseflies were held in 35-cm^3 aluminum sleeve cages (BioQuip Products, Rancho Dominguez, CA) and fed on 75% sugar and 25% milk powder; 2- to 4-day-old adults of both sexes were used in the experiments. Cockroaches (adult males only) were held in glass aquaria and fed on dog kibble. Camel crickets (late-stage nymphal males and females) were held in glass aquaria and provided with dog kibble and apple. To avoid contamination, all insect aquaria and cages were sterilized with a 10% bleach solution and washed with 70% ethanol followed by DNA-free H_2O. A single person maintained all three species and wore gloves whenever feeding and handling these insects; cage interiors were exposed to ambient air only momentarily.

Sampling Locations

Samples were collected from multiple sites as also described in Toothman et al. (9) within a large (12,300 m^2) four-story academic building containing offices, and research and instructional laboratories (The Trani Center for Life Sciences, Virginia Commonwealth University, Richmond, VA). Locations were selected on the basis of accessibility, the availability of flat surfaces, and the number of typical occupants. "Offices" were occupied regularly by one person with frequent visitors and categorized as "low-traffic" locations. "Laboratories" were typically occupied by five to 10 researchers and categorized as "medium-traffic" locations. "Classrooms" were instructional laboratories occupied by *c.* 100 people each weekday and categorized as "high-traffic" locations. Three surfaces ("replications") were sampled within each location, and dust level on each was categorized qualitatively as "unapparent," "low," "medium," or "high" as described in Toothman et al. (9).

Foraging Experiments

The ability of foraging adult insects to acquire and deliver detectable human DNA was tested in two separate experiments. In Experiment 1, we tested the hypothesis that adult houseflies and German cockroaches would acquire human DNA by foraging on dusty indoor surfaces at variable dust and traffic levels. PCR amplification with mtDNA and nuclear DNA primers was used to determine the presence or absence of human DNA in nucleic acids purified from experimental insects. Twenty-four groups of houseflies and cockroaches, each with five individuals, foraged within test arenas with an unapparent, low, medium, or high level of dust, within eight locations that varied in human traffic level (five "low," two "medium," and one "high"), for a total of 120 individuals of each species. Negative controls included an additional two to five individuals of each species.

In Experiment 2, we tested the ability of adults of the common housefly, German cockroach, and immature camel crickets to collect human DNA by foraging on surfaces with a medium dust level within six locations, three with a high traffic level (classrooms) and three with a low traffic level (offices). The quantity of human DNA recovered by individual insects was quantified by qPCR (see "Molecular Assays" below). Quality of insect-borne human DNA was assessed by subjecting each sample that yielded a detectable quantity of human DNA to STR analysis (see "Molecular Assays" below). In high-traffic locations (classrooms), three surfaces (replicates) were sampled, whereas only one surface was sampled in the smaller low-traffic locations (offices) due to the lack of available surfaces, for a total of 60 individuals of each of the three species (total $n = 180$). An additional two to five individuals of each species that were not permitted to forage served as negative controls.

In both experiments, insects were chill-anesthetized, and five individuals of the same species were placed under a $18 \times 32 \times 10$ cm sterile transparent plastic box (Sterilite®; Sterilite Corporation, Townsend, MA) and allowed to forage on the 576-cm^2 exposed surface (counter top, desk, or bookshelf) for 1 h ± 5 min. Insects were removed from the sampling area by inserting a clean sterile sheet of rigid paper stock between the surface and the box. Recovered insects, grouped by box, were sacrificed by freezing at −20°C and later transferred individually to sterile 1.5-mL tubes within 2 days.

DNA Extraction

Each insect sample was partially homogenized using a sterile pellet pestle in 400 μL B1 Cell Lysis Solution from the Mo Bio UltraClean™ BloodSpin™ purification kit (Mo Bio, Inc., Carlsbad, CA) previously shown to collect any material adhering to the exterior or ingested while avoiding potential inhibitory co-extracts (8). Insect exoskeleton and other solids were allowed to settle at room temperature for 1 min after which all liquid was transferred to a

sterile 1.5-mL tube for DNA extraction. Total DNA was extracted from samples using the Mo Bio UltraClean™ BloodSpin™ purification kit. All other operations were performed according to the manufacturer's instructions resulting in a final elution volume of 50 μL per insect specimen. This material was used directly as template for all assays. Absence of kit-based and operator-induced contamination was verified by performing kit extraction blanks with DNase-free water along with each set of DNA extractions.

Molecular Assays

Assaying Purified Samples for Presence and Quality of Human DNA—The presence and quality of human DNA recovered from insects was evaluated by traditional PCR using nuclear and mitochondrial primers. In Experiment 1, samples were assayed for the presence of human nuclear DNA using primers that amplified the region flanking the polymorphic *Alu* sequence in the tissue plasminogen activator gene on human chromosome 8 (*TPA*25) (18). mtDNA was assayed using two mtDNA primer sets consisting of one forward primer (F16140 = "mtDNA-A" or F16190 = "mtDNA-B") and reverse primer R16420 (19,20). In Experiment 2, samples were assayed for the presence of human nuclear DNA using the ABI Quantifiler™ Human DNA Quantification Kit (Applied Biosystems, Inc., Foster City, CA). In Experiment 2, the mtDNA primers were combined to perform a single duplexed reaction per sample.

All PCRs contained the following: three parts JumpStart™ REDTaq™ ReadyMix™ PCR Reaction Mix (Sigma, St. Louis, MO), one part forward + reverse primer mix at 5 mM concentration per primer (Integrated DNA Technologies, Coralville, IA), and two parts template DNA. All PCRs were conducted with an initial polymerase activation step at 94°C for 3 min 30 sec, followed by 40 cycles of 94°C for 30 sec, 57°C for 30 sec, and 72° C for 20 sec. Absence of PCR master mix contamination was verified by performing negative PCR controls (H_2O used as template) with every set of reactions. The products of *TPA25* PCRs were visualized on 6% polyacrylamide gels (PAGE); mtDNA products were visualized on PAGE or 2% e-Gels (Invitrogen, Carlsbad, CA), and Quantifiler™ products were assayed using the Bio-Rad iCycler (Bio-Rad, Hercules, CA).

Quantitation of Human DNA Recovered from Insects—Quantitation of human DNA was performed for all samples in triplicate using the QuantifilerTM Human DNA Quantification Kit (Applied Biosystems) with duplicate standard human DNA dilutions on every plate. The dynamic range of the assay covered four orders of magnitude, ranging from 0.023 to 50 ng/μL. Each of the three insect species was run on each of 10 assay plates. To ensure consistency of quantification estimates across assays, insect replicates were performed in different plates. Assays were performed using a Bio-Rad iCycler-iQ™ Real-Time PCR Detection System. Reaction conditions were as recommended by the manufacturer with one exception: input of each sample was 1.6 μL in 20-μL total reaction volume. Optimization was limited to increasing the number of cycles from the standard 40–45 cycles to accommodate observed low quantities of human DNA. Correlation coefficients for standard curve reactions averaged 0.976 (±0.055) for each assay. Protocols for the iCycler-iQTM were based on those recommended for the ABI platform.

STR Analysis of Positive Samples

All insect samples yielding human DNA from the qPCR assays (n = 34) were subjected to STR analysis. Nine human loci were amplified using AmpFℓSTR® Profiler PlusTM PCR Amplification Kit (Applied Biosystems) as per the manufacturer's instructions. PCRs were performed using a PTC-100 Thermal Cycler (MJ Research, Inc., Watertown, MA) and were resolved primarily using ultrathin polyacrylamide automated genotyping on an MJ BaseStation 51™ (MJ Bioworks, Inc., Sauk City, WI), under standard conditions, specifically a 30-sec constant injection at 4000 V and a collection run totaling 6000 scans. Allele analyses were performed using Cartographer v1.2.6sg software (MJ Bioworks). To determine concordance across capillary platforms, 10% of all Profiler Plus™ reactions were also analyzed on an ABI Prism® 3100-*Avant*™, following standard default conditions for fragment separation, including a 5-sec injection time. The detection threshold for all Profiler Plus™ reactions was 75 RFU (relative fluorescence unit) and 200 RFU for all MJ BaseStation reactions.

Contamination Control Measures

Control measures were implemented to ensure that recovered human DNA was acquired by insects through experimental exposure to dusty surfaces only and not from handling. With the exception of the foraging trials, all preamplification procedures were conducted under a laminar flow hood. Long gloves over long sleeves were worn during all manipulations, and surfaces and instruments were cleaned with 10% bleach followed by 70% ethanol. Aerosol-barrier pipette tips and other sterile consumables were opened, used, and closed by one technician only. Frequently used reagents were aliquotted into smaller tubes, and remainders discarded after use. All negative controls, including unexposed insects, DNA extraction blanks, and PCR negative control reactions tested negative, confirming the absence of human DNA contamination in reagents and test samples. An STR profile was generated for the individual who maintained all insects and performed most of the analyses.

Data Analyses

To determine whether the percentage of individuals within each group that tested positive for human mtDNA and human nuclear DNA differed between insect species, among locations, or between insect species with respect to location, data from Experiment 1 were subjected to analysis with a two-way analysis of variance (ANOVA) (SPSS v.14.0.2; SPSS Inc., Chicago, IL), and resulting means were compared using Tukey's HSD. Prior to analyses, data were transformed by the arcsine of the square root when necessary to correct for non-normality; otherwise, all assumptions for parametric analysis were met. Similar analyses were used to compare the percentage of human mtDNA-positive individuals in Experiment 2, except that results for the smaller low-traffic areas, sampled from one surface rather than three, were analyzed in a separate one-way ANOVA. The percentage of individuals that tested positive for human nuclear DNA in at least one of the triplicate qPCR was compared among the three species within each of the two location groups (classrooms and offices) and within each of the two location groups in separate Kruskal–Wallis rank tests (SigmaStat v.3.1; SysStat Software, Inc., San Jose, CA). Likewise, DNA quantity was compared among insect species and locations in separate Kruskal–Wallis rank tests (SigmaStat v.3.1). In addition, group means were calculated as the percentage of positive individuals within each group of five individuals.

Results

Presence of Human DNA

Housefly and Cockroach Foragers at Variable Traffic and Dust Levels (Experiment 1)—Results support the hypothesis that

foraging insects can acquire human DNA from environmental dust; however, the proportion of positive samples did not vary with respect to human traffic or dust level. Overall, 85% of individual cockroaches and 87% of all houseflies tested positive for human DNA ($n = 120$ for each species). More houseflies (75%) tested positive for mtDNA-A or mtDNA-B than cockroaches (59%) ($p \leq 0.018$; Table 1). The percentage of human mtDNA-positive individuals did not differ among locations ($p = 0.287$), nor between insect species with respect to location ($p = 0.331$) (Fig. 1*A*). Likewise, the percentage of individuals (26.2 ± 3.5%) that tested positive for the human nuclear locus *TPA*25 did not differ significantly between insect species, among sampling locations ($p = 0.827$), nor between species with respect to location ($p = 0.948$) (Fig. 1*B*). The mean detection rate for human nuclear DNA across the three replicated samples taken at each location was 71% for houseflies, 95% for cockroaches, and 100% for comparable swab samples (Table 1). Human DNA was not detected in any of the control insects or PCRs.

Housefly, Cockroach, and Cricket Foragers at Two Traffic Levels and One Dust Level (Experiment 2)—Results provide a replicated test of the hypothesis that foraging insects can acquire human DNA from environmental dust; however, the informative value of human DNA samples did not vary with respect to human traffic. Human DNA was recovered from 73 to 88% of insects ($n = 60$ for each species) that foraged on surfaces with a medium dust level in high- or low-traffic locations. At "high-traffic" locations (classrooms), the percentage of individual insects that tested positive for human DNA with mtDNA-A or mtDNA-B differed among the three insect species ($p = 0.03$). More ($p = 0.034$) cockroaches (69%) tested positive for human mtDNA than camel crickets (38%), but there was no difference ($p \geq 0.074$) between cockroaches and houseflies (44%) or between houseflies and crickets (Table 2). The percentage of individuals that tested positive for human mtDNA differed significantly ($p = 0.039$) among locations, but not among species with respect to location ($p = 0.666$). In low-traffic areas (offices), the percentage of human mtDNA-positive individuals did not differ among the three insect species ($p = 0.579$) nor the 12 sample locations ($p = 0.118$) (Table 2). The mean mtDNA detection rate for all three insect species was 100%, compared to 75% for comparable dust samples (Table 2). The proportion of nuclear human DNA-positive individuals differed among insect species ($p = 0.018$) with more cockroaches (60%) testing positive than camel crickets (20%); neither cockroaches and houseflies (40%) nor houseflies and crickets differed ($p \geq 0.05$) (Table 2). The percentage of human nuclear DNA-positive individuals did not differ ($p = 0.812$) within high-traffic classrooms nor within low-traffic offices ($p = 0.812$). Overall, human nuclear DNA was detected in 89% of the locations sampled by insects, including one sublocation (classroom 2–1) for which dust samples were negative (Table 2).

Quantitation of Insect-borne Human DNA (Experiment 2)—Reproducibility of 20 standard curves across 10 assay plates (Fig. 2) using the same dilution series was high, as indicated by the relatively small standard errors. Internal positive controls indicated no evidence of inhibition associated with insect extracts. Ct values for 65 of 66 specimens ranged from 30.15 to 37.45 (Ct = 17.29 for the outlier), and deviation across replicate assays was in general <3% (Fig. 2). The quantity of human DNA recovered from insect foragers was estimated to range from <0.001 ng to 0.181 ng per individual, with the exception of a single housefly that yielded 418.75 ng ($n = 66$ positive insects; Table 2). Overall, the mean quantity of human DNA was higher in housefly (0.028 ± 0.007 ng) and cockroach (0.027 ± 0.007 ng) samples than in camel cricket (0.011 ± 0.005 ng) samples ($p = 0.006$); comparable dust samples yielded a mean of 2.448 ± 0.556 ng of human DNA (Table 2). The mean quantity of human DNA among the three insect samples did not differ among the low-dust offices ($p = 0.074$) nor among high-dust classrooms ($p = 0.850$). Of 531

TABLE 1—*Insect recovery of human DNA from indoor surfaces at variable dust and human traffic levels (Experiment 1). Insects were exposed to a 576-cm² dust-covered area for 60 ± 5 min. Data represent the percentage of individuals* (n = 5) *of each insect species in three replications that tested positive for human mtDNA or human nuclear DNA. Results for comparative surface swab samples ("Dust") are from Toothman et al. (9).*

				Human mtDNA (% Positive)			Human Nuclear DNA (% Positive)		
Sample Name	Replicate	Traffic Level	Dust Level	Dust	Fly	Roach	Dust	Fly	Roach
Classroom 1	1	High	Unapparent	100	80	30	33.3	20	60
	2	High	High	33.3	70	70	66.7	20	20
	3	High	Medium	100	70	70	66.7	40	20
Office 1	1	Medium	High	100	80	70	33.3	40	60
	2	Medium	Low	100	50	60	66.7	20	20
	3	Medium	High	66.7	90	90	33.3	40	20
Office 2	1	Medium	High	100	100	70	66.7	20	20
	2	Medium	High	100	100	80	100	60	20
	3	Medium	Low	0	90	90	33.3	0	60
Office 3	1	Medium	Unapparent	100	90	40	100	0	20
	2	Medium	Unapparent	100	40	60	66.7	20	40
	3	Medium	Low	100	60	80	66.7	20	20
Laboratory 1	1	Low	Medium	100	100	60	66.7	40	20
	2	Low	High	100	70	50	33.3	0	40
	3	Low	High	100	60	80	66.7	0	40
Laboratory 2	1	Medium	Low	100	80	30	100	20	0
	2	Medium	Low	100	40	50	66.7	0	20
	3	Medium	Low	100	50	80	100	20	60
Laboratory 3	1	Low	Low	100	100	10	66.7	40	20
	2	Low	Low	100	90	50	100	40	20
	3	Low	Medium	100	70	20	66.7	0	20

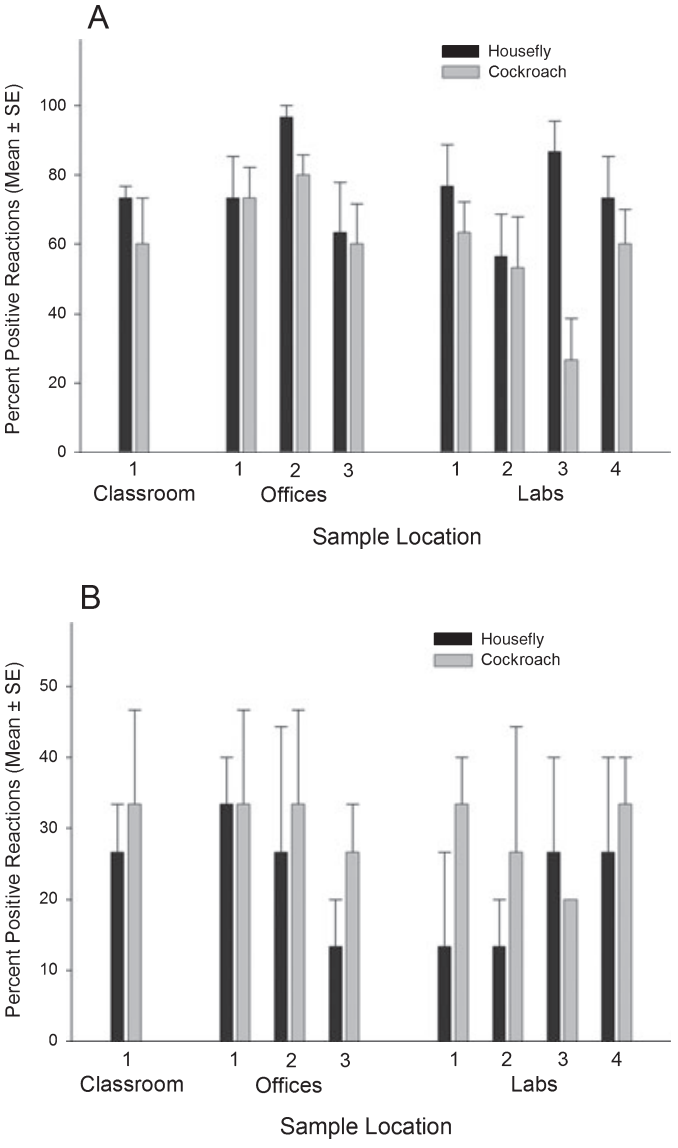

FIG. 1—*Delivery of human DNA by adults of the common housefly and German cockroach after foraging on indoor surfaces with variable dust levels in rooms with variable traffic levels (Experiment 1). (A) Human mtDNA. The percentage of positive individuals in each group of five (21 groups of each species) did not differ* ($p > 0.05$) *between species, among sample locations, or by the interaction of these effects. (B) Human nuclear DNA. The percentage of positive individuals in each group of five (21 groups of each species) did not differ* ($p > 0.05$) *between species, among sample locations, or by the interaction of these effects. See Table 1 for dust and traffic levels at each sample location.*

total reactions (each sample tested in triplicate), 17.3% ± 3.2% yielded quantifiable human DNA, and 37.3% ± 7.1% of 177 insect samples tested positive in at least one of three replicate reactions. Of these 66 samples, 9% tested positive in all three reactions, 21% tested positive in two reactions, and 70% tested positive in only one reaction. All positive control samples tested positive, and all negative control samples tested negative for human DNA.

STR Analyses

Of the 34 positive insect samples (13 roaches, 12 flies, and 9 crickets) subjected to AmpFℓSTR® Profiler Plus™ PCR amplification, 41% yielded STR alleles; five (12%) yielded at least one allele call for one or more loci; and three (24%) exhibited mixtures of three to five alleles (Table 3). The profile of alleles for the individual who maintained insects and performed molecular genetic analyses was not detected among the suite of alleles that amplified for any insect sample. Most allele signals were near or below 500 RFU; additionally, distinct peaks were present in many samples that could be discerned from background noise but were below the detection threshold. Seven representative reactions run on the MJ BaseStation 51™ were also visualized on an ABI Prism® 3100-*Avant*™ to test concordance with a forensics industry standard machine (Table 4, Fig. 3). Concordance between the two analysis platforms was 80%, and one of six samples had four of five allele designations matching between the two platforms. Lack of concordance was attributable to loss of detectable alleles below the ABI Prism® 3100-*Avant*™ scoring threshold, not to mislabeling or misscoring.

Discussion

Presence of Human DNA in Dust Acquired by Insects

This study provides the first evidence that foraging insects can serve as human DNA collectors. All three species tested, the common housefly, German cockroach, and camel cricket, acquired detectable human mtDNA and human nuclear DNA while foraging on dusty indoor surfaces. Overall, human mtDNA was detected more readily than human nuclear DNA. The mean number of human mtDNA-positive individuals in each species group of five ranged from one to five individuals (20–100% positive), resulting in the detection of human mtDNA at all 16 of the sample locations (i.e., a 100% detection rate). In contrast, the percentage of individuals within each group that tested positive for human nuclear DNA ranged from 0 to 100%, and human nuclear DNA was detected in 89% of the sample locations. Similar differences were reported for comparative dust samples with very small quantities of human DNA (9). Nevertheless, this study demonstrates that insect samplers can provide evidence of human habitation and potentially more complete information about the identity of the human occupants in downstream forensic analyses. Further, this study demonstrates the utility of insects as environmental samplers of molecular evidence in general.

Detection of Human DNA with Respect to Insect Species

All three insect species delivered evidence of human DNA after exposure to dusty indoor surfaces. In Experiment 1, more houseflies (75%) tested positive for human mtDNA-A or mtDNA-B than cockroaches (59%) ($p = 0.05$). In contrast, only 44% of houseflies tested positive in Experiment 2, compared to 58% of cockroaches and 38% of camel crickets (houseflies vs. cockroaches, $p = 0.074$; houseflies vs. crickets, $p = 0.05$; cockroaches vs. crickets, $p = 0.05$). Differences in housefly delivery of human DNA between the two experiments may reflect timing of the experiments with respect to the circadian periodicity of foraging activity. Houseflies are diurnal, and, serendipitously, Experiment 1 was conducted on a summer afternoon, and Experiment 2 was conducted on an early evening in autumn. This illustrates the importance of appropriate knowledge of the life history and ecology of insects employed as environmental samplers. Additional factors that could affect foraging activity include insect age or physiological state, environmental factors, such as light intensity and quality, relative humidity and temperature, or the quantity of human DNA in the environment.

TABLE 2—*Insect recovery of human DNA from indoor surfaces with medium dust levels in classrooms (''class'') with high human traffic levels and offices (''office'') with low human traffic levels (Experiment 2). Insects were exposed to a 576-cm^2 dust-covered area for 60 ± 5 min. Data represent the mean percentage of individuals* (n = 5) *in three replicated groups of each insect species that tested positive for human mtDNA or human nuclear DNA. Quantity of human DNA (ng/sample) was determined by qPCR.*

	Human mtDNA (% Positive)				Human Nuclear DNA (% Positive)				Human DNA Recovered (x ± SD) (ng/sample)			
Sample	Dust	Fly	Roach	Cricket	Dust	Fly	Roach	Cricket	Dust	Fly	Roach	Cricket
Class 2–1	0	40	100	40	0	40	60	0	N/A	0.011 ± 0.024	0.077 ± 0.104	N/A
Class 2–2	100	40	100	60	100	20	80	40	2.389 ± 1.350	0.015 ± 0.033	0.027 ± 0.027	0.054 ± 0.110
Class 2–3	100	100	100	60	100	80	60	0	5.656 ± 3.403	0.041 ± 0.040	0.021 ± 0.217	N/A
Class 3–1	100	100	100	100	100	80	60	0	4.734 ± 0.994	0.042 ± 0.030	0.038 ± 0.041	N/A
Class 3–2	0	100	100	60	100	40	20	40	0.797 ± 0.681	0.034 ± 0.055	0.012 ± 0.027	0.012 ± 0.017
Class 3–3	100	100	100	40	100	40	20	20	2.203 ± 1.657	0.023 ± 0.034	0.008 ± 0.019	0.009 ± 0.019
Class 4–1	100	20	20	60	100	40	60	20	1.112 ± 0.172	0.015 ± 0.022	0.015 ± 0.020	0.001 ± 0.003
Class 4–2	100	100	100	100	100	0	40	20	2.222 ± 0.420	N/A	0.033 ± 0.048	0.017 ± 0.038
Class 4–3	100	80	100	20	100	40	60	40	1.995 ± 0.042	0.044 ± 0.080[*]	0.060 ± 0.109	0.025 ± 0.050
Office 4	100	60	40	40	100	40	20	40	4.828 ± 1.438	0.001 ± 0.002[†]	0.060 ± 0.109	0.004 ± 0.008
Office 5	0	80	100	60	100	40	40	20	0.062 ± 0.005	0.001 ± 0.002	0.004 ± 0.007	0.003 ± 0.006
Office 6	100	60	20	40	100	40	40	20	0.926 ± 0.484	0.091 ± 0.133	0.012 ± 0.019	0.002 ± 0.005

[*]This group includes the individual noted in Tables 3 and 4, and Fig. 3.
[†]One individual yielding 418.75 ng of human DNA was omitted as an outlier (n = 4).

Detection of Human DNA with Respect to Location

DNA was acquired by insect foragers from all locations sampled in the two experiments; however, no consistent pattern of human DNA collection was revealed with respect to traffic level. Owing to the restrictions of the experimental design and available locations for sampling, traffic levels (assigned by location) were not sampled equally, so the effect of human traffic level on insect sampling efficiency is difficult to infer; however, one of the three locations with high traffic and medium dust levels yielded a consistently higher percentage of insects with detectable human DNA (classrooms; Table 2, Fig. 3). Similar results were found in the quantity of human DNA that can be recovered from environmental isolates composed primarily of dust (9). Thus, an important message garnered from these studies is that high human traffic conveys a high likelihood of detecting three or more people but, at the same time, low human traffic does not necessarily limit the availability of detectable human DNA.

Detection, Quantitation, and STR Analysis of Human DNA Acquired by Insects

This study demonstrates that omnivorous scavenging insects can acquire detectable human DNA from the environment. Previously, the gut contents of necrophagous species have been utilized as a source of human DNA (21,22). In addition, human DNA has been recovered from three hemophagous species, a mosquito (23), the human body louse (24), and bed bug (25). In the present study, 63% of adult houseflies, 54% of adult cockroaches, and 21% of immature camel crickets acquired and delivered detectable human DNA by foraging on dusty indoor surfaces (Tables 1 and 2). The group-wise detection rate (at least one of five individuals in the same group tested positive) for human mtDNA was 100% for all three insect species over 33 sample locations. In comparison, 88% of comparable dust samples taken from adjacent areas in the same sample locations tested positive in at least one of three replicated reactions for human mtDNA. Results demonstrate the potential use of free-foraging insects for the collection of forensic evidence.

We offer several suggestions relating to applications involving insect samplers of environmental human DNA. Samples should be assayed first for the presence of human DNA using traditional PCR before performing more expensive qPCR. As expected, the multi-locus *TPA*25 was more sensitive than qPCR for detecting the presence of human DNA. With regard to extrapolating below the lowest human DNA standard in the qPCR assay, despite concerns expressed previously (26), we found that detection below the lower standard amount appeared to be an acceptable indication (deviation <3%) that sufficient intact human DNA was present in insect isolates to result in STR signals. Based on the range of human DNA detected after insects were allowed to forage for 1 h, we suggest that when qPCR is used to assay samples suspected to have a very small quantity of human DNA within an extremely large quantity of background DNA, the dilution curve should be extended by including lower quantities of standard DNA and, further, that the number of human DNA standard replicates should be increased to three per plate. In combination, these two measures should alleviate the need to extrapolate starting quantities of samples.

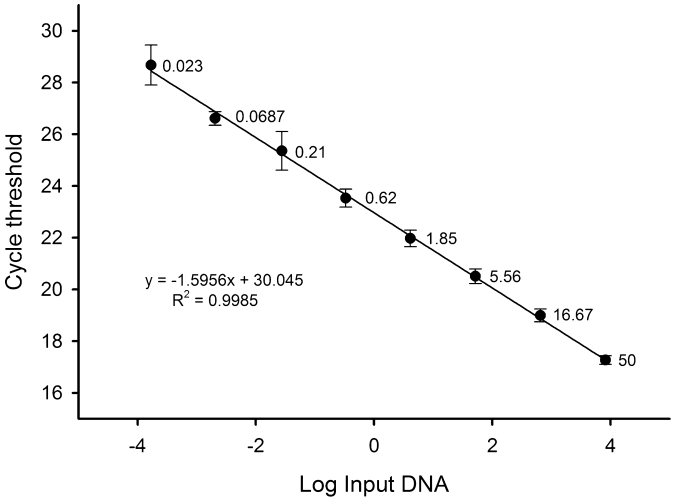

FIG. 2—*Calibration curves across 10 qPCR plates utilized to quantify human DNA recovered from insects. Points represent the mean ± SE for n = 20 replicates (two per plate); actual amounts of input human DNA (ng/μL) are shown to the right of each point.*

TABLE 3—*Allelic data for 12 insect samples that tested positive for human DNA, assayed using AmpFℓSTR® Profiler Plus™ and resolved on MJ BaseStation 51™. Numbers represent the number of alleles observed at each locus (e.g., "5" indicates where five alleles were detected for vWA from a roach in Classroom 3, indicating that more than two people were detected). Dashes indicate where no alleles were observed for a locus.*

Insect Species	Sample Location	Traffic Level	Input DNA (pg/μL)	Amelogenin	FGA	vWA	D3 S1358	D5 S818	D7 S820	D8 S1179	D13 S317	D18 S51	D21 S11
Fly*	Classroom 4	High	3.669 ± 3.301	X	–	2	2	–	–	3	–	–	1
Fly	Office 3	Low	8.375 ± 14.506	–	–	–	–	–	–	–	–	–	–
Roach	Classroom 1	High	0.496 ± 0.859	–	–	–	–	–	–	–	–	–	–
Roach	Classroom 2	High	5.092 ± 1.839	X	1	1	3	–	–	2	–	–	–
Roach	Classroom 3	High	1.190 ± 2.061	X	3	5	2	–	–	3	–	1	5
Roach	Classroom 3	High	1.246 ± 2.596	X	–	–	–	–	–	–	–	–	–
Roach	Classroom 4	High	0.767 ± 1.328	X	–	–	1	–	–	–	–	–	1
Roach	Classroom 4	High	2.106 ± 3.595	–	–	–	–	–	–	–	–	–	–
Roach	Classroom 4	High	5.097 ± 7.031	X	–	–	–	–	–	–	–	–	–
Cricket	Classroom 1	High	0.429 ± 0.744	–	–	–	–	–	–	–	–	–	–
Cricket	Classroom 2	High	5.004 ± 5.088	X	–	1	–	–	–	1	–	–	–
Cricket	Office 3	Low	0.054 ± 1.164	–	–	–	–	–	–	–	–	–	–

*Same individual as noted in Tables 2 and 4, and Fig. 3.

TABLE 4—*Comparison of six AmpFℓSTR® Profiler Plus™ reactions analyzed on two platforms, ABI Prism® 3100-*Avant™*, and MJ BaseStation 51™. Concordance between the two platforms was 80%. Table contains the total number of alleles observed for each locus. Dashes indicate where no alleles were observed for a locus.*

Platform	Insect Species	Sample Location	Amelogenin	FGA	vWA	D3 S1358	D5 S818	D7 S820	D8 S1179	D13 S317	D18 S51	D21 S11
ABI	Fly*	Classroom 4	X,X	1	2	2	2	–	1	–	–	1
MJ			X	–	2	2	–	–	3	–	–	1
ABI	Fly	Office 3	–	–	–	–	–	–	–	–	–	–
MJ			–	–	–	–	–	–	–	–	–	–
ABI	Roach	Classroom 2	–	–	–	–	1	–	1	–	–	1
MJ			X	1	1	3	–	–	2	–	–	–
ABI	Roach	Classroom 3	–	–	–	–	1	–	–	–	–	–
MJ			X	3	5	2	–	–	3	–	1	5
ABI	Roach	Classroom 4	–	–	–	–	–	–	–	–	–	–
MJ			–	–	–	–	–	–	–	–	–	–
ABI	Cricket	Classroom 2	–	–	–	–	–	–	–	–	–	–
MJ			X	–	1	–	–	–	1	–	–	–

*Same individual as noted in Tables 2 and 4, and Fig. 3.

Insect samplers with as little as 0.8–5.1 pg/μL of input human DNA yielded interpretable STR profiles (Table 3). This illuminates the need for documenting standards for forensic DNA practice (9,26) and validating methods for the collection of human DNA evidence provided by insects. At present, the use of insects for the collection of environmental human DNA for STR analysis is limited by inconsistency of acquisition and apparent quality of human DNA. These limitations could be overcome by pooling individual insect samples prior to analysis, resulting in a fivefold increase in human DNA quantity. Alternatively, enzymatic/assay enrichment of the small quantities of human DNA by whole genome amplification (WGA) or low copy number PCR (LCN-PCR) could be used to increase the potential for detecting human habitation of a particular space.

Implications

Results indicate that the use of insect samplers has limited application at the present time for routine forensic casework where the purpose of testing is to identify a specific human. However, this study demonstrates the potential use of free-roaming insects as environmental samplers of human DNA and other molecular evidence, thus potentially expanding the applications of forensic entomology to include general surveillance of human groups and for verifying human activity within enclosed areas. In particular, this approach may prove useful for biological and homeland security cases where stealth is indicated. Because insects passively acquire environmental evidence, multiple organic (e.g., pathogens) and inorganic (e.g., explosives) materials can be collected simultaneously with human DNA. Although insects delivered much smaller quantities of human nuclear DNA (<0.001–0.181 ng per individual) than direct surface swabbing of the entire sampling area (9–28 ng/cm^2) (9), insects can sample locations that are physically inaccessible to human investigators. For example, indigenous or released insects could be captured from an adjacent structure under surveillance, potentially offering information about past or present inhabitants. Because synanthropic insects, such as houseflies, German cockroaches, and camel crickets, are inherent components of human habitats, they are not likely to cause suspicion. With advancements in analytical technology and statistical deconvolution, the role of insect samplers in forensic and medico-legal investigations will increase in value and new applications are likely to arise.

Acknowledgments

We thank Drs. Wes Watson and Coby Schal (North Carolina State University) for supplying houseflies and cockroaches, Jarrod Champagne (VCU) for technical support, and Dr. William Eggleston (VCU) for critical review of an earlier version of this manuscript. Finally, we appreciate two anonymous reviewers for

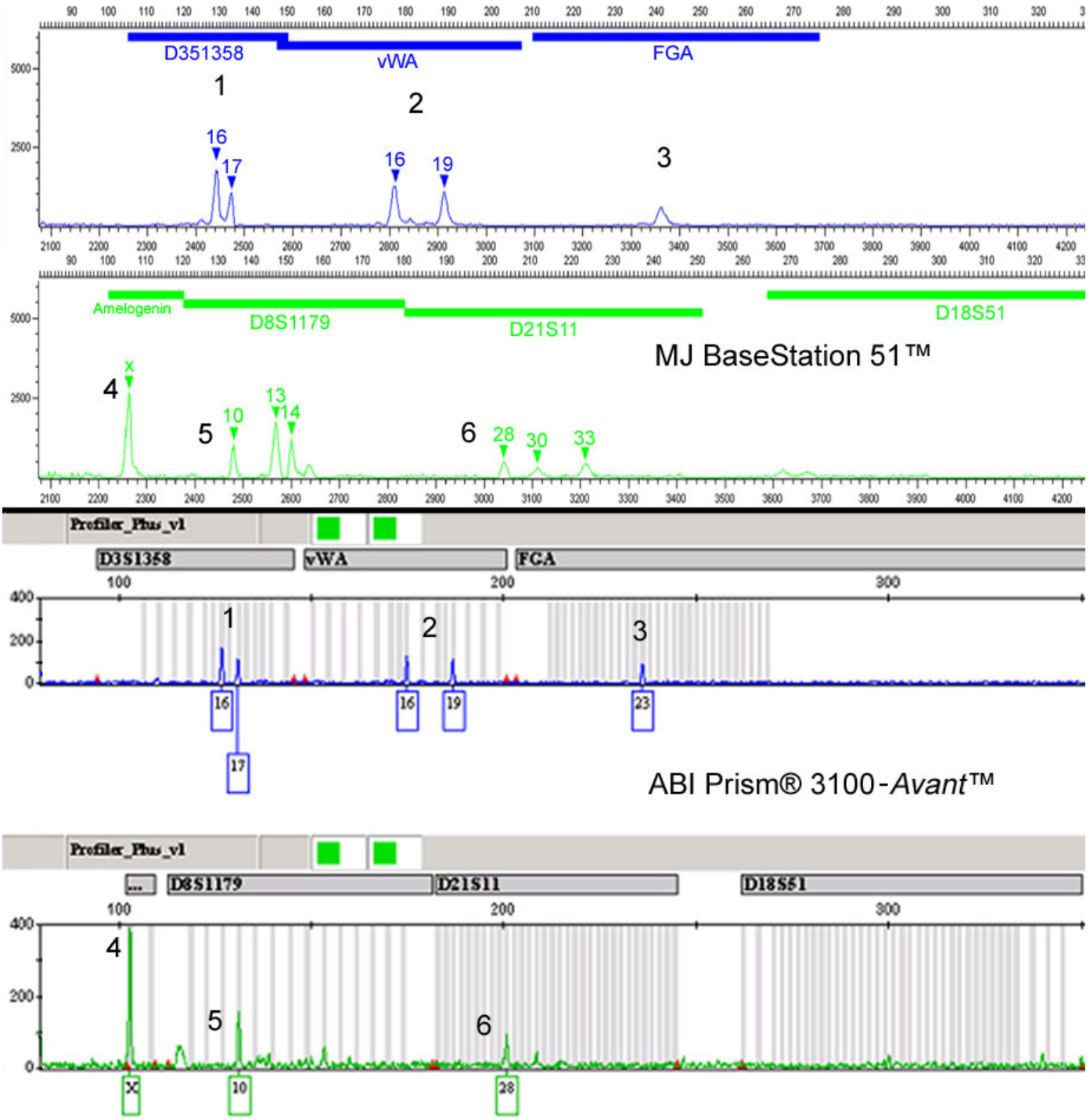

FIG. 3—*Comparison of a AmpFℓSTR® Profiler PlusTM reaction (housefly, classroom 4) run on MJ BaseStation 51™ and ABI Prism® 3100-*Avant™. *Concordance between the two platforms was 80%. Corresponding loci on the chromatograms are labeled 1–6.*

their thoughtful and helpful recommendations for improving this manuscript.

References

1. Byrd JH, Castner JL. Insects of forensic importance. In: Byrd JH, Castner JL, editors. Forensic entomology: the utility of arthropods in legal investigations. Boca Raton, FL: CRC Press, Inc, 2000;121–42.
2. Greenberg B, Kunich JC. Entomology and the law: flies as forensic indicators. New York, NY: Cambridge University Press, 2002.
3. Amendt J, Krettek R, Zehner R. Forensic entomology. Naturwissenschaften 2004;9(2):51–65.
4. Wells JD, Introna F, Di Vella G, Campobasso CP, Hayes J, Sperling FAH. Human and insect mitochondrial DNA analysis from maggots. J Forensic Sci 2001;46(3):685–7.
5. Clery JM. Stability of prostate specific antigen (PSA), and subsequent Y-STR typing, of *Lucilia (Phaenicia) sericata* (Meigen) (Diptera: Calliphoridae) maggots reared from a simulated postmortem sexual assault. Forensic Sci Int 2001;120(1-2):72–6.
6. Campobasso CP, Linville JG, Wells JD, Introna F. Forensic genetic analysis of insect gut contents. Am J Forensic Med Pathol 2005;26(2):161–5.

7. Wells JD, Stevens JR. Applications of DNA-based methods in forensic entomology. Annu Rev Entomol 2008;53:103–20.
8. Kester KM, Brown BL, Jackman J, Theodore M, Le M, Shanholtz L. Methods and molecular tools for analysis of BW agents delivered by insect sentinels. In: Proceedings of the 2003 Joint Service Scientific Conference on Chemical and Biological Defense Research, 2003 Nov 17-20; Towson (MD). Available by request or https://www.cbrniac.apgea.army.mil/Products/Catalog/Pages/ViewItem.aspx?ID=SOAR-06-18 (accessed July 8, 2010).
9. Toothman MH, Kester KM, Dawson Cruz T, Champagne J, Street WS, Brown BL. Characterization of human DNA in indoor environmental samples. Forensic Sci Int 2008;178:7–15.
10. West LS. The housefly, its natural history, medical importance, and control. Ithaca, NY: Comstock Pub. Co., 1951.
11. Graczyk TK, Knight R, Gilman RH, Cranfield MR. The role of non-biting flies in the epidemiology of human infectious diseases. Microbes Infect 2001;3:231–5.
12. Zurek L, Denning SS, Schal C, Watson DW. Vector potential of the house fly, Musca domestica L. (Diptera: Muscidae) for Yersinia pseudotuberculosis. J Med Entomol 2001;38(2):333–5.
13. Otake S, Dee SA, Moon RD, Rossow KD, Trincado C, Farnham M, et al. Survival of porcine reproductive and respiratory syndrome virus in houseflies. Can J Vet Res 2003;67(3):198–203.
14. Robinson WH, editor. Blattaria. In: Urban insects and arachnids: a handbook of urban entomology. Cambridge, MA: Cambridge University Press, 2005;35–64.
15. Brenner RJ. Economics and medical importance of German cockroaches. In: Rust MK, Owens JM, Reierson DA, editors. Understanding and controlling the German cockroach. New York, NY: Oxford University Press, 1995;77–92.
16. Zurek L, Schal C. Evaluation of the German cockroach (*Blatella germanica*) as a vector for verotoxigenic *Escherichia coli* F18 in confined swine production. Vet Microbiol 2004;101(4):263–7.
17. Taylor SJ, Krejca JK, Denight ML. Foraging range and habitat use of *Ceuthophilus secretus* (Orthoptera: Rhaphidophoridae), a key trogloxene in central Texas cave communities. Am Midl Nat 2005;154(1):97–114.
18. García-Obregón S, Alfonso-Sánchez MS, Pérez-Miranda AM, Vidales C, Arroyo D, Peña JA. Genetic position of Valencia (Spain) in the Mediterranean Basin according to *Alu* insertions. Am J Human Biol 2006;18(2):187–95.
19. Kline MC, Vallone PM, Redman JW, Duewer DL, Calloway CD, Butler JW. Mitochondrial DNA typing screens with control region and coding region SNPs. J Forensic Sci 2005;50(2):377–85.
20. Luciani S, Fornaciari G, Rickards O, Martínez Labarga O, Rollo F. Molecular characterization of a Pre-Columbian mummy and *in situ* coprolite. Am J Phys Anth 2006;129:620–9.
21. Zehner R, Amendt DJ, Krettek R. STR typing of human DNA from fly larvae fed on decomposing bodies. J Forensic Sci 2004;49(2):337–40.
22. Linville JG, Hayes J, Wells JD. Mitochondrial DNA and STR analysis of maggot crop contents: effect of specimen preservation technique. J Forensic Sci 2004;49(2):341–4.
23. Ansell J, Hu JT, Gilbert SC, Hamilton KA, Hill AV, Lindsay SW. Improved method for distinguishing the human source of mosquito blood meals between close family members. Trans R Soc Trop Med Hyg 2000;94(5):572–4.
24. Mumcuoglu KY, Gallili N, Reshef A, Brauner P, Grant H. Use of human lice in forensic entomology. J Med Entomol 2004;4(4):803–6.
25. Szalanski AL, Austin JW, McKern JA, Steelman CD, Miller DM, Gold RE. Isolation and characterization of human DNA from bed bug, ''Cimex lectularius'' L., (Hemiptera: Cimicidae) blood meals. J Agric Urban Entomol 2006;23(3):189–94.
26. Cupples CM, Champagne JR, Lewis KE, Dawson-Cruz T. STR profiles from DNA samples with ''undetected'' or low Quantifiler™ results. J Forensic Sci 2009;54(1):103–7.

Additional information and reprint requests:
Karen M. Kester, Ph.D.
Virginia Commonwealth University
Department of Biology
1000 W. Cary St.
Richmond, VA 23284-2012
E-mail: kmkester@vcu.edu

JOURNAL OF FORENSIC SCIENCES

J Forensic Sci, November 2010, Vol. 55, No. 6
doi: 10.1111/j.1556-4029.2010.01488.x
Available online at: onlinelibrary.wiley.com

PAPER

PSYCHIATRY & BEHAVIORAL SCIENCES

Hanna Putkonen,[1] *M.D., Ph.D.; Ghitta Weizmann-Henelius,*[1] *Ph.D.; Eila Repo-Tiihonen,*[2] *M.D., Ph.D.; Nina Lindberg,*[3] *M.D., Ph.D.; Tuula Saarela,*[4] *M.D., Ph.D.; Markku Eronen,*[1] *M.D., Ph.D.; and Helinä Häkkänen-Nyholm,*[5,6] *Ph.D.*

Homicide, Psychopathy, and Aging—A Nationwide Register-based Case-comparison Study of Homicide Offenders Aged 60 Years or Older*

ABSTRACT: With populations aging there have been some concerns on elderly offending. We compared elderly homicide offenders with a younger comparison group with special emphasis on psychopathy. We analyzed nationwide register-based material on all homicide offenders aged 60 or older who were in a forensic psychiatric examination in Finland 1995–2004 and their gender-matched comparison group of younger homicide offenders. The offenders 60 years or older were diagnosed less often than the younger ones with drug dependence and personality disorders and more often with dementia and physical illnesses. The mean Psychopathy Checklist—Revised total scores as well as factor and facet scores were lower in the 60 or older age group. The group 60 years or older had significantly lower scores on eight individual items of social deviance. The interpersonal/affective factor 1 scores did not differ. Understanding the possible underlying phenomena of violent behavior may provide help for developing services for the elderly.

KEYWORDS: forensic science, psychopathy, homicide, PCL-R, aging, elderly

The risk of homicidal offending decreases with increasing age from middle age onward (1). There are several reasons for this: symptoms of personality disorders mellow down, physical frailty, and lessened social contacts, and so on. Furthermore, offenders with antisocial personality have high mortality rates (2). Yet, there have been concerns about increasing numbers of elderly offenders and prisoners (3–7). In Finland, the number of homicide offenders aged 60 or older has remained quite stable during the past decades. In 1960–1974, the proportion was 6.5% and in 2003–2007 it was 5.8% of all homicide offenders (8).

Psychiatric illness has been found prevalent among elderly offenders and prisoners (4,7,9,10). The prevalence of specific diagnoses has varied in different studies. Some studies have found depression common among elderly prisoners (10,11), while others have not (12). Furthermore, Rosner et al. (12) found schizophrenia, personality disorders, and alcoholism prevalent among geriatric offenders, while Fazel and Grann (13) found a Swedish offender population with a lesser likelihood of schizophrenia or personality disorders and a higher likelihood of dementia or affective psychosis. In addition, Taylor and Parrot (9) found a lesser prevalence of personality disorders among elderly offenders. Alcohol abuse is widespread among elderly offenders, like within the younger ones (6,14).

Psychopathy is an important concept in explaining criminal behavior, particularly violent criminality (15). Egocentricity and impulsivity, lack of empathy and remorse, as well as shallow and labile affects are typical personality traits in psychopathy alongside violation of social norms (15). The most commonly used operational definition of psychopathy is the Hare Psychopathy Checklist—Revised (PCL-R) (15). The prevalence of antisocial personality disorder and PCL-defined psychopathy has been found to decline with age (16,17). Although research on psychopathy is rather extensive, to our knowledge no previous studies on psychopathy of aging homicide offenders exist.

Because the populations of many Western countries are aging, it is necessary to have multifaceted knowledge on issues associated with elderly homicide. Yet, previous studies have been limited by a lack of standardized diagnostic instruments and by selection bias (3). Because psychopathy is an important concept in explaining violent behavior, it should also be used in explaining elderly violence. In the present nationwide study, we compared elderly offenders with younger ones regarding demographics, past and present offenses, and psychiatric morbidity. Our special aim was to

[1]Vanha Vaasa Hospital, PO Box 13, 65381 Vaasa, Finland.
[2]Department of Forensic Psychiatry, University of Kuopio, Niuvanniemi Hospital, F1-70240 Kuopio, Finland.
[3]Helsinki University Central Hospital, Department of Adolescent Psychiatry, PO Box 590, 00027 MUS, Helsinki, Finland.
[4]Psychiatric Department, Helsinki Health Centre, PO Box 6000, 00899 Helsinki, Finland.
[5]Department of Psychology, University of Helsinki, Helsinki, Finland.
[6]Forensic Laboratory, National Bureau of Investigation, PO Box 285, Vantaa, Finland.

*Dr. Lindberg received travel funds from Novartis and Bristol-Myers Squibb during 2008; Dr. Eronen received speakers honoraria from Bristol-Myers Squibb, Astra Zeneca, Orion and Novartis; Dr. Saarela from Jansen-Cilag and Pfizer; and Dr. Häkkänen from Bristol-Myers Squibb. These are all single occasions with minor economic significance.

Received 24 July 2009; accepted 26 Sept. 2009.

compare their scores on psychopathy. We hypothesized that the elderly homicide offenders would score less on psychopathy than the younger ones.

Methods

Study Sample

The material of this study was register-based, comprehensive, and nationwide. It consisted of all Finnish forensic psychiatric examination reports for offenders prosecuted for homicide between 1995 and 2004 ($N = 749$). These 749 offenders were prosecuted for 700 homicidal events with 757 victims. For this study, cases with an offender at least 60 years of age ($n = 25$) were identified and gathered for analyses. There were three such women and 22 men. Of the remaining offenders in the national data, a random sample of 25 gender-matched offenders formed the comparison group. The data file was sorted by time, and each case received her/his comparison as the next consecutive gender-matched offender. Three (12%) older and seven (28%) younger offenders were prosecuted for murder, and 22 (88%) older and 18 (72%) younger for (voluntary) manslaughter. The mean age of the older offenders was 66.8 (SD 5.7, 60–82) and of the younger 34.8 (SD 10.8, 19–59). We chose the age 60 to match previous forensic research on the elderly (7,13,18,19).

Data Sources

The average age of Finnish male homicide offenders is 37.5 years and that of female homicide offenders 38.8 years. The homicide rate of Finns 60 years or older is ca. 0.1 per 100,000 women/year and slightly over 1 per 100,000 men/year (20).

In Finland between 1995 and 2004, the mean clearance rate for homicide was 92% (21). Hardly any victims of homicide remain unknown to the police (22). Furthermore, during 1995–2004, a total of 1046 people were prosecuted for homicide (23), and 749 (71%) of these were referred to a forensic psychiatric examination. According to Finnish law, the courts decide if a forensic psychiatric examination is required. These examinations are thorough inpatient evaluations, including exhaustive data collected from various sources, and psychiatric and psychological assessments. The forensic psychiatric reports have effectively been used as study material before and their reliability is deemed high by both courts and scientists (24,25). Furthermore, the National Authority for Medicolegal Affairs (NAMA) instructs and controls the standards of the examinations. All reports for this study were carefully analyzed for variables related to psychosocial and mental health issues: offenders' socio-demographic variables, adulthood criminality, use of mental health services, suicidal behavior, and the results of the forensic psychiatric examination, including crime scene variables and psychiatric diagnoses. Inter-rater reliability of variables was assessed in our previous studies, with partially the same data and data collection procedure (26). Only variables with a substantial or perfect agreement were included in the study.

PCL-R (15) is a 20-item rating scale based on a semi-structured interview and a review of collateral information. The items are rated on a three-point scale consistent with the degree to which the personality and behavior matches the item description. The total score adds up to 40. In addition to the diagnostic cutoff score of 30 recommended by Hare (15), a second cutoff score of 25 is frequently used in European studies (27,28) and others to enable comparison (29). In this study, we reported both. The revised scale has a two-factor structure, the interpersonal/affective and social deviance, and four facets, interpersonal, affective, lifestyle and antisocial (15). In this study, we reviewed forensic evaluation reports of the offenders, and the PCL-R was retrospectively rated by trained raters. Studies have shown that file-only PCL-R ratings can be used for research purposes with solid reliability, but they are likely to result in lower PCL-R scores (28,30). Furthermore, our raters were blind to case versus comparison group status.

To further evaluate inter-rater agreement of the PCL-R, 20 reports were randomly chosen from the total national data and rated by all raters after preparation in workshop attendance and numerous training sessions. The inter-rater agreement was assessed using intraclass correlation $ICC_{(2,1)}$. The ICC (for absolute agreement for a single rater) was 0.898 for the PCL-R total score; 0.735 for factor 1 and 0.920 for factor 2 scores. All correlations were significant ($p < 0.001$). The internal consistency, as measured by Cronbach's alpha, was 0.89 for all items, 0.86 for factor 1 and 0.79 for factor 2, 0.84 for facet 1, 0.83 for facet 2, 0.87 for facet 3, and 0.64 for facet 4.

The NAMA and the Ministry of the Interior approved the study procedures.

Statistical Analyses

Data analyses were made with SPSS 16.0 statistical software package. Chi-square analysis and Fisher's exact test were used to compare differences in frequencies between groups. Differences in mean PCL-R scores were assessed by Mann–Whitney *U*-test. The independent samples *t*-test was used to compare differences in mean of ages. Effect sizes were calculated using Cohen's *d*. Findings were considered significant if $p < 0.05$.

Results

As shown in Table 1, there were no significant differences between the older and younger groups in demographic variables, psychiatric treatment history, previous suicidal behavior or criminality, and only one difference in the crime scene variables. The mean age of the victims of the older offenders was 54.9 years (SD 13.8, 29–86) and of the younger ones 39.1 years (SD 14.3, 12–69). This difference in means was significant ($p < 0.001$, *t*-test). The

TABLE 1—*Comparison of older and younger homicide offenders—descriptive information.*

	60 Years or Older $N = 25$	Comparison $N = 25$
	n (%)	*n* (%)
Demographic variables		
In a live-in relationship	11 (44)	7 (28)
Had children	16 (70)	11 (46)
Previous mental health treatment	14 (56)	13 (52)
Previous criminal offending	12 (48)	18 (72)
Violent offending	9 (36)	13 (52)
Crime scene variables		
Motive: quarrel	14 (56)	14 (56)
Method: stabbing	15 (60)	15 (60)
Method: shooting	2 (8)	4 (16)
Intoxicated with alcohol	20 (80)	22 (88)
Intoxicated with drugs	1 (4)	8 (32)*
Victim: female	9 (36)	9 (36)
Victim: intimate partner	8 (32)	5 (20)
Attempted suicide at scene	3 (12)	3 (12)

*$p < 0.05$, Fisher's exact test, two-sided.

offenders' diagnoses are shown in Table 2. Four older offenders and three younger ones were assessed in need of involuntary psychiatric hospital treatment.

The elderly offenders with previous criminal offending differed from those without in two ways: the previously offended elderly had more often alcohol abuse/dependence (75% vs. 31%, $p < 0.05$) and were diagnosed more often with a personality disorder (67% vs. 23%, $p < 0.05$). Further, three older and one younger offender had previously committed homicide. All three elderly reoffenders were men within the age limit 65–80 years, diagnosed with alcohol dependence and a personality disorder and committed the index homicide while intoxicated with alcohol, during a drinking situation.

The group 60 years or older scored lower than the comparison group on the mean PCL-R total, factor, and facet scores, prorated for missing items. The mean PCL-R total score for the older group was 9.2 (SD 8.7, 0–35) and for the comparison group 17.6 (SD 9.4, 2–37.8). The difference was significant ($U_{(1)} = 142.5$, $p < 0.002$; $d = 0.93$). One (4%) older and six (24%) younger offenders received a score of 30 or over ($p = 0.044$). Two older and six younger offenders received a score of 25 or more.

The mean for factor 1 (interpersonal/affective) score in the older offender group was 4.8 (SD 4.0, 0–15) and in the comparison group 6.6 (SD 4.2, 1–16). The difference was not significant. The mean for factor 2 (social deviance) score in the older offenders was 4.1 (SD 5.2, 0–16) and in the comparison group 10.2 (SD 6.1, 0–20). This difference was significant ($U_{(1)} = 127.5$, $p < 0.001$; $d = 1.08$). Similar differences were found in the mean scores of facet 3 (lifestyle; $U_{(1)} = 153.5$, $p < 0.002$; $d = 1.0$), the mean in the older group was 2.5 (SD 3.1, 0–10) and in the comparison group 5.7 (SD 3.3, 0–10). The difference in mean scores of facet 4 (antisocial behavior) was also significant ($U_{(1)} = 132.5$, $p < 0.003$; $d = 0.96$). The mean score of facet 4 was 1.7 (SD 2.3, 0–7.5) in the older group and 4.5 (SD 3.1, 0–9) in the comparison group. The difference in the scores on facet 1 and 2 was not significant.

There were significant differences between the older and younger groups in the frequencies of scoring 1 or 2 on the PCL-R in eight of the 20 individual items (Table 3). All eight differences were within the nine items of factor 2 (social deviance). No significant

TABLE 2—*Comparison of older and younger homicide offenders—results of the forensic psychiatric examination.*

	60 Years or Older $N = 25$	Comparison $N = 25$	
	n (%)	*n* (%)	$d^{\dagger}$
Diagnosis			
Psychotic diagnosis	3 (12)	4 (16)	–
Schizophrenia	1 (4)	1 (4)	–
Psychotic depression	0 (0)	1 (4)	–
Alcohol dependence/abuse	13 (52)	18 (72)	–
Drug dependence/abuse	0 (0)	9 (36)*	1.06
Any personality disorder	11 (44)	19 (76)*	0.69
Antisocial personality	2 (8)	7 (28)	–
Borderline personality	2 (8)	2 (8)	–
Dementia	5 (20)	0 (0)*	0.71
Any chronic physical illness	12 (48)	3 (12)*	0.85
Criminal responsibility			
Full	11 (44)	18 (72)	–
Diminished	10 (40)	4 (16)	–
None	4 (16)	3 (12)	–

*$p < 0.05$, Fisher's exact test, two-sided.
†Effect size Cohen's d was defined "small, $d = 0.2$", "medium = 0.5", and "large = 0.8".

TABLE 3—*PCL-R scores item-by-item—homicide offenders 60 years or older and comparison group (n = 25 in both groups).*

Item	≥60 Years-group %	Comparison-group %	p*	$d^{\dagger}$
1. Glibness/superficial charm				
Score 0	84.0	76.0		
Scores 1 and 2	16.0	24.0	ns	–
2. Grandiose sense of self worth			ns	–
Score 0	76.0	64.0		
Scores 1 and 2	24.0	36.0		
3. Need for stimulation			0.001	1.22
Score 0	72.0	20.0		
Scores 1 and 2	28.0	80.0		
4. Pathological lying			ns	–
Score 0	91.3	69.6		
Scores 1 and 2	8.7	30.4		
5. Conning/manipulative			ns	–
Score 0	87.5	72.0		
Scores 1 and 2	12.5	28.0		
6. Lack of remorse or guilt			ns	–
Score 0	40.0	40.0		
Scores 1 and 2	60.0	60.0		
7. Shallow affect			ns	–
Score 0	16.0	12.0		
Scores 1 and 2	84.0	88.0		
8. Callous/lack of empathy			ns	–
Score 0	40.0	24.0		
Scores 1 and 2	60.0	76.0		
9. Parasitic lifestyle			0.008	0.88
Score 0	79.2	37.5		
Scores 1 and 2	20.8	62.5		
10. Poor behavioral controls			ns	–
Score 0	36.0	12.0		
Scores 1 and 2	64.0	88.0		
11. Promiscuous sexual behavior			ns	–
Score 0	83.3	80.0		
Scores 1 and 2	16.7	20.0		
12. Early behavior problems			0.005	1.15
Score 0	87.5	45.8		
Scores 1 and 2	12.5	54.2		
13. Lack of realistic goals			0.004	0.88
Score 0	64.0	20.8		
Scores 1 and 2	36.0	79.2		
14. Impulsivity			0.012	0.85
Score 0	48.0	12.0		
Scores 1 and 2	52.0	88.0		
15. Irresponsibility			0.002	1.10
Score 0	72.0	24.0		
Scores 1 and 2	28.0	76.0		
16. Failure to accept responsibility			ns	–
Score 0	40.0	16.0		
Scores 1 and 2	60.0	84.0		
17. Many short-term marital relationships			ns	–
Score 0	88.0	73.9		
Scores 1 and 2	12.0	26.1		
18. Juvenile delinquency			0.023	0.72
Score 0	95.7	66.7		
Scores 1 and 2	4.3	33.3		
19. Revocation of conditional release			ns	–
Score 0	86.7	68.4		
Scores 1 and 2	13.3	31.6		
20. Criminal versatility			0.000	1.24
Score 0	87.5	32.0		
Scores 1 and 2	12.5	68.0		

PCL-R, Psychopathy Checklist—Revised.
*Chi-square test, df = 2, two tailed, ns = not significant.
†Cohen's d.

differences were found on any factor 1 (interpersonal/affective) items.

Discussion

In this nationwide study, we found that the Finnish homicide offenders 60 years or older do indeed differ from the other homicide offenders. Yet, this age group might also include offenders more like their younger counterparts. As a whole, the older group scored significantly lower than the younger group on the PCL-R. Specifically noteworthy was the significant difference in factor 2, social deviance, and the lack of difference in factor 1, interpersonal/affective.

The only psychiatric diagnoses with significant differences between the two age groups were drug dependence/abuse, personality disorders, and dementia. No one in the elderly group received a diagnosis of drug dependence/abuse. This is in line with previous findings (6,7). Yet, over half of the elderly offenders were diagnosed with alcohol abuse/dependence, not significantly less than the younger offenders. In fact, alcohol misuse in the elderly is commonly missed or inadequately managed (31), and substance abuse services need to apply to all age groups (6). This is especially true in a country like Finland, where alcohol use has increased during the past decades, especially among the elderly (32).

A personality disorder was diagnosed in 11 (44%) of our elderly offenders, significantly less than in the younger ones (76%). This was in line with a study on a secure forensic psychiatry inpatient services (7). Moreover, the prevalence of antisocial personality has been found to decrease with age (16).

In our study, depression did not emerge in the diagnoses. Previously, there have been inconsistent results on depression and elderly homicide (10,12). Finland is notorious for not only high homicide but also suicide figures, and elderly homicide has been found more often than non-elderly homicide to precede suicide (18). Perhaps some depressed offenders escaped the data because of suicide. Our methodology did not allow further study on this.

Dementia was diagnosed in 20% of the older offenders. Irritability, episodic aggression and violence sometimes accompany dementia (33,34). The vast majority of aggressive incidents involving patients with dementia are minor (35). Homicide is a very rare event among patients with dementia. Yet, it has even been considered a potential risk factor for homicide (14). In Finland, dementia is diagnosed by neurologists and geriatrics, sometimes by geriatric psychiatrists. Treatment is divided among several units and fields, including home nursing. All these professionals should acknowledge the opportunity to assess the threat of violence and address issues related to it in treatment. As the population gets older, also the infrequent events of dementia should be recognized.

We found no significant differences between the two age groups in the studied mental health and criminal history or the social background variables. This was in line with previous studies (36). Almost half of the elderly offenders had a criminal history, approximating previous results (18). However, the offenders with previous offending may present a different subgroup of offenders than those without. They had more alcohol dependence and personality disorders, not unlike the typical Finnish homicide offender, a substance-abusing, marginalized, and antisocial man (20). Taxonomic analyses with larger data are needed to study this further.

It was clear that the older group scored lower on the PCL-R than the younger one. As this was the first study to report PCL-R scores of elderly homicide offenders, there is no previous literature with which to compare our results. Yet, on a general level, although with a younger population than ours, it has been observed that factor 1 (interpersonal/affective) scores (items) are stable across the age-span while mean scores on factor 2 (social deviance) decline with age (17,37). Our results showed differences between the age groups within the factor 2 items and facets 3 and 4, in line with the study by Huchzermeier et al. (16). As they concluded, it seems that different aspects of psychopathy follow different developmental courses. In a way, some of the elderly offenders in our study may have calmed down; they had less need for stimulation, less impulsive or antisocial behavior, and more responsibility. Obviously, with our cross-sectional data this remains hypothetical. Furthermore, besides actual psychological differences, the differences in items "juvenile delinquency" and "early behavior problems" might also reflect two things: an earlier era of youth with stricter conformity demands and the bias of lapsed time. It seemed essential that there were no differences in the items measuring interpersonal and affective features, the so-called core personality features, while there indeed were significant differences in the impulsive and irresponsible behavioral features. Harpur & Hare (17) have suggested that age-related differences in traits associated with impulsivity and social deviance are not necessarily paralleled by other psychopathic traits. The assumption that the core personality traits of psychopathy persist into middle age and late adulthood (15) might explain some of the homicide offending by elderly offenders. Certainly an association has been found between factor 1 and violence (38), and these issues should be addressed in the treatment of patients of all ages.

Strengths and Limitations

Elderly homicide has been a challenging topic for research mainly because of small data. This was a unique nationwide, comprehensive study, which is a definite strength. We studied all the forensic psychiatric examinations for homicide in Finland 1995–2004. The Finnish clearance rate for homicide and the tradition of thorough forensic psychiatric examinations and statistics form a solid basis for register-based study. The diagnoses of the Finnish forensic psychiatric examinations are always based on exhaustive examination and specific criteria and are considered reliable for study purposes (25,39). However, the fact that this study was retrospective and register-based does present some obvious limitations, though mostly same limitations apply both the elderly and the comparison group. Yet, it is possible that some early-life data on the elderly offenders are missing because of aged registers and faded memories. Clearly, the small number of cases limits statistical analyses with multiple and confounding variables, but the effect sizes of the observed differences were mostly very large. Whether or not our results can be generalized over countries other than Finland requires further research.

The assessment of psychopathic traits was performed using the 20-item Hare PCL-R (15), which has become the standard for assessing psychopathy in forensic settings. The PCL-R has been shown to be a reliable and valid instrument for measuring psychopathy (28,40), and the psychometric properties of the PCL-R appear to be similar in different countries (40). Furthermore, our data was comprehensive and included both women and men, which we consider a strength. Most previous studies using the PCL-R, just like most homicide studies, have been performed on men only, few on women only. Certain gender differences in psychopathy have been noted (41) but having a total population with gender-matched controls minimizes this problem. Yet, gender differences may be an uncontrolled source of variation in scores on variables of interest. Further, research has consistently shown that PCL–R assessments based solely on file information are highly similar to ratings including an interview, provided there is sufficient file information, and

therefore file-based assessment has been seen appropriate for research purposes (28,30). In this study, raters received the information in the forensic psychiatric examination reports, i.e., objective statements for court procedures, and they were blind to case versus comparison group status. Various bias issues were attended to in training.

Conclusion

Only the elderly commit serious violence infrequently, which has caused them to be ignored as a focus for research and service development (31). Specialist old age psychiatric forensic services have been previously suggested (4). Suitable facilities for older offenders requiring ongoing nursing care and the ability to manage risky behavior have been called for to prevent older offenders being stuck in inappropriate facilities (5). Based on our results, it seems that the elderly and their risk for violence should be remembered in both the population and the forensic services. As the elderly offenders seemed to have problems with (factor 1) issues related to interpersonal and affective traits, perhaps these issues need to be addressed more in the treatment of patients of all ages. Longitudinal studies to determine the stability of impulsive and antisocial traits of psychopathy would produce valuable information on the elderly offenders. As the populations of many Western countries are aging, the number of elderly offenders might increase. This should be taken into consideration in both planning services for the older adults as well as future studies to enhance prevention of elderly homicide.

Acknowledgments

We thank the National Authority for Medicolegal Affairs for co-operation in data collecting and Dr. Lehti for providing statistics.

References

1. Hare RD, McPherson LM. Violent and aggressive behavior by criminal psychopaths. Int J Law Psychiatry 1984;7(1):35–50.
2. Repo-Tiihonen E, Virkkunen M, Tiihonen J. Mortality of antisocial male criminals. J Forensic Psychiatry 2001;12:677–83.
3. Fazel S, Jacoby R. The elderly criminal. Int J Geriatr Psychiatry 2000;15(3):201–2.
4. Tomar R, Treasaden IH, Shah AK. Is there a case for a specialist forensic psychiatry service for the elderly? Int J Geriatr Psychiatry 2005; 20(1):51–6.
5. Yorston GA, Taylor PJ. Commentary: older offenders—no place to go? J Am Acad Psychiatry Law 2006;34(3):333–7.
6. Arndt S, Turvey CL, Flaum M. Older offenders, substance abuse, and treatment. Am J Geriatr Psychiatry 2002;10(6):733–9.
7. Coid J, Fazel S, Kahtan N. Elderly patients admitted to secure forensic psychiatry services. J Forensic Psychiatry 2002;13:416–27.
8. Lehti M. Homicide database. Helsinki, Finland: The National Research Institute of Legal Policy, 2008.
9. Taylor PJ, Parrott JM. Elderly offenders. A study of age-related factors among custodially remanded prisoners. Br J Psychiatry 1988;152:340–6.
10. Fazel S, Hope T, O'Donnell I, Jacoby R. Hidden psychiatric morbidity in elderly prisoners. Br J Psychiatry 2001;179:535–9.
11. Barak Y, Perry Y, Elizur A. Elderly criminals: a study of the first criminal offence in old age. Int J Geriatr Psychiatry 1995;10(6):511–6.
12. Rosner R, Wiederlight M, Harmon RB, Cahn DJ. Geriatric offenders examined at a forensic psychiatry clinic. J Forensic Sci 1991;36(6): 1722–31.
13. Fazel S, Grann M. Older criminals: a descriptive study of psychiatrically examined offenders in Sweden. Int J Geriatr Psychiatry 2002;17(10):907–13.
14. Rayel MG, Land WB, Gutheil TG. Dementia as a risk factor for homicide. J Forensic Sci 1999;44(3):565–7.
15. Hare RD. The Hare psychopathy checklist—revised (PCL-R), 2nd edn. Toronto: Multi-Health Systems, 2003.
16. Huchzermeier C, Geiger F, Kohler D, Bruss E, Godt N, Hinrichs G, et al. Are there age-related effects in antisocial personality disorders and psychopathy? J Forensic Leg Med 2008;15(4):213–8.
17. Harpur TJ, Hare RD. Assessment of psychopathy as a function of age. J Abnorm Psychol 1994;103(4):604–9.
18. Fazel S, Bond M, Gulati G, O'Donnell I. Elderly homicide in Chicago: a research note. Behav Sci Law 2007;25(5):629–39.
19. Lewis CF, Fields C, Rainey E. A study of geriatric forensic evaluees: who are the violent elderly? J Am Acad Psychiatry Law 2006;34(3):324–32.
20. Kivivuori J, Lehti M, Aaltonen M. Homicide in Finland, 2002–2006 a description based on the Finnish homicide monitoring system (FHMS). Web reviews 3/2007. Helsinki: Oikeuspoliittinen tutkimuslaitos, 2007, http://www.optula.om.fi/uploads/coixzx0dv6vk7ih.pdf (accessed May 5, 2009).
21. Statistics Finland. Crime Statistics, Rikokset ja niiden selvittäminen 1995–2004. http://www.stat.fi/tup/tilastotietokannat/index_en.html (accessed November 6, 2007).
22. Pajuoja J, Salminen M. Kadonneet henkilöt [Missing persons]. Helsinki, Finland: Keskusrikospoliisi, 1996.
23. Statistics Finland. Crimes recorded by the police. Helsinki, Finland: Statistics Finland, 2006.
24. Eronen M, Hakola P, Tiihonen J. Mental disorders and homicidal behavior in Finland. Arch Gen Psychiatry 1996;53(6):497–501.
25. Putkonen H, Komulainen EJ, Virkkunen M, Eronen M, Lönnqvist J. Risk of repeat offending among violent female offenders with psychotic and personality disorders. Am J Psychiatry 2003;160(5):947–51.
26. Laajasalo T, Häkkänen H. Background characteristics of mentally ill homicide offenders: a comparison of five diagnostic groups. J Forens Psychiatr Psychol 2004;15:451–74.
27. Cooke DJ. Psychopathy across cultures. In: Cooke DJ, Forth AE, Hare RD, editors. Psychopathy: theory, research and implications for society. Amsterdam: Kluwer Academic Publishers, 1998;13–45.
28. Grann M, Långström N, Tengström A, Stålenheim EG. Reliability of file-based retrospective ratings of psychopathy with the PCL-R. J Pers Assess 1998;70(3):416–26.
29. Warren JI, Burnette ML, South SC, Chauhan P, Bale R, Friend R, et al. Psychopathy in women: structural modeling and comorbidity. Int J Law Psychiatry 2003;26(3):223–42.
30. Wong S. Is Hare's psychopathy checklist reliable without the interview? Psychol Rep 1988;62:931–4.
31. Yorston G. Aged and dangerous. Old-age forensic psychiatry. Br J Psychiatry 1999;174:193–5.
32. Sulander T. Functional ability and health behaviours: trends and associations among elderly people, 1985–2003. Helsinki, Finland: National Public Health Institute, 2005.
33. Patel V, Hope T. Aggressive behaviour in elderly people with dementia: a review. Int J Geriatr Psychiatry 1993;8:457–72.
34. Siever LJ. Neurobiology of aggression and violence. Am J Psychiatry 2008;165(4):429–42.
35. Patel V, Hope RA. Aggressive behaviour in elderly psychiatric inpatients. Acta Psychiatr Scand 1992;85(2):131–5.
36. Goetting A. Patterns of homicide among the elderly. Violence Vict 1992;7(3):203–15.
37. Brandt JRKW, Patrick CJ, Curtin JJ. Assessment of psychopathy in a population of incarcerated adolescent offenders. Psychol Assess 1997;9(4):429–35.
38. Hemphill JF, Hare RD, Wong S. Psychopathy and recidivism: a review. Leg Criminol Psychol 1998;3:139–70.
39. Eronen M. Mental disorders and homicidal behavior in female subjects. Am J Psychiatry 1995;152(8):1216–8.
40. Hare RD, Clark D, Grann M, Thornton D. Psychopathy and the predictive validity of the PCL-R: an international perspective. Behav Sci Law 2000;18(5):623–45.
41. Jackson R, Richards H. Psychopathy in women: a valid construct with clear implications. In: Herve H, Yuille JC, editors. The psychopath theory, research, and practice. Mahwah, New Jersey: LawrenceErlbaum Associates, Inc, 2007;389–410.

Additional information and reprint requests:
Hanna Putkonen, M.D., Ph.D.
Vanha Vaasa Hospital
PO Box 13
FI-65381 Vaasa
Finland
E-mail: hanna.putkonen@vvs.fi

JOURNAL OF FORENSIC SCIENCES

J Forensic Sci, November 2010, Vol. 55, No. 6
doi: 10.1111/j.1556-4029.2010.01530.x
Available online at: onlinelibrary.wiley.com

TECHNICAL NOTE
ANTHROPOLOGY

Hugo F. V. Cardoso,[1,2] *Ph.D.*

Testing Discriminant Functions for Sex Determination from Deciduous Teeth*,†

ABSTRACT: Three studies have proposed discriminant functions for sex determination from deciduous tooth crown dimensions, and this study tests the existing functions on a sample of 46 Portuguese immature skeletons of known sex, aged from birth to 10 years. Deciduous teeth were measured in their mesiodistal and faciolingual crown dimensions, and percentage of correct allocation accuracy in determining sex using each specific function was determined. Discriminant functions were also calculated from data collected for this study and tested using cross-validation. Results show poor overall accuracy (33.3–75%) and poor cross-validation (46.2–60.0%). This is related to low sexual dimorphism in deciduous tooth crown size, as well as differences in degree of sexual dimorphism and in overall tooth size between different samples. For these reasons, deciduous crown size does not seem to show significant forensic value as discriminator of sex, particularly when methods developed on one population are applied to individuals of another population.

KEYWORDS: forensic science, forensic anthropology, human identification, sex determination, deciduous dentition, odontometrics

Determining the sex of human immature skeletal remains is a known problem in forensic practice and bioarcheological studies. A few techniques have been tentatively employed for the determination of sex of immature skeletal remains, of which one is odontometrics. Traditionally, assessing sex differences in tooth size has involved mesiodistal and buccolingual diameters of tooth crowns. A number of studies have established significant sexual dimorphism in size of the permanent (1–6) and deciduous crowns (7–13), but seldom have these differences been explored for their forensic or bioarcheological value in determining sex. For the deciduous dentition, the exceptions to this are the studies by Black (14), DeVito and Saunders (15), and Żądzińska et al. (16).

DeVito and Saunders (15) published a series of discriminant functions for sex determination of deciduous teeth, and these seem to provide the greatest percentage of correct sex allocation accuracy (>75%). These equations have been developed using a sample of living children—the Burlington growth study—and their accuracy was determined using a holdout sample comprised of related groups of known sex cases of the same sample. Black (14) also developed a series of discriminant functions for sex determination of deciduous teeth using a sample of living children—the University School Growth Study from the University of Michigan—but the accuracy obtained is considerably lower, between 63.9 and 68.4%. Żądzińska et al. (16) provide one single discriminant function (75% of correct sex allocation accuracy) derived from a sample of 113 immature remains from a Medieval site in Poland, where sex was genetically determined. Although most of these methods do not provide very high correct sex allocation accuracies, they have never been systematically tested on independent samples.

The purpose of this study is to test the discriminate functions proposed by Black, (14), DeVito and Saunders (15), and Żądzińska et al. (16) for sex determination from deciduous crown dimensions and briefly discuss the potential pitfalls of using sexual dimorphism in deciduous tooth size for developing reliable discriminant functions for sex determination. Testing these functions provides a measure of the reliability of their use in a forensic context, because in an actual forensic case, the expert may not or cannot determine whether the case is comparable with the Burlington Growth Study group of children or any of the other samples of children. Therefore, it is important to assess cross-sample applicability of methods, but samples of nonadult skeletons of known sex and age are not easily accessible. This study provides such an opportunity using a large sample of Portuguese fully documented immature skeletal remains.

Materials and Methods

The discriminant functions developed by Black (14), DeVito and Saunders (15), and Żądzińska et al. (16) were tested on a sample of 46 immature skeletons (males = 20; females = 26), aged from birth to 10 years (Table 1), who were born between 1911 and 1971 in Portugal. Skeletons in the sample were selected from the identified skeletal collection curated at the National Museum of Natural History in Lisbon, Portugal (17). Specimens were selected if at least one deciduous tooth was present with the crown completely formed down to the cementoenamel junction. For each individual, all available deciduous teeth were measured in their mesiodistal and faciolingual crown dimensions with a Mitutoyo digital sliding caliper and recorded to two decimal places. The mesiodistal width measures the maximum width of the crown in the mesiodistal plane

[1]Departamento de Zoologia e Antropologia, Museu Nacional de História Natural & Centro de Biologia Ambiental, Lisboa, Portugal.
[2]Faculdade de Medicina, Universidade do Porto, Porto, Portugal.
*Funding was partly provided by a Doctoral Fellowship from the *Fundação para a Ciência e Tecnologia* (grant # SFRH/BD/4917/2001) and by a Postdoctoral Fellowship from the same institution (grant # SFRH/BPD/22142/2005).
†Presented at the 2008 Annual Meeting of the Canadian Association for Physical Anthropology, November 5-8, 2008, in Hamilton, Ontario.
Received 9 Aug. 2009; and in revised form 23 Sept. 2009; accepted 8 Oct. 2009.

TABLE 1—*Age and sex distribution of the individuals in the study sample.*

Age (years)	Females	Males	Total
0–0.9	1	0	1
1.0–1.9	3	8	11
2.0–2.9	1	7	8
3.0–3.9	2	3	5
4.0–4.9	5	3	8
5.0–5.9	2	1	3
6.0–6.9	2	1	3
7.0–7.9	1	2	3
8.0–8.9	1	0	1
9.0–9.9	1	1	2
10.0–10.9	1	0	1
Total	20	26	46

between the contact points of each crown, and the faciolingual measures the maximum width of the crown perpendicular to the mesiodistal plane (4). This description is consistent with the measurements taken by DeVito and Saunders (15) and Żądzińska et al. (16), but it is not clear what definition was utilized by Black (14). Only the measurements from the left side were considered, unless the left side was unavailable in which case the right side was measured. To assess intraobserver error, five random individuals were selected, and their mesiodistal and faciolingual crown dimensions remeasured on all available teeth several months after the beginning of the study. Measurements from the first and second sessions were compared by calculating the intraclass correlation coefficient (ICC) using SPSS (SPSS Inc., Chicago, IL).

Percentage of correct allocation accuracy in determining sex using the equations developed by Black (14), DeVito and Saunders (15), and Żądzińska et al. (16) were calculated for females and males separately and for the total sample. Owing to preservation, sample sizes vary for each discriminant function tested. Percent dimorphism for each tooth was also calculated and was expressed as the male/female ratio minus one (2). The average dimorphism percentage was calculated for the overall dentition and compared to that reported in or calculated from data in Black (14), DeVito and Saunders (15), and Żądzińska et al. (16).

To assess whether it is possible to generate accurate sex models from data collected for this study, discriminant functions were calculated and tested using cross-validation. This was performed using SPSS, and the leave-one-out method was chosen to calculate the cross-validation error rate. Functions were calculated for single and combinations of variables. The four crown dimensions with the greatest percentage of sexual dimorphism were used in isolation to generate four discriminant functions. When combining variables, one function was generated entering each of the previous four variables independently and one other function was generated by running a stepwise analysis to determine the best combination of variables to discriminate sex.

Results and Discussion

The first step in this study is to assess the reliability of odontometric data. Intraobserver error results were pooled from different teeth, and mesiodistal and faciolingual crown dimensions were compared separately. The ICC for mesiodistal measurements is 0.997 (95% CI: 0.995–0.998), and for faciolingual measurements, it is 0.991 (95% CI: 0.984–0.996), indicating that the variance owing to measurement error is very small or practically inexistent.

Table 2 shows the female and male mean for each tooth diameter and the percentage of sexual dimorphism. The male mean is greater than the female mean for all variables, except for some

TABLE 2—*Mean diameters for the female and male samples and percentage of sexual dimorphism (SD).*

Tooth	Female Mean	Male Mean	SD
Mesiodistal diameter			
m^2	8.65	8.93	3.19
m^1	6.88	7.02	2.03
c'	6.75	6.88	1.92
i^2	5.04	5.00	−0.69
i^1	6.25	6.27	0.39
m_2	9.57	10.03	4.77
m_1	7.87	7.94	0.89
c,	5.83	5.87	0.71
i_2	4.62	4.44	−3.99
i_1	4.20	4.01	−4.47
Buccolingual diameter			
m^2	9.50	9.88	3.96
m^1	8.44	8.42	−0.29
c'	5.92	6.04	2.00
i^2	4.76	4.65	−2.24
i^1	4.98	4.89	−1.68
m_2	8.62	8.63	0.09
m_1	6.84	7.03	2.83
c,	5.47	5.47	0.11
i_2	4.25	4.18	−1.50
i_1	3.81	3.70	−2.82

diameters. Similarly to Black (14), some dimensions are greater in females than in males. This finding alone strongly suggests that sex determination methods based on deciduous tooth size may not be successful. The ''inverse'' sexual dimorphism obtained is partially explained by the small sample size of one or both of the sexes for the respective diameter, but it should still reflect those occasions where females show greater diameters than males, and vice versa, thus increasing misclassifications as to sex. This is confirmed by the test of discriminant functions, which is shown in Table 3. Equations developed by Black (14) range in accuracy from 33.3 to 75.0% in the total sample. In the function with the greatest correct sex allocation, accuracy for females (66.6%) was considerably lower than that for males (83.3%). DeVito and Saunders' (15) equations classified correctly as to sex between 35.7 and 45.9% of cases. The last three equations achieved the greatest sex differences in allocation accuracy, with the females showing 85.7% and males

TABLE 3—*Sex allocation accuracy (%) for each discriminant function tested (original correct sex allocation is shown in parentheses).*

	Females		Males		Total	
Equation	Correct	Incorrect	Correct	Incorrect	Correct	Incorrect
Black (1978)						
Eq. 1 (63.9%)	28.6	71.4	36.4	63.6	33.3	66.7
Eq. 2 (66.2%)	63.6	36.4	22.8	77.8	45.0	55.0
Eq. 3 (68.4%)	66.6	33.3	83.3	16.7	75.0	25.0
Eq. 4 (64.7%)	33.3	66.7	44.4	56.0	38.9	61.1
Eq. 5 (67.7%)	40.0	60.0	50.0	50.0	45.5	54.5
DeVito and Saunders (1990)						
Eq. A (90.5%)	40.0	60.0	33.3	66.7	35.7	64.3
Eq. B (80.0%)	40.0	60.0	33.3	66.7	35.7	64.3
Eq. D (73.8%)	33.3	66.7	44.4	55.6	40.0	60.0
Eq. A (76.2%)	42.9	57.1	33.3	66.7	37.5	62.5
Eq. B (72.5%)	42.9	57.1	33.3	66.7	37.5	62.5
Eq. D (76.2%)	50.0	50.0	33.3	66.7	41.2	58.3
Eq. A (71.4%)	85.7	14.3	21.7	78.3	45.9	54.1
Eq. B (65.0%)	85.7	14.3	21.7	78.3	45.9	54.1
Eq. D (71.4%)	85.7	14.3	21.7	78.3	45.9	54.1
Żądzińska et al. (2008)						
Eq. (78.0%)	38.5	61.5	73.3	26.7	59.3	40.7

21.7% of correctly allocated cases. The single equation provided by Żądzińska et al. (16) only classified 59.3% of the cases correctly, where males were correctly classified in 73.3% of cases and females in 38.5% of cases.

Besides poor overall allocation accuracy, both sexes showed very unequal classification rates. Equations from different studies do not provide any consistent pattern, except that of DeVito and Saunders (15), which shows a high accuracy in females (>80%) when using three equations. However, different equations from the same study correctly classify more males than females in one instance, but more females than males in another. Not only did functions not perform significantly better than chance, but occasionally they were also found to show the opposite association with sex. That is, in some cases, females scored more consistently than males and vice versa, as shown by total allocation accuracies under 50%. This is partly related to the fact that female dimensions are occasionally greater than male dimensions and, in the case of the correctly classified males from DeVito and Saunders' (15) equations, they may also reflect the reality of the original sample, namely absolute tooth size and sexual dimorphism.

Compared to this study, where mean percent sexual dimorphism is 2.03%, teeth in the sample of children utilized by DeVito and Saunders (15) are not only greater in overall crown diameter (interpolated from their charts) but also show greater sexual dimorphism (3.67%). Therefore, when using DeVito and Saunders' (15) discriminant functions, more males are incorrectly classified as females, while a greater proportion of females are also correctly classified. Comparatively, mean deciduous tooth crown size in Black's (14) study shows lower sexual dimorphism (1.55%) but are, on average, 1.4% greater in absolute size. This means that there would be some instances where females would also be correctly classified more frequently. This, however, did not occur, and the inverse has been obtained, possibly because females show greater mean values for some crown diameters. In the study by Żądzińska et al. (16), size of deciduous tooth crowns shows similar sexual dimorphism (2.09%) to that of this study but are, on average, 0.5% smaller in absolute size. However, the small sex differences in tooth size do not provide enough discrimination to consistently classify cases in one sex or the other.

The relative inaccuracy of the different methods is confirmed by the cross-validation rates obtained from discriminant functions generated in this study (Table 4). Equations 1–4 are based on single variables showing the greatest sexual dimorphism, whereas equations 5 and 6 are derived from combinations of variables. In Table 4 classification rates from cross-validation are compared to those calculated from the original sample. Overall, there is a reduction in correct sex allocation when using cross-validation, but the functions were already poor discriminators of sex in the original sample. Functions based on single variables are only able to correctly classify as to sex in 54.7–60.0% of the cases, whereas the rate for functions generated from combinations of variables is 46.2%.

In a worldwide survey, Harris and Lease (12) show that sexual dimorphism is low in the primary dentition, averaging 2% in mesiodistal diameter across all 10 tooth types. However, mean sexual dimorphism can vary greatly. For example, average sexual dimorphism in crown diameters is 1.13% in a sample of Javanese children (11) or 1.62% in a sample of children from South Australia (10), whereas sexual dimorphism is 3.07% in a sample of Australian Aboriginal children (7) or 3.67% in the Burlington Growth Study children (15). In addition, unlike what is found in the permanent dentition (4), the tooth that shows greatest degree of sexual dimorphism is not consistently the same across the different studies. For example, in Farmer and Townsend (10), it is the buccolingual diameter of the maxillary lateral incisor, whereas in Margetts and Brown (7), it is the buccolingual diameter of the mandibular first molar. In DeVito and Saunders (15), it is the buccolingual diameter of the lateral maxillary incisor, and in Black (14), it is the buccolingual diameter of the mandibular first molar as well as in Żądzińska et al. (16). In this study, it is the mesiodistal diameter of the mandibular second molar, which shows greater percentage of sexual dimorphism (4.77). With such a low degree of sexual dimorphism, with large population variation in degree of sexual variation, and with no particular tooth or teeth showing the greatest degree of difference, it is of no surprise that the discriminant functions tested in this study performed so poorly.

These population variations may result from differences in the quality of the environment during growth and development, namely maternal health, which may influence tooth size. For example, Garn et al. (18) have shown that children with low birthweight and low birthlength show significantly smaller deciduous tooth crowns. Similarly, Seow and Wan (19) have found that very low birthweight children showed the smallest deciduous crown dimensions, compared to the normal birthweights who showed the largest, with the low birthweight children showing intermediate dimensions. Therefore, population differences in crown dimensions might be brought about by selective survival, differential perinatal mortality and changing proportions of the developmentally immature surviving into the later years (18). In addition to reducing overall tooth crown size, poor environmental conditions during prenatal life may also decrease sex differences by affecting males most significantly (20).

The study sample is comprised of dead children, who died at a younger age of poor health and grew up under poor environmental conditions (21,22) that may have affected their tooth crown sizes. Results with the Lisbon collection show that absolute size and absolute sexual dimorphism in deciduous tooth crown size are smaller in this skeletal sample than in the sample of living children utilized by DeVito and Saunders (15). Consequently, sex in the study sample could not be accurately determined from discriminant

TABLE 4—*Sex allocation accuracy (%) for each discriminant function generated from data collected in this study, tested on the original sample and using cross-validation.*

	Females		Males		Total	
Equation	Correct	Incorrect	Correct	Incorrect	Correct	Incorrect
Original sample						
Eq. 1	52.0	48.0	57.7	42.3	54.9	45.1
Eq. 2	50.0	50.0	61.9	38.1	56.4	43.6
Eq. 3	56.5	43.5	63.0	37.0	60.0	40.0
Eq. 4	57.1	42.9	46.9	53.1	54.7	45.3
Eq. 5	27.3	72.7	66.7	33.3	50.0	50.0
Eq. 6	53.8	46.2	69.2	30.8	61.5	38.5
Cross-validation						
Eq. 1	52.0	48.0	57.7	42.3	54.9	45.1
Eq. 2	50.0	50.0	61.9	38.1	56.4	43.6
Eq. 3	56.5	43.5	63.0	37.0	60.0	40.0
Eq. 4	57.1	42.9	46.9	53.1	54.7	45.3
Eq. 5	0.0	100.0	80.0	20.0	46.2	53.8
Eq. 6	53.8	46.2	38.5	61.5	46.2	53.8

Eq. 1 is generated from the mesiodistal diameter of m^2; Eq. 2 is generated from the mesiodistal diameter of m_2; Eq. 3 is generated from the buccolingual diameter of m^2; Eq. 4 is generated from the buccolingual diameter of m_1; Eq. 5 is generated from a stepwise analysis that selected the buccolingual diameter of i^2 and the buccolingual diameter of c'; Eq. 6 is generated from the combination of variables in Eqs. 1, 2, 3, and 4.

function of deciduous teeth. Although the Portuguese sample is composed of children who were dead, sexual dimorphism is actually greater in magnitude than that in the living sample used by Black (14). In addition to crown size, it is the amount of sexual dimorphism that is decisive for successful and accurate sex estimation. The influence of low sexual dimorphism is clearly shown by the poor results obtained from cross-validation of functions calculated from data collected for this study. Therefore, the inconsistency of results suggests that deciduous tooth crown dimensions show insufficient sexual dimorphism, which added to variations in size because of environmental circumstances, make for their unreliable use in forensic practice.

Conclusion

This study shows that deciduous crown dimensions are a poor discriminator of sex and that the results shown here do not confirm the, albeit low, allocation accuracies reported for the discriminant function by the original studies. The only exception is one equation developed by Black (14), which provided a slight greater accuracy than that of its original sample. Overall, results suggest that there are very few sex differences in crown dimensions of deciduous teeth to warrant a reliable use of statistical techniques that quantify these differences for sex prediction. Results also suggest that absolute tooth size and the degree and/or sign of sexual dimorphism are important confounders in the cross-sample application of these techniques. This study confirms the concerns of Harris and Lease (12), who state that there are two important obstacles in the forensic value of the primary dentition for sex determination: (i) primary crown dimensions are less sexually dimorphic than permanent tooth dimensions; and (ii) the degree of dimorphism within and among populations varies.

Acknowledgments

I thank the anonymous reviewers for their helpful comments and corrections.

References

1. Moorrees CF, Thomsen SO, Jensen E, Yen PK. Mesiodistal crown diameters of the deciduous and permanent teeth in individuals. J Dent Res 1957;36:39–47.
2. Garn SM, Lewis AB, Swindler DR, Kerewsky RS. Genetic control of sexual dimorphism in tooth size. J Dent Res 1967;46:963–72.
3. Stroud JL, Buschang PH, Goaz PW. Sexual dimorphism in mesiodistal dentin and enamel thickness. Dentomaxillofac Radiol 1994;23:169–71.
4. Hillson SW. Dental anthropology. Cambridge: Cambridge University Press, 1996.
5. Schwartz GT, Dean MC. Sexual dimorphism in modern human permanent teeth. Am J Phys Anthropol 2005;128:312–7.
6. Ditch LE, Rose JC. A multivariate dental sexing technique. Am J Phys Anthropol 1972;37:61–4.
7. Margetts B, Brown T. Crown diameters of the deciduous teeth in Australian Aboriginals. Am J Phys Anthropol 1978;48:493–502.
8. Lysell L, Myrberg N. Mesiodistal tooth size in the deciduous and permanent dentitions. Eur J Orthod 1982;4:113–22.
9. Axelsson G, Kirveskari P. Crown size of deciduous teeth in Icelanders. Acta Odontol Scand 1984;42:339–43.
10. Farmer V, Townsend G. Crown size variability in the deciduous dentition of South Australian children. Am J Hum Biol 1993;5:681–90.
11. Kuswandari S, Nishino M. The mesiodistal crown diameters of primary dentition in Indonesian Javanese children. Arch Oral Biol 2004;49:217–22.
12. Harris EF, Lease LR. Mesiodistal tooth crown dimensions of the primary dentition: a worldwide survey. Am J Phys Anthropol 2005;128:593–607.
13. Clinch LM. A longitudinal study of the mediodistal crown diameters of the deciduous teeth and their permanent successors. Eur J Orthod 2007;29(Suppl. 1):i75–81.
14. Black TK. Sexual dimorphism in the tooth-crown diameters of the deciduous teeth. Am J Phys Anthropol 1978;48:77–82.
15. DeVito C, Saunders SR. A discriminant function analysis of deciduous teeth to determine sex. J Forensic Sci 1990;35:845–58.
16. Żądzińska E, Karasińska M, Jedrychowska-Dańska K, Watala C, Witas HW. Sex diagnosis of subadult specimens from Medieval Polish archaeological sites: metric analysis of deciduous dentition. Homo 2008;59:175–87.
17. Cardoso HFV. The collection of identified human skeletons housed at the Bocage Museum (National Museum of Natural History), Lisbon, Portugal. Am J Phys Anthropol 2006;129:173–6.
18. Garn SM, Osborne RH, McCabe KD. The effect of prenatal factors on crown dimensions. Am J Phys Anthropol 1979;51:665–78.
19. Seow WK, Wan A. A controlled study of the morphometric changes in the primary dentition of pre-term, very-low-birthweight children. J Dent Res 2000;79:63–9.
20. Stinson S. Sex differences in environmental sensitivity during growth and development. Yearb Phys Anthropol 1985;28:123–47.
21. Cardoso HFV. Patterns of growth and development of the human skeleton and dentition in relation to environmental quality [dissertation]. Hamilton (ON): McMaster University, 2005.
22. Cardoso HFV. Environmental effects on skeletal versus dental development: using a documented subadult skeletal sample to test a basic assumption in human osteological research. Am J Phys Anthropol 2007;132:223–33.

Additional information and reprint requests:
Hugo F. V. Cardoso, Ph.D.
Departamento de Zoologia e Antropologia
Museu Nacional de História Natural & Centro de Biologia Ambiental
Universidade de Lisboa
Rua da Escola Politécnica 56/58
1250-102 Lisboa
Portugal
E-mail: hfcardoso@fc.ul.pt

JOURNAL OF FORENSIC SCIENCES

J Forensic Sci, November 2010, Vol. 55, No. 6
doi: 10.1111/j.1556-4029.2010.01468.x
Available online at: onlinelibrary.wiley.com

TECHNICAL NOTE

PHYSICAL ANTHROPOLOGY

Laurel E. Freas,[1] *M.A.*

Assessment of Wear-Related Features of the Kerf Wall from Saw Marks in Bone*†

ABSTRACT: Analyses of saw marks in bone may yield important information about the class characteristics of saws used in postmortem dismemberments, yet little research has been directed at identifying saws' individualizing characteristics. This study adds to existing saw mark analysis methodologies by examining wear-related features of kerf walls using light- and environmental scanning electron microscopy. A crosscut saw and hacksaw were used to create sequences of 30 cuts in bone; these sequences reveal patterns of progressive loss of fine details of kerf wall morphology with increasing saw blade wear, because of the rounding of sharp points and edges. Nevertheless, diagnostic kerf wall features used to establish class characteristics persist despite these wear-related changes. Unsuccessful attempts at statistical analysis of wear-related changes, based on striae width and density, suggest these patterns are not readily quantifiable. Additionally, despite the scanning electron microscope's superior imaging capabilities, it provided few practical, methodological gains over traditional light microscopy.

KEYWORDS: forensic science, forensic anthropology, toolmark analysis, postmortem dismemberment, cutmark, kerf, scanning electron microscopy

The importance of competent toolmark analysis to forensic investigations has long been understood. One of the more challenging types of toolmark analysis encountered by forensic anthropologists is the interpretation of saw marks in cases of postmortem dismemberment. Although the literature on toolmark analysis dates from the early part of the 20th century, saw marks have received very little attention for much of the intervening period, as it was long thought that "saw teeth erase identifiable characteristics with every consecutive stroke as the tool progresses through the cut" ([1], p. 390; [2,3]). Bonte's seminal 1975 paper (2), however, outlined an approach for determining the class characteristics of the saw from microscopic features of the cutmark. More importantly, Bonte's study, along with those that would follow (i.e., [1,3–6]), demonstrated that the

> continuous or reciprocating actions of saws enhance, rather than erase, details necessary for saw class identification. Saws' repetitive actions will commonly produce more diagnostic features than, for example, the penetration and removal of a knife associated with a single stab wound. ([1] p. 390)

The last 30 years have witnessed striking gains in both the quantity and quality of research on the microscopic analysis of saw marks in bone. It is now widely accepted that through careful microscopic examination of the cutmark, a competent forensic anthropologist can potentially determine a number of key class characteristics of the saw in question, including (i) set type and width; (ii) tooth shape and size; (iii) direction of the cut; and (iv) whether the saw is a hand- or power-saw (1–5). Despite the increase in research, however, little effort has been directed at isolating features of cutmarks that can be correlated with the individual characteristics of a particular saw blade. The paucity of research is owed to two related factors: the complexity of the saw's "edge" and the complexity of the sawing process. In contrast to single-edged tools, an individual saw possesses hundreds of cutting edges (one on each tooth), each of which may interact with the substrate in a slightly different way during each cutting stroke. It may require dozens of cutting strokes to complete a single saw cut through a bone, and each stroke may vary in speed, pressure, and angle of approach. When taken in combination, these factors create an amount of variation—even between cuts produced by the same saw—that can easily overwhelm a search for patterns created by the unique individual characteristics, such as edge imperfections, of a particular individual saw (3).

Most efforts at the individuation of saws within a class have taken a broader approach, focusing instead on features of the kerf that are connected to wear-related changes in the condition of the saw blade (1–4). Andahl (4) discusses several distinctive shapes of false-start kerfs that may give clues as to the condition of the saw teeth and blade. However, false-start kerfs are not the only type of saw mark that should yield information about the saw's condition. The kerf walls contain a tremendous amount of information about the saw that created them, as a result of the mechanics of the sawing motion (3,5). As a typical hand-held reciprocating saw is pushed through the kerf on the cutting stroke, it moves deeper into the substrate on a slightly angled trajectory, because of each tooth cutting slightly deeper than the one before it. The individual saw teeth leave fine striae on the kerf

[1]Department of Anthropology, University of Florida, PO Box 117305, Gainesville, FL 32611.

*Presented in part at the 56th Annual Meeting of the American Academy of Forensic Sciences, February 20, 2004, in Dallas, TX, and in part at the 58th Annual Meeting of the American Academy of Forensic Sciences, February 23, 2006, in Seattle, WA.

†Supported by a National Science Foundation Graduate Research Fellowship (2002-2005) and by a Forensic Sciences Foundation Acorn Grant (2005).

Received 11 Jan. 2009; and in revised form 31 Aug. 2009; accepted 6 Sept. 2009.

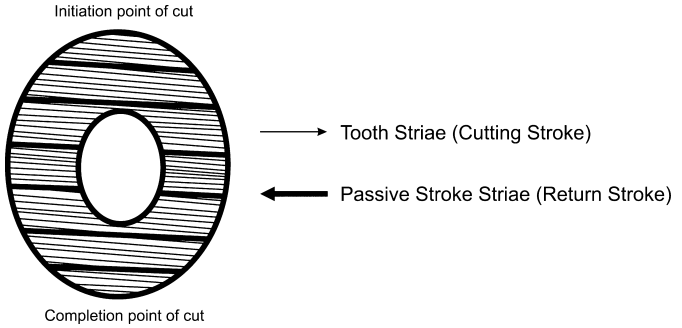

FIG. 1—*Schematic drawing of a kerf wall produced by a reciprocating saw, showing the repetitive pattern of fine tooth striae (created on the cutting stroke) between two coarser passive stroke striae (created on the return stroke).*

walls (tooth striae) as they cut through the substrate. On the passive (return) stroke, the teeth are all pulled through the kerf at roughly the same level as the saw is repositioned for the next cutting stroke. The reciprocating action creates residual kerf striae organized in a repetitive pattern of groups of slightly diagonal, narrow, parallel tooth striae between more level, coarser passive (return) stroke striae (Fig. 1) (3). To date, however, there have been no published studies evaluating wear-related indicators of saw blade condition within complete saw cuts.

In view of this gap in the literature, the aim of this study is to examine the relationship between a saw's degree of wear and the appearance of the kerf wall, with regard to the following questions:

- Can cuts made by a new, unworn saw be distinguished from cuts made by a saw which has been used and now shows some degree of wear, based on the appearance of the kerf wall? Can corresponding differences be observed in the appearance/condition of the saw itself? How will wear-related patterns differ between saws of different classes with different characteristics (i.e., crosscut saws vs. hacksaws; alternating vs. wavy set; filed vs. chisel-shaped teeth)?
- Is there a difference between saw blade wear generated by use on bone and wear generated by use on the saw's intended substrate (i.e., wood for carpentry saws such as crosscut saws; metal for hacksaws)? Correspondingly, will there be differences between kerf walls created by saws used only on bone and those used first on the intended substrate and then on bone, beyond any wear-related differences?
- Can any observed wear-related differences in kerf wall morphology between cuts created by new, unworn saws and cuts created by worn saws be quantified?

Scanning Electron Microscopy

To investigate these questions, the added imaging power of a scanning electron microscope (SEM) was enlisted. Traditionally, forensic scientists have relied solely on light microscopy at low powers (10× to 100×) for the examination of tool marks. It has been suggested, however, that the enhanced image-capture capabilities of SEMs (i.e., greater detail resolution, depth of field, and range of magnification) may be of considerable utility to forensic tool mark analysis. As SEMs are specifically designed to capture highly detailed, nearly three-dimensional images of an object's surface, they would seem to be particularly suited to this application (7–10).

In recent years, SEM imaging has been used frequently and to great advantage by archeologists and paleoanthropologists in their analyses of bone modification patterns from their respective contexts (11–18). Such studies have yielded important insights on many aspects of cutmark analysis including: (i) differentiation of true cutmarks from cutmark "mimics" produced by scavenging animals, root etching, sedimentary abrasion, and other taphonomic processes (11–13); (ii) determination of the directionality and sequence of individual cutmarks (13,14); and (iii) distinguishing among cutmarks produced by tools made of different materials (i.e., stone vs. metal blades) (16,18).

Despite the potential advantages of employing electron microscopy in forensic toolmark analyses, only a few such studies exist (7,8,19–23). Of these, only two investigate the use of SEM imaging for the identification of individualizing characteristics in saw marks in bone (22,23). The reasons for this limited use of SEM imaging of cutmarks in bone are manifold, and most are equally compelling as the reasons favoring the use of SEM imaging in toolmark analysis. Foremost among these are the high-vacuum environment of the SEM chamber, which is often problematic for organic, porous materials such as bone, and the restrictions placed on sample size by the dimensions of the SEM chamber. Evidentiary concerns may also be raised by the common practice of "sputter coating" the sample with a thin layer of gold alloy to enhance the quality of the SEM images (9–11,17). While these concerns can be overcome by making a silicone mold of the toolmark, this is also not without risks as the molding process, even if done carefully, may also damage the feature or surface being replicated (11,17,24).

Fortunately, recent advances in SEM technology can ameliorate many of these concerns. SEM units known as environmental SEMs now exist which can provide the desired image quality while operating at partial vacuum and while using the natural moisture content of an organic sample to facilitate conductance of the electron beam, obviating the need for desiccation and sputter coating (10,17,25). Additionally, SEMs are increasingly accessible and can now be found at most major research universities, the largest of which may have several units on campus. Thus, a fuller incorporation of scanning electron microscopy into the analyses of saw marks in bone may now be possible.

The purposes of the current study, then, are twofold: first, to consider patterns of wear-related changes in the kerf wall, and their impact on the interpretation of saw marks in bone; and second, to evaluate the utility of environmental SEM imaging for qualitative and quantitative analyses of such cut marks.

Materials and Methods

The sequences of saw cuts examined in this study were generated using new blades of two common classes of saws (see Symes [3] and Symes et al. [1] for a discussion of the general features of each class of saw):

- Craftsman 15-inch, 12 teeth per inch (TPI) Alternate-Set Crosscut Saw (Sears, Roebuck and Co, Hoffman Estates, IL)
- Vermont American 12-inch, 24 TPI Wave-Set Bimetal Hacksaw (Bosch Tool Corporation, Mt. Prospect, IL)

These types of saws were selected because they are relatively inexpensive (<$20 each), readily available at any local hardware store, and are fairly general-purpose in their design. These characteristics make them likely to be found in any given household and, by extension, likely candidates for forensic scrutiny.

Each saw was used to make a sequence of 30 cuts in defleshed, fresh adult white-tailed deer (*Odocoileus virginianus*) tibiae. Both right and left tibiae were used, and all cuts proceeded through the bone in a latero-medial direction. All sequences of cuts began at

the proximal end of the bone, ensuring that all cuts passed through the diaphyseal cortical bone, rather than through the expanded cancellous bone in the metaphyses. Each cut produced a slice of bone approximately 1.5 cm thick; two tibiae were required for each sequence of 30 cuts. After each cut, the saw blade was visually examined to document wear-related changes in its condition. After the sawing was complete, the 30 bone slices from each sequence were degreased for 10-15 min in a solution of hot water and soap following Shipman and Rose ([13], p. 65) and Symes ([3], p. 21).

As a control measure, an identical crosscut saw and hacksaw were used to make sequences of 30 cuts in the saws' intended substrates, to create a degree of wear resulting from normal usage of these saws, such as might be seen on any saw readily at-hand in a given household. The "control" crosscut saw was used to make cuts through a 2×2 pine board, and the "control" hacksaw was used to make cuts through a length of 3⁄4-inch diameter "Type-L" hard copper tubing, as these represent materials which might commonly be cut with saws of these types. The saw blade was visually examined after each cut to document wear-related changes in its condition. These control saws were then used to make a series of five cuts through deer tibiae; the resulting bone slices were degreased as described earlier.

All kerf walls were examined under a stereoscopic light microscope at powers of 10× to 40×, using a dual-arm fiber-optic light source to provide a high degree of contrast in light and shadow across the kerf wall. Individual bone slices were examined sequentially, noting any changes in appearance of, or distinguishing features present on, the kerf wall; special attention was paid to the depth and clarity of the striae on each kerf wall.

After examination under light microscopy, the kerf walls of cut numbers 1, 6, 12, 18, 24, and 30 from the cut sequences were photographed through a light microscope equipped with a 35 mm camera mount, at 10× magnification, and then submitted for environmental SEM imaging. These cut numbers were selected because it was felt that they provided good coverage of the cut sequences and were sufficiently demonstrative of the changes in kerf wall morphology occurring over the course of the cut sequences. Environmental SEM imaging was performed in a Hitachi VP-SEM 3000N scanning electron microscope (Hitachi High-Technologies America, Life Sciences Division, San Jose, CA) operated by the Department of Civil and Coastal Engineering, University of Florida. This SEM unit is well suited for forensic toolmark research, as it operates at a partial vacuum and can therefore image the bone surface directly rather than requiring that the specimen be sputter coated or cast prior to imaging. The SEM images were generated at a beam setting of 5.0 kV, with a magnification of 120× and working distances of 13.3–15.6 mm (two of the samples were imaged at working distances of 18.1 and 18.3 mm).

At these settings, the amount of surface area captured in the SEM image (the "spot size") was slightly less than 1 mm^2 (approximately 800 by 1100 μm). Because of the complexity of kerf wall striation patterns, it was determined that a larger area of each kerf wall needed to be imaged to obtain a true impression of the characteristics of each cutmark. To accomplish this, each kerf wall was imaged in a series of rows of overlapping frames. As it would have required an excessively large number of such images to cover the entire kerf wall, it was decided that only one quadrant of the kerf wall would be scanned. Each kerf wall was divided by a horizontal line, which separated the wall into upper and lower halves, and by a vertical line, which separated the kerf wall into entrance (the side of the cut where the saw teeth enter the kerf) and exit (the side of the cut where the saw teeth exit the kerf) halves (Fig. 2). From the four possible quadrants, the "lower, exit" quadrant was selected for imaging because it is believed that the saw is most stable in this portion of the cut (3). Therefore, the amount of irregular striae or "noise" introduced into the normal pattern of residual kerf striae by any erratic movements of the saw should be minimized in this quadrant, and thus the features observed on the kerf wall should primarily reflect the physical condition of the saw blade.

Once the individual images were generated, they were assembled in Adobe Photoshop 7.0 (Adobe Systems Incorporated, San Jose, CA) to create a composite image of the "lower, exit" quadrant of each kerf wall. Each composite is composed of approximately 25–30 separate images. These composite images allowed side-by-side comparison of the sequence of kerf walls for the purposes of evaluating any changes in the appearance and patterning of the residual kerf striae on each kerf wall.

In recognition of the growing drive within the forensic science community to develop quantitative analytical methods (largely in response to *Daubert* [26]), two separate approaches to quantitative assessment of the wear-related changes observed in the SEM

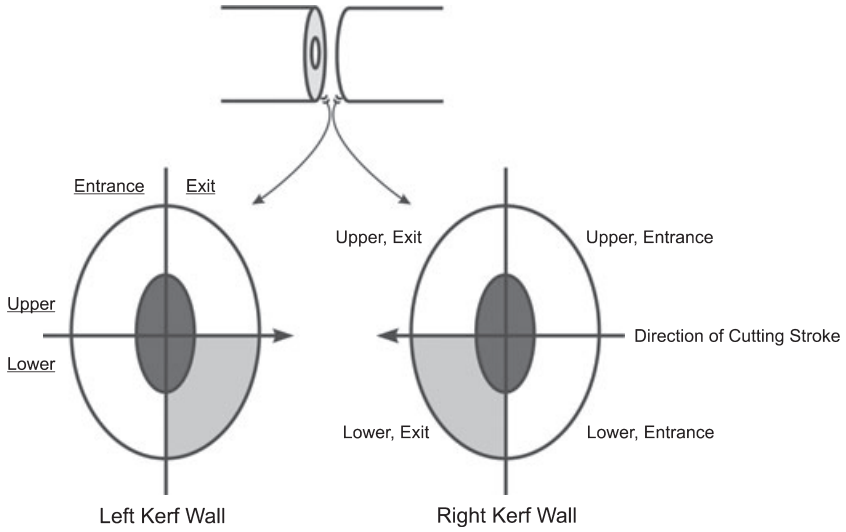

FIG. 2—*Schematic drawing of the quadrants of a kerf wall. Shaded quadrants were submitted for scanning electron microscope imaging. Note that left and right kerf walls are mirror opposites with respect to the orientation of the quadrants.*

images were attempted. These approaches intended to quantify any changes in (i) the mean widths of tooth striae over the course of the cut sequences and (ii) the number of tooth striae visible within each cycle of cutting and passive (return) strokes.

Results and Discussion

Light Microscopic Analysis

The early cuts in the crosscut saw sequence clearly demonstrate features typical of saw marks produced by this class of saw: cuts are smooth and even as a result of the slicing action of the diagonally filed individual teeth, with groups of evenly spaced, slightly diagonal, medium-fine tooth striae alternating with coarser passive (return) stroke striae. As the series of cuts progresses, the finer details of the kerf wall become increasingly smoother, more shallow, and indistinct, and the kerf walls gradually take on a "polished" appearance. By the last cut of the sequence, very few, if any, tooth striae are visible on the kerf wall, and the passive stroke striae are very shallow.

In total, a distinct pattern of decreasing amounts of fine detail on the kerf walls can be seen over the course of the cut sequence. This pattern can be correlated with observed wear-related changes in the saw blade's condition. As the cut sequence progressed, the sharp edges at the most projecting points of the individual teeth became increasingly rounded. Beginning near the middle of the cut sequence, an increasing degree of polishing was observed on the sides of the saw, starting first at the tips of the saw teeth and gradually spreading up the body of the teeth as the cut sequence progressed. The decreasing degree of fine detail present on the kerf walls is thus most likely the result of both the gradual rounding off of sharp edges and points along the margins of the teeth and the polishing of metal surfaces that are in contact with bone. As the rounding and polish became more pronounced, the sharp edges and points responsible for creating the fine striae disappeared, and the fine striae themselves became less distinct.

This pattern of saw blade wear is very similar in nature to the pattern of wear observed on the control crosscut saw. The only noted difference was in the degree of wear present at the end of the cut sequences, with the control saw showing slightly less wear. This is unsurprising given that pine is less dense than bone and should impart less wear to the saw blade. Concordantly, the kerf walls in bone produced by the control saw after 30 cuts through wood were similar in overall morphology to the kerf walls in the last third of the bone-only cut sequences. These observations suggest that a crosscut saw used only to cut bone wears more quickly, but in exactly the same manner, as a crosscut saw used to cut wood, and both will produce highly similar cutmarks in bone.

The pattern of wear-related changes in kerf wall morphology in the hacksaw sequence was very similar to the pattern seen in the crosscut saw sequence, with very clear, fine striae at the beginning of the sequence becoming increasingly shallow and indistinct as the sequence progresses. Unlike the crosscut saw sequence, however, the total degree of decline in fine detail over the course of the hacksaw sequence was very slight. Although there was some deterioration in the sharpness of tooth striae over the course of the sequence, they nevertheless were present and relatively distinct in cuts at the end of the series.

As was expected, the hacksaw blade itself also showed few signs of wear. This is likely because of the specially hardened metal of the hacksaw blades, which provides the durability and strength necessary to allow the blades to cut other metals. Use on bone therefore does not impart as great a degree of wear on hacksaw blades as it does on carpentry saws such as crosscut saws. The wear pattern was also affected by the hacksaw's wavy set, which places fewer teeth in direct contact with the kerf wall. Most of the observable wear-related changes in the blade stem from the transfer of paint from the widest parts of the wavy set to the surface of the kerf wall. This parallels the pattern of polishing observed on the sides of the crosscut saw. There was also some very slight rounding of the sharp edges of the teeth, accounting for the equally slight changes in the appearance of the kerf wall striae; but overall, the evidence of wear on the blade was minimal. The control hacksaw showed a slightly greater degree of wear than the hacksaw used to cut only bone, owing to the greater hardness and density of the copper tubing relative to bone. The kerf walls in bone produced by the control saw after 30 cuts through copper tubing showed a corresponding decrease in fine detail beyond that seen in the final cuts of the bone-only sequence. As with the crosscut saw, however, the overall morphology (beyond wear-related differences) of the kerf walls produced by the two hacksaws was highly similar.

SEM Analysis

In the composite SEM image of the first cut from the crosscut saw sequence (Fig. 3), several sets of fine, more or less evenly spaced tooth striae are clearly visible, bounded above and below by deeper passive (return) stroke striae—precisely the features anticipated in a cutmark generated by a brand-new saw. The majority of

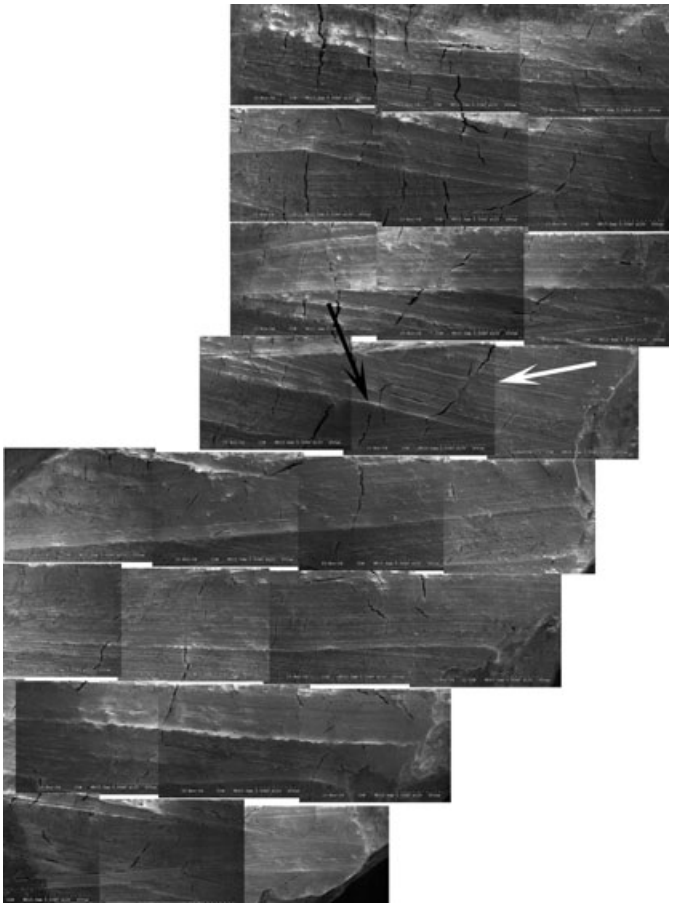

FIG. 3—*Composite scanning electron microscope image of left kerf wall from the first cut of the crosscut sequence. Note sets of fine tooth striae (light arrow) bounded above and below by deeper, coarser passive stroke striae (dark arrow).*

individual tooth striae are delineated by sharp margins, and the passive stroke striae are well defined and readily distinguished from one another and from the tooth striae. Overall, there is substantial surface relief, with the deepest parts of individual striae quite distinct from the overall surface of the kerf wall.

At this level of magnification and image resolution, the variability between each stroke of the sawing motion becomes apparent. In Fig. 3, note the differing angles at which each set of tooth striae and the associated passive stroke stria are oriented relative to the striae of other stroke cycles. This is because of variations in the angle of attack of each cutting stroke during the sawing process. Although this phenomenon was visible under light microscopy, it is far more conspicuous in the SEM composite images. This variation would prove problematic during attempts at quantitative analysis of the kerf walls (discussed in the following section).

The SEM images of the subsequent cuts in the crosscut saw sequence continue to show the anticipated pattern of a decreasing loss of fine detail over the course of the sequence. For example, the SEM images of the sixth cut show a fair number of tooth striae, and although many are still characterized by relatively sharp margins, they are generally less distinct than the tooth striae in the first cut. The tooth striae in the sixth cut also appear somewhat broader and shallower and are not as densely spaced as those in the first cut. This suggests that some of the sharp edges and fine points along the margins of the saw teeth had already been blunted by this early point in the cut series. Over the remainder of the cutmark sequence, the tooth striae become progressively more shallow and less clearly defined, such that by the later cuts almost no tooth striae are discernible. In cut 30 (Fig. 4), for example, the only striae visible in the SEM image are the passive stroke striae, and even these are very shallow.

With the loss of the fine tooth striae and the increasing shallowness of the passive stroke striae, there is an associated loss in the overall topography of the kerf walls. The kerf walls from cuts 24 and 30 appear rather smooth when compared to the kerf wall from the first cut. This smoothness was noted under light microscopic examination and was attributed to polishing from increased surface contact and friction with the flat sides of the saw teeth after the sharp edges and points had been worn away. Under electron microscopy, it becomes apparent that some of this apparent smoothness may also be because of an increasing amount of smearing of the bone surface. Smearing has been previously described by both Bromage and Boyde (14) and Houck (19), in their analyses of SEM images of knife marks, as areas of bone that adhered to the side of the blade and were subsequently compressed and displaced down the length of the cutmark as the knife passed. This same phenomenon is likely occurring on the kerf walls of the crosscut saw sequence. As the sharp edges and fine points of the saw teeth were worn away, increasing contact between the sides of the saw teeth and the kerf wall resulted in a greater degrees of smearing, obscuring any fine tooth striae present in those areas.

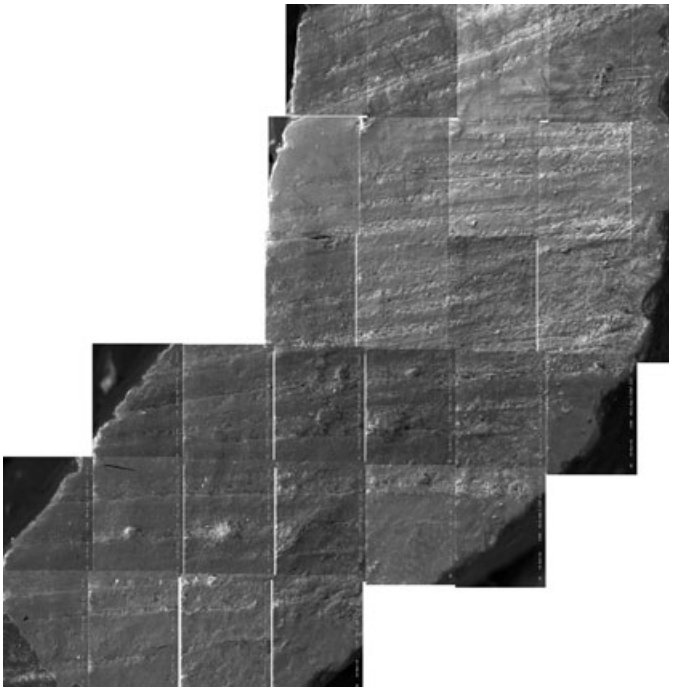

FIG. 4—*Composite scanning electron microscope image of left kerf wall from cut 30 of the crosscut sequence. Note the shallow passive stroke striae and the lack of fine tooth striae.*

Example composite SEM images of selected kerf walls from the hacksaw sequence are presented in Figs. 5 through 7. These images also reveal the expected pattern of wear-related changes in the appearance of the kerf wall. As was observed in the crosscut sequence, the tooth striae become less and less distinct, with an increase in bone smearing toward the end of the sequence. The SEM images of the hacksaw cuts also confirm that the total amount of change over the course of this sequence is far less than the amount of change observed over the crosscut sequence. Additionally, the composite images of kerf walls from cut 12 (not shown) and cut 18 (Fig. 6) both show areas of tooth hop, recognizable in the images as broad, wavy lines with a regular pattern of peaks and troughs. This feature of the kerf wall has been identified by Andahl (4) and Symes (3) as providing important clues about number of TPI on the associated saw blade. It is encouraging to see that, despite an advancing degree of wear on the saw blade, this feature is still clearly discernible and thus useable for diagnostic purposes.

Quantitative Analysis

As was noted earlier, two separate approaches to quantifying wear-related changes in kerf wall morphology were attempted using the composite SEM images. However, each approach proved to be unworkable. The first approach attempted to quantify changes in the mean width of the tooth striae over the course of the cut sequences. This approach was based on observations of apparent increases in tooth striae width as the cut sequences progressed, because of the progressive dulling of saw tooth edges. The expectation was that there would be statistically significant differences in mean tooth striae width between the earlier cuts (i.e., cuts 1 and 6) and the later cuts (i.e., cuts 24 and 30) within each of the sequences. However, problems with this approach were encountered almost immediately.

Foremost was the issue of obtaining a valid, unbiased sample of striae widths. The initial attempt at data collection focused on isolating several areas of each kerf wall where the tooth striae were the clearest. It quickly became obvious, though, that this would introduce a significant bias into the sample, because the clearest striae on each kerf wall were not necessarily representative of the overall appearance of that particular cut. These problems could have been solved by taking measurements of striae widths from several standardized areas on each kerf wall. Unfortunately, because each kerf wall has a different shape and different

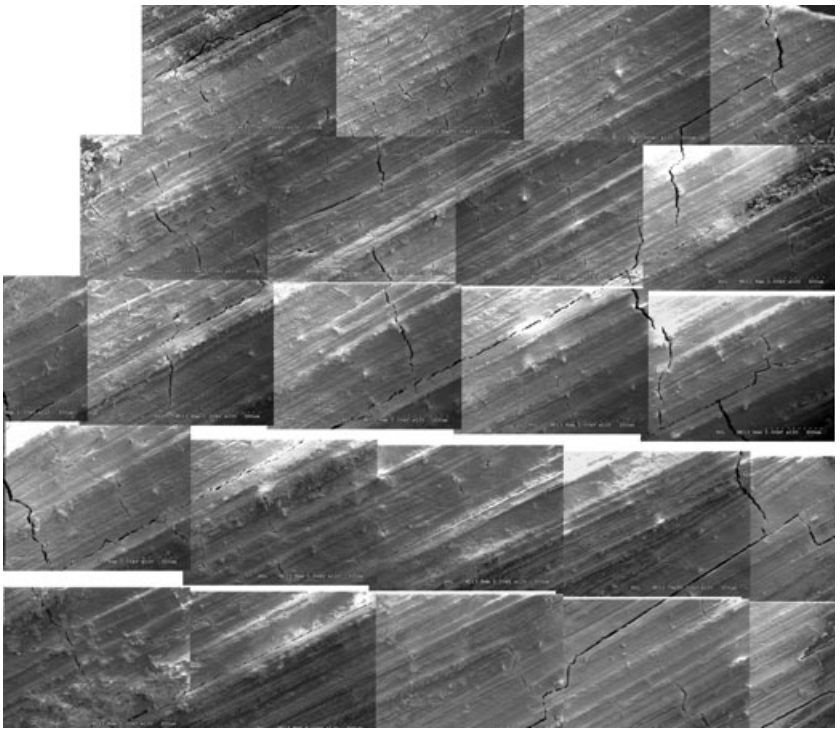

FIG. 5—*Composite scanning electron microscope image of right kerf wall of the sixth cut of the hacksaw sequence.*

configuration of striae, there are no consistent "landmarks" on the images that could have served as points of reference for such standardizations. This would have caused further problems with establishing the replicability of the data collection process.

Even had these sampling problems been overcome, additional problems would have arisen in the course of obtaining a sufficient number of accurate measurements for statistical analysis. As the cut sequences progress, the tooth striae lose their sharp margins and become more and more poorly defined, making accurate measurement of their widths increasingly difficult. These difficulties in appreciating the margins of the striations are compounded by the tendency, in later cuts, for the details of the microstructure of the bone to visually overwhelm patterns of striations. Moreover, as almost no tooth striae were even discernible in the later cuts from the crosscut sequence, it would have been nearly impossible to collect any usable measurements. In light of these difficulties, this approach to quantification was abandoned.

The second attempt at statistical analysis focused on quantifying the number of tooth striae visible within each stroke cycle on the kerf wall. The rationale behind this approach was that as the saw teeth become blunted, there ought to be fewer sharp points and edges to create tooth striae on each cutting stroke, leading to a significant decrease in the numbers of tooth striae within each stroke cycle as the cut sequence progresses. Once again, however, sampling problems were encountered almost immediately.

Because of the variability in the length and pressure of each cutting stroke, there is great variation in the number of teeth that passed through the kerf and the amount of bone that was cut away on any given cutting stroke. Thus, on each kerf wall, there are stroke cycles of varying heights, raising the question of which stroke cycles should be selected for the purposes of striae counting. As with the prior attempts to measure striae widths, there are no convenient reference points by which to standardize the selection of stroke cycles. Furthermore, because the angle of attack was not consistent throughout the process of making each cut, each stroke cycle varies in height over the width of the kerf wall. The only way to ensure that one is counting the full number of tooth striae in a given cutting stroke is to count the striae in the area of the greatest height of the stroke cycle. Unfortunately, that area may not be in the area that was imaged by the SEM, and if it is not, then one is not actually counting the full number of striae within that cutting stroke.

The difficulties encountered in these two attempts at quantification of the observed wear-related changes suggest that such cutmarks are perhaps not suited to a statistical analysis. The fundamental issue is that there are too many variables—such as stroke length, angle of attack, and stroke pressure—involved in the creation of the cut sequences that could not readily be controlled.

Conclusion

It had been anticipated that SEM imaging would shed additional light on observed patterns of wear-related changes in the appearance of kerf walls—an endeavor that met with a fair degree of success. The SEM images confirm the pattern of wear-related changes in kerf wall morphology first observed under light microscopy as an increasing loss of fine striae on the kerf walls over the course of the cut sequences. These images also support the interpretation that such changes are because of the blunting of sharp edges and points along the cutting margins of the saw teeth. The loss of clearly delineated tooth striae over the course of the sequences also goes toward refuting Bonte's (2) assertion that the number of striae within a stroke cycle is approximately equal to two-thirds the number of teeth on the saw, an assertion that has also been questioned by Symes (3). Nevertheless, other diagnostic features of the kerf wall, such as tooth hop, persist in spite of these wear-related changes in the saw teeth, indicating that even worn saw blades will still yield clues as to their class identification. This research suggests that, although investigators might do well to take wear-related features of the kerf wall into consideration during their analyses, such features do not necessarily

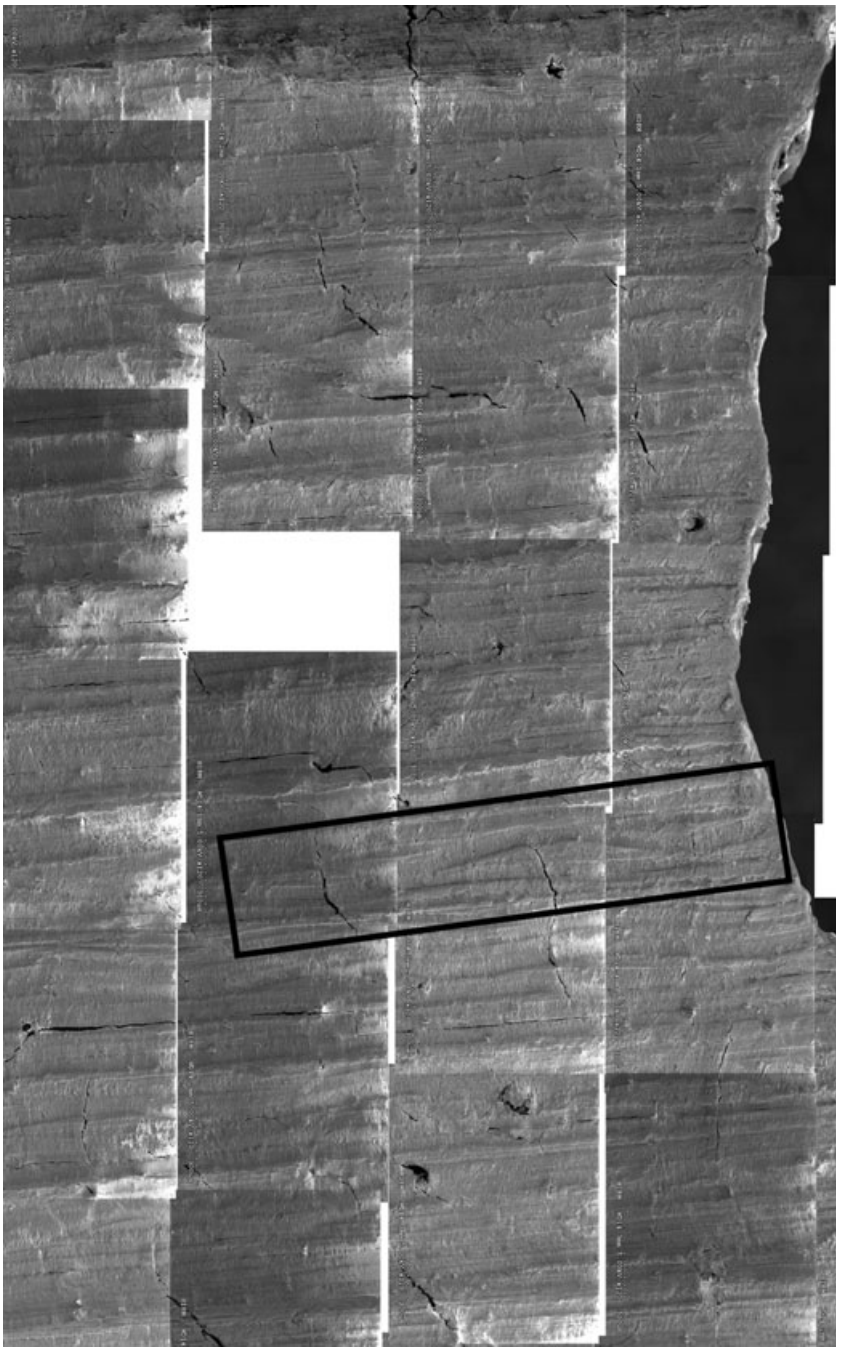

FIG. 6—*Composite scanning electron microscope image of right kerf wall of cut 18 of the hacksaw sequence. Note tooth hop (black rectangle).*

undermine the utility of the established methods for determining the class characteristics of the saw in question.

This study also illustrated the shortcomings of using SEM imaging in forensic toolmark analysis. It is commonly thought that the greatly increased amount of surface detail presented in SEM images may allow improved quantification of kerf wall features, thereby facilitating statistical analysis of the observed patterns of wear-related changes. This was not the case. Some patterns simply do not readily yield to quantification, and that may well be the case here. However, some of the problems with the quantitative analyses attempted here also stem from the realization that while the enhanced detail of the SEM images allowed clear visualization of the residual kerf striae in the early cuts, this same detail tended to overwhelm the striation patterns in later cuts, as the details of microstructure of the bone itself began to swamp the details of the increasingly faint striae.

Furthermore, the fundamental character of SEM imaging still makes it somewhat impractical for forensic toolmark analysis. As with so many aspects of forensic anthropology analyses, the analysis of toolmark evidence recognition is, at its core, a matter of pattern recognition. The highly focused image-capture capabilities of the SEM, which make it so well suited to the investigation of so many microscopic phenomena, also make it perhaps less than ideal for the analysis of patterns so broad and variable as kerf walls in bone. In saw mark analysis, it is a truth that the whole is greater than the sum of the parts, and in attempting to use the high resolution and magnification of SEM images to atomize the kerf wall into quantifiable parts, the diagnostic value of the whole is lost.

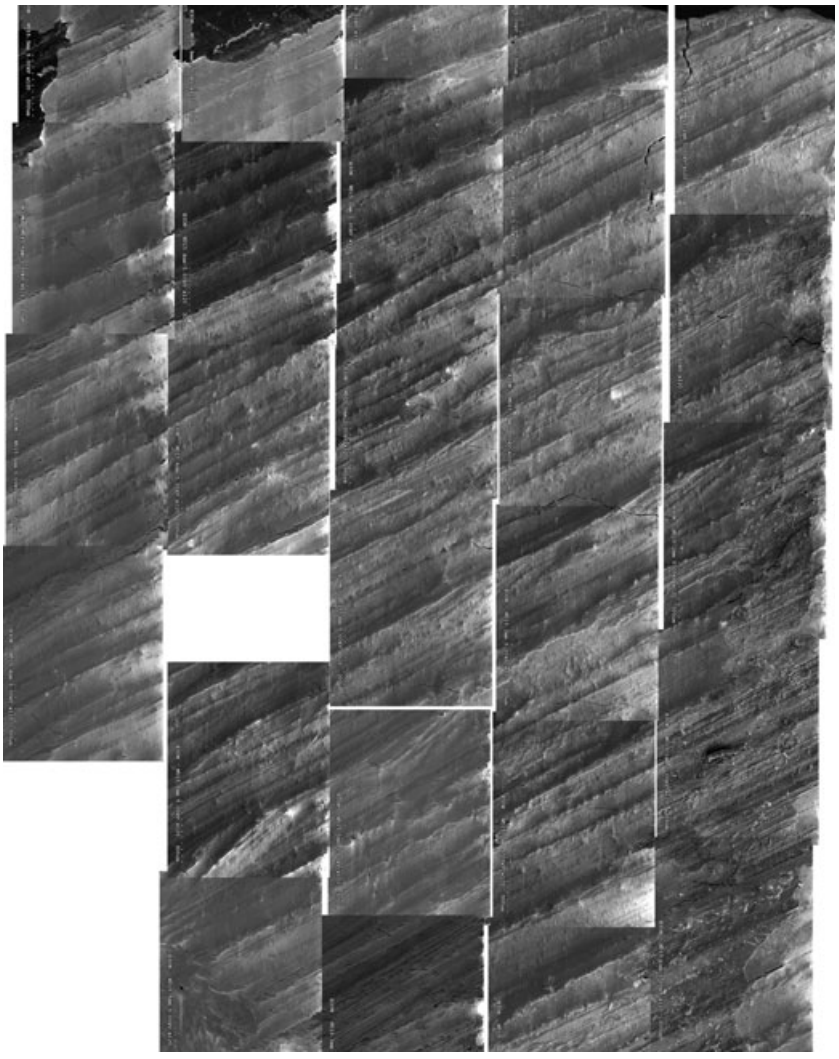

FIG. 7—*Composite scanning electron microscope image of right kerf wall of cut 30 of the hacksaw sequence.*

Of course, this is not to say in the least that the SEM analysis of these cutmarks was completely unproductive. As noted earlier, the SEM images created in this study confirmed several important light microscopic observations of the characteristics of kerf walls. But perhaps an even more important gain is the understanding that the SEM images reveal little about the appearance of the kerf walls that cannot also be seen under light microscopy. Additionally, the difficulties encountered in the quantitative analysis of the SEM images further suggest that this imaging modality may not be of significant advantage to the forensic analysis of saw marks in bone. This is enlightening news for forensic anthropologists involved in toolmark research and analysis, who may be concerned that their analyses might be made easier, more accurate, or more reliable by the use of SEM imaging.

Acknowledgments

The author thanks Dr. Andrew Boyd and Tanya Reidhammer of the Department of Civil and Costal Engineering, University of Florida, for their efforts in generating the SEM images for this study. Deepest thanks are also owed to Dr. Michael Warren, Dr. Steven Symes, Dr. Kenneth Kennedy, and Dr. Elias Kontanis for their superb guidance and invaluable advice along the way.

References

1. Symes SA, Berryman HE, Smith OC. Saw marks in bone: introduction and examination of residual kerf contour. In: Reichs KJ, editor. Forensic osteology: advances in the identification of human remains, 2nd edn. Springfield, IL: Charles C. Thomas, 1998;389–409.
2. Bonte W. Tool marks in bone and cartilage. J Forensic Sci 1975;20:315–25.
3. Symes SA. Morphology of saw marks in human bone: identification of class characteristics [dissertation]. Knoxville (TN): Univ. of Tennessee, 1992.
4. Andahl RO. The examination of saw marks. J Forensic Sci Soc 1978;18: 31–46.
5. Symes SA, Berryman HE, Smith OC, Blake C. Saw dismemberment of human bone: characteristics indicative of saw class and type. Proceedings of the 44th Annual Meeting of the American Academy of Forensic Sciences; 1992 February 17–22; New Orleans, LA. Colorado Springs, CO: American Academy of Forensic Sciences, 1992;166.
6. Reichs KJ. Postmortem dismemberment: recovery, analysis and interpretation. In: Reichs KJ, editor. Forensic osteology: advances in the identification of human remains, 2nd edn. Springfield, IL: Charles C. Thomas, 1998;353–88.
7. Singh RP, Aggarwal HR. Identification of wires and the cutting tool by scanning electron microscopy. Forensic Sci Int 1984;26:115–21.
8. Sehgal VN, Singh SR, Dey A, Kumar MR, Jain CK, Grover SK, et al. Tool marks comparison of a wire cut ends by scanning electron microscopy: a forensic study. Forensic Sci Int 1988;36:21–9.
9. Gilbert WH, Richards GD. Digital imaging of bone and tooth modification. Anat Rec (New Anat) 2000;261:237–46.

10. Stokes DJ. Recent advances in electron imaging, image interpretation and applications: environmental scanning electron microscopy. Philos Transact A Math Phys Eng Sci 2003;361:2771–87.
11. Shipman P. Applications of scanning electron microscopy to taphonomic problems. Ann N Y Acad Sci 1981;276:357–85.
12. Shipman P. Life history of a fossil: an introduction to taphonomy and paleoecology. Cambridge, MA: Harvard University Press, 1981.
13. Shipman P, Rose JJ. Early hominid hunting, butchering and carcass processing behaviors: approaches to the fossil record. J Anthropol Archaeol 1983;2:57–98.
14. Bromage TG, Boyde A. Microscopic criteria for the determination of directionality of cutmarks on bone. Am J Phys Anthropol 1984;65:359–66.
15. Olsen SL. Applications of scanning electron microscopy in archaeology. Adv Electron El Phys 1988;71:357–80.
16. Olsen SL. The identification of stone and metal tool marks on bone. In: Olsen SL, editor. Scanning electron microscopy in archaeology. BAR International Series, No. 452. Oxford: British Archaeological Reports, 1988;337–60.
17. Olsen SL. Introduction: applications of scanning electron microscopy to archaeology. In: Olsen SL, editor. Scanning electron microscopy in archaeology. BAR International Series, No. 452. Oxford, United Kingdom: British Archaeological Reports, 1988;3–7.
18. Greenfield HJ. The origins of metallurgy: distinguishing stone from metal cut-marks on bones from archaeological sites. J Archaeol Sci 1999;26:797–808.
19. Houck MM. Skeletal trauma and the individualization of knife marks in bones. In: Reichs KJ, editor. Forensic osteology: advances in the identification of human remains, 2nd edn. Springfield, IL: Charles C. Thomas, 1998;410–24.
20. Tucker BK, Hutchinson DL, Gilliland MFG, Charles TM, Daniel HJ, Wolfe LD. Microscopic characteristics of hacking trauma. J Forensic Sci 2001;46:234–40.
21. Bartelink EJ, Wiersema JM, Demaree RS. Quantitative analysis of sharp force trauma: an application of scanning electron microscopy in forensic anthropology. J Forensic Sci 2001;46:1288–93.
22. Saville PA, Hainsworth SV, Rutty GN. Cutting crime: the analysis of the ''uniqueness'' of sawmarks on bone. Int J Legal Med 2007;121:349–57.
23. Bush PJ. SEM analysis of saw marks in bone. Proceedings of the 61st Annual Meeting of the American Academy of Forensic Sciences; 2009 February 16–21; Denver, CO. Colorado Springs, CO: American Academy of Forensic Sciences, 2009;83–4.
24. Rose JJ. A replication technique for scanning electron microscopy: applications for anthropologists. Am J Phys Anthropol 1983;62:255–61.
25. Claugher D. Preparative methods, replicating and viewing of uncoated materials. In: Olsen SL, editor. Scanning electron microscopy in archaeology. BAR International Series, No. 452. Oxford, United Kingdom: British Archaeological Reports, 1988;9–21.
26. *Daubert v. Merrell Dow Pharmaceuticals, Inc.*, 113 S.Ct 278, 1993.

Additional information and reprint requests:
Laurel E. Freas, M.A.
Department of Anthropology
University of Florida
PO Box 117305
Gainesville, FL 32611
E-mail: lef6@ufl.edu

JOURNAL OF FORENSIC SCIENCES

J Forensic Sci, November 2010, Vol. 55, No. 6
doi: 10.1111/j.1556-4029.2010.01529.x
Available online at: onlinelibrary.wiley.com

TECHNICAL NOTE
CRIMINALISTICS

Jarrah R. Myers,[1] *M.S.F.S.*

Validation of a DNA Quantitation Method on the Biomek® 3000

ABSTRACT: Laboratory automation has the ability to increase the throughput and efficiency of laboratory processes to keep pace with current backlogs and requests for analysis. This paper addresses the specific studies employed to properly evaluate an automated method for DNA quantitation setup using Applied Biosystems Quantifiler™ Human DNA Quantification kit on a Biomek® 3000. The calibration of robotic pipetting as well as comparison with manually performed steps confirmed the accuracy of the automated methods used. Reproducibility studies evaluated differences between robotic and manually prepared human DNA standard curves. Additional studies examined DNA samples of known quantities, extract storage formats, sensitivity, and an assessment of contamination. The Biomek® 3000 not only demonstrated reproducibility and accuracy that equaled or surpassed the manual method but also revealed a contamination-free method to replace the multiple pipetting steps required during quantitation setup.

KEYWORDS: forensic science, DNA, automation, quantitation, Biomek® 3000, calibration

A number of automated or robotic instruments have been developed recently that are capable of performing a variety of tasks ranging from rapid extraction robots to laboratory automation workstations that can handle upward of 384 samples. No matter how complex the automation chosen, each has the potential to dramatically increase the laboratory's current throughput of samples requiring DNA analysis.

The DNA analysis process consists of multiple transfers of liquids containing either reagent or DNA from one place to another. Any step in the process that requires a liquid transfer by hand-pipetting is amenable to automation, which includes DNA extraction, DNA quantitation setup, normalization of DNA extracts for amplification, amplification setup, and preparation for injection on a genetic analyzer. The utilization of liquid-handling robots not only has the potential to increase throughput but also decrease the human error involved in repetitive tasks (1). Laboratory automation workstations, such as Beckman Coulter, Inc.'s Biomek® 3000, have the potential to replace many of the aforementioned liquid transfer steps that encompass the entire DNA analysis process. The major challenge with the implementation of automation into the DNA analysis workflow is the daunting task of completing a thorough internal validation on a method that is novel to that particular laboratory. This paper will discuss in detail the validation of an automated method for a half-volume DNA quantitation setup using Applied Biosystems (ABI) Quantifiler™ Human DNA Quantification kit.

The internal validation studies performed fell into five main categories: accuracy, reproducibility, known samples, sensitivity, and contamination, which were derived from the Scientific Working Group for DNA Analysis Methods (SWGDAM) guidelines for internal validation (2). Verifying the accuracy of the previously optimized pipetting techniques was initially accomplished through calibration. A specific technique was designed for each critical volume range applied during quantitation setup. The reproducibility studies evaluated the ability of the automated method to consistently generate valid results, with the focus on the human DNA standard curve used for DNA quantitation. Known samples were compared using automated and manual methods for quantitation setup, and the results of the sensitivity study were compared to previously generated data. Finally, contamination studies were performed to assess whether the automated method introduced contamination into the DNA extract (source) or quantitation (destination) wells.

The validation of the Biomek® 3000 method for DNA quantitation setup demonstrated that a robotically performed quantitation setup method was just as reliable as a manually performed quantitation setup procedure.

To better understand the validation using the Biomek® 3000, one must be briefly introduced to the manner in which the transfer of liquids is controlled on a Biomek® 3000. The Biomek® 3000 is an automated liquid-handling workstation that pipettes desired volumes of liquids by an air displacement mechanism, similar to hand pipettes. The Biomek® 3000 software is icon based that enables a smooth transition to the programming of methods. The Biomek® 3000 software controls the action of pipetting on three basic levels: *liquid class, pipetting technique,* and *pipetting template* (3). The *liquid class* can be altered for the unique properties possessed by the liquid by using the liquid type editor. Properties, such as viscosity, and bubble formation of an extraction reagent require certain attention during pipetting. Viscosity can be controlled by the blow-out volume (a leading air gap drawn up that helps to dispense the entire volume of liquid in the tip) and the trailing air gap (drawn up following aspiration of the liquid), which is applicable for liquids that drip. The speed of the aspiration, dispense, and mix steps can also be optimized within the liquid type editor. Each programmed step in a method requires the selection of the desired liquid (3,4).

[1]Kansas City Police Crime Laboratory, 6633 Troost Avenue, Kansas City, MO 64131.

Received 14 May 2009; and in revised form 3 Aug. 2009; accepted 15 Aug. 2009.

The next level of control is the *pipetting technique,* which is also chosen in each transfer step or aspirate and dispense step in a method. The pipetting technique can be edited under the technique browser. Pipetting technique enables the programmer to control the aspiration, dispense, and mixing of any liquid type, and the pipetting technique can override the liquid class settings if desired. Additional factors under the control of the pipetting technique are the height from the bottom of the labware for aspiration and dispensing steps. One of the most important aspects of the pipetting technique is the calibration settings for that specific technique. Depending on the volume, tool, and tip type chosen, a programmed pipetting step may or may not be dispensing the desired volume. The calibration tab within the pipetting technique editor enables the application of the determined calibration settings to be applied such that the dispensed volume is accurate (4).

The final, and most specific, level of control is the *pipetting template*. The pipetting template is chosen within each pipetting technique and can be modified by the pipetting template editor. Pipetting template allows one to control each movement of the pipette tip within the well using icon-based tools. These specific movements are speed, degree, and depth of the tip during and between aspiration, mixing, and dispensing steps (3).

Methods

The Quantifiler™ Human DNA Quantification kit in combination with the ABI Prism® 7000 SDS and SDS software was used to generate all internal validation data for this study. Select samples were amplified using ABI's Cofiler® amplification kit, injected on an ABI 310 Genetic Analyzer, and analyzed using ABI's GeneMapper® ID v1.0 software.

General

Before calibrating each pipetting technique and before conducting the validation studies, it was necessary to learn how to write methods that would control the movements of the instrument. Each pipetting technique was optimized based on the liquid chosen. Optimization parameters included aspiration and dispensing speeds, blowout volumes, and "tip dips" to remove any liquid remaining on the tip. It was also discovered that 50-µL tips were the most accurate for the pipetting of small volumes for either the P20 or P200 tools.

Accuracy

The initial challenge with determining the accuracy of the automated pipetting techniques was caused by the small volume of DNA required for quantitation reactions. Although the Biomek® 3000 was developmentally validated to pipette as little as 2 µL of liquids, half-volume quantitation reactions require only 1 µL of DNA extract. The other pipetting techniques determined to have critical volumes in need of calibration were used in the preparation of the human DNA standard curve: 10, 20, and 30 µL.

This method of calibration required a dye with an absorbance range that can be measured with a spectrophotometer or plate reader available in your laboratory. The dye chosen must have an absorbance range compatible with the filters on the spectrophotometer. The first step in calibration was to create a standard curve by hand-pipetting a range of values surrounding the target volume. For example, 0.5, 0.75, 1.0, 1.25, and 1.50 µL volumes were used to prepare a standard curve for the 1-µL pipetting technique. The absorbance values generated by the spectrophotometer or plate reader were plotted against the corresponding volume to create a standard curve.

The second step evaluated the accuracy of the robotic pipetting technique compared to the standard curve generated manually as described in the first step above. The automated method was programmed to dispense the target volume along with several volumes surrounding the target (as had been performed in the preparation of the standard curve) in at least 24 replicates. A volume calibration curve was determined from the average absorbance values for each volume pipetted robotically by plotting the displaced volume versus the actual volume dispensed (refer to Fig. 1). The scaling factor (slope = m) and offset value (y-intercept = b) were changed from a default of 1.0 and 0 in the calibration tab for each pipetting method calibrated based on the volume calibration curve generated.

The final step evaluated the accuracy of the newly calibrated technique. Multiple replicates (n = 48) of the target volume were dispensed by the robotic method, and the absorbance values were used to verify the accuracy of the newly calibrated technique versus the standard curve generated in the first step.

Some key aspects concerning the calibration of pipetting techniques involved bringing the total volume to 100 µL. Some manipulation of the dye concentration may also be needed to fall into the sensitivity range of the plate reader or spectrophotometer used. Eosin Y (Sigma-Aldrich, St. Louis, MO) dye was diluted with sterile deionized water, and absorbance values were detected using a Sunrise Plate Reader (Tecan Austria GmbH, Grodig/Salzburg, Austria), wavelengths 420–650 nm, in conjunction with a Tecan® Evo workstation (Tecan, Männedorf, Switzerland) and Magellan software (Tecan Austria GmbH, Grodig/Salzburg, Austria). Finally, the standard curve (prepared by hand), calibration and verification steps should be performed on the same day from the same stock of dye to minimize variation in absorbance values.

Reproducibility

The reproducibility studies consisted of the evaluation of the accuracy and precision of the automated method within and between runs. Of note, the master mix was robotically aliquoted for the entire quantitation plate, even for those samples manually loaded onto the plate for each study performed in the internal validation. Therefore, the only variation that should have been detected by the quantitation results was the difference between the manual

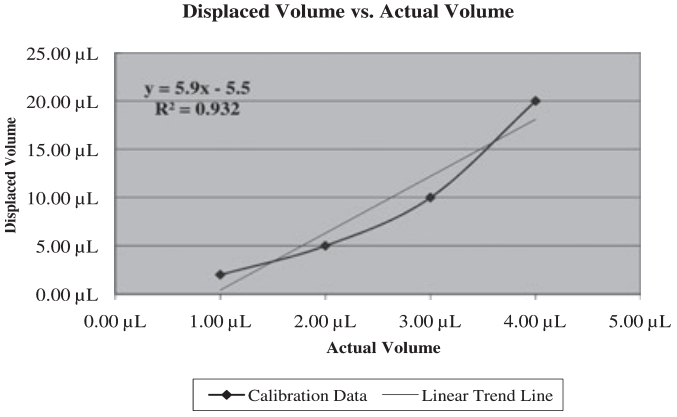

FIG. 1—*Graphical depiction of the generation of a new scaling factor and offset value for a calibrated robotic pipetting technique. The calibration line corresponds to the required adjustment in accuracy to be made based upon the volume displaced during robotic pipetting as opposed to the desired volume.*

or robotic pipetting. Section quality assurance criteria were applied to each quantitation run. Data were compiled for the human DNA standard curves, individual points within the standard dilution series, and the DNA standard, to be referred to as "030321," on three separate quantitation runs. The DNA standard "030321" has demonstrated a consistent cycle threshold (Ct) value of approximately 25 and has been used as a quality control check when verifying new Quantifiler™ lots. Reproducibility plates consisted of one manually prepared set of human DNA standard curves loaded in duplicate along with three Biomek® 3000 prepared human DNA standard curves each loaded in duplicate. The DNA standard "030321" was loaded in six replicates each for manual and robotic methods.

The replicates of "030321" and each curve generated, whether automated or manual, were statistically compared to evaluate the reproducibility of the Biomek® 3000.

As part of the Taqman™ probe technology employed in ABI's Quantifiler™ Human kit, the FAM dye serves as the reporter dye for estimating the quantity of template DNA present in the quantitation reaction (5). Ct(FAM) values for each point in the human DNA standard curve were also statistically compared. The statistic used to evaluate the variability of each curve (automated or manual) and individual point was the %CV, coefficient of variation:

$$\%\text{CV} = \frac{\text{standard deviation}}{\text{average}}$$

Percentage of CV is a statistical evaluation of the dispersion of values around the mean. Percentage of CV was an appropriate statistic to use because it was able to compare multiple data sets to evaluate the reproducibility of different aspects of the robotic method, such as the Ct(FAM) values, for each point in the standard curve and of the internal DNA standard, "030321."

Known Samples

A total of 32 DNA extracts of known origin (previously amplified and detected or from a known source), varying sample type, and of a range of concentrations were quantitated using an automated method. These same known extracts were also quantitated on the same plate by manual addition to allow for a within plate comparison. Just as with the reproducibility study, the master mix was robotically aliquoted for the entire quantitation plate, even for those samples manually added to the plate.

Current storage format for DNA extracts is in a 1.5-mL tube with attached screw cap (with o-ring), which is not compatible with an automated method. Two format changes were examined: 1.5-mL nonattached screw cap (with o-ring) and 96-deep-well plate. The 1.5-mL tubes were left uncapped during automated methods, while the 96-deep-well plate was covered with aluminum sealing film. Reproducibility of the known samples was also examined while determining the best extract storage format.

Sensitivity

Previous studies evaluating the sensitivity of manual quantitation runs involved the serial dilution of the internal DNA standard, "030321." This dilution series was prepared by hand and added manually and robotically to a quantitation plate in which the master mix was added using an automated method. The quantitation results of the robotic pipetting of this sensitivity series were compared to the manually added sensitivity series as well as to previously generated sensitivity data.

Contamination

Multiple contamination studies were performed by the automated method to demonstrate whether the source or destination wells were contaminated during robotic pipetting. Checkerboard and zebra-stripe patterns were applied to the source plate (DNA extracts in tube or plate format) and destination (quantitation plate) wells to determine whether any carryover of DNA occurred between wells containing a high level of DNA to wells containing only reagents or blanks (TE^{-4}). Quantitation results from the reagent-only wells on the destination plate and the amplification of blank samples from the source plate were evaluated to determine whether contamination could be attributed to the automated method.

Results and Discussion

Reproducibility

Each Biomek® 3000 human DNA standard curve generated passed quality assurance criteria for Quantifiler™ in reference to the slope range, y-intercept, and R^2 values (>0.98; R^2 statistic evaluates the fit of the individual points when compared to a linear regression line of the points).

The average reproducibility of the Biomek® 3000's robotic preparation and addition of each standard in the human DNA standard dilution series for DNA quantitation was 0.77%, which consisted of nine separate curves added in duplicate across three quantitation runs (Table 1). The average %CV for each standard in the manually generated human DNA standard dilution series across the three quantitation runs was 1.29%. The within run reproducibility of the robotic and manual preparation of the human DNA standard curves for quantitation is demonstrated graphically in Fig. 2. Similarly, Fig. 3 demonstrated the variation between standard curves generated for both manual and robotic curves. The evaluation of the reproducibility was graphed based on the %CV values calculated from each duplicate standard curve.

The average Ct(FAM) value using the 1-μL robotic pipetting technique for the DNA standard, "030321," during the reproducibility runs was 24.77 when compared to 25.11 for the manually added DNA standard yielding a percent difference of 1.35%. The average %CV of robotic pipetting for 1 μL of "030321" was 0.38% when compared to 0.39% for manual pipetting.

The reproducibility results demonstrated that the automated platform for quantitation setup was slightly more precise than a manually performed setup because of a lower %CV value. Evaluation of the accuracy of robotically performed pipetting could only be compared to the results of manually loaded samples and standards. One

TABLE 1—*Reproducibility of human DNA standard curve for quantitation.*

	Robotic Method			Manual Method		
Standard Point	Average Ct(FAM)	STDEV	%CV	Average Ct(FAM)	STDEV	%CV
50 ng	22.68	0.204	0.90	22.86	0.243	1.06
16.7 ng	24.35	0.096	0.40	24.36	0.157	0.64
5.56 ng	25.92	0.121	0.47	26.02	0.280	1.07
1.85 ng	27.58	0.206	0.75	27.51	0.176	0.64
0.62 ng	29.18	0.127	0.43	28.86	0.365	1.27
0.21 ng	30.64	0.259	0.85	30.15	0.365	1.21
0.068 ng	31.98	0.301	0.94	32.10	0.409	1.27
0.023 ng	33.58	0.484	1.44	33.45	1.063	3.18
		Average	0.77		Average	1.29

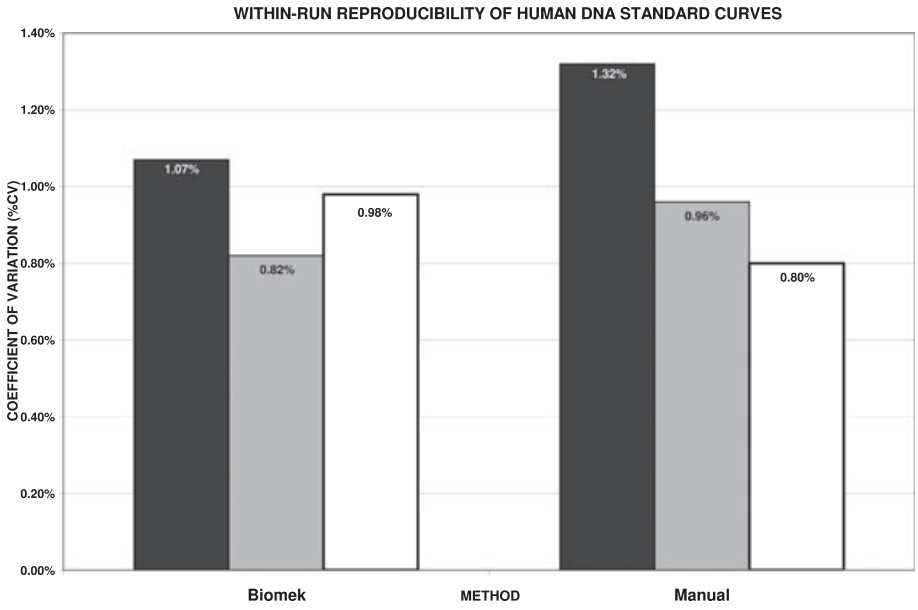

FIG. 2—*Variation of robotically prepared curves (in duplicate) versus one manual curve (in duplicate) per quantitation run. %CV corresponds to the average variation between duplicate values for each standard curve prepared robotically and manually.*

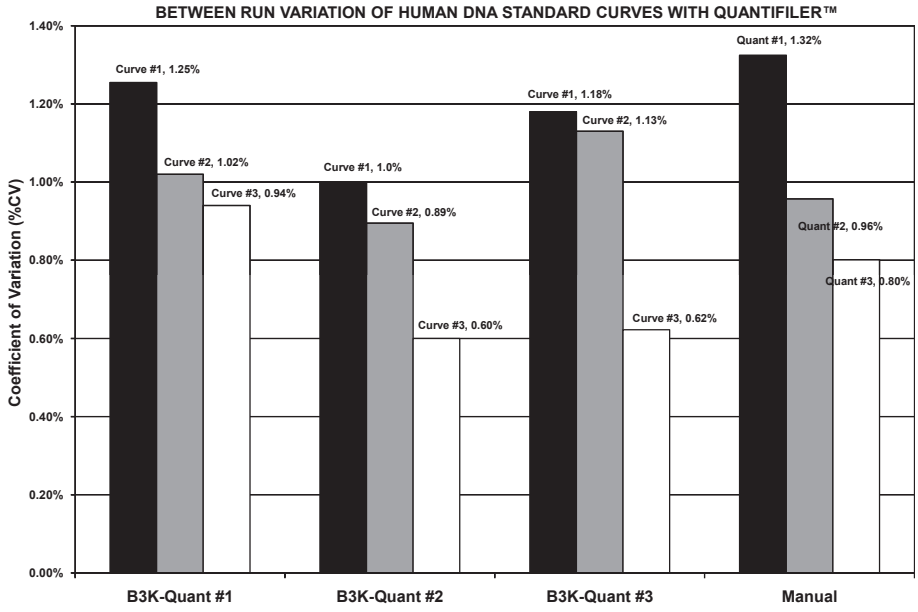

FIG. 3—*An evaluation of the variation of all duplicate standard curves (manual or robotic) prepared for the reproducibility study. Three standard curves (in duplicate) per quantitation run were prepared robotically, while only one standard curve (in duplicate) was prepared manually per quantitation run.*

would expect similar variation between multiple quantitation runs of the same sample or standard.

An additional reproducibility study (referred to as Reproducibility #2) performed during another aspect of the validation also evaluated accuracy of the robotic pipetting of 1 μL of the internal DNA standard, "030321." Refer to Table 2 for the comparison of the reproducibility results for "030321" developed as well as the percent difference between both automated reproducibility studies and the values obtained from manual pipetting. The results demonstrate that automated pipetting of 1 μL of sample is not only reproducible but accurate as supported by minimal percent differences between manual and robotic pipetting Ct values.

Known Samples

For the 32 known samples quantitated robotically and manually, the percent difference was 1.18%. Concordant results were demonstrated by inhibited samples for both manual and automated methods in which the Ct value for the internal passive control was undetermined.

Format verification studies using the known samples in 1.5-mL nonattached screw cap tubes and 96-deep-well plates demonstrated accurate quantitation results consistent with previously developed results from the manual method. The reproducibility across three quantitation runs containing the same known samples in different

TABLE 2—*Internal DNA standard (030321) comparison.*

Study	Average Ct(FAM)	STDEV	%CV	% Difference
Reproducibility	24.77	0.0950	0.38	1.35
Reproducibility #2	24.92	0.1630	0.65	0.76
Manual	25.11	0.0967	0.39	NA

storage formats was measured by an average %CV of 1.34% and an average percent difference of 1.29%. The minimal percent difference in combination with the reproducibility of quantitation results between formats supports the conclusion that consistent quantitation results are independent of the extract format.

Because of successful quantitation results from previously discussed studies, the remaining aspects of the validation only evaluated the performance of the automated quantitation setup method.

Sensitivity

Automated quantitation setup results for the dilution series of "030321" demonstrated a limit of detection equivalent to the 1:1024 dilution of stock "030321." The quantitation result of this dilution was 13.5 pg/μL as opposed to the expected result of 9.77 pg/μL, such that the quantitation result slightly overestimated the actual quantity of the sample.

The lower limit of detection of the automated method was consistent with previously determined detection limits of 13 and 9.5 pg/μL from the manual Quantifiler™ validation and manual half-volume verification study.

Contamination

The results of the zebra-stripe and checkerboard-patterned quantitation runs evaluating the possibility of contamination of the quantitation plate and source DNA plates demonstrated that 145 of 148 total blank wells yielded undetermined results. The results of the three wells that yielded a Ct(FAM) result were 35.32, 37.92, and 36.83. Quantitation results with such high Ct values could easily correspond to normal background fluorescence that varies well to well and run to run.

As DNA quantitation is an end-step process, the most important aspect of assessing possible contamination through the robotic setup was the evaluation of the source plates containing extracted DNA as these tubes or wells remain open on the deck throughout the automated method. The workflow of the robotic tool and tip in itself is a means of preventing contamination. DNA extracts, whether in tube racks or 96-well plates, are placed on the rear of the deck, while the destination and reagent tubes are placed on the front of the deck such that a used tip will never travel over DNA-containing tubes or wells.

Further investigation of possible source contamination was evaluated by the performance of an automated quantitation setup method from a checkerboard pattern of DNA and blank samples from both 24-tube rack and 96-well plate formats. Quantitation results for samples containing DNA and blank samples from these source racks demonstrated undetermined or undetectable amounts of DNA. Ten blanks from each source DNA extract format were chosen for downstream amplification. All 20 samples were in the path of tip travel between aspiration from the source plate toward the quantitation plate. No genetic information was developed from the amplification and detection of these 20 blank samples.

Conclusions

The estimation of the quantity of amplifiable human DNA is an important step in the DNA analysis process because future manipulations of the sample can be determined based upon the results of this step. Such decisions include whether to treat the sample for the possible presence of PCR inhibitors, whether or not to stop the analysis as well as how much extract to amplify. The goal of this internal validation was not only to validate an automated system for quantitation setup but also to demonstrate that this automated system maintained the desired quality and reliability that has been demonstrated with manual quantitation setup.

The Biomek® 3000, using calibrated pipetting techniques, demonstrated the ability to accurately and reproducibly quantify the amount of amplifiable human DNA from extracted DNA samples in a 1.5-mL screw cap (nonattached) format and 96-well plate format. Although sometimes implied by the word automation, the Biomek® 3000 empirically demonstrated that the most impressive aspect of its operation was the reproducibility that it demonstrated through repeated preparations of human DNA standard curves as well as the reproducible pipetting of 1 μL of DNA.

The measurements of variation (and therefore reproducibility) were below 2%, and the percent differences between automated and manual setup were also below 2%. The minimal amount of variation between repeated tasks as well as between automated and manual techniques further supports the conclusion that the Biomek® 3000 reliably performs the protocols for quantitation of human DNA (6).

Another important goal in demonstrating the quality and reliability of this automated platform was to evaluate the possibility of contamination, whether it occurred at the source (DNA) or destination (quantitation plate). Contamination was evaluated by the amplification of blank samples adjacent to DNA-containing tubes or wells. No DNA was detected in these blank samples through quantitation, while amplification results further demonstrated that contamination does not occur during robotic methods, supporting previous validation work (7–10).

Acknowledgments

Thanks are given to Amy Gibson from Beckman Coulter for her constant support during the initial phases of this validation study. Additional acknowledgements are given to Ann Mallot of the Kansas City Police Crime Laboratory for her assistance with the graphics and figures.

References

1. Butler JM. Forensic DNA typing—biology, technology and genetics of STR markers, 2nd edn. MA: Elsevier, 2005.
2. Scientific Working Group for DNA Analysis Methods. Revised validation guidelines. Forensic Sci Commun 2004;6(3).
3. Beckman Coulter, Inc. Biomek Software Version 3.3 user's manual. Fullerton, CA: Beckman Coulter, Inc., 2006.
4. Beckman Coulter, Inc. Biomek® 3000 Laboratory Automation Workstation user's manual. Fullerton, CA: Beckman Coulter, Inc., 2006.
5. Applied Biosystems. Quantifiler™ Kits user's manual. Foster City, CA: Applied Biosystems, 2005.
6. Mandrekar P, Flanagan L, McLaren R, Tereba A. Automation of DNA isolation, quantitation and PCR setup. Madison, WI: Promega Corporation, http://www.promega.com/geneticidproc/ussymp13proc/contents/mandrekar.pdf (accessed July 2009).
7. Greenspoon SA, Ban J. Robotic extraction of mock sexual assault samples using the BioMek® 2000 and the DNA IQ™ System. Profiles in DNA 2002;5:3–5.
8. Greenspoon SA, Ban JD, Sykes K, Ballard EJ, Edler SS, Baisden M, et al. Application of the BioMek® 2000 Laboratory Automation

workstation and the DNA IQ™ System to the extraction of forensic casework samples. J Forensic Sci 2004;49:29–39.
9. Crouse CA, Yeung S, Greenspoon S, McGuckian A, Sikorsky J, Ban J, et al. Improving efficiency of a small forensic DNA laboratory: validation of robotic assays and evaluation of microcapillary array device. Croat Med J 2005;46:563–77.
10. Frégeau CJ, Lett M, Elliott J, Bowen KL, White T, Fourney RM. Adoption of automated DNA processing for high volume DNA casework: a combined approach using magnetic beads and real-time PCR. In: Amorim A, Corte-Real F, Morling N, editors. Progress in Forensic Genetics 11. Proceedings of the 21st International ISFG Congress; 2005 Sept 13–16; Ponta Delgada, The Azores, Portugal: Intl. Congress Series 1288 2006;688–90.

Additional information and reprint requests:
Jarrah R. Myers, M.S.F.S.
Kansas City Police Department Crime Laboratory
6633 Troost Avenue
Kansas City, MO 64131
E-mail: jarrah.myers@kcpd.org

JOURNAL OF FORENSIC SCIENCES

J Forensic Sci, November 2010, Vol. 55, No. 6
doi: 10.1111/j.1556-4029.2010.01503.x
Available online at: onlinelibrary.wiley.com

TECHNICAL NOTE

CRIMINALISTICS

Masaru Asari,[1] Ph.D.; Tomohiro Omura,[1] Ph.D.; Chikatoshi Maseda,[1] Ph.D.; Kazuo Matsubara,[2] Ph.D.; Hiroshi Shiono,[1] M.D., Ph.D.; and Keiko Shimizu,[1] M.D., Ph.D.

A New Method for Human ABO Genotyping Using a Universal Reporter Primer System

ABSTRACT: We developed a new method for forensic ABO genotyping based on a universal reporter primer (URP) system. This allows for the simultaneous detection of six single nucleotide polymorphism (SNP) sites in the ABO gene (nucleotide positions 261, 297, 526, 703, 796, and 803). This URP system provides obvious peaks, ranging from 82 to 151 bp in length. ABO genotypes were classified and successfully genotyped by our method, including minor alleles that may cause a discrepancy between the genetic data and serological phenotypes. Full profiles were identified using as little as 0.1 ng (0.05 ng/reaction) of standard K562 and 9947A DNA. Moreover, the success rate of genotyping from a URP system was much higher than that from a conventional primer extension method in degraded DNA. This method enables simple and rapid detection of multiple SNP sites on human ABO genes and is highly specific and sensitive when using limited and degraded DNA.

KEYWORDS: forensic sciences, ABO blood group, DNA typing, single nucleotide polymorphism (SNP), universal reporter primer system, degraded DNA

The ABO blood system has been routinely analyzed for use as a forensic identification tool. For cases in which serological typing is unclear, genotyping of single nucleotide polymorphisms (SNPs) on the ABO gene, which encodes glycosyltransferases on chromosome 9, is an alternative and useful method, even if residual DNA in forensic materials is limited and/or degraded. In recent years, an increasing number of variations have been found on this gene, especially in exons 6 and 7 (1,2). Some of these variations cause amino acids substitutions, resulting in different ABO serological phenotypes. In addition to the frequently observed standard classification (A, B, AB, and O), classification of many subgroups is possible because of different combinations of identified SNPs (3). However, from a forensic perspective, we must select SNPs and obtain genetic results of ABO types that correspond to phenotypes from serological tests. Although nucleotide positions (nps) 261 and 703 are representative SNP sites for ABO grouping (4), other sites, such as nps 220, 802, and 803, are useful to avoid discrepancies between genetic and serological tests (5).

Numerous techniques are available for SNP genotyping, and the polymerase chain reaction–restriction fragment length polymorphism (PCR–RFLP) method or primer extension assay has been used for the detection of multiple SNPs in the forensic field (4–9). However, these techniques are time consuming. Although standard allele-specific amplification and subsequent gel electrophoresis detection is also a popular strategy for SNP genotyping, false-positive results sometimes occur (10), and this technique requires high specificity in the design of primers and exact conditions for amplification. SNP genotyping using a universal reporter primer (URP) system is a simple and rapid fluorescence-based method (11) consisting of two-phase amplification and subsequent electrophoretic analysis. The amplification reaction is performed using characteristic nonlabeled locus-specific primers combined with URPs and fluorescence-labeled universal primers. In recent years, this technique has been reported to be useful for degraded DNA from forensic samples (11). We also reported successful identification of severely degraded DNA from a 4-year formalin-fixed tissue using allele-specific amplification with URPs (12).

In this study, we developed a simple and rapid method for forensic ABO genotyping using a URP system, and herein report the specificity of amplification primers and the sensitivity in limited and degraded DNA.

Materials and Methods

Buccal cells were collected from 26 healthy Japanese individuals, and DNA was extracted using the QIAamp DNA Blood Mini Kit (Qiagen, Hilden, Germany) according to the manufacturer's instructions. DNA concentration was determined using Nano Drop ND-1000 (Nano Drop Technologies, Wilmington, DE). We selected six SNP sites (nps 261 and 297 from exon 6 and nps 526, 703, 796, and 803 from exon 7) identified in human ABO genes, and designed amplification primers for phase I and II reactions as described previously (11). The principle of two-phase amplification using a URP system was illustrated in Fig. 1. The phase I reaction was performed using two allele-specific forward primers and one reverse primer in each locus (Table 1). These primers were designed using universal sequences upstream of locus-specific sequences with SNP alleles at the 3′ terminus. The forward primers contained universal 9 tails (uni9) or universal 11 tails (uni11), and the reverse primers contained universal 13 tails (uni13). Two fluorescence-labeled universal primers were used in the phase II reaction, and the 5′ terminus of uni9 and uni11 was tagged with FAM

[1]Department of Legal Medicine, Asahikawa Medical College, Asahikawa, 078-8510 Japan.
[2]Department of Hospital Pharmacy & Pharmacology, Asahikawa Medical College, Asahikawa 078-8510, Japan.

Received 3 June 2009; and in revised form 27 July 2009; accepted 11 Sept. 2009.

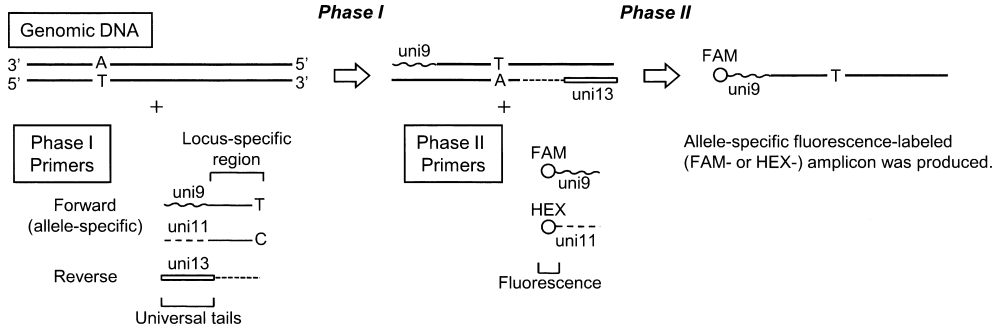

FIG. 1—*Schematic of two-phase amplification using a URP system.*

TABLE 1—*Primer sequences for the phase I reaction.*

Region	Nucleotide Position	SNP	Sequence (5′-3′)*	Fragment Size of Target Genome (colors)	Amount (pmol/20 μL)
Exon 6	261	G	uni9-GAAGGATGTCCTCGTGGTG	79 bp (blue)	1.0
		del G	uni11-GGAAGGATGTCCTCGTGGTA	79 bp (green)	2.0
			uni13-TCGTTGAGGATGTCGATGTT		2.0
	297	A	uni9-GTTGAGGATGTCGATGTTGgAT†	52 bp (blue)	1.0
		G	uni11-GTTGAGGATGTCGATGTTGgAC†	52 bp (green)	1.0
			uni13-TTGGCTGGCTCCCATTGT		1.0
Exon 7	526	C	uni9- AGCTGTCAGTGCTGGAGGTGC	86 bp (blue)	1.8
		G	uni11-AGCTGTCAGTGCTGGAGGTGG	86 bp (green)	1.8
			uni13-ACGCACACCAGGTAATCCAC		1.8
	703	G	uni9-CGGCTGCTTCCGTAGAAGCC	115 bp (blue)	3.0
		A	uni11-CGGCTGCTTCCGTAGAAGCT	115 bp (green)	3.0
			uni13-ATTACCTGGTGTGCGTGGAC		3.0
	796	C	uni9-ACGAGGGCGATTTCTACTACC	98 bp (blue)	1.8
		A	uni11-CGAGGGCGATTTCTACTACA	97 bp (green)	1.8
			uni13- GTCGACCATCATGGCCTAGT		1.8
	803	G	uni9- ACCGACCCCCCGAAGAACC	48 bp (blue)	2.0
		C	uni11- ACCGACCCCCCGAAGAACG	48 bp (green)	2.0
			uni13- GGACGAGGGCGATTTCTACT		2.0

*Each primer contains universal sequences upstream of locus-specific sequences: uni9 (CGACGTGGTGGATGTGCTAT) or uni11 (TGACGTGGCTGACCTGAGAC) for forward primers and uni13 (CAAGCTGGTGGCTGTGCAAG) for the reverse primer in each SNP locus.
†Small letters indicate nucleotides mismatched to the reference exon 6 sequences.

(blue) and HEX (green), respectively. Primers for the phase I reaction were classified into two sets (nps 261, 526, and 796 for set A and 297, 703, and 803 for set B) and mixed in each set before PCR. Up to 1 ng of DNA extracts was amplified in a total volume of 20 μL containing an optimized concentration of phase I primer mix (set A or set B), and the reagent of the multiplex PCR kit (Qiagen) using the following conditions: 95°C for 15 min; seven cycles of 94°C/30 sec, 60°C/15 sec, 72°C/15 sec, 60°C/15 sec, 72°C/15 sec, 60°C/15 sec, 72°C/15 sec; and 32 cycles of 94°C/30 sec, 76°C/105 sec. Using 0.5 μL of sets A and 1.5 μL of set B products after phase I, phase II amplification was performed in total volume of 20 μL containing 0.8 pmol of phase II primers, and 0.5 units of AmpliTaq Gold DNA polymerase (Applied Biosystems, Foster City, CA) using the following conditions: 95°C for 11 min; and two cycles of 94°C/60 sec, 60°C/30 sec, 76°C/60 sec, followed by a 4°C hold. The PCR product (0.5 μL) was added to 10 μL of Hi-Di Formamide (Applied Biosystems) containing 0.3 μL of GeneScan HD400 ROX Size Standard (Applied Biosystems). Samples were analyzed using an ABI PRISM 310 Genetic Analyzer (Applied Biosystems). The sequence of exons 6 and 7 was analyzed to determine alleles of each locus. The sequencing reaction was performed using the BigDye Terminator v1.1 Cycle Sequencing Kit (Applied Biosystems), according to the manufacturer's instructions. To examine the specificity of the genotyping reaction in homozygous and heterozygous alleles, we used the discrimination factor (DF) for evaluation. The duplicate peak heights of relative fluorescence units data from the electropherograms were averaged to obtain mean heights (H), and the DF was calculated using the following normalizing algorithm: $DF = (H_{blue\ peak} - H_{green\ peak})/(H_{blue\ peak} + H_{green\ peak})$. To confirm the sensitivity of this system, we also analyzed ABO genotypes using standard DNA (K562 and 9947A), and applied this system to degraded DNA from forensic samples. DNA was extracted by the standard phenol/chloroform method after decalcification or QIAamp DNA Micro kit (Qiagen) according to the manufacturer's instructions. We used 0.5 μL of DNA extracts for two multiplex reactions and followed the detection method as described earlier.

Results and Discussion

The URP system provided different labeled products corresponding to the existing alleles in a two-phase amplification reaction. The 3′end of phase I primers was located in the targeted SNPs in each locus, and an allele-specific amplicon with uni9 and/or uni11 tails was obtained after the phase I reaction. In the phase II reaction, FAM-label or HEX-label was added to the products by amplification using fluorescence-labeled universal primers. Two-phase amplification and fluorescence-based detection provided obvious peaks of six SNPs in exons 6 (nps 261 and 297) and 7 (nps 526, 703, 796, and 803) on human ABO genes. Electropherograms of

common ABO genotypes (AA, AO, BB, BO, AB, and OO) are shown in Fig. 2. Corresponding to existing allele(s) of genomic DNA, the blue (FAM-labeled) and/or green (HEX-labeled) peaks with the same fragment sizes were identified in each locus, except for np 796. At np 796 alone, one base difference that was consistent with the difference of the primer length was observed between C and A alleles. Electropherogram of the OO genotype contains a nonspecific blue peak near the green peak derived from O allele at np 261. However, the size of this nonspecific peak is shorter than that of the green peak, and the blue/green peaks observed can distinguish this OO genotype from other genotypes including heterozygous alleles at np 261. Although the size of the target genomes ranged from 48 to 115 bp, the final products also contain 40 bp of universal sequences. All peaks ranged from 82 to 151 bp in the electropherogram, and the actual sizes of peaks were close to the expected sizes of amplicon.

DNA genotyping results do not always reflect the phenotype, and some minor alleles do not contain typical sequences in major groups. For example, O303 lacks the single-base deletion at np 261 (13), which is commonly observed in the O allele, and A204 contains the substitution of A at np 703 characteristic of the B allele (14,15). In addition to these alleles, cis-AB02 (16) and O207 (17) also contain SNP sites that cause possible mistyping. The ABO grouping using the six SNPs selected in this study is shown in

TABLE 2—*ABO grouping using six single nucleotide polymorphisms.*

		Nucleotide Position					
Group	Allele	261	297	526	703	796	803
A	A101*	G	A	C	G	C	G
	A113			G			
	A204		G	G	A		
B	B101*		G	G	A	A	C
	B107		G		A	A	C
	B108			G	A	A	C
	B(A)01		G	G		A	C
cisAB	cis-AB01						C
	cis-AB02		G	G	A		C
O	O101*	delG					
	O201*	delG	G				
	O207	delG	G	G	A	A	C
	O303		G	G			

*Representative allele with indicated single nucleotide polymophisms.

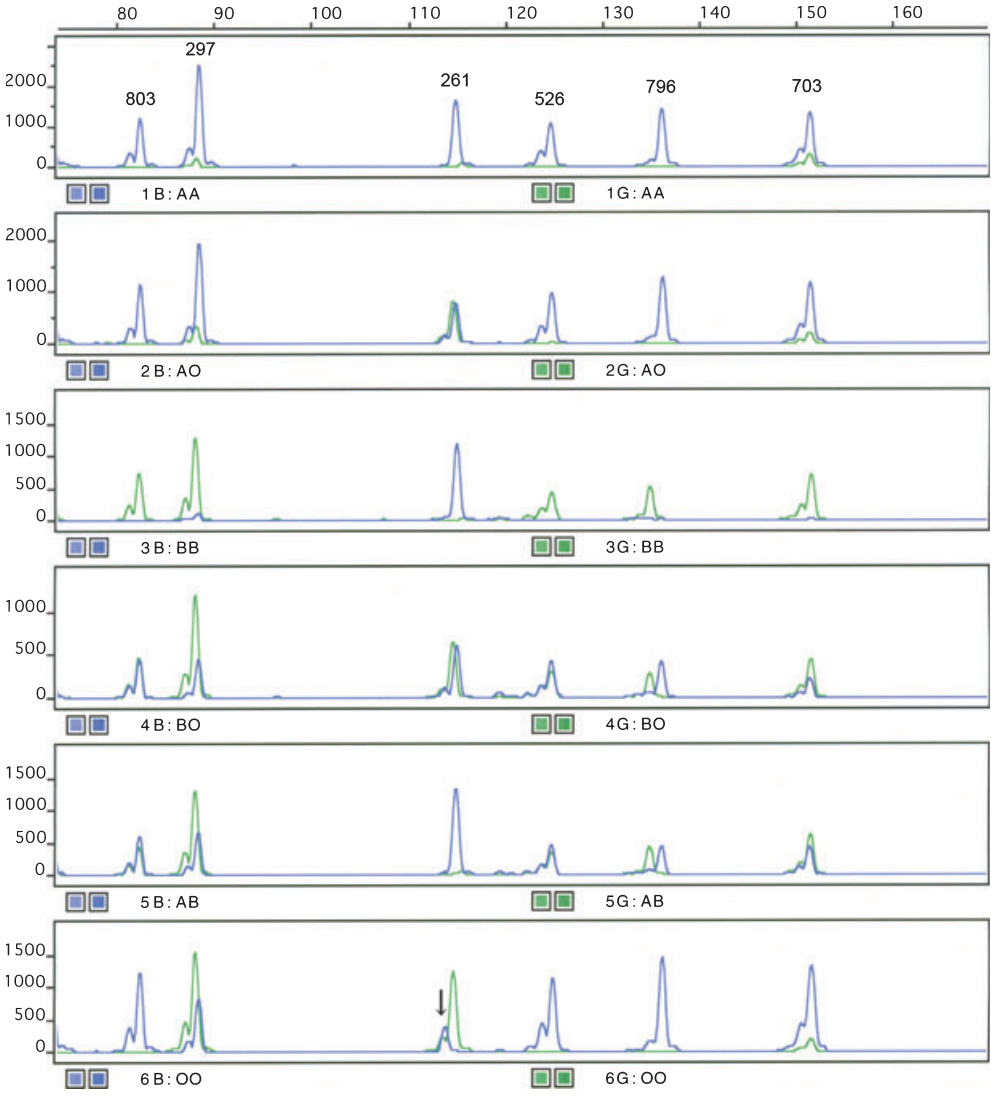

FIG. 2—*Electropherograms of common ABO genotypes by a URP system. The SNP profiles of six genotypes (AA, AO, BB, BO, AB, and OO) are shown, and the number above the peak in AA genotype indicates each SNP locus of the ABO gene. The X-axis indicates the length of the DNA fragment, and the Y-axis indicates relative fluorescence units. The arrowhead indicates a nonspecific peak identified in the OO genotype.*

TABLE 3—*Color of peaks observed in representative allele pairs.*

Phenotype	Allele Pair	Nucleotide Position					
		261	297	526	703	796	803
A	A101/A101	B	B	B	B	B	B
	A101/O101	B/G	B	B	B	B	B
	A101/O201	B/G	B/G	B	B	B	B
B	B101/B101	B	G	G	G	G	G
	B101/O101	B/G	B/G	B/G	B/G	B/G	B/G
	B101/O201	B/G	G	B/G	B/G	B/G	B/G
AB	A101/B101	B	B/G	B/G	B/G	B/G	B/G
O	O101/O101	G	B	B	B	B	B
	O101/O201	G	B/G	B	B	B	B
	O201/O201	G	G	B	B	B	B

B and G indicate the blue and green peaks of each amplicon, respectively.

Table 2, and expected color of peaks in representative pairs of alleles were shown in Table 3. ABO genotypes were classified and successfully genotyped by our method, including minor alleles that may cause a discrepancy between the genetic data and serological phenotypes. Moreover, some variations (e.g., np 802) targeted in other studies are rare in the Japanese population (5,18), and a validation study could not be performed conclusively in these sites. On the other hand, the six selected SNPs are common in various populations, and classification based on these SNPs is easy to validate with genotyping.

To elucidate the specificity of amplification primers, we determined the DFs using homozygous and heterozygous alleles of 26 Japanese individuals. The DFs at the six SNP sites are shown in Fig. 3. The value was expected to be close to 1.00 or −1.00 in the two homozygous alleles and 0 in the heterozygous allele. The DFs from one homozygous allele ranged from 1.00 to 0.63 among the six SNP sites, and the other homozygous allele ranged from −0.85 to −1.00. The averages DFs in the homozygous alleles were 0.90 and −0.95, respectively. On the other hand, the DFs from heterozygous alleles ranged from 0.18 to −0.28 among the six SNP sites, and the average was −0.02. The 297A/G primers have G at the third nucleotide from the 3′ terminus, which is mismatched to exon 6 sequences, and the specificity of the genotyping reaction increased significantly compared with the perfectly matched primers (data not shown). Our results indicated that all SNP sites showed clear differentiation between homozygotes and heterozygotes.

To clarify the lower limit, we performed SNP genotyping using diluted templates of standard K562 and 9947A DNA. Diluted templates (1, 0.5, 0.1, and 0.05 ng) of standard DNA were amplified for two multiplex reactions of sets A and B primer mix, and each dilution was typed for five replicates (Table 4). Full profiles were identified using as little as 0.1 ng (0.05 ng/reaction) of standard DNA. Amplification using 0.05 ng (0.025 ng/reaction) of DNA caused nonspecific product or dropout of expected alleles.

We applied this method to forensic samples (tooth, bone, and nail) collected from 24 cases. At first, these samples were analyzed by a conventional primer extension method using the SNaPshot kit

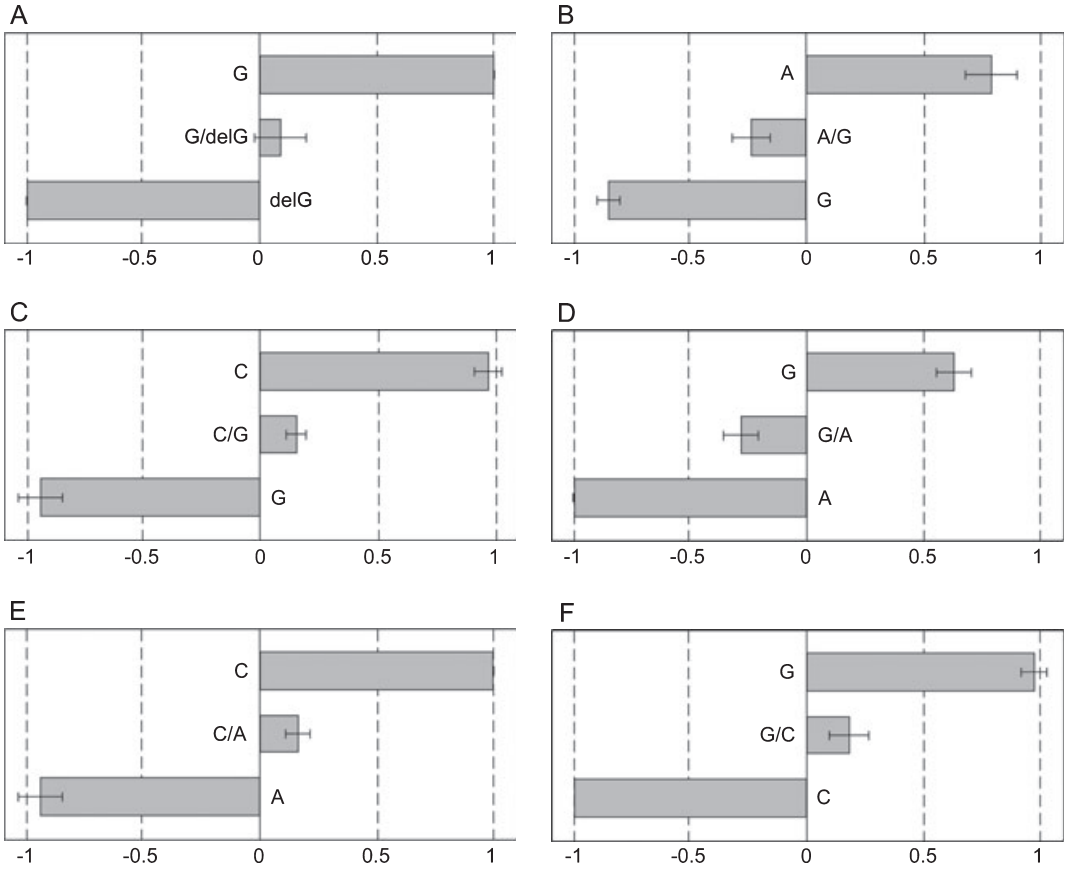

FIG. 3—*Discrimination factors (DFs) in homozygous and heterozygous alleles at six SNP sites. (A) np 261; (B) np 297; (C) np 526; (D) np 703; (E) np 796; and (F) np 803. Each column represents the average ± SD of the DFs by analysis of 26 Japanese individuals.*

TABLE 4—*Sensitivity of six SNPs genotyping using standard K562 and 9947A.*

Template DNA(ng)	Nucleotide Position					
	261	297	526	703	796	803
K562 (Amplicon peak	G	B	B	B	B	B)
1.0	532	1604	927	821	1104	1222
0.5	564	1360	947	798	1098	1073
0.1	468	476	599	575	748	644
0.05	457	386	565	511	671	NR
9947A (Amplicon peak	B/G	B/G	B/G	B/G	B/G	B/G)
1.0	382/287	406/1120	473/547	419/281	375/267	350/550
0.5	372/239	304/971	440/498	401/241	390/276	292/507
0.1	345/218	160/598	468/423	393/241	417/212	251/405
0.05	412/232	275/701	227/327	NR	NR	386/398

Template DNA indicates total amount for two multiplex reaction of sets A and B primer mix, and each template was typed for five replicates. Each reaction was performed using half sizes of the indicated amount of DNA.

The values shown are the average peak heights of each SNP in relative fluorescence units, and NR (no results) indicates that nonspecific products or dropout of expected alleles are observed in three or more replicates.

B and G of amplicon peaks indicate the blue and green peaks, respectively.

(Applied Biosystems) described previously (7), and ABO genotypes were successfully determined in 14 samples. Of the remaining 10 samples, obvious peaks were not identified, suggesting that the residual DNA was heavily degraded; complete locus drop-outs were observed. On the other hand, the success rate of genotyping from a URP system was much higher than that from a primer extension method, and our genotyping method gave full profiles in 22 samples. Duplicate analysis using degraded DNA showed the different DFs of homozygous and heterozygous alleles, and the interpretation with two or more genotyping would be needed for possible mutations in analysis of degraded DNA.

This approach is a simple, rapid, highly specific, and sensitive technique for forensic ABO genotyping. The reaction only requires multiplex PCR reagents and nonlabeled and fluorescence-labeled characteristic primers, and amplification using six designed primers performed in two multiplex reactions with identical thermal cycling condition. Reaction mixture for two-phase amplification can be easily prepared, and a series of amplification, which can provide fluorescence-labeled products in multiple SNP loci, was performed within 3 h. Two amplicons are simultaneously detectable in a Genetic Analyzer, which is widely used in forensic application, and the sizes of fragments and the detectable color of peaks make it easy to determine existing alleles of each SNP. Moreover, fluorescence-based genotyping using a URP system can avoid false-positive results, which are sometimes caused by standard allele-specific amplification and subsequent agarose gel electrophoresis (10). Instead, the product size from electropherograms is exactly determined for each locus, and we can easily distinguish whether the expected peak occurs or not. PCR–RFLP is one of the most popular methods for forensic SNP genotyping (4,6), but multiple SNPs detection is unsuitable because simultaneous use of restriction enzyme is sometimes difficult. The primer extension technique is also popular and easily provides SNP determinations with fluorescence labeling of existing alleles (5,7–9). However, this assay is robust and consists of four multistep reactions. Moreover, the signal strengths of the fluorescence labeling are not well balanced, which make it difficult to distinguish between homozygous and heterozygous alleles. Although newly introduced SNP genotyping tools, such as MALDI/TOF-MS (19), Taqman PCR (20), and DNA array (21), can be also applied for forensic use, these methods require expensive equipment.

In conclusion, we developed a new technique based on a URP system for forensic ABO genotyping. This method allows simple and rapid detection of multiple SNP sites on the human ABO gene. In addition, genotyping using the designed primers is highly specific and sensitive in analysis of limited and degraded DNA.

References

1. Yamamoto F, Clausen H, White T, Marken J, Hakomori S, Yamamoto F, et al. Molecular genetic basis of the histo-blood group ABO system. Nature 1990;345:229–33.
2. Yip SP. Sequence variation at the human ABO locus. Ann Hum Genet 2002;66:1–27.
3. Hosseini-Maaf B, Hellberg A, Chester MA, Olsson ML. An extensive polymerase chain reaction-allele-specific polymorphism strategy for clinical ABO blood group genotyping that avoids potential errors caused by null, subgroup, and hybrid alleles. Transfusion 2007;47: 2110–25.
4. Lee JC, Chang JG. ABO genotyping by polymerase chain reaction. J Forensic Sci 1992;37:1269–75.
5. Shintani-Ishida K, Zhu BL, Maeda H, Uemura K, Yoshida K. A new method for ABO genotyping to avoid discrepancy between genetic and serological determinations. Int J Legal Med 2008;122:7–9.
6. Fukumori Y, Ohnoki S, Shibata H, Yamaguchi H, Nishimukai H. Genotyping of ABO blood groups by PCR and RFLP analysis of 5 nucleotide positions. Int J Legal Med 1995;107:179–82.
7. Doi Y, Yamamoto Y, Inagaki S, Shigeta Y, Miyaishi S, Ishizu H. A new method for ABO genotyping using a multiplex single-base primer extension reaction and its application to forensic casework samples. Leg Med 2004;6:213–23.
8. Inagaki S, Yamamoto Y, Doi Y, Takata T, Ishikawa T, Imabayashi K, et al. A new 39-plex analysis method for SNPs including 15 blood group loci. Forensic Sci Int 2004;144:45–57.
9. Ferri G, Bini C, Ceccardi S, Pelotti S. ABO genotyping by minisequencing analysis. Transfusion 2004;44:943–4.
10. Yaku H, Yukimasa T, Nakano S, Sugimoto N, Oka H. Design of allele-specific primers and detection of the human ABO genotyping to avoid the pseudopositive problem. Electrophoresis 2008;29:4130–40.
11. Hussain J, Gill P, Long A, Dixon L, Hinton K, Hughes J, et al. Rapid preparation of SNP multiplexes utilising universal reporter primers and their detection by gel electrophoresis and microfabricated arrays. Int Congr Ser 2003;1239:5–8.
12. Asari M, Watanabe S, Matsubara K, Shiono H, Shimizu K. Single nucleotide polymorphism genotyping by mini-primer allele-specific amplification with universal reporter primers for identification of degraded DNA. Anal Biochem 2009;386:85–90.
13. Grunnet N, Steffensen R, Bennett EP, Clausen H. Evaluation of histo-blood group ABO genotyping in a Danish population: frequency of a novel O allele defined as O2. Vox Sang 1994;67:210–5.
14. Ogasawara K, Yabe R, Uchikawa M, Saitou N, Bannai M, Nakata K, et al. Molecular genetic analysis of variant phenotypes of the ABO blood group system. Blood 1996;88:2732–7.
15. Ogasawara K, Yabe R, Uchikawa M, Bannai M, Nakata K, Takenaka M, et al. Different alleles cause an imbalance in A2 and A2B phenotypes of the ABO blood group. Vox Sang 1998;74:242–7.
16. Mifsud NA, Watt JM, Condon JA, Haddad AP, Sparrow RL. A novel cis-AB variant allele arising from a nucleotide substitution A796C in the B transferase gene. Transfusion 2000;40:1276–7.
17. Roubinet F, Kermarrec N, Despiau S, Apoil PA, Dugoujon JM, Blancher A. Molecular polymorphism of O alleles in five populations of different ethnic origins. Immunogenetics 2001;53:95–104.
18. Watanabe G, Umetsu K, Yuasa I, Suzuki T. Amplified product length polymorphism (APLP): a novel strategy for genotyping the ABO blood group. Hum Genet 1997;99:34–7.

19. Petkovski E, Keyser-Tracqui C, Hienne R, Ludes B. SNPs and MALDI-TOF MS: tools for DNA typing in forensic paternity testing and anthropology. J Forensic Sci 2005;50:535–41.
20. Lee LG, Livak KJ, Mullah B, Graham RJ, Vinayak RS, Woudenberg TM. Seven-color, homogeneous detection of six PCR products. BioTechniques 1999;27:342–9.
21. Divne AM, Allen M. A DNA microarray system for forensic SNP analysis. Forensic Sci Int 2005;154:111–21.

Additional information and reprint requests:
Masaru Asari, Ph.D.
Department of Legal Medicine
Asahikawa Medical College
2-1-1-1 Midorigaokahigashi
Asahikawa 078-8510
Japan
E-mail: asari@asahikawa-med.ac.jp

JOURNAL OF FORENSIC SCIENCES

J Forensic Sci, November 2010, Vol. 55, No. 6
doi: 10.1111/j.1556-4029.2010.01522.x
Available online at: onlinelibrary.wiley.com

TECHNICAL NOTE

CRIMINALISTICS

Greg W. Cook,[1] *Ph.D.; Peter T. LaPuma,*[1] *Ph.D.; Gary L. Hook,*[2] *Ph.D.; and Brian A. Eckenrode,*[3] *Ph.D.*

Using Gas Chromatography with Ion Mobility Spectrometry to Resolve Explosive Compounds in the Presence of Interferents*

ABSTRACT: Ion mobility spectrometry (IMS) is a valued field detection technology because of its speed and high sensitivity, but IMS cannot easily resolve analytes of interest within mixtures. Coupling gas chromatography (GC) to IMS adds a separation capability to resolve complex matrices. A GC-IONSCAN® operated in IMS and GC/IMS modes was evaluated with combinations of five explosives and four interferents. In 100 explosive/interferent combinations, IMS yielded 21 false positives while GC/IMS substantially reduced the occurrence of false positives to one. In addition, the results indicate that through redesign or modification of the preconcentrator there would be significant advantages to using GC/IMS, such as enhancement of the linear dynamic range (LDR) in some situations. By balancing sensitivity with LDR, GC/IMS could prove to be a very advantageous tool when addressing real world complex mixture situations.

KEYWORDS: forensic science, explosives, ion mobility, ion mobility spectrometry, gas chromatography, portable, contraband, screening

An important challenge facing law enforcement and military personnel is the ability to detect, correctly identify, and interdict the illegal possession of explosives intended to initiate terror and harm citizens, both nationally and internationally. Ion mobility spectrometry (IMS) is a proven technology for trace screening of explosive compounds in field settings (1–16). Some of the advantages with IMS include the following: low detection limits for single-component samples (nanogram detection limits); fast analysis time (provides output data in seconds); no required sample pretreatment of solids or analytes in solution; operates at atmospheric pressure eliminating bulky vacuum systems, detects both positive and negative ions, which provides good selectivity; can be miniaturized and battery operated; and is comparably less expensive to purchase and operate than other trace detection technologies (1,2,4,5,10,17,18). As of 2005, more than 15,000 field portable IMS instruments are in use for explosives detection (12).

While many IMS instruments are used in the field to locate explosives, as with all detection techniques, there are limitations. IMS does not handle chemical mixtures adequately because of the complex interactions in the IMS source that leads to obscure or less distinct plasmagrams (19–21). IMS instruments are prone to inaccurate detection and false positive responses when chemical interferents are present in samples. IMS instruments are also relatively easy to saturate resulting in a linear response range that is often limited to one to two orders of magnitude. Thus, sample size must be carefully controlled at the instrument's entrance to prevent saturation or nonlinear response (5,12,20,22–24). If these limitations can be mitigated, IMS can be a more powerful tool in detecting explosives under a variety of confounding sampling situations.

One way to overcome IMS limitations is by coupling a gas chromatograph (GC) to the IMS detector (25–29). While two chemicals can have identical IMS ion mobilities, the chemicals typically have different GC retention times, which helps separate chemicals prior to entering an IMS (30,31). The addition of GC to IMS has demonstrated improved trace organic chemical detection through better resolution, lower detection limits, reduced detector saturation, and increased IMS linear range (32,33). GC provides the advantage of separating analyte mixtures into individual components for detection, but the addition of GC increases system complexity, power consumption, and analysis time which all work against the advantages of IMS alone (34,35). Consequently, if GC is to be added to an IMS detector for field applications, the disadvantages should be eliminated or reduced.

The objective of this research was to compare GC/IMS and IMS for the detection of explosive compounds in the presence of interferents. The performance characteristics of IMS mode and GC/IMS mode were evaluated to determine the method detection limit (MDL), accuracy, and precision in the detection of five explosive compounds amidst four complex chemical mixtures as interferents.

Materials and Methods

Instrumentation

The instrument used in this research, a Smiths Detection GC-IONSCAN® (Warren, NJ), can be operated in IMS mode or

[1]Department of Preventive Medicine and Biometrics, Uniformed Services University of the Health Sciences, 4301 Jones Bridge Road, Bethesda, MD 20814.
[2]Defense Threat Reduction Agency, 1600 Texas Street Se, Albuquerque, NM 87117-0001.
[3]Federal Bureau of Investigation, Counterterrorism and Forensic Science Research Unit, 1 J Edgar Hoover Road, Quantico, VA 22135-0001.

*Official Disclaimer: The views expressed in this article are those of the authors and do not reflect the official policy or position of the Department of the Navy, Department of Defense, Federal Bureau of Investigation, or the United States Government.

Received 31 July 2008; and in revised form 10 Aug. 2009; accepted 26 Sept. 2009.

GC/IMS mode with the ability to switch between positive or negative ion mode. In the IMS mode, analytes are thermally desorbed in a solid phase desorber (SPD) and combined with makeup gas (filtered ambient air). The GC column is bypassed permitting relatively fast (<15 sec), direct analysis of samples. In the GC/IMS mode, thermally desorbed analytes enter a sample loop (10 cm MXT-1; 0.53 mm internal diameter; 7.0 μm film thickness) which acts as a preconcentrator for GC separation. The sample loop (preconcentrator) is subsequently heated and sample vapors are carried into the GC (15 m MXT-1; 0.53 mm internal diameter; 1.0 μm film thickness). In the positive ion mode, a trace amount of nicotinamide is automatically added into the ionization region as an internal calibrant. In the negative ion mode, a trace amount of 4-nitro-benzylnitrile is automatically added as an internal calibrant. In each mode, the software uses the internal calibrant drift time to correct for the expected ion mobilities (K_o) of targeted compounds.

The GC-IONSCAN® was used in accordance with the user's manual and manufacturer recommendations. Data acquisition parameters for each of the five explosives analyzed are listed in Table 1. When operated in IMS mode, sample carrier gas and drift gas (350 mL/min) were ambient air purified with activated charcoal and a desiccant in the instrument's purification unit. When operated in GC/IMS mode, BIP® helium (Airgas, Salem, NH) was used as the carrier gas. All methods and data were analyzed and processed using the GC-IONSCAN® software (Instrument Manager version 5.114). HMTD and TATP were not part of the original onboard library for the GC-IONSCAN®; however, they were added using method parameters obtained from the manufacturer.

Explosives Sample Preparation

The following explosive materials (all 99% or greater in purity) were provided by the FBI Explosives Unit of the Laboratory Division (Quantico, VA) and dissolved to concentrations of 500, 100, 50, 10, 5, 1, and 0.1 ng/μL of solvent.

- Hexamethylene triperoxide diamine (HMTD) dissolved in acetone
- Pentaerythritol tetranitrate (PETN) dissolved in methanol
- 1,3,5-Trinitro-1,3,5-triazine (RDX) dissolved in methanol
- Triacetone triperoxide (TATP) dissolved in methanol
- 2,4,6-Trinitrotoluene (TNT) dissolved in methanol.

To accurately transfer a known quantity of explosive to each swab, 1 μL of a dissolved explosives solution was directly deposited onto Teflon® swabs (Smiths Detection, Warren, NJ). The solvent was allowed to evaporate (*c.* 5 sec), leaving the desired mass load of explosive on the swab before it was placed into the instrument's SPD. The sum of the analyte's maximum peak amplitudes was recorded and used for comparisons.

Interferents

Four common commercial products (two beverages, a moisturizer, and fertilizer) that could be used in real world explosive concealment attempts were selected as interferents to evaluate the effect of chemical matrix interferents. The identity of the interferents are withheld in the interest of security. Interferents #1 and #2 were deposited onto swabs in 5-μL aliquots and allowed to dry. The average dry weight of Interferent #1 and Interferent #2 deposited on the Teflon® swab was 700 and 420 μg, respectively. The weight was determined by weighing five of each interferent containing swab and calculating the mean. A 100-mg droplet of Interferent #3 was placed on a 10 square inch clean pane of glass and spread as evenly as possible using a gloved finger. Swab wipes (1 cm swipe) were collected from the glass pane. The average weight of Interferent #3 collected on the Teflon® swab was 500 μg. For Interferent #4, 25 mg of dry particles was placed inside a 0.5-L plastic bag and shaken. One-centimeter swab wipes were collected from the bag interior. The average dry weight of Interferent #4 collected on a swab was 450 μg. The relative quantity of each interferent was designed to simulate real world situations at disguising explosive compounds.

Explosives with Interferents

Sample swabs were prepared with the four interferents, as previously described, and subsequently spiked with a known mass of

TABLE 1— *GC-IONSCAN® data acquisition parameters.*

	HMTD*	PETN	RDX	TATP*	2,4,6-TNT
			IMS Experimental Conditions		
Operating mode	Negative	Negative	Negative	Positive	Negative
Sampling time (sec)			10		
SPD temperature (°C)	225	227	227	220	227
Inlet temperature (°C)	240	242	242	225	242
Drift tube temperature (°C)	105	112	112	150	112
Electric field gradient (V/cm)	200	200	200	175	200
			GC/IMS Experimental Conditions		
Loop (preconcentrator) cycle program (sec)			Sample (10); Heat (3); Purge (15); Cool (15)		
Loop (preconcentrator) temperature (°C)	220	220	220	240	220
Valve temperature (°C)	200	200	200	220	200
Oven initial temperature (°C)	120	120	120	80	120
Oven initial hold (sec)	20	20	20	120	20
Oven ramp rate (°C/min)	40	40	40	40	40
Oven final temperature (°C)	240	240	240	120	240
Final hold (sec)	20	20	20	20	20
Transfer line temperature (°C)	180	220	220	240	220
Analysis duration (sec)			220		
Product ion retention time (sec) (variability)	90	114	117	71	100

*TATP and HMTD were not part of the original onboard library. Analysis was performed using parameters obtained from Smiths Detection.

TABLE 2—*Mass load of explosive compound and interferent prepared on sample swabs. The spiked concentration (mass loading level) of each explosive compound was at least one order of magnitude higher than the observed MDL under pure (exemplars) conditions.*

Explosive	Mass of Interferent on Sample Swab (μg)	Mass of Explosive on Sample Swab for IMS Analysis (ng)	Mass of Explosive on Sample Swab for GC/IMS Analysis (ng)
HMTD	#1 700	10	500
	#2 420	10	500
	#3 500	10	500
	#4 450	10	500
PETN	#1 700	10	100
	#2 420	10	100
	#3 500	10	100
	#4 450	10	100
RDX	#1 700	10	10
	#2 420	10	10
	#3 500	10	10
	#4 450	10	10
TATP	#1 700	10	500
	#2 420	10	500
	#3 500	10	500
	#4 450	10	500
2,4,6-TNT	#1 700	10	10
	#2 420	10	10
	#3 500	10	10
	#4 450	10	10

the explosive compound (see Table 2). The spiked concentration (mass loading level) of each explosive compound was at least one serial dilution concentration higher than the observed MDL under pure (exemplars) conditions.

Results and Discussion

Linear Dynamic Range

The IMS and GC/IMS operational modes of the instrument were evaluated to determine whether the addition of a GC affects the linear dynamic range (LDR) of the IMS. Response curves are shown in Fig. 1 for the five selected explosive compounds. GC/IMS was expected to limit the amount of sample entering the IMS at any one time and thereby prevent saturation of the IMS. In all five cases, the GC/IMS mode had lower signal intensity than IMS mode resulting in decreased sensitivity. This effect is most likely due to the limited capacity of the instrument's sample loop (preconcentrator), which is only used during the GC/IMS mode.

In GC/IMS mode, the instrument is designed to pass sample and carrier gas for a preset period of time through a preconcentrator, described earlier, that essentially acts as a trapping medium. Subsequently, a six-port valve reverses flow and the preconcentrator is simultaneously heated to desorb and transfer the analytes into the GC column for chemical separation. All preconcentrators have a limited trapping capacity, which can differ among compounds. Once a preconcentrator reaches its maximum trapping capacity for an analyte, any subsequent analyte will simply pass through (breakthrough) and may never be transferred into the GC column or, in this case, the IMS.

The GC/IMS response in Fig. 1*a–e* has a lower peak amplitude than the IMS response at nearly all concentrations even though the IMS settings remained the same. The decreased signal response for GC/IMS at the same concentrations may be primarily attributed to the limiting effect of the sample loop. As mentioned, analyte is lost when the preconcentrator reaches its maximum trapping capacity. The decreased response may also be because of inefficient transfer of sample vapors into the GC or the IMS. With analysis of RDX (Fig. 1*a*), it appears that in IMS mode the initial response (slope or sensitivity) ends at *c.* 5 ng whereas for GC/IMS the initial response curve ends at *c.* 10 ng. This difference is minor and it would be difficult to suggest that the instrument in this configuration has a greater LDR under GC/IMS conditions over that of IMS alone (the sensitivities are approximately equivalent). The steep slope indicates that sensitivity is good, but at the same time the LDR is poor. This is one of the major limitations with IMS, especially in field environments. However, in the analysis of PETN, TATP, and HMTD (Fig. 1*b,d,e*), the differences are substantial. For example, in the analysis of PETN with IMS alone, the linear response ends at *c.* 10–15 ng. In GC/IMS mode, the LDR is beyond the data set even though the sensitivity is considerably lower. These data indicate that the LDR can be substantially improved, at a sacrifice to sensitivity, by employing a preconcentrator in GC/IMS mode. The IMS, as the detector for the GC, will only receive less analyte mass per unit time as the separation proceeds and thus will not reach the upper curve (reactant ion depletion) until the preconcentrator trapping efficiency is improved for a wider variety of explosive compounds. These results are extremely important for future GC/IMS designs that may balance sensitivity requirements with dynamic range advantages. In other words, if the IMS signal nearly immediately saturates for a given analyte, it would be beneficial if the system was not depleted of reactant ions so that other components could still be measured and not missed. This is very important for conditions when there is a complex sample matrix as in this experimental design.

These observations clearly point to several design considerations for future GC/IMS systems. The preconcentrator could be designed to collect more analyte if the PDMS-coated sample loop was replaced or modified by using: (i) a thicker phase, (ii) a longer sample loop, (iii) an alternate coating, (iv) multiple stationary phase coatings in series, or (v) use of a different sample collection medium that will preferentially trap the explosive compounds and thereby provide overall a more efficient transfer of sample vapors into the column and subsequently into the IMS. A second approach to improve preconcentrator efficiency could be to recirculate sample flow back through the preconcentrator to increase its trapping efficiency. Another design to improve GC/IMS performance would be to replace the air circulation heated column with a resistively heated column or a short column with improved temperature programming rates that allow for more rapid, improved chromatography. This modification would lower analysis times and if wide-bore open tubular columns are used could provide a more efficient transfer of sample vapors into the IMS (36,37). Improvements to the trapping efficiency and separation technology at the front end will reduce analyte losses and allow more analyte to be introduced to the IMS detector which will increase the signal intensity and thus improve sensitivity while simultaneously increasing the LDR over that of IMS alone.

Interferent Analysis

The four commercial products selected to evaluate the effect of chemical matrix interferents on IMS and GC/IMS detection of the five explosive compounds consisted of multiple chemical mixtures and represent items commonly found in field settings. Each of the four interferents was individually applied to a swab, as previously discussed, and analyzed with IMS and GC/IMS. Ten samples were analyzed for each interferent. Table 3 summarizes the results of "interferent only" sample analysis. A false positive was defined as an alarm for an explosive compound when there actually was no

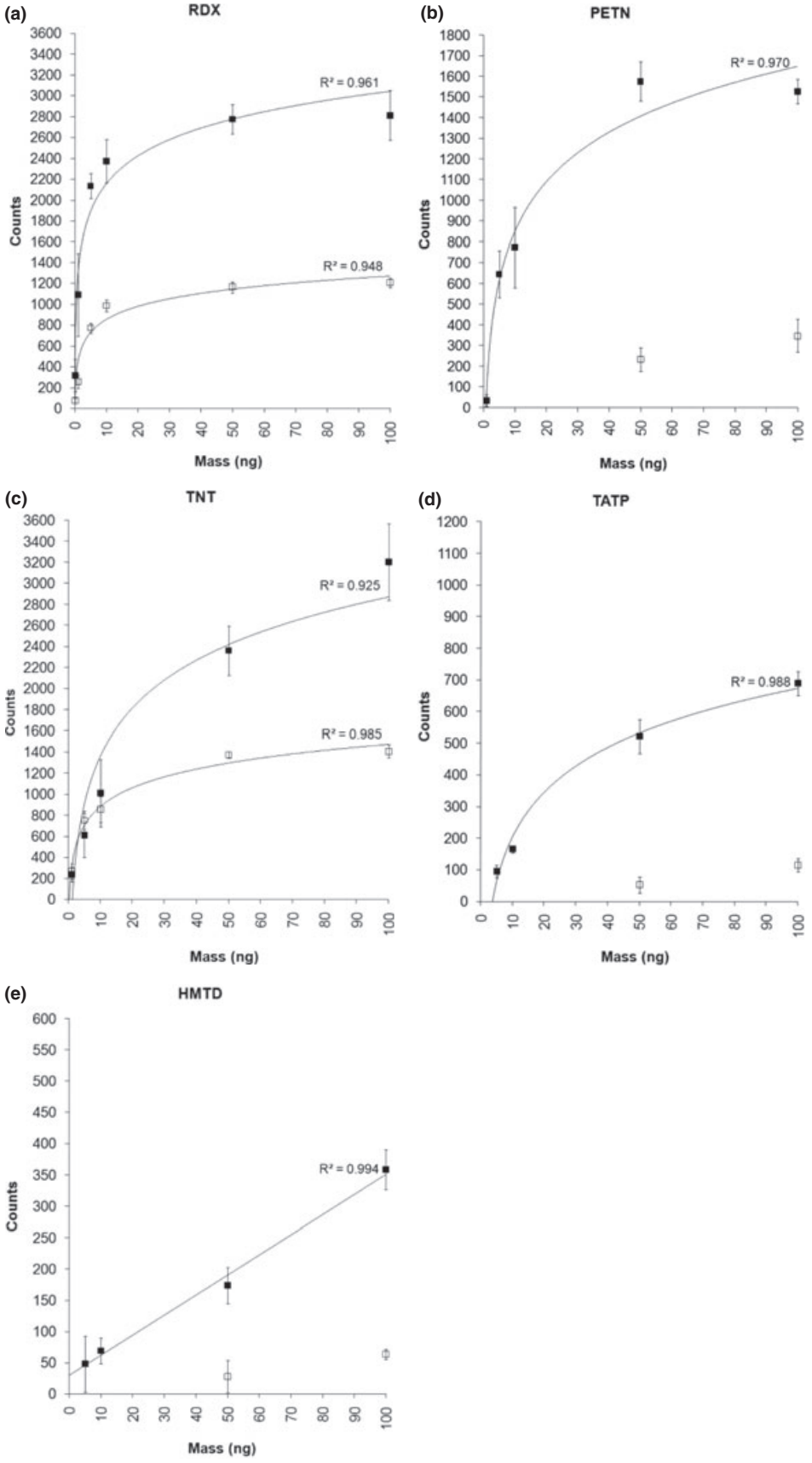

FIG. 1—*Response curves for (a) RDX, (b) PETN, (c) TNT, (d) TATP, and (e) HMTD with IMS ■ and GC/IMS □. Data points represent the mean (*n = *5). Error bars represent one standard deviation. Note for PETN, TATP, and HMTD GC/IMS measurements below 50 ng were indistinguishable from noise.*

TABLE 3—*Summary of chemical matrix interferents analyzed by IMS and GC/IMS using the GC-IONSCAN®.*

	Interferent #1		Interferent #2		Interferent #3		Interferent #4	
Interferent Only	IMS	GC/IMS	IMS	GC/IMS	IMS	GC/IMS	IMS	GC/IMS
Number of samples	10	10	10	10	10	10	10	10
Number of false positives	0	0	2	0	5	0	0	0

explosive compound in the sample. "Interferent only" samples analyzed by IMS resulted in seven false positives (two with Interferent #2 and five with Interferent #3). The false positive responses occurred because an interferent constituent had the same drift time as an explosive compound in the instrument's library. GC/IMS analysis of "interferent only" samples resulted in zero false positives. The proportion of false positives was significantly higher for IMS (7/40) than for GC/IMS (0/40) ($p = 0.012$, Fisher's exact test).

Plasmagrams of the "interferent only" samples collected by IMS analysis were complex because of the multicomponent chemical makeup of the interferents. Figure 2 shows an IMS plasmagram for Interferent #3 analysis. Note that the $(H_2O)_nO_2^-$ and $(H_2O)_3Cl^-$ reactant ions rapidly decreased in intensity as the product ions created from Interferent #3 components increased in intensity. $(H_2O)Cl^-$ reactant ions were nearly depleted for a brief period during the analysis. Depletion of reactant ions by an interferent, such as this, can suppress or prevent detection of targeted analyte(s) because no reactant ions would be available to transfer charge to the analyte(s) (38).

Figure 3 shows GC/IMS analysis of Interferent #3 and illustrates that the separation provided by GC prevented reaction ion saturation within the IMS ionization region. The preseparation of Interferent #3 chemicals minimized the number of chemicals present at any one time and prevented complete depletion of the number density of reactant ions. The GC separation of Interferent #3 chemicals can be observed in Fig. 3 by the discrete analyte peaks in the individual IMS scans, collected from front to back.

Figure 4 shows IMS analysis of Interferent #4. $(H_2O)_nO_2^-$ and $(H_2O)_nCl^-$ reactant ions decreased in intensity as the product ions

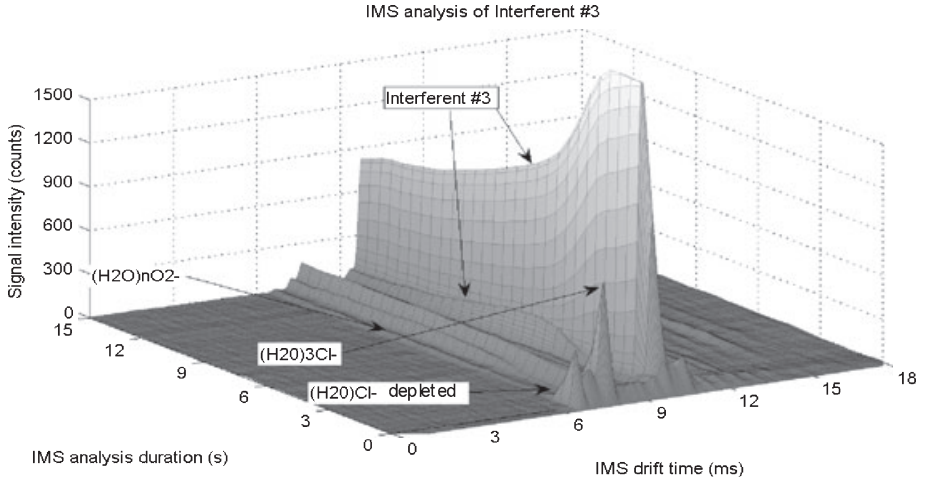

FIG. 2—*IMS analysis of Interferent #3.*

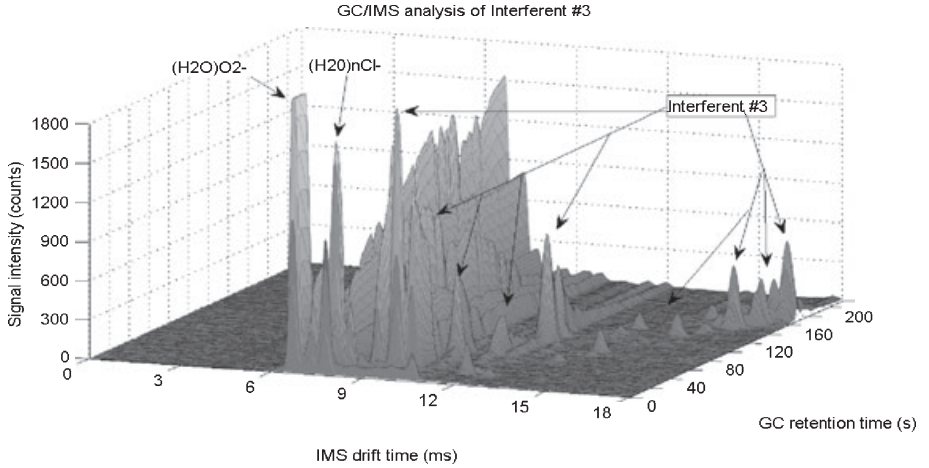

FIG. 3—*GC/IMS analysis of Interferent #3.*

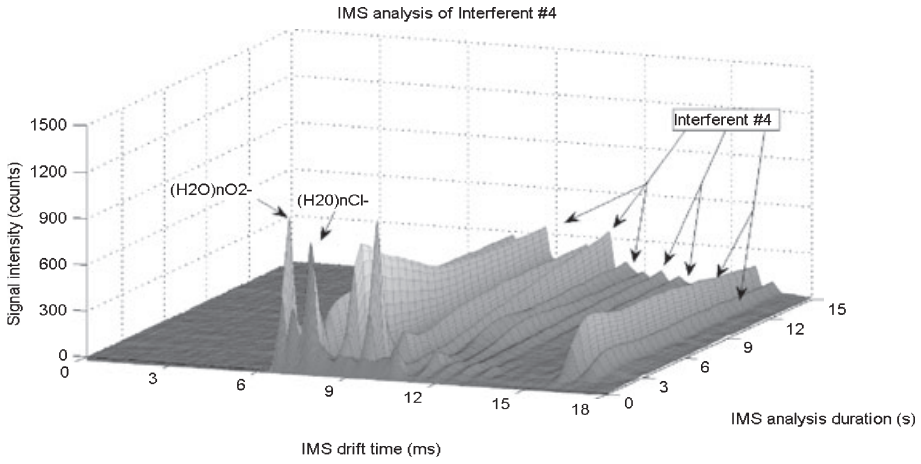

FIG. 4—*IMS analysis of Interferent #4.*

created from Interferent #4 components increased in intensity. Interferent #4 components remained in the IMS for the duration of analysis. Frequently, the interferent components remained in the IMS for most of the duration of analysis (see Figs. 2 and 4). This resulted in carry-over of the interferents into instrument blanks which were collected after each sample analysis. After intervals, ranging from 30 sec to 5 min, the drift gas was able to purge the interferent components from the instrument and the original number of reactant ions was restored. Subsequent IMS analyses could then be continued. The same phenomenon was observed for Interferents #1 and #2.

Figure 5 shows GC/IMS analysis of Interferent #4. The separation of Interferent #4 components can be clearly observed by the separated peaks in the individual IMS scans. Unlike IMS alone (Fig. 4), nearly all Interferent #4 components have been purged from the detector by the end of the GC/IMS analysis duration. The reactant ion(s) have also re-intensified as Interferent #4 components passed through the drift region and charge transfer reactions were completed. A relatively quick recovery of GC/IMS was observed for all four interferents tested.

GC/IMS analysis of "interferent only" samples (Figs. 3 and 5) did not result in carry-over of the interferents into the instrument blanks collected after GC/IMS analysis. Near complete restoration of the baseline and original number of reactant ions occurred toward the end of the analysis (*c.* 3 min) and delays in subsequent GC/IMS analysis were not experienced. This is most likely attributed to the preferential sample loop collection properties and GC separation of interferent components, which prevented saturation and suppression of the IMS signals and enabled the drift gas to purge the interferent more rapidly. Separately, the longer analysis duration of GC/IMS enabled the drift gas to purge the interferent during the entire analysis. Instrument blanks were collected before and after each "interferent only" sample analysis to ensure restoration of the baseline, restoration of the original reactant ion intensity, and absence of carry-over.

Explosive Detection in the Presence of Interferents

After evaluating the detection capabilities of IMS and GC/IMS with each of the five explosives and each of the four interferents separately, the detection of explosives in the presence of interferents was tested. One interferent per swab was prepared and analyzed, as previously described ($n = 10$). A false positive (+) is defined as an instrument alarm when no explosive compound is present or identifying the incorrect explosive compound. A false negative (−) is defined as an instrument response in which the technology did not alarm for the explosive compound in the mixture. For IMS and GC/IMS to identify a chemical, an analyte

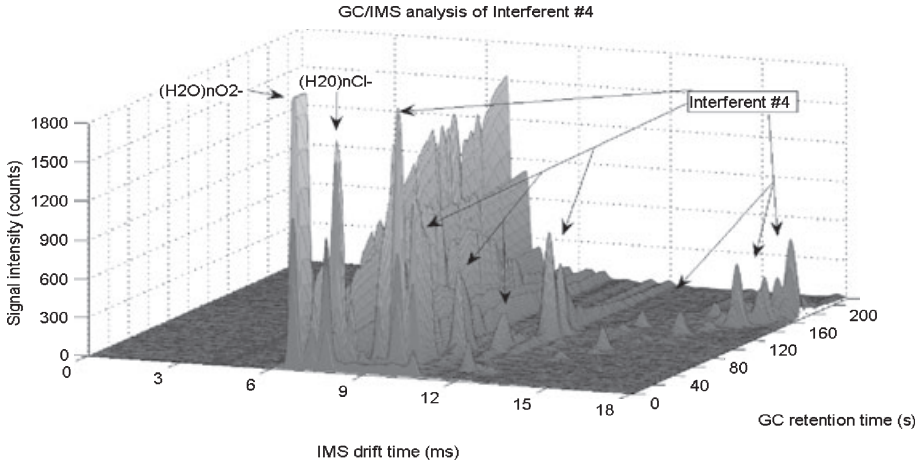

FIG. 5—*GC/IMS analysis of Interferent #4.*

peak(s) must conform to the detection algorithm parameters in the instrument's library. The concentration for each explosive compound in the presence of interferents was set at least one serial dilution concentration higher than the observed MDL. The results are summarized in Table 4.

False Positives

IMS analysis yielded 21 false positive alarms in 100 interferent/explosive combination samples. Of the 21 false positives, 12 occurred when the instrument identified the correct explosive in the sample, but also identified additional explosive compound(s) that were not in the sample. For the remaining nine false positives, the instrument incorrectly identified an explosive that was not in the sample and did not identify the actual explosive compound in the sample. Some false positives occurred because the interferent ion peak(s) had the same drift time as an explosive compound in the instrument's library. The failure to identify the correct explosive compound in four of the nine false positive responses occurred because the detection algorithm was set to search for more than one analyte peak, rather than a single analyte peak to confirm identification, and the criterion for detecting multiple analyte peaks was not met. The use of multiple analyte peak detection is a widely used IMS technique to improve selectivity and minimize false positives. Collectively, these results highlight the fact that IMS has limited capabilities when analyzing complex mixtures and tend toward false positive responses.

Using GC/IMS, the number of false positive responses was substantially reduced to one false positive in 100 interferent/explosive combination samples. For this single false positive response, GC/IMS did not alarm for RDX, but for an explosive compound(s) that was not in the sample. The false positive occurred because the RDX peak amplitude was below the minimum threshold set in the detection algorithm. The mean GC/IMS signal response to 10 ng pure RDX was 57% lower than the mean IMS signal response that triggered an alarm. Loss of sample mostly likely occurred via the GC/IMS sample preconcentrator. A more efficient transfer of sample vapors into the column and the detector with GC/IMS may improve or optimize signal response and further reduce the occurrence of false positives because of lower GC/IMS signal response.

False Negatives

Both IMS and GC/IMS resulted in 11 false negative responses each in 100 interferent/explosive combination samples. The false negative responses by IMS were triggered by one of three conditions:

- The instrument was programmed to alarm when the detection algorithm criterion was met for all analyte peak(s); however, one of the analyte peak(s) was below the minimum threshold set in the detection algorithm criteria.
- The analyte peak was not resolved from an interferent component. The analyte peak did not meet the detection algorithm

TABLE 4—*Summary of GC-IONSCAN® IMS and GC/IMS analysis of explosive compounds in the presence of interferents. The dry weight of Interferents #1, #2, #3, and #4 deposited on a sample swab was* c. *700, 420, 500, and 450 μg, respectively.*

	IMS			GC/IMS			IMS and GC/IMS Used in Sequence		
Interferent	Correct	False (+)	False (−)	Correct	False (+)	False (−)	Correct	False (+)	False (−)
HMTD IMS (10 ng)									
GC/IMS (500 ng)									
#1	4	–	1	5	–	–	5	–	–
#2	5	1*	–	5	–	–	5	–	–
#3	5	3*	–	5	–	–	5	–	–
#4	0	3†	2	5	–	–	5	–	–
PETN IMS (10 ng)									
GC/IMS (100 ng)									
#1	5	–	–	4	–	1	5	–	–
#2	4	1†	–	4	–	1	5	–	–
#3	2	1†	2	5	–	–	5	–	–
#4	0	2†	3	5	–	–	5	–	–
RDX IMS (10 ng)									
GC/IMS (10 ng)									
#1	5	–	–	5	–	–	5	–	–
#2	5	–	–	4	1†	–	5	–	–
#3	5	–	–	5	–	–	5	–	–
#4	5	5*	–	5	–	–	5	–	–
TATP IMS (10 ng)									
GC/IMS (500 ng)									
#1	5	–	–	5	–	–	5	–	–
#2	5	–	–	5	–	–	5	–	–
#3	5	–	–	5	–	–	5	–	–
#4	5	–	–	1	–	4	5	–	–
TNT IMS (10 ng)									
GC/IMS (10 ng)									
#1	5	–	–	5	–	–	5	–	–
#2	5	–	–	0	–	5	5	–	–
#3	0	2†	3	5	–	–	5	–	–
#4	2	3*	–	5	–	–	5	–	–
Total	77 of 100	21	11	88 of 100	1	11	100 of 100	0	0

*Instrument did alarm for the correct explosive in the sample; however, the instrument also alarmed for an additional explosive compound(s) that was not in the sample.

†Instrument alarmed for an explosive compound(s) that was not in the sample.

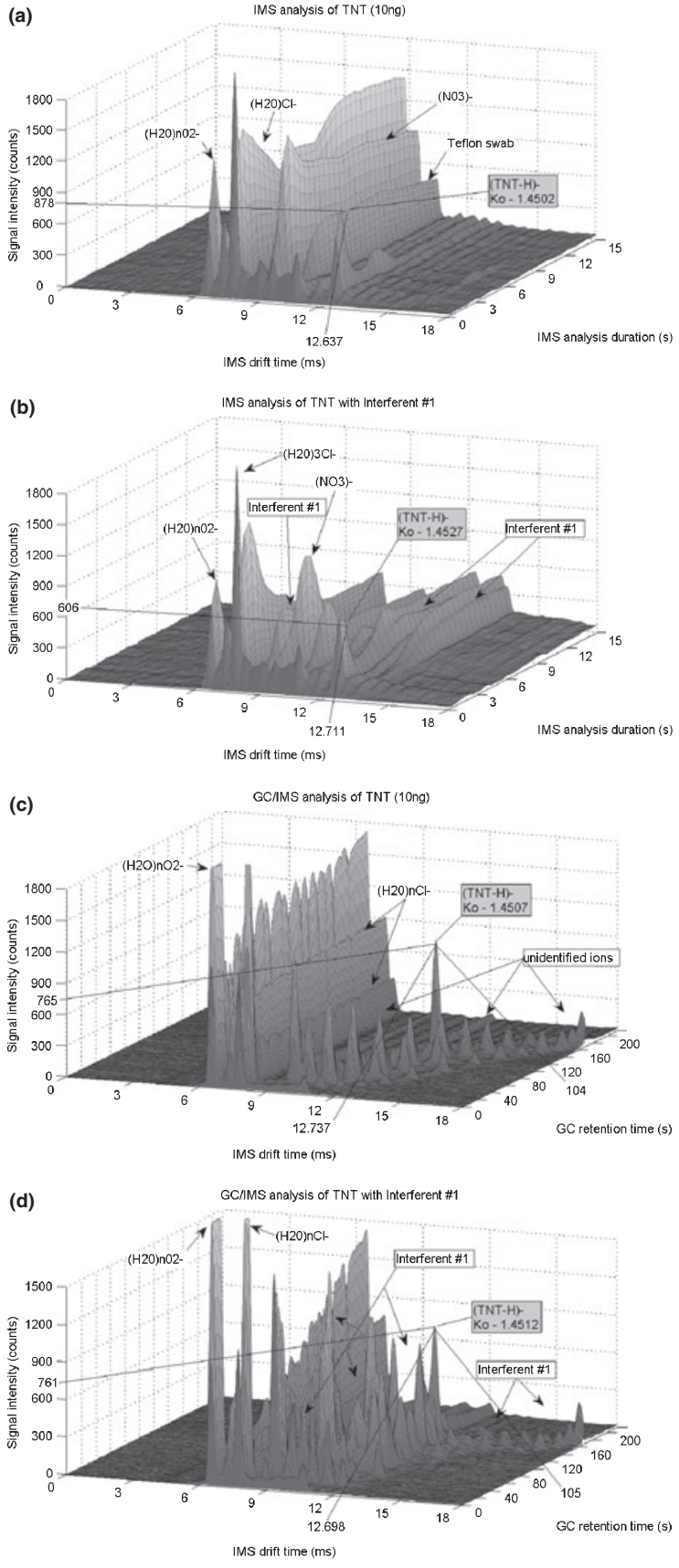

FIG. 6—*(a) IMS analysis of 10 ng TNT. (b) IMS analysis of 10 ng TNT with 700 ug Interferent #1. (c) GC/IMS analysis of 10 ng TNT. (d) GC/IMS analysis of 10 ng TNT with 700 ug Interferent #1.*

criteria for the peak width at half the maximum amplitude because the analyte peak was too broad.
- The analyte peak was present in only a single IMS scan, and the instrument was programmed to identify an analyte only if the analyte peak was present on two successive IMS scans.

The false negative responses by GC/IMS were triggered only by conditions 1 and 2 above.

The effect of analyte peaks not meeting the minimum detection threshold with GC/IMS, may be corrected by redesigning or replacing the sample preconcentrator with a new sample collection medium (trap) for a more efficient transfer of targeted analytes into the column. The effect of peak broadening with GC/IMS can be corrected by improving column temperature control to enhance the chromatography.

Signal Response Suppression

The interferents used in this study also suppressed IMS signal response for the explosive compounds. The suppression of the IMS signal response for the explosive was because of the inability of IMS to separate the complex multicomponent interferents in the samples. IMS plasmagrams and GC/IMS chromatograms from analysis of pure 10 ng TNT and 10 ng TNT with *c.* 700 μg Interferent #1 are shown in Fig. 6 to illustrate how GC separates complex multicomponent interferents.

Figure 6*a* shows IMS analysis of 10 ng TNT ($(TNT\text{-}H)^-$ was detected at 12.637 msec). The maximum peak amplitude recorded for TNT in this sample was 878 counts. Note that when the sample enters the IMS detector the reactant ion peaks decrease in intensity as charge transfer reactions occur. The reactant ion peaks re-intensify as sample molecules pass through the system and charge transfer reactions complete. Some unknown contaminants are present in the plasmagram, which is typical of field analysis.

In Fig. 6*b*, IMS analysis of 10 ng TNT sample with *c.* 700 μg Interferent #1 shows that TNT was also detected at a similar drift time (12.711 msec). The presence of Interferent #1 components resulted in a suppression of signal response to TNT. The maximum peak amplitude recorded for TNT in this sample was 606 counts versus 878 counts with no interferent. This corresponds to a 31% drop in signal intensity for the TNT in this sample. The mean drop in signal intensity ($n = 5$) for TNT with Interferent #1 versus pure TNT was 46%, which was more than one standard deviation of signal response to pure TNT. Note that when the TNT sample with Interferent #1 enters the IMS detector the reactant ion peak decreases in intensity, but do not re-intensify, as interferent constituent molecules pass through the system during the entire analysis. This presence of interferent constituents resulted in carry-over and delay in subsequent sample analysis until interferents were purged from the instrument.

Figure 6*c* shows the addition of GC to IMS for analysis of 10 ng TNT. The chromatogram shows the three-dimensional analysis of GC retention time and IMS drift time plotted against signal intensity. The TNT peak is clearly observed at 104 sec GC retention time and 12.737 msec IMS drift time. The maximum peak amplitude recorded for TNT in this sample was 765 counts. GC/IMS signal response was consistently less than the IMS signal response for all five explosives, which is likely due to loss of analyte. Additional peaks of unknown contaminants of little analytical interest can also be observed in the GC/IMS chromatogram, which is typical of field analysis.

GC/IMS analysis of 10 ng TNT with *c.* 700 μg Interferent #1 (Fig. 6*d*) shows that TNT was detected at a similar GC retention time (105 sec) and IMS drift time (12.698 msec) as 10 ng TNT without Interferent #1 (Fig. 6*c*). The introduction of column effluent into the IMS spread the competitive distribution of charge into the individual IMS scans. Many separate analyte peaks, resulting from Interferent #1 components, were measured between 7 and 15 msec during the first 110 sec of analysis. This is unlike IMS analysis of TNT with Interferent #1 (Fig. 6*b*) in which three distinct analyte peaks were observed for the duration of analysis. The maximum peak amplitude recorded for TNT in this GC/IMS sample analysis was 761 counts versus 765 counts with no interferent (Fig. 6*c*). This corresponds to <1% drop in signal intensity by GC/IMS for the TNT in the sample. The mean drop in signal intensity ($n = 5$) with GC/IMS for TNT with Interferent #1 versus pure TNT was 13%, which was within one standard deviation of signal response to GC/IMS analysis of TNT with no interferent. This was unlike IMS-only analysis which resulted in a 46% drop in mean signal intensity. Further studies involving chemical matrix interferents and the reactant ions they produce in IMS is warranted based on these findings.

Conclusions

There was not an apparent advantage with GC/IMS with regard to false negatives. Both IMS and GC/IMS resulted in 11 false negative responses in 100 interferent/explosive combination samples. However, the low signal response is likely due to limitations with the sample preconcentrator design. This suggests the performance of GC/IMS can be improved with an enhanced sample preconcentrator design that has increased capacity and/or higher affinity for chemicals of concern. This is a correctable situation that could reduce the false negative responses for GC/IMS.

There was an observed advantage with GC/IMS in reducing the number of false positives. There were seven false positive results in 40 "interferent only" samples with IMS compared to no false positives in 40 "interferent only" samples with GC/IMS. When explosive compounds were tested in the presence of interferents, IMS analysis had 21 false positive responses in 100 interferent/explosive combination samples whereas GC/IMS had only one in 100 samples. The reduction in false positives demonstrates a significant advantage of adding a chemical separation technology prior to IMS analysis.

The combination of GC with IMS shows the potential to overcome the difficulties in sampling mixtures with IMS. The potential for extending the LDR through improved sample delivery and preconcentrator design may prove critical for enhancing the performance of field IMS systems. The combined technologies of GC and IMS should be seen as a step in improving the complex problem of reducing false positive and false negative responses where many nontargeted substances create complex matrices and interfere with IMS detection. GC/IMS could be used as a practical intermediate screening tool for validating "IMS only" positive responses in detecting explosive compounds among airport passengers and baggage, cargo shipping containers, buildings, or improvised explosive devices. GC/IMS could also increase Transportation Security Administration, military, law enforcement, and other personnel's confidence with primary screening technology; reduce the effect of complacency when IMS false alarms persist; and provide additional information, with better capability, in a questionable situation.

Acknowledgments

The authors would like to thank Mrs. Kelly Mount and Mr. David McCollam, Federal Bureau of Investigation, Laboratory

Division, Explosives Unit (Quantico, VA), Dr. Mark Miller, Federal Bureau of Investigation, Laboratory Division, Counterterrorism and Forensic Science Research Unit (Quantico, VA), and Dr. Sabatino Nacson and Dr. Alexander Grigoriev, Smiths Detection (Mississauga, Ontario) for their technical support.

References

1. Karasek FW, Kilpatrick WD, Cohen MJ. Qualitative studies of trace constituents by plasma chromatography. Anal Chem 1971;43:1441–7.
2. Karasek FW, Keller RA. Gas chromatograph/plasma chromatograph interface and its performance in the detection of musk ambrette. J Chromatogr Sci 1972;10:626–8.
3. Carr TW. Comparison of the negative reactant ions formed in the plasma chromatograph by nitrogen, air, and sulfur hexafluoride as the drift gas with air as the carrier gas. Anal Chem 1979;51(6):705–11.
4. Baim MA, Hill HH. Halogenated compound response in an oxygen doped ion mobility detector for capillary gas chromatography. J High Resolut Chromatogr Chromatogr Commun 1983;6:4–10.
5. Baumbach JI, Eiceman GA. Ion mobility spectrometry: arriving on site and moving beyond low profile. Appl Spectrosc 1999;53(9):338A–55A.
6. Mieczkowski T. The utilization of ion mobility spectrometry in a criminal justice field. Drug Test Technol 1999;67:73–89.
7. Ewing RG, Atkinson DA, Eiceman GA, Ewing GJ. A critical review of ion mobility spectrometry for the detection of explosives and explosive related compounds. Talanta 2001;54(3):515–29.
8. Yinon J. Field detection and monitoring of explosives. Trends Analyt Chem 2002;21(4):292–301.
9. Buttigieg GA, Knight AK, Denson S, Pommier C, Bonner Denton M. Characterization of the explosive triacetone triperoxide and detection by ion mobility spectrometry. Forensic Sci Int 2003;135:53–9.
10. Eiceman GA, Stone JA. Ion mobility spectrometers in national defense. Anal Chem 2004;76(21):390A–6A.
11. Tam M, Hill HH. Secondary electrospray ionization-ion mobility spectrometry for explosive vapor detection. Anal Chem 2004;76:2741–7.
12. Eiceman GA, Karpas Z. Ion mobility spectrometry, 2nd rev. edn. Boca Rotan, FL: Taylor and Francis, 2005.
13. Perr JM, Furton KG, Almirall JR. Solid phase microextraction ion mobility spectrometer interface for explosive and taggant detection. J Sep Sci 2006;28(2):177–83.
14. Borsdorf H, Eiceman GA. Ion mobility spectrometry: principles and applications. Appl Spectrosc Rev 2006;41(4):323–75.
15. Oxley JC, Smith JL, Kirschenbaum LJ, Marimganti S, Vadlamannati S. Detection of explosives in hair using ion mobility spectrometry. J Forensic Sci 2008;53(3):690–3.
16. Rasanen RM, Nousiainen M, Perakorpi K, Sillanpaa M, Polari L, Anttalainen O, et al. Determination of gas phase triacetone triperoxide with aspiration ion mobility spectrometry and gas chromatography-mass spectrometry. Anal Chim Acta 2008;623:59–65.
17. Karasek FW. The plasma chromatograph research/development. Research/Development 1970;21:34–7.
18. Carr TW, Needham CD. Analysis of organic surface contamination by plasma chromatography/mass spectroscopy. New York, NY: Plenum Publishing Corporation, 1979.
19. Fytche LM, Hupe M, Kovar JB, Pilon P. Ion mobility spectrometry of drugs of abuse in customs scenarios: concentration and temperature study. J Forensic Sci 1992;37(6):1550–66.
20. Eiceman GA, Wang YF, Harden CS, Shoff DB. Enhanced selectivity in ion mobility spectrometry analysis of complex mixtures by alternate reagent gas chemistry. Anal Chem 1995;306:21–33.
21. Spangler GE, Carrico JP, Campbell DN. Recent advances in ion mobility spectrometry for explosives vapor detection. J Test Eval 1985;13:234–40.
22. Hill HH, Siems WF, Louis RH. Ion mobility spectrometry. Anal Chem 1990;62(23):1201A–9A. December 1, 1990.
23. Snyder AP, Harden CS. Portable hand-held gas chromatography/ion mobility spectrometry device. Anal Chem 1993;65:299–306.
24. Matz LM, Tornatore PS, Hill HH. Evaluation of suspected interferents for TNT detection by ion mobility spectrometry. Talanta 2004;54:171–9.
25. Baim MA, Herbert HH. Tunable selective detection for capillary gas chromatography. Anal Chem 1982;54:38–43.
26. Snyder PA, Maswadeh WM, Parsons JA, Tripathi A, Meuzelaar HLC, Doworzanski JP, et al. Field detection of Bacillus spore aerosols with stand-alone pyrolysis-gas chromatography-ion mobility spectrometry. Field Analyt Chem Technol 1999;3(4–5):315–26.
27. Dindal AB, Bayne CK, Jenkins RA, Koglin EN. Explosives detection technology. Barringer Instruments GC-IONSCAN, 2000, Interagency Agreement Number DW89937854, Document Number EPA-VS-SCM-45.
28. Luo Y, Harrington PB. Forensic application of gas chromatography-differential mobility spectrometry with two-way classification of ignitable liquids from fire debris. Anal Chem 2007;79(17):6752–9.
29. Kanu AB, Hill HH. Ion mobility spectrometry detection for gas chromatography. J Chromatogr A 2008;1177:12–27.
30. Rhykerd CL, Hannum DW, Murray DW, Parmeter JE. Guide for the selection of commercial explosives detection systems for law enforcement applications. Washington, DC: National Institute of Justice, 1999 Sept; Report No.: 100-99, Interagency Agreement No 94-IJ-R-004, Project No 97-028-CTT, Document Number NIH Guide 100-99.
31. LaFontaine P, Pilon P, Morrison R, Neudorfl P. The use of GC-IMS to analyze high volume vapour samples from cargo containers. Int J Ion Mobil Spectrom 2001;4(1):34–6.
32. Meuzelaar HLC, McClennen WH, Dworzanski JP, Sheya SA, Snyder AP, Harden CS, et al. Hyphenated techniques; the next generation of field-portable analytical instruments. Proceedings of the Ninth International Symposium on Field Screening Methods for Hazardous Wastes and Toxic Chemicals; 1995 Feb 22–24; Las Vegas, NV. Pittsburgh, PA: Air and Waste Management Association, 1995;38–47.
33. Arnold NS, Hall DL, Wilson R, Snyder AP. A new hand-portable gas chromatography/ion mobility spectrometry system for chemical detection applications. In: Berg DA, editor. Proceedings of the 1996 ERDEC Scientific Conference on Chemical and Biological Defense Research; 1996 Nov 19–22; Aberdeen Proving Ground, MD. Springfield, VA: National Technical Information Service, 1996;225–31.
34. Erickson RP, Tripathi A, Maswadeh WM, Snyder AP, Smith PA. Closed tube sample introduction for gas chromatography-ion mobility spectrometry analysis of water contaminated with a chemical warfare agent surrogate compound. Anal Chim Acta Vol 2006;556(2):455–61.
35. Kanu AB, Ching W, Hill HH. Rapid preseparation of interferences for ion mobility spectrometry. Anal Chim Acta 2008;610:125–34.
36. Sloan KM, Mustacich RV, Eckenrode BA. Development and evaluation of a low thermal mass gas chromatograph for rapid forensic GC-MS analyses. Field Analyt Chem Technol 2001;5(6):288–301.
37. Smith PA, Sng MT, Eckenrode BA, Leow SY, Koch D, Erickson RP, et al. Towards smaller and faster gas chromatography–mass spectrometry systems for field chemical detection. J Chromatogr A 2005;1067:285–94.
38. DeBono R, Grigoriev A, Jackson R, James R, Kuja F, Loveless A, et al. Separation of mixtures using gas chromatography coupled to ion mobility spectrometry. Int J Ion Mobil Spectrom 2002;5(2):194–201.

Additional information and reprints requests:
Brian A. Eckenrode, Ph.D.
Federal Bureau of Investigation
Counterterrorism and Forensic Science Research Unit
Building 12
Quantico, VA 22135
E-mail: baeckenrode@fbiacademy.edu

JOURNAL OF FORENSIC SCIENCES

J Forensic Sci, November 2010, Vol. 55, No. 6
doi: 10.1111/j.1556-4029.2010.01473.x
Available online at: onlinelibrary.wiley.com

TECHNICAL NOTE

GENERAL; PATHOLOGY/BIOLOGY

Kiesha Warren-Gordon,[1] *Ph.D.; Bryan D. Byers,*[1] *Ph.D.; Stephen J. Brodt,*[1] *Ph.D.; Melissa Wartak,*[1] *B.S.; and Brian Biskupski,*[1] *B.S.*

Murder Followed by Suicide: A Newspaper Surveillance Study Using the *New York Times Index*

ABSTRACT: Murder–suicide is a relatively uncommon event but as reported by the *New York Times*, it has occurred and continues to occur yearly. Previous research has indicated that those who commit murder–suicides tend to be men, are in or have been in an intimate relationship with the victim, victims tend to be women, and a firearm is most likely to be used. This study uses a newspaper surveillance methodology to examine such cases. Articles from the *New York Times* as found in the *New York Times Index* were coded, analyzed, and examined. The cases, 166 in total, support the findings from prior research. The trend data was examined by cross tabulations and chi-square analysis. The findings suggest that murder–suicides are rare events and when they occur they usually involve a male perpetrator and an intimate partner victim who is either a wife or girlfriend with the event occurring in a private home. A firearm is the most commonly used method for both murders and suicides, particularly if there was more than one murder victim. The authors conclude by suggesting that future research should focus on using the forthcoming data resource in the CDC's National Violent Death Reporting System (NVDRS) to examine the occurrence of murder–suicide.

KEYWORDS: forensic science, murder–suicide, *New York Times Index*, newspaper surveillance, filicide-suicides, newspaper accounts of suicides

Murders followed by suicide, often referred to as "murder–suicides," are relatively rare events. The rarity of these events, however, does not diminish the devastation of these events on families and the psychological trauma produced among societal members when the news of a murder–suicide reaches them. Several researchers have examined this type of interpersonal violence using a variety of approaches. We examine murders followed by suicide using a newspaper surveillance approach that has been used by others. This study builds on previous research and also extends previous research. It extends previous research given that no other researchers have attempted to conduct a large-scale study of murder–suicide, which examines multiple decades and centuries. We review relevant literature on murders followed by suicide, discuss our newspaper surveillance methodology, present our findings, and offer a discussion and conclusions.

Literature Review

A number of studies have addressed the issue of homicide followed by suicide. Researchers have relied on two main sources when studying murder–suicides. The two sources are (1) local death records and (2) newspaper accounts for a specific geographic area. National data on murder–suicide is not yet fully available for the United States. The Centers for Disease Control (CDC), however, is piloting a project to create a national "violent death" dataset, which will show such connections statistically. At this writing, however, this dataset is not yet available for most geographic areas. Data is available for select areas within the United States for years 2003, 2004, 2005; however, the lack of available sources of data has resulted in researchers relying upon newspaper and media reports along with local records produced by coroners and medical examiners to study murder–suicides.

Our examination of the literature, therefore, purposely focuses on studies using newspaper surveillance given the scope of our study. The use of newspapers reports to examine murder–suicides has been an accepted technique because of the lack of statistical datasets available. The use of newspaper reports has been utilized to examine various aspects of murder–suicides (1–4). In a previous study that examined the relationship between media reporting of suicide and actual suicide in Australia, the authors found that there was a significant relationship between the increase in suicides and attempted suicides in the period following the media report (2). Another study used a newspaper surveillance approach for their data collection (5). They examined a 3-year period between 1997 and 1999 using 191 national newspapers. Classifications were made using a modified Hanzlick-Koponen typology (6). Five relationships between the perpetrator and victim were used along with 13 probable motivations. The majority of the murder–suicides involved intimate partners and guns and were perpetrated by men. Researchers examined murder–suicides in Galveston County, Texas, for an 18-year period. All but one of the perpetrators within the data were men, all but four of the victims were women, all victims and perpetrators were from the same ethnic group, with about half being Caucasian (7). The typical relationships between the victims and the offenders could be considered "intimate," given that the victims

[1]Department of Criminal Justice and Criminology, Ball State University, North Quad 248, Muncie, IN 47306.

Received 14 Mar. 2009; and in revised form 10 Aug. 2009; accepted 5 Sept. 2009.

tended to be a current or ex-girlfriend or spouse. Most of the offenders were very possessive in the relationship and alcohol use was prevalent.

Two commissioned national studies also examined this topic. The Violence Policy Center examined newspaper reports of murder–suicide from January 1, 2001 to June 30, 2001 (8). Operationally, they further stipulated that the suicide had to occur within 24 h of the murder. They point out, as we have, that there is no national tracking system for murder–suicides as well as the fact that murder–suicides might be underestimated. They delineated murder–suicides by state and examined the murder or suicide method, gender of the perpetrator, relationship of the perpetrator to the victim or victims, age of the perpetrator, and the location of the event. Florida had the most murder–suicides with 35 murder–suicides. Ninety-four percent of the total incidents involved a firearm, most offenders were men, most of the relationships were with inmate partners, offenders were older than their victims, most incidents occurred in homes, and the gender of the offender is a predictor of who is murdered. Women tended to kill only the children and themselves, while a man is more likely to murder the entire family. This study also found a higher number of murder–suicide among law enforcement officers.

The National Institute of Justice along with the National Institute on Drug Abuse and the National Institute on Alcohol Abuse and Alcoholism funded a study that also focused on domestic violence as the cause of murder–suicides (9). Using a Danger Assessment instrument, they found that they could reasonably predict those more likely to be killed by their intimate partner. Over 80% of the women killed had a high score, but of those not killed, 40% had a high score. They did find a correlation between being threatened with a gun and being killed. Therefore, some history of interpersonal conflict and domestic violence appeared to precede murder–suicides.

On the other end of the age spectrum, authors looked at spousal murder–suicides in the elderly (10). The factors that were examined in this study were age, the relationship of the perpetrator to the victim or victims, as well as the supposed motivation of murder–suicides. The idea of "suicide pacts" among older couples as being the cause for murder–suicides is actually extremely rare according to their findings. Depression was the most important factor in contributing to murder–suicides, with the healthy partner feeling overworked with care-giving responsibilities on behalf of the ill partner. All the men in the study used a firearm for both the murder and suicide, but the affective disorder of depression was shown to be an important contributing factor to the murder–suicide. Studies have also found that close relationships, such as a wife or a girlfriend, are usually found within the context of a murder–suicide. The relationships are chaotic, being torn between love and hate (11). Morbid jealousy is also present most times, with a proposed separation or actual separation setting off the event. This separation will usually send the offender into a depression, making him feel helpless. After the murder, the offender feels guilt, which is what can lead to the suicide. This process also applies to parents who kill their children.

Previous studies have had several limitations. All of them cover a very limited period of time. Most cover only a few years, with a few covering up to 50 years. A few of these studies examined murder–suicides by state, but none looked at any smaller unit of analysis than a county. Several of the studies were completed overseas, mostly in Australia. Most of the studies conducted in the United States were on a very small analytical level such as a county. They are recorded as two separate events—a murder and a suicide. Because the two crimes are not linked in the records, it makes it difficult to search for such cases as one event.

While previous research has shed light on the characteristics of murder–suicide, these studies may underestimate the frequency and incidence of such events. The current study adds to the social scientific understanding of murder–suicide by examining the reporting of murder–suicides in a national news outlet. This study also adds to the literature that recognizes the value of media to examine social phenomenon such as murder–suicide. In particular, the use of *The New York Times* as the media source for analysis in this study contributes to the body of literature that recognizes this newspaper as a valuable source of data (1). Researchers contend that *The New York Times* is the newspaper of the "national political elite" (1). Researchers argue that the content of *The New York Times* is rich with contemporary events that cannot be matched by other national print media outlets (1).

Methodology

Newspaper Surveillance

Using an approach similar to previous research, a content analysis was conducted of stories about murder–suicides from the *New York Times Index* archives as far back as possible; the *New York Times Index* includes newspaper articles beginning from 1850, the first year examined within this study. The term "murder-suicide" was searched electronically under of a number of different combinations (e.g., "murder-suicide," "murder suicide," "murder and suicide,") to reveal usable cases for analysis. Both murder and suicide articles were returned with nearly 600 total results or "hits" for the inclusive years of 1850 and 2003 (the latest year available at the time of the search). Cases were excluded if the murder–suicide was not confirmed, if only a murder occurred, if only a suicide occurred, or the story was not about an actual event of interest for this study, such as an article about the topic for a book or some fictionalized account. One hundred and sixty-six ($n = 166$) individual cases remained, and these were examined in detail. They ranged in date from December of 1858 to September of 2003. Given there were no murder–suicide statistics available for this time period, comparison could not be made to fully validate the frequency of these cases as reported in the *New York Times* during this period (please see discussion above regarding the CDC data effort).

Variables

From each article, which was treated as the unit of analysis, certain variables were extracted and coded for analysis. The variables were the month of the incident, the day of the incident, the year of the incident, the gender of the perpetrator, the gender of the first victim, the gender of the second victim, the gender of the third victim, the gender of the fourth victim, the location of the first murder, the location of the suicide, the relationship of the first victim to the perpetrator, the relationship of the second victim to the perpetrator, the relationship of the third victim to the perpetrator, the relationship of the fourth victim to the perpetrator, the location of the second murder, the location of the third murder, the location of the fourth murder, the murder method for the first victim, the suicide method for the perpetrator, the state in which incident occurred, the city where the incident occurred, the murder method for the second victim, the murder method for the third victim, the murder method for the fourth victim, the relationship of the fifth victim to the perpetrator, the location of the fifth murder, the murder method for the fifth victim, the gender of the fifth victim, the gender of the sixth victim, the relationship between the sixth victim and the perpetrator, the murder method for the sixth victim, and the location of the sixth murder.

Coding

Obviously, not all variable attributes were present in all cases, but all information that was available was coded. Characteristics from each of the case incidents, by variable, were first entered on to a code sheet. All coded variables were then transferred from the code sheets to SPSS (SPSS Inc., Chicago, IL) for purposes of statistical analysis. The coding method was based on the variables present in the majority of the newspaper articles.

Analysis and Findings

Univariate Findings

Looking at each month, the most murder–suicides occurred during the month of December with a frequency of 14.5% (n = 24), August followed December with 12.0% (n = 20) of cases, and September with 10.8% (n = 18). The perpetrator's gender in 86.1% (n = 143) of the cases was male. Women represent a mere 13.3% of murder–suicide perpetrators. Geographically, the cases represented in the *New York Times* for this analysis occurred all over the nation. However, there was some loading of cases in certain geographic areas. For example, as can be found in Table 1, over 60% of the articles appeared in the Middle Atlantic division. Another 12% came from the New England division. Thus, nearly 63% of the cases reported in the *Times* occurred in the Northeast region of the country. However, the Northeast was not the only region represented with murder–suicide cases. Nearly 8% came from the Midwest region, over 7% occurred in the South region, and another 11.43% came from the West region.

We also examine victims of murder–suicides by gender as shown in Table 2. Over 75% (n = 126) of the first victims were women. For the second victim, it was just as likely to be a man as a woman, being an even split with 22 cases with male second victims and 22 cases with female second victims. Women were the third victim 60% (n = 9) of the time.

Table 2 shows the locations of the first through third murders. The location of both murders and suicides tended to be in private homes or residences. The frequency of the first murder in a private home was 78.5% (n = 124). The more victims there were, the more likely the murder occurred in a private home. The location of the second murder took place in a private home 88.6% (n = 39) of the time, 95.8% (n = 23) of the time for the third murder, and 100% of the time with the fourth and fifth murders. The typical location of the suicide, then, tended to be in the same private home. The suicide frequency in a private home was 73.4% (n = 113). It should be noted that the majority of murder–suicide cases involve one murder and one suicide.

Table 3 presents the murder methods for the first, second, and third victims as well as the perpetrator's method of suicide. The most used murder and suicide instrument was a gun or firearm. The murder method for the first victim was a firearm in 77.6% (n = 125) of the cases. It was the murder method used against the second victim in 73.8% (n = 31) of the cases and 66.7% (n = 16) for the third murder victim. A firearm was used in 77.1% (n = 121) of suicides with other methods being less common.

Table 4 presents the relationship between the first and second victims and the perpetrator. The relationship between the first

TABLE 1—*Cases by national region and division.*

Region Frequency	*n* (%)
Northeast	
Division	
New England (Connecticut, Maine, Massachusetts, New Hampshire, Rhode Island, Vermont)	20 (12.05)
Middle Atlantic (New Jersey, New York, Pennsylvania)	101 (60.84)
Midwest	
Division	
East North Central (Illinois, Indiana, Michigan, Ohio, Wisconsin)	11 (6.62)
West North Central (Iowa, Kansas, Minnesota, Missouri, Nebraska, North Dakota, South Dakota)	2 (1.20)
South	
Division	
South Atlantic (Delaware, District of Columbia, Florida, Georgia, Maryland, North Carolina, South Carolina, Virginia, West Virginia)	6 (3.61)
East South Central (Alabama, Kentucky, Mississippi, Tennessee)	3 (1.80)
West South Central (Arkansas, Louisiana, Oklahoma, Texas)	4 (2.40)
West	
Division	
Mountain (Arizona, Colorado, Idaho, Montana, Nevada, New Mexico, Utah, Wyoming)	4 (2.40)
Pacific (Alaska, California, Hawaii, Oregon, Washington)	15 (9.03)
Total	166 (99.95)*

*Percentages do not sum to 100% because of rounding.

TABLE 2—*Gender and location of murder victim, by victim number.*

	Victims		
	Victim 1	Victim 2	Victim 3
Gender			
Male	23.2% (38)	50.0% (22)	40.0% (6)
Female	76.8 (126)	50.0 (22)	60.0 (9)
Total (*n*)	100.00% (164)	100.00% (44)	100.00% (15)
Location			
Private home	78.5% (124)	88.6% (39)	95.8% (23)
Public place	7.0 (11)	4.5 (2)	4.2 (1)
Business	8.9 (14)	0.0 (0)	0.0 (0)
Woods	2.5 (4)	0.0 (0)	0.0 (0)
Church	0.6 (1)	0.0 (0)	0.0 (0)
Aircraft	1.3 (2)	0.0 (0)	0.0 (0)
Hotel room	1.3 (2)	0.0 (0)	0.0 (0)
Other	0.0 (0)	6.8 (3)	0.0 (0)
Total (*n*)	100.0% (158)	100.00% (44)	100.00% (24)

TABLE 3—*Murder methods by victim number and perpetrator suicide method.*

Method of Murder	Victims			Suicide Method
	Victim 1	Victim 2	Victim 3	Perpetrator
Firearm	77.6% (125)	73.8% (31)	66.7% (16)	77.1% (121)
Knife	8.7 (14)	4.8 (2)	4.2 (1)	5.7 (9)
Asphyxiation	1.9 (3)	0.0 (0)	0.0 (0)	6.4 (10)*
Drowning	1.2 (2)	0.0 (0)	0.0 (0)	1.3 (2)
Poisoning	2.5 (4)	9.5 (4)	8.3 (2)	3.2 (5)
Blunt object	1.9 (3)	0.0 (0)	0.0 (0)	0.0 (0)
Carbon monoxide poisoning	1.9 (3)	2.4 (1)	8.3 (2)	2.5 (4)
Arson	1.2 (2)	2.4 (1)	4.2 (1)	1.9 (3)
Purposely crashing auto	0.6 (1)	2.4 (1)	4.2 (1)	1.9 (3)
Unknown	2.5 (4)	4.8 (2)	4.2 (1)	0.0 (0)
Total (*n*)	100.00% (161)	100.00% (42)	100.00% (24)	100.00% (157)

*While victims died of asphyxiation because of strangulation, perpetrators died of asphyxiation because of hanging.

TABLE 4—*Relationship of first and second victims to the perpetrator.*

Victim Relationship to Perpetrator	Victims	
	Victim 1	Victim 2
Wife	38.0% (63)	0.0 (0)
Girlfriend	12.0 (20)	0.0 (0)
Husband	3.0 (5)	0.0 (0)
Boyfriend	1.2 (2)	0.0 (0)
Acquaintance	3.0 (5)	0.0 (0)
Employer	1.2 (2)	9.4 (3)
Daughter	7.2 (12)	28.1 (9)
Son	4.2 (7)	43.8 (14)
Friend	3.6 (6)	6.3 (2)
Fiancé	0.6 (1)	0.0 (0)
Neighbor	1.8 (3)	0.0 (0)
Other relative	4.8 (8)	12.5 (4)
Business associate	0.6 (1)	0.0 (0)
Co-worker	2.4 (4)	0.0 (0)
Unknown/not reported	16.3 (27)	0.0 (0)
Total (*n*)	100.00% (166)	100.00% (32)

TABLE 5—*Gender of the first victim, by gender of the perpetrator.*

	Perpetrator Gender	
	Male	Female
Victim gender		
Male	19.0% (27)	50.0% (11)
Female	81.0 (115)	50.0 (11)
Total (*n*)	100.0% (142)	100.0% (22)
Relationship of first victim to the perpetrator		
Wife	52.5% (63)	0.0% (0)
Girlfriend	16.7 (20)	0.0 (0)
Husband	0.0 (0)	26.3 (5)
Boyfriend	0.0 (0)	10.5 (2)
Acquaintance	4.2 (5)	0.0 (0)
Employer/co-worker/business associate	5.8 (7)	0.0 (0)
Daughter	3.3 (4)	42.1 (8)
Son	5.0 (6)	5.3 (1)
Friend	3.3 (4)	10.5 (2)
Fiancé	0.0 (0)	5.3 (1)
Neighbor	2.5 (3)	0.0 (0)
Other relative	6.7 (8)	0.0 (0)
Total (*n*)	100.00% (120)	100.00% (19)

victim and the perpetrator was an "intimate" one in most of the cases, with wife and girlfriend being the most prominent. Wives accounted for 38% ($n = 63$) of the first victim cases and girlfriends comprising 12% ($n = 20$) of first victim cases. Sons were found to be the most common second victim at 43.8% ($n = 14$) with daughters being the second most common at 28.1% ($n = 9$).

Bivariate Findings

In examining the bivariate findings, the relationship between the perpetrator's gender and the first victim's gender was found to be statistically significant. In 81% ($n = 115$) of cases, the perpetrator was a man and the first victim was a woman. Female perpetrators were shown to have murdered men and women equally. Table 5 shows this relationship.

The Pearson chi-square test was significant for this relationship ($p < 0.001$). Analyses were conducted on the relationship between the perpetrator's gender and the gender of all other victim types (second through sixth), and no significant relationship was found among these other combinations.

Another factor that was examined was the method of murder and the method of suicide. In this case, murder method was treated as an independent variable and suicide method was treated as a dependent variable because of the temporal order of these events within each case. The percentage of murder–suicide cases where a firearm was used for both the murder and the suicide was 95.2% or the vast majority (chi-square $p < 0.001$). No table is presented for these data given the large number of cells and the heavy loading of cases for two attributes.

The next relationship examined is that of the perpetrator's gender and the relationship the perpetrator had with the first victim. Table 5 shows these findings. As before, we know from our analyses that the most frequent perpetrator is a man. When examining this relationship, it is shown that the most common perpetrator is not only a man but most often kills either a wife or a girlfriend (chi-square $p < 0.001$). Female perpetrators, likewise, most often kill husbands. While the cell sizes are small, it is noteworthy that female perpetrators kill daughters and friends more often than they kill men.

Another relationship examined is the location of the first murder and the location of the suicide. The location of the first murder was treated as an independent variable and the location of the suicide was treated as a dependent variable due, again, to the temporal order of these events. The private home was the most frequent location for both the location of the first murder and the location of the suicide, occurring 93.4% of the time (chi-square $p < 0.001$). No table is provided for this relationship given the large number of cells and the heavy case loading on two attributes.

Trend Data

Given the *New York Times Index* extends to 1850, we also examine trends in the characteristics of murders followed by suicide. Between 1850 and 1900, there were only seven cases of murder followed by suicide reported in the *Times* with the first case being reported in 1858. From 1901 through 1950, there were a total of 17 cases reported. The largest number of cases appeared in the *Times* from 1951 through 2003. During this period, 142 cases of murder followed by suicide were reported. To create three equal 20-year intervals, we examined 1944–1963, 1964–1983, and 1984–2003. We did this for two reasons. First, the majority of murders followed by suicide occurred in the latter half of the 20th century (along with the first few years of the 21st century). Second, we wished to condense the data in such a way that would enable us to present meaningful trend-based discussion regarding a number of murder–suicide case characteristics.

Trend data is presented in Table 6, which includes five separate cross tabulations. There is very little difference concerning perpetrators among the intervals. The vast majority of perpetrators were men in all three intervals. We also found no difference between the intervals regarding the gender of the first victim. The majority were women. The next three relationships do provide some interesting differences. In the first, location of the first murder and private residences (including hotel rooms) remain the most common. However, murders, accompanied later by a suicide, have occurred more often in public places and in business environments and less frequently in rural locations such as a woods ($\chi^2 = 0.042$). Concerning the murder method, firearms remained popular during each of the intervals; however, firearms became more popular in the last interval from 1984 to 2003. Poisoning has become less common over time, and the use of a knife peaked from 1964 to 1983 ($\chi^2 = 0.014$). Finally, the location of the suicide followed a similar pattern to the location of the first murder ($\chi^2 = 0.034$).

TABLE 6—*Chi-square analyses for gender of perpetrator, gender of first victim, location of first murder, murder method, and location of suicide, by three two-decade intervals.*

	Interval		
	1944–1963	1964–1983	1984–2003
Perpetrator			
Male	88.9% (16)	81.4% (35)	90.4% (75)
Female	11.1 (2)	18.6 (8)	9.6 (8)
Total (*n*)	100.00% (18)	100.00% (43)	100.00% (83)
		$p = 0.347$, n.s.	
First victim			
Male	11.1% (2)	31.0% (13)	20.5% (17)
Female	88.9 (16)	69.0 (29)	79.5 (66)
Total (*n*)	100.00% (18)	100.00% (42)	100.00% (83)
		$p = 0.195$, n.s.	
Location of first murder			
Private home/hotel room	77.8% (14)	85.4% (35)	79.5% (62)
Public place/business	11.1 (2)	12.2 (5)	20.5 (16)
Woods	11.1 (2)	2.4 (1)	0.0 (0)
Total (*n*)	100.00% (18)	100.00% (41)	100.00% (78)
		$p = 0.042$*	
Murder method			
Firearm	70.6% (12)	70.7% (29)	87.2% (68)
Knife	5.9 (1)	14.6 (6)	6.4 (5)
Poison	17.6 (3)	4.9 (2)	0.0 (0)
Other	5.9 (1)	9.8 (4)	6.4 (5)
Total (*n*)	100.00% (1817)	100.00% (41)	100.00% (78)
		$p = 0.014$*	
Suicide location			
Private home/hotel room	72.2% (13)	90.2% (37)	82.2% (60)
Public place/business	16.7 (3)	7.3 (3)	17.8 (13)
Woods	11.1 (2)	2.4 (1)	0.0 (0)
Total (*n*)	100.00% (18)	100.00% (41)	100.00% (73)
		$p = 0.034$*	

*Statistically significant chi-square relationship in the bivariate crosstabulation.

Discussion

Most murder–suicides occur during the month of December and also within August and September. The perpetrator's gender was male in most cases. This is not surprising as men are usually the perpetrators of violent crime. The following results are supported by research that has been compiled on the topic of murder followed by suicide (12). The victims, in most cases, were the wives and girlfriends of the perpetrator. In very few cases were the perpetrator and victim or victims strangers. In the cases with more than one victim, the gender and relationship between the perpetrator and victims varied, but usually the relationship was familial. It can be concluded here, as has been demonstrated in previous research, that the majority of murder–suicides occurred within intimate relationships. The location of both murders and suicides tended to be in private homes or residences. The more victims there were, the more likely the murder occurred in a private home. The private home was the most common location not only for first victim but it was also most common for most other victims. This is consistent with prior research given that most participants are family members or are well known to each other. Also when murdering one or more family members, a private home allows the perpetrator to complete the homicide and suicide in relative privacy. A gun or firearm was the most common method for both murder and suicide. In the cases with more than one victim, multiple murder methods were used in some of the cases, but this was rare. Firearms are readily available, relatively quick, and efficient. Moreover, men are more likely to use firearms to commit suicide, so it should not be surprising that such a means is used. Further, firearms tend to be a very "lethal" vehicle for interpersonal aggression. For these reasons and if a firearm is used, the outcome is more likely to be final. As has been found in previous studies, a gun or firearm was the most common murder and subsequent suicide method. Men comprised most of the perpetrators, women made up most of the victims. In the bivariate relationships, gender played a key role in who was killed by male perpetrators, but not for female perpetrators. Male perpetrators were more likely to kill intimate partners such as a wife or girlfriend, while women were more likely than men to kill their children. This finding is consistent with previous research as well.

Finally, we present some trend data. When examining 20-year intervals beginning in 1944 and ending in 2003, we found that the gender of the perpetrator and the gender of the first victim did not change over time. However, we did find significant relationships for the location of the first murder, the murder method, and the suicide location by time interval. While the private residence for the first murder (again most murder–suicides involve one victim) was most common over time, there was an increasing prevalence of murders (followed by suicide) occurring in public places and businesses. While the firearm remained the most common murder instrument over time, it did increase in popularity over the intervals. Also poisoning decreased in popularity as a murder method and the use of knives peaked from 1964 to 1983. Finally, the location of the suicide normally was a private home or hotel room, and we saw similar trends with the location of the suicide as we did with the location of the first murder.

Conclusion

Murder–suicides are rare events. When they do occur, they usually involve a male perpetrator and an intimate partner victim who is either a wife or girlfriend. If there are multiple victims involved beyond an "intimate" other, it is usually children. A firearm is the most commonly used method for both murders and suicides, particularly if there was more than one murder victim. Most murder–suicides occur in a private home or residence. While the plurality of murder–suicides took place in the month of December in this study, this is not believed to be a central factor in murder–suicide incidents. The main characteristic typifying the murder–suicide incident is that these events tend to involve a male perpetrator who kills his "intimate" (or ex-) companion and then turns the gun on himself.

Future researchers should examine the intimate relationships between murder–suicide perpetrators and victims to learn more about events that might lead up to these most devastating incidents. In particular, it would be useful for future researchers to examine murder–suicide cases, retrospectively, to examine the characteristics of such incidents vis-à-vis long-standing domestic violence patterns within tumultuous relationships. Researchers might also examine potential warning signs in interpersonal relationships that could lead to murder–suicide. While it is impossible to predict many forms of violent behavior, there could be a fruitful research agenda in examining potential markers in murder–suicide cases as possible predictors of this lethal interpersonal dynamic. Future researchers also have a potentially valuable and forthcoming data resource in the CDC's National Violent Death Reporting System (NVDRS). This will allow researchers to link homicides and suicides within the same case and permit more detailed, reliable, and useful analyses of murder–suicides.

References

1. Chesebro J, McMahan D. Media constructions of mass murder–suicides as drama: the New York Times' symbolic construction of mass murder–suicides. Commun Q 2006;54:407–25.
2. Pirkis J, Burgess P, Francis C, Blood W, Jolley D. The relationship between media reporting of suicide and actual suicide in Australia. Soc Sci Med 2006;62:2874–86.
3. Nikunen M. Parenthood in murder-suicide news. Idealized fathers and murderous mums. J Scand Stud Criminol Crime Prev 2006;7:164–84.
4. Liem M, Koenraadt F. Homicide-suicide in the Netherlands: a study of newspaper reports, 1992–2005. J Forens Psychiatry Psychol 2007;4: 482–93.
5. Malphur JE, Cohen D. A newspaper surveillance study of homicide-suicide in the United States. Am J Forensic Med Pathol 2001;23:142–8.
6. Hanzlick R, Koponen M. Murder-suicide in Fulton County, Georgia, 1988–1991: comparision with a recent report and proposed typology. Am J Forensic Med Pathol 1994;15:168–73.
7. Felthous AR, Hempel AG, Heredia A, Freeman E, Goodness K, Holzer C. Combined homicide-suicide in Galveston County. J Forensic Sci 2001;46:586–92.
8. Brock K, Bishop C, Burgess S. American roulette: the untold story of murder-suicide in the United States. Washington, DC: Violence Policy Center, 2002; 1–18.
9. Campbell JC, Webster D, Koziol-McLain J, Block CR, Campbell D, Curry MA. Assessing risk factors for intimate partner homicide. Natl Inst Justice J 2003;250:15–9.
10. Malphur JE, Cohen D. A statewide case–control study of spousal homicide-suicide in older persons. Am J Geriatr Psychiatry 2005;3:211–7.
11. Stack S. Homicide followed by suicide: an analysis of Chicago data. Criminology 1997;35(3):435–53.
12. Lester D. Why people kill themselves: a 2000 summary of research on suicide, 4th edn. Springfield, IL: Charles C. Thomas, 2000.

Additional information and reprint requests:
Kiesha Warren-Gordon, Ph.D.
Department of Criminal Justice and Criminology
Ball State University
North Quad 256
Muncie, IN 47306
E-mail: kwarrengordo@bsu.edu

JOURNAL OF FORENSIC SCIENCES

J Forensic Sci, November 2010, Vol. 55, No. 6
doi: 10.1111/j.1556-4029.2010.01527.x
Available online at: onlinelibrary.wiley.com

TECHNICAL NOTE

PATHOLOGY/BIOLOGY; GENERAL

Lars Uhrenholt,[1] *Ph.D., D.C. and Lene W. T. Boel,*[1] *Ph.D., M.D.*

Contributions from Forensic Imaging to the Investigation of Upper Cervical Fractures

ABSTRACT: Injuries to the upper cervical spine (UCS) are common in traumatic deaths and postmortem computed tomography (PMCT) may contribute to the forensic investigation. This study presents PMCT in comparison with autopsy in the examination of UCS injury. Thirteen consecutive cases with UCS fracture and/or cranio-cervical dislocation were examined with PMCT and autopsy, and the findings were correlated. Neither of the techniques identified all UCS injuries. Fractures of atlas and axis were best visualized with PMCT whereas cranio-cervical dislocation was better identified during autopsy. Serious injuries were present after both high- and low-energy trauma. Medico-legal autopsy in combination with PMCT produced a thorough evaluation of UCS injuries. By combining these procedures detailed investigations, including accident reconstruction and injury pattern analysis, can be performed. This study supports the routine application of PMCT, as a supplement to the medico-legal autopsy of deaths with UCS injuries.

KEYWORDS: forensic science, forensic radiology, computed tomography, forensic pathology, upper cervical spine, injury, virtopsy

Injuries to the upper cervical spine (UCS) are a common consequence of serious traumatic loading of the UCS complex because of traffic crashes, falls from heights, and assaults. In traumatic deaths, UCS injuries are common and therefore often identified during autopsy. Although not always fatal, these types of injuries are serious and carry a high risk of spinal cord injury and death. In the acute stage of UCS injury, death may be instantaneous because of respiratory arrest or spinal chock. Survivors from such injuries are likely to suffer from sequelae, particularly because of spinal cord injury, despite efficient surgical stabilizing intervention, and secondary complications may arise thereby increasing the risk of delayed death (1,2). The UCS includes atlas C1 and axis C2, and UCS injuries include primarily fractures of the osseous structures (3,4), cranio-cervical dislocation (4), articular cartilage injury (4,5), ligamentous injury with or without subsequent instability (6), vascular injury (7,8), and neurological injury (9,10). These injuries may be present as solitary lesions or in combination. For obvious reasons, identification of UCS injury is of high concern in clinical settings. The therapeutic approach of clinicians and surgeons is based upon knowledge of pathoanatomical conditions, types of injury, prevalence, and methods of identification. Similar to clinicians and surgeons, forensic pathologists need to be able to identify UCS injuries as they most often contribute significantly to the cause of death. During medico-legal autopsy, identification of UCS injuries may be difficult, especially if procedures displaying the cranial vault and the UCS from the anterior and posterior aspects cannot be utilized. UCS injuries may be subtle and are sometimes disguised by absent bleeding and undisplaced fractures. Hence, supplemental autopsy procedures are necessary to improve the sensitivity of the investigation. Advanced postmortem diagnostic imaging procedures, including postmortem computed tomography (PMCT) and magnetic resonance imaging (MRI), have the unique potential of displaying the UCS in great detail. Numerous studies have described the general advantages of postmortem diagnostic imaging, including also conventional X-ray techniques. However, only limited data are available concerning the contributions from advanced postmortem diagnostic imaging procedures in the investigation of upper cervical fractures (11).

In this study, findings from PMCT were correlated with autopsy findings in 13 consecutive cases who had suffered UCS fracture and/or cranio-cervical dislocation. The aim of this study was to identify and discuss advantages and limitations of these adjunct procedures.

Methods

We conducted a review of a database at the Department of Forensic Medicine, University of Aarhus, for UCS fractures over a period of 12 months. Included were cases where subjects' had been exposed to a broad range of traumatic events (road traffic crashes, falls, and assaults) leading to death. The manner of death was suicide, homicide, or accidental, and all natural deaths were excluded. Only cases with an UCS fracture (atlas C1 and/or axis C2), identified during the medico-legal investigation either by autopsy and/or PMCT, had to be present. Only cases where PMCT examination had been performed after the death were included, thereby excluding cases with antemortem CT scanning or lack of CT scanning. Each case was reviewed with regard to mechanism of trauma, time of death after the traumatic event, findings during autopsy, and CT findings.

Postmortem Computed Tomography

PMCT was performed at the Department of Forensic Medicine, University of Aarhus. For the PMCT examination, the bodies were scanned as they arrived at the department, i.e., wearing their clothes, jewelry, and in some cases antemortem hospital treatment

[1]Department of Forensic Medicine, University of Aarhus, Aarhus, Denmark.

Received 30 June 2009; and in revised form 22 Sept. 2009; accepted 4 Oct. 2009.

devices (intubation tubes, catheters, etc.). An in-house Siemens Definition 64 slice scanner (Siemens Healthcare, Ballerup, Denmark) was used performing whole-body scanning. The examination was divided topographically into three body parts (head and neck, torso and abdomen, and lower extremity), each with specific console settings, which could then be performed in one undisturbed sequence. The head and neck sequences used a slice thickness of 1 mm, and in some cases, additional reconstructions with a slice thickness of 0.64 mm were produced. Console standard settings were 140 kV, 500 mAs, and 0.75 pitch. From the PMCT data reconstructions were made using different algorithms (H20S smooth and H60S sharp), available in the workstation software provided by the manufacturer. Each PMCT examination took approximately 20 min, including transportation of the deceased, scout view of the body, whole-body CT, and completion of the predetermined reconstruction sequences. The PMCT images were initially evaluated by an experienced forensic pathologist in all cases, and in four selected cases, a senior radiologist with postmortem radiology experience also evaluated the images. Following the initial evaluation, each of the cases was reviewed by the authors to complete a detailed description and classification of the injuries identified according to previously published classification systems (4,12–14).

Medico-legal Autopsy

The deceased were examined at autopsy, within 1–2 h after the PMCT examination, using routine procedures. In all cases, an anterior Y-incision approach was utilized, according to previously described procedures, allowing visualization of the anterior part of the UCS (15).

Evaluation of the Postmortem Computed Tomography and Medico-legal Autopsy Findings

The data obtained from the PMCT examination and the findings from the autopsy were compared.

Results

The retrospective study of deceased with UCS fractures following trauma resulted in inclusion of 13 cases (five women and eight men, mean age 44 years, range 15–64 years), who had all been examined after death with CT scanning and medico-legal autopsy. The manner of death was homicide in two cases, accidental in 11 cases (seven traffic related, three falls, and one blow to the head from aeroplane wing). The time from trauma to death ranged between 0 and 20 days (mean 2.3 days, median 0 days). In three cases, an antemortem CT scanning had been performed prior to the death. There were consistent CT findings in the three cases where antemortem and PMCT scanning had been performed.

There were three cases with cranio-cervical fracture/dislocation, three cases with atlas fractures, and nine cases with axis fractures (four odontoid process fractures). There was agreement between the autopsy findings and the PMCT findings in 10 cases; in one case, autopsy was more sensitive and in two cases, PMCT revealed more findings (Table 1). Autopsy revealed a cranio-cervical dislocation with a fracture of C1 in a case of a 45-year-old male motorcycle driver who crashed into a motor vehicle. Although there was bleeding and fragmentation from a fracture of the clivus/occipital condyle, no displacement was observed of the cranium over the atlas on the PMCT images and cranio-cervical dislocation could

TABLE 1—*Case-specific demographics regarding autopsy and PMCT findings of the UCS.*

Case #	Gender	Age	Mechanism of Trauma	Autopsy Findings (UCS Only)	PMCT Findings (UCS Only)
1	Female	22	Ejectee from motor vehicle	Fracture of the odontoid process of C2	Fracture of the odontoid process of C2 (type II) with anterior displacement of the fragment
2	Male	55	Hit from behind by an aeroplane wing during taxi	Sequelae following spondylodesis of C0–C3 secondary to fracture of C1 and C2	Sequelae to spondylodesis of C0-C3. Fracture of C1 anteriorly and posteriorly, and fracture of the odontoid process of C2 (type III)
3	Female	64	Fall from wheelchair	Fracture of the odontoid process of C2	Undisplaced fracture of the odontoid process of C2 (type III)
4	Male	45	Crash on bicycle	Oblique fracture of the odontoid process of C2	Fracture of the odontoid process of C2 (type II)
5	Male	45	Motorbike collision into motor vehicle	Cranio-cervical dislocation and fracture of C1	No injury detected
6	Male	43	Motor vehicle collision (driver of van)	Fracture of C1	Fracture of the left lateral mass of C1
7	Male	18	Motor vehicle collision into a truck followed by fire (deceased was driver of vehicle)	Fracture of body of C2	Fracture of the body of C2 posteriorly extending into the pedicles bilaterally and left posterior arch of C1
8	Male	41	Homicide by shooting with shotgun using a Brennecke-bullet	Fracture of C2	Fracture of the right laminae of C2
9	Female	15	Pedestrian hit by a motor vehicle	Cranio-cervical dislocation with localized bleeding	Cranio-cervical dislocation and fracture of the right anterior arch of C1
10	Female	55	Motor vehicle collision (hit from the front right during a left turn)	Cranio-cervical dislocation	Cranio-cervical dislocation
11	Female	45	Homicide (killed by knifestabbing)	Fracture of the laminae (posterior arch) of C2 (posterior arch)	Fracture of the laminae of C2
12	Male	63	Fall from stairways	Fracture of C2	Fracture of the body of C2
13	Male	60	Fall from tree	Fracture of the odontoid process of C2	Multifragmentary fracture (comminuted) of the body and posterior aspects of C2

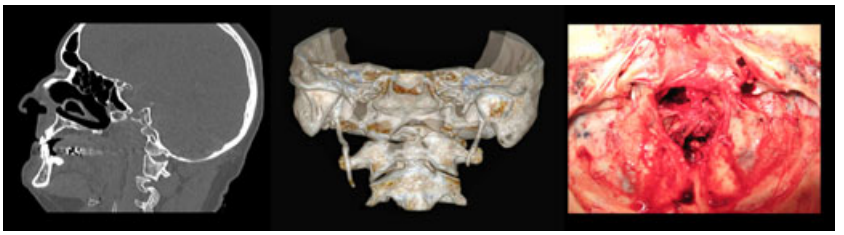

FIG. 1—*Sagittal and three-dimensional reconstructed PMCT images (left and center) of an undisplaced cranio-cervical dislocation that was undiagnosed on PMCT. Fragmentation of a clivus/condylar fracture is evident in the foramen magnum on the macroscopic photograph (right) through the foramen magnum viewed from above, as well as on the sagittal images.*

not be identified (Fig. 1). Neither was a discrete fracture of C1 identified on PMCT imaging. PMCT revealed two cases with C1 fractures that were not identified during autopsy. In one case, a 15-year-old female pedestrian was hit by a motor vehicle, from which she suffered a cranio-cervical dislocation, which was identified during autopsy, as well as a fracture of the right anterior arch of C1 with insignificant bleeding which could only be seen on the PMCT images. In the other case, an 18-year-old male driver of a motor vehicle collided with a truck after which his vehicle completely burned out. He suffered a fracture of the body of C2, but also a fracture of the posterior arch of C1. The C1 fracture was not identified during the autopsy.

PMCT allowed detailed description of the different types of fractures, i.e., C2 fractures: two type II and two type III odontoid, two body, two posterior arch, and one multifragmentary fracture of the body and posterior aspects (Fig. 2), and C1 fractures: one Jefferson, one anterior arch, one posterior arch, and one lateral mass fracture. Furthermore, visualization of postsurgical intervention was clearly visible using the PMCT images (Figs 3 and 4).

Discussion

This review of 13 consecutive unique cases with UCS fractures revealed that postmortem forensic imaging procedures in combination with medico-legal autopsy produced a thorough evaluation and precise classification of fractures. Fractures of atlas and axis were best visualized with imaging procedures, and in some cases only identified with such. However, cranio-cervical fracture/dislocation was better identified with autopsy. Fractures of the UCS complex were present after both high- and low-energy trauma and contribute significantly to the cause of death.

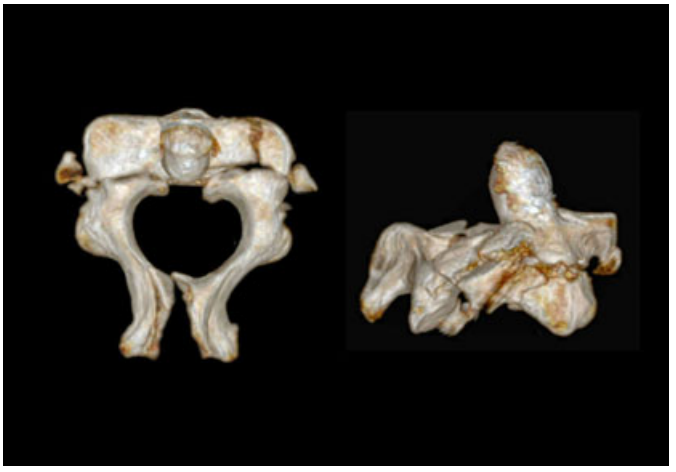

FIG. 2—*Carefully enhanced three-dimensional reconstructions of PMCT images showing the second cervical spine vertebrae (axis C2) from above (left) and from the right side slightly angled (right). A multi-fragmentary fracture (comminuted) is present, involving the body, the transition between the body and the pedicles, the transverse processes and the spinous process.*

Cranio-cervical Dislocation

Fracture/dislocation of the cranio-cervical region was reported in three cases based on the autopsy and one of these could not be identified with PMCT. The discrepancy is likely because of the fact that autopsy also allows manual testing of stability which is not possible during PMCT. In the case with the missed cranio-cervical dislocation, there was no distortion of the cranio-cervical structures. In contrary, a fragment from the clivus/occipital condyle fracture may have disturbed the interpretation as the localized bleeding was thought to arise from this fracture, hindering identification of the dislocation on PMCT scanning (Fig. 1; [4]). Hence, it is very unlikely that a cranio-cervical dislocation remains undiagnosed during medico-legal autopsy; however, these findings suggest that relying solely on postmortem diagnostic imaging findings in a medico-legal investigation carry the risk of missing this significant injury.

Atlas C1 Fractures

Fractures of the atlas C1 were difficult to visualize during the medico-legal autopsy, particularly at the posterior arch, which is not displayed during routine autopsy procedures. Although the posterior aspect may be displayed during autopsy, this requires more invasive procedures which are not routinely performed (11).

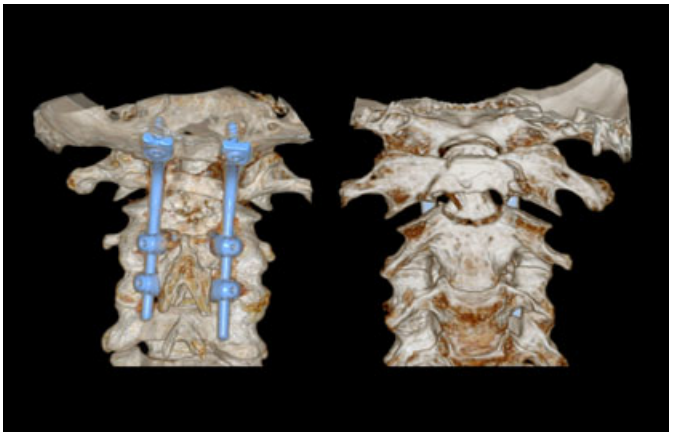

FIG. 3—*Three-dimensional formatted images of PMCT showing correctly placed surgical stabilization of atlas and axis fractures by spondylodesis of the cranio-cervical region (metal brackets). Furthermore, an odontoid process fracture (type II) and atlas fractures are visualized. Viewed from the back (left) and the front (right).*

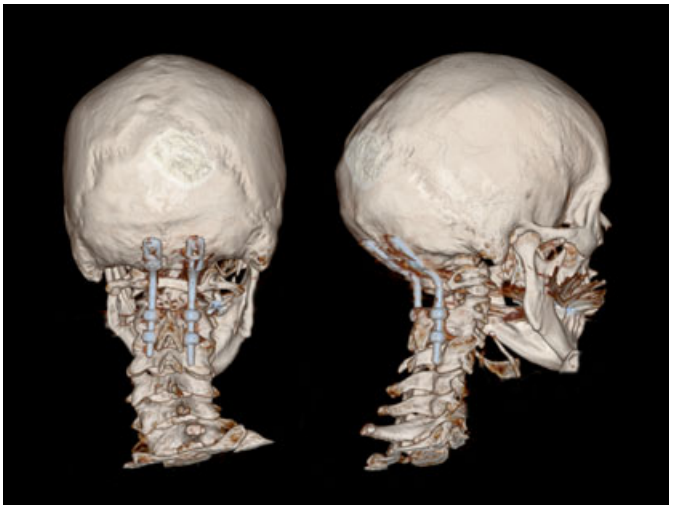

FIG. 4—*Three-dimensional formatted images of PMCT providing images for the analysis of surgical intervention.*

Although discrete in nature, atlas fractures should be identifiable on both routine autopsy and PMCT. Nonetheless, there was disagreement between autopsy and PMCT with regard to the presence of three atlas fractures, which is somewhat anticipatable with regard to the aforementioned posterior undisclosed anatomical region. Precise description and classification of the fractures, according to the most commonly used classification systems (4,12,14), was possible using the PMCT images.

The importance of a distinct classification of an atlas fracture in a forensic context may seem trivial at first hand. However, beyond the necessary accuracy of the forensic report, this has importance for the purpose of epidemiological documentation. In selected cases, identification of unique fractures improves the likelihood of accurate reconstruction of loading characteristics and description of circumstances of any particular event (11,12). As with other types of objective evidence of injury this may have judicial relevance in cases with conflicting evidence (16–18).

Axis C2 Fractures

The most common type of fracture in this study was axis C2 fractures, and all nine cases with axis fractures were identified with both autopsy and PMCT. The odontoid process, which was fractured in four cases, is often exposed during high-energy hyperextension loading of the cervical spine, but also minor trauma, such as a fall from a wheelchair, may also produce this type of injury (Table 1). Most often, significant fractures through the basis of the odontoid process, or through the corpus of C2, are associated with localized bleeding leading the pathologist to the diagnosis. All cases in this study used an anterior dissection approach only, and it is possibly that using a posterior dissection approach would supply additional information to the forensic pathologist. However, in each case, the pathologist found that sufficient information had been retrieved based on PMCT data and the autopsy findings. In this study, the exact classification of odontoid process fractures, according to the system proposed by Anderson and D'Alonzo (3,4,13), was only possible by examination of the CT images in comparison with routine autopsy procedures. Removal of tissue samples for more detailed macroscopic and microscopic examination does however allow this identification and classification, although this involves a more invasive approach (11). Interestingly, one case with bilateral fractures of the transverse processes of C2 was reported as a part of a multifragmentary fracture (Fig. 2). Such injuries are associated with injury to the vertebral arteries, being an important part of the cranio-cervical blood supply, and this may have contributed to the cause of death (7).

Postmortem Computed Tomography

By focusing solely on the UCS in this study, it was possible to confirm some of the advantages of PMCT primarily that it allows a very detailed visualization of UCS fractures, thereby improving the precision and quality of the medico-legal investigation. Furthermore, by reducing the slice thickness to 0.64 mm, highly detailed images may be produced, further improving the quality of the volume rendered images through the three-dimensional reformatting processes. Such images are extremely illustrative, and for the purpose of medico-legal judicial presentation of findings, this offers a unique opportunity to present detailed data for the court. Albeit expensive, PMCT is a practicable tool requesting limited time-resources for the individual investigation, and implementation in the forensic community is recommended (19,20).

Despite the favorable outcome of the CT procedures in this study, other studies have identified a number of limitations with regard to resolution, sensitivity, and specificity (11,21,22), and we also identified injuries during autopsy that could not be visualized using PMCT. Although this study did not utilize conventional radiography, the literature shows that this procedure is associated with an even higher degree of limitations than PMCT. Hence, it is possible that some of the injuries detected in this study, for example the cases with laminar fractures and cranio-cervical dislocation, would have been missed using conventional radiological examination of the cervical spine (19,21–24).

PMCT is regarded as an adjunct procedure to the forensic autopsy whereby the highest level of precision of the medico-legal investigation can be maintained. PMCT does not visualize articular cartilage or the ligamentous complex in any great detail, and discrete osseous injuries may remain undiagnosed (21). With recent advances in CT (dual source CT scanners), simultaneous scanning in two energy levels may improve visualization of structures with different Houndsfield unit characteristics in the same scanning sequence. Currently, however, these structures are best examined with MRI although this also suffers from limitations with sensitivity (11,21,25). An additional advantage of PMCT in forensic settings is the detailed visualization of surgical intervention, as shown in Figs 3 and 4. The PMCT images are particularly useful and contribute with very detailed information to the forensic pathologist's analysis of surgical intervention which is often problematic.

Relevance of Findings

Continuous improvement in the knowledge of UCS pathoanatomy is necessary for optimal management strategies of casualties in clinical settings as well as in the reporting of these injuries in forensic settings. It is clear from this study that advanced diagnostic imaging procedures contributes significantly to the medico-legal investigation of UCS fractures following trauma. Unfortunately, there appears to be an underreporting of UCS injuries in Denmark because of the low number of medico-legal autopsies performed of people killed in traffic crashes, as less than 20% of road traffic crash fatalities are investigated with postmortem autopsy (26,27). To gain more precise insight into the extent of UCS injuries in traffic-related deaths, both increases in number of autopsies performed and increased utilization of adjunct diagnostic imaging procedures are needed. As relatively minor-energy transfer trauma,

such as a simple fall from same level, is also capable of producing fractures of the UCS, such injuries need to be suspected in a range of traumatic exposures relating to death (28,29). Routine utilization of PMCT in the examination of traumatic deaths seems to be a logic integration of this sensitive diagnostic tool to the medico-legal investigation.

Conclusions

This study of PMCT and autopsy findings from 13 consecutive cases with UCS fracture and/or cranio-cervical dislocation revealed that these procedures in combination produce a thorough evaluation and precise classification of fractures. Neither of the techniques identified all UCS injuries. Fractures of atlas and axis were best visualized with imaging procedures whereas cranio-cervical dislocation was better identified with autopsy. Fractures of the UCS complex were present after both high- and low-energy trauma. This study supports the implementation of PMCT in forensic settings on a routine basis as a supplement to the medico-legal autopsy which remains the most central element of the medico-legal investigation.

Acknowledgments

The authors thank senior consultant, A.G. Jurik, DMSc., Department of Radiology, Aarhus University Hospital, Aarhus Sygehus, Denmark, for her participation in the PMCT interpretation and Professor Annie Vesterby, DMSc., for having commented on the manuscript.

References

1. Soden RJ, Walsh J, Middleton JW, Craven ML, Rutkowski SB, Yeo JD. Causes of death after spinal cord injury. Spinal Cord 2000;38(10):604–10.
2. Lidal IB, Snekkevik H, Aamodt G, Hjeltnes N, Biering-Sorensen F, Stanghelle JK. Mortality after spinal cord injury in Norway. J Rehabil Med 2007;39(2):145–51.
3. Clark CR, White AA III. Fractures of the dens. A multicenter study. J Bone Joint Surg Am 1985;67(9):1340–8.
4. Pathria M. Physical injury: Spine. In: Resnick D, Kransdorf M, editors. Bone and joint imaging, 3rd edn. Philapelphia, PA: Elsevier Saunders, 2005;879–904.
5. Schonstrom N, Twomey L, Taylor J. The lateral atlanto-axial joints and their synovial folds: an in vitro study of soft tissue injuries and fractures. J Trauma 1993;35(6):886–92.
6. Krakenes J, Kaale BR. Magnetic resonance imaging assessment of craniovertebral ligaments and membranes after whiplash trauma. Spine 2006;31(24):2820–6.
7. Inamasu J, Guiot BH. Vertebral artery injury after blunt cervical trauma: an update. Surg Neurol 2006;65(3):238–45.
8. Nedeltchev K, Baumgartner RW. Traumatic cervical artery dissection. Front Neurol Neurosci 2005;20:54–63.
9. Taylor JR, Twomey LT, Kakulas BA. Dorsal root ganglion injuries in 109 blunt trauma fatalities. Injury 1998;29(5):335–9.
10. McKinley W, Santos K, Meade M, Brooke K. Incidence and outcomes of spinal cord injury clinical syndromes. J Spinal Cord Med 2007;30(3):215–24.
11. Yen K, Sonnenschein M, Thali MJ, Ozdoba C, Weis J, Zwygart K, et al. Postmortem multislice computed tomography and magnetic resonance imaging of odontoid fractures, atlantoaxial distractions and ascending medullary edema. Int J Legal Med 2005;119(3):129–36.
12. Levine AM, Edwards CC. Fractures of the atlas. J Bone Joint Surg Am 1991;73(5):680–91.
13. Anderson LD, D'Alonzo RT. Fractures of the odontoid process of the axis. J Bone Joint Surg Am 1974;56(8):1663–74.
14. Jefferson G. Fracture of the atlas. Report of four cases, and review of those previously recorded. Br J Surg 1920;7:407–22.
15. Vanezis P. Pathology of neck injury. London, UK: Butterworth & Co. (Publishers) Ltd., 1989.
16. Freeman MD, Rossignol AM, Hand ML. Forensic epidemiology: a systematic approach to probabilistic determinations in disputed matters. J Forensic Leg Med 2008;15(5):281–90.
17. Freeman MD, Nelson C. Injury pattern analysis as a means of driver identification in a vehicular homicide; a case study. Forensic Exam 2004;13(1):24–8.
18. Buck U, Christe A, Naether S, Ross S, Thali MJ. Virtopsy—noninvasive detection of occult bone lesions in postmortem MRI: additional information for traffic accident reconstruction. Int J Legal Med 2009;123(3):221–6.
19. Thomsen AH, Jurik AG, Uhrenholt L, Vesterby A. An alternative approach to computerized tomography (CT) in forensic pathology. Forensic Sci Int 2009;183(1–3):87–90.
20. Poulsen K, Simonsen J. Computed tomography as routine in connection with medico-legal autopsies. Forensic Sci Int 2007;171(2–3):190–7.
21. Uhrenholt L, Nielsen E, Vesterby Charles A, Hauge E, Gregersen M. Imaging occult lesions in the cervical spine facet joints. Am J Forensic Med Pathol 2009;30(2):142–7.
22. Iwase H, Yamamoto S, Yajima D, Hayakawa M, Kobayashi K, Otsuka K, et al. Can cervical spine injury be correctly diagnosed by postmortem computed tomography? Leg Med (Tokyo) 2009;11(4):168–74.
23. Holmes JF, Akkinepalli R. Computed tomography versus plain radiography to screen for cervical spine injury: a meta-analysis. J Trauma 2005;58(5):902–5.
24. Griffen MM, Frykberg ER, Kerwin AJ, Schinco MA, Tepas JJ, Rowe K, et al. Radiographic clearance of blunt cervical spine injury: plain radiograph or computed tomography scan? J Trauma 2003;55(2):222–6.
25. Friedrich KM, Trattnig S, Millington SA, Friedrich M, Groschmidt K, Pretterklieber ML. High-field magnetic resonance imaging of meniscoids in the zygapophyseal joints of the human cervical spine. Spine 2007;32(2):244–8.
26. Uhrenholt L, Gregersen M. Hvorfor obduceres så få trafikdræbte? Dansk Politi 2003;5:30–1.
27. Uhrenholt L, Schumacher B, Freeman M. Road trafffic fatalities in Aarhus Police District in 2000-2004—medical investigations and legal consequences. Copenhagen, Denmark: Ugeskr Laeger. In press.
28. Ejlersen JA, Dalstra M, Uhrenholt L, Charles AV. An unusual case of sudden unexpected death: postmortem investigation and biomechanical analysis of the cervical spine. J Forensic Sci 2007;52(2):462–6.
29. Freeman MD, Croft AC, Nicodemus CN, Centeno CJ, Elkins WL. Significant spinal injury resulting from low-level accelerations: a case series of roller coaster injuries. Arch Phys Med Rehabil 2005;86(11):2126–30.

Additional information and reprint requests:
Lars Uhrenholt, Ph.D.
Assistant Professor
Department of Forensic Medicine
University of Aarhus
Brendstrupgaardsvej 100
8200 Aarhus N
Denmark
E-mail: lu@forensic.au.dk

JOURNAL OF FORENSIC SCIENCES

J Forensic Sci, November 2010, Vol. 55, No. 6
doi: 10.1111/j.1556-4029.2010.01502.x
Available online at: onlinelibrary.wiley.com

TECHNICAL NOTE

PATHOLOGY/BIOLOGY

Graziela M. Biavati,[1] *M.Sc.; Fernando H. de Assis Santana,*[1] *M.Sc.; and José R. Pujol-Luz,*[1] *Ph.D.*

A Checklist of Calliphoridae Blowflies (Insecta, Diptera) Associated with a Pig Carrion in Central Brazil*

ABSTRACT: Although the Cerrado is the second major Brazilian biome, few studies have been undertaken about its entomofauna. Blowflies have an important role in forensic entomology, helping in the determination of *postmortem* intervals. The main goal of this exploratory study was to identify and to catalog the blowfly species associated with a pig carcass. The study was conducted in a pasture in Brasília, Distrito Federal. A pig (*Sus scrofa*) was killed with a .22 caliber shot in the frontal region of the head. Adult blowflies were surveyed daily from June 1 through 30, 2004. A total of 14,910 adult calliphorids were collected, representing eight species: *Chrysomya albiceps, C. megacephala, Cochliomyia macellaria, Chloroprocta idioidea, Hemilucilia semidiaphana, H. segmentaria, Lucilia cuprina,* and *L. eximia*. *C. albiceps* was the most frequent species, amounting to 94.76% of the catch. Five decomposition stages were observed, and for calliphorids, the most attractive stage was the bloated one.

KEYWORDS: forensic science, Cerrado, savanna highlands, biodiversity, insect succession, forensic entomology, necrophagous insects

The Cerrado is considered one of the world's biodiversity hotspots. Although it represents the second major Brazilian biome, occupying 21% of the national territory (1,2), little attention has been given to its arthropods. Few studies have been made about its entomofauna (3–7) and still less about its dipterofauna (8). Checklists of species associated with cadavers/carcasses are scanty (9–12) added to a general lack of information about Diptera diversity in the Cerrado of Central Brazil (13,14).

Blowfly actively participate in organic matter decomposition (15), conferring to this group an important role in forensic entomology (16). Diptera and Coleoptera are the main groups of necrophagous insects involved in decomposition processes (17,18). Flies are generally the first to reach the substrate, and Calliphoridae, Muscidae, Fanniidae, and Sarcophagidae are the main families responsible for the cadaver/carcass decomposition (19–22). In Brazil, studies about human and animal corpses began in the 20th century but substantial development has only been attained in the last few years (24,25).

Studies addressing succession patterns have been used both in temperate/subtropical and tropical environments (16,24). Those studies described the entomological succession patterns, demonstrating that species composition varies in relation to the geographic location and abiotic factors (23). This variation has been helpful in the determination of *postmortem* intervals (PMI) (25–28) but the decomposition process has pertinent ecological implications: the availability of nutrients and carbon produced in decomposition has direct effects on the flora and fauna associated with the background soil, increasing fertility and microbial biomass and activity (29).

This exploratory study is the first one undertaken in Brazilian savanna highlands (Cerrado), and the main goal is to identify and catalog the species of blowflies associated with a pig carcass and the relation between the presence of adults of calliphorids and the decomposition stages exhibited by the carcass.

Methods

The study was carried out in a 1600 m^2 pasture-inactivated area, surrounded by Cerrado *sensu stricto*, at Brasília, Distrito Federal (15°56′22″S; 47°54′54″W). A carcass of *Sus scrofa* in decomposition, with approximately 15 kg, was used to attract insects. The pig was killed with a .22 caliber shot in the frontal region of the head and placed undressed in a metal cage with 1.5 m of diameter and 2 m of height, suspended about 10 cm above the ground, and covered with a Shannon trap. The blowfly collects lasted 15 min and was performed daily between June 1 and 30, 2004.

The captured insects were identified with the help of McAlpine's key (30) and Calliphoridae species with the keys of Dear (31), Carvalho and Ribeiro (32), and Mello (33). Part of the collected material was deposited in the Entomological Collection of the Departamento de Zoologia da Universidade de Brasília. The experiment was authorized by the Ethics Committee for Animal Use of the Instituto de Biologia of the same University.

Results

A total of 14,910 adult individuals were collected. *Chrysomya albiceps* was the most frequent species in the carcass, amounting to 94.76% of the individuals, followed by *C. megacephala* (3.04%),

[1]Núcleo de Entomologia Urbana e Forense, Departamento de Zoologia, Instituto de Ciências Biológicas, Universidade de Brasília, Campus Darcy Ribeiro, CEP 70.910-900, Brasília-DF, Brasil.

*Financial support provided by Conselho Nacional de Desenvolvimento Científico e Tecnológico—CNPq for the Grants 308636/2007-4 and 474081/2007-9 to JRPL. Also the Coordenação de Aperfeiçoamento de Pessoal de Nível Superior—CAPES for the graduate fellowship to FHAS and the CNPq graduate fellowship to GMB.

Received 25 June 2009; and in revised form 20 Aug. 2009; accepted 11 Sept. 2009.

Chloroprocta idioidea (1.08%), *Cochliomyia macellaria* (0.91%), *Lucilia eximia* (0.15%), *Hemilucilia semidiaphana* (0.03%), *H. segmentaria* (0.02%), and *L. cuprina* (0.01%).

As observed by Early and Goff (34), there are five decomposition stages: initial, during 1 day; bloated, 8 days; decay, 13 days; postdecay, 9 days; and dry, which started at the last day of the experiment. All of them, with the exception of *L. cuprina*, were collected in the bloated stage, *C. albiceps* being the most frequent species (Fig. 1). Likewise, all the species, with the exception of the two species of *Hemilucilia*, were collected in the decay stage. *C. albiceps* was the only species occurring in the dry stage. There was no capture of blowflies at the initial and dry stages (Fig. 2).

Discussion

Calliphorid blowflies are the main active agents of pig carcasses decomposition (15,21,35); some genera are used in forensic entomology as they provide significant data on PMI (23). *C. albiceps*, *C. megacephala*, and *C. putoria* are introduced species and may cause some impact on the native community of necrophagous dipterans (36). During the 1970s, they spread out to the states of Goiás, Minas Gerais and Pará, reaching some cities in the northeast of Brazil (37).

C. albiceps was the most frequent species in the carcass during the postdecay stage. The same results were found in Goiás (13) and Southeastern Brazil (9,17,38). This species is considered by

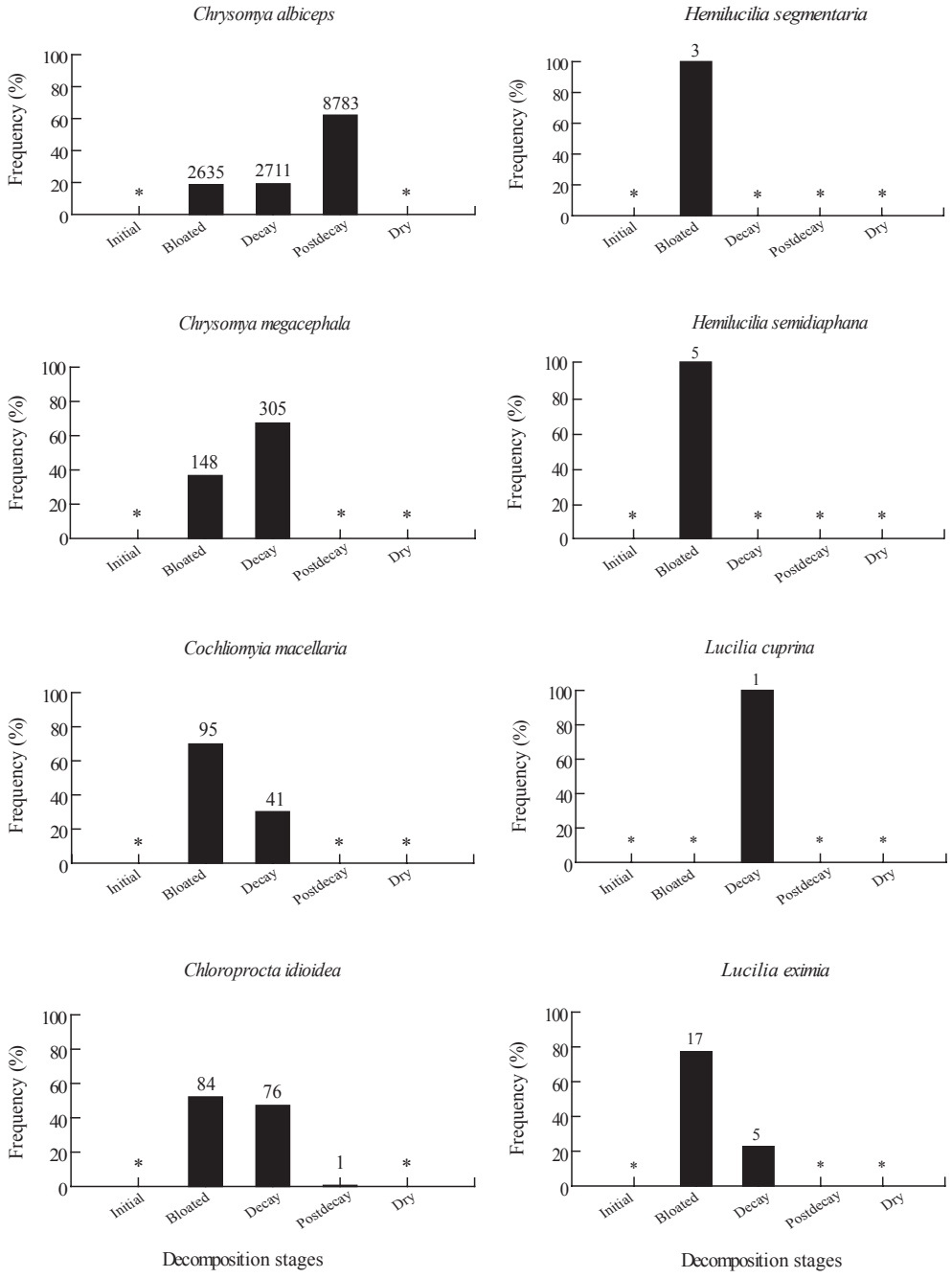

FIG. 1—*Calliphorid species recorded during the five decomposition stages of Sus scrofa in June 2004 at the Cerrado. *no data. The number above the bar represent the number of collected individuals.*

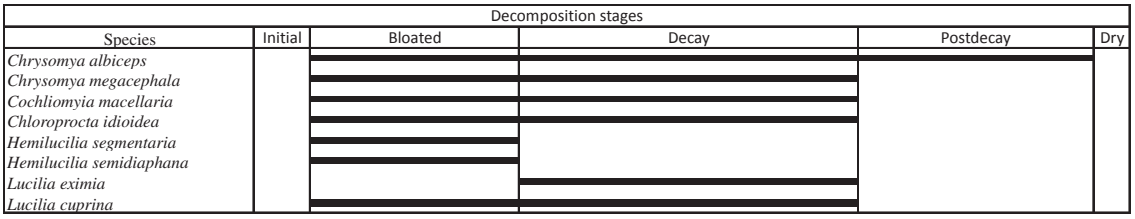

FIG. 2—*Calliphorid species succession patterns during the five decomposition stages of Sus scrofa in June 2004 at the Cerrado.*

these authors as a carrion fly. Although the frequency of *C. megacephala*, *C. macellaria*, *C. idioidea*, *H. semidiaphana*, *H. segmentaria*, *L. eximia,* and *L. cuprina* was not representative, all the species collected in this study are also considered good forensics indicators (10,39,40).

In Brazil, *C. macellaria* was considered the most frequent species in cadaver colonization (41), but with the introduction of *Chrysomya* in this country, it suffered a populational drop, probably because of predatory behavior and larval competition with species such as *C. albiceps* (39,42,43). Andrade et al. (43) observed that *C. macellaria* larval aggregation decreases when *C. albiceps* is present and that the larval aggregation of the latter increases with the presence of *C. macellaria.*

The presence of *C. idioidea* adults was observed along the bloated, decay, and postdecay stages of the carcass. Its presence along several stages of the decomposition process suggests that this species could be an important forensic indicator. It has been collected in fragments of secondary Atlantic Forest in Southeastern Brazil (44–47). Sousa (48) observed a frequency of 88.06% of collected individuals in the state of Amazonas, indicating that this species in an important faunistic component in that area. There is no information about *C. idioidea* at the Cerrado.

Three adults of *H. segmentaria* and five of *H. semidiaphana* were collected. Other studies using animal baits also detected a low frequency of *H. segmentaria* adults (39,49,50). Moura et al. (10) and Carvalho et al. (22) observed that *H. semidiaphana* occurs in greater frequency in forest environments. The low frequency found in the Cerrado may therefore be explained by the presence of open areas and the great solar incidence. Oliveira-Costa (23) considers this species a good forensic indicator for rural zones.

Lucilia was represented by the species *L. cuprina* and *L. eximia*. The former with only four individuals collected. Oliveira-Costa et al. (40) also collected a small number of *L. cuprina* in human corpses; the indication of this species is not frequently mentioned in the existing checklists. Adults of *L. eximia* were collected at the beginning of the decomposition of the pig carcass, being present along all stages, but disappearing in the dry stage. This species is known as one of the first muscoid species to colonize animal carcass (22,38,39,49). Although adults occurred in small number in carcasses, their colonization was abundant, being collected both in forest and in urban environments (23).

Acknowledgments

We thank Nelson Papavero and Marta Wolff for useful comments and suggestions that improved the clarity and content of the manuscript. We are also indebted to the Instituto de Biologia and the Estação Experimental Fazenda Água Limpa of the Universidade de Brasília for academic and scientific support.

References

1. Myers N, Mittermeier RA, Mittermeier CG, Fonseca GAB, Kent J. Biodiversity hotspots for conservation priorities. Nature 2000;403:853–8.
2. Klink CA, Machado RB. A conservação do Cerrado brasileiro. Megadiversidade 2005;1:147–55.
3. Diniz IR, Kitayama K. Seasonality of vespid species (Hymenoptera: Vespidae) in a central Brazilian Cerrado. Rev Biol Trop 1998;46:1–4.
4. Machado ABM. *Lauromacromia bedei* sp. nov. from the State of Minas Gerais, Brazil (Odonata: Corduliidae). Rev Bras Entomol 2005;49: 453–6.
5. Calderon RA, Constantino R. A survey of the termite fauna (Isoptera) of an eucalypt plantation in Central Brazil. Neotrop Entomol 2007;36: 391–5.
6. Camargo AJA. A new species of *Hylesia* Hüber (Lepidoptera: Saturniidae: Hemileucinae) from Brazilian Cerrado. Rev Bras Zool 2007; 24(1):199–203.
7. Pessoa-Queiroz R, Morais HC, Diniz IR. Abundance and temporal distribution of *Gonioterma exquisita* Duckworth (Lepidoptera: Elachistidae: Stenomatinae) on *Byrsonima pachyphylla* Griseb. (Malpighiaceae) in the Brazilian Cerrado. Rev Bras Entomol 2008;52:62–7.
8. Diniz IR, Morais HC, Gonçalves RG. Insetos. In APA de Cafuringa: a última fronteira natural do Distrito Federal. Brasília: Secretaria de Meio Ambiente e Recursos Hídricos - SEMARH, 2006; Volume 1, 219–23.
9. Souza AM, Linhares AX. Diptera and Coleoptera of potential forensic importance in Southeastern Brazil: relative abundance and seasonality. Med Vet Entomol 1997;11:8–12.
10. Moura MO, Carvalho CJB, Monteiro-Filho ELA. A preliminary analysis of insects of medico-legal importance in Curitiba, State of Paraná. Mem Inst Oswaldo Cruz 1997;92:269–74.
11. Carvalho LML, Thyssen PJ, Goff ML, Linhares AX. Observations on the succession patterns of necrophagous insects on a pig carcass in an urban area of Southeastern Brazil. Aggrawal's Internet J Forensic Med Toxicol 2004;5:33–9.
12. Carvalho CJB, Mello-Patiu CA. Key to the adults of the most common forensic species of Diptera in South America. Rev Bras Entomol 2008;52:390–406.
13. Marchiori CH, Castro MEV, Paiva TCG, Teixeira FF, Silva CG. Dípteros muscóides de importância médica e veterinária e seus parasitóides em Goiás. Arq Bras Med Vet Zootecnia 2000;52:350–3.
14. Barros RM, Mello-Patiu CA, Pujol-Luz JR. Sarcophagidae (Insecta: Diptera) associados à decomposição de carcaças de *Sus scrofa* Linnaeus (Suidae) em área de Cerrado do Distrito Federal, Brasil. Rev Bras Entomol 2008;52:606–9.
15. Smith KGV. A manual of forensic entomology. London: British Museum (Natural History), 1986.
16. Amendt J, Krettek R, Zehner R. Forensic entomology. Naturwissenschaften 2004;91:51–65.
17. Carvalho LM, Linhares AX. Seasonality of insect succession and pig carcass decomposition in a natural forest in Southeastern Brazil. J Forensic Sci 2001;46:604–8.
18. Turchetto M, Vanin S. Forensic entomology and climatic change. Forensic Sci Int 2004;146:S207–9.
19. Linhares AX. Synanthropy of Muscidae, Fanniidae and Anthomyiidae (Diptera) in the city of Campinas, São Paulo, Brazil. Rev Bras Entomol 1981;25:231–43.
20. Greenberg B. Flies as forensic indicators. J Med Entomol 1991;28: 565–77.
21. Catts EP, Goff ML. Forensic entomology in criminal investigations. Annu Rev Entomol 1992;37:253–72.
22. Carvalho LM, Thyssen PJ, Linhares AX, Palhares FAB. A checklist of arthropods associated with pig carrion and human corpses in Southeastern Brazil. Mem Inst Oswaldo Cruz 2000;95:135–8.

23. Oliveira-Costa J. Entomologia Forense: quando os insetos são vestígios. Campinas (SP): Millennium, 2008.
24. Pujol-Luz JR, Arantes LC, Constantino R. Cem anos da Entomologia Forense no Brasil (1908-2008). Rev Bras Entomol 2008;52:485–92.
25. Goff ML. Estimation of postmortem interval using arthropod development and successional patterns. Forensic Sci Rev 1993;5:81–94.
26. Benecke M, Lessig R. Child neglect and forensic entomology. Forensic Sci Int 2001;120:155–9.
27. Oliveira-Costa J, Mello-Patiu CA. Application of forensic entomology to estimate of the postmortem interval (IPM) in homicide investigation by the Rio de Janeiro Police Department in Brazil. Aggrawal's Internet J Forensic Med Toxicol 2004;5:40–4.
28. Pujol-Luz JR, Marques H, Ururahy-Rodrigues A, Rafael JA, Santana FHA, Arantes LC, et al. A forensic entomology case from the Amazon Rain Forest of Brazil. J Forensic Sci 2006;51:1151–3.
29. Carter DO, Yellowlees D, Tibbett M. Cadaver decomposition in terrestrial ecosystems. Naturwissenschaften 2007;94:12–24.
30. McAlpine JF. Key to families—adults. In: McAlpine JF, Peterson BV, Shewell GE, Teskey HJ, Vockrth JR, Wood DM, editors. Manual of Neartic Diptera. Ottawa, Canada: Research Branch, 1981;1.
31. Dear JP. A revision of world Chrysomyini (Diptera: Calliphoridae). Rev Bras Zool 1985;3:109–69.
32. Carvalho CJB, Ribeiro PB. Chave de identificação das espécies de Calliphoridae (Diptera) do sul do Brasil. Rev Bras Parasitol Vet 2000;9: 169–73.
33. Mello RP. Chave para identificação das formas adultas das espécies da família Calliphoridae (Diptera: Brachycera: Cyclorrapha) encontradas no Brasil. Entomologia y Vectores 2003;10:255–68.
34. Early M, Goff ML. Arthropod succession patterns in exposed carrion on the island of O'ahu, Hawaiian Islands, USA. J Med Entomol 1986;23:520–31.
35. Souza AM. Sucessão entomológica na decomposição de carcaça animal, com ênfase nas famílias Calliphoridae e Sarcophagidae (Diptera) [dissertation]. Campinas (SP): UNICAMP, 1994.
36. Wells JD, Greenberg B. Laboratory interaction between introduced *Chrysomya rufifacies* and native *Cochliomyia macellaria* (Diptera: Calliphoridae). Environ Entomol 1992;21:640–5.
37. Guimarães JH, Prado AP, Buralli GM. Dispersal and distribution of three newly introduced species of *Chrysomya* Robineau-Desvoidy in Brazil (Diptera: Calliphoridae). Rev Bras Entomol 1979;23:245–55.
38. Carvalho LM, Linhares AX, Trigo JK. Determination of drug levels and the effect of diazepan on the growth of necrophagous flies of forensic importance in Southeastern Brazil. Forensic Sci Int 2001;120:140–4.
39. Salviano RJB. Sucessão de Diptera caliptrata em carcaça de *Sus scrofa* Linnaeus, Rio de Janeiro [dissertation]. Rio de Janeiro (RJ): UFRRJ, 1996.
40. Oliveira-Costa J, Mello-Patiu CA, Lopes SM. Dípteros muscóides associados com cadáveres humanos na cena da morte no estado do Rio de Janeiro, Brasil. Bol Mus Nac Zool, Rio de Janeiro 2001;464:1–6.
41. Freire O. Algumas notas para o estudo da fauna cadavérica da Bahia. Gaz Méd da Bahia 1914;46:110–25.
42. V Aguiar-Coelho VM, Queiroz MMC, Milward-de-Azevedo EMV. Associação entre larvas de *Chrysomya megacephala* (Fabricius), *Chrysomya albiceps* (Wiedemann) e *Cochliomyia macellaria* (Fabricius) (Calliphoridae: Diptera) sob condições de laboratório. Rev Bras Zool 1995;12:983–90.
43. Andrade JB, Rocha FA, Rodrigues P, Rosa GS, Faria LDB, Zuben CJV, et al. Larval dispersal and predation in experimental populations of *Chrysomya albiceps* and *Cochliomyia macellaria* (Diptera: Calliphoridae). Mem Inst Oswaldo Cruz 2002;97:1137–40.
44. Leandro MJF, D'Almeida JM. Levantamento de Calliphoridae, Fanniidae, Muscidae e Sarcophagidae em um fragmento de mata na Ilha do Governador, Rio de Janeiro, Brasil. Iheringia 2005;95:377–81.
45. Furusawa GP, Cassino PCR. Ocorrência e distribuição de Calliphoridae (Diptera: Oestroidea) em um fragmento de Mata Atlântica Secundária no Município de Engenheiro Paulo de Frontin, Médio Paraíba. Rev Biol Ciênc da Terra 2006;6:152–64.
46. Guimarães RR. Sazonalidade da fauna de Calliphoridae (Insecta: Diptera) e ocorrência de microhimenópteros parasitóides (Insecta: Hymenoptera) de Cochliomyia hominivorax (Coquerel, 1858) (Diptera: Calliphoridae), na região da Baixada Fluminense, Estado do Rio de Janeiro, Brasil [dissertation]. Rio de Janeiro (RJ): UFRRJ, 2006.
47. Marinho CR, Barbosa LS, Azevedo ACG, Queiroz MMC, Valgode MA, Aguiar-Coelho VM. Diversity of Calliphoridae (Diptera) in Brazil's Tinguá Biological Reserve. Braz J Biol 2006;66:95–100.
48. Sousa JRP. Fauna de califorídeos e sarcofagídeos (Insecta: Diptera) das matas e clareiras com diferentes coberturas vegetais da base de extração petrolífera, Bacia do Rio Urucu, Coari, Amazonas [dissertation]. Belém (PA): Mus Paraense Emílio Goeldi/UFPA, 2008.
49. D'Almeida JM, Lopes HS. Sinantropia de dípteros muscóides (Calliphoridae) no Estado do Rio de Janeiro. Arq Univ Fed Rur do Rio de Janeiro 1983;6:39–48.
50. D'Almeida JM. Substratos utilizados para a criação de dípteros caliptratos no Jardim Zoológico do Rio de Janeiro (Rio-Zoo). Mem Inst Oswaldo Cruz 1989;84:257–64.

Additional information reprints not available from author:
José Roberto Pujol-Luz, Ph.D.
Titular Professor
Núcleo de Entomologia Urbana e Forense
Departamento de Zoologia
Instituto de Ciências Biológicas
Universidade de Brasília
Campus Darcy Ribeiro
CEP 70.910-900, Brasília-DF
Brasil
E-mail: jrpujol@unb.br

JOURNAL OF FORENSIC SCIENCES

J Forensic Sci, November 2010, Vol. 55, No. 6
doi: 10.1111/j.1556-4029.2010.01474.x
Available online at: onlinelibrary.wiley.com

TECHNICAL NOTE

PSYCHIATRY & BEHAVIORAL SCIENCES

Ewout H. Meijer,[1] *Ph.D.; Fren T. Y. Smulders,*[1] *Ph.D.; and Harald L. G. J. Merckelbach,*[1] *Ph.D.*

Extracting Concealed Information from Groups*

ABSTRACT: Lie detection procedures are typically aimed at determining guilt or innocence of a single suspect. Serious security threats, however, often involve groups, such as terrorist networks or criminal organizations. In this report, we describe a variant of the skin conductance-based Concealed Information Test (CIT) that allows for the extraction of critical information from such groups. Twelve participants were given information about an upcoming (mock) terrorist attack, with specific instructions not to reveal this information to anyone. Next, each subject was subjected to a CIT, with questions pertaining to the details of the attack. Results showed that for every question, the average skin conductance response to the correct answer option differed significantly ($p < 0.05$) from those to all other options. These results show that the information about the upcoming attack could be extracted from the group of terror suspects as a whole.

KEYWORDS: forensic science, terrorism, lie detection, polygraph, concealed information test, CIT, Guilty Knowledge Test, network analysis

Lie detection procedures are typically aimed at determining guilt or innocence of a single suspect. Many of today's security threats, however, do not come from individuals, but from organized groups such as terrorist networks or criminal organizations. In this report, we describe a technique that can be used to extract critical information from such groups; and in this way, we help to increase the security of citizens.

This technique is based on the Concealed Information Test (CIT; also known as the Guilty Knowledge Test [1,2]). This test aims to detect the presence or absence of crime-related information in a suspect's memory. In a typical CIT, questions concern crime details known only to the police and the perpetrator, but not to an innocent suspect. With each question, several answer options are presented serially, while psychophysiological parameters, such as skin conductance, are recorded. Answer options include the correct, but also several plausible but incorrect ones (e.g., "Was the victim killed with a … (i) gun, (ii) knife, (iii) rope, (iv) bat, (v) screw driver"). For innocent suspects, all options are equally plausible and will elicit similar physiological responses. However, for a guilty suspect, the correct option is salient and elicits an enhanced response. Thus, consistent stronger physiological responding to the correct answer options indicates knowledge of intimate crime details, from which guilt can be inferred. This use of the CIT is supported by research on the human orienting reflex (3), has good validity (4), and is widely used as a forensic tool in Japan (5,6).

An alternative application of the CIT is the so-called Searching Peak of Tension Test (SPOT [6,7]). This variant can be employed when the correct alternative is not known to the investigative authorities, but rather is the topic of investigation. If that is the case, a series of answer options are presented to the suspect, and the option that evokes the largest response is considered to be the one that warrants further investigation. In this way, the CIT can be used to discover, for example, the location of the body of a murder victim when the perpetrator is known.

In organized crime and terrorism, there are often multiple suspects who are likely to possess the same critical information. The question arises whether this critical information can be extracted by presenting the same questions to multiple suspects. The correct alternative should evoke the largest response in the majority of them. Screening for answer options that, on average, evoke the largest response in a group could then provide a reliable method for determining concealed information unknown to the investigative authorities, for example about a terrorist plan.

Method

Twelve male undergraduate students of Maastricht University (mean age 22.4 years, SD = 2.9) were asked to participate in an experiment. They read and signed an informed consent and received financial compensation for their participation. The experiment was approved by the ethical committee of the Faculty of Psychology and Neuroscience, Maastricht University. Upon arrival in the laboratory, the participant was told that the experiment entailed role playing and that he had to pretend he was a member of a terrorist organization. Next, the participant was given an envelope that contained instruction to go to a bar located inside the university building for a briefing. In the bar, he found an envelope labeled "top secret." This envelope contained the details of an upcoming terrorist attack (target, location, and date), with specific instructions to make sure not to reveal these details to anyone. Next, the participant returned to the laboratory.

Upon return to the laboratory, the participant was told that he was suspected of being a member of a terrorist organization,

[1]Faculty of Psychology and Neuroscience, Maastricht University, The Netherlands.

*Presented at the 18th Conference of the European Association for Psychology and Law, July 2–5, 2008, in Maastricht, The Netherlands, and the 21st Annual Meeting of the Association for Psychological Science, May 22–25, 2009, in San Franscisco, CA.

Received 6 May 2009; and in revised form 10 Aug. 2009; accepted 5 Sept. 2009.

possessing important information about an upcoming attack, and was therefore asked to undergo a lie detection test. After attachment of the sensors, the participant was again reminded to keep any information secret. To increase motivation, participants were promised a €5 reward for beating the test. The test consisted of one practice question and three test questions. The practice question referred to the day of the week and served to familiarize the participant with the procedure. The test questions pertained to the target, the location, and the date of the upcoming attack. All questions were presented on a computer monitor. With each question, six answer options were presented serially, each for 2 sec, with an interstimulus interval of 25 sec (e.g., "On what date will the attack take place?" February 2, October 8, April 20, November 22, March 27, August 15). The first answer option presented was never the correct one and served to absorb novelty orienting responses. The remaining five answer options were presented in random order. Participants responded to the presentation of each answer option with a verbal "no." The order of the questions was determined by a balanced latin square (8). All testing took place in a sound-proof laboratory, and participants were monitored from a control room by means of a video surveillance camera and a microphone.

Skin conductance was measured in microsiemens (μS) using a 24 bit DC 0.5 Volt system (Contact Precision Instruments, London, U.K.) with a sampling rate of 60 Hz. Two Beckmann silver/silver chloride (Ag-AgCl) electrodes (8 mm in diameter) were placed on the medial phalanges of the first and second fingers of the participants' nondominant hand. Electrodes were filled with isotonic electrode paste (0.9% NaCl). Skin conductance responses (SCRs) were computed as the maximum positive deflection between 1 sec and 5 sec following stimulus onset. To eliminate individual differences in responsivity, within-question standardized scores were computed by subtracting the mean of all five responses (excluding the buffer option) from the response to each answer option and dividing that by the standard deviation of all five responses (9). Three separate univariate repeated-measures ANOVAs were carried out on these z-scores, one for each question. The original degrees of freedom are reported with the Greenhouse-Geisser adjusted p-value and Greenhouse-Geisser Epsilon value (ε).

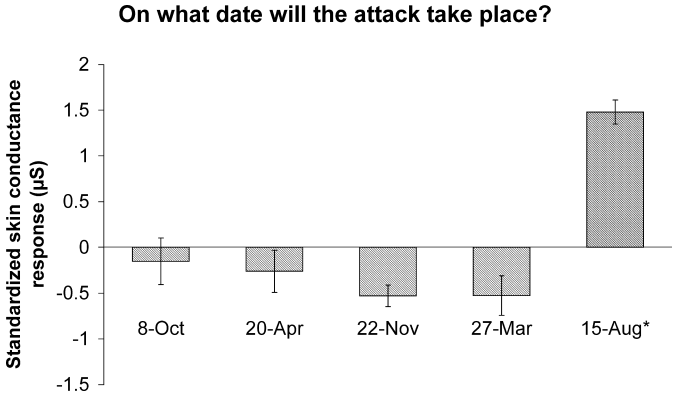

FIG. 1—*Mean standardized skin conductance response to answer options for the question about the date of the upcoming attack. *Denotes the correct option. Error bars represent standard errors of the mean.*

Results and Discussion

All three repeated-measures ANOVAs performed on the SCRs elicited by the different options revealed a main effect (date: [$F_{4,44} = 14.5$, $p < 0.001$, $\varepsilon = 0.66$], city: [$F_{4,44} = 14.5$, $p < 0.001$, $\varepsilon = 0.73$], target: [$F_{4,44} = 5.46$, $p = 0.004$, $\varepsilon = 0.75$], for an example see Fig. 1). *Post hoc* comparisons showed that for every question, responses to the correct answer option differed significantly ($p < 0.05$) from those to all other options, while, with one exception, responses to incorrect answer options did not differ from each other (see Table 1).

These results show that with the CIT, one can extract critical information about an upcoming terrorist attack from a group of terror suspects. In this way, this network variant of the CIT (N-CIT) may help to prevent terrorist attacks, but it may also be useful in revealing the location of drug laboratories, weapons or persons, or identify details of money laundry operations. This way, it may help to increase security and may serve as an alternative to controversial interrogation techniques.

Even though the current experiment was performed under ideal conditions (e.g., all participants possessing the information), our results likely generalize to the field. CIT research typically shows very large effect sizes. Mock crime studies that best mimic real life situations have found a Cohen's d of 3.12 (4), and an estimation of Cohen's d for the current study is 2.45 (for the estimation procedure see [10]). Such high effect sizes create leeway for use under suboptimal circumstances, like a smaller group of suspects, or a group of suspects in whom not everyone possesses the critical information. In any case, the N-CIT can be used as a challenge test. If no differences are found, this should be interpreted with caution. If one option does differ, however, further investigation into that option is warranted.

Investigative authorities already put considerable effort into mapping criminal networks (11). Additionally, the N-CIT requires that plausible answer options are limited in number. In some cases, the number of available options may be naturally limited; in others, the available options need to be reduced by police work. If this can be achieved, the N-CIT may prove a valuable tool for information gathering from groups of suspects.

TABLE 1—p-*values for the* post hoc *comparisons for the three questions.*

Question														
	Date					Location					Target			
	20 Apr	22 Nov	27 Mar	15 Aug*		Den Haag	Eindhoven	Utrecht	Rotterdam*		C&A	HEMA	H&M	V&D*
8 Oct	0.80	0.22	0.32	0.001	Den Bosch	0.18	0.75	0.05	<0.001	Bijenkorf	0.24	1	0.90	0.02
20 Apr		0.33	0.52	<0.001	Den Haag		0.44	0.52	0.001	C&A		0.22	0.14	<0.001
22 Nov			0.99	<0.001	Eindhoven			0.13	<0.001	HEMA			0.88	0.01
27 Mar				<0.001	Utrecht				0.001	H&M				0.002

*Denotes the correct answer.

The different locations represent large cities in the Netherlands. The targets all refer to department stores that can be found in these cities.

References

1. Lykken DT. The GSR in the detection of guilt. J Appl Psychol 1959;43:385–8.
2. Lykken DT. A tremor in the blood. New York, NY: Plenum Press, 1998.
3. Verschuere B, Crombez G, De Clercq A, Koster EH. Autonomic and behavioral responding to concealed information: differentiating orienting and defensive responses. Psychophysiology 2004;41:461–6.
4. Ben-Shakhar G, Elaad E. The validity of psychophysiological detection of information with the Guilty Knowledge Test: a meta-analytic review. J Appl Psychol 2003;88:131–51.
5. Hira S, Furumitsu I. Polygraphic examinations in Japan: application of the guilty knowledge test in forensic investigations. Int J Police Sci Manag 2002;4:16–27.
6. Nakayama M. Practical use of the concealed information test for criminal investigation in Japan. In: Kleiner M, editor. Handbook of polygraph testing. San Diego, CA: Academic Press, 2002;49–86.
7. Raskin DC. Polygraph techniques for the detection of deception. In: Raskin DC, editor. Psychological methods in criminal investigation and evidence. New York, NY: Springer, 1989;247–96.
8. Williams EJ. Experimental designs balanced for the estimation of residual effects of treatments. Aust J Sci Res 1949;2:149–68.
9. Ben-Shakhar G. Standardization within individuals: a simple method to neutralize individual differences in skin conductance. Psychophysiology 1985;22:292–9.
10. Meijer EH, Smulders FTY, Johnston JE, Merckelbach HLGJ. Combining skin conductance and forced choice in the detection of deception. Psychophysiology 2007;44:814–22.
11. Borgatti SP, Mehra A, Brass DJ, Labianca G. Network analysis in the social sciences. Science 2009;323:892–5.

Additional information and reprint requests:
Ewout H. Meijer, Ph.D.
Faculty of Psychology and Neuroscience
Department of Clinical Psychological Science
Maastricht University
P.O. Box 616
6200 MD Maastricht
The Netherlands
E-mail: eh.meijer@maastrichtuniversity.nl

JOURNAL OF FORENSIC SCIENCES

J Forensic Sci, November 2010, Vol. 55, No. 6
doi: 10.1111/j.1556-4029.2010.01466.x
Available online at: onlinelibrary.wiley.com

CASE REPORT
CRIMINALISTICS

Jin-Wen Chen,[1] *Ph.D.; Cornelius E. Uboh,*[1,2] *Ph.D.; Lawrence R. Soma,*[1] *V.M.D.; Xiaoqing Li,*[1] *M.S.; Fuyu Guan,*[1] *Ph.D.; Youwen You,*[1] *Ph.D.; and Ying Liu,*[1] *Ph.D.*

Determining the Source of Equine Bloodstains by Dinucleotide Repeats*

ABSTRACT: A novel multiplex of independent dinucleotide tandem repeat (DTR) loci was previously described that is capable of not only discriminating human and equine DNA, but of identifying a single equine source. We report a case in which a bloodstained syringe and two needles were found during inspection of a barn by inspectors of the Pennsylvania Racing Commissions. Using the multiplex and single-locus detection, all 21 equine DTR markers were detected in a suspect horse and two evidence samples, indicating the evidence samples came from the suspect animal. Only six markers were detected in the third evidence sample because the volume of blood was limited. Following whole-genome amplification and single-locus PCR, the third evidence sample detected a total of 17 markers and the likelihood of identity (probability from suspect horse/probability from a random pacer) was 7.0×10^6. The DTR multiplex has some technical limitations, but it is already practical for casework.

KEYWORDS: forensic science, racehorses, sample identification, bloodstains, short tandem repeats, multiplex polymerase chain reaction, whole-genome amplification

There are several ways to prevent doping of race horses, which adversely affects their welfare. These include testing of blood or urine postcompetition and the prohibition of needles and syringes from racetracks, except when they are used by practicing veterinarians. The PA Racing Commissions may require testing a biologic sample for presence of drugs whether it has been obtained from a horse or from a syringe or needle found after unannounced barn searches. A sample's chain-of-custody documentation may be challenged so that it is important to identify the source of the sample. The origin of a sample from a needle or syringe may be equine or human, and some blood samples may be limited in quantity or degraded. Therefore, it is important to examine the sample DNA for species and individual by robust methods. Recently, analysis of 21 equine dinucleotide tandem repeat (DTR) loci (1) and whole-genome amplification (WGA) (2) have permitted identifications with almost no (3.1×10^{-13}) error. In this article, we describe an actual case to demonstrate how dried blood from a needle and syringe was analyzed and shown to be from a suspect horse.

[1]University of Pennsylvania School of Veterinary Medicine, New Bolton Center Campus, 382 West Street Road, Kennett Square, PA 19348.
[2]Pennsylvania Equine Toxicology & Research Center, West Chester University, 220 E Rosedale Avenue, West Chester, PA 19382.
*Financial support for this study was provided by the PA Racing Commissions and the PA Harness Horsemen Association at Pocono and Chester Downs, Meadows Standardbred Owners Association and Horsemen Benevolent and Protection Association at Penn National and Presque Isles Downs.

Received 20 Mar. 2009; and in revised form 14 Aug. 2009; accepted 15 Aug. 2009.

Materials and Methods

Samples

A suspect blood sample, one syringe and two needles containing bloodstains were received in the laboratory for identifying the source of blood. Evidence and suspect samples were collected during a routine barn search at a racetrack in PA.

DNA Isolation and Quantification

Bloodstains were recovered from the syringe and needles by suspending in TE buffer. Total DNA was isolated by Genorise DNA Purification System (Genorise Scientific, PA) (1). DNA was verified on 0.8% agarose gel, and the quantity was estimated by TL100 software as well as OD_{260} measurement (1,3). DNA quantity recovered from the suspect horse sample was 10.23 μg per 0.3 mL blood, 1.12 μg from syringe, 300 ng from needle #1, but no quantifiable DNA was recovered from needle #2.

Whole-Genome Amplification

To recover quantifiably sufficient DNA for PCR analysis on needle #2, multiple displacement amplification (MDA) was conducted to amplify entire genomic DNA from the isolate using REPLi-g mini kit (Qiagen, CA) (2). A total of 1.2 μg DNA was obtained following WGA.

PCR Amplification

A previously developed short tandem repeat (STR) typing method with minor modification was used in generating DTR profile for each sample by HotStar Taq DNA Polymerase Master Mix (Qiagen) (1). Briefly, A single tube of 15-μl reaction was

TABLE 1—*Equine and human (*) short tandem repeat (STR) loci, dye assignment, sequences and concentrations (nM) of PCR primers, and PCR product size (bp).*

STR	Dye	Primer 1	Primer 2	nM	Size
VHL20	D4	caagtcctcttacttgaagactag	aactcagggagaatcttcctcag	70	90–110
UMNe156	D2	agactagcttcaaattgcccc	cctatgcttgaaggagtgtg	90	102–124
HTG4	D3	ctatctcagtcttcgttgcaggac	ctccctccctccctctgttctc	40	128–140
AHT4	D2	aaccgcctgagcaaggaagt	tcccagagagtttaccctgg	90	146–162
HMS6	D3	gaagctgccagtattcaaccattg	ctccatcttgtgaagtgtaactca	70	160–170
HMS7	D4	caggaaactcatgttgataccatc	tgttgttgaaacataccttgactgt	70	175–185
ASB9	D2	tttcctcctccactacacac	tcccttatcacaatagagcag	100	201–215
ASB2	D3	ccttccgtagtttaagcttctg	cttccccagaagttagagcag	90	190–226
COR045	D4	taccgcaagtgaaaccagttc	ttgtgggactgagcccttaac	70	217–233
HMS3	D2	ccaactctttgtcacataacaaga	catcagtcagaagctgcgaacc	90	243–265
UMNe222	D3	accaagctatgagtcaggag	agcatcttcatgtcctctgc	60	249–267
LEX074	D4	ccccttaaattcagaaagagagcc	ggaatttggagattatctgtgggc	15	273–291
TH01*	D2	ctgttcctcccttatttccc	ggtacctggaaatgacactg	100	281–297
COR008	D3	aggacactgaagggctgaaag	tagatagcgtctggagggttc	90	297–321
HMS2	D2	acggtggcaactgccaaggaag	gatctctagctcagtaaatcacagg	100	305–325
UM015	Cy5	agtctggctgaggatactg	tttgctgtcacattagaggg	40	330–346
COR018	D2	tgagtcttctgtactcctgg	ccacatctgggagtactaga	90	343–368
UMNe116	D3	ctggctaaactcttattcc	acatgggagaaaatacacac	90	364–378
UMNe479	D4	gagatggatggaatagcttg	tgcccagcctgaaagatttc	60	377–385
HMS1	D2	cacttatcagagaggccctcc	gtcatcccactctatcagggg	90	399–409
TPOX*	D2	cacagcttgatctcctcatg	tgaactcctcaggtccaatc	100	425–445
UMNe191	D3	tgtcctcacttggcatgagtcc	ccagatggtgaaacaaggggc	100	414–442
LEX073	D4	ttcagaacatcatccagcatcccc	cccaccactcaaatgtactaggc	40	462–492
D18S51*	D3	actgcacttcactctgagtg	cactttagccgacaaaaggc	100	470–494

assembled by 1× Master Mix, 3 mM $MgCl_2$, 20–50 ng DNA template, 40–100 nM primers, 67 μg/mL BSA, and 667 μg/mL Triton X-100. PCR amplification was subjected to 95°C for 15 min, 30 cycles of 94°C for 30 sec, 57°C for 30 sec, and 72°C for 1 min with final extension at 72°C for 10 min in a TC-512 Thermal Cycler (Techne, NJ). The 24-plex PCR was conducted to detect 21 equine DTR loci (Table 1) and three human tetranucleotide tandem repeat (TTR) loci to detect contamination of equine sample by human DNA. To amplify each of 21 loci in the suspect and evidence samples, a single-locus PCR was conducted using the same conditions as in the multiplex method.

Detection of Amplified DTR Loci and Allele Designation

Amplified markers were measured for size using capillary electrophoresis (CE) by a CEQ8800 Genetic Analysis System (Beckman Coulter, Brea, CA) (1,3). Individually amplified STR loci for each sample were pooled in one well of a 96-well plate for fragment analysis. Allelic size was determined by comparing to an internal size standard-600 containing 33 fragments (60–640 nucleotides) with 10–20 nucleotides apart and by fragment analysis software (Beckman Coulter) (1). An allele was designated as number of repeat motif plus 0.1 for partial repeat (one nucleotide) (1,3,4).

DNA Sequencing

Allele 20 and stutter products at locus HMS1 were sequenced using GenomeLab™ Dye Terminator Cycle Sequencing (DTCS) Quick Start Kit (Beckman Coulter) as described previously (1). A single PCR product of allele or stutter was isolated from 6% polyacrylamide gel prior to sequencing.

Statistical Analysis

The random match probability (RMP) and likelihood ratio (LHR) were used to estimate the probability of sample matching (5). RMP evaluates the probability of having a match under the following defense hypothesis: a random horse (not the suspect) is the contributor of the DNA sample, which is obtained as a product of genotype frequencies for Pacer Standardbred population. To compare two typical samples, a product of genotype frequencies of which independent loci have identical or distinct genotypes was calculated and LHR was obtained.

Results and Discussion

Multiplex PCR Revealed Detection of 20 Equine DTR Loci in the Suspect and Two Evidence Samples

Multiplex PCR indicated that all equine DTR markers except locus HMS1 were clearly detected in suspect horse, syringe, and needle #1 (data not shown). Results obtained from multiplexing were consistent with those from single-locus detection. Human TTR loci were not detected in the samples, suggesting that the source of the bloodstains was a horse not human.

A 24-plex STR method was developed as a novel approach to identify racehorse sample and contamination by human DNA (1). Although the method still uses DTR and internal size standard instead of allelic ladder, it had demonstrable advantages: higher power of identification, use of conventional allelic designation, and detection of contamination by human DNA. Multiplexing conditions were optimized according to DNA template, concentrations of magnesium and primer, and cycling parameters. We noted that it was helpful to include BSA and Triton in the multiplex assay to improve DNA amplification of challenging samples such as these case samples. These two reagents did not show any adverse effect on fragment sizes and thus, should not affect genotype results. Three human TTR markers in the 24-plex panel were human specific and did not recognize equine DNA (1). Based on the results at hand, it is clear that bloodstains in the syringe or needle #1 shared the same source with the suspect sample.

In the previous study, no deficiency of detection was observed for HMS1 locus in 261 samples. Difficulty in detecting HMS1

may suggest a rare mutation in the primer binding site in these case samples. It would be advisable to remove HMS1 from the panel if it continued to show deficiency in its detection.

Detection of 17 Equine DTR Loci in Needle #2

Only six markers were detected from needle #2 in 24-plex PCR (not shown). Following WGA of the DNA sample, eight more markers were detected while seven others showed weak or no signals by multiplexing. However, by single-locus PCR, DTR profiles for three additional markers (COR018, HMS1, and UMNe191) were observed. Altogether, 17 markers were detected in needle #2 although sufficient DNA was generated following WGA. The incomplete DNA profile may be attributed to low quality or DNA damage.

DNA quantity contributes to the success of multiplexing and low DNA template such as 1 ng made some alleles undetectable (1). Needle #2 presented difficulty in the multiplex detection of equine DTR markers although the addition of BSA and Triton improved amplification. In addition, the result of this study indicated that WGA could improve DNA yield to cause some alleles to become detectable. WGA is a great approach for limited forensic samples that contain low level DNA (2). However, WGA may not recover or repair damaged DNA template, and thus has limitations in improving PCR assay if the template is damaged. Seven markers were heterozygotes in the suspect and two evidence samples, but were detected as homozygote in needle #2. Although it was not readily evident as to whether this high rate of homozygote was due to the limited detection of the difficult sample, allelic dropout in WGA treated sample may not necessarily indicate that WGA caused such effect. Evidence has shown that WGA did not eliminate but improved allelic detection of HMS1 when diluted DNA samples were subjected to WGA (not shown). Moreover, ø29 DNA polymerase used for MDA has an error rate of 1 in 10^6–10^7 (6). If the absence of other alleles was because of the DNA damage or low quality, this sample may share common source with other three samples.

Locus HMS1 Was Detectable with Single-Locus PCR

Locus HMS1 was not detectable in multiplexing but was in single-locus PCR in all four samples (not shown). These four samples showed an identical product of allele 20 that was confirmed by DNA sequencing. Interestingly, the allele at locus HMS1 was not detected in the previous study in 171 Standardbred horses (1). Stutter peaks present in all samples were sequenced and were one repeat unit smaller. Needle #2 also showed two additional stutter products that were two and three repeat units smaller than the allelic product. Multiple stutter peaks in needle #2 may be related to low DNA quality.

While multiplex PCR showed difficulty in amplifying some markers in extreme circumstances such as degraded samples, a single-locus PCR may overcome this difficulty. It is necessary for multiplex method to reveal complete STR profile; however, this may not be always true especially in extremely difficult samples as presented in this case study. Although the robustness of the multiplex assay is in high demand in forensic science, this casework showed that single-locus detection is useful as an alternative approach when difficult DNA template is presented. However, single-locus amplification may not be needed if multiplexing can reveal complete STR profile.

Identification of Allelic and Stutter Peaks

All allelic peaks were identified by multiplex and single-locus PCR and by CE. They were identical between single and multiplex detections. Stutter peaks were observed in 17 of 21 markers. For instance, at locus ASB2, an identical peak pattern was observed between suspect (Fig. 1*A*) and syringe (Fig. 1*C*) samples. In both samples, the highest peak was designated allele 26. The third highest peak in the suspect sample and the second highest peak in the syringe were both three repeat units larger than the first allelic peak, and thus were designated as allele 29. Peak 216 (arrow) was one repeat unit smaller than the corresponding allelic peak and thus it was considered a stutter peak in both suspect and evidence

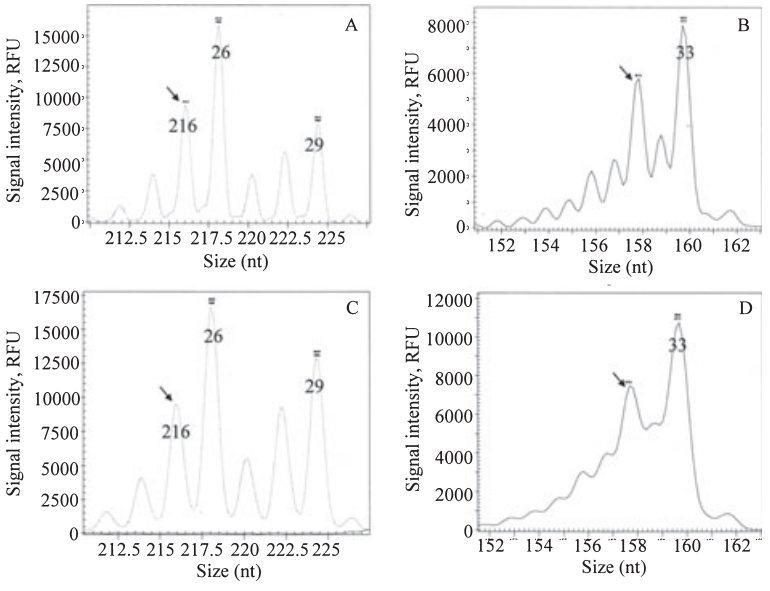

FIG. 1—*Detection of stutter activity. In suspect (A, B) and evidence (C, D) samples, stutter peaks were detected at loci ASB2 (A, C) and AHT4 (B, D). Allelic peaks were labeled and designated by number of repeat unit determined by DNA sequencing. Typical stutter peaks are indicated by arrows and other minor peaks are characterized as non-allelic peaks (not labeled).*

samples. The other minor peaks appeared as stutter or nonallelic products. Both samples (suspect and syringe) showed identical STR profile that was a heterozygote at locus ASB2. Locus AHT4 also showed an identical peak pattern between suspect (Fig. 1*B*) and syringe (Fig. 1*D*). In both samples, the highest peak was allele 33, the second highest peak that was one repeat unit smaller was considered a stutter product. The other minor peaks were smaller in size and one nucleotide apart and appeared as nonallelic products. Both samples (suspect and syringe) exhibited an identical genotype that was a homozygote at locus AHT4.

While DTR loci were employed to identify disputed samples, nonallelic peaks such as stutter peaks need to be clearly identified and interpreted. Stutter peak usually appear as one or more repeat unit smaller in size (7,8) and is defined as an artifact of PCR amplification (8). Multiple stutter peaks with partial repeat unit (single bp) apart were also observed (Fig. 1*B*). These irregular artifact peaks were much smaller than the regular stutter peaks with peak area ratio (PAR) of 0.28–0.44 to the allelic peaks (not shown). Stutter product was previously identified as shadow band by amplification of DTR loci, a nonallelic product probably from amplification slippage caused by a pause in DNA chain elongation (8). Occurrence of stutter activity depends on the nature of *Taq* DNA polymerase with processivity of approximately 40 (8). It was expected that a more processive thermostable DNA polymerase could reduce or eliminate stutter activity. In TTR locus, stutter activity mostly occurred as one repeat unit smaller than the corresponding allele (9). However, in DTR locus, nonspecific amplification often represents reduction by multiples of the repeat unit (8). Although stutter activity was very common, some markers (UMNe222, COR018, UMNe479, and UMNe191) showed minimal to no artifact activity. DNA templates from bloodstains and suspect sample showed no difference in stutter activity as a sign of the same nature of these samples.

With amplification of TTR loci, PAR of the stutter peak was usually less than 15% of allelic peak (7,9,10). In DTR loci, however, stutter peaks were often comparable to allelic peaks according to peak areas. This undesired activity may complicate interpretation of the results. However, in this case study, conclusion can be easily drawn because both evidence and suspect samples had identical peak patterns. Because of the disadvantages of DTR, it would be important to develop a method for detection of equine TTR for more effective forensic DNA testing. The drawback is that there are only few equine TTR sequences published with little information of its feasibility in forensic testing. Cloning and polymorphism characterization of more TTR sequences would definitely benefit the horse racing industry in sample identification and doping control.

Comparisons of Genotypes between the Suspect and the Evidence

The suspect and two evidence samples exhibited identical profiles (Table 2). Among 17 markers detected in needle #2, 79% alleles were identical to the other samples. Among 21 DTR markers, 14 loci accounting for 67% were heterozygote in the suspect and two evidence samples. In needle #2, only three markers showed distinct alleles that accounted for 28% heterozygote. The overall PAR was similar between the suspect and two evidence samples with an average of approximately 0.70.

Random Match Probability and Likelihood Ratio

Except for alleles at locus HMS1, alleles at all other loci were present at frequency of 0.01–0.63 (1). All samples presented a new allele (20) at locus HMS1 with calculated allele frequency of 0.006 (n = 172). With allele frequencies defined in the Standardbred Pacer racehorse (Table 3) (1), RMP was 3.1×10^{-13} between the suspect and two evidence samples, and 1.5×10^{-10} between evidence 3 and other samples, assuming a random horse is the contributor of the DNA sample (5).

To estimate match probability between suspect and evidence samples, LHR was also calculated. LHR for the match between suspect and two evidence samples was 3.2×10^{12}. LHR for the match between needle #2 and other samples was 7.0×10^{6} although such a match is less likely compared with the one between the suspect and remaining two evidence samples.

TABLE 2—*Comparisons of short tandem repeat (STR) profiles between suspect and evidence.*

	Suspect	Syringe	Needle #1	Needle #2
VHL20	18/23.1	18/23.1	18/23.1	18/23.1
UMNe156	21/21	21/21	21/21	21/21
HTG4	16/20	16/20	16/20	16/20
AHT4	33/33	33/33	33/33	33/33
HMS6	17/19	17/19	17/19	ND/ND
HMS7	20/20	20/20	20/20	20/20
ASB9	15/15	15/15	15/15	ND/ND
ASB2	26/29	26/29	26/29	29/29
COR045	21/22	21/22	21/22	21/22
HMS3	23/25.1	23/25.1	23/25.1	25.1/25.1
UMNe222	10/16	10/16	10/16	ND/ND
LEX074	19/20	19/20	19/20	19/19
COR008	19/24	19/24	19/24	19/19
HMS2	18/18	18/18	18/18	ND/ND
UM015	14/18	14/18	14/18	14/14
COR018	16/17	16/17	16/17	16/16
UMNe116	19/20	19/20	19/20	19/19
UMNe479	24/24	24/24	24/24	24/24
HMS1	20/20	20/20	20/20	20/20
UMNe191	13/17	13/17	13/17	13/17
LEX073	34.1/34.1	34.1/34.1	34.1/34.1	34.1/34.1

TABLE 3—*Allele frequencies for alleles detected in the suspect and evidence samples (n = 172).*

STR	Allele	Frequency	Allele	Frequency
VHL20*	18	0.377	23.1	0.044
UMNe156	21	0.544	NA	NA
HTG4	16	0.436	20	0.099
AHT4*	33	0.474	NA	NA
HMS6*	17	0.152	19	0.447
HMS7*	20	0.377	NA	NA
ASB9	15	0.301	NA	NA
ASB2*	26	0.257	29	0.196
COR045	21	0.146	22	0.386
HMS3*	23	0.383	25.1	0.056
UMNe222	10	0.175	16	0.693
LEX074	19	0.023	20	0.281
COR008	19	0.091	24	0.477
HMS2*	18	0.386	NA	NA
UM015*	14	0.395	18	0.155
COR018*	16	0.187	17	0.594
UMNe116*	19	0.184	20	0.360
UMNe479*	24	0.711	NA	NA
HMS1	20	0.006	NA	NA
UMNe191*	13	0.237	17	0.243
LEX073*	34.1	0.126	NA	NA

*Random match probability (RMP) and likelihood ratio (LHR) were calculated over 13 independent loci.

STR, short tandem repeat; NA, not applicable.

Equine sample identification with proper interpretation of the result is rarely reported (11). Most alleles shown in these case samples were common in the Standardbred Pacer horses (Table 3). Among 42 alleles in 21 loci, six alleles appeared less than 10 in 100 horses in the limited population especially the alleles at locus HMS1 was detected for the first time. Although the RMP and LHR were calculated based on the allele frequency observed in the limited population, an accurate matching probability could be drawn if a larger population was observed.

References

1. Chen J-W, Uboh CE, Soma LR, Li X, Guan F, You Y, et al. Identification of racehorse and sample contamination by novel 24-plex STR system. Forensic Sci Int Genet 2010;4(3):158–67.
2. Dean FB, Hosono S, Fang L, Wu X, Faruqi AF, Bray-Ward P, et al. Comprehensive human genome amplification using multiple displacement amplification. Proc Natl Acad Sci U S A 2002;99(8):5261–6.
3. Chen J-W, Uboh CE, Soma LR, Li X, Guan F, You Y. Microsatellite loci in urine supernatant and stored samples from racehorses. Am J Vet Res 2008;70(5):648–57.
4. Budowle B, Garofano P, Hellman A, Ketchum M, Kanthaswamy S, Parson W, et al. Recommendations for animal DNA forensic and identity testing. Int J Legal Med 2005;119(5):295–302.
5. Fung WK, Hu YQ, Chung YK. On statistical analysis of forensic DNA: theory, methods and computer programs. Forensic Sci Int 2006;162: 17–23.
6. Esteban JA, Salas M, Blanco L. Fidelity of phi 29 DNA polymerase. Comparison between protein-primed initiation and DNA polymerization. J Biol Chem 1993;268(4):2719–26.
7. Walsh PS, Fildes NJ, Reynolds R. Sequence analysis and characterization of stutter products at the tetranucleotide repeat locus vWA. Nucleic Acids Res 1996;24(14):2807–12.
8. Murray V, Monchawin C, England PR. The determination of the sequences present in the shadow bands of a dinucleotide repeat PCR. Nucleic Acids Res 1993;21(10):2395–8.
9. Urquhart A, Oldroyd NJ, Kimpton CP, Gill P. Highly discriminating heptaplex short tandem repeat PCR system for forensic identification. BioTechniques 1995;18(1):116–8. 20-1.
10. Gill P, Sparkes B, Buckleton JS. Interpretation of simple mixtures of when artefacts such as stutters are present—with special reference to multiplex STRs used by the Forensic Science Service. Forensic Sci Int 1998;95:213–24.
11. Tobe SS, Reid SJ, Linacre AM. Successful DNA typing of a drug positive urine sample from a race horse. Forensic Sci Int 2007;173:85–86.

Additional information and reprint requests:
Cornelius E. Uboh, Ph.D.
University of Pennsylvania School of Veterinary Medicine
New Bolton Center Campus
382 West Street Road
Kennett Square, PA 19348
E-mail: ubohcorn@vet.upenn.edu

JOURNAL OF FORENSIC SCIENCES

J Forensic Sci, November 2010, Vol. 55, No. 6
doi: 10.1111/j.1556-4029.2010.01445.x
Available online at: interscience.wiley.com

CASE REPORT

ENGINEERING SCIENCES

Jiri Adamec,[1] *Ph.D.; Karel Jelen,*[2] *Ph.D.; Petr Kubovy,*[2] *Ing.; Frantisek Lopot,*[2] *Ph.D.; and Erich Schuller,*[1] *Ph.D.*

Forensic Biomechanical Analysis of Falls from Height Using Numerical Human Body Models*

ABSTRACT: This article describes the method of using human body models developed originally for the use in automotive safety in forensic reconstructions of falls from height. The MADYMO® software package and multibody human body models were used in forensic analyses of two real cases—a fatal fall from a window *c.* 13.8 m above the ground and a fall into a *c.* 2.5-m deep cellar pit resulting in isolated ankle joint injury. The performed series of numerical simulations helped to reconstruct the events and to resolve legally relevant questions concerning various aspects of the falls. The benefits as well as limitations and potential biases associated with the use of numerical simulation in forensic biomechanical settings are discussed. The method has proven to be effective under specific circumstances, though the cost (both financial and temporal) still prevents it from wider use.

KEYWORDS: forensic science, forensic biomechanics, fall from height, numerical simulation, human body model, multibody modeling

Falls from height—onto a solid surface as well as into a fluid body—have been recognized as a relevant biomechanical research area (1–3). They occur frequently and are associated with substantial costs both financial and to society. Legal issues are often raised by falls that require the clarification of their causation.

Biomechanical analysis plays a significant role in the forensic investigation especially in unwitnessed falls from height and in suspected homicide cases. The crucial task of the forensic experts is to resolve—or to help resolve—whether the fall resulted from an accident, a suicidal action, or an assault.

In order to get insight into the studied event and assess its various legally relevant aspects, reconstructions of many accidents and/or crime types are performed. In addition to classic reconstruction methods including staging and experiment, the importance of numerical simulation has grown continuously over the last decades primarily as a result of increasing computer performance. From a biomechanical point of view, a reconstruction of an event (fall from height) means finding such a time history of the kinematical and dynamical parameters describing the movement and interaction of the human body with the surrounding structures that is in accordance with all the available evidence. Sometimes the statements of involved persons—witnesses, victims, suspects—must be taken into account.

[1]Ludwig-Maximilian-University Munich, Institute for Legal Medicine, Nussbaumst. 26, 80336 Munich, Germany.
[2]Charles University—Department of Anatomy and Biomechanics, Prague, Czech Republic.
*Part of this study was supported by grant agencies GACR—106/03/0464 and GAUK—111/C/2006.

Received 2 Mar. 2009; and in revised form 20 May 2009; accepted 1 Aug. 2009.

The typical process of a forensic reconstruction goes backwards with respect to time, i.e., from the known final state of the involved systems and from the available evidence information about the course of the event, and the initial configuration is extracted. This holds also for the widely spread computational car accident reconstruction—from the car end locations, observable deformations, and other evidence the car motion during and prior to the crash is reconstructed by using the laws of impact mechanics. In falls, there is generally not an unambiguous relationship between the initial conditions of the fall and the evidence, i.e., the same final body position and injury pattern can be the result of a wide variety of different initial conditions and several versions of the reconstruction of the same fall can thus be consistent with the known traces, especially if there are only a few. As a result, it is not possible to use a kind of an inverse computational technique to reconstruct the initial conditions from the known final state on the scene.

The conceptual formulation of numerical simulation with human body models is opposite to the classic reconstruction process—based on a definition of the systems (human bodies and surrounding structures) and their initial conditions, the mechanics of the event is computed forward to the final state. From this point of view, numerical simulation does not seem to be a suitable reconstruction method because it requires the most important (and not objectively known) information as an input. However, numerical simulation can be a very valuable tool in forensic biomechanical analyses of certain kinds of problems if used adequately; the aim of this article is to give an overview of the current possibilities in this area and demonstrate its potential by means of two examples with high-end biomechanical human body models.

Many legally relevant aspects concerning falls are related to testimonies of involved persons (both victims and suspects) and their biomechanical plausibility. Questions arise whether the description

of the incident—related by its nature mostly to the actions preceding the fall—is consistent with the evidence. In this type of question, the use of numerical simulation with human body models can be very beneficial.

Numerical Simulation

Thanks to the relative simplicity of the movement of a free falling body, falls from height were traditionally analyzed by using basic laws of physics governing the kinematics of the center of gravity of the (whole human) body with the air resistance neglected. However, many of the real cases involve an interaction between the human body and the surrounding structures at the beginning or during the fall (i.e., impacts of various body parts on rigid or deformable structures), and the reconstruction of the kinematics becomes thus very intricate. Numerical simulation is a method that can shed light even on highly nontrivial events. Thanks to very powerful visualization tools, the movements and their various aspects can be shown and interrelations explained. Thus, even biomechanical laymen—lawyers, judges, jury etc.—can get a clear idea of the studied incident and understand better its relevant aspects. Moreover, it is easy to modify the input parameters and thus assess various different scenarios of the studied event. The results of numerical simulations are objective in the sense that the movements and interactions are governed by the laws of mechanics and thus independent of personal experiences or opinions of the expert. Another huge benefit of numerical simulation is its capability to provide quantitative data regarding the temporal, spatial, and (as far as the model permits) even dynamical patterns of the incident.

Having named the main advantages of numerical simulation in forensic biomechanical analysis of falls, it must be stressed that its use is fraught with many pitfalls. Apart from the problems of general nature common for all kinds of numerical simulation of dynamic processes, there are some specific issues regarding the use of human body models. As with any other models, their validity is absolutely essential. For a human body model to reach sufficient predictive, structural, and replicative validity, it must reflect the mechanical properties of the real human body (the one that is being studied, i.e., an individual!) and it must be proven to reproduce the experimentally ascertained data in situations consistent with the studied incident.

A very important point that needs to be handled is the capability of the human bodies to generate movements and/or forces through muscular contraction. Muscular contractions—voluntary as well as reflective—influence the kinematical and dynamical parameters of human movements and must be taken into account in forensic analyses. Although models of a human body with implemented muscle models including muscle geometry as well as activation and contraction dynamics have already been developed, their use in forensic biomechanics is not practicable. The reason is the need of the input data, i.e., of the signals coming from the central nervous system to the muscles. The timing and amplitude of the signals sent to individual muscles during the analyzed event cannot be ascertained ex post. In fact, even if we measure the kinematics of all body segments of an individual and all the reaction forces resulting from his interaction with the surroundings directly during the incident in question, we would not be able to generate the inputs for the muscle activity (the neural controls)—a general problem referred to as the inverse dynamics problem of neuromuscular control that was proven to be ill posed from a mathematical point of view and thus not solvable (4). For forensic reconstructions, it implies that the muscle activation pattern, i.e., a reliable input for the muscle activity modeling, can never be found. The practical consequence for forensic analyses is that only situations with only marginal influence of muscle activity on the output can be studied or other ways of its modeling have to be found. Obviously, the latter concerns only predictable and simple kinematical effects like postural stability of the relative positions of body segments (simple refers not to the physiological fundamentals of postural activity but to its observable output). First steps in this direction have been undertaken in the field of automotive safety—an occupant model with stabilizing spine was introduced (5). The same model in combination with ''active'' limbs, i.e., arms and legs with implemented muscles controlled in a very easy manner by sensors was used to imitate known driver reactions (6). It must be noted that this approach was used only for the reconstruction of known—measured—typical reactions and as such it is applicable only in this particular kind of situation.

The MADYMO® Human Body Models

The essential property of a computer model of a human body with regard to forensic analyses of falls is the ability to represent its kinematics and interactions with the surroundings. High demands for validity with respect to both kinematical and dynamical response to impacts entail immense development costs that exceed the resources of forensic experts by several orders of magnitude in both temporal and monetary terms. While there are hardly ever going to be means available for the development of a special model for forensic analyses, the experts could take advantage of the already existing and continually improved products designed primarily for other purposes.

Several types of advanced numerical human body models have been developed recently for use in traffic accident analyses and reconstructions as well as in the development and optimization of passive safety systems.

MADYMO® (MAthematical DYnamical MOdels) (7) is a numerical simulation software tool developed for use in automotive safety that incorporates both multibody and finite element techniques. A database of human body models of various kinds (occupant, pedestrian) and sizes is available and ready to use. Because of their robustness, the multibody models seem to be especially suitable for the analysis of falls. Their anthropometry is based on the RAMSIS database (8); it is important to stress that although meant for use primarily in the automotive industry, they represent real human bodies and not technical devices such as anthropomorphic testing devices (ATDs). The properties of joints connecting individual body segments—range of motion, joint restraint forces etc.—reflect literature findings on living subjects. The rheological properties of the segments (stiffness, damping, hysteresis) are also based on the data found in literature and they were optimized and validated in simulations of postmortem human subjects (PMHS) impactor tests. The kinematical response to one or multiple consequent impacts (for example car-to-pedestrian accident) was validated by means of a series of volunteer tests for low-range loads and by several types of PMHS tests for high loads. The validation process included various impact directions as well as various body parts (pelvis, abdomen, thorax, shoulder, lower extremity); details can be found in (7,9,10). The validity of the kinematical and dynamical response of the models proven in both volunteer and PMHS testing—not only in short-term severe impacts but also in scenarios designated by lower loading and longer duration—qualifies the model for usage in forensic analyses. Further validation of the models for specific situations of forensic relevance is possible and can be strongly recommended.

Methods

Forensic Biomechanical Analysis Using Numerical Human Models

The general methodology of the application of human body models in forensic biomechanics should consist of the following steps:

- problem definition
- extraction of relevant systems (components)
- choice of the human model
- modeling of other relevant systems (components)
- definition of the initial conditions and the range of variation of unknown parameters
- pilot simulation
- series of simulations with variable parameters
- interpretation of results
- conclusions

The problem definition involves both the forensic part aiming at the answer of the legally relevant questions and its reformulation to a problem that can be solved by means of a numerical simulation. Examples of such transformation are given in the real case demonstrations presented later.

The effectiveness of modeling and numerical simulation depends to a vast extent on the ability of the expert to discern what is relevant and must be included in the model and what is not. The art of modeling (or the science of it) consists in constructing models complex enough to account for all major elements and, at the same time, easy enough for efficient use and clear interpretation of results.

In forensic biomechanical analyses, the most critical system is the human body. From the wide selection of advanced human models already available, the most suitable should be chosen. For the analysis of falls, the MADYMO® model family seems to be very appropriate. The models represent the kinematics of the human body with a high degree of validity experimentally proven by means of both volunteer and PMHS testing, the contact properties are defined in the models and there are several different anthropometries available.

Another advantage of the MADYMO® package is the easy way to model various systems surrounding the human body—both using multibody technique with simple geometries and finite element method if a high degree of detail is needed. It is possible to implement in MADYMO® the contact characteristics of any geometry by using force/deflection characteristics—an example of contact characteristics definition for compact earth and grass ground usable in a numerical simulation is given in (11). Damping, hysteresis, and other phenomena can be represented in the model, provided the necessary parameters are known.

The initial conditions are sometimes described by one of the involved persons; in unwitnessed falls they are completely unknown. Even if a "precise" verbal description is available, the initial conditions have got a stochastic character and must be subjected to a variation. Principally, every single parameter defining the initial conditions (position of a body or a segment relative to other systems/components, initial velocities—magnitudes as well as directions, etc.) should be subjected to variation in the whole range of its possible (realistic) values. Care must be taken that every set of parameters is consistent, i.e., the values can occur simultaneously in reality. In very intricate cases, some experimental validation (imitation of the initial phase in the laboratory etc.) might be necessary. The number of levels of each parameter as well as the range of possible values of each parameter depends on the nature of the parameter. If n denotes the number of parameters subjected to variation and m_i, $i = 1, \ldots, n$ the number of various levels of the ith parameter, it is necessary to perform $m_1 . m_2 . \ldots . m_n$ simulation runs to explore the whole space of possible versions of the event.

The purpose of the pilot simulation with freely chosen initial values of the parameters is the check of the system models, the contact interaction definition, and the stability of the numerical model. All modifications of the model should be performed prior to the parameter variations because any change of the model at a later stage would require the modification and re-calculation of all the already performed simulations.

The interpretation of the results is the critical part of the expert work. Apart from the forensic and biomechanical background, a comprehensive knowledge of numerical simulation is required in order to assess the results correctly. Care must be taken especially regarding the simplifications of the model with respect to the real setting and regarding the deviations of the human body model from the real individual.

The conclusions drawn should clarify the legal issues and supply the court with the expert information needed.

Case Description

Two real forensic cases were included in the current study, with the first one having two considered scenarios.

Case 1—A 58-year-old man reported to have fallen into a 2.5-m-deep cellar pit on an insufficiently secured building site when walking his dog during night hours. He stated in evidence that he "unexpectedly took a step into an empty space," landed on his right foot and suffered a Weber type-B fracture of the ankle. There were no other injuries whatsoever. The lawyers of the defendant insisted that the injury cannot originate from the described event. A forensic biomechanical expert was called in to assess whether the isolated right ankle injury is in line with the description of the accident. Based on the characteristic of the injury, the eversion of the right foot was identified as the injury mechanism. The MADYMO® model of the pit consisting of several planes is shown in Fig. 1. Please note that the staircase was modeled as a simple plane (the slant face of the pit). It would have been possible to model the individual steps, but only the general shape of the pit was of importance in the forensic analysis.

Case 2—A 25-year-old female person fell out of a window located 13.8 m above the ground and suffered lethal injuries. The investigators pointed out a discrepancy between the testimony of the only eye witness of the fall and the findings at the scene. The

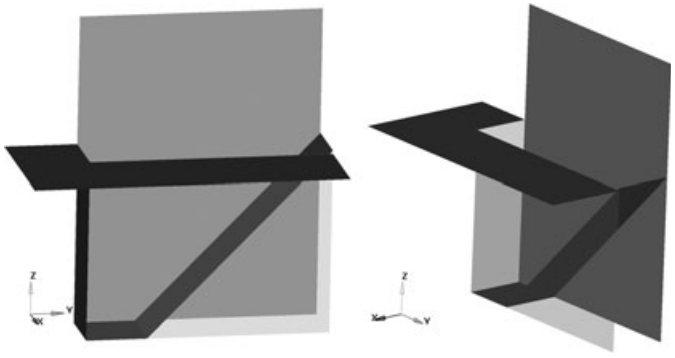

FIG. 1—*The multibody model of the pit. For a better overview, the front plane is displayed translucent.*

eye witness, who was together with the victim in the room during the incident, stated in evidence that the (drunken) victim stood in the open window, lost balance, tried to catch on the window frame and/or the window sill but failed to hold and slipped downward. In contrast to the expectations of the investigators, the body was not found close to the base of the house, the horizontal distance between the house wall and the body lying parallel to the house wall was as long as 2.0—2.8 m (the body was found by persons who reported somewhat different body locations; the victim was moved immediately as the first aid was provided). Another witness—a person living one storey below the victim—reported to have heard an impact on her window sill (the sheet metal was found slightly deformed), so the falling body might have interacted with this structure. In Fig. 2, the geometry of the relevant structures in the corresponding MADYMO® model is shown. Please note that redundant geometrical elements were used for the definition of the geometry of the house. This was done in order to ensure that the contacts between the nodes of the human model body surface and the other geometries work well. From the upper window, only the window sill was modeled and another ellipsoid was used to mark the height of the window. In Fig. 2, it is apparent that the window sills (in each floor of the house) overreach the contour of the house wall by *c.* 4 cm.

The question to answer by a forensic biomechanics expert was whether the evidence can be brought in accordance with the testimony of the eye witness (who was suspected of a homicide). The autopsy report stated that the injuries including subarachnoidal hemorrhage, clavicle, sternum, and left humerus fracture, multiple rib fractures, comminuted fracture of the 11th thoracic vertebra, rupture of the intervertebral disc between the 10th and 11th thoracic vertebrae, lung and heart contusion were consistent with landing on the back slightly rotated to the left. No injuries inconsistent with a fall from height were reported (signs of sharp violence, throttling, gunshot wounds etc.). At the time of the fall, the victim had a blood alcohol content of 1.76 g/kg.

Numerical Simulation

The MADYMO package was used to perform the simulation together with the MADYMO human body models—in the first case, the multibody pedestrian model the geometry of which consists of 64 ellipsoids and 2 planes, and in the second case, the multibody occupant model with the outer surface described by about 2000 triangular elements defined as a null material (facet surface) connecting *c.* 1000 nodes. Table 1 shows the basic anthropometric characteristics of the victims and of the used human models; as both models represented the average human man, their basic body parameters are the same.

TABLE 1—*Anthropometric characteristics of the victims and of the used human models.*

	Case 1	Case 2	Model
Body mass (kg)	77	68	76
Body height (m)	1.70	1.76	1.74

Based on the measurements and findings on the scene, models of relevant surrounding structures were created using multibody technique and simple geometrical shapes—ellipsoids, cylinders, and planes. As the structures interacting with the human body were very unyielding (concrete or paved surfaces, walls etc.), they were modeled as rigid, and the contact calculation was driven by the characteristics of the softer human body. In all simulations, the gravity was modeled as an acceleration field in the vertical (z) direction of $-9.81/\text{ms}^2$. Air resistance was neglected because of low expected movement velocities of the human body.

Results

Case 1

The injured person submitted a description of the accident, and all the relevant parameters of the surrounding structures were measured and incorporated into a simulation model. In the pilot simulation, the degrees of freedom of the individual segments of the model were deliberately chosen in a way that a support phase on the left foot during gait was imitated. The left foot was on the ground and the right foot was located 5 cm in front of the verge of the pit (i.e., the distance of the last support of the stance leg from the verge of the pit was 45 cm). The human body model was oriented along the long axis of the pit and its horizontal velocity was set at 1.0/ms—an estimation of these parameters based on the statement of the injured. In the next step, the input parameters that were not exactly known, i.e., the ones derived from the description of the injured person—the orientation of the model, the location of the last support relative to the verge of the pit and the gait velocity—were subjected to variation within the range of possible values. The orientation of the body was also considered as deviating 20° in each direction from the long axis of the pit. In all simulations, it was assumed that the person walked forward perpendicular

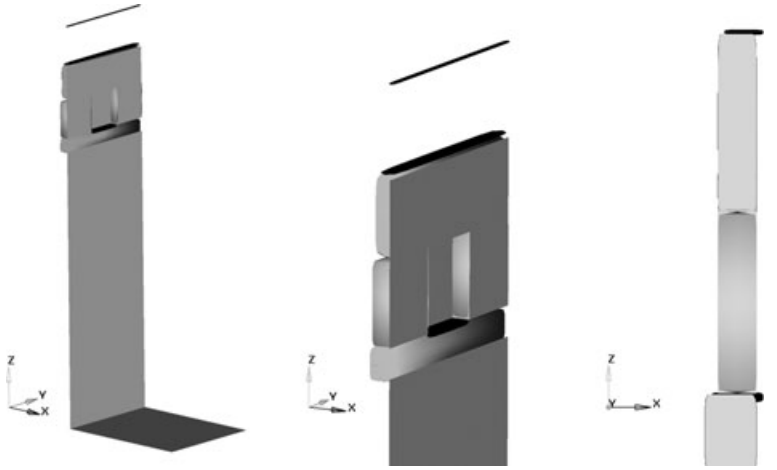

FIG. 2—*The multibody model of the house wall and the ground. The ellipsoids representing window sills are colored black.*

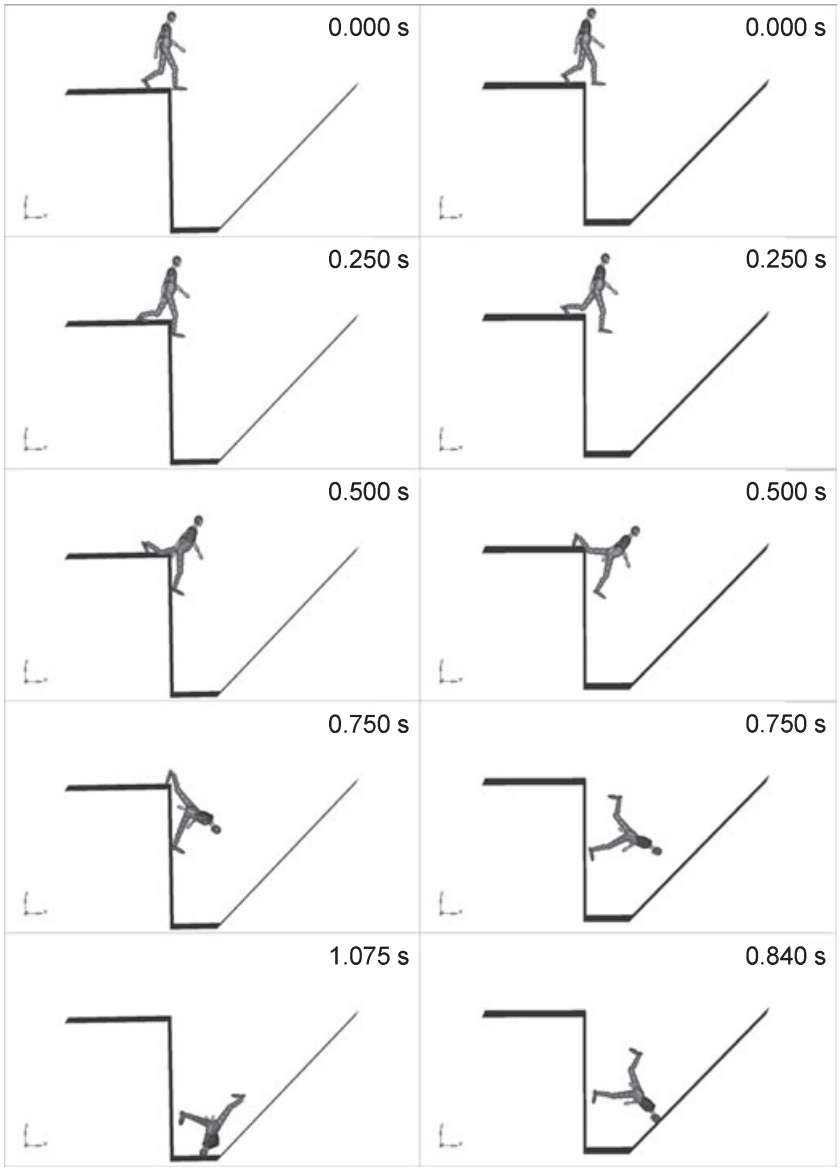

FIG. 3—*The human body model kinematics—screenshots from two simulation runs. Left higher initial velocity and greater distance between the last support and the verge of the pit.*

to the coronal plane of the body and the initial velocity of the center of gravity was defined in this direction. Two locations of the last support of the stance leg were considered −30 cm and 45 cm from the verge of the pit. The gait velocity was also considered in two levels −0.2/ms representing "slow" and 1.0/ms representing "normal" gait (the velocity was described as "not high"). The simulation matrix contained $3 \times 2 \times 2 = 12$ simulation runs.

All simulation results predicted similar model kinematics with a head impact; two examples are shown in Fig. 3. The location of the head impact varied, but there was no simulation run indicating the possibility of suffering isolated leg injury.

Please note that the simulation results cannot be interpreted as a reliable prediction of head injuries. The human body model is passive, real human beings would most probably protect the head instinctively with the arms and thus upper extremity injuries should be expected (exclusively or in addition to head injuries) although they are not predicted by the numerical model.

Based on the numerical simulation, it was stated in evidence that the description of the accident was not plausible from the biomechanical point of view and the described accident could not explain the diagnosed isolated ankle fracture.

In the course of the trial, the plaintiff changed his testimony and offered a new description of the kinematics—he was allegedly walking backwards perpendicular to the long axis of the pit. In order to verify this version, a new series of simulations was performed. The same parameters were subjected to variation as in the previous analysis; the step length and the gait velocity were lowered to account for backward locomotion. The kinematics of the human body model was substantially different and as shown in Fig. 4, in one of the simulation runs the kinematics predicting an isolated injury of the right ankle was obtained. Please note that the injury prediction is based on the kinematics of the body, i.e., on the fact that the model lands on the right foot and shows a clear tendency toward an eversion and, at the same time, no impacts suggesting possible injuries to other body regions were detected. A quantitative analysis of the acting forces was not performed—it was obvious that after a fall from *c.* 2.5 m, the impact force can exceed the tolerance of the ankle bones/ligaments.

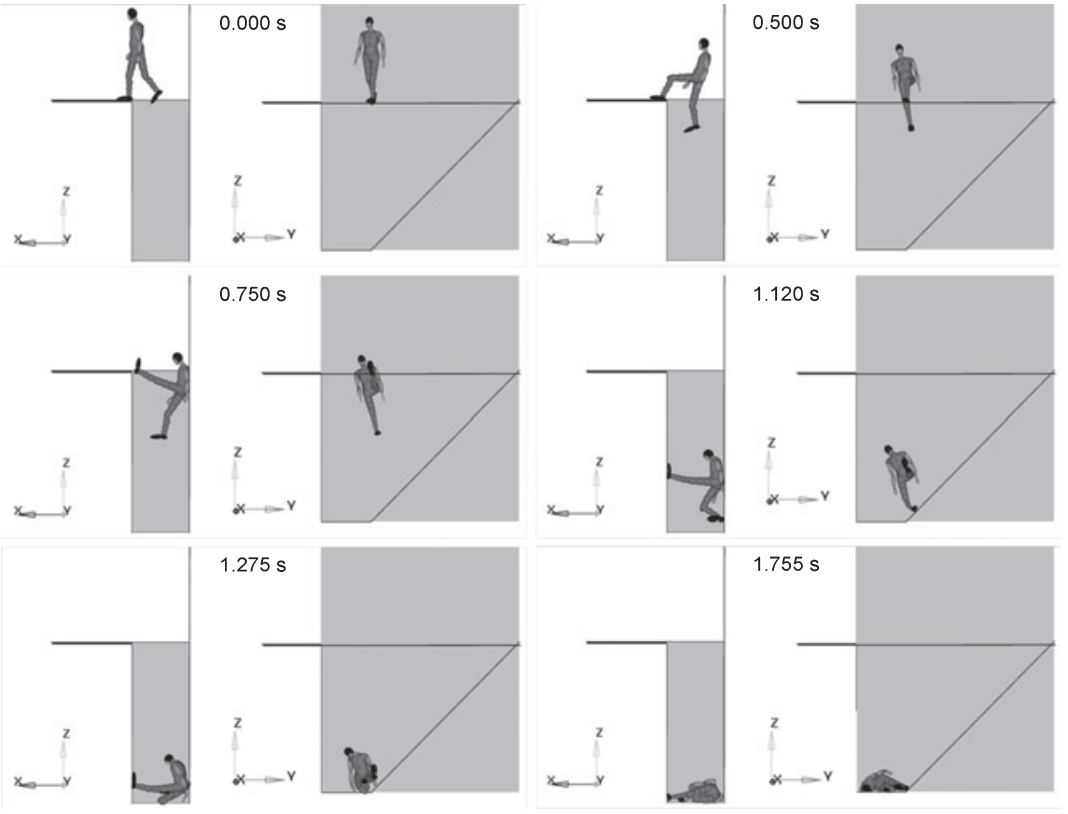

FIG. 4—*The kinematics of the human body predicting isolated injury of the right ankle (screenshots arranged left to right, top to bottom).*

Case 2

The testimony of the accused contained only a very general description of the body position of the victim during the first phase of the fall after the loss of balance (the presumed loss of balance was allegedly not seen by him). The only detail clearly remembered was the attempt to hold onto the window frame; the last body part to be seen was one arm sliding over the window sill. The number of uncertain parameters was very high and they would have had to be subjected to a very fine variation of steps within their ranges of possible values, because even a small difference in the initial state could be because of many possible interactions between the body and the house structures leading to a substantially different kinematics of the falling body. A complete simulation matrix would have contained a huge number of simulation runs that would make the computation as well as the evaluation infeasible within an acceptable time span. For this reason, an iterative process was used with the pilot simulation representing a deliberately chosen parameter selection as a starting point. Based on the results, the initial parameters that were believed to be most relevant were varied in several levels (the parameters as well as the number of their levels were different in each iterative step). The most promising simulations in terms of conformity between the kinematics of the model and the evidence were further modified until a reasonable level of agreement was achieved. Figure 5 shows screenshots from a simulation run (designated Version 1) that reflects all relevant features of the accident, i.e., the initial kinematics is in agreement with the description of the accused, the human body model lands on its back in accordance with the autopsy findings, and the model hits the ground at a distance from the house (represented by the X-component of the linear displacement of the pelvis, see Fig. 8) that lies within the range specified by the witnesses who found the body. Screenshots from another simulation are provided in Fig. 6. A slight change of the initial body position with respect to the previously described simulation (the body was rotated in the frontal plane and the position of the left arm was adjusted accordingly so that it touches the window sill) lead through different contact interactions to a different human body model kinematics during the flight phase. However, the results are also in agreement with the evidence and Version 2 must thus be regarded as another possible reconstruction of the event. The differences in the kinematics are demonstrated in Figs. 7 and 8 showing the vertical (*Z*-) component of the linear velocity of the head and the pelvis and the horizontal (*X*-) distance of these body segments travelled during the fall, respectively. Whereas in Version 1, the feet of the human model interact with the window sill of the lower apartment, in Version 2 the model shows a contact with the buttocks that leads to a vertical velocity peak of the pelvis observable in Fig. 7. As no evidence was found that would help to ascertain what body part hit the window sill both versions should be treated equally. The biomechanical analysis by means of numerical simulation proved that a fall kinematics consistent with the description of the accused as well as with the final body position reported by the witnesses can be the result of a fall with zero initial horizontal velocity, i.e., of an accidental fall.

A total number of 173 simulation runs was performed during the analysis of this case.

In the simulation, the occupant facet model was chosen because a complex interaction between various structures of the house was expected and the body surface is modeled in a more detailed fashion than in the pedestrian model. The model worked well except for the final part of the simulation; because of extremely high emerging forces during the landing of the model instabilities occurred in many individual runs.

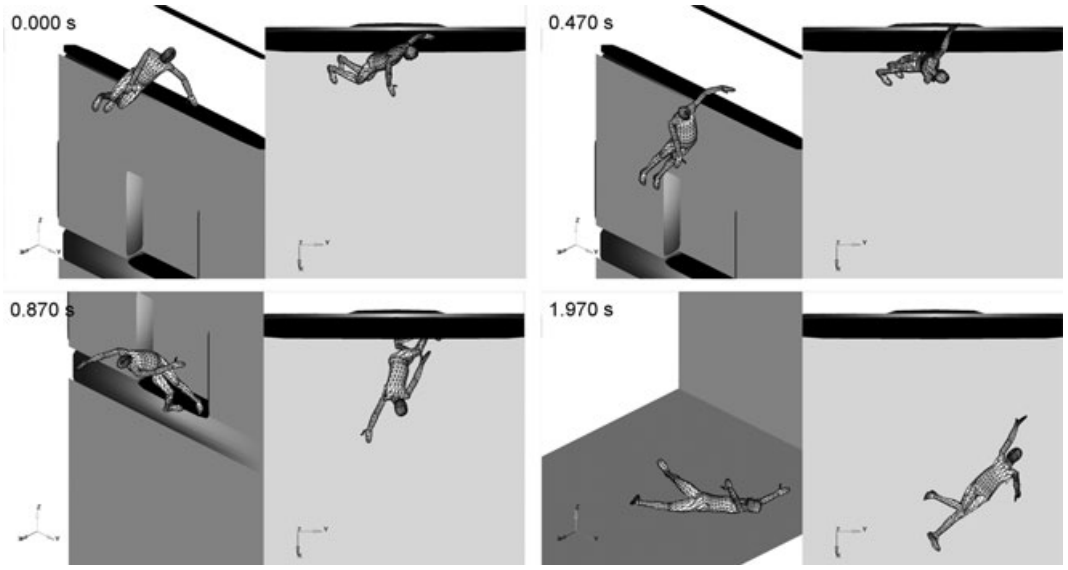

FIG. 5—*Screenshots from a simulation run consistent with the evidence—Version 1.*

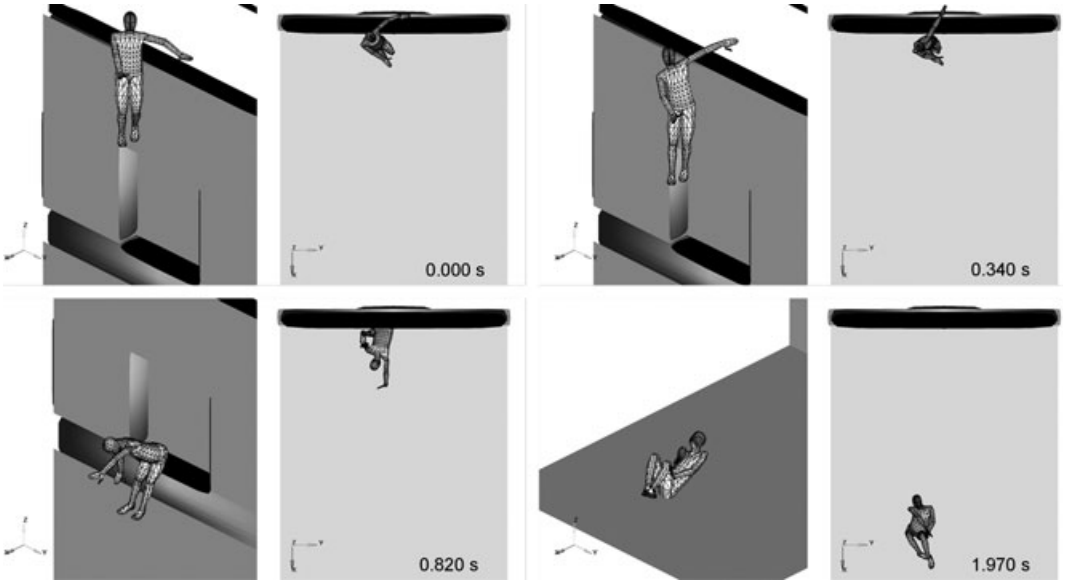

FIG. 6—*Screenshots from a simulation run consistent with the evidence—Version 2.*

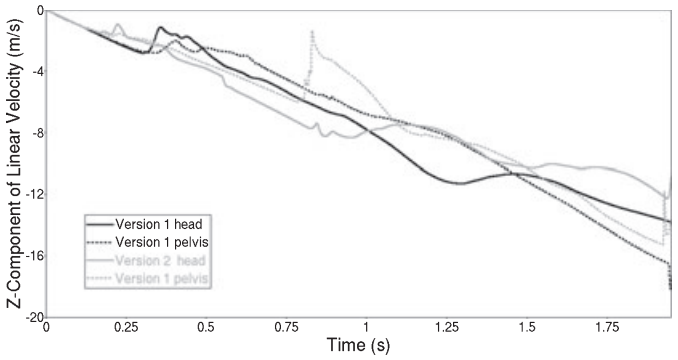

FIG. 7—*The vertical (Z-) component of the linear velocity of the head and the pelvis for both versions of the fall.*

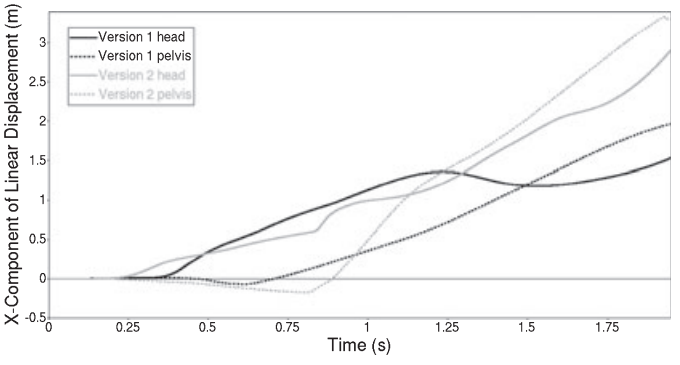

FIG. 8—*The horizontal (X-) component of the linear displacement of the head and the pelvis in both versions of the fall (measured from the beginning of the simulation).*

Discussion

In both the presented cases, numerical simulation was used to verify the descriptions of the fall. In case 1, the description was detailed, the number of uncertain parameters limited, and the kinematics in all simulation runs rather simple in terms of interactions between the human body and its surroundings and similar to each other within both parts of the study. The kinematics in case 2 was characterized by many ramifications depending on the interaction between the human body and the house structures. The number of uncertain parameters was so high and the ranges of their possible values so wide that a comprehensive analysis of all potential versions of the fall would not have been feasible. If a simulation conforming to the evidence had not been found, it could not have been interpreted as a refutation of the statement of the accused, because all possibilities were not taken into account. In contrast, by finding a simulation conforming both to the physical evidence and the statement of the accused, his version cannot be regarded as confirmed—there is still a possibility that the victim was pushed from the window, and the final position of the body and the injuries were generated in a different way. The numerical simulation only showed that (in contrast to the statement of the plaintiff) the evidence does not necessarily contradict an accidental fall as described by the accused. Apart from that, through the evaluation of multiple simulation runs of the same fall with only minor differences in the initial conditions, the range of possible kinematics became apparent.

In unwitnessed falls, the reconstruction is based solely on the physical evidence found on the scene. The crucial question whether the fall was the result of a suicidal action, a self-inflicted accident, or if other persons were involved can be unambiguously answered by means of a biomechanical analysis only under certain circumstances. Numerical simulation with human models can help to ascertain whether all the evidence can be explained as a result of a suicidal jump or an accident. The existence of such a solution—found in an iterative process starting at deliberately chosen initial conditions with following parameter variation—does not automatically exclude an intervention of another person (i.e., a homicide). For example, a low initial horizontal velocity necessary for the model to reach the known body impact location on the ground might be the result of an active step as well as of a push through another person. Only after a thorough analysis of all the (biomechanical as well as nonbiomechanical) evidence, the event could be classified as a suicidal jump, an accident, or an assault.

Especially in falls with little evidence regarding the human body movements (in an extreme case, only the landing position of the body can be reconstructed based on the suffered injuries), more than one plausible version of the same fall can be found.

As documented by the two real world examples, numerical simulation using human body models does not constitute a reconstruction method on its own. On the contrary, computational methods can be meaningfully used only after as many biomechanical aspects of the incident are known as possible. The classic biomechanical reconstruction of falls, i.e., determination of the body orientation at the time of impact from suffered injuries and the process of working backwards from the final position to the starting position utilizing physical evidence, cannot be replaced by numerical simulation. The results of the ''conventional'' biomechanical reconstructions are treated as a reference and new insights are obtained through the comparison between the numerical simulation results and the observed or assessed biomechanical features of the incident.

If information regarding the initiation of the fall is available (the description of involved persons or witnesses etc.), numerical simulation can produce the resulting motion and the biomechanical plausibility of the statements can be verified.

Although visualization capabilities of numerical simulation allow very realistic display of the results, they must always be treated as what they are—not a reality but its simplified model. Thus, it is necessary to explain the deviations from reality and their potential influence on the outcomes.

The model should be representative of the individual person of interest. Currently, most of the models including the MADYMO® family are available in discrete sizes corresponding to the population average as used in the automotive industry (the anthropometry of the 5th percentile woman, 50th percentile man, 95th percentile man etc.). Individuals substantially different from the average body composition—especially very lean or adipose persons—do not have adequate representations. Various scaling tools and methods are being developed so this problem will likely be overcome to a certain degree in the foreseeable future. The ultimate forensic investigation tool—a detailed numerical model of the studied individual with all its particularities—is not feasible because apart from anthropometrical measurements, it would require extensive testing of the subject including loading beyond its biomechanical tolerance. On the other hand, it is worth mentioning that some legal problems relate to whole populations and the use of an ''average'' human body is preferred over characteristics of one subject that might deviate from most of other individuals in the population; an example of such a problem is the analysis of hazards and potential injury risks involved in particular situations.

It was already mentioned that the implementation of muscle activity in the models in a physiological manner, i.e., the usage of computational models of muscle activation and contraction dynamics, would be based solely on estimates and thus obviously not objective. However, the simulation packages offer many possibilities how to imitate specific effects of muscle activity. A hand grip on a certain object (window sill, branch of a tree etc.) can be imitated by using a restraint (spring and damper) between the palm of the hand and the structure, the stance can be imitated by (temporarily) locking some of the lower extremity joints degrees of freedom, an active jump can be imitated by introducing corresponding initial velocity of the center of gravity of the human body and the corresponding definition of the initial degrees of freedom of joints etc. However, care must be taken so that the simulation reflects reality. In many cases, it is advisable to perform the simulation with a passive model and assess the potential effects of muscle activity on the observed results; an example hereof is the injury prediction in case 1—based on the simulation only, head injuries were predicted; taking muscle activity into account, also upper extremity injuries can be expected.

Even in the first steps toward the usage of numerical simulation in forensic analyses of falls with a very simple 2D model, representing only the kinematics of a chain of a small number of rigid bodies with no impact properties (12), it was already demonstrated that computational models can facilitate forensic biomechanical analysis of falls. From problems of forensic nature, the first situations to be studied with advanced numerical human body models developed primarily for automotive safety were obviously traffic accidents (13). Recently, MADYMO® human body models were successfully used in reconstructions of falls (14); based on numerical simulation of well-documented falls, the kinematics as well as the impact on the ground were reconstructed, and head injury analysis was performed.

As individual organs/tissues are not represented in the multibody models, no detailed mechanisms of injury can be analyzed. The

injury prediction is thus limited to the assessment of the model kinematics and interactions with other systems. For a detailed analysis of individual injuries, the body segment of interest could be replaced by its detailed version (this is possible in MADYMO® because detailed finite element models of the head/neck and the lower and upper extremities are available for some of the models) or the impact of interest could be simulated again by using the kinematical information from multibody simulation (i.e., the impact direction, velocity etc.) and a detailed model of the particular body part. An example of such analysis that goes beyond a typical forensic biomechanical reconstruction of a fall from height is demonstrated in (15).

The use of numerical simulation in forensic biomechanical analyses is obviously associated with costs that fall basically into two main categories. Although the license cost of the software and the human body models is still high at the moment, and forensic simulations are therefore performed almost exclusively in high-priority cases (train and airplane crashes etc.), decrease in licence fees can be assumed because of ongoing progress and competition in this rapidly developing field. The time costs relate both to the additional work needed for the preparation and evaluation of the simulation and to the computational time. The former depends to a high degree on the skills and experience of the expert and should not exceed several hours if simple multibody systems are generated (more time consuming might be the measurement and assessment/validation of the material properties and possible initial conditions to be used). The latter depends on the used model and computer (or cluster). The human body models used in this study proved to be very efficient—single simulation runs on a single Dual-XEON-Server (2 × 2800 MHz) took no more than 30 min for the simulation time of 1 sec. For more demanding simulations, parallel processing can be used.

There are of course general limitations of numerical simulation in the reconstruction of falls from height. With increasing fall height, the predictability of the kinematics and thus the meaningfulness of the usage of a numerical simulation decrease (also, air resistance would need to be implemented in the model). The same holds for a high number of interactions between the human body and the surrounding structures at the beginning and during the fall (fall on a staircase with multiple rolling etc.). However, in such scenarios, numerical simulation could effectively help to define the range of possible kinematical responses. A very challenging task would represent a numerical simulation of impact with fluid bodies. Because of the immense intricacy and time cost of such simulation, it would be advisable to simulate the fall kinematics only up to the point of impact.

In falls from severe heights, impact forces acting on the body during the impact on the ground can easily exceed the range for which the model was validated. Gross destruction of segments (head crush etc.) cannot be reproduced by the current models. Thus, very high energy impacts are presumably more elastic in the model than in real humans; this should be accounted for in the interpretation of the results. It must be noted that it is possible to modify the models according to the specific needs of the investigator. Thus, having the knowledge of the human body response to extreme loading, the appropriate loading curve (plus hysteresis, damping etc.) could easily be implemented.

Obviously, numerical simulation using human body models constitutes only a small part in the investigation puzzle aimed at the biomechanical aspects of the event. A complete forensic analysis is multidimensional and requires the cooperation of experts from various fields.

Conclusions

The numerical simulation with the MADYMO® human models proved to be a useful tool in forensic biomechanical analyses of falls from height. The primary advantages of the method are its objectivity, quantitative character of the analysis, and powerful visualization capabilities enabling insight even for biomechanical laymen.

The simulation results must be interpreted with great caution; the main sources of potential errors are the model simplifications, deviations from the individual's anthropometry, lack of muscle activity of the numerical model, and potentially erroneous initial conditions of the simulation.

The costs—both monetary in terms of licenses for simulation software and human body models and temporal in terms of time necessary for the pre- and postprocessing as well as computational time—are currently hampering wider use of this method in forensic day-to-day business. However, with the ongoing progress in numerical simulation especially in the field of human body kinematics and impact modeling, an increase in the employment of this method can be expected in the future.

References

1. Lallier M, Bouchard S, St-Vil D, Dupont J, Tucci M. Falls from heights among children: a retrospective review. J Pediatr Surg 1999;34:1060–3.
2. Sawyer J, Flynn J, Dormans J, Catalano J, Drummond D. Fracture patterns in children and young adults who fall from significant heights. J Pediatr Orthop 2000;20:197–202.
3. Snyder RG, Snow CS. Fatal injuries resulting from extreme water impact. Aerosp Med 1967;38:779–83.
4. Hatze H. The inverse dynamic problem of neuromuscular control. Biol Cybern 2000;82:133–41.
5. Cappon H, Mordaka J, van Rooij L A computational human model with stabilizing spine: a step towards active safety. SAE paper 2007;2007-01-1171.
6. Meijer R, Rodarius C, Adamec J, van Nunen E, van Rooij L. A first step in computer modelling of the active human response in a far side impact. Int J Crashworthiness 2008;13(6):643–52.
7. Madymo BV. MADYMO, Version 6.3. Delft: MADYMO BV, 2005.
8. RAMSIS. RAMSIS Manual version 3.1. Kaiserslautern: Tecmath Gmbh, 1997.
9. de Lange R, van Rooij L, Mooi H, Wismans JSHM. Objective biofidelity rating of a numerical human occupant model in frontal to lateral impact. Stapp Car Crash J 2005;49:457–80.
10. van Hoof J, de Lange R, Wismans JSHM. Improving pedestrian safety using numerical human models. Stapp Car Crash Journal 2003;47:401–36.
11. Davidson PL, Chalmers DJ, Stephenson SC. Prediction of distal radius fracture in children using a biomechanical impact model and case-control data on playground free falls. J Biomech 2005;39(3):503–9.
12. Sloan GD, Talbott JA. Forensic application of computer simulation of falls. J Forensic Sci 1996;41(5):782–5.
13. Adamec J, Schuller E, Praxl N, Schönpflug M. Possible driver injury causation/aggravation by the unbelted back seat passenger in a frontal crash—a simulation study. Forensic Sci Int 2003;136(Suppl 1):194–5.
14. O'Riordain K, Thomas PM, Phillips JP, Gilchrist MD. Reconstruction of real world head injury accidents resulting from falls using multibody dynamics. Clin Biomech 2003;18:590–600.
15. Raul JS, Baumgartner D, Willinger R, Ludes B. Finite element modelling of human head injuries caused by a fall. Int J Legal Med 2005;120(4):212–8.

Additional information and reprint requests:
Jiri Adamec, Ph.D.
Ludwig-Maximilian-University Munich
Institute for Legal Medicine
Nussbaumst. 26
80336 Munich
Germany
Email: jiri.adamec@med.uni-muenchen.de

JOURNAL OF FORENSIC SCIENCES

J Forensic Sci, November 2010, Vol. 55, No. 6
doi: 10.1111/j.1556-4029.2010.01526.x
Available online at: onlinelibrary.wiley.com

CASE REPORT

GENERAL; ANTHROPOLOGY

Ayaka Sakuma,[1] D.D.S.; Masuko Ishii,[2] M.Sc.; Seiji Yamamoto,[3] M.D., Ph.D.; Ryota Shimofusa,[3] M.D., Ph.D.; Kazuhiro Kobayashi,[1] M.Sc.; Hisako Motani,[1] D.D.S., Ph.D.; Mutsumi Hayakawa,[1] M.D., Ph.D.; Daisuke Yajima,[1] M.D., Ph.D.; Hisako Takeichi,[1] Ph.D.; and Hirotaro Iwase,[1] M.D., Ph.D.

Application of Postmortem 3D-CT Facial Reconstruction for Personal Identification*

ABSTRACT: Postmortem computed tomography (CT) images can show internal findings related to the cause of death, and it can be a useful method for forensic diagnosis. In this study, we scanned a ready-made box by helical CT on 2-mm slices in a mobile CT scanner and measured each side of the box to assess whether reconstructed images are useful for superimposition. The mean difference between the actual measurements and the measurements on the three-dimensional (3D) reconstructed images (3D-CT images) is 0.9 mm; we regarded it as having no effect on reconstruction for the superimposition method. Furthermore, we could get 3D-CT images of the skull, which were consistent with the actual skull, indicating that CT images can be applied to superimposition for identification. This study suggested that postmortem CT images can be applied as superimpositions for unidentified cases, and thinner slices or cone beam CT can be a more precise tool.

KEYWORDS: forensic science, forensic diagnosis, postmortem images, computed tomography, three-dimensional reconstruction, superimposition

Postmortem computed tomography (CT) imaging is a useful method for forensic diagnosis, and it is now being introduced in the field of forensic medicine rapidly. In Japan, as the infrastructure for the investigation into the cause of death is insufficient, CT is expected to be a screening test for cadavers, which must be subjected to medico-legal autopsy. We examine whether CT can be useful as a screening test and how it should be used in our system. Our CT scanner is in a van, which has been used as a medical examination car for almost 20 years. Recently, we have been using CT for all cases, which are subjected to forensic autopsies. With postmortem CT imaging, we can obtain information on the pneumothorax, pleural effusion, ascites, cardiac tamponades, gunshot wounds, and so on before an autopsy; it can support the diagnosis of the cause of death (1). In the case of an unidentified body, the superimposition method has been used as a part of personal identification (2). In the superimposition method, a skeletonized skull is compared to an antemortem picture of the victim, and the thickness of soft tissues or the anatomic structure is analyzed. The precision of three-dimensional (3D) reconstructed images is important for the superimposition method. In this study, we examined whether 3D-CT images obtained by a CT scanner can be applied to the superimposition method using a ready-made box and a skeletonized skull. We assessed the precision of the CT scanner by a statistical comparison of the difference between the actual measurements and the measurements on the 3D-CT images. Furthermore, 3D reconstructed images of a drowned body, a burned body, and a mummified body that had soft tissue on the skull were also examined.

[1]Department of Legal Medicine, Graduate School of Medicine, Chiba University, 1-8-1 Inohana, Chuo-ku, Chiba 260-8670, Japan.
[2]Forensic Science Laboratory, Chiba Prefecture Police Headquarters, 1-71-1 Chuominato, Chuo-ku, Chiba 260-0024, Japan.
[3]Department of Radiology, Graduate School of Medicine, Chiba University, 1-8-1 Inohana, Chuo-ku, Chiba 260-8677, Japan.

*Funded in part by a "Protecting Children from Crime" grant from the Research Institute of Science and Technology for Society (RISTEX) of the Japan Science and Technology Agency (JST).

Received 3 April 2009; and in revised form 20 Aug. 2009; accepted 7 Sep. 2009.

Materials and Methods

Mobile CT Scanner

We used a mobile CT scanner in a van (CT-W950SR: 1990; Hitachi Medico, Tokyo, Japan). It was a single helical CT system. All subjects were scanned on 2-mm slices, 140 mA, 120 kV, 2.0 sec, revealing data sets of the neck. To confirm the precision of 3D-CT images using CT-W950SR, we compared the actual measurements of a ready-made box with measurements of 3D reconstructed images.

Precision of 3D-CT Images

First, a ready-made box (79.6 cm wide, 87.1 cm deep, and 115.3 cm high) was measured with a caliper. Then, the box was scanned in four directions, and we measured each side by taking 3D-CT images with the 3D measuring function of Virtualplace Fuujin (AZE, Tokyo, Japan). Three sides of each direction were measured twice by three examiners. To evaluate the extent of error between the actual measurements and the measurements of 3D reconstructed images on the screen, these data were tested using The Data Analysis and Graphing Workspace software Origin 6.0

(Origin Lab, Northampton, MA). Also, the between-examiner variation was tested with one-way analysis of variance (ANOVA) (3).

Cases

The four cadavers that were brought to Department of Legal Medicine, Graduate School of Medicine, Chiba University for forensic examination were scanned before forensic autopsy—a body with a skeletonized skull, a drowned body, a burned body, and a mummified body.

- A body with a skeletonized skull that was found by the police in a house had been dead for 1–6 months, and the soft tissue had not adhered to the skull.
- A drowned body floating in a river was found by someone walking along the riverside. It had been dead for 1–6 months, and highly putrefactive soft tissue was still adhering to the face.
- A burned body that was found at the scene of a fire had been dead for a couple of weeks or months; the soft tissue was carbonized and indurated.
- A mummified body that was found by a neighbor in a house had been dead for 2–4 months; the soft tissue was dehydrated, indurated, and partially parched.

These crania were set in a supine position and scanned with the CT scanner on 2-mm slices, 140 mA, 120 kV, and 2.0 sec. Then, DICOM data from CT images were imported from Vol-Rugle (Medic Engineering, Kyoto, Japan), and these images were changed to the form of field data and constructed into 3D polygon data using MicroAVS (KGT, Tokyo, Japan) and Virtualplace Lexus (AZE). The 3D images were superimposed on the skull or antemortem pictures of the victim, and we analyzed replication of the hard tissue.

Results

Evaluation of the Extent of Error

From the results of the statistics, the mean measurements of the box on the 3D reconstructed images are 78.78 mm in width, 86.20 mm in depth, and 114.40 mm in height. Standard errors are 0.187 in width, 0.223 in depth, and 0.236 in height. The differences between the actual measurements and the measurements of the 3D reconstructed images are *c.* 0.9 mm on every side (Table 1). The test using one-way ANOVA that confirms whether there are significant differences between examiners resulted in "the means are NOT significantly different" (Table 2).

Reconstruction of CT Images

In the case of the skeletonized skull, a scalariform artifact was seen because of the 2-mm-thick slices in the 3D-CT images, but the anatomic structure was replicated (Fig. 1). The average difference at 10 landmarks (the minimum width of the forehead, the maximum width of the forehead, the distance between the nasion to the edge of the maxilla, the width of the zygomatic arch, the distance between the left orbit to the right orbit, the height of the orbit, the width of the orbit, and the nasal height) of a skull between the actual measurements and 3D reconstructed images was 1.25 cm.

Superimposing and comparing the 3D images with the actual skull, it was considered that the 3D images were substantially consistent with the actual skull except the occipital region, which was deleted for trimming the fixation apparatus of the skull from the faded image (Fig. 2; [4]). In the vertical wiped image at midline, the 3D images and the actual skull seem to be consistent at the parietal region and frontonasal suture (Fig. 3). At the maximum width of the orbit, the 3D images and actual skull seem to be consistent at the supraorbital and infraorbital margins. In the horizontal wiped image at the maximum zygomatic diameter, the 3D images and actual skull seem to be consistent at the lateral margin of the anterior nasal aperture; and at the middle of the orbit, the 3D

TABLE 2—*Differences of measurements between examiners.*

	Mean			Variance		
	X	*Y*	*Z*	*X*	*Y*	*Z*
Examiner 1	78.89	86.35	114.55	0.15	0.22	0.37
Examiner 2	78.71	86.01	114.50	0.12	0.32	0.43
Examiner 3	78.74	86.14	114.16	0.15	0.32	0.73

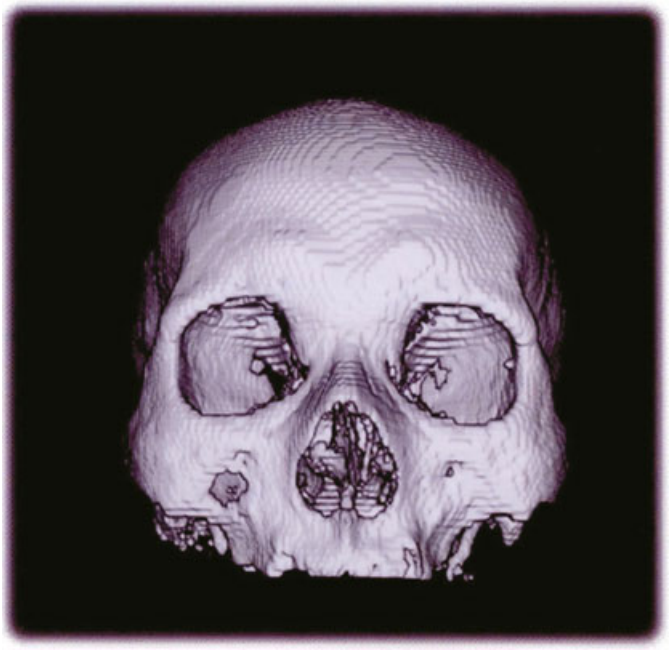

FIG. 1—*3D reconstructed image of the skull. The scalariform was seen because of the slice thickness in the 3D-CT images; however, the anatomic structure was replicated.*

TABLE 1—*Differences between the actual measurements and the measurements of 3D reconstructed images.*

	AM	Mean	Difference	SD	SE	Min	Max	Range	Sum	*N*
Width	79.6	78.78	0.82	0.895	0.187	78.0	79.2	1.2	1890.7	24
Depth	87.1	86.20	0.90	1.068	0.223	85.1	86.9	1.8	2068.0	24
Height	115.3	114.40	0.90	1.130	0.236	112.8	115.4	2.6	2745.7	24

AM, actual measurement.

FIG. 2—*Faded image of the 3D-CT images and the actual skull. It is considered that the 3D-CT images were substantially consistent with the actual skull.*

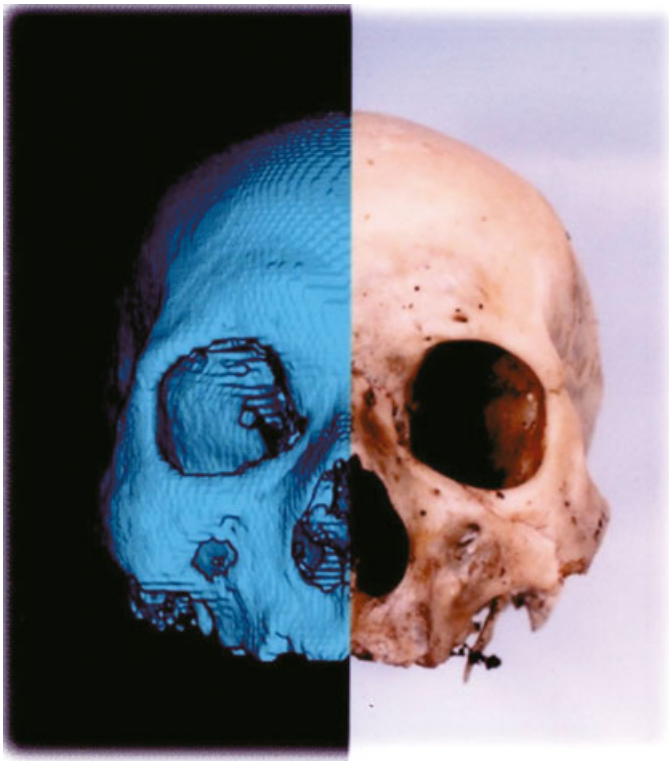

FIG. 3—*Wiped image of the 3D-CT images and the actual skull. In the vertical wiped image at midline, the 3D-CT images and the actual skull seem to be consistent at the parietal region and frontonasal suture.*

images and the macerated skull were consistent at the nasomaxillary suture and orbital margin. The 3D-CT images and the antemortem picture of the victim were superimposed and compared. In the vertical wiped image at the maximum width of the orbit, it seems that the eyebrow was located on the supraorbital margin, and the palpebral fissure that links the angulus oculi medialis and argulus oculi lateralis was located on the height under 1/3 of the orbit. In the horizontal wiped image above the palpebral fissure, the angulus oculi medialis was located on the interior to inferomedial margin of the orbit, and the argulus oculi lateralis was located on the lateral margin of the orbit (Fig. 4*a*). In the horizontal wiped image at the maximum width of the lateral margin of the anterior nasal aperture, the ala of the nose could be seen at the exterior of the lateral margin of the anterior nasal aperture. In the faded image of the 3D image and the antemortem picture of the victim, the thickness of the soft tissue was measured at the zygomatic diameter, at the distance between the angulus oculi medialis and inferomedial margin of the orbit, at the distance between the argulus oculi lateralis and lateral margin of the orbit, at the distance between the subnasal and extremitas inferior of the anterior nasal aperture, and at the distance between the ala of the nose and lateral margin of the anterior nasal aperture (Fig. 4*b*; [5,6]). In this study, these data were not used for practical personal identification using the superimposition method, considering that the data of the thickness of the soft tissue of the Japanese cranial part were old, and the number of subjects was too few to ignore dispersion of the data. However, with this study, we could confirm that CT images can be applied to the superimposition method or to measuring the thickness of the soft tissue for data collection (7,8). As for the drowned body with highly putrefactive soft tissue, the scalp from the front to the parietal was defective, and there was a prosthetic appliance from the left canine tooth to the right second molar tooth of the lower jaw. In the 3D-CT images, there was a radial artifact because of the metal of the prosthetic appliance but it did not affect the representation of the bone (Fig. 5). In regard to the burned body, which had deep burns at the cranial part, there was no metal artifact because of the edentulous jaw, and the bones were reconstructed completely as a squamous suture appeared clearly (Fig. 6). As for the mummified body in the 3D-CT images, a coronal suture and lambdoid suture were reconstructed rather well (Fig. 7; [9,10]).

Discussion

Concerning the results of the box measurements, it was scanned 2-mm slices, and the spatial resolution was FOV/512 pixels, so there would be a 0.49 mm error/pixel if FOV was 250 mm. However, in this study, the difference between the actual box measurements and the measurements of the 3D reconstructed images is about 0.9 mm. Therefore, we regarded these results as having no effect on the 3D reconstruction of the craniofacial part or the superimposition method for identification (11,12).

Although it has been about 20 years since our mobile CT was made, and each image thickness was 2 mm, we could reconstruct 3D-CT images of bone that were consistent with the actual skull. Consequently, it was confirmed that a 3D-CT scan can reproduce the bone structure of the head or face well. Therefore, 3D-CT images can be applied to the superimposition method as a tool for personal identification (13,14). In superimposing and comparing the 3D-CT images of the skeletonized skull with the antemortem picture of the victim, there was compatibility in the results of the thickness of the soft tissue. In this case, the victim was finally identified by DNA testing using a toothbrush and fingernail that remained near the body. The superimposition method was practically not used for identification because more data that can sustain the accuracy of the superimposition method using CT should be collected further. Also, computing software, which can set up a suitable position of the

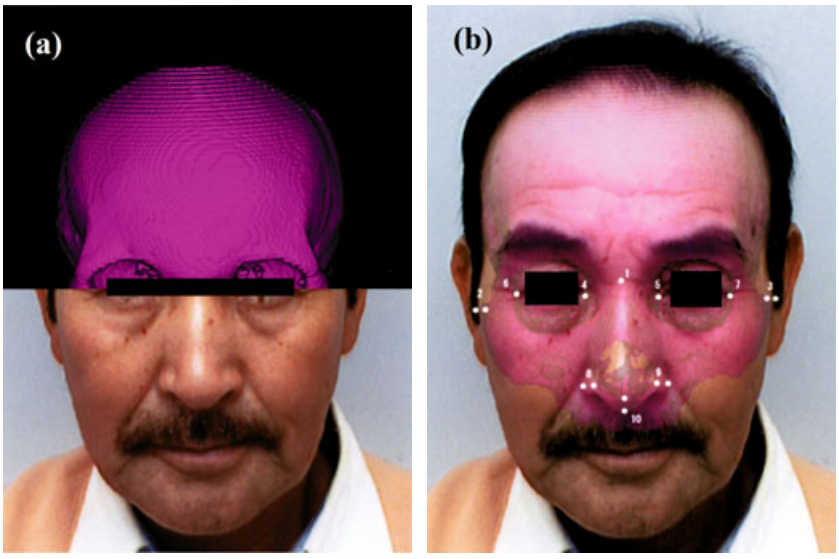

FIG. 4—*Superimposition of 3D-CT images and the antemortem picture of the victim: (a) the horizontal wiped image above the palpebral fissure, and (b) the faded image.*

FIG. 5—*The case of the drowned body: (a) 3D-CT image, and (b) the picture in forensic autopsy.*

inferior maxilla for the superimposition method, has yet to be developed. In the presented case, the position of the inferior maxilla was ignored because of instability due to the deficiency of teeth therein. However, measurements of the distance between points in the inferior maxilla are necessary to apply 3D-CT to the superimposition method, and it is necessary to reconstruct the contour from the forehead to the mental region, which is good for identification in the case of an edentulous jaw or unknown articulation. The CT scan has made it possible to reconstruct bone structure, which indicates that 3D-CT images can be applied for personal identification by the superimposition method in the case of a drowned body, burned body, and mummified body, the bones of which so far had to be bleached for the purpose of the superimposition method. Collecting data from 3D-CT images is far easier than the conventional way of bleaching, and the images can be saved in the computer for a long time while the bones are subjected to smashing to pieces for the purpose of DNA analysis (15).

In the case of the burned body and mummified body, there was the possibility that accentuation of impermeability would affect the scanning of hard tissues. In the process from combustio erythematosa to charring, the soft tissues gradually contract and sclerose. Also, in the process of mummification, the soft tissues dehydrate and sclerose. So the density of the CT images became higher in comparison with usual ones. The influence on the reconstruction of the hard tissues relative to the degree of carbonization or mummification must be considered (16,17). In this study, we got good results from 2-mm slices. Now multislice CT has been innovated to take slices 0.5 mm in thickness, and improvement in partial volume effects can produce more information about hard tissue like bone. Also, cone beam CT used in clinics can produce slices down

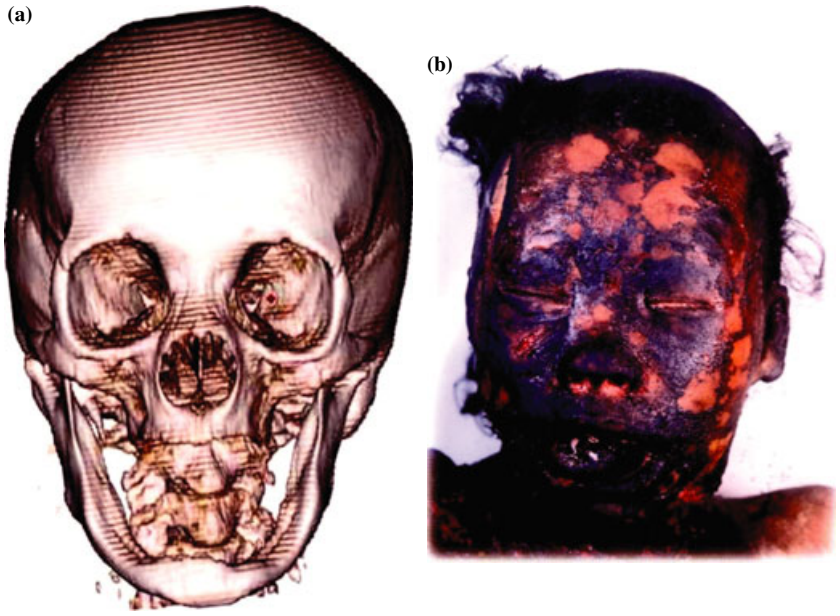

FIG. 6—*The case of the burned body: (a) 3D-CT image, and (b) the picture in forensic autopsy.*

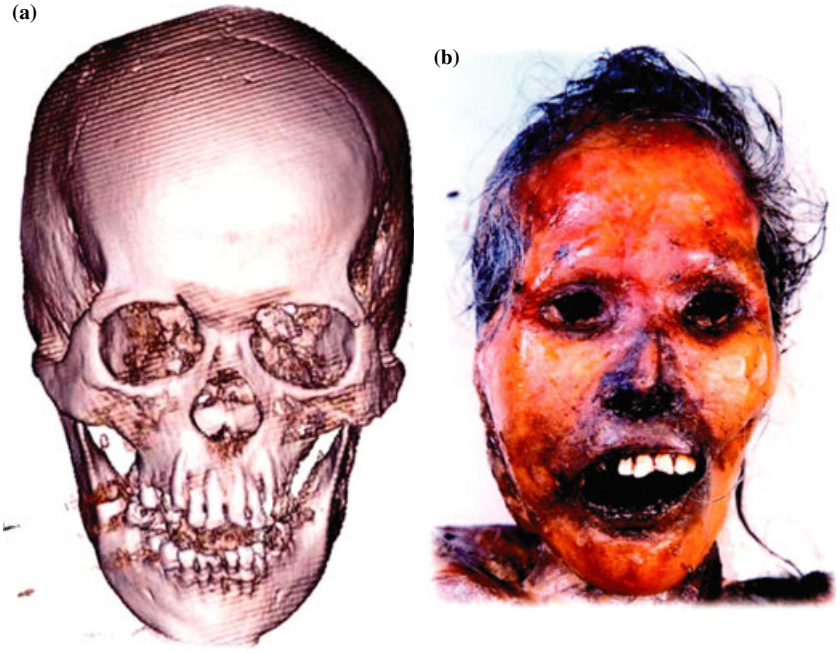

FIG. 7—*The case of the mummified body: (a) 3D-CT image, and (b) the picture in forensic autopsy.*

to 0.1–0.2 mm, and detailed measurement points can be analyzed by superimposition. Compared with multislice CT, cone beam CT can reduce metal artifacts, so it can reconstruct images of the roots of teeth, coronal restoration and caries, which are important for personal identification from the point of view of dentists (18). Postmortem CT images should be utilized with superimposition for unidentified cases.

References

1. Hayakawa M, Yamamoto S, Motani H, Yajima D, Sato Y, Iwase H. Does imaging technology overcome problems of conventional postmortem examination? A trial of computed tomography imaging for postmortem examination. Int J Legal Med 2006;120:24–6.
2. Dedouit F, Telmon N, Costagliola R, Otal P, Florence LL, Joffre F, et al. New identification possibilities with postmortem multislice computed tomography. Int J Legal Med 2007;121:507–10.
3. Ross AH, Williams S. Testing repeatability and error of coordinate landmark data acquired from crania. J Forensic Sci 2008;53(4):782–5.
4. Smith DR, Limbird KG, Hoffman JM. Identification of human skeletal remains by comparison of bony details of the cranium using computerized tomographic (CT) scans. J Forensic Sci 2004;47(5): 937–9.
5. Seda S, Yoshino M. Judgement of skeleton. Tokyo, Japan: Reibunsha Corp., 1990.

6. Yoshino M. Cranio-facial identification. Jpn J Forensic Sci Technol 1997;2(2):45–6.
7. Phillips VM, Smuts NA. Facial reconstruction: utilization of computerized tomography to measure facial tissue thickness in a mixed racial population. Forensic Sci Int 1996;83:51–9.
8. Kim KD, Ruprecht A, Wang G, Lee JB, Dawson DV, Vannier MW. Accuracy of facial soft tissue thickness measurements in personal computer-based multiplanar reconstructed computed tomographic images. Forensic Sci Int 2005;155:28–34.
9. Yoshino M, Matsuda H, Kubota S, Imaizumi K, Miyasaka S. Assessment of computer-assisted comparison between 3D and 2D facial images. Jpn J Forensic Sci Technol 2000;5(1):9–15.
10. Calvalcanti MG, Vannier MW. Quantitative analysis of spiral computed tomography for craniofacial clinical applications. Dentomaxillofac Radiol 1998;27(6):344–50.
11. Cavalcanti MG, Rocha SS, Vannier MW. Craniofacial measurements based on 3D-CT volume rendering: implications for clinical applications. Dentomaxillofac Radiol 2004;33(3):170–6.
12. Rocha SS, Ramos DLP, Cavalcanti MGP. Applicability of 3D-CT facial reconstruction for forensic individual identification. Pesqui Odontol Bras 2003;17(1):24–8.
13. Haglund WD, Fligner CL. Confirmation of human identification using computerized tomography (CT). J Forensic Sci 1993;38(3):708–12.
14. Eliasova H, Krsek P. Superimposition and projective transformation of 3D object. Forensic Sci Int 2007;167:146–53.
15. De Greef S, Willems G. Three-dimensional reconstruction in forensic identification: latest progress and new tendencies in the 21st century. J Forensic Sci 2005;50(1):12–7.
16. Yoshino M, Miyasaka S. Facial identification in forensic science for searching. Tokyo, Japan: Reibunsha Corp., 2000.
17. Miyasaka S. Progress in facial reconstruction technology. Forensic Sci Rev 1999;11:52–87.
18. Pohlenz P, Blessmann M, Oesterhelweg L, Habermannc CR, Begemannc PGC, Schmidgunstd C, et al. 3D C-arm as an alternative modality to CT in postmortem imaging: technical feasibility. Forensic Sci Int 2008;175(2):134–9.

Additional information and reprint requests:
Ayaka Sakuma, D.D.S.
Department of Legal Medicine
Graduate School of Medicine
Chiba University
1-8-1 Inohana, Chuo-ku
Chiba 260-8670
Japan
E-mail: a.sakuma@graduate.chiba-u.jp

JOURNAL OF FORENSIC SCIENCES

J Forensic Sci, November 2010, Vol. 55, No. 6
doi: 10.1111/j.1556-4029.2010.01472.x
Available online at: onlinelibrary.wiley.com

CASE REPORT
ODONTOLOGY

Susumu Ohtani,[1] *Ph.D. and Toshiharu Yamamoto,*[2] *Ph.D.*

Age Estimation by Amino Acid Racemization in Human Teeth

ABSTRACT: When an unidentified body is found, it is essential to establish the personal identity of the body in addition to investigating the cause of death. Identification is one of the most important functions of forensic dentistry. Fingerprint, dental, and DNA analysis can be used to accurately identify a body. However, if no information is available for identification, age estimation can contribute to the resolution of a case. The authors have been using aspartic acid racemization rates in dentin (D-aspartic acid/L-aspartic acid**:** D/L Asp) as an index for age estimation and have obtained satisfactory results. We report five cases of age estimation using the racemization method. In all five cases, estimated ages were accurate within a range ±3 years. We conclude that the racemization method is a reliable and practical method for estimating age.

KEYWORDS: forensic science, age estimation, teeth, racemization, D-amino acid, dentin

In many cases, age estimation of an unidentified body is determined by morphological changes such as the eruption stage of primary and permanent teeth, level of attrition and abrasion, and palatal and cranial sutures. However, because of the large estimation range of these methods, the results are not always accurate. In 1975, it was found that there was a high correlation ($r = 0.921$) between racemization rates in enamel and actual age (1), and that aspartic acid (Asp) has the most rapid racemization reaction speed of all the amino acids. In 1976, it was observed that this correlation ($r = 0.979$) is higher in crown dentin (2) than in enamel. The authors (3,4) have extensively studied the amino acid racemization method, examining different areas in the dentin, and have applied this method to actual age estimation. However, few reports exist in the literature about this topic (5). Therefore, we present five cases in which the amino acid racemization technique was used for actual age estimation.

Materials and Methods

Figure 1 illustrates the procedures for analyzing dentin amino acids from the hydrolysis of samples to the sample injection in a gas chromatograph (GC-17A; Shimazu, Kyoto, Japan). Teeth with no dentinal dental caries that were extracted because of periodontal disease were used for testing. Dentin was sectioned either labiolingually (incisors and canines) or buccolingually (premolars and molars) using a low-speed cross-section saw (Isomet, Buchler Co. Ltd, Lake Bluff, IL) to fabricate longitudinal sections *c.* 1 mm thick (Fig. 2). Dentin only was collected from the sectioned samples. The sections were then ultrasonically washed sequentially with 0.2 M hydrochloric acid, distilled water (three times), ethanol, and ether for 5 min each. The dentin sections were powdered and mixed together with an agate mortar, and then 5–10 mg dentin powder was collected for testing (6).

Separation of D, L-amino Acids

One of the most important points in this study was achieving clear separation of D, L-amino acids and setting the conditions to make a sharp peak in the chromatogram. After isolating N-trifluoroacetyl (TFA)-isopropyl ester from the amino acid sample, a capillary column (15 m in length, 0.3 mm in inner diameter), an optically active stationary phase coated with L-t-Leu-L-α-naftil ethylamide-polysiloxan, was fabricated to obtain racemization rates (7).

Figure 3 represents a gas chromatogram of the amino acids in dentin. Actual examinations require detection of amino acids in a short period of time. In cases of Asp detection only, the result was obtained in only 4 min. Racemization rates were calculated by converting to $\{1n[(1+D/L)/(1-D/L)]\}$.

Summary of Cases

Case 1

A female skeletonized body was found in a dry riverbed covered with daylilies. Because this was a possible homicide and the individual responsible had hidden the body, it was vital to identify the victim. The estimated age was calculated to be between 15 and 25 years from methods obtained by autopsy. The dental acid racemization technique estimated her age to be 21 ± 3 years. After 10 days of investigation, it was determined that the victim was an 18-year-old woman whose house was only 300 m from where the body was found (Table 1).

Case 2

An adipocere female body covered by a blue plastic sheet was found in the ground at a residential development site. The

[1]Institute for Frontier Oral Science, Kanagawa Dental College, 82 Inaoka-cho, Yokosuka, 238-8580 Kanagawa, Japan.
[2]Department of Human Biology, Kanagawa Dental College, 82 Inaoka-cho, Yokosuka, 238-8580 Kanagawa, Japan.

Received 12 July 2009; and in revised form 3 Sept. 2009; accepted 6 Sept. 2009.

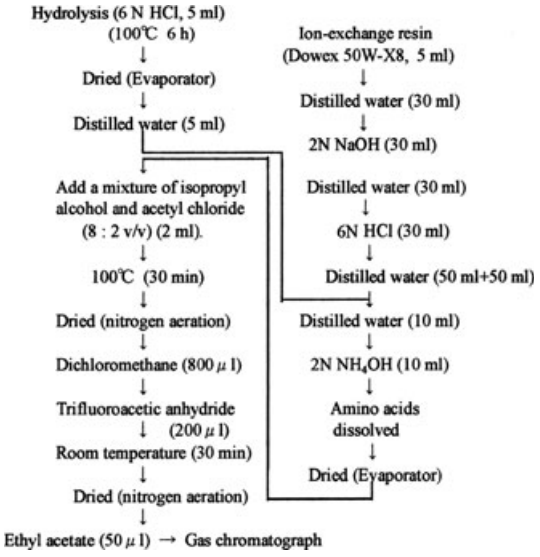

FIG. 1—*Our standard procedures for measuring D/L ratios.*

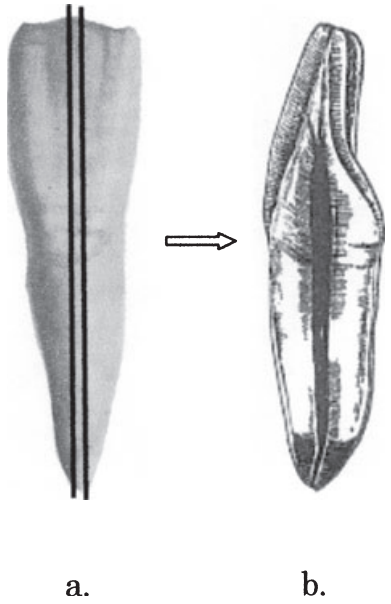

FIG. 2—*Sites used for determining the aspartic acid D/L ratio in dentin. (a) The block bars indicate cutting lines; (b) the cut face of the mandibular central incisor.*

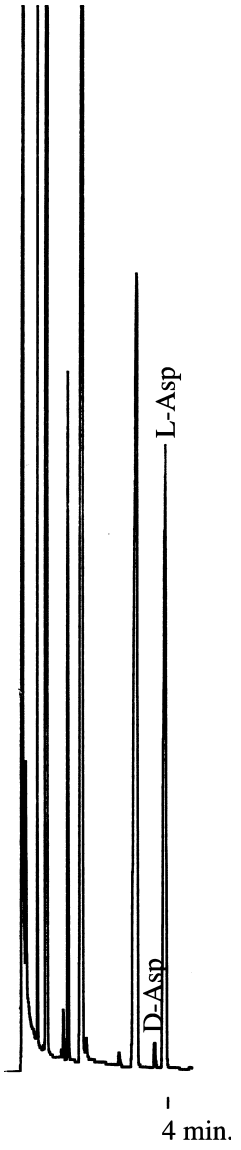

FIG. 3—*Gas chromatogram of N-trifluoroacetyl isopropyl esters of amino acids in dentin. Column temperature, 110°C, 1 min hold, and then programmed to 190°C at 2°C /min; injection temperature, 240°C; carrier gas, helium; split ratio, 40:1.*

estimated age was between 30 and 40 years as determined by the autopsy. The estimated age by racemization was 39 ± 3 years. After 9 days, the body was identified as a 41-year-old woman who managed a hotel.

Case 3

An adult skeletonized female body covered by concrete was found in a cedar forest. The evidence suggested that a hole had been dug, the body placed inside, and concrete poured on top, confirming the likelihood that the victim had been murdered and the body abandoned. The estimated age determined by autopsy was 20 to 30 years. The estimated age determined by racemization was 19 ± 3 years. Information obtained from the body such as height and blood type was similar to a missing person (known as S), aged 21 years, whose dental chart and radiographs matched the body. The body was therefore positively identified as S.

Case 4

A naked female body covered with fallen leaves was found on the slope of a path through a forest. The estimated age determined by autopsy was between 35 and 45 years. Racemization analysis produced an estimate of 57 ± 3 years. After 5 days, a man reported that the body could be that of his missing wife, aged 55 years. Dental information then confirmed that the body was his wife.

Case 5

A naked decomposed female body bound hand and foot with ropes was found floating in the sea attached to a lead diving belt.

TABLE 1—*Five cases of age estimation from teeth using amino acid racemization.*

	Materials Investigated	Actual Age	ln[(1+D/L)/(1−D/L)]	Age Calculation Formula	Age Estimated from Teeth
Case Report 1 (18 years of age)					
A	Mandibular lateral incisor (right)	40	0.1598	Y = 231.38X−2.21 r = 0.996 n = 5	39
	Mandibular lateral incisor (left)	50	0.2136		51
	Mandibular lateral incisor (right)	58	0.2406		57
	Mandibular lateral incisor (right)	63	0.2618		62
	Mandibular lateral incisor (right)	67	0.2780		66
B	Mandibular lateral incisor (left)	?	0.0818		21
	Mandibular lateral incisor (right)	?	0.0814		21
Case Report 2 (41 years of age)					
A	Mandibular first premolar (right)	17	0.0502	Y = 680.81X−18.49 r = 0.994 n = 5	15
	Mandibular first premolar (left)	47	0.1008		50
	Mandibular first premolar (right)	61	0.1156		60
	Mandibular first premolar (left)	67	0.1284		68
	Mandibular first premolar (right)	78	0.1374		75
B	Mandibular first premolar (left)	?	0.0858		39
	Mandibular first premolar (right)	?	0.0852		39
Case Report 3 (21 years of age)					
A	Mandibular central incisor (right)	31	0.0784	Y = 832.57X−33.29 r = 0.998 n = 5	31
	Mandibular central incisor (left)	41	0.0876		39
	Mandibular central incisor (left)	52	0.1032		52
	Mandibular central incisor (right)	69	0.1100		58
	Mandibular central incisor (left)	67	0.1210		67
B	Mandibular central incisor (left)	?	0.0630		19
	Mandibular central incisor (right)	?	0.0634		19
Case Report 4 (55 years of age)					
A	Mandibular lateral incisor (right)	39	0.0772	Y = 815.00X−22.44 r = 0.986 n = 6	40
	Mandibular lateral incisor (left)	48	0.0844		46
	Mandibular lateral incisor (right)	52	0.0922		52
	Mandibular lateral incisor (right)	54	0.0928		53
	Mandibular lateral incisor (right)	57	0.0964		56
	Mandibular lateral incisor (left)	61	0.1038		62
B	Mandibular lateral incisor (right)	?	0.0976		57
Case Report 5 (66 years of age)					
A	Mandibular first premolar (left)	31	0.0744	Y = 806.40X−29.96 r = 0.995 n = 6	30
	Mandibular first premolar (left)	42	0.0910		43
	Mandibular first premolar (left)	45	0.0930		45
	Mandibular first premolar (left)	50	0.1008		51
	Mandibular first premolar (right)	55	0.1038		54
	Mandibular first premolar (right)	63	0.1146		63
B	Mandibular first premolar (left)	?	0.1228		69
	Mandibular first premolar (right)	?	0.1210		68
A	Mandibular second premolar (right)	36	0.0760	Y = 733.07X−21.30 r = 0.992 n = 5	34
	Mandibular second premolar (right)	42	0.0874		43
	Mandibular second premolar (left)	46	0.0942		48
	Mandibular second premolar (left)	52	0.1002		52
	Mandibular second premolar (right)	65	0.1162		64
B	Mandibular second premolar (left)	?	0.1186		66
	Mandibular second premolar (right)	?	0.1176		65

A, Teeth used for standards; B, cases; Y, age; X, ln[(1+D/L)/(1−D/L)]; r, coefficient of correlation.

The body had been stabbed more than 10 times with a knife in the chest and abdomen. It was believed that the body had been moved from the murder site and dumped into the sea from a cliff. The estimated age determined by autopsy was 45 to 60 years. The estimated age by racemization analysis was 67 ± 3 years. The body was later identified as a 66-year-old woman from dental findings and blood type.

Discussion

Dentin is used for age estimation using racemization. To obtain an accurate age, more than four control teeth of the same type from individuals of known age are required. This is the same procedure used with DNA fingerprinting when examining a subject with a control (size marker). Age estimation equations (linear equations by the least square method) are obtained using racemization rates from the control teeth, and the age is estimated by substituting the racemization rates into that equation each time.

After fabrication of longitudinal tooth sections, the entire sectioned dentin parts are completely powdered and mixed to collect 5–10 mg of powder (as little as 2–3 mg may be sufficient). Single-rooted teeth such as mandibular incisors or mandibular premolars are ideal for this technique as they have a relatively small volume, making it easy to collect the entire dentin sample. In addition, the process of racemization is almost completely halted by death, because of the rapid decrease in body temperature. Therefore, an estimated age at the time of death can generally be obtained from bodies 10 years or more after death. Age estimates can be accurately obtained from burned bodies if the surface color phases of the teeth are the same as live teeth (8).

This method is extremely reliable in comparison with conventional age estimation methods, and it has been suggested that the

method be adopted as an international standard (9). However, except for the authors, almost no researchers are applying this method in Japan. Possible reasons for the lack of popularity of this method include: (i) several control teeth of known age are required; (ii) it is difficult to fabricate a column that will achieve excellent separation; and (iii) it is difficult to separate the dentin from the other components of teeth. Currently, the authors are trying to fabricate a capillary column that is able to completely and clearly separate D-Asp and L-Asp in a short period of time for accurate and simple testing (7). We hope this method will become widely used for age estimation of unidentified bodies.

References

1. Helfman PM, Bada JL. Aspartic acid racemisation in tooth enamel from living humans. Proc Nat Acad Sci USA 1975;72:2891–4.
2. Helfman PM, Bada JL. Aspartic acid racemisation in dentine as a measure of ageing. Nature 1976;262:279–81.
3. Ohtani S. Different racemization ratios in dentin from different locations within a tooth. Growth Dev Aging 1997;61:93–9.
4. Ohtani S, Ito R, Yamamoto T. Differences in the D/L aspartic acid ratios in dentin among different types of teeth from the same individual and estimated age. Int J Legal Med 2003;117:149–52.
5. Ohtani S. Estimation of age from the teeth of unidentified corpses using the amino acid racemization method with reference to actual cases. Am J Forensic Med Pathol 1995;16:238–42.
6. Ohtani S, Yamamoto T. Strategy for the estimation of chronological age using the aspartic acid racemization method with special reference to coefficient of correlation between D/L ratios and ages. J Forensic Sci 2005;50:1020–7.
7. Abe I, Ohtani S. Novel chiral selectors anchored on polydimethylsiloxane as stationary phases for separation of derivatized amino acid enantiomers by capillary gas chromatography. J Sep Sci 2006;29:319–24.
8. Ohtani S, Sugeno H, Marumo T, Yamamoto K. Two cases of age estimation from teeth of burned body using amino acid racemization. Jpn J Legal Med 1989;43:191–7. (in Japanese).
9. Waite ER, Collins MJ, Ritz ST, Schutz HW, Cattaneo C, Borrman HIM. A review of the methodological aspects of aspartic acid racemization analysis for use in forensic science. Forensic Sci Int 1999;103:113–24.

Additional information and reprint requests:
Susumu Ohtani, Ph.D.
Institute for Frontier Oral Science
Kanagawa Dental College, 82 Inaoka-cho
Yokosuka, 238-8580
Kanagawa
Japan
E-mail: ohtanisu@kdcnet.ac.jp

JOURNAL OF FORENSIC SCIENCES

J Forensic Sci, November 2010, Vol. 55, No. 6
doi: 10.1111/j.1556-4029.2010.01525.x
Available online at: onlinelibrary.wiley.com

CASE REPORT

ODONTOLOGY; ANTHROPOLOGY

Emilio Nuzzolese,[1] *D.D.S., Ph.D. and Matteo Borrini,*[2] *M.S.*

Forensic Approach to an Archaeological Casework of ''Vampire'' Skeletal Remains in Venice: Odontological and Anthropological Prospectus*

ABSTRACT: During the years 2006–2007, the Archeological Superintendent of Veneto (Italy) promoted a research project on mass graves located on Nuovo Lazzaretto in Venice, where the corpses of plague deaths were buried during the 16th and 17th centuries. The burials were of different stages and are believed to be the remains of plague victims from the numerous outbreaks of pestilence, which occurred between the 15th and 17th centuries. Among the fragmented and commingled human bones, an unusual burial was found. The body was laid supine, with the top half of the thorax intact, arms parallel to the rachis axis, the articulations were anatomically unaltered. Both the skull morphology and the dimensions of the *caput omeris* suggest the body was a woman. A brick of moderate size was found inside the oral cavity, keeping the mandible wide open. The data collected by the anthropologist were used to generate a taphonomic profile, which precluded the positioning of the brick being accidental. Likewise, the probability of the brick having come from the surrounding burial sediment was rejected, as the only other inclusions found were bone fragments from previous burials in the same area. The data collected by the odontologist were employed for age estimation and radiological dental assessment. The forensic profile was based conceptually on the ''circumstances of death'' and concluded that the positioning of the brick was intentional, and attributed to a symbolic burial ritual. This ritual confirms the intimate belief held at those times, between the plague and the mythological character of the vampire.

KEYWORDS: forensic science, forensic odontology, forensic anthropology, forensic radiology, vampirism, forensic archaeology

Paleopathological examination of skeletal remains of suspected ''vampires'' coming from ancient sites may shed light on reasons for a vampire folk belief and for the ways in which these corpses were treated in terms of burial rites. To this end, taphonomy plays an important role here (1,2).

Belief in the vampire myth is widespread throughout the world. Greece has a long tradition of vampires. Examples of the Greek ''undead'' date back to the ancient world with creatures, such as Efialtae, Striges, Lamiae, Empoussai, Epopidae, Yello, and Mormo. In Homer's Odyssey, it is clearly stated that the dead like drinking blood (3). There also existed special festivals in the honor of the dead, the Anthesteria and in Roman times, the Lemuria. In Byzantium, Slavic influence, in conjunction with the precepts of the Greek Orthodox Church, form the legend of a Greek vampire species called ''Vrykolakas,'' the Slavic word for werewolf. The word became directly associated with vampires out of the belief that all werewolves would be vampires after death (3,4). The presence of vampires also exists in medieval Greek texts, novels, manuscripts, ecclesiastical laws, exorcisms, and folk songs (5). Forensic pathology proposes that most, if not all, of the beliefs surrounding the ''vampire'' can be explained in terms of folk misconceptions based on the processes of decomposition of the cadaver after death.

[1]Viale JF Kennedy 77, 70124 Bari, Italy.
[2]Via Del Mattone 17/A, 19131 Cadimare (SP), Italy.

*Presented at the 61st Annual Meeting of the American Academy of Forensic Sciences, February 16–21, 2009, in Denver, CO.

Received 3 June 2009; and in revised form 21 July 2009; accepted 15 Aug. 2009.

Finally, in the clinical–pathological record, conditions producing symptoms that are similar to vampiric attributes include rabies, anthrax, photosensitivity, and serious psychological disorders (5–8). Against the popular misconception that nails and hair keep growing after death, it is a consequence of a back shrinkage of the skin. Also swelling, which sometimes is extreme, is the main reason why the cadaver is pinned, tied, or weighed down in its grave, and the ''vampire'' corpse is often killed by piercing. The revenant cannot cross the water because, as a result of extreme swelling, the body will emerge and float (1).

Background

During the years 2006–2007, the Archeological Superintendent of Veneto (Italy) promoted research project on mass graves located on Nuovo Lazzaretto in Venice, where the corpses of plague deaths were buried during the 16th and 17th centuries.

The project was part of a summer work camp by Archeoclub (Venice Section) and was carried out with sponsorship of the International Centre of Archaeological Research (CIRA) and the Radix Project ''Venetian archaeological sites to be saved,'' with the assistance of La Spezia Archaeological Group (G.A.SP.)

The excavation area is located in a cemetery site positioned around an ancient wall built after a health and quarantine decree of the Republic Senate dated July 8, 1468 meaning to establish a bulwark against epidemics.

At the excavation site, the recovery stage was performed applying traditional archaeological techniques along with modern

forensic archaeology/anthropology protocols in order to improve accuracy and data collection.

Two stratigraphic macro-units were discovered: one unit contained mixed disjointed skeletal remains with ancient *postmortem* fragmentation and sharp/blunt breaks; the other unit contained human remains of primary deposition, generally showing no postburial disturbance.

The stratigraphic data and the finding of devotional medals coined on the 1600 Jubilee allowed pinpointing of the intact bodies to the 17th century plague. Those corpses were buried by digging into previous graves that may be dated to the previous Venetian plague in 1576.

Archaeological and Anthropological Considerations

The taphonomic evaluation allowed the reconstruction of the various decomposition phases of each corpse as well as the understanding of the stratigraphical seriation because of piling of bodies during burial and its relevance to shrouds, cloths used to wrap a body for burial. Sharp/blunt breaks on the bones can be explained by the work of gravediggers with their spades. Within these two macro-stratigraphic units (16th and 17th centuries), we can also spot different phases of body depositions, with postburial disturbances and intersection of skeletons.

Among the burials that have been studied using this approach, there is a body that appears as particularly interesting: the skeleton is preserved from half the chest to the skull because it was cut at the humeral diaphyses when later graves were dug (Fig. 1).

The individual (classified as number ID 6), currently still under analysis, is at the moment identified as an adult woman by the general skull morphology and *caput humeris* size (9). The skeleton was interred supine in a simple burial pit (covered space), with her arms parallel to the rachis axis; the anatomical relationships between bones are well preserved, all joints persist in an anatomical order except for a slight verticalization of the left clavicle because of a wall effect produced by a shroud (which also caused small slumping and splaying of ribs).

The distinctiveness of the ID 6 grave is that a moderate-size piece of brick is inside the oral cavity, keeping the mandible wide open while still articulated in the glenoid cavity (Figs 2 and 3). A thanatological and taphonomic profile rules out postmortem displacement of bones (10) and a subsequent collapse of the object inside the oral cavity. Also, it is highly unlikely that pieces of bricks were part of the sediments that were used to fill the burial, because the only "substantial" elements in the soil are bone fragments related to more ancient depositions, destroyed by the continuous activities in the graveyard.

As the insertion of the brick into the dead woman's mouth must be considered intentional, this practice probably had such a symbolic and ritual value, that the sextons working in the graveyard during the plague handled the corpse that way, despite the danger of infection.

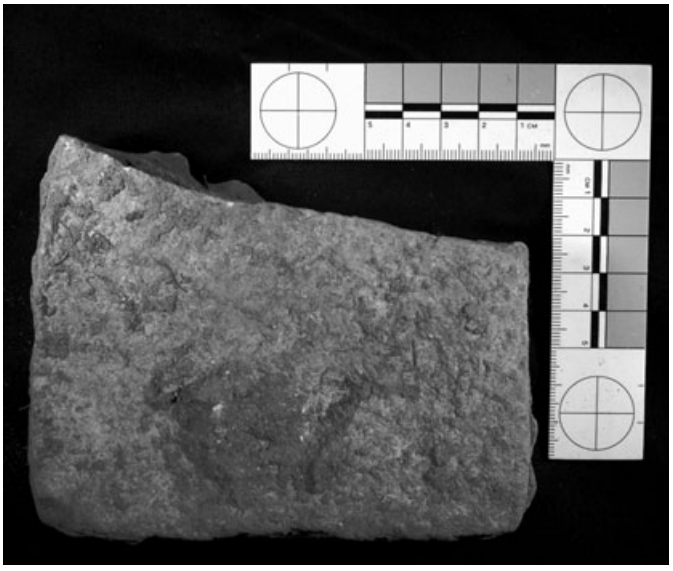

FIG. 1—*Brick found in the oral cavity.*

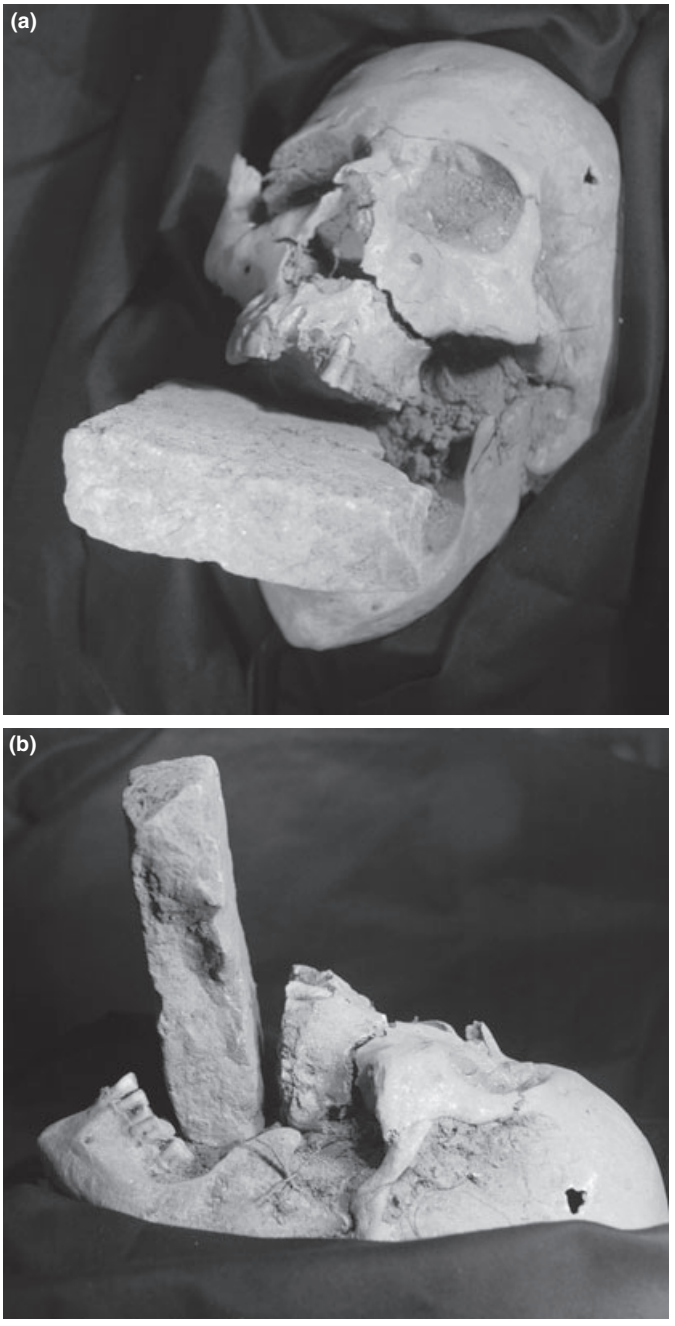

FIG. 2—*(a) The skull as it appeared in the excavation site with brick repositioned in the oral cavity. (b)* Lateral view.

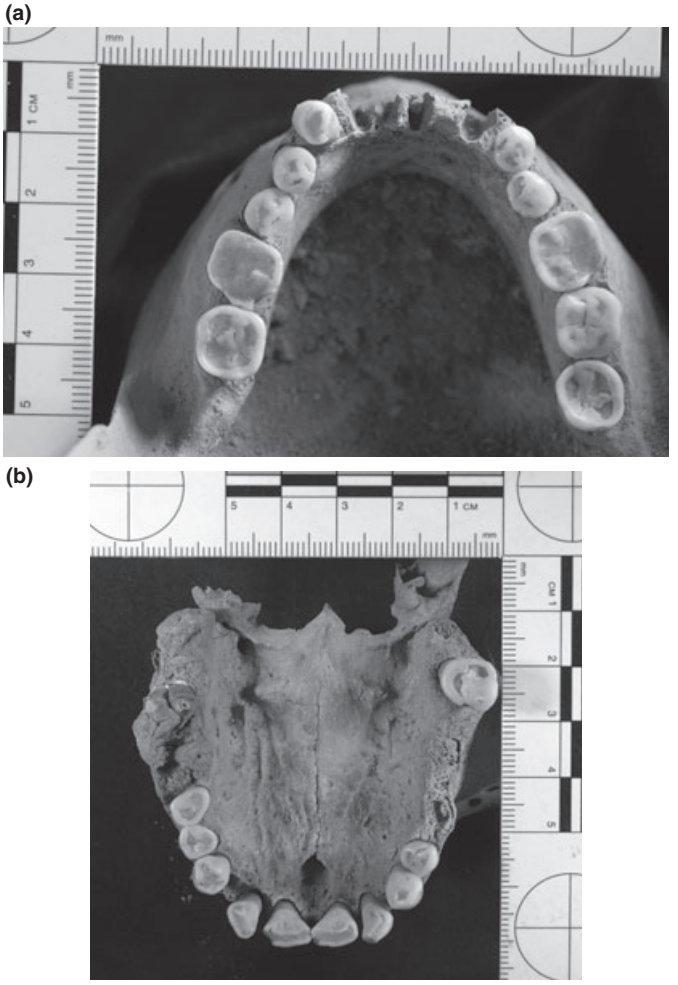

FIG. 3—*(a) Photographs of the oral cavity area: occlusal upper view. (b) Occlusal lower view.*

Odontological Study

The material was analyzed macroscopically before and after the sediment removal (Fig. 3) in the Museum of Prehistory in Florence, where the remains and skull are temporarily stored. Found teeth were repositioned finding the right alveolus. The macroscopic analysis revealed almost complete arches, no dental treatments, a high degree of abrasion of occlusal surfaces, lack of enamel hypoplastic defects, and inferior incisors lost postmortem. Both arches underwent digital photographs and periapical radiological imaging using Nomad X-Ray portable device (Aribex Inc., Orem, UT) and Radiovideography sensor (Trophy, Vincennes, France) connected to a computer, with 0.05-sec exposure time and 68 Kv (Fig. 4). Dental wear, which is widely used in anthropology, could not be a reliable method for age estimation. Age assessment method proposed by Cameriere et al. was employed (11–13). This method uses the apposition of secondary dentine that is proven to be reliable, regardless of the historical period of the specimen, and particularly suitable for adults individuals. The canines periapical X-ray images (Fig. 5) were employed together with Adobe Photoshop to determinate the area of the pulp chamber of the canine and its entire area thus applying the regression formulae to evaluate chronological age as suggested by Cameriere et al. (11–13). Using this method, we obtained an estimated age of 61 ± 5 years.

The dental analysis revealed the individuals did not suffer any sustained periods of childhood stress from malnutrition or disease.

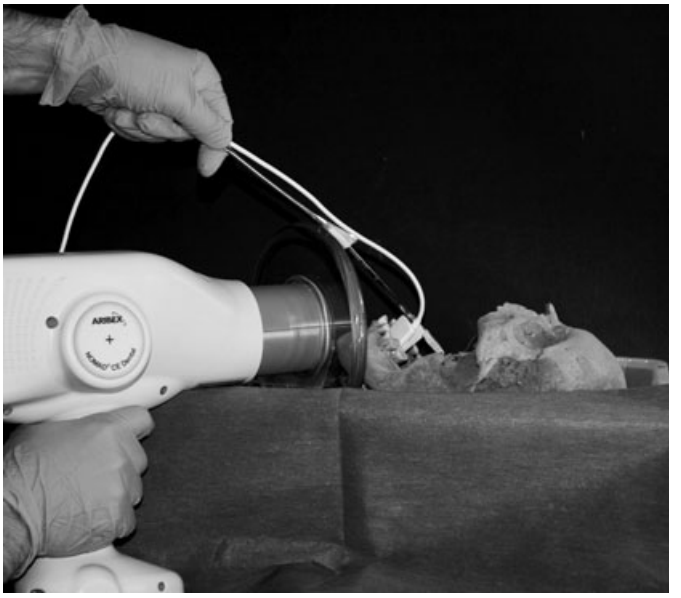

FIG. 4—*Nomad X-ray portable device combined with a sensor connected to a notebook, while examining the skull, stored in the Museum of Prehistory in Florence.*

FIG. 5—*Periapical X-ray image of upper right canine for Cameriere et al's. age estimation method.*

Conclusion

We assume that during the digging of a hole in the ground for a person who had just died of the plague, the gravediggers cut off the ID 6 deposition. They noticed the shroud (its presence is suggested by the verticalization of the clavicle) and a hole, which corresponded with the mouth. As the body appeared as quite intact, they probably recognized in that body the so-called *vampire,* responsible for plague by chewing her shroud. As a consequence, they inserted a brick in her mouth. The sequence of those events

(*time since death*) can be deduced by the lack of alteration on the skeleton joints, so that we can suppose that the gravediggers dealt with the corpse when it was not disjointed yet. The insertion of the brick into the mouth at the time of the primary deposition can be ruled out because we have no reference, even folkloric, for such a practice in that historical and cultural context.

It is not strange that superstitions concerning vampires were widespread in the 16th to 17th centuries even in a ''cosmopolitan'' and evolved city like Venice. It is surprising, however, that this exorcism ritual has been clearly recognized in an archaeological context: the ID 6 grave could well be the first ''vampire'' burial archaeologically attested and studied by a forensic odontological and anthropological approach.

Final Remarks

Forensic science is a fast-evolving cluster of applied disciplines that operate independently as well as interdisciplinarly. Fields like anthropology and odontology develop and expand incorporating new methods and theories. As a result, the boundaries between forensic science disciplines become blurred allowing a multidisciplinary involvement and approach, especially when skulls are involved.

References

1. Barber P. Forensic pathology and the European vampire. In: Dundes A, editor. The vampire: a casebook. Madison, WI: The University of Wisconsin Press, 1998;109–42.
2. Haglund WD, Sorg MH, editors. Forensic taphonomy: the post-mortem faith of human remains. Boca Raton, FL: CRC Press, 1997.
3. Davias O. Montague summers: o ellin vrykolax, ekd. Delfini: Athina, 1995.
4. Tsaliki A. Vampires beyond legend: a bioarchaeological approach. Proceedings of the XIII European Meeting of the Paleopathology Association; 2000 Sept 18–23; Chieti, Italy. Teramo: Edigrafital S.p.A, 2001;295–300.
5. Gomez-Alonso J. Rabies: a possible explanation for the vampire legend. Neurology 1998;51:856–9.
6. Jaffe PD, Dicataldo F. Clinical vampirism: blending myth and reality. In: Dundes A, editor. The vampire: a casebook. Madison, WI: The University of Wisconsin Press, 1998;143–58.
7. Lutwick LI. G-Docs and X-files. Infect Med 1998;3:165–7, 210.
8. Sledzik PS, Bellantoni N. Brief communication: bioarcheological and biocultural evidence for the New England vampire folk belief. Am J Phys Anthropol 1994;94(2):269–74.
9. Borrini M. Archeologia forense: metodo e tecniche per il recupero dei resti umani: compendio per l'investigazione scientifica. Bologna: Editrice Lo Scarabeo, 2007 (in Italian).
10. Roksandic M. Position of skeletal remains as a key to understanding mortuary behaviour. In: Haglund WD, Sorg MH, editors. Advances in forensic taphonomy. Boca Raton, FL: CRC Press, 2001;99–117.
11. Mincer HH, Chaudhry J, Blankenship JA, Turner EW. Postmortem dental radiography. J Forensic Sci 2008;53(2):405–7.
12. Cameriere R, Brogi G, Ferrante L, Mirtella D, Vultaggio C, Cingolani M, et al. Reliability in age determination by pulp/tooth ratio in upper canines in skeletal remains. J Forensic Sci 2006;51(4):861–4.
13. Cameriere R, Ferrante L, Belcastro MG, Bonfigli B, Rastelli E, Cingolani M. Age estimation by pulp/tooth ratio in canines by mesial and vestibular peri-apical x-rays. J Forensic Sci 2007;52(5):1151–5.

Additional information and reprint requests:
Matteo Borrini, M.S.
Via del Mattone 17/a
19131 Cadimare (SP)
Italy
E-mail: matteo.borrini@gmail.com

JOURNAL OF FORENSIC SCIENCES

J Forensic Sci, November 2010, Vol. 55, No. 6
doi: 10.1111/j.1556-4029.2010.01469.x
Available online at: onlinelibrary.wiley.com

CASE REPORT

PATHOLOGY AND BIOLOGY

Meredith A. Lann,[1] *M.D. and Amy Martin,*[2] *M.D.*

An Unusual Death Involving a Sensory Deprivation Tank*

ABSTRACT: Deaths involving sensory deprivation tanks are very rare. We describe a unique case in which a previously healthy 50-year-old woman apparently died while floating in a sensory deprivation tank at her residence. Autopsy failed to reveal definitive anatomical abnormalities pointing to the cause of death. A thorough scene investigation, full medicolegal autopsy to include toxicological analyses, and a complete investigation into the equipment at the scene, were conducted. Blood toxicologic studies were significant for the presence of ethanol (0.27%) and a mixture of over-the-counter sedating medications and prescription drugs. The cause of death was ruled as acute mixed drug and ethanol toxicity combined with probable environmental hyperthermia; manner was accident. This case report will help the forensic community understand the intended use of flotation tanks, as well as possible risks associated with improper use.

KEYWORDS: forensic science, forensic pathology, relaxation, sensory deprivation, toxicity, flotation tank

Sensory deprivation tanks, also known as isolation tanks or flotation baths, are lightless, soundproof chambers in which a subject can float in a virtually stimulation-free environment. The flotation tank consists of a small chamber filled with water only about 30-cm (10 inches) deep, resembling a large garden tub with a metal roof containing a single door for entry and exit. This environment greatly reduces visual, auditory, and tactile stimulation. To reduce skin sensation, subjects usually float nude and adjust the water temperature to that of skin temperature (93–96°F). Magnesium sulfate salts added to the water (*c.* 25% concentration) increase buoyancy and allow the subject to float supine while keeping the face and upper chest above the water. Some units possess a ring-shaped heating coil underneath, which creates a subtle convection current that, when heated, keeps the subject in the center of the pool and minimizes contact with the sides of the chamber. Tanks may be used at home or in flotation centers and spas, which offer use of a flotation tank for a fee.

Here, we describe a unique death that occurred inside a sensory deprivation tank. We include a discussion of the intended uses of sensory deprivation and flotation therapy, as well as special considerations for the scene investigation and when performing autopsy in this type of death.

Case Report

A 50-year-old woman was found dead within the basement of her residence, her body floating supine inside a closed sensory deprivation tank (Fig. 1). The scene was secure, and there was no evidence of foul play. The deceased was previously healthy and had no significant medical history. The deceased reportedly drank alcohol, sometimes mixing alcohol with both prescription and over-the-counter medications. However, she did not use illicit drugs currently. According to family and friends, she had never mentioned nor attempted suicide, although had been feeling increasingly stressed. She was last known to be alive *c.* 2 days prior to being found, after conversing by phone with a friend.

The deceased was found nude, floating supine in the tank with the face and upper chest clearly above the surface of the water. The depth of the water was *c.* 18 inches. Early to moderate decomposition changes were noted, consisting of marbling and patchy skin slippage that was more prominent over the submerged portions of the body (Fig. 2). The door to the tank was working properly; there were no abnormalities that would prevent one from exiting the tank. The external pump filtration system was situated alongside the tank (Fig. 3) and was still running when the body was found. It should be noted that the deceased had reportedly never used the flotation tank before, and likely was not familiar with the appropriate use of the device.

A full medicolegal autopsy revealed the body of a normally developed, normally nourished Caucasian woman with mild decomposition changes as described previously. A thin film of dry, white powdery material was seen over submerged portions of the body consistent with submersion in water containing magnesium salts. Petechiae over the face or mucosae were absent. The extremities showed marked pruning of the fingers and feet. On internal examination, the organs were pale and somewhat firm and the musculature was firm and pink–brown, consistent with exposure to external heat. There was no hemorrhage or fracture in the neck. The tongue was free of bite marks or other lesions. Diffuse hemolytic staining was present on all endothelial and endocardial surfaces. Pulmonary emboli were absent, and the airways were clear of significant debris or fluid. The heart weight was 400 g; significant atherosclerotic stenosis or thrombosis were not present in the coronary arteries. Both lungs were moderately heavy (right 750 g,

[1]Southwestern Institute of Forensic Sciences, Dallas, TX.
[2]Denver Office of the Medical Examiner, Denver, CO.
*Presented at the 61st Annual Meeting of the American Academy of Forensic Sciences, February 16–21, 2009, in Denver, CO.

Received 14 May 2009; and in revised form 4 Sept. 2009; accepted 6 Sept. 2009.

FIG. 1—*Scene photo. The body was floating supine in the flotation tank and exhibited moderate decompositional changes, which are more prominent in the submerged portions of the body.*

FIG. 2—*Scene photo. Close-up view of the body illustrating the face and nose are above the level of the water.*

left 610 g), with congestion and edema. Significant abnormalities of the calvarium and brain (1370 g) were absent. Light microscopic examination of hematoxylin and eosin-stained sections of all vital organs was consistent with the observed state of decomposition and otherwise noncontributory.

Toxicologic analyses of peripheral blood and urine were performed. Doxylamine, an over-the-counter antihistamine sedative, was detected in the blood at a level of 1.35 ug/mL. The over-the-counter antihistamine diphenhydramine was detected in the blood at 14 ng/mL. For comparison, the peak blood level in healthy persons after ingestion of a single oral therapeutic dose of 25 mg doxylamine is 99 ug/L, and the peak blood level after oral ingestion of 50 mg of diphenhydramine is 66 ug/L (1). A low level of sertraline at 31 ng/mL was also detected in the blood using liquid–liquid extraction and gas chromatography with mass spectrometry (courtesy El Paso County Coroner's Office Toxicology Lab, Colorado Springs, CO). The blood ethanol level was 0.270%. Chemical analysis of the vitreous revealed an elevated creatinine of 5.2 mg/dL.

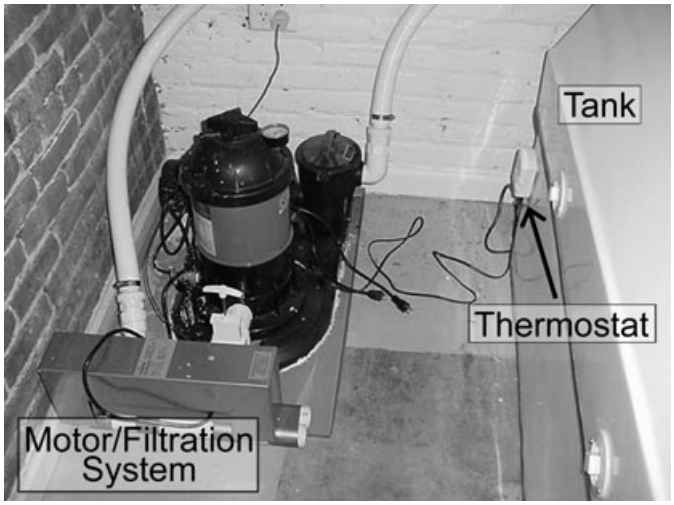

FIG. 3—*Scene photo. The filtration pump and motor (left) were inadvertently left on while using the flotation tank, resulting in heat transfer from the motor to the nearby tank (right).*

Discussion

Deaths involving sensory deprivation tanks are very rare. A thorough literature search using PubMed and Ovid MEDLINE search engines yielded no reported cases in the medical literature; however, one recent online news article describes the death of a 30-year-old man in the United Kingdom who purportedly drowned during a flotation session after ingestion of ketamine (2).

Different forms of sensory deprivation have been practiced since the days of ancient Greece. The flotation tank was created by neuropsychiatric researcher Dr. John C. Lilly in the 1950s, and was used in his studies on human consciousness. In the mid-1960s, a technique called flotation reduced environmental stimulation therapy (REST) emerged as a methodology for investigation into psychiatric and personality disorders. Recently, many stress reduction or behavioral modification programs use flotation REST, as reportedly this environment engenders optimism, euphoria, and positive inner well-being that is conducive to enhanced learning states and behavioral change (3–5). Flotation REST has been increasingly employed as an alternative therapy for chronic medical conditions such as systemic hypertension, chronic headache, joint and low back pain, chronic whiplash syndrome, ankylosing spondylitis, and fibromyalgia (6–8). Controlled studies on the efficacy of therapeutic flotation REST are very limited; a few small controlled studies describe significant decreases in heart rate and blood pressure both during and after flotation sessions (6,9) and detectable electroencephalographic changes similar to dream sequences (10,11).

It is important to note that the filtration system is not supposed to be on during flotation sessions. Not only does the pump motor tend to create unwanted noise, but the pump can reach very high temperatures (up to 130°F) while running. The temperature of water in the tank at the time of scene investigation was *c.* 20°F higher than the usual target temperature. This close-coupled pump has a built-in motor with the motor drive and the pump impeller on the same shaft, and therefore the heat generated from the motor can be transferred to the fluid within the tank. The temperature of the water in the tank at the time of scene investigation was 116°F, approximately 20 degrees higher than the set target temperature of 97°F. The thermostat of the water heater was found to be functioning properly as it consistently turned off as the water temperature

approached the high set point. However, there was no safety device to shut the pump off if water temperatures elevated to an unsafe level. Indeed, a test run of the unit demonstrated that the water temperature in the tank could be significantly increased solely from heat transfer from the motor, from 67.4° to 96.2°F, over 20-h time. With an estimated postmortem interval of 24–36 h, the pump motor alone would have been capable of raising the water temperature in the tank from the presumed temperature of 97°F during the decedent's session to the 116°F (change in temperature of 19°F), when she was discovered.

A complete inspection of the equipment was performed by a certified electrician familiar with this type of motor and filtration system and heated water tanks. The pump apparatus, filtration system, and UV light were found to have no electrical hazard or abnormal current.

Flotation tank deaths are similar in many regards to hot tub deaths. Similar health hazards exist; for both types of deaths, one must consider similar differential causes of death to include drowning, electrocution, natural causes, and hyperthermia. However, the buoyancy provided by the addition of magnesium sulfate salts in flotation tanks greatly reduces the likelihood of drowning. The physiologic changes that occur with heat transfer during immersion in warm water include increased peripheral vasodilation and perspiration, effectively decreasing peripheral blood volume and increasing blood viscosity. One author describes various electrocardiographic abnormalities that may occur, and possibly increase risk for adverse outcomes such as syncope or inherent arrhythmia, especially in elderly individuals or individuals with preexisting cardiovascular disease (12). Furthermore, the use of alcohol, cocaine, or medications that affect temperature-regulating mechanisms may exacerbate these complications; therefore, toxicologic studies are imperative for these types of deaths.

We suspect that as the decedent was not accustomed to using this device, she likely did not know to turn the pump off during use. It appears she fell asleep during her session and was henceforth unable to respond appropriately to the hyperthermic conditions. The combination of ethanol and sleep-enhancing medications of doxylamine and diphenhydramine were likely contributory in this regard. One may hypothesize that these substances may have even acted synergistically in blunting her response to the increased temperature of the water.

As there are no specific diagnostic anatomical criteria for death by hyperthermia (13), our conclusions were made after consideration of the circumstances surrounding the death. Drowning is difficult to define based on anatomic findings. However, drowning seemed unlikely in this case given the decedent's nose and mouth were clearly above water level and the lungs did not take on the typical distended, heavy nature that is typically seen in drownings. Furthermore, the airways and stomach were free of significant fluid collection. Other possible natural causes of death to include arrhythmia, myocardial infarction, and seizure were considered, but also considered unlikely given this was a healthy woman with no known prior medical conditions and no significant anatomical findings at autopsy. Electrocution was also deemed unlikely given there was no identifiable abnormal current in the device.

Although they are rare, deaths in flotation tanks can occur. It is critical to perform a full medicolegal autopsy and complete toxicological analyses in these types of cases. Moreover, scene investigation into sensory deprivation tank deaths calls for special considerations and safety precautions to avoid injury to individuals present during the investigation. And as for any equipment-related death, it is critical that experts who are familiar with the equipment inspect the unit in question for potential hazards such as electrical short-circuiting or other functional defects. No such functional defects were found in this case.

Ultimately, after assessing the circumstances surrounding the death and the findings at the scene and autopsy, the cause of death was determined as a result of complications of acute mixed drug and alcohol toxicity combined with probable environmental hyperthermia. The manner was ruled as accident.

References

1. Baselt RC. Disposition of toxic drugs and chemicals in man, 8th edn. Foster City, CA: Biomedical Publications, 2008;489–91, 520–2.
2. http://www.getreading.co.uk/news/s/2032922_floatation_tank_horror (accessed June 28, 2009).
3. Cooper GD, Adams HB. Studies in REST, II. An overview of REST technology. J Subst Abuse Treat 1988;5:69–75.
4. Adams HB. Studies in REST, III. REST, arousability, and the nature of alcohol and substance abuse. J Subst Abuse Treat 1988;5:77–81.
5. Forgays DG. Flotation REST as a smoking intervention. Addict Behav 1987;12:85–90.
6. Bood SA, Sundequist U, Kjellgren A, Nordstrom G, Norlander T. Effects of flotation-restricted environmental stimulation technique on stress-related muscle pain: what makes the difference in therapy—attention-placebo or the relaxation response? Pain Res Manag 2005; 10(4):201–9.
7. Hill S, Eckett MJH, Paterson C, Harkness EF. A pilot study to evaluate the effects of floatation spa treatment on patients with osteoarthritis. Complement Ther Med 1999;7:235–8.
8. Edebol H, Bood SA, Norlander T. Chronic whiplash-associated disorders and their treatment using flotation-REST (Restricted Environmental Stimulation Technique). Qual Health Res 2008;18(4):480–8.
9. Jacobs GD, Heilbronner RL, Stanley JM. The effects of short term flotation rest on relaxation: a controlled study. Health Psychol 1984;3(2):99–112.
10. Iwata K, Nakao M, Yamamoto M, Kimura M. Quantitative characteristic of alpha and theta EEG sctivities during sensory deprivation. Psychiatry Clin Neurosci 2001;55:191–2.
11. Jacobs GD, Benson H, Friedman R. Topographic EEG mapping of the relaxation response. Biofeedback Self Regul 1996;21(2):121–9.
12. Press E. The health hazards of saunas and spas and how to minimize them. Am J Public Health 1991;81(8):1034–7.
13. DiMaio VJ, DiMaio D. Forensic pathology, 2nd edn. New York, NY: CRC Press LLC, 2001;425–6.

Additional information and reprint requests:
Meredith A. Lann, M.D.
Southwestern Institute of Forensic Sciences
5230 Southwestern Medical Avenue
Dallas, TX 75235
E-mail: malann@dallascounty.org

JOURNAL OF FORENSIC SCIENCES

J Forensic Sci, November 2010, Vol. 55, No. 6
doi: 10.1111/j.1556-4029.2010.01521.x
Available online at: onlinelibrary.wiley.com

CASE REPORT

PATHOLOGY/BIOLOGY

Lisa B.E. Shields,[1] *M.D.; Cristin M. Rolf,*[2] *M.D.; Gregory J. Davis,*[2] *M.D.; and John C. Hunsaker III,*[2] *M.D., J.D.*

Sudden and Unexpected Death in Three Cases of Ehlers-Danlos Syndrome Type IV*

ABSTRACT: Ehlers–Danlos syndrome (EDS) type IV is a connective tissue disorder characterized by the inability to produce sufficient amounts of collagen or a defect in the structure of collagen. The most serious complications include a rupture of a viscus or vascular rupture with or without mural dissection. Death may result from internal hemorrhage. This report describes three cases of sudden and unexpected death caused by EDS type IV. Two cases involved hemothorax as a result of dissection of the subclavian artery and aorta, respectively. The third case represented spontaneous pulmonary rupture and hemorrhage. A detailed family history should be sought, and additional specimens collected to confirm the diagnosis, including skin fibroblasts for collagen testing and blood for DNA testing. The forensic pathologist should consider the possibility of EDS type IV upon discovery of spontaneous visceral or arterial rupture and should alert the family members of this hereditary and potentially fatal condition.

KEYWORDS: forensic science, forensic pathology, Ehlers–Danlos syndrome, sudden death, connective tissue disorder, hereditary

The initial description of the triad of skin laxity and fragility as well as joint hypermobility was published in Russia in 1892 (1). This condition was subsequently reported by Ehlers and Danlos in 1901 and 1908, respectively, and the Ehlers–Danlos syndrome (EDS) was formally introduced (2,3). This syndrome is a heterogeneous group of connective tissue disorders that have been classified into 11 various subtypes with further simplification into six major types (4,5). The spectrum of EDS encompasses a host of disorders with various clinical features, modes of inheritance, biochemical defects, and prognostic implications. However, overlapping signs and symptoms may prevent an individual from being assigned to a distinct type (4–7). The reported incidence has ranged from one in 5000 births to one in every 20,000 births (5,8).

EDS type IV, the vascular type, is marked by the following four clinical characteristics: (i) easy bruising/hematomas, (ii) thin skin with visible veins, (iii) distinctive facial features, and (iv) rupture of the vessels and/or viscera (4,8,9). While representing only 4% of the EDS cases, type IV poses the risk of premature death from spontaneous arterial, intestinal, or uterine rupture and may not be diagnosed until postmortem examination (6,8,10). Approximately 25% of patients with the vascular type experienced the first complication by the age of 20, while 80% of patients had at least one complication by the age of 40 (10). The median survival is 48 years (10). The vascular type is inherited in an autosomal dominant manner; however, several reports have described autosomal recessive transmission (8,11). Furthermore, the incidence of neomutations is likely to the degree that sporadic cases represent half of reported cases (8). In addition, as with other heritable connective tissue diseases, there is a large degree of variability among members of the same family carrying the same mutation (5).

We report three cases of sudden and unexpected death caused by EDS type IV. Each case was diagnosed postmortem. Two decedents underwent postmortem DNA molecular studies revealing the abnormalities in type III collagen, while the third decedent was diagnosed on a clinicopathologic basis. We will highlight the classic features and recognized risk of visceral and vascular rupture associated with EDS type IV and will describe the diagnostic techniques utilized in confirming this disorder.

Case 1

Case History

A 33-year-old white female was admitted in asystole to the emergency department (ED) after awaking suddenly during the night and stated that she "was passing out." Despite advanced cardiac life support protocol, she was unable to be resuscitated. She had been admitted to the hospital 8 days prior to her death with complaints of headache, photophobia, and gastrointestinal symptoms, including nausea, vomiting, and abdominal pain. Upper gastrointestinal endoscopy revealed gastritis and chronic enteritis of the duodenum, and colonoscopy was grossly significant for a small cluster of dark red polyps clinically suspicious for either juvenile polyps or hamartoma. Laboratory studies demonstrated a microcytic hypochromic anemia. She underwent two blood transfusions. There was no family history of adverse vascular events.

[1]Medicolegal Research Associate, Norton Neuroscience Institute, 210 E. Gray Street, Suite 1105, Louisville, KY.
[2]Office of the Associate Chief Medical Examiner, Frankfort, KY and Department of Pathology and Laboratory Medicine, University of Kentucky College of Medicine, Lexington, KY.
*Presented in part at the 56th Annual Meeting of the American Academy of Forensic Sciences, February 16–21, 2004, in Dallas, TX.

Received 31 July 2009; and in revised form 8 Oct. 2009; accepted 15 Oct. 2009.

Autopsy Findings

The decedent was a well-nourished asthenic woman appearing older than her offered age of 33. She measured 4 feet 11 inches and weighed 92 pounds. External appearance demonstrated thin and transparent skin of the trunk and extremities, which afforded easy visual recognition of the subcutaneous vasculature (Fig. 1). Internal findings included unusual friability of the vasculature, soft tissues, and viscera. With traction, the aorta tore into ring-like segments. There was a dissection of the left subclavian artery with adventitial hemorrhage; the false, intramural channel extended from its origin at the aorta to 10 cm distal in the upper arm (Fig. 2). A left hemothorax of 1050 mL and visceral pallor were noted. There was a rupture of the wall of the middle colic and inferior mesenteric arteries supplying the transverse colon with endoluminal thrombosis and segmental early necrosis of the colon. Microscopical evaluation revealed a dissection of the outer third of the muscle wall of the left subclavian artery and the left renal artery. The decedent's skin tore upon restoration of the body following autopsy, and the embalmers reported severe friability of the vasculature and difficulty in the intravascular embalming procedure.

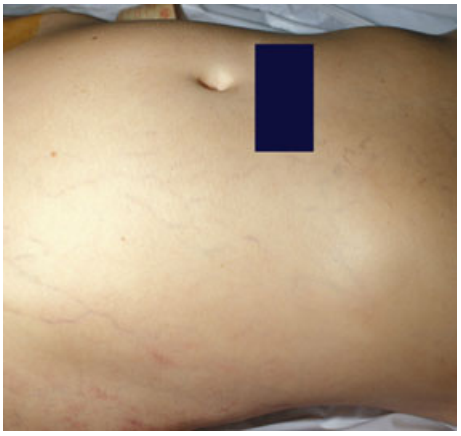

FIG. 1—*Thin and transparent skin of the trunk revealing the subcutaneous vasculature (Case 1).*

FIG. 2—*Left subclavian artery with intramural dissection and separation of the walls (Case 1).*

DNA Molecular Studies

Samples of the lung, skin, and kidney were obtained during autopsy. Fibroblast cultures were grown at the Cytogenetics Laboratory, University of Kentucky, Lexington, KY. The cultures were subsequently submitted to the Collagen Diagnostic Laboratory, University of Washington, Seattle, WA. Electrophoretic mobilities of the collagen produced by cultured fibroblasts revealed diminished type III procollagen and intracellular storage of abnormal type III procollagen. cDNA responsible for encoding pro alpha 1(III) chains of the type III procollagen was synthesized from RNA isolated from the patient's fibroblast culture. The DNA molecular studies identified a mutation in one allele of the COL3A1 gene, specifically, the second nucleotide of intron 14 (IVS14 + 2T->A).

The cause of death was left hemothorax by dissection with rupture of the left subclavian artery owing to EDS type IV.

Case 2

Case History

A 14-year-old white boy presented to the ED with the sudden onset of back and abdominal pain of 1-h duration. On the day of his death, he had been playing basketball and preparing for a family trip. During the examination at the ED, the patient emitted a "large scream/yell" and suddenly collapsed. Following the collapse, he was apneic and pulseless. The victim had a negative medical history except for a physician's appointment for the flu 3 years earlier.

Autopsy Finding

The decedent was a well-nourished, well-developed boy, who was 5 feet 2 inches tall and weighed 137 pounds. The skin was of normal turgor with small subepidermal vessels apparent on the upper chest and around the eyelids. He had mild musculature atrophy of the lower legs as well as healed, surgically repaired corrections of the lower legs and feet for congenital talipes calcaneus deformities.

The internal organs including the aorta, liver, kidneys, heart, and spleen were extremely soft and friable, and there was pallor of the viscera (Fig. 3). The aorta broke into multiple rings upon traction, and paraesophageal hemorrhage was seen. Stanford type B aortic dissection (12) was evident and encompassed the outer third muscular layer of the ascending and descending aorta and origins of the three major branches arising from the arch (Fig. 4). In addition to multiple ring-like intimal tears of the descending aorta, there was a rupture of the ascending aorta into the pericardial sac (100 mL) and right pleural space (1700 mL). Blood also dissected underneath the entire right parietal pleura and a portion of the left parietal pleura.

DNA Molecular Studies

Tissues of lung, kidney, and skin were collected during autopsy. Fibroblast cultures were grown at the Cytogenetics Laboratory, University of Kentucky, Lexington, KY and were subsequently submitted for a collagen diagnostic evaluation at the Collagen Diagnostic Laboratory, University of Washington, Seattle, WA. The amount of type III procollagen secreted by the cells was significantly diminished, and there was an intracellular storage of abnormal type III procollagen. The decrease in synthesis and increase in intracellular storage reflect a structural defect in the pro alpha 1(III) chains of the type III procollagen encoded by one allele (G184V)

FIG. 3—*Excessive friability of the wall of the thoracoabdominal aorta with evidence of a paraaortic hematoma (Case 2).*

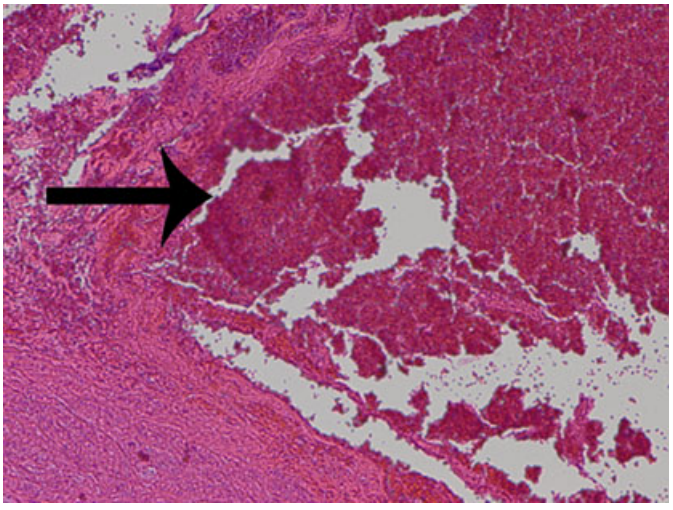

FIG. 4—*A photomicrograph of a Stanford type B aortic dissection. The aorta demonstrates a dissection of its outer third layer. Red blood cells are seen dividing the layers in a wedge-like fashion (Case 2).*

of the COL3A1 gene. Thus, the biochemical studies were consistent with the clinical diagnosis of the vascular form of EDS type IV.

The cause of death was right hemothorax and hemopericardium resulting from aortic dissection (Stanford type B) and rupture caused by EDS type IV.

Case 3

Case History

A 19-year-old white man was found dead in his bed in the morning by his father. The victim had spoken with his father the previous night and had been in "good spirits." The decedent had recently complained of severe headaches, including one the night prior to death. There was no known drug or alcohol abuse and no reported history of medications. The victim had been clinically diagnosed with von Willebrand disease 1 year prior to death per Coroner's report. Interviews with the victim's family indicated that

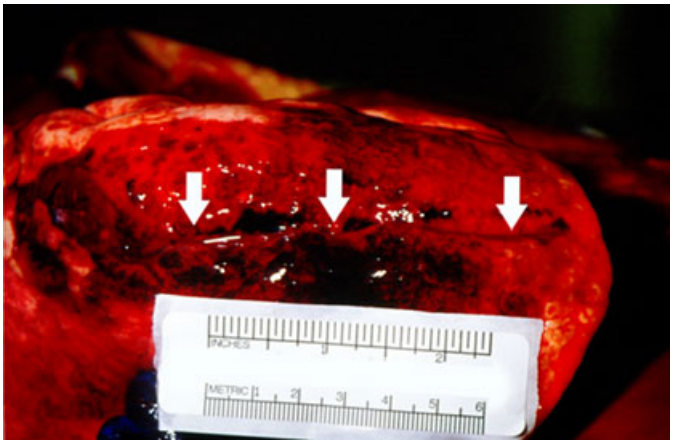

FIG. 5—*Pleural/parenchymal tear of the posterior aspect of the lower lobe of the right lung measuring 4 inches vertical up to 2 inches deep (arrows) (Case 3).*

he was "very double-jointed and able to contort himself." In addition, he had a history of umbilical and bilateral inguinal hernias as well as easy bruisability.

Autopsy Findings

The decedent was a normally developed and adequately nourished man with a height of 5 feet 11 inches and a weight of 168 pounds. The entirety of the soft tissues and viscera exhibited moderate-marked softening without stigmata of decomposition. Examination and palpation of the spine, ribs, shoulder girdle, and pelvis revealed marked looseness and hypermobility of the costovertebral joints and sharp anterior angulation of the posterior aspect of ribs 2–6 bilaterally. Sections of the right posterior ribs revealed them to be narrow with posterior bony protuberances up to 0.2 inches in greatest diameter. There was evidence of a pleural/parenchymal tear of the posterior aspect of the lower lobe of the right lung measuring 4 inches vertical up to 2 inches deep (Fig. 5). Approximately 1600 mL of clotted and nonclotted blood was collected within the smooth right pleural space. The victim did not undergo collagen diagnostic studies for confirmation of EDS.

The cause of death—based on the clinicopathologic diagnosis—was right hemothorax caused by pulmonary rupture sustained as the result of EDS.

Family Investigation

Following the victim's death, further investigation was conducted involving his family members. The decedent's father did not have either a history or clinical findings to suggest that he may have a connective tissue disorder. However, the victim's mother's history and physical examination were suggestive of a connective tissue disorder. She underwent fibroblast collagen studies, which were submitted to the Collagen Diagnostic Laboratory, University of Washington, Seattle, WA. Biochemical genetic analysis did not detect any abnormality with type I and type III procollagen.

Discussion

Several studies in the literature have discussed the lethal nature of EDS type IV, specifically, as a result of rupture of arteries, uterus, or intestines (6,10). Arterial rupture accounts for the majority of the deaths, while fatalities involving the colon are less

common (8,10). Pregnancy represents a significant risk for women with EDS type IV because of uterine or vascular rupture, commonly encountered in the peripartum period or within 2 weeks after delivery (8,10). In light of a maternal mortality rate of approximately 12% (10,13), an early cesarean section is recommended to decrease the risk during labor (14).

In Pepin et al.'s (10) landmark study of 220 patients with EDS type IV and their 199 affected relatives, most of the deaths were caused by arterial dissection or rupture. Of the 103 deaths caused by arterial rupture, 78 involved a thoracic or abdominal vessel and nine were caused by hemorrhage of the central nervous system; the artery was not specified in 16 cases. Thirteen individuals died as a result of organ rupture, as follows: uterus, five cases; heart, three cases; and liver or spleen, five cases. Bowel rupture and sepsis represented 8% of all deaths (10 cases of gastrointestinal rupture).

Sudden death caused by a rupture of an artery or organ attributed to EDS type IV has been discussed in several studies. Prahlow and Wagner (15) reported three cases of EDS type IV diagnosed postmortem. One case was determined to be spontaneous vascular laceration because of connective tissue disease with various abnormalities noted during exploratory surgery prior to death, including a partially detached spleen with associated hemorrhage as well as lacerations of the renal artery and aorta. Prahlow and Wagner (15) utilized the term "laceration" in this case, which was initiated by the mechanical trauma of cross-clamping the aorta. Another case involved hemoperitoneum (2500 mL) associated with abdominal aortic dissection and rupture, and the third case was ruled as left iliac artery rupture in a woman in the 35th week of pregnancy. Fibroblast culture, which was performed in two cases, confirmed EDS type IV.

Wimmer et al. (16) reported the case of a 15-year-old boy who had not been diagnosed with EDS type IV until autopsy. His cause of death was caused by rupture of the right subclavian artery and right vertebral artery as well as "laceration" of the right brachiocephalic vein. A right paraclavicular hematoma amounting to 3 L of clotted blood extended to the neck, face, and chest, and a ruptured, dissecting aneurysm of the transverse aortic arch was also noted. Gilchrist and Duflou reported the case of a 30-year-old man who died because of cardiac tamponade from myocardial rupture complicating transmural myocardial infarction (17). The decedent had been previously diagnosed with EDS type IV, which, they hypothesized, may have played a role in his coronary atherosclerosis and subsequent myocardial rupture. Additional cases of vascular EDS determined postmortem include brainstem infarction with hemorrhage resulting from basilar artery thrombosis (18), subarachnoid hemorrhage in a 5-month-old infant (19), and splenic rupture (20,21).

The definitive diagnosis of EDS type IV is made by culturing skin fibroblasts to assess abnormalities of type III procollagen or by identifying a mutation in the gene for type III procollagen (COL3A1) (7,10,21). This analysis identifies >95% of individuals with a defect of type III collagen, by detecting either the quantitative (reduced amounts of collagen type III) or qualitative (structurally abnormal type III collagen) defects (22). Type III collagen is found predominantly in the skin, blood vessels, and the bowel wall (21), accounting for the pathology noted in these bodily areas in individuals with EDS type IV. There are no diagnostic hematologic, serum chemistry, immunologic, or microscopic pathologic findings (6,21). Histology and electron microscopy may demonstrate the findings of arterial wall thinning, decreased collagen content, and distorted collagen fibril structure (10). To elucidate further the pathogenesis of vascular lesions associated with vascular-type EDS, Boutouyrie et al. (23) conducted a study from a biomechanical approach. They determined that an abnormally low intima-media thickness caused a higher wall stress in an elastic artery (such as the common carotid) in patients with the EDS type IV compared with controls and opined the relative medial attenuation is likely to increase the risk of arterial dissection and rupture (23).

The facial features commonly associated with the vascular-type EDS appear in various patterns and may include the following: slenderness, prominent bones and eyes, sunken cheeks, periorbital pigmentation with telangiectasias on the eyelids, and thin lips (8). While hyperextensibility of the skin and hypermobility of the joints are not commonly encountered in patients with this condition, thin and translucent skin with visible underlying vasculature is often noted (8,21). The incidence of congenital hip dysplasia, congenital clubfoot, and inguinal hernias is higher in individuals with EDS type IV than the general population (10,22,24).

The first two cases in this study involved arterial rupture. The cause of death of Case #1 was dissection of the left subclavian artery resulting in a left hemothorax of 1050 mL. Furthermore, the aorta tore into ring-like pieces with traction. In the second case, right hemothorax and hemopericardium were noted with rupture of aortic dissection (Stanford type B). There were multiple ring-like intimal tears of the descending aorta and rupture of the aorta into the pericardial sac (100 mL) and right pleural space (1700 mL). Both of these individuals underwent skin fibroblast collagen studies to confirm the postmortem diagnosis of EDS type IV. Soft and friable internal organs as well as thin and transparent skin revealing the subcutaneous vasculature were noted during the autopsies. Other findings associated with EDS type IV demonstrated in these cases included the tearing of the skin upon restoration of the body after autopsy and friability of the vasculature during the embalming procedure in Case #1, and a history of congenital talipes calcaneus deformities of the lower legs and feet with remote surgical corrections in Case #2.

Medical procedures, such as arteriography and endoscopy, should be avoided in individuals with EDS type IV (8). Arteriography has been associated with a 67% risk of complications, including hematomas, thrombosis, persistent bleeding, and death (25). The victim in Case #1 underwent antemortem endoscopy and colonoscopy prior to death that revealed the extent of her gastric and colonic pathology. As she was not diagnosed with EDS type IV until postmortem, the physicians who evaluated her in the hospital 8 days prior to her death unknowingly performed invasive tests that are contraindicated in an individual with her condition.

There is a high likelihood of excessive bruising and a tendency to form hematomas in EDS type IV owing to the fragility of capillaries and perivascular connective tissues (6,22). However, these features are not specific to vascular EDS, as they are often encountered in many disorders of coagulation and/or platelets, including hemophilia A and B, von Willebrand disease, and all subtypes of EDS (22). Furthermore, several characteristics of osteogenesis imperfecta mimic EDS type IV, including thin skin, joint laxity, susceptibility to sustaining fractures, fragile large blood vessels, and various cardiac abnormalities, such as aortic regurgitation (5). The victim in Case #3 had been clinically diagnosed with von Willebrand disease 1 year prior to his death per Coroner's report, perhaps owing to his history of easy bruisability. However, his history of facile contortions coupled with inguinal hernias and the findings demonstrated at autopsy, specifically, a pulmonary rupture in association with softening of the soft tissues and viscera as well as hypermobility of the joints and ribs suggest that he may have had EDS type IV misdiagnosed as von Willebrand disease.

Furthermore, to our knowledge, Case #3 represents the first reported case in the literature of sudden death caused by pulmonary

rupture in probable EDS type IV. The rupture of the lung was not artifact as it was observed upon opening of the chest cavity. We hypothesize that a pulmonary arterial branch (i) ruptured spontaneously, (ii) leaked blood, (iii) formed a progressively and rapidly expanding intraparynchmal hematoma that mechanically disrupted the normal pulmonary interstitium, sustentacular tissues, and visceral pleura, and (iv) resulted in a pulmonary tear with a large hemothorax. Massive tissue destruction disallowed confirmation by microscopy.

Rupture of the lung has seldom been described in the literature (24,26). Yost et al. (26) reported a case of a 27-year-old man with an initial clinical presentation of spontaneous onset of hemiparesis. He underwent a thoracotomy with a left lower lobectomy for massive focal hemoptysis, with friable lung parenchyma noted during surgery. The victim was subsequently diagnosed with EDS type IV through skin collagen testing. Following a 6-year duration of hemoptysis and paralysis, he was found unresponsive at home. The autopsy demonstrated friability of the fibroconnective tissue and aorta as well as a massive hemorrhage of the right lung and left upper lobe with tracheal aspiration. Pulmonary microscopic findings revealed marked acute diffuse alveolar hemorrhage, pulmonary capillaritis, hemosiderosis, and focal osseous metaplasia.

Conclusion

EDS type IV, the vascular type, represents a heritable connective tissue disorder marked by type III procollagen abnormalities caused by a mutation of the COL3A1 gene. It poses the risk of sudden death from spontaneous arterial, intestinal, or uterine rupture. Individuals may not be diagnosed with the condition during life or may be misdiagnosed with another connective tissue or coagulation disorder. Therefore, it is of utmost importance for the forensic pathologist to be aware of EDS upon discovery of an individual with characteristic facial features, thin and transparent skin with apparent subcutaneous vasculature, and excessively friable vasculature, soft tissues, and viscera. The forensic pathologist should obtain specimens during autopsy for collagen fibroblast testing to receive a confirmatory diagnosis. Postmortem fibroblast cultures may be submitted to the Collagen Diagnostic Laboratory at the University of Washington for specialized testing. The contact information may be retrieved at http://www.pathology.washington.edu/clinical/collagen. Because of the autosomal dominant nature of this condition, family members should be apprised of the decedent's EDS diagnosis and undergo testing themselves. Family members with EDS will need to make informed decisions in their own lives with respect to obstetric complications, greater regard for safety in everyday activities including strenuous physical activity and aggressive sports, as well as documentation of their medical condition, such as wearing a medical bracelet and informing personal physicians.

Acknowledgments

We acknowledge Melanie Pepin, MS, CGC, Genetic Counselor, and Peter H. Byers, MD, Professor of the Departments of Pathology and Medicine (Medical Genetics), at the Collagen Diagnostic Laboratory, University of Washington, Seattle, WA. We also thank Anjana Pettigrew, MD, Associate Professor of the Department of Pathology and Laboratory Medicine, University of Kentucky, Lexington, KY who grew the fibroblast cultures at the Cytogenetics Laboratory.

References

1. Chernogubow N. Cutis laxa. Mhft Prakt Dermatol 1892;14:76.
2. Ehlers E. Dansiche dermatologische gesellschaft. Dermatol Z 1901;8:173–5.
3. Danlos M. Un cas de cutis laxa avec tumeurs par contusion chronique des coudes et des genoux. Bull Soc Fr Dematol Syphiligr 1908;19:70–2.
4. Beighton P, De Paepe A, Steinmann B, Tsipouras P, Wenstrup RJ. Ehlers-Danlos syndromes: revised nosology, Villefranche, 1997. Ehlers-Danlos National Foundation (USA) and Ehlers-Danlos Support Group (UK). Am J Med Genet 1998;77:31–7.
5. Prockop DJ, Czarny-Ratajczak M Heritable disorders of connective tissue. In: Fauci AS, Braunwald E, Kasper DL, Hauser SL, Longo DL, Jameson JL, et al., editors. Harrison's principles of internal medicine, 17th edn. New York, NY: McGraw-Hill Companies, Inc., 2008;2461–9.
6. Oderich GS, Panneton JM, Bower TC, Lindor NM, Cherry KJ, Noel AA, et al. The spectrum, management and clinical outcome of Ehlers-Danlos syndrome type IV: a 30-year experience. J Vasc Surg 2005;42:98–106.
7. Pope FM, Martin GR, Lichtenstein JR, Penttinen R, Gerson B, Rowe DM, et al. Patients with Ehlers-Danlos syndrome type IV lack type III collagen. Proc Natl Acad Sci USA 1975;72:1314–6.
8. Germain DP. Clinical and genetic features of vascular Ehlers-Danlos syndrome. Ann Vasc Surg 2001;16:391–7.
9. Pope FM, Narcisi P, Nicholls AC, Germaine D, Pals G, Richards AJ. COL3A1 mutations cause variable clinical phenotypes including acrogeria and vascular rupture. Br J Dermatol 1996;135:163–81.
10. Pepin M, Schwarze U, Superti-Furga A, Byers PH. Clinical and genetic features of Ehlers-Danlos syndrome type IV, the vascular type. N Engl J Med 2000;342:673–80.
11. Pope FM, Nicholls AC, Jones PM, Wells RS, Lawrence D. EDS IV (acrogeria): new autosomal dominant and recessive types. J R Soc Med 1980;73:180–6.
12. Daily PO, Trueblood HW, Stinson EB, Wuerflein RD, Shumway NE. Management of acute aortic dissections. Ann Thorac Surg 1970;10(3):237–47.
13. Pope FM, Nicholls AC. Pregnancy and Ehlers-Danlos syndrome type IV. Lancet 1983;1:249–50.
14. Erez Y, Ezra Y, Rojansky N. Ehlers-Danlos type IV in pregnancy: a case report and a literature review. Fetal Diagn Ther 2008;23:7–9.
15. Prahlow JA, Wagner SA. Death due to Ehlers-Danlos syndrome type IV. Am J Forensic Med Pathol 2005;26(1):78–82.
16. Wimmer PJ, Howes DS, Rumoro DP, Carbone M. Fatal vascular catastrophe in Ehlers-Danlos syndrome: a case report and review. J Emerg Med 1996;14(1):25–31.
17. Gilchrist ER, Duflou JA. Incidental myocardial infarction in Ehlers-Danlos syndrome type IV? J Forensic Sci 2005;50(2):461–4.
18. Jarmulowicz M, Phillips WG. Vascular Ehlers-Danlos syndrome undiagnosed during life. J R Soc Med 2001;94:28–30.
19. Byard RW, Keeley FW, Smith CR. Type IV Ehlers-Danlos syndrome presenting as sudden infant death. Am J Clin Pathol 1990;93:579–82.
20. Harris SC, Slater DN, Austin CA. Fatal splenic rupture in Ehlers-Danlos syndrome. Postgrad Med J 1985;61:259–60.
21. Kaufman JA. SIR 2005 annual meeting film panel case: vascular type Ehlers-Danlos syndrome. J Vasc Interv Radiol 2005;16:645–9.
22. De Paepe A, Malfait F. Bleeding and bruising in patients with Ehlers-Danlos syndrome and other collagen vascular disorders. Br J Haematol 2004;127:491–500.
23. Boutouyrie P, Germain DP, Fiessinger JN, Laloux B, Perdu J, Laurent S. Increased carotid wall stress in vascular Ehlers-Danlos syndrome. Circulation 2004;109:1530–5.
24. Ludwig J. Handbook of autopsy practice, 3rd edn. Totowa: Humana Press, 2002.
25. Mattar SG, Kumar AG, Lumsden AB. Vascular complications in Ehlers-Danlos syndrome. Am Surg 1994;60:827–31.
26. Yost BA, Vogelsang JP, Lie JT. Fatal hemoptysis in Ehlers-Danlos syndrome. Chest 1995;107:1465–7.

Additional information and reprint requests:
John C. Hunsaker III, M.D., J.D.
Office of the Associate Chief Medical Examiner
100 Sower Boulevard, Suite 202
Frankfort, KY 40601-8272
E-mail: John.Hunsaker@ky.gov

JOURNAL OF FORENSIC SCIENCES

J Forensic Sci, November 2010, Vol. 55, No. 6
doi: 10.1111/j.1556-4029.2010.01471.x
Available online at: onlinelibrary.wiley.com

CASE REPORT

PATHOLOGY AND BIOLOGY

Hajime Mizukami,[1,2] *M.D., Ph.D.; Tomonori Nagai,*[2,3] *M.D., Ph.D.; Shinjiro Mori,*[2] *M.D., Ph.D.; Shuichi Hara,*[1] *Ph.D.; Tatsushige Fukunaga,*[2] *M.D., Ph.D.; and Takahiko Endo,*[1,2] *M.D., Ph.D.*

An Autopsy Case in Which Self-Bloodletting Via a Cervical Blood Access Led to a Fatal Outcome*

ABSTRACT: A 48-year-old woman was found dead on a chair in her living room. She had received dialysis every day because of chronic renal failure for the past 15 years. On a table beside her, there was a mirror and 10-mL syringe on a napkin. A stopper was out of place in a portion of a three-way blood access tube established in the right cervical region, and blood coagulation was noted in the lumen. There was a bloodstained measuring cup on the floor. Autopsy findings included a large number of shunt traces in the bilateral infraclavicular fossae and upper limbs, as well as the cervical blood access terminal reaching the right atrium via the internal jugular vein to superior vena cava. Various organs showed anemia. Neither a fatal lesion nor injury was noted in the main organs. Therefore, this patient may have committed suicide by self-bloodletting via a cervical blood access.

KEYWORDS: forensic science, suicide, self-bloodletting, dialysis, cervical blood access, autopsy

In patients requiring long-term dialysis, such as those with chronic renal failure, it is essential to maintain a blood access. In most patients, arteriovenous fistula (A/V fistula) or internal shunt, in which artificial vasodilative area formation is performed using a graft, is mainly employed as a blood access because of frequent dialysis. However, in patients in whom internal shunt is impossible or puncture is difficult, an indwelling catheter to be inserted into the internal jugular vein for a long period is often used (1). In this study, we report an autopsied patient who possibly committed suicide by self-bloodletting via a cervical blood access.

Case Report

The case was a 48-year-old unmarried woman, without an occupation. She had undergone dialysis over the past 15 years because of kidney dysfunction related to chronic renal failure (the etiology was unclear). Recently, she had gone to a hospital for dialysis every day but had not received any oral agent. In addition to hypotension, anemia, and yellow ligament osteosis (surgery was performed 10 years previously), she had been diagnosed with bone marrow dysplasia syndrome. However, the details were unclear. At the age of 23, cibophobia was noted. At the age of 42–43, hyperphagia was observed with a body weight twice that at the time of death. She had undergone stomach-reducing surgery. On the day of her death, she went to the hospital for dialysis as usual and took the hospital's car to the shopping street *c.* 200 m from her home at 1:45 PM. She had a shopping receipt issued at 3:40 PM. At 7:10 PM, her younger brother found her dying on her back on a chair in her living room, with her arms hanging down. Blood coagulation was noted in the lumen of a portion of a three-way blood access tube, which was established in the right cervical region 1 month before, and a stopper was out of place. However, there was no blood leakage. On a table beside her, there was a mirror and needle-free 10-mL syringe on a napkin. In addition, a bloodstained measuring cup was on the floor (Fig. 1). The chest area of her clothes was bloodstained, and a bloodstain measuring 30 cm in diameter was observed on a tablecloth. On the floor, there were also two bloodstains measuring 15 cm in diameter. However, the total volume of blood was unclear precisely. As the situation leading to the fatal outcome was unclear, a medicolegal autopsy was performed 40 h after death.

At autopsy, the height and body weight were 151 cm and 43 kg, respectively. The skin was pale. Slight purple-red livor mortis was observed on the dorsal surface and discolored under digital compression. Rigidity was systemically marked. In the right cervical region, a blood access with a three-way catheter had been established and blood was noted in the lumen of one tube (Fig. 2). In the bilateral subclavicular regions, elbows, and forearms, there were a large number of old dialytic traces. Old surgical traces were observed on the median abdomen, median superior dorsal surface, and right back. No trauma was observed.

Concerning internal findings, macroscopically, the main organs in the thoracic and abdominal cavities were anemic. The cervical catheter reached the right atrium via the internal jugular vein to superior vena cava (Fig. 3). In the pericardial cavity, 30 mL of

[1]Department of Forensic Medicine, Tokyo Medical University, 6-1-1 Shinjuku, Shinjuku-ku, 160-8402 Tokyo, Japan.
[2]Tokyo Medical Examiner's Office, Tokyo Metropolitan Government, 4-21-18 Otsuka, Bunkyo-ku, 112-0012 Tokyo, Japan.
[3]Department of Forensic Medicine, Jikei University School of Medicine, 3-25-8 Nishishinbashi, Minato-ku, 105-8461 Tokyo, Japan.
*Presented at the 92nd Congress of the Japanese Society of Legal Medicine, April 23–25, 2008, in Nagasaki, Japan.

Received 16 July 2009; and in revised form 17 Aug. 2009; accepted 6 Sept. 2009.

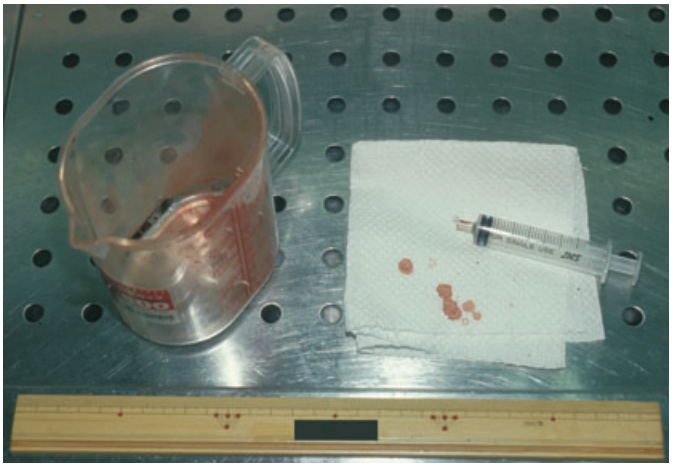

FIG. 1—*A 10-mL syringe and napkin on the table, as well as a blood-stained measuring cup on the floor.*

FIG. 2—*Blood access established in the right cervical region (blood was detected in the lumen of a portion [red label] of the three-way catheter) and a dialytic trace in the right subclavicular vein.*

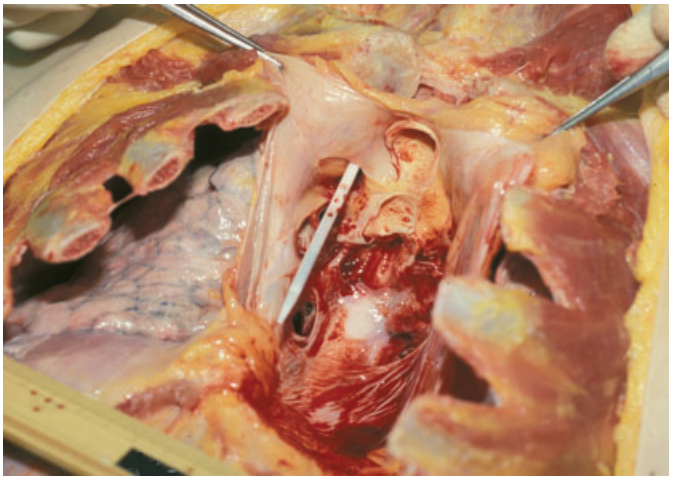

FIG. 3—*Superior vena cava and the end of the catheter after heart extirpation.*

light-yellow transparent liquid was present. The heart weight was 270 g. After the heart was extirpated, dark-red, fluid blood remained in the pericardial cavity. Its volume was *c.* 30 mL. The right ventricle was dilated, and neither macroscopic nor histological investigation revealed any myocardial arrangement abnormalities or ischemic changes. Coronary sclerosis was slight. The bilateral pleurae showed adhesion in some areas. The left and right lungs weighed 303 and 275 g, respectively. There was no marked alveolar/bronchial change nor pneumonia. The liver weight was 1114 g, with a flat surface. The surface and cut surface were red-brown. Neither fatty droplet infiltration nor chronic hepatitis was noted. The left kidney weight was 128 g. The right kidney had been extirpated. The glomeruli were partially organized. The afferent and efferent glomerular arterioles showed moderate hyaloid changes. There was no proliferation of mesangium cells, marked change in the uriniferous tubule, nor infiltration of inflammatory cells. The 1/2 area of the pyloric-side stomach had been extirpated and reconstructed using the Billroth II procedure. There were no marked macroscopic/histological changes in the bone marrow. No air embolism was shown in any examined organs. No air embolism was shown with any organs that we inspected.

Any drugs were not detected from gastric contents or blood. Neither ethanol nor acetone was detected in the blood. A biochemical test could not be conducted because of postmortem changes.

Discussion

In patients with chronic renal failure, arteriovenous anastomosis and internal shunt with a graft are mainly employed as a blood access for frequent dialysis. However, an indwelling catheter to be inserted into the internal jugular vein, subclavicular vein, or femoral vein for a long period is used in patients urgently requiring blood purification; those in whom it is impossible to establish an internal shunt because of serious occlusive peripheral arterial disorders, severe chronic heart failure, hypotension, or disturbance of superficial veins of the limbs; those in whom it is impossible to maintain blood flow via the superficial area; and those in whom dementia, restlessness, or movements make internal shunt puncture/fixation difficult (1).

In the present case, the actual volume of blood loss was unclear. However, the cervical catheter's cap was out of place, and the main organs showed anemia. In addition, the volume of blood remaining in the heart was small. There was no other trauma or lesion that may have caused the death. Therefore, the patient may have died from self-bloodletting via the cervical blood access. The right kidney had been extirpated, and there was also a possibility that chronic renal failure-related anemia accelerated the death. However, the histology of the kidney showed that the glomeruli were relatively well maintained. As the patient had undergone stomach-reducing surgery, malabsorption syndrome may have promoted agastric anemia. Furthermore, bone marrow findings did not suggest any hematopoietic cell abnormalities.

As serious medical accidents related to dialysis, several studies have indicated hemorrhage associated with the needle coming out during dialysis or circuit blockage, blood access perforation in the presence of infection, and fatal hemorrhage related to the external shunt being displaced (2). On the other hand, psychiatric symptoms such as depression and anxiety are frequent in patients undergoing dialysis. The relative risk of suicide including dialysis refusal is higher than in the general population (2,3). Suicide methods under conditions specific to these patients include exsanguinations by disconnecting or otherwise interrupting the shunt and an excessive ingestion of salt, fluid, or potassium (2). In addition, as blood access-associated death, a patient who committed suicide by directly injuring the internal shunt site of the medial elbow with a razor, was reported (4). In the present case, the possibility of an

accident related to hemorrhage at the shunt site was ruled out based on the state of death. The presence of a mirror on the table suggests the patient's premeditated behavior, and we estimated that the patient opened the cervical catheter and used the syringe to withdraw blood, which was then placed in the measuring cup. Therefore, she may have committed suicide.

Concerning self-exsanguination, a large number of patients with Münchhausen syndrome (5–7), including fatal cases (8), have been reported. Women comprised the greater portion, including health professionals. In these patients, self-exsanguination with a syringe resulted in factitious anemia. However, these were not suicide attempts. According to our knowledge, this is the first case of death related to self-exsanguination with a syringe via an indwelling catheter.

References

1. Ohira S, Naito H, Amano I, Azuma N, Ikeda K, Kukita K, et al. Japanese Society for Dialysis Therapy. 2005 Japanese Society for Dialysis Therapy guidelines for vascular access construction and repair for chronic hemodialysis. Ther Apher Dial 2006;10:449–62.
2. Cohle SD, Graham MA. Sudden death in hemodialysis patients. J Forensic Sci 1985;30:158–66.
3. Haenel T, Brunner F, Battegay R. Renal dialysis and suicide: occurrence in Switzerland and in Europe. Compr Psychiatry 1980;21:140–5.
4. Marc B, Baudry F, Zerrouki L, Ghaith A, Garnier M. Suicidal incised wound of a fistula for hemodialysis access in an elderly woman: case report. Am J Forensic Med Pathol 2001;22:212–3.
5. Haddad SA, Winer KK, Gupta A, Chakrabarti S, Noel P, Klein HG. A puzzling case of anemia. Transfusion 2002;42:1610–3.
6. Saed G, Potalivo S, Panzini L, Bisetti A. Munchausen's syndrome. A case of factitious hemoptysis. Panminerva Med 1999;41:62–7.
7. Zahner J, Schneider W. Munchausen syndrome in hematology: case reports of three variants and review of the literature. Ann Hematol 1994;68:303–6.
8. Hirayama Y, Sakamaki S, Tsuji Y, Sagawa T, Takayanagi N, Chiba H, et al. Fatality caused by self-bloodletting in a patient with factitious anemia. Int J Hematol 2003;78:146–8.

Additional information and reprint requests:
Hajime Mizukami, M.D., Ph.D.
Department of Forensic Medicine
Tokyo Medical University
6-1-1 Shinjuku, Shinjuku-ku
Tokyo 160-8402
Japan
E-mail: mizukamh@tokyo-med.ac.jp

JOURNAL OF FORENSIC SCIENCES

J Forensic Sci, November 2010, Vol. 55, No. 6
doi: 10.1111/j.1556-4029.2010.01470.x
Available online at: onlinelibrary.wiley.com

CASE REPORT

PATHOLOGY AND BIOLOGY

Kelly G. Devers,[1] *M.D. and Jeffrey S. Nine,*[2] *M.D.*

Autopsy Findings in Botulinum Toxin Poisoning

ABSTRACT: In the United States, foodborne botulism is most commonly associated with home-canned food products. Between 1950 and 2005, 405 separate outbreaks of botulism were reported to the Centers for Disease Control and Prevention (CDC). Approximately 8% of these outbreaks were attributed to commercially produced canned food products. Overall, 5–10% of persons ingesting botulinum toxin die. Few reports exist pertaining to autopsy findings in cases of foodborne botulism. Here, we report the autopsy findings of a man who died after a prolonged illness caused by botulinum toxin exposure likely attributable to a commercially prepared food source. Despite extensive testing, our histopathologic findings were nonspecific. We therefore conclude that the forensic pathologist must become familiar with the neurotoxicity syndrome associated with this illness. Maintaining vigilance for botulism by carefully reviewing the decedent's clinical history will aid in the early identification and control of outbreaks, either foodborne or terrorism-related.

KEYWORDS: forensic science, *Clostridium botulinum*, foodborne botulism, botulism, botulism poisoning, food poisoning, neurotoxin syndromes

Clostridium botulinum is a spore-forming bacterium found worldwide in soil and marine environments. The bacteria can survive indefinitely in spore form. When environmental conditions are hospitable, the bacteria can germinate and produce neurotoxins. The primary types of botulism poisoning are foodborne botulism, wound botulism (usually associated with black-tar heroin injection in IV drug abusers), and infant botulism (often associated with ingesting of botulinum spores in products such as honey or inhalation of contaminated dust particles). Foodborne botulism sources include commercially prepared foods as well as both canned and noncanned home-prepared foods. Failure to refrigerate freshly cooked foods (both commercial and home-made) is an important cause of noncanned foodborne botulism cases (1).

In 2007, a total of 144 cases of botulism were reported to the Centers for Disease Control and Prevention (CDC). Foodborne botulism accounted for 18% of total cases, with the majority of cases attributed to infant botulism. Five cases of unknown etiology were reported. Of the foodborne and unknown cases, five deaths were confirmed. Foodborne sources included beaver tail, seal oil, fermented beluga, whale blubber, fish stinkheads, home-canned foods, and commercially prepared foods including hot dog chili sauce and chili with beans (2,3).

Botulinum toxins are released when food contaminated with *C. botulinum* bacteria is ingested. The toxins attack nerve synapses, causing a descending paralysis, usually beginning with the oculomotor nerves. The onset of symptoms varies from 12 to 35 h after exposure but can be delayed up to 2 weeks. The patient is usually not febrile. Initial complaints of dizziness, diplopia, dry mouth, and diarrhea are common. As the muscle paralysis continues to descend, many patients become ventilator dependent. A single dose of *C. botulinum* antitoxin is the treatment of choice. Complete recovery is possible but may take up to 1 year, depending on the baseline status of the patient (1,3,4).

Case Report

A 52-year-old man was found stuporous on the floor of his home by a family member and was taken immediately to a nearby emergency room (ER). He had complained to a relative of feeling "ill" for a period of 2 weeks prior to this event. In the emergency room, he reported difficulty swallowing, diplopia, and inability to walk. Soon after arrival, his respiratory status rapidly declined, and he required urgent intubation. A magnetic resonance imaging/magnetic resonance angiography brain scan showed no evidence of stroke. Testing of his spinal fluid revealed no evidence of meningitis. He was examined by a neurologist who diagnosed possible foodborne botulism poisoning. In July of 2007, the CDC issued a warning regarding an outbreak of botulism poisoning linked to commercially prepared canned chili products (2,3). The patient told his clinicians he had eaten canned chili within the past month. *Clostridium botulinum* antitoxin was administered within 30 h of presentation. A stool specimen sent to the CDC later tested positive for *C. botulinum* toxin Type A. Like many patients stricken with foodborne botulism poisoning, he required long-term ventilator support. Within 3 weeks, he was transferred to a long-term care facility for ventilator weaning and physical rehabilitation. Unfortunately, the patient went into cardiopulmonary arrest and died 40 days after his initial ER presentation.

Materials and Methods

The general autopsy was performed at the New Mexico Office of the Medical Investigator in Albuquerque, New Mexico. The brain was fixed in 10% formalin for 2 weeks and examined

[1]University of New Mexico Health Sciences Center, Department of Pathology, MSC08 4640, 1 University of New Mexico, Albuquerque, NM 87131.
[2]University of New Mexico School of Medicine, Office of the Medical Investigator, MSC11 6030, 1 University of New Mexico, Albuquerque, NM 87131.

Received 9 June 2009; and in revised form 30 Aug. 2009; accepted 6 Sept. 2009.

macroscopically, and tissue blocks were dissected for microscopic examinations. Frozen muscle tissue sections were also examined microscopically. The tissue sections were stained with hematoxylin and eosin. Frozen sections of sural nerve, peroneal nerve, and deltoid muscle were sent to the CDC in Atlanta. The CDC did not report any significant histopathologic findings in the muscle and nerve specimens. Stool sent to the CDC tested positive for *C. botulinum* toxin Type A. Agents from the New Mexico Health Department searched the decedent's home but were unsuccessful in finding either canned chili products or receipts for those products.

Results

Autopsy findings included a 1.0-cm pulmonary embolus adherent to the left lower lobe pulmonary artery. The lungs displayed diffuse congestion with chronic inflammation. An adherent thrombus was also present in the left posterior tibial vein. The heart was mildly enlarged (440 g) with mild atherosclerotic and hypertensive cardiac disease. There was a maximum of 75% focal narrowing of the right coronary artery and a maximum of 50% focal narrowing of the left anterior descending coronary artery. Other findings included a patent foramen ovale (0.2 cm in diameter) and mild hepatosplenomegaly. Findings attributed to botulinum toxin exposure included grossly apparent diffuse muscular atrophy of the upper and lower extremities. Microscopically, sections of quadriceps and gastrocnemius muscle showed scattered degenerating muscle fibers with basophilic change along with scattered angular atrophic fibers. Sural and peroneal nerves displayed no significant histopathology. The official cause of death was listed as complications of *C. botulinum* toxin poisoning.

Discussion

In the United States, foodborne botulism poisoning is most commonly associated with home-canned foods such as vegetables. A total of 405 separate outbreaks of botulism poisoning were reported to the CDC between 1950 and 2005. Approximately 8% of these outbreaks were attributed to commercially prepared canned food products, including canned tuna, vichyssoise, liver paste, and beef stew (3). In 2007, a total of 144 cases of botulism were reported to the CDC. Foodborne botulism accounted for 18% of total cases, with the majority of cases attributed to infant botulism. Three percent of cases were of unknown etiology. For the year 2007, New Mexico reported two cases of infant botulism and one case of botulism from an unknown source (our case) to the CDC (2,3).

In late July of 2007, the FDA issued a warning and recall regarding canned hot dog chili sauce made by a single commercial manufacturer. In early July, five cases of foodborne botulism were reported: two in Texas, one in California, and two in Indiana. Stool samples from these patients tested positive for *C. botulinum* Type A. On July 21, additional brands of hot dog chili and certain types of dog food were added to the recall list. Cans of chili from the recalled lots were all found to be contaminated with *C. botulinum* toxin Type A. The CDC in Atlanta, GA, issued a warning on 30 July 2007 regarding this foodborne botulism outbreak (2).

In our case, the patient told his doctors that he had eaten canned chili within the month before he became ill. According to his family, his food preparation practices were not particularly sanitary, owing to a previous head injury. The patient's stool specimen tested positive for *C. botulinum* toxin Type A, the same type of toxin that was found in the other canned chili botulism cases. He became sick in late July 2007.

If an undiagnosed patient dies weeks to months after infection, botulism poisoning as the primary cause of death can be extremely difficult to determine. The differential diagnosis of botulism includes Guillain–Barre syndrome, myasthenia gravis, tick paralysis, Lambert–Eaton syndrome, stroke, meningitis, and drug/alcohol toxicity as well as many other less common causes (5–7). A careful review of clinical history may help guide the pathologist at autopsy. Most often cited are the symptoms of the "diagnostic pentad" of botulism, which includes: nausea and vomiting, dysphagia, diplopia, dry mouth, and fixed/dilated pupils. On physical examination, cranial nerve palsies such as ophthalmoplegia, ptosis, and slurred speech are essential for the diagnosis and must be present before the onset of other neurological symptoms. These findings may, or may not, be followed by symmetrical descending flaccid paralysis and subsequent respiratory failure (5–7). In a study of 706 patients hospitalized for botulism in the Republic of Georgia, 8% died. The most common causes of death among these patients were cardiac arrest (74%) and respiratory failure (21%) (4,8). Ante-mortem radiologic, routine chemistry, hematologic, and cerebrospinal fluid studies are usually all normal. Untreated patients may display only a few minor cranial nerve deficits or may progress to complete paralysis and respiratory arrest. The time frame of symptomatic manifestations in untreated cases ranges from a few hours to a few days and appears to be dose-related. Notably, as patients progress to respiratory arrest, the usual signs of hypoxemia (e.g., agitated state) are absent owing to muscle paralysis (7).

Postmortem specimens can be of diagnostic utility in suspected botulism cases. Currently, the gold standard for the detection of botulinum toxin is the mouse bioassay, which is performed by designated BSL-3 containment facilities (6). Acceptable postmortem specimens include intestinal contents, gastric contents, tissue samples (in cases of wound or adult intestinal toxemia botulism), nasal swabs (in cases of inhalational botulism), stool, and serum (6). Fagan et al. (9) found that botulinum toxin Type B could be detected in serum for up to 12 days after toxin ingestion and at least up to 4 days in Type A. Woodruff et al. found that stool culture for botulinum toxin is more sensitive than the mouse assay when specimens are obtained later in the illness. No studies currently exist demonstrating when circulating toxin is no longer detectable in either untreated or treated patients (10). In the present case, the stool specimen that tested positive for botulinum toxin Type A was collected *c.* 16 days after the patient's self-reported onset of symptoms. This finding suggests that botulinum toxin Type A may persist in stool longer than 4 days, as previously reported.

Few studies exist pertaining to significant histopathologic findings in cases of foodborne botulism. Various human and animal studies published from the late 1800s to the early 1980s have most consistently reported microscopic hemorrhages and vascular engorgement in multiple areas of the central nervous system (6,11,12). Today, these findings are considered by most researchers to be nonspecific and likely attributable to shock, other postmortem changes, or processing artifact. Muscle atrophy of varying degrees is to be expected in prolonged cases of paralysis or immobility. Thus, the primary role of autopsy histopathology in foodborne botulism cases currently lies in the exclusion of other disease processes (1,6,13,14).

The CDC has designated *C. botulinum* as a Class A biological agent. Botulinum toxins are the deadliest of all known toxins. Deliberate inoculations of commercial food and beverages or release via aerosolization are the most likely methods to be employed by terrorists (15). Therefore, clinicians and pathologists alike should always consider botulism poisoning if the clinical

presentation warrants such investigation. Numerous clinical studies have demonstrated an array of signs and symptoms that should create a high index of suspicion. If there is any concern for botulism poisoning, a call should be placed immediately to the state health department, so that an epidemiologic investigation can be initiated. The CDC has a 24-h on-call consultant available to provide guidance regarding specimen testing sites and shipment requirements (1,14,16). Early identification and reporting of suspected botulism cases is vital in the prevention of accidental or intentional widespread outbreaks. The autopsy pathologist can play a vital role in this surveillance process.

References

1. Infectious Diseases Society of America. Botulism: current, comprehensive information on pathogenesis, microbiology, epidemiology, diagnosis, and treatment. Botulism Fact Sheet. (Rev Feb.5, 2009):1-32, http://www.cidrap.umn.edu/idsa/bt/botulism/biofacts/botulismfactsheet.html (accessed March 25, 2009).
2. The Centers for Disease Control and Prevention. Atlanta, Georgia. Botulism associated with commercially canned chili sauce—Texas and Indiana, July 2007. MMWR Morb Mortal Wkly Rep 2007;56(30):767–9.
3. The Centers for Disease Control and Prevention, The National Surveillance Team, Enteric Diseases Epidemiology Branch, Atlanta, Georgia. Summary of botulism cases. http://www.cdc.gov/nationalsurveillance/PDFs/Botulism_CSTE_2007.pdf, (accessed March 15, 2009).
4. Gottleib S, Kretsinger K, Tarkhashvili N, Chakvetadze N, Chokheli M, Chubinidze M, et al. Long-term outcomes of 217 botulism cases in the Republic of Georgia. Clin Infect Dis 2007;45(2):174–80.
5. Sobel J, Tucker N, Sulka A, McLaughlin J, Maslanka S. Foodborne botulism in the United States, 1990–2000. Emerg Infect Dis 2004;10(9):1606–11.
6. Dembek ZF, Smith LA, Rusnak JM. Botulism: cause, effects, diagnosis, clinical and laboratory identification, and treatment modalities. Disaster Med Public Health Prep 2007;2:122–34.
7. Hughes JM, Blumenthal JR, Merson MH, Lombard GL, Dowell VR Jr, Gangarosa EJ. Clinical features of types A and B food-borne botulism. Ann Intern Med 1981;95(4):442–5.
8. Sobel J. Botulism Clin Infect Dis 2005;41(8):1167–73.
9. Fagan R, McLaughlin J, Middaugh J. Persistence of botulinum toxin in patients' serum: Alaska, 1959–2007. J Infect Dis 2009;199:1029–31.
10. Woodruff BA, Griffin PM, McCroskey LM, Smart JF, Wainwright RB, Bryant RG, et al. Clinical and laboratory comparison of botulism from toxin types A, B, and E in the United States, 1975–1988. J Infect Dis 1992;166(6):1281–6.
11. France MP. Histological examination of the central nervous system in the diagnosis of botulism. J Comp Pathol 1989;101(1):101–8.
12. Wilbur RL, Ophuls W. Botulism: a report of food poisoning apparently due to eating of canned stringbeans with pathological report of a fatal case. Arch Pathol 1914;14:589–604.
13. Varma J, Katsitadze G, Moiscrafishvili M, Zardiashvili T, Chokheli M, Tarkhashvili N, et al. Signs and symptoms predictive of death in patients with foodborne botulism—Republic of Georgia, 1980–2002. Clin Infect Dis 2004;39:357–62.
14. Shapiro D, Weissfeld S, Baselski V, Carey R, Gilligan P, Snyder J, et al. Sentinel laboratory guidelines for suspected agents of bioterrorism: botulinum toxin. American Society for Microbiology. (Rev July 2003):1–6, http://www.asm.org/images/pdf/Botulism.pdf (accessed March 5, 2009).
15. Arnon SS, Schechter R, Inglesby TV, Henderson DA, Bartlett JG, Ascher MS, et al. Botulinum toxin as a biological weapon: medical and public health management. J Am Med Assoc 2001;285:1059–70.
16. The Centers for Disease Control and Prevention. Atlanta, Georgia. Botulism in the United States, 1899–1996: handbook for epidemiologists, clinicians and laboratory workers. CDC Division of Bacterial and Mycotic Diseases 1998;1–43, http://www.cdc.gov/nczved/dfbmd/disease_listing/files/botulism.pdf (accessed March 10, 2009).

Additional information and reprint requests:
Kelly Devers, M.D.
Department of Pathology
University of New Mexico Health Sciences Center
MSC08 4640, 1 University of New Mexico
Albuquerque, NM 87131
E-mail: kdevers@salud.unm.edu

JOURNAL OF FORENSIC SCIENCES

J Forensic Sci, November 2010, Vol. 55, No. 6
doi: 10.1111/j.1556-4029.2010.01506.x
Available online at: onlinelibrary.wiley.com

CASE REPORT

PATHOLOGY/BIOLOGY

Marta I. Saloña,[1] Ph.D.; M. Lourdes Moraza,[2] Ph.D.; Miguel Carles-Tolrá,[3] Ph.D.; Victor Iraola,[4] Ph.D.; Pablo Bahillo,[5] Ph.D.; Tomás Yélamos,[6] Ph.D.; Raimundo Outerelo,[7] Ph.D.; and Rafael Alcaraz,[8] M.D.

Searching the Soil: Forensic Importance of Edaphic Fauna After the Removal of a Corpse

ABSTRACT: Arthropods at different stages of development collected from human remains in an advanced stage of decomposition (following autopsy) and from the soil at the scene are reported. The corpse was found in a mixed deciduous forest of Biscay (northern Spain). Soil fauna was extracted by sieving the soil where the corpse lay and placing the remains in Berlese–Tullgren funnels. Necrophagous fauna on the human remains was dominated by the fly Piophilidae: *Stearibia nigriceps* (Meigen, 1826), mites Ascidae: *Proctolaelaps epuraeae* (Hirschmann, 1963), Laelapidae: *Hypoaspis (Gaeolaelaps) aculeifer* (Canestrini, 1884), and the beetle Cleridae: *Necrobia rufipes* (de Geer, 1775). We confirm the importance of edaphic fauna, especially if the deceased is discovered in natural environs. Related fauna may remain for days after corpse removal and reveal information related to the circumstances of death. The species Nitidulidae: *Omosita depressa* (Linnaeus, 1758), Acaridae: *Sancassania berlesei* (Michael, 1903), Ascidae: *Zerconopsis remiger* (Kramer, 1876) and *P. epuraeae*, Urodinychidae: *Uroobovella pulchella* (Berlese, 1904), and Macrochelidae: *Glyptholaspis americana* (Berlese, 1888) were recorded for the first time in the Iberian Peninsula.

KEYWORDS: forensic science, forensic entomology, human corpse, edaphic fauna, *Stearibia nigriceps, Glyptholaspis americana, Hypoaspis (G.) aculeifer, Proctolaelaps epuraeae, Sancassania berlesei, Uroobovella pulchella, Zerconopsis remiger*

A corpse generates new biological processes that evolve according to the environment in which it is found as it produces important changes in the soil (1). The natural inhabitants of undisturbed soils disappear and new organisms take their place, resulting in a new ecosystem dominated by the cadaveric fauna (1,2). The study of the dynamics of colonization, development, and succession patterns of necrophagous fauna on a corpse or carrion is at the heart of medico-criminal entomology (2). Moreover, for corpses found in advanced stages of decomposition, arthropods may provide the only method available for estimating a minimum postmortem interval (PMI) (3). It should be noted, however, that the estimate of PMI for a corpse in an advanced stage of decomposition may be unreliable as successional waves elapse over time and numerous environmental factors come into play that may diminish the accuracy of the estimate (3,4). Indeed, corpses in an advanced stage of decomposition can provide important information relating to succession periods rarely reported (5–8).

[1]Department de Zoología y Biología Celular Animal, Facultad Ciencia y Tecnología, UPV-EHU, Campus de Leioa, Barrio de Sarriena s/n, E-48940 Bilbao, Spain.
[2]Department de Zoología y Ecología, Facultad de Ciencias, Universidad de Navarra Apdo. 177, E-31080 Pamplona, Spain.
[3]Avda. Príncipe de Asturias 30, ático 1, E-08012 Barcelona, Spain.
[4]Laboratorios LETI, S.L. C/ Sol 5, E-28760 Tres Cantos, Madrid, Spain.
[5]IES Baracaldo, Bizkaia, Spain.
[6]Calle Balmes, nº 61, ppl. 3ª, E-08007 Barcelona, Spain.
[7]Department Zoología y Antropología Física, Universidad Complutense de Madrid, E-28040 Madrid, Spain.
[8]Servicio de Patología Forense, Instituto Anatómico Forense, C/ Barroeta Aldamar 10, E-48001 Bilbao, Spain.

Received 7 April 2009; and in revised form 5 June 2009; accepted 11 Aug. 2009.

This paper presents the first forensic case where arthropods have been collected from a corpse in an advanced stage of decomposition in the Basque Country (north of Spain) and where soil biota has been previously studied under natural conditions (9,10). This was the first chance to gather important information about arthropods associated with a body in an advanced stage of decomposition in this area and it highlights the need to carefully examine a broad perimeter adjacent to the human remains to avoid losing, ignoring, or underestimating critical forensic evidence.

Material and Methods

Case Description

In August 2003, the remains of a young man were discovered near the edge of a mixed deciduous forest in a rural area of Biscay (northern Spain). The corpse was lying on the ground, completely dressed, reduced to a skeleton bearing the remains of dried soft tissue, and covered with mites and insects. The deceased had last been seen alive 3 months prior to the discovery of the corpse. Unfortunately, the body had already been removed from the scene before authorization was received from the magistrate to collect entomological evidence. Nevertheless, evidence was eventually gathered from the site following removal of the corpse and this included organisms of forensic interest.

Methodology

A medico-legal autopsy was performed by the Forensic Pathology Service of Bilbao in accordance with international standards (11).

Beetles, fly larvae, and mites were collected from the skeletal remains held at the Forensic Pathology Service and preserved in 70% ethanol.

Nine (3 × 3) samples of ground litter and soil (500 cc/sample, taken to a depth of 5 cm) were collected from the scene and sieved. Large arthropods were removed with forceps, and soil mesofauna was extracted from aliquots of the sieved soil (100 cc) using Berlese–Tullgren funnels (12). All fauna was preserved in 70% ethanol for later identification.

Approximately half of the fly larvae collected from the corpse and the soil at the scene were incubated at 23°C in natural daylight in the laboratory to confirm their identification (13). The remaining maggots (n = 20) were placed in hot water for 1 min before preservation in 80% ethanol (14).

Results and Discussion

The autopsy revealed the existence of a skull injury, 1 cm in diameter, with significant hematoma in the corresponding area of the brain. Evidence suggested that death had been caused by a violent attack.

The site was a mixed deciduous forest with an adequate preservation of the canopy and ground cover, extremely closed, dark, and wet. These forests are relict in the area because of intensive farming activities (15). A diagram with weather data collected from the nearest meteorological station is included in Fig. 1.

A total of 29 species was collected and identified from soil samples taken at the crime scene; there was a direct correspondence between the five species collected from the corpse after autopsy that were also present in the soil samples (Table 1).

The corpse was covered in the larvae of Piophilidae (Diptera). The maggots were active in the soil samples together with pupae, and adults were emerging from the soil. Specimens reared from larvae collected in soil confirmed the consistency of the evidence. Adults emerging from the soil and the reared larvae were identified as *Stearibia nigriceps* (Meigen, 1826), the dominant fly found in the removed corpse. In simulations previously carried out using pigs in northern Spain, this species has been found in lower frequency and abundance than the similar species *Piophila casei* (Linnaeus, 1758), the cheese skipper (16).

The presence of *Necrobia rufipes* (de Geer, 1775) (Coleoptera, Cleridae), in both the corpse and in the soil was also noteworthy; adults were reared from preimaginal stages collected from the soil. In addition, adults of *Necrobia violacea* (Linnaeus, 1758) were also collected from soil samples. Other beetle larvae were found in the soil but rearing in the laboratory proved unsuccessful.

Finally, three mite species were collected from the corpse and their presence was confirmed in the soil. The most abundant mite species on the corpse was *Proctolaelaps epuraeae* (Hirschmann, 1963) (Mesostigmata, Ascidae), a species previously cited associated with *Epuraea fuscicollis* (Stephens, 1832) (Coleoptera, Nitdulidae) in Europe (17). We also found adults of *Hypoaspis (Gaeolaelaps) aculeifer* (Canestrini, 1884) (Mesostigmata, Laelapidae) and one deutonymph of the phoretic mite *Uroobovella pulchella* (Berlese, 1904) (Mesostigmata, Urodinychidae). The absence of other species on the remains may be explained by the long delay between the corpse being found and permission being granted for the collection of evidence in the morgue. The complementary information reported from the soil may be of importance for future forensic cases. We therefore give a detail list of all the species and instars found in this research in Table 1.

Despite some previous research carried out in our region, there is still a lack of knowledge concerning the distribution of local necrophagous species and their biology. This makes it difficult to formulate precise conclusions based on the morphology of the corpse and the structure of the community. The numerous factors that influence the dynamics of the decomposition process can

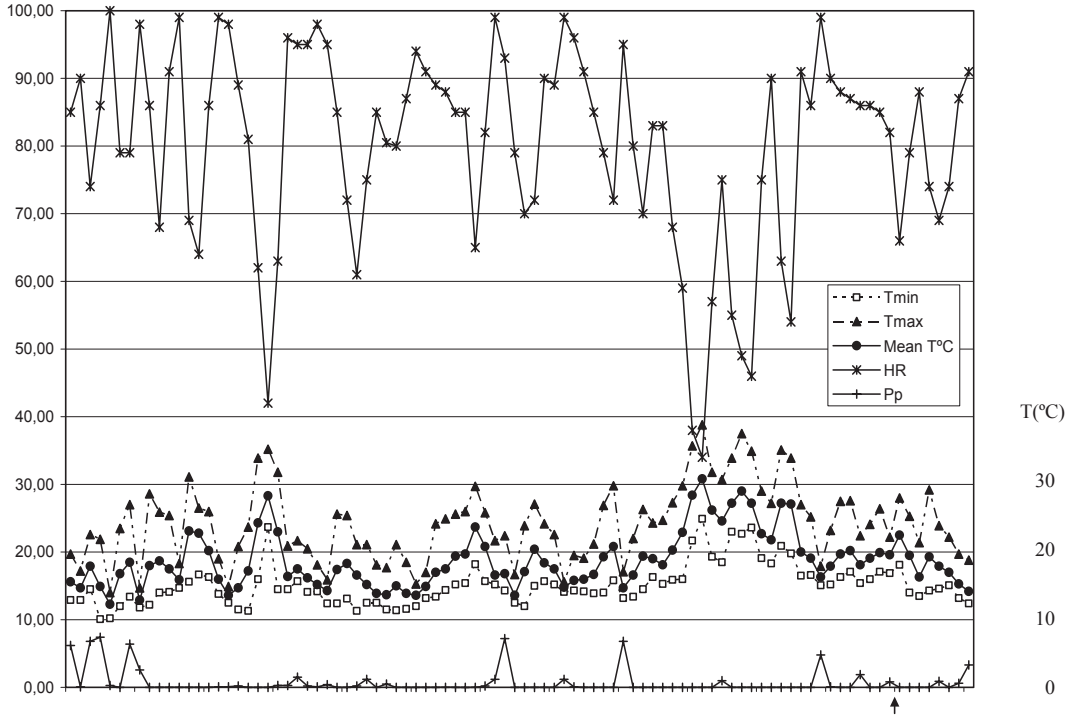

FIG. 1—*Ombrotermic diagram after data recorded at the closest meteorological station. T, temperature; min, minimum; max, maximum; HR, relative humidity (%); Pp, precipitation (mm/m²); ↑ corpse discovery day.*

TABLE 1—*Species collected from soil samples extracted at the scene (soil) and directly from the corpse.*

Order	Family	Species	Corpse	Soil	NR
Diptera	Piophilidae	*Stearibia nigriceps* (Meigen, 1826)	L Ad	L P Ad	BC
Coleoptera	Cleridae	*Necrobia rufipes* (de Geer, 1775)	Ad	L P Ad	
		Necrobia violacea (Linnaeus, 1758)		Ad	
	Histeridae	*Carcinops pumilio* (Erichson, 1834)		Ad	
		Margarinotus (*Paralister*) *ignobilis* (Marseul, 1854)		Ad	
	Nitidulidae	*Omosita colon* (Linnaeus, 1758)		Ad	IP
		Omosita depressa (Linnaeus, 1758)		Ad	
	Silphidae	Unidentified larvae		L	
	Staphylinidae	*Acrotona aterrima* (Gravenhorst, 1802)		Ad	
		Atheta (Atheta) coriaria (Kraatz, 1858)		Ad	BC
		Dimetrota cinnamoptera (Thomson, 1856)		Ad	
		Carpelimus (Trogophloeus) corticinus (Gravenhorst, 1806)		Ad	BC
		Gyrohypnus fracticornis (O. Muller,1776)		Ad	BC
		Habrocerus capillaricornis (Gravenhorst, 1806)		Ad	BC
		Lithocharis ochracea (Gravenhorst, 1802)		Ad	
		Oligota parva (Kraatz, 1858)		Ad	
		Philonthus discoideus (Gravenhorst, 1802)		Ad	
		Platystethus arenarius (Geoffroy, 1785)		Ad	
		Rugilus orbiculatus (Paykull, 1789)		Ad	
Collembola	Unidentified species		Ad		
Astigmata	Acaridae	*Sancassania berlesei* (Michael, 1903)		N Ad	IP
Oribatida	Camisiidae	*Platynothrus peltifer* (C.L. Koch, 1839)		Ad	
	Mycobatidae	*Minunthozetes semirufus* (C.L. Koch, 1841),		Ad	
Mesostigmata	Ascidae	*Proctolaelaps epuraeae* (Hirschmann, 1963)	Ad	N Ad	IP
		Zerconopsis remiger (Kramer, 1876)		Ad	IP
	Laelapidae	*Hypoaspis (G.) aculeifer* (Canestrini, 1884)	Ad	N Ad	BC
	Urodinychidae	*Uroobovella pulchella* (Berlese, 1904)	Ad	N Ad	IP
	Parasitidae	*Paragamasus* sp.		N	
	Macrochelidae	*Glyptholaspis americana* (Berlese, 1888)		Ad	IP
Chilopoda	Unidentified species		Ad		
Diplopoda	Unidentified species		Ad		
Isopoda	Unidentified species		Ad		

L, larvae; P, pupae; Ad, Adult; NR, new record; BC, Basque Country; IP, Iberian Peninsula.

significantly impact the succession models (3,4). Nevertheless, observations of arthropod fauna associated with human remains in advanced stages of decomposition are not frequently reported in scientific literature. Indeed, this is the first time that a detailed list of species of forensic interest associated with human remains in an advanced stage of decomposition (nearly skeletonized) has been recorded in the Basque Country (north of Spain).

Although 10 days had passed since the removal of the corpse, the same species extracted from the corpse itself were also identified in soil samples taken from where the corpse had been found. The community was dominated by larvae of *S. nigriceps* (fly identified after incubation). Pupae and emerging adults of this species were also present in the soil and this helped to substantiate the evidence collected at the scene. *S. nigriceps* is recognized as an important forensic indicator, arriving late in the decomposition process, usually after saponification (18,19). Larvae of this species have been previously reported in Venice (6), with a PMI estimated at 2 months. The community structure was also consistent with a previous case reported from the Hawaiian Islands of a corpse in an advanced stage of decomposition (5). In both cases, only third instars of the Piophilidae were found on the corpses (5,6). We also collected adults emerging from the soil that confirm at least one complete development cycle of the fly in the soil and fits well with the estimated PMI (3 months).

With respect to the seasonality of the community structure, we should note that *Margarinotus ignobilis* (Marseul, 1854), rarely found in late summer, supports the estimated time of death, given at the end of May or beginning June. The presence of *Carcinops pumilio* (Erichson, 1834) confirms an advanced stage of decomposition, and the complete development of the Piophilidae, with adults emerging from the soil, is in accordance with a minimum PMI estimation of 2 months, which is consistent with a simulation recently performed in our region (unpublished data).

However, the lack of complementary records of environmental data prior to the removal of the corpse prevents a more accurate estimation of this interval. Therefore, further simulations using animal models are needed in our region.

Mites are usually overlooked in forensic research, although they are present in nearly every stage of decomposition and are directly associated with other species of forensic interest (20). The most abundant mite species collected from the corpse, *P. epuraeae*, is a phoretic mite from Nitidulidae previously described (17); *U. pulchella* also uses insects for phoresis. *H. (G.) aculeifer* is known as a generalist predator of soil invertebrates (21) and is used in the biological control of soil pests (22). Furthermore, the presence of all the developmental stages of *P. epuraeae* supports a long-term association of the mite with the remains. From cases in Belgium, the coexistence of *Proctolaelaps* and *Hypoaspis* (23) as well as the presence of *Sancassania berlesei* (Michael, 1903) have been reported previously. This third species has also been identified in conditions similar to those of the case described here, that is, on a corpse exposed to high levels of humidity for 3–3.5 months (23).

In this paper, we confirm both an association of some mite species with a specific period of decomposition and the potential for using mites as indicators of environmental conditions (20,23).

While oribatids are the dominant group of mites in our natural soils (9,10), they usually disappear during the decomposition of a corpse (24). Accordingly, in this case, when comparing the oribatid fauna collected from the soil immediately adjacent to the corpse with that inhabiting undisturbed soils in the same area, significant

differences were found. More than 30 species had previously been collected from undisturbed soils from mixed deciduous forests in this area (9,10). However, of these species, only two were found in the soil samples taken from the location where the corpse was discovered and they were poorly represented. Notably, one of them, *Platynothrus peltifer* (C.L. Koch, 1839), is a species that typically remains in disturbed soils (9,10) and, moreover, has previously been identified on dog carcasses in Tennessee (USA) (25). The relevance of these species in forensic research should therefore be more fully explored.

The case reported here provides novel information regarding the structure of the arthropod community associated with a corpse in an advanced state of decomposition; at the same time, it adds to the overall body of knowledge, having identified species not previously reported from this geographical area. Specifically, in this paper, *Omosita depressa* (Linnaeus, 1758) (26), together with *P. epuraeae* (Hirschmann, 1963), *S. berlesei* (Michael, 1903), *Zerconopsis remiger* (Kramer, 1876), *U. pulchella* (Berlese, 1904), and *Glyptholaspis americana* (Berlese, 1888) are recorded for the first time in the Iberian Peninsula. Table 1 includes references to the additional new records for our region.

Acknowledgments

Our special thanks go to the magistrate and police for the facilities provided for the research and publication of the results; to Dr. H. Braig for his critical review, comments and suggestions that improved the contents of the manuscript, and to J.B. Dickerson and Ideas Need Communicating Language Services for the final revision of the manuscript.

References

1. Bornemissza GF. An analysis of arthropod succession in carrion and the effect of its decomposition on the soil fauna. Aust J Zool 1957;5:1–12.
2. Hall RD. Introduction: perceptions and status of forensic entomology. In: Byrd JH, Castner JL, editors. Forensic entomology: the utility of arthropods in legal investigations. Boca Raton, FL: CRC Press, 2001;1–15.
3. Anderson GS. Insect succession on carrion and its relationship to determining time of death. In: Byrd JH, Castner JL, editors. Forensic entomology: the utility of arthropods in legal investigations. Boca Raton, FL: CRC Press, 2001;143–75.
4. Archer MS, Bassed RB, Briggs CA, Lynch MJ. Social isolation and delayed discovery of bodies in houses: the value of forensic pathology, anthropology, odontology and entomology in the medico-legal investigation. Forensic Sci Int 2005;15:259–65.
5. Goff ML, Flynn MM. Determination of postmortem interval by arthropod succession: a case study from the Hawaiian Islands. J Forensic Sci 1991;36:607–13.
6. Turchetto M, Lafisca S, Constantini G. Postmortem interval PMI determined by study sarcophagous biocenoses: three cases from the province of Venice Italy. Forensic Sci Int 2001;120:18–31.
7. Arnaldos MI, García MD, Romera E, Presa JJ, Luna A. Estimation of postmortem interval in real cases based on experimentally obtained entomological evidence. Forensic Sci Int 2005;149:57–65.
8. Merritt RW, Snider R, de Jong JL, Benbow ME, Kimbirauskas RK, Kolar RE. Collembola of the grave: a cold case history involving arthropods 28 years after death. J Forensic Sci 2007;52:1359–61.
9. Saloña Bordas MI, Iturrondobeitia JC. Estudio de las comunidades de oribátidos *Acari, Oribatei* de varios ecosistemas de Vizcaya y una zona próxima. 3. Análisis comparado de las afinidades cenóticas e interespecíficas. Rev Ecol Biol Sol now Eur J Soil Biol 1991;27:185–203.
10. Saloña Bordas MI, Iturrondobeitia JC. A comparative study of the soil mite communities *Acari* of Woodland and non-Woodland areas in the Basque Country. In: Watkins C, editor. Ecological effects of afforestation. Oxon: CABI Pbl, 1993;153–63.
11. Council of Europe. Recommendation Nr R 99.3 on the harmonisation of medico-legal autopsy rules and its explanatory memorandum. Strasbourg, Germany: CDBI/INF 7, 1999;6–29.
12. Steyskall GC, Murphy WL, Hoover EM, editors. Collecting and preserving insects and mites: tools and techniques. USDA Misc. Publication No. 1443. Washington, DC: Agriculture Research Service, 1986.
13. Amendt J, Campobasso CP, Gaudry E, Reiter C, LeBlanc HN, Hall MJR. Best practices in forensic entomology. Standards and guidelines. Int J Legal Med 2007;121:90–104.
14. Adams ZJO, Hall MJR. Methods used for the killing and preservation of blowfly larvae, and their effect on post-mortem larval length. Forensic Sci Int 2003;138:50–61.
15. Duñabeitia M, Rodríguez N, Salcedo I, Sarrionandia E. Field mycorrhization and its influence on the establishment and development of the seedlings in a broadleaf plantation in the Basque Country. For Ecol Manage 2004;195:129–39.
16. Castillo M. Estudio de la entomofauna asociada a cadáveres en el Alto Aragón España. Bol Soc Entomol Aragonesa 2002;6:1–93.
17. Karg W. Acari (Acarina), Milben. Parasitiformes (Anactinochaeta). Cohors Gamasina Leach. Raubmilben. 2nd ed. Die Tierwelt Deutschlands 1993;59:1–523.
18. Anderson G, Van Laerhoven SL. Initial studies on insect succession on carrion in Southwestern British Columbia. J Forensic Sci 1996;41:617–25.
19. Martinez E, Duque P, Wolff M. Succession pattern of carrion-feeding insects in Paramo, Colombia. Forensic Sci Int 2007;166:182–9.
20. Braig HR, Perotti MA. Carcasses and mites. Exp Appl Acarol 2009;49:45–84.
21. Heckmann LH, Ruf A, Nienstedt KM, Krogh PH. Reproductive performance of the generalist predator *Hypoaspis aculeifer* (Acari: Gamasida) when foraging on different invertebrate prey. Appl Soil Ecol 2007;36:130–5.
22. Berndt O, Meyhöfer R, Poehling HM. The edaphic phase in the ontogenesis of *Frankliniella occidentalis* and comparison of *Hypoaspis* mites and *Hypoaspis aculeifer* as predators of soil-dwelling thrips stages. Biol Control 2004;30:17–24.
23. Leclercq M, Verstraetten C. Entomologie et Médecine légale. Datation de la mort. Acariens trouvés sur des cadavres humains. Bull Ann Soc Belge Ent 1988;124:195–200.
24. Goff ML. Gamasid mites as potential indicators of postmortem interval. In: Channabasavanna GP, Viraktamath CA, editors. Progress in acarology. New Delhi, India: Oxford & IBH Publishing Co, 1989;443–50.
25. Reed HB. A study of dog carcass communities in Tennessee, with special reference to insects. Am Midl Nat 1958;59:213–45.
26. Bahillo de la Puebla P, Colón JI, Saloña M. Confirmación de la presencia de *Omosita depressa* (Linnaeus, 1758) en la Península Ibérica (Coleoptera, Nitidulidae). Bol SEA 2004;34:161–2.

Additional information and reprint requests:
Marta I. Saloña, Ph.D.
Department de Zoología y Biología Celular Animal
Facultad Ciencia y Tecnología
UPV-EHU, Campus de Leioa
Barrio de Sarriena s/n
E-48940 Bilbao
Spain
E-mail: m.salona@ehu.es

JOURNAL OF FORENSIC SCIENCES

J Forensic Sci, November 2010, Vol. 55, No. 6
doi: 10.1111/j.1556-4029.2010.01485.x
Available online at: onlinelibrary.wiley.com

CASE REPORT

PATHOLOGY/BIOLOGY

Kumara Thevan,[1] *B.Sc.; Abu Hassan Ahmad,*[1] *Ph.D.; Che Salmah Md. Rawi,*[1] *Ph.D.; and Bhupinder Singh,*[2] *M.B.B.S.*

Growth of *Chrysomya megacephala* (Fabricius) Maggots in a Morgue Cooler*

ABSTRACT: In estimating the postmortem interval (PMI) using maggots obtained during autopsy, the forensic entomologist makes decisions regarding the effects of low-temperature storage of the body on the insects. In this case report, a corpse was found in an abandoned house in the residential area of Bukit Mertajam, Penang, Malaysia. The maggots were found to be alive inside the mouth of the deceased although the corpse had been in the morgue cooler for 12 days. The maggots were reared and identified as *Chrysomya megacephala* (Fabricius). The emerged adult flies were kept as a stock colony, and the duration of development under the indoor fluctuating temperature regime was studied. The total duration of developmental process of this species was 9.5 ± 0.5 days, and the PMI estimated was 3.2 ± 0.6 days. This case report demonstrates the survival of *Ch. megacephala* maggots for 12 days and their growth inside the morgue cooler.

KEYWORDS: forensic science, forensic entomology, Calliphoridae, postmortem interval, maggot mass, Malaysia

The growth and development of calliphorid (Diptera: Calliphoridae) larvae is of great interest to forensic science, especially for estimation of a postmortem interval (PMI) (1). To obtain an estimate of the minimum PMI, one requires accurate identification of the species recovered from the case, data on the temperature regime prior to the taking of the samples, and relevant information on the duration of development of the species at various temperatures (2). Furthermore, the developmental rate of calliphorid larvae is influenced by the temperature of their immediate environment (1). There are two main physiological responses to low temperatures: diapause and quiescence (3,4). Diapause is a delay in development evolved in response to regularly recurring periods of adverse environmental conditions (3), whereas quiescence mainly stops development for a short time and acts like an anesthetic. Quiescence is induced by the immediate effect of temperatures ranging from 0 to 10°C and involves a deceleration of insect metabolic activity (4). However, when a "maggot mass" is formed, the maggot mass temperature may be sufficient to allow continued development and is essential in allowing development (5). The objectives of this case study were to highlight (i) the importance of the case history in PMI estimation and (ii) the growth of blowfly maggots stored in a morgue cooler.

Case Report

On July 25, 2007, an unknown male corpse was found in an empty house in the residential area of Bukit Mertajam, Penang, Malaysia (5° 21′N, 100° 28′E). The corpse was in active decay stage and fully clothed. The autopsy was performed on the same day the corpse was found, and no entomological specimens were collected. After 5 days of the corpse being kept in the morgue cooler, we were informed that maggots had infested the corpse. The entomological specimens were collected on July 30, 2007, at 12.30 pm. Specimens taken were nonhairy maggots, which were collected from the mouth (alive) and on the legs (dead). On attempting rearing, the maggots failed to survive. Pending police investigations, the corpse was still kept in the mortuary. On August 6, 2007, at 11.30 am, the second sampling was carried out. The samples were one newly emerged adult (wings not developed), and nonhairy pupae were found outside the morgue cooler (14 pupae). Then, 34 nonhairy live maggots were taken from the mouth (Fig. 1). There were no live maggots found inside the morgue cooler beside the one in the mouth of the deceased. On rearing, these live maggots survived and were identified as *Ch. megacephala* (Fabricius) using taxonomic keys provided by Greenberg & Kunich (6). The temperature of the morgue cooler was at 4 ± 3°C, and the temperature of the maggot mass inside the mouth was 12°C. Unfortunately, the temperature of the scene of death was not available.

In Malaysia, there is a lack of any published data regarding the development time of *Ch. megacephala* under indoor fluctuating temperature of Malaysian tropical climate. For the purpose of this study, the emerged adults were maintained as a colony, and the immature life cycle of this species was studied at room temperature to simulate the scene of death. In this experiment, beef meat was used as the rearing medium, and nine replicates were made. The eggs were collected from the colony and were transferred into the rearing containers [11.5 (h) × 10.0 (w) × 10.0 (L) cm] with 2.5 m thick soil inside it. The maggots were fed with fresh beef meat *ad libitum*. The developmental data, temperatures, and relative humidity of the rearing were recorded from the time the eggs were collected until the emergence. From each replicate, an average of

[1]School of Biological Sciences, Universiti Sains Malaysia, 11800 Penang, Malaysia.
[2]Institute of Forensic Medicine (Northern Region), Penang Hospital, 10990 Residensi Road, Penang, Malaysia.
*Funding provided by Universiti Sains Malaysia (USM) RU research grant 1001/PBiology/815009.

Received 22 April 2009; and in revised form 6 Aug. 2009; accepted 13 Sept. 2009.

FIG. 1—*The live maggot mass of* Chrysomya megacephala *(arrow) forming froths in the mouth of the corpse (photo taken during the first sampling).*

five maggots was randomly collected, every morning and evening until the maggots reached the pupal stage. These maggots were warm-water killed (52 ± 10°C) and preserved in Kahle's solution. The instar stages of the preserved maggots were recorded by determining the number of posterior spiracles slits under the stereomicroscope, and the lengths of the maggots were measured. For the first and second instar, a slide of the posterior spiracles was prepared and observed under the light microscope. After the rearings were completed, the developmental times (days) were calculated as shown in Table 1, and the graph of larval length against developmental time (hours) was constructed (Fig. 2).

Results and Discussions

The average length of the dead *Ch. megacephala* (Fabricius) maggots found on the legs during the first specimen collection was 13 mm (third instar). The recently emerged adult found outside the body freezer failed to develop its wings and died. The 14 pupae collected from outside the morgue cooler emerged on August 8, 2007, between 10 am and 4 pm. The live larvae that were collected from the mouth of the deceased on first sample collection averaged 10 mm in length (third instar), and on the second sampling, the length of the maggots was 13.5 mm (third instar). The reared live larvae that were collected on second sampling turned into pupae on August 8, 2007, at 4 pm and emerged on August 11, 2007, at 5 pm. The developmental time of the maggots from the time of second sample collection until the pupal stage was 52.5 h. The pupation period was 73 h (3 days). The mean temperature of the rearing room was 29.5 ± 1°C, and the relative humidity was 61–79%.

Ch. megacephala also known as the Oriental latrines fly, is a species of medical importance (7) and has been identified playing an important role in forensic cases (8). This species, formerly Australasian and Pacific in distribution, is now widespread in Africa and the Americas (9). In Malaysia, *Ch. megacephala* is now the predominant species infesting human corpses (10). In this case report, during the sampling periods, the live maggots were observed to form froths above the maggot mass in the mouth (Fig. 1). When the corpse was taken out from the morgue cooler, the maggots went deep into the throat, and we managed to extract 34 maggots only. The maggots grew 3.5 mm in length between the first and second sample collection period (6 days). Under sub-optimal conditions, blowfly larvae can delay pupariation (9). In this case study, the maggots of *Ch. megacephala* were found alive, infesting the corpse placed in the morgue cooler for a total of 12 days in darkness (except during the sampling period), inside the mouth of the deceased at the ambient temperature of 4 ± 3°C. A potential error of 8.6–12.8% in PMI estimation was reported, if the assumption that no insect development takes place during the preautopsy refrigeration is made (11); while others found low temperature (4°C) because of refrigeration affects the normal development of blowflies (12). This probably explains the shortened pupal period from normal 3.9 days (Table 1) to 3.0 days (case specimens). In this case study, the PMI was estimated by comparing their length with the graph constructed in Fig. 2 because of several reasons: (i) the most accurate estimation would be using the size of the oldest dead

TABLE 1—*The accumulated developmental time (days) of* Chrysomya megacephala *at the indoor rearing temperature of 29 ± 2°C and relative humidity of 59–75%.*

Immature Stages	Eggs/First Instar	Second Instar	Third Instar	Post Feeding	Pupa	Emergence
Accumulated developmental time (days)	0.8 ± 0.2	1.6 ± 0.0	3.3 ± 1.3	4.5 ± 0.4	5.1 ± 0.5	9.0 ± 0.5

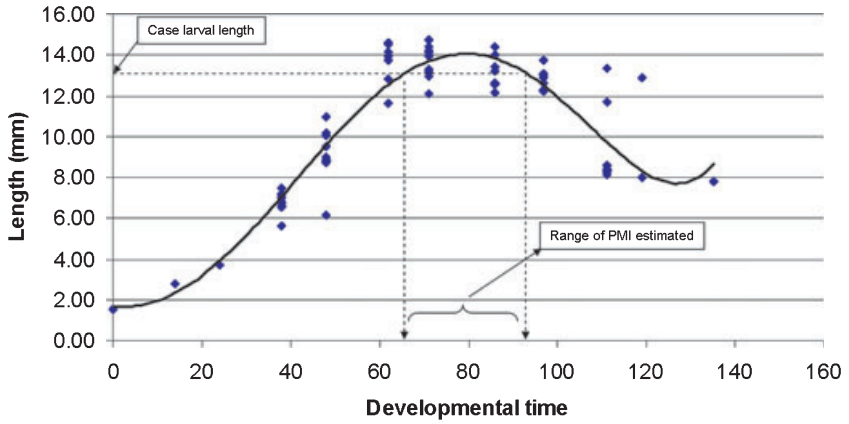

FIG. 2—*The larval length against developmental time (hours) of* Chrysomya megacephala *(nine replicates) at 29 ± 2°C.*

maggots collected in the first sampling because there was no degree-day reference data of this species at 12°C available; (ii) we did not know the exact temperature experienced by the maggots throughout the 12-day period for the degree-days method to be used, and there is evidence that maggots can thermoregulate their temperature when maggot mass formed (13,14); (iii) the corpse was found indoors and temperature data from nearby weather data cannot be used while the temperature data of the scene of death was not recorded; (iv) the use of larval length to determine PMI was acceptable if both the scene of death and reference data were at the almost similar environment (indoors) where the temperature fluctuates little (15). The PMI was estimated between 64 h (2.6 days) and 94 h (3.9 days) based on the length of the dead maggots collected in the first sampling. If the PMI estimation on the case was carried out using the length of live *Ch. megacephala* maggots collected from the second sample (13.5 mm), the PMI estimated would be still within the range estimated earlier; however, in reality the maggots were actually more than 12 days old. Thus, the potential for blowfly larvae to undergo significant development while being stored in the morgue is a possibility that forensic entomologists should consider during an investigation involving samples collected from autopsy (11). It was suggested that if the time of death may be of interest in cases with insects' colonization of human corpses, preferably a person with experience in the field of forensic entomology should be present at the crime scene or at least during the autopsy (16,17). However, this is not a standard practice in Malaysia, and without the knowledge of the case history and the thermal history of the maggots, the forensic entomologist must be cautious in estimating the PMI.

Acknowledgments

We thank Mr. Chan Kok Cheng, Mr. Mahashim Mahamud, and Mr. Abdullah Shaari for their help during the period of sample collections. Lastly, we thank Dr. R.H.L. Disney for comments on the manuscript.

References

1. Catts EP, Goff ML. Forensic entomology in criminal investigation. Annu Rev Entomol 1992;37:253–72.
2. Disney RHL. Duration of development of two species of carrion-breeding scuttle flies and forensic implications. Med Vet Entomol 2005;19:229–35.
3. Chapman RF. The insects: structure and function, 4th edn. Cambridge, UK: Cambridge University Press, 1998.
4. Denlinger DL, Joplin KH, Chen CP, Lee RE. Cold shock and heat shock. In: Richard J, Lee E, Denlinger DL, editors. Insect at low temperature. New York, NY: Chapman & Hall, 1991; 131–48.
5. Higley LG, Haskell NH. Insect development and forensic entomology. In: Byrd JH, Castner JL, editors. Forensic entomology—the utility of arthropods in legal investigations. Boca Raton, FL: CRC Press, 2001; 67.
6. Greenberg B, Kunich JC. Entomology and the law: flies as forensic indicators. Cambridge, UK: Cambridge University Press, 2002.
7. Sukontason KL, Sukontason K, Piangjai S, Boonchu N, Chaiwong T, Vogtsberger RC, et al. Larval morphology of *Chrysomya megacephala* (Fabricius) (Diptera:Calliphirodae) using scanning electron microscope. J Vector Ecol 2003;28(1):47–52.
8. Smith KGV. A manual of forensic entomology. London, UK: Cornell University Press, 1986.
9. Wells JD, Kurahashi H. *Chrysomya megacephala* (Fabricius) (Diptera: Calliphoridae) development: rate, variation and the implications for forensic entomology. Japan J Sanit Zool 1994;45(4):303–9.
10. Lee HL, Krishnasamy M, Abdullah AG, Jeffrey J. Review of forensically important entomological specimens in the period of 1972-2002. J Trop Biomed 2004;21:69–75.
11. Huntington TE, Higley LG, Baxendale FP. Maggot development during morgue storage and its effect on estimation the postmortem interval. J Forensic Sci 2007;52(2):453–8.
12. Myskowiak JB, Doums C. Effects of refrigeration on the biometry and development of *Protophormia terraenovae* (Robineau-Desvoidy) (Diptera: Calliphoridae) and its consequences in estimating post-mortem interval in forensic investigations. Forensic Sci Int 2002;125:254–61.
13. Slone DH, Gruner SV. Thermoregulation in larval aggregations of carrion-feeding blow flies (Diptera: Calliphoridae). J Med Entomol 2007;44(3):516–23.
14. Byrd JH, Butler JF. Effects of temperature on *Chrysomya rufifacies* (Diptera: Calliphoridae) development. J Med Entomol 1997;34(3):353–8.
15. Gennard DE. Forensic entomology—an introduction. Chichester, UK: John Wiley & Sons, 2007.
16. Haskell NH. Entomological collection techniques at autopsy and for specific environments. In: Catts EP, Haskell NH, editors. Entomology & death: a procedural guide. South Carolina: Clemson, 1990;98–109.
17. Klotzbach H, Schroeder H, Augustin C, Pueschel K. Information is everything—a case report demonstrating the necessity of entomological knowledge at the crime scene. Anil Aggrawal's Int J Forensic Med Toxicol 2004;5(1):19–21.

Additional information and reprint requests:
Prof. Abu Hassan Ahmad, Ph.D.
School of Biological Sciences
Universiti Sains Malaysia
11800 Penang
Malaysia
E-mail: aahassan@usm.my

JOURNAL OF FORENSIC SCIENCES

J Forensic Sci, November 2010, Vol. 55, No. 6
doi: 10.1111/j.1556-4029.2010.01483.x
Available online at: onlinelibrary.wiley.com

CASE REPORT

PSYCHIATRY & BEHAVIORAL SCIENCES

Gilles Gavaudan,[1,2] M.D.; David Magalon,[2] M.D.; Julien Cohen,[2] M.D.; Christophe Lançon,[2] M.D., Ph.D; Georges Léonetti,[1] M.D., Ph.D; and Anne-Laure Pélissier-Alicot,[1] M.D., Ph.D.

Partial Agonist Therapy in Schizophrenia: Relevance to Diminished Criminal Responsibility

ABSTRACT: Pathological gambling (PG), classified in the DSM-IV among impulse control disorders, is defined as inappropriate, persistent gaming for money with serious personal, family, and social consequences. Offenses are frequently committed to obtain money for gambling. Pathological gambling, a planned and structured behavioral disorder, has often been described as a complication of dopamine agonist treatment in patients with Parkinson's disease. It has never been described in patients with schizophrenia receiving dopamine agonists. We present two patients with schizophrenia, previously treated with antipsychotic drugs without any suggestion of PG, who a short time after starting aripiprazole, a dopamine partial agonist, developed PG and criminal behavior, which totally resolved when aripiprazole was discontinued. Based on recent advances in research on PG and adverse drug reactions to dopamine agonists in Parkinson's disease, we postulate a link between aripiprazole and PG in both our patients with schizophrenia and raise the question of criminal responsibility.

KEYWORDS: forensic science, pathological gambling, schizophrenia, aripiprazole, dopamine, criminal responsibility

According to the Diagnostic and Statistical Manual of Mental Disorders (1), pathological gambling (PG) is a persistent and recurrent maladaptive behavior that is characterized by at least five of the following symptoms: preoccupation with gambling; use of increasing amounts of money; inability to control, cut back, or stop gambling; irritability if not gambling; committing illegal acts to finance the behavior; lies to family or other persons to conceal the behavior; gambling to escape other problems; jeopardizing relationships (personal and professional); or relying on others to relieve desperate financial situations caused by the behavior. Evidence supports the existence of a causal relationship between criminal behavior and PG to maintain habitual gambling behaviors (2).

In the general population, the prevalence of PG ranges from 0.42% (3) to 1.93% (4). A higher frequency of 4.4% has been reported in patients with Parkinson's disease, rising to 8% with dopamine agonist therapy (5). This result is in line with many published case reports that identified PG as a complication of dopamine agonist therapy in Parkinson's disease (see [6] for review) and also in restless legs syndrome (7). Taken together, these observations support the hypothesis of a link between PG and dopaminergic neurotransmission (8). They raise the possibility that a complex behavioral disturbance such as PG could be related to dopamine drugs.

To the best of our knowledge, PG has never been described as a complication of drug treatment in schizophrenia. We report two patients with schizophrenia who developed PG and committed theft secondary to treatment with aripiprazole, a dopamine partial agonist.

[1]Service de Médecine Légale, Faculté de Médecine, Université de la Méditerranée, F-13005 Marseille, France.
[2]SHU de Psychiatrie d'Adultes et Centre des Addictions, Hôpital Sainte-Marguerite, F-13009 Marseille, France.

Received 29 April 2009; and in revised form 27 Aug. 2009; accepted 11 Sept. 2009.

Case 1

A 46-year-old man presented the first symptoms of paranoid schizophrenia, essentially characterized by active delusions and auditory hallucinations, at the age of 20. Over a 12-year period, he experienced several psychotic episodes and was frequently admitted to hospital. He received various typical antipsychotic drugs, and also clozapine, without a complete recovery. Depot haloperidol was the most effective drug in obtaining partial remission, although the patient continued to have chronic delusions and auditory hallucinations. As positive symptoms improved, negative symptoms progressively increased and led to a deficit syndrome. Except for nicotine dependence, there was no history of substance abuse and no comorbid condition such as personality disorder. Neurological examination was normal. No psychiatric disorder or PG was reported in the family.

Since 2000, his symptoms had remained stable. For 5 years, his pharmacological treatment did not change and consisted of haloperidol (a monthly 200 mg intramuscular depot injection) and prazepam (60 mg/day). He was seen by a psychiatrist once a month. The patient lived with his sister and was a low-frequency recreational gambler (lottery scratch cards) without financial consequences. In November 2005, he started a new treatment in association with haloperidol. Aripiprazole (15 mg/day) was initiated to improve positive and negative symptoms. A few days later, the patient's sister observed that he spent increasing amounts of money to buy lottery scratch cards, up to 300 euros

(*c.* 400 U.S. dollars) per day. She also observed that he showed increasing anxiety. When she tried to decrease his spending, the patient became nervous and aggressive. His gambling intensified to such an extent that he began to steal from his sister. She discovered the thefts and tried to hide money. But 3 weeks after the last visit to his psychiatrist, the patient physically assaulted his sister to obtain money. Informed of this pathological behavior, we asked for a clinical examination of the patient 1 week before the next planned visit. He presented anxiety without exacerbation of his schizophrenic symptoms. He also had a craving to gamble that decreased his anxiety briefly. PG was diagnosed, and as the disorder had started with the introduction of aripiprazole, we decided to discontinue this drug and to increase prazepam to 80 mg/day. One week later, a second clinical examination showed that PG and anxiety had entirely disappeared after the discontinuation of aripiprazole. The dose of prazepam was decreased to 60 mg/day, and depot haloperidol was continued. After 3 weeks, the patient's symptoms returned to the same level as before the introduction of aripiprazole. No further pathological behavior was reported.

Case 2

A young 19-year-old man with schizophrenia developed PG while treated with aripiprazole and committed theft. He had first sought psychiatric advice at the age of 17. He presented a severe persecutory delusional syndrome associated with auditory hallucinations and mental automatism. Two days after the onset of symptoms, he stabbed his father, who he was convinced would kill the entire family. Fortunately, he caused only minor physical injury. Transferred to a psychiatric high-security hospital, he was found not criminally responsible because of insanity. Amisulpride (800 mg/day) and diazepam (30 mg/day) were the two medications initially given.

Six weeks later, the treatment had resulted in such improvement of the patient's psychotic symptoms that amisulpride was progressively decreased to 400 mg/day, and diazepam was discontinued. He was transferred to our conventional inpatient care unit. A first clinical examination found no delusional or hallucinatory symptoms, but he presented negative symptoms such as affective flattening, avolition, and attentional impairment. Upon further review, the patient's parents reported that these deficit symptoms had begun 6 months earlier and were associated with an increasing and severe level of cannabis abuse. He began to avoid social contact, discontinued recreational activities and dropped out of school. Family psychiatric history revealed paranoid schizophrenia (three psychotic episodes) in a sister, in full remission with risperidone treatment. One month after his transfer from the high-security hospital, the patient was discharged and returned home. He was referred to our outpatient clinic and started a job in a transitional employment program. One month after discharge, as the negative symptoms did not sufficiently decrease, we introduced aripiprazole (10 mg/day) as adjuvant therapy. A few weeks later, he began to bet very small amounts of money on soccer games and to buy lottery scratch cards with his friends in a recreational way. Five months later, he bet 2 euros on a soccer game and won 50 euros (*c.* 68 U.S. dollars). At this point, he became a high-frequency gambler. He believed he could earn a living in this way and constantly asked his parents for large sums of money. We were not aware of this behavior. During the visits with the medical staff, the patient and his parents did not spontaneously report such symptoms. Seven weeks after his "big win," the patient committed a theft. He physically assaulted a woman in the street to steal her mobile phone. A few minutes later, the police arrested him trying to sell the mobile phone in a betting shop.

Because of the patient's history, the judge appointed a psychiatric court expert to assess his legal responsibility. The sentence was deferred. The patient was placed on conditional liberty during this period and immediately attended the outpatient clinic with his parents. He appeared unconcerned about the theft and its effect on the victim, merely arguing that he was in need of money. We decided to change his treatment completely. Amisulpride and aripiprazole were discontinued, and risperidone was initiated (4 mg/day). Three weeks later, PG had ceased and the patient started to show concern about his aggressive behavior. The court expert allowed partial criminal responsibility on account of his schizophrenia, making no reference to PG and the link with criminal behavior. The patient was sentenced only to a 6-month suspended prison sentence. Four months later, he continued his transitional employment program and showed no further symptoms of PG.

Discussion and Conclusion

Research has shown the existence of a causal relationship between criminal behavior and PG (9). A high percentage of subjects commit offenses to finance their gambling. Addictive gambling directly influences the intensity of criminal behavior. It seems to be the most important criminogenic factor, more influential than antisocial personality (9). To our knowledge, this is the first time that PG has been described secondary to dopamine partial agonist therapy in patients with schizophrenia and has led to criminal behavior.

PG has already been reported as a complication of dopamine agonists in patients with Parkinson's disease (9). The central role of dopaminergic drug therapy strengthens the hypothesis that PG is caused by altered function of the dopaminergic reward system (8,10). Decreased dopamine cerebrospinal fluid concentration and increase in its metabolites, 3,4-dihydroxyphenylacetic acid and homovanillic acid, have been found in patients with PG compared with normal controls (11). This finding is thought to be related to increased dopamine turnover and release in the brain of pathological gamblers (11). It has been speculated that stimulation of mesolimbic dopamine receptors may result in gambling behavior in patients with Parkinson's disease who receive dopaminergic treatment. In the genetic field, research has shown that variants of the *DRD2* gene, coding for D2 receptors, have also been associated with gambling (12). It is hypothesized that *DRD2* is a reinforcement or reward gene (10). Moreover, the role of the dopamine D3 receptor has also been argued. In Parkinson's disease, dopamine agonists, especially pramipexole, are the largest independent risk factor for developing PG (6). The relative selectivity of dopamine agonists for the D3 dopamine receptor has been postulated as a mechanism for their association with impulse control disorder (13). Thus, PG may be an adverse event relating to more continuous dopamine D3 receptor stimulation, this receptor being found in the mesolimbic pathways implicated in motivation, emotion, and reward behaviors.

In both the cases we present, PG did not occur with dopamine agonists but with the new antipsychotic, aripiprazole, that has partial agonist properties on D2-D3 dopamine receptors. Almost all antipsychotic agents, such as haloperidol and amisulpride, are D2 dopamine receptor antagonists. On the other hand, dopamine partial agonists are a new class of antipsychotic agents that offer an attractive option for the treatment of schizophrenia (14). They may act as a functional antagonist in the mesolimbic dopamine pathway, where excessive dopamine activity is thought to cause positive symptoms, but they show functional agonist activity in the

mesocortical pathway, where reduced dopamine activity is thought to be associated with negative symptoms and cognitive impairment. In clinical trials, aripiprazole-treated patients showed significantly greater improvements in negative symptoms (15). This result led us to start aripiprazole for our two patients to improve their negative symptoms. They both were given a stable regimen of dopamine antagonist (for 5 years in case one and for three and a half months in case two), leading to a hypodopaminergic state. Thus, aripiprazole, despite its partial agonist activity, may have disrupted dopaminergic tonus by stimulating dopamine receptors in this particular context, thus causing PG.

Both cases present strong arguments in favor of an adverse drug reaction, which can be assessed through seven criteria: (i) time to onset, (ii) dechallenge, (iii) rechallenge, (iv) search for non-drug-related causes, (v) risk factors for drug reaction, (vi) reaction at site of application or relevant and reliable laboratory test strongly in favor of the drug's responsibility, and (vii) previous reports of similar drug–event associations (15). In our first case, PG started very early, a few days after initiation of aripiprazole, whereas in the second case, the onset was 5 months later. This discrepancy is in line with clinical observations in Parkinson's disease. Gallagher et al. (6) reported that the latency of onset of PG after dopamine agonist initiation ranges from <1 to 84 months. Furthermore, in both our cases, PG rapidly resolved once dopamine partial agonist was discontinued. This close time relationship suggests a causal association. Neurological examination, laboratory tests, and brain imaging did not reveal any other cause. It should also be noted that both premorbid gambling (case one) and a history of drug use (nicotine for case one and cannabis for case two) are considered to be associated with high-risk individuals (3,6), whereas schizophrenia is not. On the other hand, we did not reintroduce aripiprazole on account of ethical considerations, and there is no laboratory test to diagnose PG. This is also the first report to present PG as a possible adverse event of dopamine partial agonist therapy. These considerations do not detract from the possibility that aripiprazole was the cause of PG.

On the other hand, a serotoninergic dysfunction seems to be involved in PG, even if the mechanisms are not yet fully elucidated. Indeed, according to Pallantini et al. (16), the acute administration of m-CPP, a nonselective serotonin 5-HT receptor agonist, induced an incremental behavioral and neurobiological response in pathological gamblers compared to controls. Now, aripiprazole appears to be a high-affinity partial agonist at the 5-HT_{1a} receptor, a high-affinity antagonist at the $5\text{-HT}_{2a/2b}$ receptors, a moderate-affinity weak partial agonist at the 5-HT_{2c} receptor, and a high-affinity weak partial agonist at the 5-HT_{7} receptor (17). Further studies are necessary to determine the way in which the serotoninergic function could be involved.

As argued by Drapier et al. (18), the remarkable point in this kind of observation is that drug treatment can be responsible for planned and structured behavioral disorders. PG is one of these disorders, and it may entail social or even legal repercussions that could be highly damaging to patients and their relatives. Research has confirmed the existence of a causal relationship between criminal behavior and PG (9). In both cases we report, physical offenses were the direct consequence of PG.

French law provides for three possibilities in the case of people with mental illness who commit offenses: (i) total responsibility as the defendant's symptoms did not affect his/her discernment and control of behavior, (ii) partial responsibility as the defendant's symptoms partially affected discernment and control, and (iii) irresponsibility as the defendant's symptoms wholly affected discernment and control. In the case of the first patient, his sister did not take legal action, but the second patient was sentenced for theft. As he was known to suffer from schizophrenia, the attorney appointed a psychiatric court expert before the trial to assess his responsibility. The expert concluded on partial responsibility related to the negative symptoms of his schizophrenia that could sometimes lead to impulsive acts of aggression toward others. The role of PG was not considered. Blaszczynski and Silove (2), considering the role of PG, observed that the judicial system is being increasingly confronted with the argument of diminished responsibility for gambling-related offenses. They concluded that a diagnosis of PG does not diminish legal responsibility but is a factor that should be considered in sentencing. The PG of our second patient occurred in association with schizophrenia and secondary to a drug treatment. We believe, in this particular case, that legal irresponsibility should have been discussed in light of the close time relationship between aripiprazole, PG, and criminal behavior.

To our knowledge, this is the first time that PG, a planned and structured behavior disturbance, has been described as occurring secondary to dopamine partial agonist therapy in patients with schizophrenia. Elsewhere, addictive gambling behavior has been shown to have a direct influence on the intensity of criminal behavior. This is in line with both our clinical observations in which patients committed physical offenses. Considering the putative link between aripiprazole and PG in these two clinical observations, criminal irresponsibility should have been argued.

References

1. American Psychiatric Association. Diagnostic and Statistical Manual of Mental Disorder, 4th edn. Washington, DC: American Psychiatric Association, 1995.
2. Blaszczynski A, Silove D. Pathological gambling: forensic issues. Aust N Z J Psychiatry 1996;30:358–69.
3. Petry NM, Stinson FS, Grant BF. Comorbidity of DSM-IV pathological gambling and other psychiatric disorders: results from the National Epidemiologic Survey on Alcohol and Related Conditions. J Clin Psychiatry 2005;66:564–74.
4. Shaffer HJ, Hall MN. Updating and refining prevalence estimates of disordered gambling behaviour in the United States and Canada. Can J Public Health 2001;92:168–72.
5. Grosset KA, Macphee G, Pal G, Stewart D, Watt A, Davie J, et al. Problematic gambling on dopamine agonists: not such a rarity. Mov Disord 2006;21:2206–8.
6. Gallagher DA, O'Sullivan SS, Evans AH, Lees AJ, Schrag A. Pathological gambling in Parkinson's disease: risk factors and differences from dopamine dysregulation. An analysis of published case series. Mov Disord 2007;22:1757–63.
7. Tippmann-Peikert M, Park JG, Boeve BF, Shepard JW, Silber MH. Pathologic gambling in patients with restless legs syndrome treated with dopaminergic agonists. Neurology 2007;68:301–3.
8. Chau DT, Roth RM, Green AI. The neural circuitry of reward and its relevance to psychiatric disorders. Curr Psychiatry Rep 2004;6: 391–9.
9. Meyer G, Stadler MA. Criminal behavior associated with pathological gambling. J Gambl Stud 1999;15:29–43.
10. Noble EP. The DRD2 gene in psychiatric and neurological disorders and its phenotypes. Pharmacogenomics 2000;1:309–33.
11. Bergh C, Eklund T, Sodersten P, Nordin C. Altered dopamine function in pathological gambling. Psychol Med 1997;27:473–5.
12. Comings DE, Rosenthal RJ, Lesieur HR, Rugle LJ, Muhleman D, Chiu C, et al. A study of the dopamine D2 receptor gene in pathological gambling. Pharmacogenetics 1996;6:223–34.
13. Dodd ML, Klos KJ, Bower JH, Geda YE, Josephs KA, Ahlskog JE. Pathological gambling caused by drugs used to treat Parkinson disease. Arch Neurol 2005;62:1377–81.
14. Lieberman JA. Dopamine partial agonists: a new class of antipsychotic. CNS Drugs 2004;18:251–67.
15. Arimone Y, Begaud B, Miremont-Salame G, Fourrier-Reglat A, Molimard M, Moore N, et al. A new method for assessing drug causation provided agreement with experts' judgment. J Clin Epidemiol 2006;59:308–14.

16. Pallantini S, Bernardi S, Quercioli M, DeCaria C, Hollander E. Serotonin dysfunction in pathological gamblers: increased prolactin response to oral m-CPP versus placebo. CNS Spectr 2006;11:956–64.
17. Kessler RM. Aripiprazole: what is the role of dopamine D2 receptor partial agonism? Am J Psychiatry 2007;164:1310–2.
18. Drapier D, Drapier S, Sauleau P, Derkinderen P, Damier P, Allain H, et al. Pathological gambling secondary to dopaminergic therapy in Parkinson's disease. Psychiatry Res 2006;144:241–4.

Additional information and reprint requests:
Anne-Laure Pélissier-Alicot, M.D., Ph.D.
Service de Médecine Légale, Faculté de Médecine
Université de la Méditerranée
13385 Marseille Cedex 5
France
E-mail: apelissier@ap-hm.fr

JOURNAL OF FORENSIC SCIENCES

J Forensic Sci, November 2010, Vol. 55, No. 6
doi: 10.1111/j.1556-4029.2010.01497.x
Available online at: onlinelibrary.wiley.com

Letter to the Editor—A Rejection of "Working Blind" as a Cure for Contextual Bias

Sir,

It seems that everywhere we now turn, we are reminded (or chided) of the fearsome dangers of contextual bias. Nearly everyone concedes that it is a potential danger, but the remedies are not so clear. Some advocate that the forensic worker be denied any information concerning the case apart from that which is absolutely necessary to conduct the indicated analysis or examination. Others have suggested that there be a sequential unmasking of the case following an initial workup, in order that the laboratory will have an opportunity to determine whether the tests that have been run have been appropriate. Others maintain that the dangers of contextual bias are overblown, and that it is adequately addressed by, or at least minimized by, the technical reviews required by accreditation programs.

Whatever the best mechanism is for quelling contextual bias, it would not seem to reside in depriving the forensic worker of full information concerning a case, the "working blind" approach. Yes, that would insulate the worker from knowing, for example, that the suspect has confessed, or being informed of other information that would not form a legitimate aspect of the forensic scientist's technical review. But this tactic presents another danger. The evidence may be submitted by an investigator, or at the behest of an attorney, neither of whom may be poised to determine precisely which tests should be run. One may have a degree in history, the other may have a few hours of physical evidence instruction, and either or both may be guessing as to what needs to be done. The evidence is nevertheless submitted, accompanied by a request to run Tests A, B, and C.

If the case is fully revealed, the laboratory may realize that Test C is silly. A rational person, and certainly a rational scientist, doesn't stand back and say, "Look what I just did, wasn't that silly? And I knew it was silly when I did it. But I did it because a lawyer asked me to!" In addition to realizing that Test C would be worthless, the laboratory may realize that what the evidence really needs, in addition to Tests A and B, are Tests D and E. The time to realize that Tests D and E are needed is at the outset, not on the eve of trial, or worse, upon cross-examination.

Furthermore, it is a fallacy to believe that if contextual bias is dealt with, in whatever fashion, the slate is wiped clean of bias and that all professional obligations have been satisfied. What about the following?

> Outcome bias, In-group bias, blind spot bias, negativity bias, selection bias, authority bias, omission bias, self-serving bias, publication bias, language bias, outcome variable selection bias, within-study reporting bias, coding bias, citation bias, gray literature bias, sampling frame bias, bogus control bias, contamination bias, compliance bias, case definition bias, previous opinion bias, one-sided reference bias, and on and on.

It is much more important to recognize them than to know the most appropriate name for them.

I reject the insinuation that we do not have the wit or the intellectual capacity to deal with bias, of whatever sort. If we are unable to acknowledge and compensate for bias, we have no business in our profession to begin with, and certainly no legitimate plea to the indulgence of the legal system. We can deal with bias, but we must work at it. Not just because the National Academy of Science is telling us that we must work at it, but because it is, and always has been, our professional responsibility. Arguably it is an ethical responsibility as well. Working at it is much to be preferred than being blinded and hobbled. And working at it does not mean burying our heads in the sand, being exposed to just a whiff of the entire case because of the trepidation of being accused of bias. As a mature profession of competent and responsible scientists, we should always countenance the possibility of bias, vanquish it when necessary, and report out our work with courage and authority.

John I. Thornton, D. Crim.,
1093 Lokoya Road,
Napa, CA 94558
E-mail: wildthorn@starband.net

JOURNAL OF FORENSIC SCIENCES

J Forensic Sci, November 2010, Vol. 55, No. 6
doi: 10.1111/j.1556-4029.2010.01495.x
Available online at: onlinelibrary.wiley.com

Commentary on: Hlastala MP. Paradigm shift for the alcohol breath test. J Forensic Sci 2010;55(2):451–6.

Sir,

The toxicology paper by Michael P. Hlastala, March, 2010, Vol 55, page 451–456, had the eye-opening title "Paradigm Shift for the Alcohol Breath Test." I searched the article for ground-breaking experimental evidence by his hand relating to the title but found none. Hlastala asserts in several places that it is erroneous to consider the air in which the ethanol is measured as representative of alveolar air, which in turn is directly equilibrating with arterial blood. So, if the ethanol source measured in breathalyzers is not ultimately the circulating blood, what is the source? Reading the paper, in one place you get the idea that the ethanol comes from the trachea and airways leading to the lungs; elsewhere in the paper, the correlation of breath air ethanol and arterial blood is acknowledged.

Hlastala's argument is like saying that the head space sampling GC used in laboratories to determine blood ethanol measures ethanol in the GC column and not in blood. There is no question that some of the ethanol coming from the lungs partitions in the airway linings. One sure evidence that the expired gas (air) is from arterial blood is the constant percent of carbon dioxide in exhaled air. Hlastala points out many things we already know, such as ethanol being water soluble, and that the partition of ethanol in air/water is temperature dependent. Hlastala states (p. 454), "Lindberg et al. (52) have shown a strong correlation between BrAC and arterial alcohol concentration," contradicting other statements in the article.

Hlastala's key evidence is Fig. 4, data calculated using a mathematical model of the human airway structure by another author whose name is not in Hlastala's current paper. The correlation of blood ethanol and a properly obtained breath sample goes back at least 50 years (as the author admits). At the last AAFS meeting this February in Seattle, a paper authored by M. R. Corbett confirmed the blood/breath ratio as an average value 2286:1 after absorption. The ratio of 2100:1 is used in standard breath testing, thereby always favoring the defendants. The ratio has been confirmed by R. Moore in J. Analytical Tox., 15, 346(1991), and many times before this.

The purpose of the breath test is not to determine blood ethanol content (BAC) accurate to the thousandth place, but to make the roads and highways safer. In achieving this end, *per se* laws have been established BAC concentrations, which presume significant impairment above either 0.08% or 0.10%, depending on the state. In most if not all USA jurisdictions, breathalyzer results are truncated to two digits and then take the lowest of duplicate results (when performed in duplicate). Consider also that the 2100:1 ratio nearly always underestimates the true BAC at the time of breath testing. The fact that there may be large percentage errors below 0.04% is of no consequence. By truncating the breath test result, some defendants get more allowance than others; however, this is a separate issue. Hlastala was concerned that smaller persons would have to provide a bigger fraction of their breath than big people and thus be treated unfairly. By that argument, everyone would need to have his/her BAC adjusted to their particular blood/body ethanol distribution ratio.

I do not believe the Hlastala paper should have been published as a regular experimental paper, but perhaps as an opinion paper. All experiments and data were from other papers, and the key information was constructed mathematically from a model of the airway. No toxicologist in recent years has advocated a change in the standard ratio, because the ratio used today, 2100:1, matches up with reality.

Theodore J. Siek,[1] Ph.D.
[1]Forensic Toxicologist, ABFT, 315 Beaver Road
Southampton, PA 18966
E-mail: Theodore.Siek@verizon.net

JOURNAL OF FORENSIC SCIENCES

J Forensic Sci, November 2010, Vol. 55, No. 6
doi: 10.1111/j.1556-4029.2010.01496.x
Available online at: onlinelibrary.wiley.com

Author's Response

Sir,

I appreciate the comments by Dr. Siek. In responding to the letter, it is clear that some further explanation is needed regarding the circulations of the lungs. Human lungs have two circulations. The pulmonary circulation brings poorly oxygenated and hypercapnic blood to the alveoli of the lungs. This systemic venous blood originates in the tissues and passes through the right heart on the way to perfusing the alveoli. In the alveoli, blood picks up oxygen from and delivers carbon dioxide to the alveolar air. The systemic arterial circulation originates from the left side of the heart. A small fraction of the systemic blood flow (about 1%) perfuses the airway tissue via the bronchial circulation with blood that is oxygenated and nutrient rich. While oxygen and carbon dioxide exchange with the pulmonary circulation, highly soluble gases like ethanol exchanges within the airways with the bronchial (systemic arterial) circulation. The alcohol measured in the breath test comes from the airway mucosa and originates from the bronchial circulation. Breath alcohol concentration more closely correlates with systemic arterial concentration during both the absorption and elimination phases.

Dr. Siek indicates that "one sure evidence that the expired gas (air) from arterial blood is the constant percent of carbon dioxide in exhaled air." Carbon dioxide has a much lower solubility in blood than alcohol. Carbon dioxide comes from venous blood and exchanges in the alveolar portions of the lungs. Alcohol, having a much greater solubility, exchanges in the airways with the systemic arterial blood. For more information, please see reference 43. The exchange of alcohol is analogous to that of water vapor, which completely exchanges with and fully saturates inhaled air before it reaches the alveoli. Exhaled carbon dioxide concentration depends on a balance between carbon dioxide production and alveolar ventilation.

Dr. Siek is concerned that the data in Fig. 4 come from another author. Dr. Hlastala is a coauthor of the paper cited (ref. 30). The first author on that paper, Ms. Tsu, did not participate in the writing of the current study.

Dr. Siek mentions that "Hlastra (sic) was concerned that smaller persons would have to provide a bigger fraction of their breath than big people and thus be treated unfairly." People with smaller lung volumes are treated unfairly by the present breath test because they have greater breath alcohol concentrations for the same blood alcohol concentration (see ref. 16). This alone is sufficient justification for modification of the breath test because it is not fair for everyone.

Dr. Siek is concerned that "no toxicologist in recent years has advocated a change in the standard ratio, because the ratio used today, 2100/1, matches up with reality." The whole point of our study is that an alcohol partition ratio for alcohol does not exist in the human lungs. "Partition" requires equilibrium, which never occurs in lungs for alcohol. The exchange of alcohol occurs in the airways during both inspiration and expiration. No steady state exists, and therefore, the term partition ratio does not apply to breath testing. Alcohol comes primarily from the airway mucosal surfaces and not the alveoli. The assumption of the alcohol breath test is that alcohol comes from the alveolus and that the concentration of alcohol in end-exhaled air is equal to the alcohol concentration in the alveolar air, which is in equilibrium with the venous blood. My study shows that this assumption is not true and that the alcohol breath test is not based on sound science. Furthermore, the use of *per se* alcohol breath measurements does not account for the known scientific error that is inherent in breath alcohol testing (or any other scientific measurement). Certainly, the scientific community would not accept data for publication without statistical analysis and a range of error for the reported results. This requirement should also apply to court proceedings.

To date, there has been no experimental evidence published to support the hypothesis that alcohol comes from the alveolus. Alveolar exchange of ethyl alcohol is an assumption that has never been validated.

Michael P. Hlastala,[1] Ph.D.
[1]Department of Medicine, Division of Pulmonary and Critical Care Medicine, University of Washington School of Medicine, Seattle, WA 98195-6522.
E-mail: hlastala@u.washington.edu

JOURNAL OF FORENSIC SCIENCES

J Forensic Sci, November 2010, Vol. 55, No. 6
doi: 10.1111/j.1556-4029.2010.01517.x
Available online at: onlinelibrary.wiley.com

Commentary on: Heaton V, Lagden A, Moffatt C, Simmons T. Predicting the Postmortem Submersion Interval for Human Remains Recovered from U.K. Waterways. J Forensic Sci 2010; 55(2):302–7.

Sir,

The authors address an interesting problem in daily forensic practice, the estimation of the postmortem submersion interval for bodies recovered from waters. They found a correlation between degree of decomposition and accumulated degree days (ADD). From this correlation, the postmortem submersion interval can be inferred by summing the average daily temperatures from the date the body was recovered retrospectively until the estimated ADD is reached (1). However, because of the wide range of ambient temperatures, only very rough estimations are possible. As far as the authors state that only few investigations have been carried out on aquatic decomposition and that there is a growing need for more systematic studies, they are obviously not aware of the investigations carried out by the German forensic pathologist Reh more than 40 years ago (2–4). This may be because of the fact that these investigations were published in German. They are widely accepted and part of the German textbooks (5–8). In 1967 and 1969, Reh published a table for the estimation of the time interval of immersion taking into account the actual water temperature and morphological findings of bodies immersed in water identified during the external or internal examination of the body. These investigations were originally carried out on 277 bodies, mainly recovered from the river Rhine, with a known postmortem interval, with the aim to answer the question if there is any correlation between time of immersion and water temperature on the one hand and signs of decomposition on the other hand. The bodies were mainly recovered from the Rhine and Rhine harbour in Düsseldorf (70%) and a smaller part (30%) from other stagnant or running waters, lakes, and pools. The water temperatures at the place and at the time of recovery were taken 0.5–1 m below the surface. Altogether 16 signs of decomposition were taken into consideration in each case (Table 1, left column). Reh found a high correlation between the progression of putrefaction and water temperature (Fig. 1). The higher the water temperature, the sooner a definite stage of decomposition is achieved, for example, in July the Rhine has a water temperature of about 18°C. It takes a minimal time of about 2–3 days for the development of gas emphysema, liquefaction of brain, or loosening of toe nails. In December, the water temperature of the Rhine is about 4°C and it takes about 28 days until the same signs of decomposition have developed.

From the average water temperature for each month and the stages of decomposition, Reh developed a table with a minimum time interval of immersion (Table 1). In the left column, the signs of decomposition (no. 1–16) and in the heading line the months are shown. Every month correlates with an average monthly water temperature (shown in the row below). As many criteria as possible should be used for estimating the minimum time interval since immersion. With more than only one or two criteria, the result gets more reliable. Every sign of putrefaction is correlated to the minimum time in which this sign can be developed. For estimating the minimum time interval of immersion, the average water

TABLE 1—*Reh's table to estimate the minimum time interval of immersion.*

	Month	Jan.	Feb.	Mar.	April	May	June	July	Aug.	Sept.	Oct.	Nov.	Dec.
Ø	Median water temperature (°C)	3.5	3.9	5.8	9.9	13.0	17.4	18.6	18.6	17.3	13.2	8.8	4.7
1.	Marbling	32	25	16 (23)	9–10	4–5	2	1–2	2	3	4–5	10	17
2.	Distension of tissues by gas	35	25	16 (23)	10	4–5	2–3	2	3	3–4	7	10	17
3.	Discoloration of the body	35	25	16 (23)	(14)	4–5	2	2	3	3–4	7	10	17
4.	Peeling of the epidermis	35	25	16 (23)	(16)	4–5	3	2	3	3–4	7	10	17
5.	Hair lost	35	25	16 (23)	10–12	4–5	2–3	2–3	3	3–4	7	10	17
6.	Hands: beginning of wrinkling	(1)	(1) 28–30	(12 h)			(6 h)			2 h		2 h	(1)
7.	Nails become loose	Over 35	(40) 30–32	23	16	5	2–3	3	3	3–4	11	17	28
8.	Peeling of skin in glove form	35	(45)	23	16	10	3	3	3–4	4	7	20	28
9.	Nails lost	Over 53	45	30 (40)	21	14	8	3	4	10	Over 11	20	Over 35
10.	Feet: beginning of wrinkling	(1)	(1)	(12 h)	(1)		(6 h)	0.5 h		2 h		2 h	(1)
11.	Nails become loose	Over 53	40	26 (35)	17	10	5	3	4	8	12	17	28
12.	Peeling of skin	Over 53	60	35	16	10	5	3	5–6	8–9	Over 11 (14)	20	28
13.	Nails lost	Over 53	Over 60	53	Over 35	Over 28	Over 10	3	Over 10	Over 10	Over 11	Over 20	Over 35
14.	Transudate in pleural cavity*	35	25 (40)	18 (35)	10	5	3–4	3	3	11	5	Over 20	
15.	Heart without blood	Over 39	32–34 (40)	23	14–15	9	4	3	3	5	11	20	28
16.	Brain liquefied	35	30 (40)	(23)	14–16	5	3–4	3	3	6	10	17	28

Left column: signs of putrefaction. First line: month. Second line: mean water temperature of the month according to measurements of Reh. Following lines: minimum time of immersion for the corresponding water temperature. Minimum time of immersion in days. Values given in parentheses, maximum time.
*>500 mL in adults.

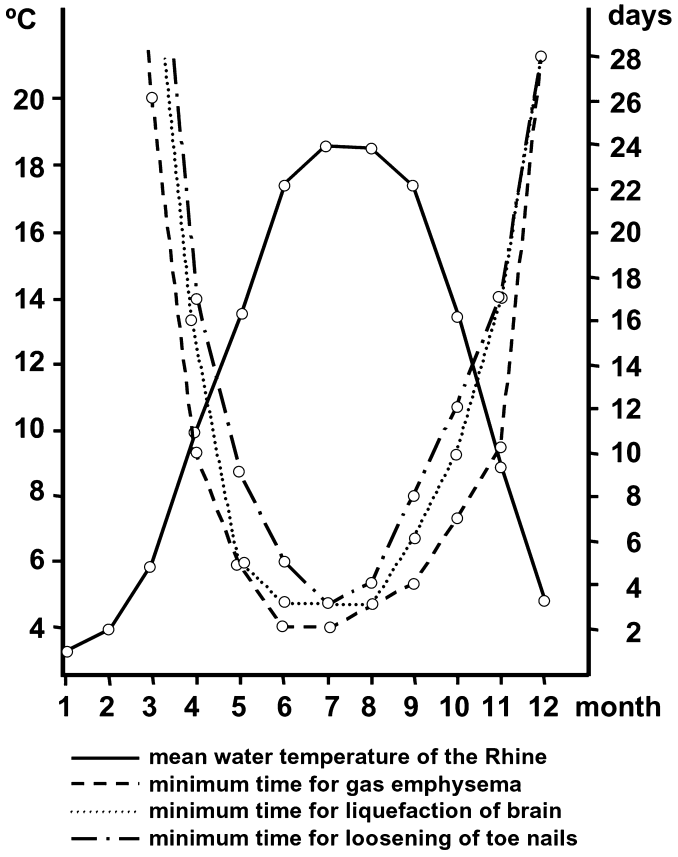

FIG. 1—*The dependence of putrefaction on water temperature and time of immersion.* X-axis: month from January to December. Left Y-axis: temperature in °C. Right Y-axis: time of immersion in days. The higher the water temperature the sooner definite stages of putrefaction develop.

temperature which is nearest to the actual water temperature at the time of recovery is considered and not the water temperature of the actual month. Reh proposes to use the water temperature of the day of recovery for the estimation. With the help of this chart, not only the minimum time interval of immersion can be estimated but also the maximum interval by considering those criteria which have not yet developed on the body.

Quite good experiences with Reh's table have been reported (9). The chart is obviously much better than the formerly used rules of thumb and takes the actual water temperature for the estimation of the time since death into consideration quantitatively. However, a recent re-evaluation of this chart revealed some shortcomings (10). The water temperatures of the river Rhine have increased during the last 40 years. For higher water temperatures (over 20°C), Reh's table is unreliable and further investigations are necessary, especially for higher water temperatures on the correlation between temperature and progression of putrefaction. For lower temperatures, the chart can be used even today. However, the actual measured water temperature of the day of recovery should be used for estimating the time of immersion. If a longer time of immersion is assumed or considerable fluctuation of water temperature has to be taken into account, the average temperature for the missing time should be used. Because of the monthly fluctuation of the water temperature, it is not advisable to estimate the time of immersion on the basis of the month of recovery without regarding the daily water temperature. The outlook of Heaton et al. that it may be feasible to construct a decomposition time table that allows investigators to estimate a more accurate postmortem submersion interval for bodies has thus already been fulfilled 40 years ago. However, as a result of its publication just in German, obviously no notice of this decomposition time table was taken. With proper and cautious application, it is a great help in routine casework.

References

1. Heaton V, Lagden A, Moffatt C, Simmons T. Predicting the postmortem submersion interval for human remains recovered from U.K. waterways. J Forensic Sci 2010;55(2):302–7.
2. Reh H. *Diagnostik des ertrinkungstodes und bestimmung der wasserzeit*. Düsseldorf: Triltsch, 1969.
3. Reh H. Anhaltspunkte für die estimmung der wasserzeit. Dtsch Z Gesamte Gerichtl Med 1967;59:235–45.
4. Reh H, Haarhoff K, Vogt CD. Die chätzung der todeszeit bei asserleichen. Z Rechtsmed 1977;79:261–6.
5. Mueller B. *Gerichtliche medizin*. Berlin, Heidelberg, New York: Springer, 1975.
6. Forster B. *Praxis der rechtsmedizin*. Stuttgart, New York: Thieme Verlag, 1986.
7. Brinkmann B, Madea B. *Handbuch gerichtliche medizin band I*. Berlin, Heidelberg, New York: Springer, 2004.
8. Madea B. *Praxis rechtsmedizin*. Berlin, Heidelberg, New York: Springer; 2. Auflage, 2007.
9. Madea B. Estimation of duration of immersion. Nordisk Rettsmedisin 2002;8:4–10.
10. Doberentz E, Madea B. Estimating the time of immersion of the bodies found in water—an evaluation of a common method to estimate the minimum time interval of immersion. Rev Esp Med Legal 2010;36(2):40–50.

Burkhard Madea, M.D.[1] and Elke Doberentz, M.D.[2]
[1]Professor of Forensic Medicine and Chairman, Institute of Forensic Medicine, University of Bonn, Stiftsplatz 12, 53111 Bonn, Germany
[2]Research Assistant, Institute of Forensic Medicine, University of Bonn, Stiftsplatz 12, 53111 Bonn, Germany
E-mail: b.madea@uni-bonn.de

JOURNAL OF FORENSIC SCIENCES

J Forensic Sci, November 2010, Vol. 55, No. 6
doi: 10.1111/j.1556-4029.2010.01518.x
Available online at: onlinelibrary.wiley.com

Authors' Response

Sir,

My co-authors and I graciously thank Madea and Doberentz for their contribution to the discussion of aqueous decomposition. We are particularly grateful to them for drawing to our attention the previously published work of Reh and others, of which we were indeed unaware because of its publication in the 1960s and 1970s in the German language. Although I (TS) read quite a few languages, alas, German is not among them. We therefore read with interest this commentary and the accompanying table derived from Reh's original research.

Madea and Doberentz contend that, based on Reh's work, the task of estimating "a more accurate postmortem submersion interval for bodies has thus already been fulfilled 40 years ago." Perhaps it might be more accurate to say that it was partially fulfilled 40 years ago for local conditions of submersion of short duration with regard to accumulated degree days (ADD) and decomposition stage. Although we agree that Reh's table would doubtless be helpful to pathologists in Germany, its main shortcoming in an anthropological perspective is that it only describes very early decomposition stages involving soft tissue changes alone, and never progresses beyond an accumulation of degree days that is quite small in magnitude. Our study integrated decomposition stages through to skeletalization and body part loss into a standardized scoring system. The maximum calculable ADD from the table provided by Madea and Doberentz is ca. 365; this occurs in the month of May, where "nails lost" occurred at "over 28 days." Since unfortunately we cannot calculate how much over 28 days this may have been, 28 days multiplied by the average water temperature of 13.0°C equals only 364 ADD. In contrast, the formulae in our study incorporated data from bodies submerged up to 2051 ADD. Furthermore, as Madea and Doberentz allude themselves, the figure of 354 ADD would only be accurate if the body was in the water solely during the month of May and not for part of April when the water was colder (9.9°C) or part of June when the water was warmer (17.4°C).

The clarity of Reh's table reproduced here is somewhat vague concerning the number of cases represented by each observation, the range of ADD when these features appeared and which features appeared congruently; I do regret being unable to read the original publication thoroughly, as no doubt the original text fills in these gaps. It would also be good to know, statistically speaking, how accurately this research has proved with new casework, and it might be very interesting indeed if Reh's original observations could be scored on the new total aquatic decomposition score (TADS) scale we presented with proper ADD's calculated from the water temperature data. We would be interested in seeing these data compared to our own and testing the predictive accuracy of our equation on the German cases.

Our research group is currently undertaking new work testing the application of our equation to: (i) calculating postmortem submersion interval (PMSI) for submersed bodies in other countries, where water temperature ranges are similar to those of the U.K.; and (ii) calculating PMSI for bodies recovered in warmer waters in the Gulf of Mexico. We hope to continue this discourse upon its completion.

Tal Simmons,[1] Ph.D.; Colin Moffatt,[1] Ph.D.;
Vivienne Heaton,[1] M.Sc.; and Abigail Lagden,[2] M.Sc.
[1]University of Central Lancashire, School of Forensic and Investigative Science, Preston PR1 2HE, UK.
[2]National Policing Improvement Agency, Crook, County Durham, UK.
E-mail: tlisimmons@uclan.ac.uk

JOURNAL OF FORENSIC SCIENCES

J Forensic Sci, November 2010, Vol. 55, No. 6
doi: 10.1111/j.1556-4029.2010.01494.x
Available online at: onlinelibrary.wiley.com

BOOK REVIEW

Peter M. Marone,[1] *M.S.*

Review of: *Implementing Quality in Laboratory Policies and Processes*

REFERENCE: Christian DR. Jr., Drilling S. Implementing quality in laboratory policies and processes using templates, project management, and six sigma. Boca Raton, FL: CRC Press, 2010, 1416 pp.

The primary audience of this text, as indicated by the authors, is the newly appointed Quality Assurance Manager. It is hoped that these folks will not be intimidated by the sheer size of the text—2.5 kg and all of 1416 pages—because, in truth, the majority of the work is a compilation of appendices that include definitions, forms, worksheets, and templates. All of these are very comprehensive and bring together a significant amount of information in a single source. As such, they are of tremendous value as a starting point for what lies ahead. The authors have provided good descriptions of the duties of the quality manager and the importance of this position not only to the overall success of the project, i.e., developing a Quality System but also to implementing and maintaining the system on a long-term basis. On the other hand, outdated language from the ASCLD/LAB "Legacy" program is used throughout the text rather than the terminology used in connection with ISO-compliant accreditation programs. This could be a source of confusion to some readers.

Chapter 3 explains project management, not in its broadest sense, but rather as what is needed to develop a systematic approach to the design of the QA methods, manuals, and procedures. This section explains planning, setting milestones, and, most importantly, setting realistic expectations. While the information regarding Six Sigma is useful and has value, its placement immediately following the project management chapter may be confusing. While Six Sigma is a powerful tool that can be used to improve process and quality, its application is usually for repetitive processes and uses a different set of nomenclature. The flow of the information to the reader would be served by relocating this information elsewhere in the text.

Chapter 5 deals with Accreditation programs and is titled, "Outsourcing Quality Assurance Programs." To make the case that quality assurance can be outsourced; the authors utilize the ASCL/DLAB Legacy program wording and compare it with wording from ISO/IEC 17025. Unfortunately, while the Legacy program still is being maintained, no new laboratories can apply for accreditation under that program. Currently, only ISO/IEC 17025 is used for accrediting forensic laboratories. The logic used is a stretch at best. Additionally, Chapter 5 indicates that one of the independent third parties providing accreditation is the International Standards Organization. This organization does not perform any accrediting.

The next few chapters deal with the development of various types of manuals, very deftly providing valuable, generic direction on policy, operational, and technical methods manuals. These are all short, half-page summaries of the various topics included in the technical methods manuals. Some of the sections such as "Error Rates and Confidence Limits" could have benefitted by providing more detail in context. Use of the terms without clarification or explanation is unfortunate, as these are of special interest to the community.

Chapter 9 deals with the creation and use of criteria files. Again, the authors compare the ASCLD/LAB 2005 Legacy program (the current version is 2008) with ISO/IEC 17025 regarding the efficacy of a document prepared to facilitate the linking of applicable policies and procedures with specific criteria (in the legacy program and standards in 17025). Again, inclusion of an accreditation document such as the ASCLD/LAB Legacy program may be confusing to some readers and is unnecessary because that program is no longer available to new accreditation applications. Additionally, there is no mention of the supplemental requirements document, which is what makes the 17025 accreditation specific to forensic science laboratories.

Despite the shortcomings, this is a great resource for those intending to or even in the midst of preparing for accreditation. The numerous forms, tables, and templates, which include a useful example of a health and safety plan, serve as good starting points, and are enhanced by some good directions and explanations.

[1]Director, Virginia Department of Forensic Science, 700 North 5th Street, Richmond, VA 23219.

JOURNAL OF FORENSIC SCIENCES

J Forensic Sci, November 2010, Vol. 55, No. 6
doi: 10.1111/j.1556-4029.2010.01499.x
Available online at: onlinelibrary.wiley.com

BOOK REVIEW

Susan M. Ballou,[1] *M.S., D-ABC*

Review of: *Crime Scene Investigation: The Forensic Technician's Field Manual*

REFERENCE: Young T, Ortmeier PJ. Crime scene investigation: the forensic technician's field manual. Upper Saddle River, NJ: Prentice Hall, Pearson Education, Inc., 2010, 433 pp.

Right at the beginning, I was unsure about the contents of this book. The cover art deceives the reader, and my first impression was that I received the wrong book to review. A double helix on a book cover generally implies the book topic will address DNA not Crime Scene Investigation as is the title of this book. I understand that the latest mantra is to test everything for DNA but basic crime scene collection is so much more than that. I also understand the desire to deviate from the common cover art, such as crime scene tape or a chalk outline of a body, but a double helix should not have been an option.

Overall, I enjoyed the layout of the book. The chapters provided quite a bit of information that was reemphasized by questions and lab exercises. The crowning glory at the end of each chapter was a case study relevant to the chapter topic. The addition of the case study provided the reality check or the substantiation for paying attention to detail and following protocols as explained in the chapter. If the reader fails to understand the severity of not collecting trace evidence, conducting poor chain of custody, or using improper lighting techniques, the case study provides the shock factor that they will be memorialized as the person that messed up and why.

I also appreciated the number of photographs provided in each chapter. Individual interpretation of an instructional paragraph can differ but the addition of pictures clarifies the writer's intent. The old saying still holds true "pictures are worth a thousand words." My disappointment was the caption limitation provided under some of the photographs. Captions were general and reading the associated chapter text did not match to what the photograph was demonstrating. Additional caption descriptors would have made the layout much more enjoyable.

I was disappointed in the limited information provided on lens filters (page 32) under the photography chapter (chapter 2) as this type of information should be practiced right at the onset and its value not left for recognition after garnering years of experience. The revelation of blood stains or pattern evidence through the use of the appropriate filter requires an individual prone to detail and knowledgeable in medium's characteristics.

Chapter 7—Special Case Crime Scenes was a good touch. The information on internal affairs is overlooked in many books on crime scenes and this brings to light the unique scenarios the crime scene technician may be responsible for.

There were errors that alluded to the authors' unfamiliarity with some of the topics. This arises when writers do not actually conduct the work but rely on a literature education. Some examples were selected to give a view of my concerns.

- Chapter 4: On page 73, the generally accepted process for proper packaging is offered, yet this is contradicted on page 88 where the instructions for collecting seminal fluid on a swab is to dry it, package it, and freeze it. This is the first mention of freezing evidence, and the reason for the deviation from the page 73 process is not offered. Federal agencies as well as some State and Local laboratories have carried out research, showing freezing does not make a difference as long as the evidence is properly dried and stored in an area with controlled humidity.
- Chapter 7: Point of origin for fire, page 181, is identified as the area usually containing the heaviest fire damage. The word "usually" should have been highlighted, bolded, put in italics, or subjected to any alternate form to pop this word to the attention of the reader. Over the past 5 years, fire research has shown that the heaviest fire damage is not generally where the fire originated and other means of determining point of origin have to be taken into consideration.
- On page 186, the reason why oral swabs are collected from a victim is when oral copulation occurred. The SANE organization is and has been collaborating with the crime laboratory personnel to determine the best way to obtain known physical evidence as un-invasive as possible. The collection of oral swabs to determine whether oral sex occurred is one of the reasons for collecting an oral swab, another reason for collecting oral swabs/buccal swabs is for obtaining the victim's DNA eliminating the need to draw blood.
- The sex crime scene information directs the reader to be alert to collect seminal fluid if the perpetrator ejaculated and did not wear a condom. These instructions should be removed from the book as they are unfounded. I have had many cases where the proposed suspect did wear a condom (as determined from interviews and subsequent identification of material evidence) and seminal fluid was still found. There are many reasons for this, such as the condom was defective, the same condom was used multiple times, and the condom was subjected to extreme factors. Basically, the crime scene technician should approach the crime scene expecting to collect all forms of evidence and not go in with blinders because of a restrictive statement, such as someone wore a condom.
- Page 193 addresses cleaned crime scenes and in this section, luminol and fluorescein are discussed. I was surprised at the

[1]Program Manager for Forensic Science, Office of Law Enforcement Standards, NIST, Gaithersburg, MD.

limited information provided. Luminol is used more often than the book suggests and it is imperative the crime scene technicians understand all aspects. For example, they should recognize the major false positives (metals, cleaning agents containing hypochlorites, such as bleach) and how these false negatives will affect the interpretation of results in a car, bathroom, or kitchen where metals and cleaning agents are regularly used. Photographs depicting a bathroom response to luminol treatment should have been included and the possible carcinogen affects of luminol and fluorescein should have been discussed.

- Chapter 10: Several erroneous statements exist in this chapter, evident that the writer does not conduct firearm examinations. For example, the chapter includes a statement that grooves in a gun barrel are bored. When in fact the grooves are cut or formed in the barrel. On page 265, the directions to safely handle a semi-automatic pistol should be revised, specifically the step-by-step direction #5 that incorrectly implies that all pistols have slide mechanisms that "lock" the slide back. The reference to the detection of nitrates by the Griess test should be corrected; the Modified Griess test identifies nitrites and reduces the carcinogen hazard. In addition, the definition of gunshot residue is incomplete. The chapter provided assumptions to the mode of death with contact wounds when the distance is only one factor taken into consideration in the investigation.
- Chapter 12: This chapter was very different from all the rest and why it was presented in its fashion eludes me. I cannot fathom why the crime scene technician should be required to understand addictions, the human response to narcotics, the ingestion pathways, and all the background information on each drug. This chapter would have been more appropriate for a basic pharmacology book. Generalization errors existed, such as the explanation of the difference between crack and powder cocaine, which is more than one is hard and the other is powder.

The impression garnered from this review is the authors had their comfort zones and relied on other information resources to fill in the gaps. Of course this is to be expected, one person should rely on other experts to supplement their knowledge. I agree this is a good book to provide to anyone interested in activities associated with crime scene investigations but it could have been an excellent book with the use of expert forensic scientists assisting with the writing and editing.

JOURNAL OF FORENSIC SCIENCES

J Forensic Sci, November 2010, Vol. 55, No. 6
doi: 10.1111/j.1556-4029.2010.01512.x
Available online at: onlinelibrary.wiley.com

BOOK REVIEW

Phoebe R. Stubblefield,[1] *Ph.D.*

Review of: *The Immortal Life of Henrietta Lacks*

REFERENCE: Skloot R. The immortal life of Henrietta Lacks. New York, NY: Crown Publishers, 2010, 370 pp.

Skloot, a science writer and historian, has produced a comprehensive description of the origins, social and cultural settings, and social and scientific outcomes surrounding the existence of the cell line labeled HeLa. This book is primarily a historical document containing not just the origin of the HeLa cell line, but also a history of those perhaps most immediately affected by the development of the cell line. Based on the title alone one might assume that the book is solely about Henrietta Lacks, her life and death, and how the HeLa cell line affected her family. Skloot provided a voice for many with a role in this story, such as the doctor who treated Mrs. Lacks' cancer, the biologist George Gey, his wife and staff who cultured the cell line, peers and friends of the Lacks' family who sought recognition and compensation for the family, and a variety of scientists and research subjects who participated in the use or misuse of the cell line.

The dominant focus and strength of this book is as a history and biography of Henrietta Lacks, beginning with slavery under the White Lacks and progressing to the events that brought them to Baltimore and Johns Hopkins. The detailed descriptions, such as of life in the Lacks' hometown of Clover, VA, and reconstructions of Henrietta's behavior and personality, demonstrate to the reader that Henrietta Lacks was a person with a life and family, who was affected by events leading to her involvement in a major scientific milestone. Skloot quotes a memorial tribute to George Gey in which he is described as the right man in the right place, etc., for the scientific discovery of the HeLa cells to have occurred. By writing this book Skloot distributes the credit more broadly and equitably. Development of the HeLa cell line involved the juxtaposition of events far beyond Gey's ingenuity, including Johns Hopkins provision of health care to the poor and deeply pigmented, a war machine that brought the Lacks to Baltimore, a poorly educated family and cultural norms that required acquiescence to medical authority, and social norms supporting scientific use of discarded tissues.

About a third of the book covers Skloot's interactions with the Lacks family and their peers, especially her connection to Deborah, Henrietta's daughter. This is where Skloot presents her own role in Henrietta Lacks' biography, despite that when relating to Deborah in particular, and the Lacks family in general, Skloot found herself to be quite the outsider. Eventually, Deborah and Skloot join forces to investigate the history of the older sister Deborah never met, the account of which being both nightmarishly horrific and encouraging to those interested in their own genealogical research. The summary result of Skloot's connection with the Lacks family and her friendship with Deborah is to reveal the deep conflict and ambivalence the Lacks family had toward the existence of the HeLa cells.

The early chapters alternate between the past and present, which supports the dominant historical theme, but weakens the sense of following scientific progress. Those interested in how the Lacks were affected by the HeLa cells and their perspective toward their role in cellular biology history will find this information spliced between interludes with the scientists, businessmen, lawyers, and politicians developing the use of the HeLa cells. Those interested in a history of HeLa-related milestones and discoveries will find a limited quantity here, and much of it presented in anecdotal form.

Skloot is clearly sympathetic to the Lacks and anyone else who has found out the hard way that they have no partnership or intellectual property in commercial discoveries derived from his or her seized or discarded tissues. A few chapters in the third part of the book address this theme, but Skloot restricts her strongest comments to the Afterword, a discussion of the most frequently asked question about the book—"Don't doctors have to tell you when they use your cells in research?" Skloot discusses the broad issue of property rights to cells, tissues, physiological processes, and DNA and presents the American Civil Liberty Union's lawsuit against Myriad's patents on the BRCA1 and 2 genes as an example of a potential shift against the prevailing attitude that commercialization promotes scientific discovery. Considering that as of this writing Myriad's patent has been overturned, Skloot's book is quite a timely entry into our public consideration of the management of our private biology.

[1]Assistant Professor and Director Forensic Science Program, University of North Dakota, Grand Forks, ND.

JOURNAL OF FORENSIC SCIENCES

J Forensic Sci, November 2010, Vol. 55, No. 6
doi: 10.1111/j.1556-4029.2010.01513.x
Available online at: onlinelibrary.wiley.com

BOOK REVIEW

Mary A. Bush,[1] *D.D.S.*

Review of: *Forensic Dentistry, 2nd edition*

REFERENCE: Senn DR, Stimson PG. Forensic dentistry, 2nd edn. Boca Raton, FL: CRC Press, 2010, 437 pp.

This volume represents a completely revised version of the 1st edition with a new editor, Dr. David Senn, joining Dr. Paul Stimson. The chapter titles have for the most part been replaced or revised, and there are new contributors. As with the 1st edition, the format of the book follows that of a scholarly text with references.

This is a lengthy volume with 18 chapters. Topics are covered that are related to forensic dentistry as well as other disciplines of forensic science.

The introductory chapter on Science, the Law and Forensic Identification, summarizes the usefulness of forensic dentistry in a legal setting from victim identification to bitemarks, with a discussion of the legal significance of DNA evidence.

In Chapter 2, History of Forensic Dentistry, the reader is provided with a collection of historical case vignettes. Chapter 3, entitled Scope of Forensic Odontology, consists of a summary of the areas that a forensic dentist would be involved with. These disciplines are covered in depth in subsequent chapters of the book.

Chapter 4 describes Death Investigation Systems, with a discussion of the current and historical context of coroners and medical examiners in the U.S.A. Chapter 5 continues with the domain of the Medical Examiner. This chapter explores the concept of establishing identity through various means including external and internal inspection, taking into account possible pathologies. The chapter is illustrated with images from the morgue and crime scene.

Fingerprints and Human Identification, Chapter 6, exposes the reader to another area of forensic science. The history and basis of fingerprint analysis is outlined and summarized, and various methods are described for collection of fingerprint data.

The authors of Chapter 7, DNA and DNA Evidence, provide a useful review of methodology of DNA analysis with relevance to dentistry. Evidence collection techniques and a glossary are included. This is a much-needed update from the 1997 1st edition.

Chapter 8 focuses on Forensic Anthropology. An encapsulated summary of this related field is given. Chapter 9, Forensic Dental Identification, provides a thorough discussion of the aspects of dental victim identification.

Chapters 10 and 11 explain the imaging modalities in forensic dentistry, those of radiography and photography. The authors of these chapters correctly deal with the transition from traditional film to digital imaging.

The reader is provided with a succinct overview of the dental role in Multiple Fatality Incidents in Chapter 12. Chapter 13 reviews the topics encompassing Age Estimation. Here, a synopsis of the common dental age estimation methods is given.

The longest chapter in the book, Bitemarks, Chapter 14, opens with a section discussing background and historical cases. In the following section entitled Problem Cases, the authors identify by name participants in a number of cases, under the pretext of helping to prevent future errors. However, naming experts provides no additional educational purpose and seems out of place in a textbook. Some of the criticism leveled here is supported only by cited personal communications. Discussion of these cases could have easily been presented without this tactic. The chapter continues with aspects of bitemark analysis including bitemark characteristics, case management, and scientific considerations.

The circumstances and frequencies of Human Abuse are summarized in Chapter 15, followed by a return to the subject of the first chapter in Chapter 16, Jurisprudence and Legal Issues. The topic of Evidence Management is covered in Chapter 17. The book concludes with a chapter entitled Future of Forensic Dentistry, a challenging subject in a field undergoing rapid change. An Appendix is provided that lists U.S. Federal and State court cases of interest in forensic odontology.

In summary, this volume contains a variety of useful and interesting information for both the novice and experienced professional. It is illustrated with numerous black and white photographs. There is also an insert that includes color photography. Although the title is *Forensic Dentistry*, it may be best described as a collection of topics within and surrounding the field of forensic dentistry. Depending on reader preference, this can be seen as an added benefit of the book as other areas outside of forensic dentistry are presented.

[1]Suny at Buffalo, School of Dental Medicine, Buffalo, NY.

JOURNAL OF FORENSIC SCIENCES

J Forensic Sci, November 2010, Vol. 55, No. 6
doi: 10.1111/j.1556-4029.2010.01514.x
Available online at: onlinelibrary.wiley.com

BOOK REVIEW

George W. Clarke,[1] *J.D.*

Review of: *The Double Helix and the Law of Evidence*

REFERENCE: Kaye DH. The double helix and the law of evidence. Cambridge, MA: Harvard University Press, 2010, 330 pp.

David Kaye, Professor of Law at Pennsylvania State University and a contributor to the history of forensic DNA typing and its interface with the legal system, has produced a thought-provoking retrospective on scientific evidence and the justice system in the United States. As described by the author, *The Double Helix and the Law of Evidence* "examines the legal and scientific controversies that swirled around DNA and earlier forms of genetic evidence." The result is an instructive survey of the events leading to judicial acceptance of DNA testing and the often-difficult relationship between forensic scientists, academics, and the world of jurisprudence.

Kaye's account begins with pre-DNA serological techniques—including ABO and protein systems—and the frequent summary treatment accorded claims of scientific difficulties by trial and appellate courts. Included are brief case histories, particularly a few judicial decisions critical of the roles of bench analysts—sometimes referred to by courts through the use of critical terms, such as "mere technicians"—in providing testimony supporting scientific reliability and acceptance of those techniques. While certainly part of the history of genetic marker typing, the author unfortunately fails to include the far greater judicial case authority noting the importance of case-level analysts in the understanding and communication of scientific acceptance, and even case law elevating analysts to greater status than academic research scientists.

However, the history provided by the author of DNA techniques and their introduction into the legal system is detailed, accurate, and particularly helpful to scientists and justice system participants alike. In chapters that are aptly named, "Trial by Mathematics," "The Intensifying Debate Over Probability and Population Genetics," and "Ending the Debate Over Population Genetics," Kaye recounts the remarkable events that surrounded the admissibility of RFLP-based technology and the accompanying population frequency data that usually provided extremely small probabilities of coincidental matching DNA profiles. In a neutral and unbiased manner, the battles between competing experts are described, as well as the transitions from one position to another that were often the hallmark of a number of the experts who played prominent roles in court hearings that resulted in decisions of admissibility or inadmissibility of DNA profiling results. Especially useful is the author's narration of the events surrounding the 1992 and 1996 reports of the National Research Council, first fueling—then extinguishing—the fires fanned by academics and others regarding the validity of statistical estimates of the rarity of matching DNA profiles. Kaye provides excellent insight into some of the differences between the fields of science and the law; notable among them is the recognition that even attaching statistics to matching genetic samples is a legal policy decision, rather than a scientific requirement.

Moving on to the development and use of PCR-based systems, the author describes the remarkable power of short tandem repeat (STR) DNA testing and its ability to be successfully used even with small and challenging samples. Further chapters and sections are devoted to DNA databasing, mitochondrial DNA, issues surrounding the interpretation of mixed DNA samples, as well as quality assurance concerns, including errors and proficiency testing of analysts and laboratories.

The author's most intriguing discussion—particularly so, for a legal system participant, such as this reviewer—confronts head-on the very treatment accorded science by courts. Kaye describes the manner by which scientific experts are selected, the significance of compensation for their services, and the question of neutrality. Like others before him, the author suggests the use of neutral, court-appointed experts to resolve questions to be answered by courts regarding the use of scientific evidence. Yet, the very nature of the adversarial system of justice, the author notes, creates substantial obstacles to the use of such witnesses; as a judicial officer, this reviewer would note the additional impediment to canonical and ethical bars on magistrates and judges becoming embroiled in the very controversies brought to court for judicial decision.

The Double Helix and the Law of Evidence underscores the difficulty of legal decision making when scientists collide with the adversarial system of justice in place in American courts. That tension is heightened when expert witnesses advance opinions that many would argue are directed toward particular social and legal policy decisions rather than the presence or absence of scientific acceptance of a theory or method. DNA typing is no exception. As the author skillfully notes regarding prior arguments about the accuracy of statistical rarity estimates, "Despite the high drama of the confrontations between the population structuralists and the defenders of independence, most of the problems with DNA testing have not been errors of high theory or the introduction of methods that did not work. Rather, they have been production-line problems in the generation of the evidence for specific cases." A concise and accurate assessment from a book this reviewer—and anyone interested in forensics—would find fascinating.

[1]Judge of Superior Court, San Diego, CA.

JOURNAL OF FORENSIC SCIENCES

J Forensic Sci, November 2010, Vol. 55, No. 6
doi: 10.1111/j.1556-4029.2010.01524.x
Available online at: onlinelibrary.wiley.com

BOOK REVIEW

Max M. Houck,[1] *Ph.D.*

Review of: *Advanced Crime Scene Photography*

REFERENCE: Duncan C. Advanced crime scene photography. Boca Raton, FL: CRC Press, 2010, 315 pp.

Photography and microscopy have much in common, using as they do lenses to image the world and make it either permanent or visible; in the case of a photomicrograph, they do both at the same time.[1] They also both suffer in the same respect when authors attempt to write about them. The books inevitably start out with a *prima facie* discussion of optics and physics, accompanied by many intricate ray diagrams showing what the light rays are doing in excruciating technical detail. Only later, about a third of the way into the book, do you get to the meat of what you want to learn and how to do it. Do not misunderstand: Those basics are critical to an understanding of both photography and microscopy, but every book does not need to start that way. If you want that kind of book, the kind that drags you through formulae and the calculus of optics, do not buy *Advanced Crime Scene Photography*. If, however, you want a well-written, comprehensive, and excellently detailed book on the practicalities of crime scene photography, then definitely buy this book.

Duncan's book begins with a well-reasoned Introduction that explains his philosophy and rationale for crime scene photography:

> The photographic documentation of crime scenes is the cornerstone of any criminal investigation. The complete and accurate portrayal of a crime scene demands that the investigators and photographers thoughtfully and purposefully record true and accurate depictions of the location and evidence...The systematic and complete photographic recording of all aspects of an investigation helps bridge the gap between an individual piece of evidence and the processing of that evidence...Consequently, crime scene photography is an important and required task that must be accomplished with dedication and skill....Frequently, the fear of venturing away from a camera's program or automatic mode settings comes from a lack of confidence. Investigators are afraid of making mistakes in exposure or composition and therefore rely too heavily on the camera....One can possess the latest and greatest camera, having all the bells and whistles imaginable, but if the command dial is never moved off the automatic mode, one may as well be documenting the scene with a disposable point-and-shoot camera. The photographer, not the camera, is responsible for taking the picture. [page 1]

I could not agree more. Fear is the mind-killer (to borrow a phrase from the science fiction novel *Dune*), and nowadays forensic professionals are very fearful. Duncan's approach to crime scene photography is a breath of cool breeze to reassure us that we can, in fact, do this.

The remaining chapters progress through equipment (Chapter 2), the basics of crime scene photography (Chapter 3), and how to take photographs that are suitable for analytical examinations, such as for shoe prints (Chapter 4, and hallelujah!). After that, Duncan then proceeds through nighttime and low-light photography (Chapter 5), flash photography (Chapter 6), and painting with light (Chapter 7; the photograph of a light-painted spider is a great reminder that many of these techniques are not scale-dependent). The book raps up with bloodstain pattern photography (Chapter 8), shooting incidents (Chapter 9), and ultraviolet and infrared photography (Chapter 10).

Duncan's style is easy-to-read without pandering and is an engaging style that will be welcomed by students and trainees alike. Duncan also provides excellent examples to make practical points link with the theoretic, such as flash casting (page 160), depth of field (page 58), and distortion in scales by angle (page 74). Moreover, Duncan does a marvelous job of taking a practical approach to teaching *photography* and not optics or physics. His examples of making your own arrows for pointers (page 26), soft box for flashes (page 29), and light boxes (page 67) are great lessons and potential assignments.

Overall, I recommend this book for professionals, students, and trainees; anyone, really, who is interested in reading from someone who has a knack for teaching (in the true "tell-show-do" paradigm). Duncan's book is a welcome addition and an excellent book on crime scene *photography*.

[1]Director, Forensic Science Initiative, West Virginia University, 1600 University Avenue, Morgantown, WV 26506.

[1]As opposed to a "microphotograph," which is a really small picture: Don't confuse the two as many "experts" do.

JOURNAL OF FORENSIC SCIENCES

J Forensic Sci, November 2010, Vol. 55, No. 6
doi: 10.1111/j.1556-4029.2010.01555.x
Available online at: onlinelibrary.wiley.com

BOOK REVIEW

Joseph P. Bono,[1] *M.A.*

Review of: *Forensic Applications of High Performance Liquid Chromatography*

REFERENCE: Bayne S, Carlin M. Forensic applications of high performance liquid chromatography, Boca Raton, FL: CRC Press, 2010, 253 pp.

This reviewer entered this project expecting to find a 253-page text describing the forensic applications of high performance liquid chromatography (HPLC) (see the title above). What I discovered was a 253-page text with approximately 30 pages describing the forensic applications of HPLC. However, in the end, this was not such a disappointing process as might be imagined. Perhaps the authors could have chosen a more descriptive title de-emphasizing the forensic applications. This text contains one of the most comprehensive and understandable descriptions of chromatography in general, and HPLC in particular that this reviewer has encountered in recent years. The authors emphasize the fundamentals of HPLC without becoming mired in math, statistics, or theory.

Each chapter presents a targeted subject area with narratives, descriptions, figures, diagrams, and tables, which are basic enough for the novice to understand and detailed enough for the expert to appreciate. At the end of each chapter, there are references that point the reader toward other sources of information. Those references, books/online publications, journal articles, and journals (general) are presented in a concise format. A review of many of these references reflects a cross-sectional approach to citing international publications in the chromatographic sciences.

The first chapter presents a brief history of chromatography and describes the fundamentals of chromatographic instrumentation. There is no abundance of information in these four pages; however, this reviewer encourages the reader not to stop. Proceed to the second chapter beginning on page 5 entitled "Basic Principles of HPLC." Here, the reader will find an excellent primer on HPLC, which is both informative and easy to understand. This chapter could serve as a stand-alone introduction to HPLC in a college chemistry instrumental analysis course. The authors take the readers through the theory of chromatography, chemical bonding and polarity and intermolecular forces.

Chapters 3 through 7 present descriptions of mobile phase preparation, the use of buffer sample preparation, modes of separation, detection system method development, and system suitability. Again, these five chapters compile the basics of what the analyst should know when performing HPLC in any laboratory. Optimizing the protocols and procedures to deliver validated results is the goal of every scientist who uses any chromatographic system. Many of the solutions to the challenges of determining the best approach to chromatographic system questions are found in these chapters.

Chapter 8 is one of the more interesting chapters in the book. The authors move the discussion of HPLC into the realm of quality assurance and conformance to the ISO/IEC 17025:2005 *General Requirements for the Competence of Testing and Calibration Laboratories*. This ISO document forms the basis for accreditation of many forensic science laboratories. It is noteworthy that the discussion in this chapter addresses the estimation of uncertainty (better described by the authors as a "level of confidence"), sources of error, and statistical evaluations. For those who have wondered what "uncertainty" means in a laboratory setting, the answer can be found in this chapter. There are also substantive descriptions of "method validation," one of which is most appropriate. Through a reference to another text, the authors describe method validation in forensic science as a requirement to ensure "that the data are reliable but also to ensure that there are no 'unjustifiable legal consequences' for the defendant in court." This is in fact what "validation" means.

Chapter 9 continues with a discussion of quality systems, accreditation, and auditing. This chapter is too brief and too basic and could have easily been eliminated from this text without losing focus on the information presented by the authors in other chapters.

Chapter 10 deals with troubleshooting HPLC systems. The format of this chapter is complete with a narrative and tables describing what to do when something goes wrong, either at the front end or the back end of an analysis. The Key Point Summary table at the end of the chapter is most informative. Many of those questions of "What is happening here?" are addressed. The reader is presented with options of where to look for the cause of the problem, and then suggestions for how to "fix it."

Finally, the reader reaches Chapter 11 entitled *Forensic Applications of HPLC*. The authors present an overview of HPLC in drug analysis, toxicology, color analysis, explosives analysis, and food and the environment. All these in 20 pages. The information in this chapter is basic at best; an expanded discussion of these analyses should have been the focus of the text. Twenty pages are not enough.

If the reader is seeking an excellent text book on chromatography, specifically HPLC, this reviewer highly recommends and will use this book, as a source of information. If the reader is seeking an overview of the forensic applications of HPLC which is limited in scope and content, this reviewer recommends the last 20 pages with the caveat that the information contained therein will be basic at best.

[1]Adjunct Instructor, Forensic and Investigative Sciences Program, Indiana University Purdue University-Indianapolis, Indianapolis, IN.

JOURNAL OF FORENSIC SCIENCES

J Forensic Sci, November 2010, Vol. 55, No. 6
doi: 10.1111/j.1556-4029.2010.01556.x
Available online at: onlinelibrary.wiley.com

BOOK REVIEW

Kenneth E. Melson,[1] *J.D.*

Review of: *Ethics and the Practice of Forensic Science*

REFERENCE: Bowen R. Ethics and the practice of forensic science. Boca Raton, FL: CRC Press, 2010, 197 pp.

Enhancing ethical behavior and professionalism within the forensic science community is a goal of ongoing efforts to improve the practice of forensic science in the United States. The National Academy of Sciences' report entitled *Strengthening Forensic Science in the United States: A Path Forward* calls for the adoption of a uniform code of ethics. ASCLD/LAB has already implemented the *Guiding Principles of Professional Responsibility for Crime Laboratories and Forensic Scientists* for its 376 accredited public and private laboratories. Robin T. Bowen's *Ethics and the Practice of Forensic Science* contributes to the knowledge base for these and other ethical practices. Her book provides the parameters for a culture of professionalism for practitioners. While acknowledging that forensic scientists are human, and therefore capable of making mistakes, Bowen promotes education and awareness to enhance the recognition of ethical issues and a framework for potentially resolving them.

The nine chapters cover the full range of ethics, starting with an analysis of just what is meant by "ethics," and then takes the reader through a progressive learning adventure about ethics and forensic science in the criminal and civil justice systems, in the courtroom, in research science, and in forensic science. Chapters 1 through 5 are general in nature, recognizing that the wide variety of situations and diversity of contexts prohibit hard and fast rules that apply to all situations. Chapters 6 and 7 explore examples of unethical behavior, most of which are widely known. Four established codes of ethics are presented in Chapter 8. Appendix B provides examples of another four codes from U.S. forensic science organizations. There is, however, no discussion, analysis, or comparison of these codes or why they were chosen for inclusion in the book from the scores of extant codes of ethics. Neither is there a resource compendium of existing codes so that readers can expand their research and comparative analyses of other codes. Unfortunately, the ASCLD/LAB code of professional responsibility, which is the most widely implemented code and the closest one to a national code, is missing.

In the author's survey of AAFS members at its 2006 Annual Meeting, a portion of which appears in Appendix A, 98% of the respondents considered ethics in forensic science to be very important or important. Nevertheless, 68% of the respondents did not think forensic scientists receive adequate training in ethics. A good foundation for this needed training appears in her last chapter, where Bowen sets out the guiding principles that she believes are the basics of ethics in forensic science. In her estimation, forensic scientists should (i) maintain technical competence; (ii) employ reliable analytical methods; (iii) confine examinations to areas of expertise; (iv) exhibit honesty regarding personal qualifications; (v) exhibit intellectual honesty regarding data generated; and (vi) objectively review evidence and deliver expert testimony.

The author also provides an extensive bibliography, but it is difficult to determine to what extent and where the bibliographic material was used to support the concepts presented in her book. There is an annoying lack of references in the text to the source material. Citations to specific studies and reports are missing, leaving the reader no avenue to check the assertion or to delve further into the subject. This is of particular concern because some of the few citations included in the body of the book are incorrect or incorrectly characterized. For example, only one other time in 40 years has this reviewer seen the case of *Frye v. United States* incorrectly referred to as a case from the United States Supreme Court, as the author does in her book. The case citation in the text clearly indicates that it is not from that court. Such a mistake regarding one of the most famous cases concerning the admissibility of scientific evidence may lead a reader to question the accuracy of other assertions and characterizations in the text, and ergo, the need for citations to specific source material.

There remains a critical need for books, other source materials, and training aids on the subject of ethics in forensic science. Robin Bowen's book provides a starting point for more discussion and will help promote widespread discourse on the important subject of ethics.

[1]The George Washington University Law School Adjunct Faculty, and Deputy Director, Bureau of Alcohol, Tobacco, Firearms and Explosives (ATF), Washington, DC.

JOURNAL OF FORENSIC SCIENCES

J Forensic Sci, November 2010, Vol. 55, No. 6
doi: 10.1111/j.1556-4029.2010.01557.x
Available online at: onlinelibrary.wiley.com

BOOK REVIEW

Carl N. Stephan,[1] *Ph.D.*

Review of: *Computer-Aided Forensic Facial Comparison*

REFERENCE: Evison PE, Vorder Bruegge RW. Computer-aided forensic facial comparison. Boca Raton, FL: CRC Press, 2009, 183 pp.

The preface of *Computer-Aided Forensic Facial Comparison* pitches this book as an initial attempt to address a number of scientific and technical issues in forensic facial comparison, and it succeeds in doing that. This edited volume reports the findings from a large-sampled 2-year research project on landmark-based analysis of 3D facial form. The book gives focus to a variety of topics across 12 chapters, including 3D face capture and human face variability. In addition to the written text, a library of raw coordinate data is also provided. As stated by the editors of the book, these data can be used for independent crime prevention and detection research and as such provide for a valuable resource. The DVD library contains coordinates of 30 landmarks on each participant's face, for >3000 living individuals. Also included are preliminary and prototypic software tools for (what is ultimately) 2D facial comparison, which were developed during the project. These generous supplements will no doubt be of value to many readers and will probably justify the outright purchase of the volume.

The book devotes prime attention to one particular type of 3D scanner—the now discontinued Geometrix FaceVision® FV802 Series Biometric Camera (ALIVE tech, Cumming, GA). Two other instruments were also employed for data collection but on a vastly reduced scale: the Cyberware® 3030PS Head and Neck Scanner (Cyberware, Inc., Monterey, CA) and the 3dMDface™ System (3dMD, Atlanta, GA). After a general introduction by the editors in Chapter 1, Goodwin et al. compare scans generated from the three aforementioned digitizers for artifacts (spikes, stretching and discrepancies in texture map alignment, etc.) and metric differences in landmark position (caliper measurements are used as the gold standard). In Chapter 3, Morecroft et al. explore 60 facial landmarks to determine which ones are optimal for 3D face scan analysis. In Chapter 4, Evison and colleagues revisit the makeup of the 3D scan sample and subject it to a principal components analysis to examine how individuals vary by sex, age, and ancestry in respect to these PCs (the first PC is given almost sole attention). In Chapter 5, Morecroft et al. explore the effects of image parameters (lighting, resolution, illumination, etc.) on the manual placement of landmarks. In Chapter 6, Goodwin et al. elucidate the patterns of visibility of 30 landmarks (arrived at in Chapter 3) with 10 degree increments of rotation between −90 to +90 degrees about two orthogonal axes (y and x). In Chapter 7, Schofield et al. explore the effect of perspective and lens distortion *in silico* by switching-out simulated lenses and changing subject–camera distances within the software environment of 3ds Max® (Autodesk®, San Rafael, CA). In Chapter 8, Maylin et al. explore the value of an active shape model to automate facial landmark placement in 3D, using 40 manually landmarked faces as a training set. In Chapter 9, Morecroft and Fieller provide solutions for missing landmarks/data. In Chapter 10, Mallett provides a very general review of the responsibilities of the expert witness and what information is admissible in court. In Chapter 11, Morecroft and Evison present a short description on the software tools included with the book, and in Chapter 12 the editors summarize the work and provide a synthesis of its major findings, the climax on p.163 being that "the 3D distribution of anthropometric landmarks studied herein, is unlikely to be sufficient to allow for identification of individuals to the exclusion of all others."

Strengths of this book lie with: the research results on 3D face variation and the total size of the sample analyzed; the breadth of different topics examined; and the supplemental data and software features included with the volume. Weaknesses are as follows: use of outdated and now discontinued technology; the preliminary and small-sampled nature of many of the sub-section studies; occasional oversights to details (text in figures is often tiny and difficult to read, color figures appear in the midst of Chapter 11, etc.). In summary, the editors' preface outlines this book nicely—it is a useful first look that draws on a large sample, but it is not an exhaustive thesis.

[1]Forensic Anthropologist and ORISE Research Participant, Joint POW/MIA Accounting Command, 310 Worchester Avenue, Hickam Air Force Base, HI.

JOURNAL OF FORENSIC SCIENCES

J Forensic Sci, November 2010, Vol. 55, No. 6
doi: 10.1111/j.1556-4029.2010.01515.x
Available online at: onlinelibrary.wiley.com

ERRATUM

REFERENCE: Jermain JD, Evans HK. Analyzing *Salvia Divinorum* and its active ingredient Salvinorin A utilizing thin layer chromatography and gas chromatography/mass spectrometry. J Forensic Sci 2009;54(3):612–16.

We have noticed an error in Figure 1. The R_1 value for salvinorin A should be $R_1 = OCOCH_3$ and not $R_1 = COCH_3$ as printed.

John D. Jermain, M.S.
Bureau of Alcohol, Tobacco,
Firearms and Explosives,
355 North Wiget Lane,
Walnut Creek, CA 94598

JOURNAL OF FORENSIC SCIENCES

J Forensic Sci, November 2010, Vol. 55, No. 6
doi: 10.1111/j.1556-4029.2010.01516.x
Available online at: onlinelibrary.wiley.com

ERRATUM

REFERENCE: Kumar O, Pradhan S, Sehgal P, Singh Y, Vijayaraghavan R. Denatured Ricin can be detected as native Ricin by immunological methods, but nontoxic *in vivo*. J Forensic Sci 2010;55(3):801–7.

Please note that a correction is required to line 5 of the Abstract for the above-referenced manuscript.

Line 5 inadvertently read: The denatured ricin did cause mortality up to 25 mg/kg, while 5 and 10 μg/kg of native ricin caused 50% and 100% mortality, respectively.

Line 5 should have read: The denatured ricin did not cause mortality up to 25 mg/kg, while 5 and 10 μg/kg of native ricin caused 50% and 100% mortality, respectively.

Om Kumar, Ph.D.
Division of Pharmacology and Toxicology,
Defense Research and Development Establishment,
Gwalior – 474002, India